

N 65-35971

(ACCESSION NUMBER)

389

(PAGES)

(THRU)

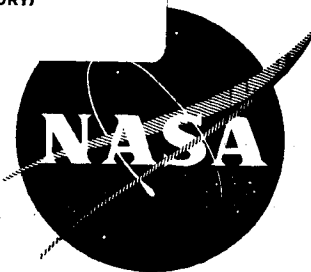
(CODE)

33

(CATEGORY)

(NASA CR OR TMX OR AD NUMBER)

NASA-CR-54739



# ALKALI METALS BOILING AND CONDENSING INVESTIGATIONS

## Quarterly Progress Report 12

GPO PRICE \$ \_\_\_\_\_

CSFTI PRICE(S) \$ \_\_\_\_\_

Hard copy (HC) 7.00Microfiche (MF) 2.00

ff 653 July 65

Edited by  
**G. L. CONVERSE**  
and  
**F. E. TIPPRETS**

prepared for  
**NATIONAL AERONAUTICS AND SPACE ADMINISTRATION**  
**CONTRACT NAS 3-2528**

**SPACE POWER AND PROPULSION SECTION**  
**MISSILE AND SPACE DIVISION**

**GENERAL  ELECTRIC**

**CINCINNATI, OHIO 45215**

NASA-CR- 54739

ALKALI METALS BOILING AND CONDENSING INVESTIGATIONS  
QUARTERLY PROGRESS REPORT 12

Covering the Period  
April 1, 1965 through June 30, 1965

Edited by

G.L. Converse  
and  
F.E. Tippetts

prepared for  
NATIONAL AERONAUTICS AND SPACE ADMINISTRATION  
Contract NAS 3-2528

July 23, 1965

Technical Management  
NASA - Lewis Research Center  
Nuclear Power Technology Branch  
Ruth N. Weltmann

SPACE POWER AND PROPULSION SECTION  
MISSILE AND SPACE DIVISION  
GENERAL ELECTRIC COMPANY  
CINCINNATI, OHIO 45215



## TABLE OF CONTENTS

	<u>Page No.</u>
Foreword	vii
List of Tables	ix
List of Illustrations	xi
Nomenclature	xvii
<u>Section</u>	
I SUMMARY	1
II 300 KW PROJECT	7
Status of Loop and Test Section	7
Status of Data Reduction	7
Status of Data Evaluation	8
Derivation of Helix Equations	8
Correlation of Single Phase Pressure	8
Drop and Heat Transfer With Inserts	
Local Results	12
III 100 KW PROJECT	17
Status of Loop and Test Section	17
Status of Data Reduction	19
Status of Data Evaluation	19
Nucleate Boiling Results	19
Critical Heat Flux, Film Boiling and	
Superheat Results	20
IV 50 KW PROJECT	31
Status of Loop and Test Section	31
Status of Data Reduction	31
Status of Data Evaluation	32
Heat Transfer	32
Liquid Vapor Interface Test	42
V FACILITIES AND INSTRUMENTATION	45
300 KW Facility	45
100 KW Facility	45
50 KW Facility	51

	<u>Page No.</u>
VI MATERIALS SUPPORT	53
Fabrication of Test Section No. 4	53
Fabrication of Test Section No. 5	55
VII ANALYSIS	59
Vapor Generation by Evaporation at Existing Liquid Vapor Interfaces	60
Vapor Generation by Vigorous Nucleate Boiling	64
Suppression of Nucleation	67
Vaporization of Potassium in a Tube Having a Uniform Heat Flux Imposed on the Tube Boundary	77
Recommended Design Procedures for Calculating Heat Transfer Coefficients at Heat Fluxes Less Than the Critical	89
REFERENCES	91
TABLES	95
ILLUSTRATIONS	105
APPENDICES	
A. Derivation of Helix Equations	189
B. 100 KW Data	197
Table B-1 100 KW Loop Test Section Instru- mentation for Test Section No. 3	199
Table B-2 Nomenclature for Tabulated 100 KW Boiling Data	200
Table B-3 100 KW Boiling Data	201
C. Condensing Test Section Mechanical Design Description (50 KW Project)	247
D. 50 KW Data	267
Table D-1 Nomenclature for Condensing Heat Transfer Results from the 50 KW Facility (5/8-inch ID Tube with Tapered Pin Insert)	269
Table D-2 Condensing Heat Transfer Results from the 50 KW Facility (5/8-inch ID Tube with Tapered Pin Insert)	272
Table D-3 Nomenclature for Condensing Heat Transfer Results from the 50 KW Facility (3/8-inch Tube, No Insert)	321
Table D-4 Condensing Heat Transfer Results from the 50 KW Facility (3/8-inch Tube, No Insert)	324

APPENDICES (Continued)

- E. Analysis of Some of the Errors Associated  
with the Measurement of Temperature  
Differences in the 100 KW Loop

369

## FOREWORD

Principal technical contribution to the program during the quarter, within the General Electric Company, was by the following individuals.

Manager, Heat Transfer Program	F.E. Tippets
300 KW Loop Project	J.R. Peterson
	D.R. Ferguson
100 KW Loop Project	J.A. Bond
50 KW Loop Project	S.G. Sawochka
Heat Transfer Mechanical Design	R.R. Oliver
Facilities	J.C. Amos
	R.A. Fuller
Instrumentation	W.H. Bennethum
Materials Support	W.R. Young
	W.H. Kearns
Analysis	G.L. Converse

## LIST OF TABLES

<u>Table No.</u>		<u>Page No.</u>
1.	Critical Heat Flux and Transition Boiling Data from 300 KW Project	95
2.	Critical Heat Flux Data from 100 KW Project	97
3.	Film Boiling and Superheat Data - 100 KW Project	98
4.	Vapor Phase Heat Transfer Coefficients-50 KW Project	99
5.	Comparison of Experimental Data and Correlation - 50 KW Project	102

## LIST OF ILLUSTRATIONS

<u>Figure No.</u>	<u>Page No.</u>
1. Experimental Friction Factors for Water Flowing in Straight Tubes Containing Helical Inserts (300 KW Project)	105
2. Summary of Friction Factor Measurements for Water Flowing in Straight Tubes Containing Helical Inserts	106
3. Correlation of Helical Flow Single Phase Friction Factors	107
4. Comparison of Predicted and Measured Helical Flow Friction Factors	108
5. Summary of Heat Transfer Measurements for Water Flowing in Straight Tubes Containing Helical Inserts	109
6. Correlation of Helical Flow Single Phase Heat Transfer Data	110
7. Critical Heat Flux Data Obtained in a 0.67-inch I.D. Tube (300 KW Facility)	111
8a. Nucleate Boiling Results, 100 KW Loop. (Test Section I.D. = 0.423 in., No Insert) $T_{sat} = 2100^{\circ}\text{F}$ , $G = 60 \text{ lb/sec-ft}^2$	112
8b. Nucleate Boiling Results, 100 KW Loop. (Test Section I.D. = 0.423 in., No Insert) $T_{sat} = 1800^{\circ}\text{F}$ and $2100^{\circ}\text{F}$ , $G = 30 \text{ lb/sec-ft}^2$	113
8c. Nucleate Boiling Results, 100 KW Loop. (Test Section I.D. = 0.423 in., No Insert) $T_{sat} = 2100^{\circ}\text{F}$ , $G = 45 \text{ lb/sec-ft}^2$	114
9. Recorder Chart Showing the Onset of the Critical Heat Flux and Film Boiling Conditions - 100 KW Loop (2/27/65)	116- 117
10. Recorder Chart Showing the Onset of the Critical Heat Flux Condition - 100 KW Loop (2/28/65)	118
11. Recorder Chart Showing the Onset of the Critical Heat Flux Condition - 100 KW Loop (3/17/65)	119

# LIST OF ILLUSTRATIONS (Continued)

<u>Figure No.</u>		<u>Page No.</u>
12.	Recorder Chart Showing the Onset of the Critical Heat Flux Condition - 100 KW Loop (3/27/65)	120
13.	Recorder Chart Showing the Critical Heat Flux Condition, Transition Boiling and Film Boiling - 100 KW Loop (3/31/65)	121
14a.	Recorder Chart Showing Changes in Boiling Regime - 100 KW Loop	122
14b.	Recorder Chart Showing Changes in Boiling Regime - 100 KW Loop (continued)	123
14c.	Recorder Chart Showing Changes in Boiling Regime - 100 KW Loop (continued)	124
15a.	Recorder Chart Showing the Onset of the Critical Heat Flux Condition - 100 KW Loop (4/1/65)	125
15b.	Repeat of Critical Heat Flux Point Shown in Figure 15a - 100 KW Loop (4/1/65)	126
16.	Comparison of Critical Heat Flux Data from the 100 KW and 300 KW Facilities	127
17.	Critical Heat Flux Parameter as a Function of Quality - 100 KW Loop	128
18.	Critical Heat Flux Parameter as a Function of Liquid Film Thickness - 100 KW Loop	129
19.	Thermal Conductivity of INCO Nickel 270 Condenser Tube	130
20.	Local Condensing Heat Transfer Coefficient for Potassium Vapor (50 KW Facility, 5/8-inch Tube Tapered Pin Insert and 3/8-inch Tube without Insert)	131
21.	Predicted Nusselt Condensing Ratio from Dukler Film Thickness	133
22.	Kinetic Theory Mass Flux	134
23.	Kinetic Theory Heat Transfer Coefficient	135
24.	Comparison of Vapor Heat Transfer Results with Kinetic Theory Prediction	137
25.	Kinetic Theory Heat Transfer Coefficient for $\sigma_e = 110$	139

# LIST OF ILLUSTRATIONS (Continued)

<u>Figure No.</u>		<u>Page No.</u>
26.	Comparison of Liquid Film and Vapor Heat Transfer Coefficient for Water and Potassium for $\sigma_c = \sigma_e = 1$	140
27.	Liquid Vapor Interface Test (50 KW Facility, 5/8-inch Tube with 1/4-inch Tubular Insert)	141
28.	Variable Automatic Power Cut Back Circuit - 100 KW Loop	142
29.	Thermocouple Junction at the End of an 11-Hole Insulator	143
30.	Thermocouple Junction in Slotted Insulator	144
31.	Transition Between 11-Hole Insulator and 2-Hole Insulator	145
32.	Cb-1Zr Test Section No. 4 for 100 KW Loop with Insert Installed	146
33.	Cb-1Zr Helical-Plug Insert for Test Section No. 4, 100 KW Loop	147
34.	Component Parts of Helix (Test Section No. 4, 100 KW Facility)	148
35.	Helix Section of Insert (Test Section No. 4, 100 KW Facility)	149
36.	Insert Plug (Test Section No. 4, 100 KW Facility)	150
37.	100 KW Test Section No. 5	151
38.	Test Section No. 5 Components, 100 KW Facility	152
39.	Boiling Nucleator (Test Section No. 5, 100 KW Facility)	153
40.	Effect of Liquid Entrainment on the Nusselt Numbers Calculated from the Film Evaporation Model	154
41.	Void Fraction as a Function of Quality for Potassium	155
42.	Slip Ratio as a Function of Quality for Potassium	156
43.	Nusselt Numbers from the Film Evaporation Model	157
44.	Film Thickness to Tube Radius Ratio as a Function of Quality	158



# LIST OF ILLUSTRATIONS (Continued)

<u>Figure No.</u>		<u>Page No.</u>
45.	Modified Film Evaporation Nusselt Numbers	159
46.	Heat Flux as a Function of $T_w - T_{sat}$ for the Forced Convection Nucleate Boiling Model	160
47.	Superheat Requirements for Incipient Boiling of Several Fluids	161
48.	Superheat Requirements for Incipient Boiling of Potassium	162
49.	Effect of Cavity Size on Superheat Requirements for Incipient Boiling of Potassium ( $T_{sat} = 1800^{\circ}\text{F}$ )	163
50a.	Micrograph of 100 KW Boiling Surface	164
50b.	Micrograph of 100 KW Boiling Surface	165
51.	Quality Requirements for Boiling Suppression ( $T_{sat} = 1800^{\circ}\text{F}$ )	166
52a.	Vaporization Regimes of Potassium (Heat Fluxes Less Than the Critical)	167
52b.	Vaporization Regimes of Potassium (Heat Fluxes Less Than the Critical)	168
53a.	Inside Wall Temperature as a Function of L/D (100 KW Test Section)	169
53b.	Heat Transfer Coefficient as a Function of L/D (100 KW Test Section)	170
54.	Inside Wall Temperature as a Function of L/D for the 100 KW Test Section (Plot Shows the Local Instability Associated with the Boiling Boundary)	171
55a.	Forced Convection Vaporization of Potassium at Low Vapor Qualities; $q'' = 29,000 \text{ Btu/hr-ft}^2$ (100 KW Data)	172
55b.	Forced Convection Vaporization of Potassium at Low Vapor Qualities; $q'' = 32,000 \text{ Btu/hr-ft}^2$ (100 KW Data)	173
55c.	Forced Convection Vaporization of Potassium at Low Vapor Qualities; $q'' = 57,000 \text{ Btu/hr-ft}^2$ (100 KW Data)	174
55d.	Forced Convection Vaporization of Potassium at Low Vapor Qualities; $q'' = 56,000 \text{ Btu/hr-ft}^2$ (100 KW Data)	175

# LIST OF ILLUSTRATIONS (Continued)

<u>Figure No.</u>		<u>Page No.</u>
56.	Nusselt Numbers as a Function of Vapor Quality (100 KW Data)	176
57.	Heat Flux as a Function of Temperature Difference for $T_{\text{sat}} = 2100^{\circ}\text{F}$ (100 KW Data)	177
58.	Heat Flux as a Function of Temperature Difference for $T_{\text{sat}} = 1990^{\circ}\text{F}$ (100 KW Data)	178
59.	Heat Flux as a Function of Temperature Difference for $T_{\text{sat}} = 1750^{\circ}\text{F}$ (100 KW Data)	179
60a.	Forced Convection Vaporization of Potassium at Intermediate Vapor Qualities; $q'' = 27,000 \text{ Btu/hr-ft}^2$ (100 KW Data)	180
60b.	Forced Convection Vaporization of Potassium at Intermediate Vapor Qualities; $q'' = 27,000 \text{ Btu/hr-ft}^2$ (100 KW Data)	181
61a.	Percent Probable Error in Inside Wall to Fluid Temperature Difference for the 100 KW Test Section (2 Wall and 3 Fluid Temperature Measurements at a Given Station)	182
61b.	Percent Probable Error in Inside Wall to Fluid Temperature Difference for the 100 KW Test Section (1 Wall and 3 Fluid Temperature Measurements at a Given Station)	183
62a.	Forced Convection Vaporization of Potassium at Intermediate Vapor Qualities; $q'' = 57,000 \text{ Btu/hr-ft}^2$ (100 KW Data)	184
62b.	Forced Convection Vaporization of Potassium at Intermediate Vapor Qualities; $q'' = 56,000 \text{ Btu/hr-ft}^2$ (100 KW Data)	185
62c.	Forced Convection Vaporization of Potassium at Intermediate Vapor Qualities; $q'' = 55,000 \text{ Btu/hr-ft}^2$ (100 KW Data)	186
62d.	Forced Convection Vaporization of Potassium at Intermediate Vapor Qualities; $q'' = 84,000 \text{ Btu/hr-ft}^2$ (100 KW Data)	187
62e.	Forced Convection Vaporization of Potassium at Intermediate Vapor Qualities; $q'' = 82,000 \text{ Btu/hr-ft}^2$ (100 KW Data)	188

## NOMENCLATURE

The symbols and units listed below are used in all derivations. The symbols listed below are occasionally used with other units in the figures, tables, or in the written text. Whenever this is done, the appropriate units are indicated.

### Simple Latin Letter Symbols

<u>Symbol</u>	<u>Quantity</u>	<u>Units</u>
A	Area	ft <sup>2</sup>
a	Radial acceleration ( $a = g/g_c$ )	Dimensionless
b	Bubble height	ft
D	Diameter	ft
E	Mass fraction of liquid entrained in the vapor core	Dimensionless
f	Darcy-Weisback friction factor	Dimensionless
G	Mass velocity (flow rate per unit flow area)	lb <sub>m</sub> /hr-ft <sup>2</sup>
g	Acceleration due to gravity	4.17 x 10 <sup>8</sup> ft/hr <sup>2</sup>
h	Heat transfer coefficient	Btu/hr-ft <sup>2</sup> -°R
J	Conversion factor (mechanical equivalent of heat)	778 ft-lb <sub>f</sub> /Btu
K	Thermal conductivity	Btu/hr-ft °R
k	Slip ratio ( $k = V_g/V_f$ )	Dimensionless
L	Length	ft
M	Molecular weight	lb <sub>m</sub> /lb <sub>m</sub> mole
P	Pressure	lb <sub>f</sub> /ft <sup>2</sup>
Q	Rate of heat flow	Btu/hr
R	Universal gas constant	1545 $\frac{\text{ft lb}_f}{\text{lb}_m \text{ mole } ^\circ\text{R}}$
r	Radius	ft
s	Arc length	ft
T	Temperature	°R
t	Time	hr
U	Overall heat transfer coefficient	Btu/hr-ft <sup>2</sup> °R
V	Velocity	ft/hr

### Simple Latin Letter Symbols (Continued)

<u>Symbol</u>	<u>Quantity</u>	<u>Units</u>
W	Flow rate	lb <sub>m</sub> /hr
X	Flowing quality ( $X = W_g/W$ )	Dimensionless
Z	Axial coordinate of the boiler	ft

### Composite Latin Letter Symbols

<u>Symbol</u>	<u>Quantity</u>	<u>Units</u>
A <sub>F</sub>	Flow area	ft <sup>2</sup>
A <sub>2</sub> /A <sub>1</sub>	Area ratio in a sudden expansion	Dimensionless
C <sub>p</sub>	Constant pressure specific heat	Btu/lb <sub>m</sub> °R
D <sub>T</sub>	Inside tube diameter	ft
g <sub>c</sub>	Conversion factor	$4.17 \times 10^8 \frac{\text{ft lb}_m}{\text{lb}_f \text{ hr}^2}$
h <sub>c</sub>	Condensing heat transfer coefficient	Btu/hr-ft <sup>2</sup> °R
h <sub>f</sub>	Liquid enthalpy	Btu/lb <sub>m</sub>
h <sub>fg</sub>	Latent heat	Btu/lb <sub>m</sub>
h <sub>g</sub>	Vapor enthalpy	Btu/lb <sub>m</sub>
K <sub>E</sub>	Irreversible loss coefficient due to sudden expansion	Dimensionless
N <sub>Nu</sub>	Nusselt number ( $N_{Nu} = h D/K$ )	Dimensionless
N <sub>Pe</sub>	Peclet number ( $N_{Pe} = G D C_p/K$ )	Dimensionless
N <sub>Pr</sub>	Prandtl number ( $N_{Pr} = \mu C_p/K$ )	Dimensionless
N <sub>Re</sub>	Reynolds number ( $N_{Re} = \rho V D/\mu$ )	Dimensionless
P <sub>w</sub>	Wetted perimeter	ft
P(X)	Probable error in X	Dimensionless
q"	Heat flux	Btu/hr-ft <sup>2</sup>
q" <sub>c</sub>	Critical heat flux	Btu/hr-ft <sup>2</sup>
r <sub>c</sub>	Cavity-mouth radius	ft

### Composite Latin Letter Symbols (Continued)

<u>Symbol</u>	<u>Quantity</u>	<u>Units</u>
$R_g$	Void fraction	Dimensionless
$v_{fg}$	Specific volume change in going from liquid to vapor	$\text{ft}^3/\text{lb}_m$
$X_c$	Quality at the critical heat flux	Dimensionless

### Simple Greek Letter Symbols

<u>Symbol</u>	<u>Quantity</u>	<u>Units</u>
$\beta$	Bubble contact angle	radians
$\Gamma$	Mass flow rate of liquid per unit circumference $\left[ \Gamma = \frac{(1-X) W}{\pi D} \right]$	$\text{lb}_m/\text{hr-ft}$
$\Delta$	Finite difference	Dimensionless
$\Delta$	Thickness of the tape wound around the centerbody of the helix	ft
$\delta$	Film thickness	ft
$\theta$	Angular displacement	radians
$\mu$	Dynamic viscosity	$\text{lb}_m/\text{hr-ft}$
$\nu$	Kinematic viscosity	$\text{ft}^2/\text{hr}$
$\rho$	Mass density	$\text{lb}_m/\text{ft}^3$
$\sigma$	Surface tension	$\text{lb}_f/\text{ft}$
$\tau$	Vapor shear stress	$\text{lb}_f/\text{ft}^2$

### Composite Greek Letter Symbols

<u>Symbol</u>	<u>Quantity</u>	<u>Units</u>
$\delta_c$	Condensation coefficient	Dimensionless
$\delta_e$	Evaporation coefficient	Dimensionless
$\tau^*$	Dimensionless Shear Stress	Dimensionless

## Subscripts

<u>Symbol</u>	<u>Quantity</u>
a	Axial velocity component
b	Bulk fluid temperature
c	Value at the critical heat flux condition
cb	Diameter of helix centerbody or probe
DNB	Departure from nucleate boiling
e	Equivalent value of a given quantity for application to helical flow
f	Indicates a liquid phase property
FB	Film boiling
FE	Film evaporation
g	Indicates a vapor phase property
H	Value referred to helix
I, i	Inside or inlet
K	Potassium
l	Refers to liquid phase
M	Maximum
Na	Sodium
NB	Nucleate boiling
o	Outlet or outside
PB	Pool boiling
s, sat	Saturation
SH	Superheat
SHV	Superheated vapor
T	Tangential
TB	Transition boiling
TP	Two-phase
TPF	Two-phase friction
v	Refers to vapor phase
w	Value at the tube wall

I SUMMARY  
F.E. Tippetts

This program is being conducted for the National Aeronautics and Space Administration under Contract NAS 3-2528 to obtain two-phase heat transfer and fluid flow data for potassium under conditions of boiling and condensing approximating those anticipated in large space turbo-electric power systems. Test equipment development, materials studies and theoretical analysis related to the experimental work are conducted as a support effort. The following items summarize the work performed during the quarter ending June 30, 1965.

300 KW Project

All boiling test data obtained with the 300 KW Facility have been reduced and reported. These data are now being analyzed and treated in preparation for a topical report covering this project.

Water pressure drop tests to obtain single-phase friction factors for the insert and non-insert test section geometries, as an aid to correlating the two-phase potassium pressure drop data obtained, have been completed and the results are reported in Section II.

Critical heat flux conditions and transition boiling heat transfer coefficients have been calculated from the data obtained with the 3/4-inch nominal diameter test section, both with and without a helical insert. These results and the analytical treatment used to derive them are presented in Section II.

The principal work under this project over the next quarter will be completion of the analytical effort and preparation of the

topical report for the project.

### 100 KW Project

Test Set No. 3, done with a 3/8-inch nominal diameter (0.42-inch I.D.) plain tube test section (no insert) were completed in early April. In addition to nucleate boiling heat transfer coefficient measurements and some boiling inception tests, several critical heat flux determinations were made at heat flux levels to 225,000 Btu/hr-ft<sup>2</sup> and heat transfer coefficient data beyond the critical heat flux point at 2100°F saturation temperature in the stable film boiling and superheated vapor regimes up to 200°F vapor superheat were obtained. All the heat transfer data of Test Set No. 3 have been reduced and the results are presented in Section III.

Test section No. 4, a 3/4-inch nominal diameter tube (0.74-inch I.D.) containing an insert composed of a smooth plug at the inlet followed by a helix of pitch-to-diameter ratio equal to two ( $P/D = 2$ ) with internal thermocouples for fluid temperature distribution measurements, was installed and tests were started in early May.

Test Set No. 4 was completed June 10, including critical heat flux determinations and measurements of nucleate boiling, film boiling and superheated vapor heat transfer coefficients at both 1800°F and 2100°F saturation temperature. In addition, boiling inception tests were performed, with special emphasis on measuring conditions in the vicinity of the boiling boundary located at the inlet-plug insert; and some adiabatic two-phase pressure drop data was obtained at 1900°F using the insert thermocouples to measure local saturation temperature for deduction of local fluid pressure.



The data from Test Set No. 4 is being reduced and will be reported in the next Quarterly Progress Report.

After completion of Test Set No. 4, Test Section No. 5 was installed and testing began early in July. Test Section No. 5 is a 3/4-inch nominal diameter tube (0.74-inch I.D.) containing a wire-wrapped inlet plug insert in combination with a continuous helical wire coil insert ( $P/D = 2$ ) together with internal thermocouples. Included as part of Test Section No. 5 is a radiant-heated artificial nucleator of the "hot-finger" type, located at the test section inlet, for additional boiling inception tests.

It is expected that Test Set No. 5 will be completed during the first half of August. Following this, the main work of this project will then be analysis and treatment of the data obtained and preparation of the topical report covering the project.

#### 50 KW Project

All of the five sets of condensing test data obtained with the 50 KW Facility have been reduced and reported. These data are now being analyzed and treated further in preparation for a topical report covering this project. Some additional treatment of the data taken with a tapered plug insert in the 5/8-inch I.D. test section (Test Set No. 2) and the data taken with the 3/8-inch I.D. plain tube test section (Test Set No. 3) was required in order to correct for error in fluid temperature measurement at the test section inlet. These data have been corrected for this error and are presented herein.

An analysis of the vapor-phase thermal resistance in condensing is given in Section IV. The analysis proceeds on the basis of

kinetic gas theory to derive the vapor-phase condensing heat transfer coefficient, which is then used for comparison with the data.

A discussion of the results obtained during a test with Test Section No. 5 to stabilize the liquid-vapor interface in the active condensing section (5/8-inch I.D. tube with instrumented tubular insert) is given in Section IV.

Over the next quarter the principal work under this project will be completion of the analytical effort and preparation of the topical report on the project.

#### Facilities, Instrumentation and Materials Support

Accountings of supporting work conducted throughout the quarter in the areas of facility maintenance and equipment changes, instrumentation, and materials are given in Sections V and VI. This work was concerned with operation of the 100 KW Facility, including test section fabrication. The fabrication of Test Sections No. 4 and No. 5 are described in detail in Section VI.

#### Analysis

Analytical treatment of nucleate boiling heat transfer is given in Section VII, including theoretical prediction of nucleate boiling heat transfer coefficients, analysis of the relationship between cavity size on the heat transfer surface and the wall superheat required to initiate bubble nucleation in potassium, comparison of theoretical predictions with data from the 100 KW Facility, and recommendation of design procedure for calculating nucleate boiling heat transfer coefficients.

300 KW Facility Modification and Test Condenser Design

Contract Modification No. 10, dated 6-18-65, adds two engineering design tasks to the program, covering:

- a) Design of a modification of the 300 KW Facility to test multiple-tube, NaK-cooled condensers at power levels to 300 KW, including addition of a tertiary loop and a 300 KW multiple-tube facility boiler,
- b) Design of two multiple-tube condensers for use in the modified 300 KW Facility.

This new work has been started and the bulk of it will be carried out over the next Quarter.

## II 300 KW PROJECT

JR Peterson/DR Ferguson

The 300 KW Facility is used to obtain potassium boiling heat transfer data. The boiling test section is a controlled temperature type, i.e., it is a two-fluid heat exchanger with the temperatures of the heat transfer fluids rather than the surface heat flux being controlled. Reference 1 presents a detailed description of the facility.

### Status of Loop and Test Section

Tests in the 300 KW Facility were completed on schedule in November 1964. The facility is in good order, awaiting firming of plans for further tests.

### Status of Data Reduction

All data obtained with the 300 KW Facility have been initially reduced, corrected and reported. Some of the early data obtained with the 1.0-inch nominal diameter boiler tubes, however, were reduced before the NRL potassium thermodynamic properties became available, and certain refinements to the calculational procedures have been made since the initial reduction. Thus, the reduced data are being re-examined and recalculated where necessary, to place all results on a common basis in preparation for the topical report on this project.

Single phase (water) pressure drop tests have been conducted in support of the two-phase potassium pressure drop analysis task. Data were taken in a 1.0-inch nominal diameter tube containing helical inserts of pitch to diameter ratios  $(P/D)^*$  of two and six, and in a 3/4-inch nominal diameter tube both without an insert and

---

\* $P/D$  = Number of pipe internal diameters per  $360^\circ$  revolution of helix.

with an insert of  $P/D = 6$ . These data are shown in Figure 1 as a plot of friction factor versus superficial Reynolds number. Also shown on the Figure is the empirical relationship for smooth tubes, which shows good agreement with the experimental data obtained without insert.

### Status of Data Evaluation

#### 1. Derivation of Helix Equations:

As a part of the analytical effort associated with the data evaluation tasks certain parameters associated with the helical inserts employed in the tests, such as equivalent diameter, helical path length, helical velocity and radial acceleration have been derived. The expressions obtained as well as the derivations employed are given in Appendix A of this report.

#### 2. Correlation of Single Phase Pressure Drop and Heat Transfer With Inserts:

It is useful in the analysis and evaluation of the boiling potassium heat transfer and pressure loss data obtained from the 300 KW Project to compare the two-phase results with the corresponding single-phase values. In view of this requirement, methods for prediction of the single phase pressure drop and gas phase heat transfer coefficients in tubes containing helical inserts were sought.

Gambill (Reference 2) has assembled single-phase heat transfer and pressure drop data for flow in tubes containing twisted tapes, and has found that the friction factors obtained under these conditions could

be correlated within approximately  $\pm 20\%$  by employing the equivalent diameter and maximum helical path length and velocity in the calculation of the friction factors and Reynold's Numbers.

This procedure was employed in an attempt to correlate the water pressure drop data presented in Figure 1 of this report for the flow of water in tubes containing helical inserts. The data obtained by Greene (Reference 3) with tubes containing helical inserts were also treated. No additional data for single-phase heat transfer or pressure drop in tubes containing helical inserts could be found in the literature.

Figure 2 shows the friction factor data of Greene together with the SPPS data obtained under this project. The data points are omitted in this latter figure for ease of comparison. The smooth curves shown represent the magnitude and range of the experimental data. Figure 3 compares this data with the prediction obtained by use of the maximum helical velocities and lengths ( $V_{HM}$  and  $L_{HM}$ ) together with the equivalent diameter ( $D_e$ ). The definitions of these quantities, based upon the derivations given in Appendix A, are given by the following equations along with the equations for the equivalent friction factor  $f_e$  and the equivalent Reynolds Number ( $N_{Re_e}$ ).

$$V_{HM} = V_a \sqrt{1 + \left(\frac{\pi D_i^2}{P}\right)} \quad (1)$$

$$L_{HM} = L \sqrt{1 + \left(\frac{\pi D_i^2}{P}\right)} \quad (2)$$

$$D_e = \frac{D_i \left[ 1 - \left(\frac{D_{cb}}{D_i}\right)^2 \right]}{1 + \frac{D_{cb}}{D_i} + \frac{1}{\pi} \left( 1 - \frac{D_{cb}}{D_i} \right)} \quad (3)$$

$$f_e = \frac{\Delta P}{\frac{L_{HM}}{D_e} \frac{\rho_f V_{HM}^2}{2g_c}} \quad (4)$$

$$(N_{Re})_e = \frac{D_e V_{HM} \rho_f}{\mu_f} \quad (5)$$

It can be seen from Figure 3 that the single-phase pressure drop data are correlated to the empirical expression for smooth tubes quite well by the approach employed, with the exception of the data obtained by Greene for the very tight twist ratio  $P/D = 0.56$ . The recommended correlation, which is the smooth tube equation (Reference 4), is given below. It should be noted that the friction factors employed in Reference 4 are defined to be smaller by a factor of four than the friction factor utilized in Equation (6).

$$f_e = \frac{0.316}{(N_{Re})_e^{\frac{1}{4}}} \quad (6)$$

A plot of the ratio of experimental to predicted friction factors, employing equation (6), is shown in

Figure 4 , where the maximum, minimum and average ratios are given as a function of  $P/D$ . The analytical technique described is seen to be valid within approximately 20% in the range  $1 \leq P/D \leq 6$ . At  $P/D = 0.56$  the friction factor is apparently over-estimated.

Greene also measured the single-phase heat transfer coefficient in his experiments with helical inserts. The data of Greene, (Reference 3), are plotted in Figure 5 as the swirl flow Nusselt Number ( $N_{Nu_i}$ ) divided by the cube root of the Prandtl Number ( $N_{Pr}$ ) versus the Reynolds Number ( $N_{Re_i}$ ), the dimensionless groups being based upon the axial velocity  $V_a$  and the tube inside diameter  $D_i$ . The prediction of the Colburn equation (Reference 4 ) for smooth tubes is shown for comparison.

Figure 6 shows the correlation of heat transfer data by use of the maximum helical velocities and lengths ( $V_{HM}$  and  $L_{HM}$ ) together with the equivalent diameter ( $D_e$ ). Equations (1), (2), (3), and (5) were employed as in the correlation of the single phase pressure drop data, for  $V_{HM}$ ,  $L_{HM}$ , and ( $N_{Re}$ ) respectively. Equation (7), following, defines the equivalent Nusselt Number ( $N_{Nu_e}$ ) that was used.

$$(N_{Nu_e}) = \frac{h D_e}{k} \quad (7)$$



It can be seen from Figure 6 that the experimental heat transfer data correlate among themselves quite well with the approach employed, but the agreement with the smooth tube prediction is not as good as was obtained in the single-phase friction factor correlation. An empirical line, shown in Figure 6, was drawn through the correlated values. This line is recommended for the prediction of single-phase heat transfer coefficients in tubes containing helical inserts. The correlation is recommended for fluids having Prandtl Numbers within an order of magnitude of the water test data used in the derivation; that is, a Prandtl Number within an order of magnitude of 1.0. The correlation is not recommended for potassium liquid, but may be used for potassium vapor. The equation for the empirical single phase heat transfer correlation is given as follows:

$$(N_{Nu_e}) = 0.359 (N_{Re_e})^{0.563} (N_{Pr})^{1/3} \quad (8)$$

The uncertainty in the vapor phase heat transfer coefficient computed for potassium from equation (8) is quite large, due to the limited number of measurements upon which the equation is based and due to the present uncertainty regarding the transport properties of potassium vapor.

### 3. Local Results

Procedures for the calculation of local heat transfer and pressure drop parameters from the 300 KW Facility boiling data, along with the results obtained from sample cases, were presented in Reference 7. These

results showed the local nucleate boiling heat transfer resistance is small in comparison to the primary fluid and boiler tube wall thermal resistances. It is therefore less important to know the nucleate boiling resistance accurately in once-through boiler design than the critical heat flux and transition and film boiling heat transfer coefficients.

Because of its relatively small magnitude, the nucleate boiling resistance cannot be obtained accurately in the two-fluid 300 KW test section, since the magnitude of expected errors in the primary fluid and boiler tube wall thermal resistance are of the same order as the nucleate boiling resistance. For these reasons, analysis and evaluation of the critical heat flux and of the transition boiling coefficients have been emphasized and less emphasis was placed on further treatment of the nucleate boiling results.

Using the calculational procedures detailed in Reference 1, critical heat flux values and transition boiling heat transfer coefficients have been computed from those data obtained with the 3/4-inch nominal diameter boiler tube in which the critical heat flux was exceeded. These results are presented in Table 1 of this report,

As a first step in the treatment of the critical heat flux data, a correlating factor to account for the effect of the helical insert was sought. Theoretical

treatment (Reference 5) and experimental studies (Reference 6) of the critical heat flux phenomenon in pool boiling indicate that the critical heat flux increases as the local acceleration or gravity increases. Specifically, the critical heat flux increases as the fourth root of the local acceleration. It is logical, therefore, to attempt correlation of forced convection critical heat flux data with vortex-generator inserts in terms of the radial acceleration at the tube wall developed by the insert.

Figure 7 shows the critical heat flux values obtained with the 3/4-inch nominal diameter boiler tube, both with and without a helical insert of pitch-to-diameter ratio equal to six ( $P/D = 6$ ). The critical heat flux values obtained with this insert were divided by the fourth root of the radial acceleration ( $a$ ), derived in Appendix A, employing a slip ratio ( $K$ ) equal to the square root of the ratio of liquid to vapor densities. It can be seen from the Figure that the correlating technique brings the data obtained with the insert into agreement with the values obtained without insert. This relationship indicates a decrease in critical heat flux as the local quality at the critical heat flux point is increased. The data shown in Figure 7 are presented in two plots, one with temperature at the critical heat flux point as a parameter, and the second with potassium mass velocity as a parameter. No definite grouping of the values with respect to either parameter is observed. Thus the effect of temperature and mass velocity upon the critical heat flux within

the range of the variables covered is less than the scatter of the data obtained. The correlating lines drawn through the data presented in Figure 7 are given by the following equation where  $q_c''$  is the critical heat flux and  $X_c$  the vapor quality at the critical point.

$$\frac{q_c'' \left( \frac{X_c}{1-X_c} \right)}{\sqrt[4]{a}} = 3.5 \times 10^5 \frac{\text{Btu}}{\text{hr-ft}^2} \quad (9)$$

The parameter  $\sqrt[4]{a}$  in equation (9) is defined as 1.0 for boiling without inserts.

More extensive and accurate data, as well as additional analysis are needed to verify and improve both the correlating technique utilized for the insert data and the conclusions cited above. These initial results are encouraging, however, and are applicable to boiler design studies, since these relationships were obtained for data which was taken under two-fluid boiling conditions similar to those which will exist in a space power system potassium boiler.

### III 100 KW PROJECT

J.A. Bond

The 100 KW Facility is a single loop system used to study heat transfer to boiling alkali metals at temperatures up to 2100°F. The radiation heated boiling test section is currently (6/30/65) a 3/4-inch Schedule 80 (0.74-inch I.D., 30-inch heated length), Cb-1%Zr pipe containing an instrumented insert. Thermocouples are attached on the outer wall of the test section and fluid temperatures are measured with insert thermocouples. A preboiler, located upstream of and in series with the test section, controls the enthalpy of the fluid entering the test section. The working fluid is potassium.

#### Status of Loop and Test Section

Tests with the 3/8-inch (0.42-inch I.D., no insert) test section were completed on April 2, 1965 (Test Set No. 3). The loop was shut down throughout April in order to install Test Section No. 4. This test section is a 3/4-inch (0.74-inch I.D., 30-inch heated length) pipe containing an instrumented plug-helix insert. The insert consists of an inlet plug (Figure 36) which forms an annular flow passage extending over half of the heated length, followed by a helix ( $P/D = 2$ ) which extends over the remaining half of the heated length downstream of the inlet plug (Figure 35). A total of five Pt-Pt10%Rh thermocouples are contained within the centerbody of the insert, distributed along the heated length. Further details of Test Section No. 4 and its instrumentation can be found in Sections V and VI of this report. Boiling operation with Test Section No. 4 began on May 10 and the planned experiments were completed on June 10. The loop was shut down during the remaining part of June for the changeover to

Test Section No. 5, the last test section in the currently contracted test program.

Test Section No. 5 is a 3/4-inch (0.74-inch I.D., 30-inch heated length) pipe containing an instrumented insert. The insert (Figure 38) consists of an inlet plug wrapped with wire which will force the potassium to flow in a helical path through the annular flow passage formed between the plug and the pipe inside wall. This geometry extends over the lower half of the 30-inch heated length. The wire coil ( $P/D = 2$ , 0.094-inch wire diameter) continues over the remaining half of the test section, but without the plug. Test Section No. 5 includes a radiant-heated nucleator of the "hot-finger" type located between the preboiler outlet and the test section heated zone inlet. The hot finger will not be used initially but will be used later for further boiling inception studies. Further details of Test Section No. 5 and its instrumentation can be found in Sections V and VI of this report.

Testing with Test Section No. 5 is scheduled to begin early in July. This is the last of the currently-contracted experimental work in the 100 KW Facility. The following table summarizes the test sections which have been used under the current program since installation of the preboiler in August, 1964.

<u>100 KW Facility Test Sections</u>			
No.	Heated Length Inches	Inside Diameter Inches	Insert
1	30	0.77	None
2	30	0.74	Helical - $P/D = 6$
3	30	0.42	None
4	30	0.74	Instrumented Plug-Helix ( $P/D = 2$ )
5	30	0.74	Instrumented Plug-Wire Coil ( $P/D = 2$ )

During the Quarter, the 100 KW Facility was operated a total of 535 hours including 450 hours under boiling conditions. Total facility operating time at the end of the Quarter was 5897 hours.

#### Status of Data Reduction

Reduction of the data obtained with the 3/8-inch (0.42-inch I.D.) test section is complete and the results are presented herein. The data obtained with Test Section No. 4 are being processed and will be reported in the next Quarterly Progress Report.

#### Status of Data Evaluation

Nucleate Boiling Results. The nucleate boiling data obtained in Test Section No. 3 (0.42 I.D.) are tabulated in Tables B-3a through B-3d. The data include points taken at two saturation temperatures, three mass velocities and three heat fluxes. The general test procedure was to hold saturation temperature, mass velocity and test section heat flux constant while the quality at the boiler exit was changed by varying the pre-boiler power. Figure 8a is a plot of the data taken at  $T_{\text{sat}} = 2100^{\circ}\text{F}$ ,  $G = 60 \text{ lb/sec-ft}^2$  with heat flux as parameter. No definite trend with heat flux is apparent, as has been previously observed in the 3/4-inch test sections. The data taken at  $G = 30 \text{ lb/sec-ft}^2$  are presented in Figure 8b which includes points taken at  $T_{\text{sat}} = 1800^{\circ}\text{F}$  and at  $T_{\text{sat}} = 2100^{\circ}\text{F}$ . The heat transfer coefficients at  $2100^{\circ}\text{F}$  are generally lower than the corresponding points at  $G = 60 \text{ lb/sec-ft}^2$ , suggesting a mass velocity effect. The data at  $T_{\text{sat}} = 1800^{\circ}\text{F}$  show a considerable scatter at the highest quality tested. The heat transfer coefficients at  $1800^{\circ}\text{F}$  are generally higher than the corresponding points at  $2100^{\circ}\text{F}$ . Figure 8c is a plot of the data taken at  $T_{\text{sat}} = 2100^{\circ}\text{F}$  and

$G = 45 \text{ lb/sec-ft}^2$ . The heat transfer coefficients appear to have a maximum at about 50% quality. Examination of these data, however, reveals that there was a considerable variation in wall temperature measured at the same axial position. For the data at  $G = 45 \text{ lb/sec-ft}^2$ , the wall-to-fluid  $\Delta T$ 's measured at an axial station approximately 2-inches from the test section outlet varied from about  $0.3^\circ\text{F}$  to  $8^\circ\text{F}$ . At the same axial location, there were circumferential variations on the order of  $3.5^\circ\text{F}$ . A detailed discussion of the probable errors in temperature measurement in the 100 KW Facility is presented in Section VIII of this report.

Critical Heat Flux, Film Boiling and Superheat Results. Due to the higher heat fluxes obtainable with the  $3/8$ -inch test section (Test Section No. 3), this test set resulted in a number of critical heat flux determinations. Also, for the first time in the 100 KW Facility, superheated vapor conditions were obtained at the test section outlet. Recorder charts showing the behavior of pertinent system parameters were made during each run in which the critical heat flux condition was reached or exceeded. Segments of these recorder charts are presented as Figures 9 through 15b.

Although there are exceptions, the general test procedure was an extension (to higher qualities) of the procedure used to obtain nucleate boiling data; i.e., the saturation temperature, mass velocity and test section heat flux were held constant while the quality was increased by slowly increasing the preboiler power until the critical quality corresponding to the test conditions was reached. During the initial runs, the test was usually terminated when the amplitude of the wall temperature oscillations reached values on the order of  $50^\circ\text{F}$  to  $100^\circ\text{F}$ . Later, after some experience was gained, it was possible to go beyond



the transition boiling regime and establish stable film boiling and superheated vapor conditions in the test section. One such run, in which superheated vapor conditions were obtained, will be discussed in detail because it illustrates the general behavior of the test section wall temperature as conditions are changed sequentially from the nucleate boiling regime into transition boiling, stable film boiling and finally into the superheated vapor condition. Deviations from this general behavior will be noted on runs in which they occurred.

Figures 14a, 14b and 14c consist of segments of recorder charts obtained during a "superheat run". The test conditions for this run were  $T_{\text{sat}} = 2100^{\circ}\text{F}$ ,  $G = 47.6 \text{ lb/sec-ft}^2$  and  $q'' = 50,000 \text{ Btu/hr-ft}^2$ . Segment - 1 of Figure 14a shows the system parameters as the test section heat flux was being increased to test conditions. Before the test section power increase, the wall temperature near the outlet was steady. After the test section power increase (Segment-1, Figure 14a) small oscillations ( $\sim 5^{\circ}\text{F}$ ) in the wall temperature began to appear, indicating that the critical heat flux condition was imminent. Segment-2 of Figure 14a shows the behavior after the test section heat flux had been increased to test conditions ( $q'' = 50,000 \text{ Btu/hr-ft}^2$ ). From this point on, the test section heat flux was held constant and the quality was varied by varying the preboiler power.

In Segment-2, the exit quality was increased from 86% to 89% with a resulting increase in the amplitude of the wall temperature oscillations. Note that immediately following the power increase (Segment-2), the amplitude of the wall temperature oscillations reached values up to about  $50^{\circ}\text{F}$  and then became

more steady. This type of behavior has been observed in most of the critical heat flux runs; i.e., the wall temperature may show relatively large oscillations immediately following a power increase and then again became steady after a short interval. In Segment-3 of Figure 14a, the exit quality was increased from 89% to 91%. At this point, the amplitude of the wall temperature oscillations increased markedly to values of about 75°F with a peak of almost 150°F, indicating that the test section outlet region was definitely in the transition boiling regime.

Figure 14b is a continuation of Figure 14a. At 1342 hrs. the exit quality was increased to 96% (Figure 14b). As can be seen, the exit wall temperature began to rise rather rapidly, indicating that the test section outlet region was going into stable film boiling. The wall temperature at the exit then recovered, oscillated a few times, again began to rise and finally leveled off in stable film boiling. During this temperature transient, the digital voltmeter was printing the wall temperature at a rate of three readings per second. The film boiling heat transfer coefficient at this point was calculated from the temperature measurements to be 228 Btu/hr-ft<sup>2</sup>-°F. Note that at this point (Figure 14b), the test section exit was in stable film boiling while the midpoint was still in the first stages of transition boiling, with random temperature oscillations of up to 50°F maximum.

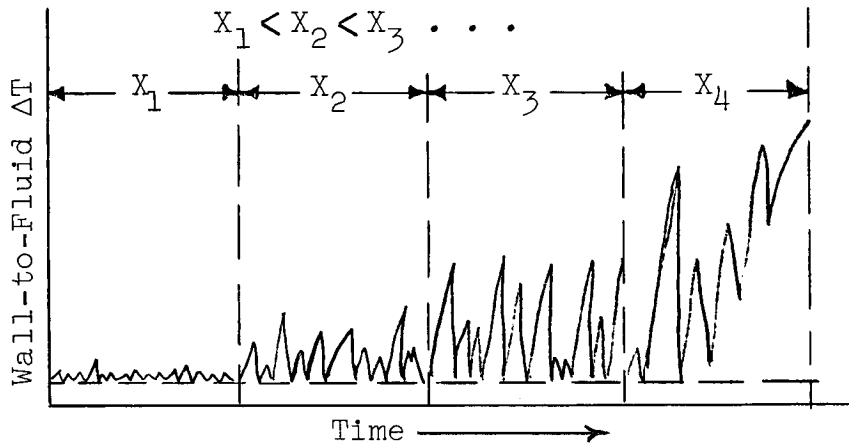
At 1349 Hrs. (Figure 14b), the preboiler power was again increased, resulting in a calculated test section exit quality greater than 100% and a measured exit vapor superheat of 25°F. When 100% exit

quality was reached, the fluid temperature at the test section outlet began to oscillate and increase, (Figure 14b). The exit wall temperature at this point is off-scale on the recorder chart. Note that the test section midpoint quality is 95% and the corresponding wall temperature oscillations have an amplitude of up to 150°F. In Segment-5 of Figure 14b, the power was increased further resulting in a vapor superheat of approximately 200°F. This was the highest exit vapor superheat reached in this test.

In Figure 14c, the quality was reduced in steps to repeat in reverse the sequence of events observed while going up in preboiler power. In Segment-7 of Figure 14c, the exit quality was reduced from 102% to 95%. At this point, the test section midpoint was back in transition boiling while the exit was still in stable film boiling. In Segment-8 of Figure 14c, the exit quality was reduced from 95% to 93%. At this point, the test section exit came out of film boiling into transition boiling. Note that this change from film to transition boiling occurred at about the same quality as the corresponding change from transition to film boiling effected earlier by increasing the quality (Segment-4 of Figure 14b). Segment-9 of Figure 14c shows the decrease in exit quality from 87% to 84%. At this point, the amplitude of the exit wall temperature oscillations dropped from values as high as 100°F down to random oscillations of about 25°F.

The general behavior of the test section wall temperature, as illustrated by the test run described above, is typical of that observed in most of the runs on which the critical heat flux condition was reached or exceeded. Although there are exceptions, it appears that after the transition boiling regime begins, the wall temperature oscillates within an envelope for

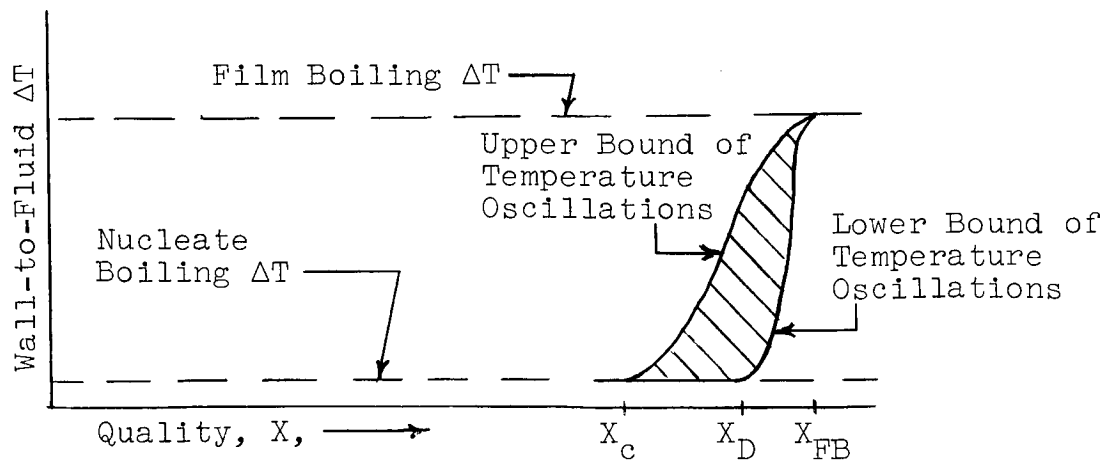
which the upper temperature bound increases with increasing quality and a lower bound which is approximately constant at the level corresponding to that for nucleate boiling, as illustrated in sketch A below.



$T_{\text{sat}}, G \text{ and } q'' \text{ constant}$

Sketch A

This same information, plotted as  $\Delta T$  vs.  $X$  might appear as shown in sketch B below:

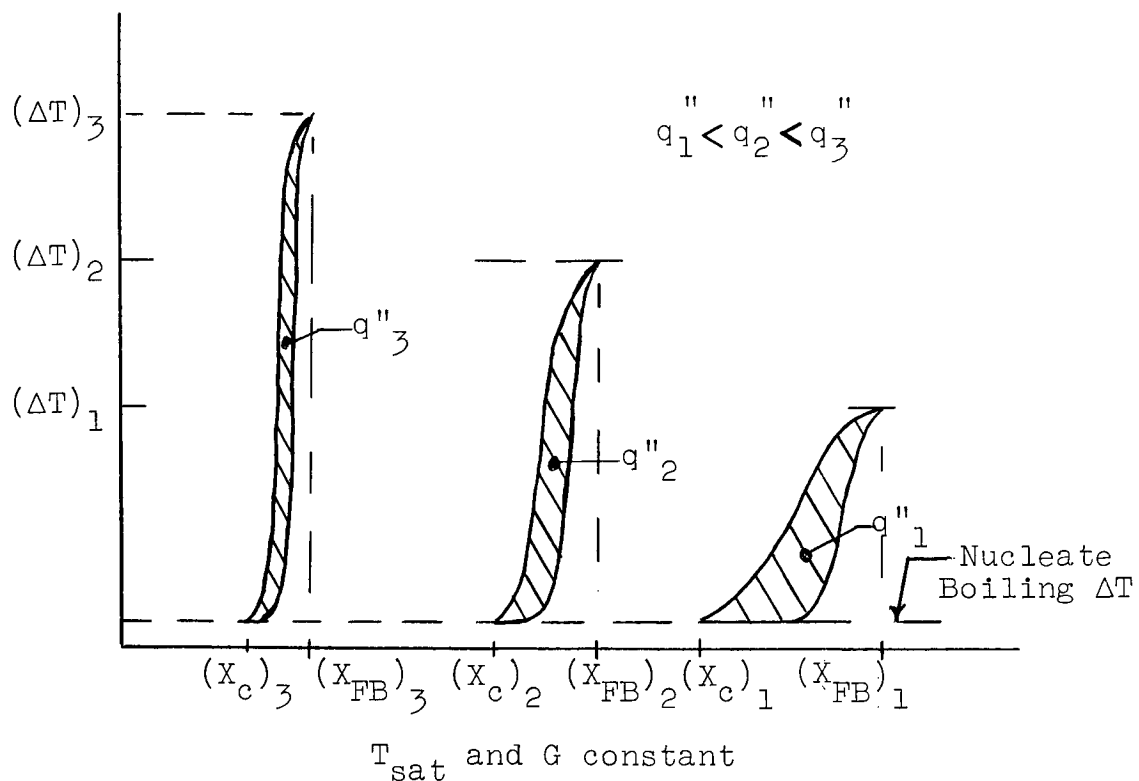


$T_{\text{sat}}, G \text{ and } q'' \text{ constant}$

Sketch B

Sketch B is undoubtedly an oversimplification because the film boiling and the nucleate boiling  $\Delta T$ 's are not necessarily independent of quality even at constant  $T_{\text{sat}}$ ,  $G$  and  $q''$ . The sketch does, however, illustrate the concept. With  $T_{\text{sat}}$ ,  $G$  and  $q''$  constant, the wall temperature apparently starts oscillating (over and above the small random oscillations associated with nucleate boiling) at some "critical quality",  $X_c$ . As the quality is increased to values greater than  $X_c$ , the amplitude of the oscillations increases but the lower bound remains essentially constant until at some higher quality  $X_D$  (see sketch B), the lower bound of the oscillations begins to increase. Above this point ( $X_D$ ), the amplitude of the oscillations begins to diminish, but the average wall temperature increases. Finally, at a quality  $X_{\text{FB}}$ , the wall temperature becomes steady at the film boiling value.

As mentioned previously, there are apparent exceptions to this general behavior. In some cases, the wall temperature will increase abruptly when the critical quality,  $X_c$ , is reached. Evidence of this phenomenon is presented in Figures 12, 15a and 15b. In Figure 15a, for example, the heat flux was constant at 211,000 Btu/hr-ft<sup>2</sup>. After the preboiler power increase (quality increase), the wall temperature began to rise rapidly ( $\sim 175^\circ\text{F}$  in 3 sec.). Presumably, if the automatic test section power trip had not reduced the heat flux, the test section would have gone into stable film boiling. This type of behavior has been observed in the runs for which the heat flux was relatively high (with correspondingly lower  $X_c$ ). A plausible explanation of the two types of behavior can be made with the aid of Sketch C.



Sketch C

Consider a hypothetical experiment in which  $T_{\text{sat}}$  and  $G$  are held constant. Three critical heat flux runs are to be made at the three heat fluxes  $q''_1$ ,  $q''_2$  and  $q''_3$  where  $q''_1 < q''_2 < q''_3$ . The results of this experiment might appear as shown in Sketch C. At the lowest heat flux, the critical quality, "film boiling quality" and film boiling  $\Delta T$  are  $(X_c)_1$ ,  $(X_{\text{FB}})_1$  and  $(\Delta T)_1$  respectively. The corresponding parameters for the other two heat fluxes are as indicated in Sketch C. If the results of this experiment were as shown in Sketch C, then the abrupt temperature rise which has been observed at the higher heat fluxes would be explained by the fact the upper bound of the  $\Delta T$  vs.  $X$  curve is so steep (at high heat fluxes) that only a small change in quality would result in a sharp rise in the wall temperature. The question to be answered is what evidence do we have to justify the relative relationships implied by Sketch C. The first implication of Sketch C is that the critical quality,  $X_c$ , decreases with increasing heat flux at constant  $T_{\text{sat}}$  and  $G$ . Although this implied relationship has nothing to do with the slope of the upper bound of the  $\Delta T$  vs.  $X$  curve, there is direct evidence that  $X_c$  does in

fact decrease with increasing heat flux for constant  $T_{\text{sat}}$  and  $G$ . This will be discussed later. The second implication of Sketch C is that the film boiling  $\Delta T$  increases with increasing heat flux. The film boiling  $\Delta T$  has been measured in the lower heat flux ranges of  $q'' = 50,000 \text{ Btu/hr-ft}^2$  and  $q'' = 100,000 \text{ Btu/hr-ft}^2$  and the results confirm that the film boiling  $\Delta T$  does increase with increasing heat flux. A third implication of Sketch C is that the quantity  $(X_{\text{FB}} - X_c)$  decreases with increasing heat flux at constant  $T_{\text{sat}}$  and  $G$ . The strongest piece of evidence to support this contention is the observation that in the relatively high heat flux runs, the wall temperature showed an abrupt rise without the oscillations discussed previously. This indicates that under those conditions (high heat flux), the critical quality,  $X_c$ , is nearly equal to the film boiling quality,  $X_{\text{FB}}$ . Further evidence of the trend of  $(X_{\text{FB}} - X_c)$  with heat flux is lacking.

The critical heat flux measurements obtained in the 100 KW Facility are tabulated in Table 2 . These include all critical heat flux determinations made with Test Sections No. 1, No. 2 and No. 3. Supporting evidence, in the form of recorder charts are presented in Figures 9 through 15b for those runs which have not been previously reported.

In most of these runs, the critical heat flux condition was indicated by wall temperature oscillations. For these runs, the question which immediately arises is what quality to call the "critical quality" for a given  $T_{\text{sat}}$ ,  $G$  and  $q''$ . Until the phenomenon is better understood, the decision must be somewhat arbitrary. The criterion which has been selected as a working definition for the present is that for a given heat flux the "critical quality" is that quality for which the "time-average" fluctuating wall-to-fluid  $\Delta T$  becomes approximately equal to twice

the corresponding steady-state nucleate boiling  $\Delta T$  based on a nucleate boiling heat transfer coefficient of  $10,000 \text{ Btu/hr-ft}^2\text{-}^\circ\text{F}$ . For example, for a heat flux of  $100,000 \text{ Btu/hr-ft}^2$  the above criterion would require that at the "critical quality" the "time-average" wall temperature be approximately  $10^\circ\text{F}$  higher than the corresponding nucleate boiling value.

For data reduction purposes, the time-average of the fluctuating wall temperature at the critical heat flux condition is estimated from the Sanborn recorder charts made for each of the test runs. The value of  $10,000 \text{ Btu/hr-ft}^2\text{-}^\circ\text{F}$  chosen as the steady-state nucleate boiling heat transfer coefficient for use in the critical heat flux condition determinations is adequately representative of the magnitudes measured in the ranges of heat fluxes, saturation temperatures and vapor qualities tested, and is taken as a constant for convenience.

The critical heat flux data in Table 2 are presented on the basis of the above definition. These data, along with the critical heat flux data from the 300 KW Facility (see Section II) are plotted in Figure 16 as  $q_c''/\sqrt[4]{a}$  vs. local quality. The relative centripetal acceleration,  $a$ , is as defined and derived in Section II of this report for use in treating the data taken with helical insert geometries. The values of  $\sqrt[4]{a}$  for the insert data are tabulated in Table 2; for the no-insert data  $\sqrt[4]{a}$  is taken to be 1.00. Use of the quantity  $\sqrt[4]{a}$  is an attempt to allow for the centrifugal action of the helical insert tending to keep liquid on the wall of the test section. Further discussion of this point is given in Section II in conjunction with treatment of the critical heat flux data from the 300 KW Facility.

The critical heat flux data presented in Figure 16 shows fairly good agreement between the data taken in the 300 KW Facility



and that taken in the 100 KW Facility considering the wide range of test conditions covered and the completely different methods used to detect the phenomenon.

Further examination of the 100 KW data suggested the presence of apparent mass velocity and saturation temperature effects. In an initial attempt to correlate these effects, the concept of a maximum rate-of-change of quality was introduced. From a simple energy balance over an increment of heated length  $d'z$ , the rate of change of quality is given by:

$$\frac{dx}{dz} = \frac{4q''}{DG h_{fg}} \quad (1)$$

The maximum rate-of-change of quality without exceeding the critical heat flux is given by:

$$\left(\frac{dx}{dz}\right)_{\max} = \frac{4q_c''}{DG h_{fg}} \quad (2)$$

The critical heat flux data have been plotted in Figure 17 with  $q_c''/DG h_{fg} \sqrt[4]{a}$  as the dependent variable and quality as the independent variable. This type of plot appears to remove the mass velocity dependence, but apparent tube diameter and temperature effects remain.

One might expect that the critical heat flux should be a function of the liquid film thickness on the wall. In another attempt to correlate the data, a liquid film thickness was calculated using the definition of the void fraction and assuming no liquid is entrained in the vapor phase. The resulting thickness,  $\delta$ , is given by:

$$\delta = 1/2 (1 - \sqrt{R_g}) D_i \quad (3)$$

The void fraction,  $R_g$ , was calculated from

$$R_g = \frac{1}{1 + K \left( \frac{\rho_g}{\rho_f} \right) \left( \frac{1-x}{x} \right)} \quad (4)$$

with the assumption that the slip ratio,  $K$ , is equal to  $\sqrt{\rho_f/\rho_g}$ . The critical heat flux data are plotted in Figure 18 as a function of liquid film thickness with  $q_c'' / DG h_{fg} \sqrt[4]{a}$  as the dependent variable. This type of correlation appears to reduce the scatter and shows the trend one might expect. Further evaluation of the data is proceeding, including comparisons with critical heat flux data obtained in the 300 KW Facility.

One aspect of the critical heat flux phenomenon which needs further evaluation is the question of flow stability. During at least two of the critical heat flux runs presented herein, flow oscillations indicated that the system stability was marginal. For example, in Figure 9, the average flow oscillations were on the order of  $\pm 7\%$  with maximum oscillations up to about  $\pm 13\%$ . Another type of possible instability is indicated in Figure 12. Here, the system pressure level dropped almost simultaneously with the sharp wall temperature excursion at the test section outlet. It is not known in this instance whether onset of the critical heat flux condition was a cause or was an effect of system instability.

In the preceding discussion, mention was made of the "film boiling quality",  $X_{FB}$ , or the quality at which "transition boiling" terminated and "stable film boiling" was established for a given set of test conditions. This data on stable film boiling inception is tabulated in Table 3 along with film boiling and superheated vapor heat transfer coefficients calculated from the measured temperatures.

#### IV 50 KW PROJECT

S.G. Sawochka

##### Status of Loop and Test Section

Completion during March 1965 of the test series with the 5/8-inch I.D. test section with 1/4-inch O.D. tubular instrumented insert (Test Set No. 5) concluded the currently planned test program in the 50 KW Facility. The facility was then shutdown, in good working order. A summary description of the test sections used for the five test sets constituting the test program under the 50 KW Project is given in Appendix G.

##### Status of Data Reduction

All data have been reported, with the last two data sets for Test Sets No. 4 and No. 5 presented in Reference 7. The data for Test Sets No. 2 and No. 3, the 5/8-inch I.D. tube with tapered pin insert and the 3/8-inch I.D. plain tube (no insert), respectively, have been re-evaluated and corrected to include the effect of the pressure change on the inlet vapor temperature due to the presence of the inlet temperature measuring probe. The re-evaluated data for Test Sets No. 2 and 3 are presented in Appendix D.

To evaluate the data for heat transfer analysis, accurate values of the thermal conductivity of the Nickel 270 condenser tube material are required. Therefore, a specimen of the material used to manufacture the tubes was sent to Battelle Memorial Institute for determination of its thermal conductivity as a function of temperature.

The method of making the thermal conductivity measurements, in brief consisted of heating one end of a specimen, measuring

the temperature gradients along the specimen, and determining the rate of heat flow through the specimen by means of a metal standard of known thermal conductivity attached to the cold end of the specimen.

Errors of thermal-conductivity measurements are estimated to not exceed  $\pm 5$  percent, the chief uncertainty being the thermal conductivity of the reference material.

The results of these measurements are given in Figure 19.

#### Status of Data Evaluation

##### A. Heat Transfer

As discussed in Reference 7, the data of Test Sets No. 1, No. 2 and No. 3, with no instrumented insert, are subject to two errors. One error is due to the presence of the temperature measuring probe at the test section inlet which had an effect on the inlet potassium pressure with a consequent error in saturation temperature measurement. The other error is due to the assumption of a linear temperature profile between the test section inlet and outlet. To determine the importance of the first error, a sample thermocouple probe was installed during Test Set No. 5, as discussed in Reference 7. The results of this test indicated that the potassium vapor temperature increased by as much as  $4^{\circ}\text{F}$  between the tip of the inlet temperature probe and a point 2-inches downstream, thereby indicating a net pressure increase, as would be obtained with single-phase flow through an expansion. The area ratio,  $A_2/A_1$ , for this test was 1.19, for the 1/4-inch O.D. probe in the 5/8-inch I.D. pipe. For application to the data of Test Sets No. 2 and No. 3, an attempt was made to correlate the experimental results using the following single phase relations.

$$p_2 - p_1 = \frac{G_1^2}{2\rho_g g_c} \left[ 1 - \left( \frac{A_1}{A_2} \right)^2 - K_E - \frac{4fL}{D} \left( \frac{A_1}{A_2} \right) \right] \quad (1)$$

For the range of vapor Reynold's numbers during the test, this equation can be approximated by

$$p_2 - p_1 = 0.21 \frac{G_1^2}{2\rho_g g_c} \quad (2)$$

The results of this comparison using equation (2) gave reasonable agreement with the test data, with a maximum deviation of 0.7°F. This procedure was then applied to Test Sets No. 2 and No. 3, and the re-evaluated data are presented in Appendix D, and in Figure 20. It was not necessary to apply this procedure to the results of Test Set No. 1 since the area ratio for this series of tests was only 1.04, thereby giving a negligible temperature increase due to the expansion.

As can be seen in Appendix D and also in Figure 20, the condensing heat transfer coefficients for Test Sets No. 2 and No. 3 are generally greater than 10,000 Btu/hr-ft-°F, which agrees in this respect with the data of Test Sets No. 1, No. 4 and No. 5. However, they exhibit a considerable amount of scatter, since a major source of error for this data was the estimate of the local potassium temperature from the measured inlet and outlet temperatures. In addition to the large scatter, a considerable number of the calculated heat transfer coefficients for Test Sets No. 2 and No. 3 are negative due to the combination of temperature measuring errors. Since this source of error was remedied during the instrumented insert data runs (Test Sets No. 4 and No. 5), no further treatment of the data for Test Sets No. 2 and No. 3 is planned.

In an initial attempt to obtain a definite reason for the departure of the experimental condensing heat transfer coefficients from the film theory predictions of Nusselt and Seban, the results for Test Sets No. 4 and No. 5, which are believed to be the most accurate, were treated in the following manner:

1. An estimate of the liquid film thickness based on the prediction of Dukler (Reference 8) was made and a liquid film heat transfer coefficient was calculated by using  $h = K/\delta$ . Although Dukler's thermal analysis of the condensing phenomenon is grossly in error for low Prandtl number fluids as has been shown by Lee (Reference 9), his hydraulic analysis which accounts for shear at the vapor-liquid interface appears to correlate film thickness data. For this reason Dukler's film thickness prediction was used to estimate the liquid film thermal resistance. The predicted liquid film Nusselt condensing ratio,  $h/(K(\sqrt{2}/g))^{1/3}$ , is presented in Figure 21 as a function of  $\tau_v^*$  using Reference 8, where

$$\tau_v^* = \frac{\tau_v}{(\rho \frac{V}{g})^{2/3}} \quad (3)$$

and

$$\tau_v = \left(\frac{dP}{dL}\right) \left(\frac{D_i - D_{cb}}{4}\right) \quad (4)$$

To determine  $h_f$  for the data of Test Sets No. 4 and No. 5, the local friction pressure gradient was estimated by

$$\left(\frac{dP}{dL}\right)_v = \frac{f}{(D_i - D_{cb})} \frac{\rho_g V_g^2}{2g_c} \quad (5)$$

where

$$V_g = \frac{4x W_K}{\rho_g \pi (D_i^2 - D_{cb}^2)} \quad (6)$$

This method gives a low-side estimate of  $\tau_v^*$  thereby maximizing the liquid film thickness and consequently its thermal resistance.

2. The experimental thermal resistance was taken to be the sum of a liquid-phase and a vapor-phase thermal resistance

$$\frac{1}{h_c} = \frac{1}{h_f} + \frac{1}{h_v} \quad (7)$$

3. A residual thermal resistance, proposed to be due to the vapor phase, was calculated by subtracting the liquid film thermal resistance from the experimental values of the total condensing thermal resistance.

In order to compare with theory the vapor-phase resistances derived from the experimental data, a theoretical prediction was formulated on the basis of kinetic gas theory following a procedure suggested by the work of Schrage and used by Rohsenow and Sukhatme (References 10 and 11), as follows.

From kinetic gas theory, the mass flow of molecules impinging on a surface is given by equation 8:

$$G = P \left( \frac{Mg_c J}{2\pi RT} \right)^{\frac{1}{2}} \quad (8)$$

The mass flux, saturation temperature relationship is shown in Figure 22 for potassium.

When equilibrium exists between a saturated gas and its liquid, the mass flux of molecules leaving the liquid surface equals the mass flux of vapor molecules condensing on the liquid surface, i.e., the net rate of heat transfer is zero. This equality is expressed by Equation 9:

$$P_S \left( \frac{Mg_c J}{2\pi RT_S} \right)^{\frac{1}{2}} = P_V \left( \frac{Mg_c J}{2\pi RT_V} \right)^{\frac{1}{2}} \quad (9)$$

However, when a net rate of mass transfer occurs such as in the case of condensation, a condition of nonequilibrium exists at the liquid-vapor interface. This nonequilibrium condition is expressed by

$$P_V \left( \frac{Mg_c J}{2\pi RT_V} \right)^{\frac{1}{2}} > P_S \left( \frac{Mg_c J}{2\pi RT_S} \right)^{\frac{1}{2}} ; \quad (10)$$

or, approximately, by

$$W/A = \sigma_c P_V \left( \frac{Mg_c J}{2\pi RT_V} \right)^{\frac{1}{2}} - \sigma_e P_S \left( \frac{Mg_c J}{2\pi RT_S} \right)^{\frac{1}{2}} \quad (11)$$

where:

- $W/A$  = mass units/unit time/unit area condensing
- $P_V$  = pressure of the saturated vapor in the bulk space
- $T_V$  = temperature of the saturated vapor in the bulk space
- $T_S$  = temperature of the liquid at the liquid vapor interface
- $P_S$  = saturation pressure corresponding to  $T_S$ .
- $\sigma_c$  = condensation coefficient, fraction of the molecules striking the surface which actually condense
- $\sigma_e$  = evaporation coefficient, fraction of the predicted molecular flux from the liquid surface which actually leaves the surface



The inequality of mass flux at the liquid-vapor interface has been expressed more accurately by Schrage who visualizes the saturated vapor stream at  $T_v$  moving toward the condensing surface at a flow rate of  $W/A$  with a counter flow of molecules at  $T_s$  from the surface as being the flow equivalent of molecules in a stationary container. Schrage's relation is given by Equation 12:

$$W/A = \sigma_c P_v \left( \frac{Mg_c J}{2\pi RT_v} \right)^{\frac{1}{2}} - \sigma_e \Gamma P_s \left( \frac{Mg_c J}{2\pi RT_s} \right)^{\frac{1}{2}} \quad (12)$$

where

$$\Gamma = \text{EXP} \left\{ -\phi^2 \right\} + \phi \pi^{\frac{1}{2}} (1 + \text{erf } \phi)$$

and

$$\phi = \frac{W/A}{\rho_g (2RT_v/g_c JM)^{\frac{1}{2}}}$$

As can be seen by examining Equations 11 and 12, the only difference that exists is a function  $\phi$  in Schrage's equation which attempts to account for the presence of a net progress velocity of the condensing gas towards the surface. The range of heat fluxes or net velocities towards the surface that were present during this test series gives very low numerical values for  $\phi$ , which yield a value of  $\Gamma$  approaching unity. For this reason Equation 12 can be simplified to yield Equation 11, which was given as the approximate relation for a simplified treatment. In order to determine a numerical value for the temperature difference between the vapor and the liquid that exists due to the presence of a net heat transfer rate, some assumption must be made regarding the values of  $\sigma_c$  and  $\sigma_e$ . It can

be shown that at equilibrium  $\sigma_c = \sigma_e$ . Therefore, under non-equilibrium conditions with a net rate of condensation, it will be assumed that the condensation and evaporation coefficients are equal. With this assumption Equation 12 can be simplified to give Equation 13:

$$W/A = \sigma_c \left[ P_v \left( \frac{Mg_c J}{2\pi RT_v} \right)^{\frac{1}{2}} - P_s \left( \frac{Mg_c J}{2\pi RT_s} \right)^{\frac{1}{2}} \right] \quad (13)$$

$$W/A = \sigma_c \Delta \left[ P \left( \frac{Mg_c J}{2\pi RT} \right)^{\frac{1}{2}} \right] \quad (14)$$

Equation (14) can be rewritten in terms of the condensing heat flux, as follows:

$$q'' = \sigma_c \Delta \left[ h_{fg} P \left( \frac{Mg_c J}{2\pi RT} \right)^{\frac{1}{2}} \right] \quad (15)$$

Since P and T are related by the saturation curve, or  $P = f(T)$ , Equation 16 is obtained as follows,

$$q'' = \sigma_c \Delta T \left( \frac{\Delta G \cdot h_{fg}}{\Delta T} \right) \quad (16)$$

$$\frac{q''}{\Delta T} = h_v = \sigma_c \left( \frac{\Delta G \cdot h_{fg}}{\Delta T} \right) \quad (17)$$

To quantitatively determine the value of  $h_v$ , the effective kinetic theory heat transfer coefficient, it is necessary to determine the value of  $\Delta G \cdot h_{fg} / \Delta T$ . Since the vapor kinetic theory mass flux can be calculated from Equation 8, its derivative with respect to temperature can be numerically determined, and the equivalent

interfacial thermal resistance can be calculated as a function of saturation temperature. The results of this calculation are presented in Figure 23 as a function of saturation temperature and  $\delta_c$ , the condensation coefficient. It should be noted that for values of  $\delta_c$  near unity, the kinetic theory heat transfer coefficient is high and would afford an insignificant thermal resistance during the condensing process. However, as the value of  $\delta_c$  decreases the effective interfacial heat transfer coefficient decreases and could afford a substantial thermal resistance if ideal kinetic theory behavior was not followed.

In Figure 24, the experimental vapor phase heat transfer coefficients of Test Sets No. 4 and No. 5 are compared to the calculated value of the vapor phase heat transfer coefficient for  $\delta_c = 0.2$ . Also included are the low-temperature data of Englebrecht (Reference 24). Reasonably good agreement between the experimental data and the theoretical prediction using the selected value  $\delta_c = 0.2$  is shown. A trend of decreasing vapor-phase condensing coefficients with decreasing saturation temperature is indicated. Table 4 lists summarized results for Test Sets No. 4 and No. 5 with the experimental values of  $\delta$  for each data point.

An alternate approach to assuming  $\delta_c = \delta_e$ , as used above for the theoretical analysis is to assume instead that deviations from ideality occur in the vapor-phase only, i.e.  $\delta_c < 1$  and  $\delta_e = 1$ . To show the effect of this, vapor heat transfer coefficients corresponding to values of the condensation coefficient 0.95 to 1.0 are presented in Figure 25. Figure 25 shows that as  $\delta_c$  is reduced from unity increasingly lower values of the vapor phase heat transfer coefficient are obtained.

Even though no rigorous basis exists for the assumption that  $\sigma_c = \sigma_e$ , the relative ease of treatment of the data use of this assumption provides justifies its use, pending development of a more rigorous theory.

Further treatment of the data in an effort to assess possible dependence of  $\sigma_c$  on additional variables omitted in the simplified treatment is beyond the scope of the current program. For this reason, the treatment of the vapor-phase heat transfer coefficients was terminated and a correlation of the condensing heat transfer coefficients in the manner suggested by Equation (7) was attempted. The dimensionless relation chosen is given by:

$$N_{NuC} = \frac{1}{\frac{1}{N_{NuCf}} + \frac{1}{N_{NuCv}}} \quad (18)$$

where

$$N_{NuCv} = \frac{\sigma_c (M/2\pi RT)^{\frac{1}{2}} (dP/dT - P/2T)}{K (\nu^2/g)^{-1/3}} \quad (19)$$

and

$N_{NuCf}$  = liquid film Nusselt number based on  $h_f = K/\delta'$

$N_{NuCv}$  = vapor Nusselt number based on kinetic theory prediction and liquid properties

After selection of this relation, the experimental data were treated statistically to determine the value of  $\sigma_c$  which gave

a minimum variance. For the tubular insert data the variance,  $S^2$ , defined by

$$S^2 = \frac{\sum_{i=1}^N \left( \frac{N_{\text{NuCP}} - N_{\text{NuCE}}}{N_{\text{NuCP}}} \right)^2}{N-1}, \quad (20)$$

was found to be relatively independent of  $\delta_c$  for  $0.17 < \delta_c < 0.22$ , with a minimum at  $\delta_c = 0.19$ , which gives a standard deviation of 27% and an average error of 22%. Deviations for each data point are listed in Table 5. When this procedure was attempted with the helical insert data, a value of  $\delta_c > 1$  was found to give a minimum variance. Since  $\delta_c > 1$  is physically unacceptable, this method of correlation was abandoned, and the data were compared directly to the predicted liquid heat transfer coefficient. The results of this comparison are presented in Table 5. A meaningful value of  $\delta_c$  was not obtained from the helical insert measurements, which was not unexpected since the method of estimating the liquid film thickness in the presence of the helical insert was a questionable extension of Dukler's theory of co-current vapor-liquid flow. As can be seen in Table 5, the condensing heat transfer coefficient predicted from Dukler's theory was always greater than the experimentally determined value with the helical insert. A value equal to 40% of that theoretically predicted from Dukler's film thickness estimate was found to correlate the experimental results with a standard error of 23% and an average error of 20%.

The relative importance of the vapor phase heat transfer resistance during the condensation of various fluids shall be discussed. From Equation 17,  $h_v$  can be calculated from vapor pressure data for any substance. For example, values of  $h_v$  for

water and potassium are presented in Figure 26, with the predicted Nusselt theory condensing heat transfer coefficient for each substance at a film Reynolds number of  $10^3$  and at a Nusselt number of 0.11. As can be seen, for  $\delta_c = 1.0$ , the vapor phase heat transfer coefficient for water is  $10^2$  to  $10^4$  times as large as the liquid film heat transfer coefficient for  $0.1 \leq p \leq 100$  psia and would therefore result in an insignificant thermal resistance during the condensing process even for a value of  $\delta_c = 0.1$ . Since a value of  $\delta_c = 0.3$  has recently been reported for water, (Reference 25) it can be seen that the vapor phase thermal resistance is negligible during the condensation of water and has, therefore, gone unnoticed. However, for potassium for  $\delta_c = 1.0$  the vapor phase and liquid film thermal resistance are equal at  $p = 1.2$  psia, and the liquid film thermal resistance is ten times as great as the vapor phase thermal resistance at 30 psia. Therefore, for potassium, the vapor phase thermal resistance is an important portion of the total condensing thermal resistance particularly for  $\delta_c < 1$  and must therefore, be considered in the correlation of condensing heat transfer data.

#### B. Liquid-Vapor Interface Test

As discussed in Reference 7 a test was performed with the tapered pin insert installed in the 5/8-inch diameter tube to determine if it was possible to raise the liquid-vapor interface into the active condensing length approximately 9 inches or 25% of the active condensing length during normal operation without experiencing rapid temperature excursions. The results of the test with the tapered pin insert showed that the liquid-vapor interface could be maintained in the active heat transfer length of the condenser but that careful control of the potassium liquid flow rate from the condenser was required. This same test was

performed with the 3/8-inch I.D. no insert tube test section and with the 5/8-inch I.D. test section with helical and tubular inserts. Figure 27 shows the response of various system parameters as the liquid vapor interface was raised into the 5/8-inch I.D. test section. The Sanborn recordings show traces of  $T_{KI}$ ,  $T_{NaI}$ ,  $T_{KO}$ ,  $W_K$ ,  $P_{BK}$ , and three temperature traces of the thermocouples located in the insert at 5-inches, 10-inches, and 15-inches from the test section exit. Constant boiler power and sodium flowrate were maintained while the liquid potassium flowrate from the condenser was gradually reduced thereby raising the liquid-vapor interface level from the surge tank into the test section. As can be seen in Figure 27, after the flow had gradually been reduced to 56 lb/hr from its initial value of 65 lbs/hr during a period of approximately 1 hr, the liquid-vapor interface entered the active heat transfer length of the condenser, as indicated by the drop in the local potassium temperature at the test section exit to approximately the sodium inlet temperature. About 30 seconds later the interface passed the thermocouple 5-inches from the test section exit. With a subsequent reduction in flow the interface was brought to a point between 10 and 15-inches from the test section exit and was stabilized for a period of about 2 hours. The thermocouple located directly above the interface position indicated approximately the potassium test section inlet temperature and the thermocouple below the interface indicated approximately the sodium inlet temperature. The difference between the two inlet temperatures was approximately 140°F during this test. As can be seen in Figure 27, the adjustment of the system to the new interface location could be brought about gradually, without any serious temperature excursions, when careful control of the potassium pump was exercised. After the interface had been maintained between 10-and 15-inches from the test section exit for the period of about an hour, the

interface was returned to the surge tank by an increase in potassium liquid flow rate from the condenser, and the system returned to its initial operating conditions. The conclusions of this test are:

1. The liquid-vapor interface can be maintained within the active heat transfer length of the test section without the system undergoing substantial temperature excursions.
2. A temperature differential corresponding to approximately the difference between the potassium inlet temperature and the sodium inlet temperature is established over a short axial length increment across the interface.
3. No unexpected system response characteristics were detected when the interface was maintained within the test section.



## V. FACILITIES AND INSTRUMENTATION

J.C. Amos/W.H. Bennethum

### 300 KW Facility

During the quarter the top cover was removed from the 300 KW gas fired sodium heater and the L-605 tube bundle was inspected visually and by a dye penetrant method. No evidence of cracks was detected by the dye penetrant inspection and the tubes showed no signs of thermal distortion. This heater has operated a total of 4,448 hours at temperatures from 800 to 1850°F.

Nine additional Inco 702, sheathed, MGO insulated, chromel-alumel thermocouples were installed on the heater tube bundle, thereby increasing the total number of thermocouples provided for monitoring tube bundle temperatures to fifteen. The six thermocouples originally installed had been located on three tubes near an access port. The nine additional ones were installed on an even circumferential distribution while access to all tubes was available during inspection of the tube bundle.

### 100 KW Facility

Planned tests with the 3/8-inch nominal diameter test section without insert (Test Section No. 3) were completed April 2, 1965. This test section was removed and Test Section No. 4, consisting of a 3/4-inch Schedule 80 pipe with a combination plug-helical insert (described in detail in Section VI), was installed. This test section was instrumented with five 0.010-inch diameter Pt10%RH-Pt thermocouples located in the helix center body tube and plug. These thermocouples were insulated with high-purity alumina beads with the junctions spaced over the active length of the test section. Thirteen 0.005-inch diameter W3%Re - W25%Re thermocouples, insulated with BeO beads, were attached to the 3/4-inch pipe wall in axial positions corresponding to the location of the insert thermocouples.

Samples of the Pt10%Rh-Pt thermocouples were calibrated in freezing point furnaces with the following results:

		<u>Error</u>
Zinc	( 787.1°F)	- 0.7°F
Aluminum	( 1220°F)	- 0.4°F
Silver	(1761.4°F)	- 1.1°F
Copper	(1981.9°F)	- 3.5°F

The alumina insulators used with the insert thermocouples were soaked in an oxidizing atmosphere at 2350°F for 2 hours to remove all contamination and were not touched with bare hands during installation.

Samples of the W3%Re - W25%Re thermocouples, made from wire removed from the spools prior to assembly of the test section thermocouples, were calibrated in a vacuum furnace against 0.020-inch diameter Pt10%Rh-Pt reference thermocouples. Initial calibrations indicated appreciable drift. However, after the thermocouples were soaked for approximately 10 hours at 2300°F repeatability to within  $\pm 3^\circ\text{F}$  was obtained. Therefore, after installation of the test section thermocouples the test section was operated for 24 hours at 2100°F prior to in-place thermocouple calibration, in order to provide thermocouple stabilization.

Calibration of an additional thermocouple made from wire removed from the spools after the test section thermocouples were assembled did not show a change in calibration with successive thermal cycles and was repeatable with  $\pm 5^\circ\text{F}$  over three cycles. It is believed that the original wire samples, for which some drift occurred at the beginning of calibration were not annealed properly

because of their relative positions on the ends of the spools. Therefore, the second calibration is probably more representative of the actual wire characteristics.

During the down-time for the change from Test Section No. 3 to No. 4, the following facility work was performed.

- a. New Cb foil was installed on the inside of the condenser louvres.
- b. The pneumatic louvre actuation was installed and checked out at room temperature.
- c. The test section heat shield, which had been used for the last three test sections was recalibrated for heat losses.
- d. A new test section heat shield, which contains ten layers of .005-inch tantalum foil, was installed and calibrated for heat losses. The additional five layers of tantalum reduced the heat losses approximately 10%.
- e. The maximum pressure head of the helical induction pump was experimentally determined to be 40 psi for 455 volts at approximately 600°F fluid temperature.
- f. The new test section no. 4 was installed and instrumented.
- g. A new 0.101-inch diameter orifice was welded into the loop and heat-treated at 2100°F for two hours.

- h. The loop was hot-flushed at a maximum temperature of 800°F, after which a sample of the potassium was analyzed. Analysis of the sample indicated 27 parts per million O<sub>2</sub>. The potassium was then hot trapped at 1200°F for 37 hours in the dump tank. Due to the low level of O<sub>2</sub> before hot trapping the potassium was not resampled after hot trapping.
- i. A control circuit was added to permit automatic power reduction during any over-temperature condition sensed by either one of two thermocouples attached to the test section wall at the last measuring station within the heated zone, in order to eliminate the possibility of over-heating the test section during critical heat flux determinations or abnormal loop operating conditions. Power cutback is adjustable from zero to approximately 75% of original power setting so that minimum interference with loop operation may be obtained. A detailed description of this circuit is presented below.

The saturable reactor core electrical control system for the test section heater is essentially a variable impedance in series with the load current. Impedance is a function of a small D.C. current through a separate winding on the reactor. The control circuit provides the D.C. current and a means of varying it to control the load current through the main reactor winding. The variable power cut-back control consists of a potentiometer identical to the normal control potentiometer used to vary D.C. output on the standard "Reactrol E" control unit. The "cut-back" potentiometer is switched into the circuit only during an over temperature condition. Power reduction is achieved by setting the "cut-back" potentiometer for a lower value of D.C. output than the standard current limit potentiometer on the "Reactrol E" unit.

The specific components of the added controls and the manner in which they tie in with the "Reactrol E" unit are shown on Figure 28. They include:

1. Two normally open switches, one each attached to a slide wire of a two pen strip chart recorder (measuring loop test section temperature),
2. A triple pole, double throw relay.
3. A 5,000 ohm potentiometer located in parallel with the "Reactrol E" current limit control through a relay contact.
4. A momentary break push button,
5. An indicating light to warn the operator that the power cut back circuit has tripped.

In operation the cut-back circuit is not functional until an over-temperature condition is reached, at which time a normally open switch mounted on one of the recorder slide wires is closed thereby activating the relay and dropping the current limit potentiometer out of the circuit and adding the cut back potentiometer. The net effect of this reaction is equivalent to manually operating the current limit control at the exact instant an over temperature condition at either of two thermocouples which are located at the last measuring station within the heated zone of the boiler is reached. The other contact on the TPDT relay is used to hold the reduced power condition until the reset push button is operated to prevent the power from returning to its original level when the thermocouple indicator falls below the set point.

Thermocouple and flow meter calibration runs for Test Section No. 4 were started on May 5, 1965 and boiling test operation was started May 10, 1965. The test plan with this test section was completed June 10, 1965. Minor interruptions of test operation were required to repair test section wall thermocouples, flow meter leads, and to remove Cb foil from the condenser coil to increase the condensing capacity for high-power test runs at 1800°F saturation temperature.

All five of the insert thermocouples installed in Test Section No. 4 survived the test program in good operating condition. Attempts to remove the thermocouple assembly from the test section at the end of the test were not successful due to the fact that the insulators became wedged in the insert tube and the center wire was broken during the attempted disassembly.

The tungsten coil preboiler radiant heater operated at a maximum gross electrical input of 60 KW and the test section tungsten rod radiant heater was operated at a maximum gross electrical power of 32 KW. The preboiler heater has operated a total of 1280 hours and will be reused for Test No. 5. The test section heater rods experienced some bowing but can be reused. However, since backup units have been prepared for both heaters, a new test section heater will be installed for Test No. 5 and the present heater retained as the back up.

Test Section No. 5 (to be described in detail in Section VI) was assembled and installed in the facility and final instrumentation is in progress. Boiling tests are scheduled to start early in July. This test section is instrumented in a manner similar to Test Section No. 4 except that the internal Pt10%Rh-Pt thermocouples are installed from both ends of the test section. This arrangement allows a total of 8 junctions to be spaced over the active length of

the test section. Figure 29 is a photograph of the thermocouple junctions made at the end of the 11-hole insulator and installed so that the center wire (0.020 Cb-1%Zr) was in contact with the end of the insert tube plug. Figure 30 is a photograph of a junction made in a slotted insulator along the length of the insert tube. The wires and junction bead were isolated from the inner tube wall by the geometry of the insulator. Figure 31 is a photograph of the transition region between 11-hole insulator and 2-hole insulator which continue to the CATS block cold junction located inside the vacuum chamber.

The 100 KW Facility operated a total of 535 hours during the quarter including 450 hours under boiling conditions. Total operating time for this facility at the end of the quarter stands at 5897 hours.

#### 50 KW Facility

There was no activity on this facility during the quarter. The facility was shutdown on March 5, 1965 in good operating condition at the completion of all contracted tests.

## VI MATERIALS SUPPORT

W.R, Young/W.H. Kearns

During this period, two test sections were fabricated and installed in the 100 KW Cb-1Zr heat transfer facility. Test Section No. 4 contained a helix and plug insert, and Test Section No. 5 contained a wire wound plug and wire coil insert. Also, new orifices were installed upstream of the preboiler for both test sections, respectively. After Test Set No. 4 was completed, the preboiler coil was removed from the facility, and the piping at the orifice location was replaced. The preboiler was reinstalled in the facility with Test Section No. 5.

All welding, except facility installations, was done in a vacuum-purged welding chamber using the tungsten arc process. The chamber was evacuated to less than  $1 \times 10^{-4}$  torr and filled with high purity helium for the welding operations. Facility installations were made using previously developed, tungsten arc field welding procedures. All structural weld joints were radiographed and helium leak checked for soundness,

### Fabrication of Test Section No. 4

This test section is shown in Figure 32. The boiler and exit tubes were 3/4-inch, Schedule 80 pipe. Test section piping was increased to 1-inch, Schedule 80 size downstream of the boiler tube to facilitate insert installation. The insert was supported at the end of the 1-inch pipe section. Access for internal insert thermocouples was provided through an opening at the end of the insert support. The test section shell was fabricated and inspected prior to installation of the boiler insert.



The insert, Figure 33 was composed of a straight plug section and a helical swirl. The inlet plug was 0.58-inch O.D. by 0.43-inch I.D. by 15-inches long. Overall length of the total insert was 50.4 inches. The helical swirl was 15 inches long with a 1.5-inch pitch on a 0.25-inch diameter center body tube.

A cap was welded to the plug tube, and centering bosses of weld metal were deposited at each end. The faces of the bosses were machined concentric with the plug to center it in the 3/4-inch boiler tube. This plug was subsequently welded to the reducer on the helical swirl as shown in Figure 33.

The helix (Figs. 34, 35) was made from nine washers cut radially. Initially, two spirals were made by welding washers end to end, four in one and five in the other. Both spirals were pulled axially to form helices. The helices were then slipped onto the 0.25-inch O.D. center tube, welded end to end, and tack welded to the tube. Reducers were welded to each end of the tube and centering wires were tack-welded to the unsupported tube section.

A 3/8-inch, Schedule 80 pipe provided rigid support for the insert (Figure 33). Weld metal deposits on this pipe were machined to produce a flange and three centering pads. This flange was machined to match the 1-inch, Schedule 80 pipe of the test section. The insert support was welded to a reducer on the helical swirl to complete the insert. A 3/8-inch diameter vent tube was also welded in position for evacuation of the hollow portion of the insert.

After the insert was placed in position, the final seal weld was made between the insert flange and the test section shell. Instrumentation thermocouples were then inserted, and the test section was positioned in the facility. Standard field welding

procedures were used to join the test section to the condenser and preboiler.

The 0.063-inch orifice used during Test Set No. 3 was removed from upstream of the preboiler and replaced with a 0.101-inch orifice by field welding. This weld was heat treated locally because it operates below the required average annealing temperature. It was heated at 2100°F for 1-hour using a small tungsten element furnace in the environmental vacuum chamber. The test section and installation field welds were heat treated at 2100°F by the potassium working fluid during the calibration runs.

#### Fabrication of Test Section No. 5

The completed test section with a boiling nucleator at the inlet is shown in Figure 37. Part of Test Section No. 4 was used for this test section. Test No. 4 boiler tube was cut off at the shell reducer leaving the insert in the pipe. The insert support section was removed by cutting through the 1-inch, Schedule 80 pipe 1.5 inches from the end. A new piece of 3/4-inch pipe was used for Test Section No. 5 boiler tube.

Two instrumented inserts were used in this test section, one installed in the exit and one in the inlet of the boiler. The test section components are shown in Figure 38.

The inlet insert was composed of a wire-wound plug followed by a helical wire coil. The plug insert at the inlet was 0.58-inch O.D. by 15.75-inches long with a 0.02-inch deep, 1.5-inch pitch helical groove machined into it to provide a seat for a wire coil. The wire coil was made of 0.094-inch diameter wire, formed to fit

tightly against the inner pipe wall, with a 1.5-inch pitch and extending the full length of the boiler section. The top half of the boiler section contained only the wire coil insert.

The boiler inlet piping included an offset formed by two special offset reducers welded back-to-back. The plug was supported on and connected to one reducer using a 0.25-inch diameter tube (Figure 38). Thermocouple instrumentation was inserted into the plug through a hole in the reducer.

The helical wire coil and the plug were inserted into the boiler tube. Downstream of the plug, the wire was attached to the tube at 2.25-inch intervals, by welding through holes in the tube, and also at the end of the tube. Subsequent X-ray inspection showed that the wire melted in two at the weld, adjacent to the plug tip. The gap in the wire, which was only about 0.16-inch, was not considered deleterious to the test. The reducers were welded together and were welded to the pipe. A boiling nucleator, Figure 39, was welded to the bottom reducer.

A thermocouple insert at the boiler exit was a piece of 0.25-inch diameter tubing seal-welded at one end with centering wires attached (Figure 38). The boiler tube was welded to the reused downstream section from Test Section 4, with the exit insert in position. The final closure weld was made in the 1-inch pipe downstream of the boiler tube.

Several orifices had been welded into the facility upstream of the preboiler coil using standard field welding procedures. Because some contamination of Cb-1Zr alloy is likely during each welding cycle, it

was decided to remove this section of piping and to replace it. Because there was no suitable location for field welding Test Section No. 5 in the facility downstream of the preboiler the preboiler coil was removed from the facility. A new section containing a thermocouple well, an orifice, and a pressure tap was fabricated. A Cb-1Zr-to-stainless steel pressure tap from the old section was used in this section. This new section was then welded to the preboiler coil in the welding chamber.

The preboiler coil and the new test section were welded together in the welding chamber. After installation of thermocouple instrumentation, the test section was field welded to the facility condenser inlet and at the preboiler inlet. The field weld and orifice section at the preboiler inlet were postweld heat treated at 1950°F for 4 hours as described previously. The test section and field weld at the condenser inlet will be heat treated during the calibration run.

## VII ANALYSIS

G.L. Converse

The analytical task during the current quarterly period has been directed primarily toward the area of forced convective boiling heat transfer. The specific area of interest is defined by the following conditions:

- A. Vertical, axially symmetric flow in a constant area tube with a uniform heat flux imposed on the tube boundary.
- B. Steady flow.
- C. Two-phase single-component flow of potassium with net vapor generation.
- D. Flow regime of the annular or annular-mist type.
- E. Heat fluxes less than the critical heat flux.

Some preliminary results of this investigation were given in Section VIII of Reference 12. In this reference two possible mechanisms of vapor generation\* in the annular or annular mist flow regimes were discussed, i.e., vapor generation by bubble formation (nucleate boiling) and/or by evaporation at the liquid vapor interfaces. These discussions included proposed methods for predicting the heat transfer coefficients for either mechanism of vapor generation. In the present section, the methods for predicting the heat transfer coefficients which were proposed in Reference 12 will first be reviewed, and some modifications and limitations to the methods will be pointed out. Some of the

---

\* The terms vaporization or vapor generation will be used to designate the production of vapors by either one or a combination of the following mechanism:

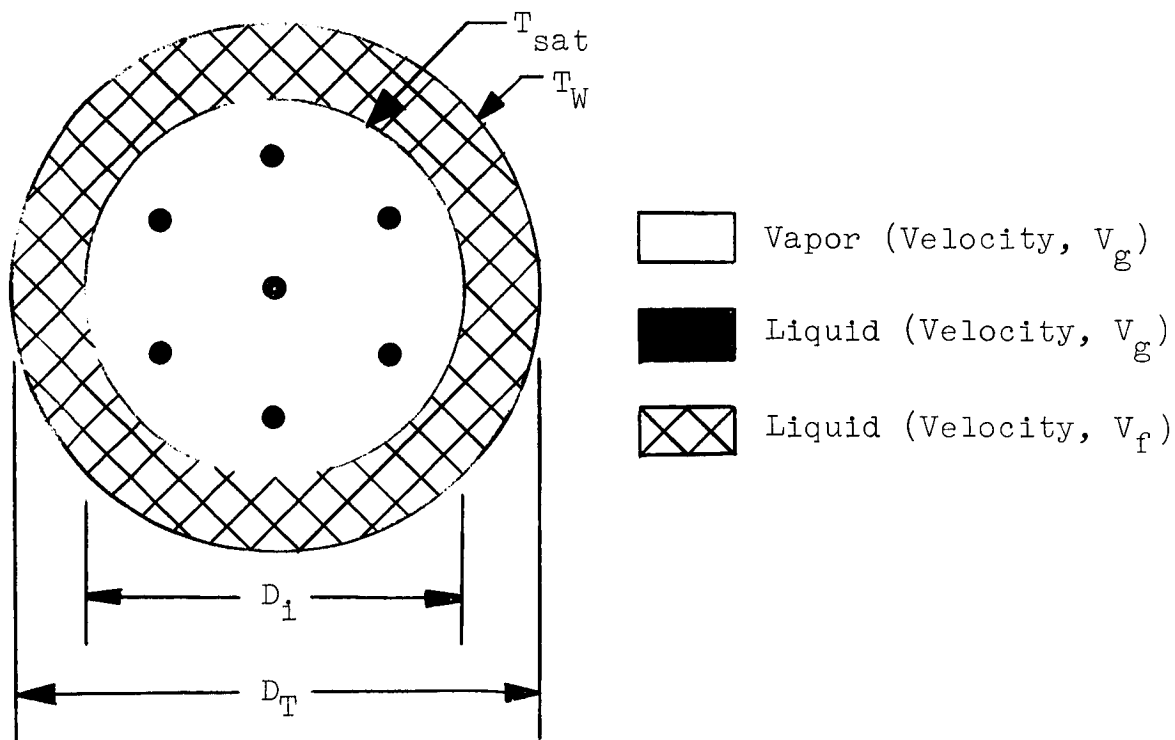
- a. Evaporation from the liquid-vapor interface
- b. Vapor production by bubble formation at the heat-transfer surface (boiling or ebullition).

factors which determine the mechanisms of vapor generation will then be discussed. Finally, the process of forced-convection vaporization of potassium inside a tube with a uniform heat flux imposed on the tube boundary will be discussed with particular reference to data from the 100 KW loop.

#### Vapor Generation by Evaporation at Existing Liquid Vapor Interfaces

For this case it was assumed that nucleate boiling was totally suppressed, and that vapor was generated by evaporation at existing liquid vapor interfaces.

The flow pattern was assumed to consist of a thin concentric layer of liquid on the wall with the remainder of the liquid entrained in the vapor core and traveling with the vapor velocity (see sketch A below).



Sketch A

The mechanism of heat transfer was assumed to be conduction from the wall to the liquid vapor interface. Evaporation of the droplets was neglected. The interface was assumed to be at the local saturation temperature.

By utilizing the expression for conduction across a cylinder with a uniform heat flux imposed on the boundary, the following equation was obtained:

$$N_{Nu} = \frac{h_{FE} D_T}{K} = \frac{2}{\ln D_T/D_i} \quad (1)$$

Equation 1 may be rewritten in terms of the average void fraction and mass fraction of entrained liquid as follows (see Reference 12).

$$N_{Nu} = \frac{h_{FE} D_T}{K} = - \frac{4}{\ln \left[ 1 - \left( \frac{1-x}{x} \right) \left( \frac{\rho_g}{\rho_f} \right) R_g (k-E) \right]} \quad (2)$$

where

$$k = \left( \frac{\rho_f}{\rho_g} \right) \left( \frac{x}{1-x} \right) \left( \frac{1-R_g}{R_g} \right) \quad (3)$$

In Reference 12 the behavior of Equation 2 was studied for several values of the slip ratio ( $k$ ) with zero entrainment ( $E$ ). In an effort to assess the effect of entrained liquid, Equation 2 was evaluated for several values of the entrainment with slip ratios of one and  $(\rho_f/\rho_g)^{\frac{1}{2}}$ . The resulting Nusselt numbers are shown in Figure 40. From this figure it can be seen that, within the limitations of the model chosen, the effect of entrainment is significant only for small values of the slip ratio, i.e., for slip ratios of order one.

In order to obtain an estimate of the slip ratio, the momentum exchange model (Reference 13) was used. In this model the relationship between quality and void fraction is given by the equation:

$$\frac{(1-x)^2}{(1-R_g)} + \frac{x^2}{R_g} \frac{\rho_f}{\rho_g} - \frac{1}{2} \frac{(1-x)^2}{(1-R_g)^2} = \frac{1}{2} \quad , \quad (4)$$

if it is assumed that  $R_g \rightarrow 0$  when  $x = 0$ .

The void fraction quality relationship calculated from equation (4) is shown in Figure 41. This void fraction quality relationship was then used in Equation 3 in order to obtain an estimate of the slip ratio. The resulting values of the slip ratio are shown in Figure 42. From Figure 42 it can be seen that, except in the low quality region, the slip ratio is quite large for range of saturation temperatures considered. In view of the above results, it was decided to use the momentum exchange model to predict the slip ratios and void fractions to be utilized in Equation 2, and to assume that the entrainment was zero. The Nusselt numbers calculated from Equation 2 utilizing the above assumptions are shown in Figure 43.

In the derivation of Equation 2, the heat was assumed to flow along a straight radial path from the tube wall to the liquid-vapor interface, i.e., the curvature of the interface in the axial direction was neglected.

$$\text{In general} \quad \frac{d\delta}{dx} = \frac{d(\delta/D)}{dx} \frac{dx}{d(\ell/D)} = \frac{4 q''}{G h_{fg}} \frac{d(\delta/D)}{dx} \quad (5)$$

Figure 44 is a plot of the ratio of film thickness to tube radius



against quality obtained from the void fraction plot in Figure 41 by assuming that all the liquid is on the tube wall. From Equation 5 it can be seen that the assumption of small interfacial curvature in the axial direction is poor in regions where either  $d(\delta/D)/dx$  or  $\frac{4q''}{Gh_{fg}}$  is large. In particular, the assumption is very poor in the low quality region, i.e., beyond the knee of the void fraction or liquid film thickness curves. In this region the Nusselt numbers shown in Figure 43 drop below the single-phase values and the solution is no longer valid. In order to remove the most undesirable feature of Figure 43, i.e., the fact that the Nusselt number drops below the single phase value in the low quality region, an interpolation formula of the form

$$\frac{h_{TP} D_T}{K} = \left[ \left( \frac{h_{\ell} D_T}{K} \right)^n + \left( \frac{h_{FE} D_T}{K} \right)^n \right]^{1/n} \quad (6)$$

was used. The Nusselt numbers calculated from this formula will approach the single phase values at low qualities and the film evaporation values at high qualities. This procedure was used in the construction of Figure 45; a single phase Nusselt number of seven was employed together with  $n = 2$ .

Although the above procedure removes the most undesirable feature of Figure 43, it in no way adequately accounts for the surface curvature in the axial direction. However, in view of the fact that the parameter  $4q''/Gh_{fg}$  is generally much less than one for potassium, it is felt that the proposed film evaporation model is adequate over most of the quality range. In the low quality region, however, both the single phase and two-phase heat transfer coefficients probably deviate somewhat from the values predicted by Equation 6.

The following qualitative trends in the two phase Nusselt number resulting from the assumption of an evaporative mechanism of vapor generation should be noted.

- a)  $N_{Nu}$  increases with increasing quality for a given saturation temperature.
- b)  $N_{Nu}$  increases with increasing liquid Peclet number (this follows from equations six and seven).
- c)  $N_{Nu}$  increases with increasing liquid entrainment in the vapor core.
- d)  $N_{Nu}$  decreases with increasing saturation temperature for a given quality.
- e)  $N_{Nu}$  is independent of heat flux for the particular analytical model chosen. However, the parameter  $\frac{4q''}{G h_{fg}}$  would probably be important if a more sophisticated analytical approach were used. This would be particularly true in the low quality region (i.e., beyond the knee of the void fraction quality curve).
- f)  $h_{FE}$  increases with decreasing tube diameter if the remaining variables are held constant.

#### Vapor Generation by Vigorous Nucleate Boiling

For this case it was assumed that vapor generation by evaporation at the liquid vapor interfaces was negligible. Vapor was assumed to be generated by the formation of vapor bubbles

at the wall of the tube, and the subsequent growth and transport of these bubbles into the vapor core.

The heat transfer coefficient was assumed to consist of that obtained by the superposition of the single phase liquid forced convective heat transfer coefficient and the nucleate pool boiling heat transfer coefficient (Reference 14).

The single phase forced convective heat transfer coefficient was calculated from the equation ( Reference 15).

$$N_{Nu} = 7 + 0.025 (N_{Pe})^{0.8} \quad (7)$$

The nucleate pool boiling heat transfer coefficient was obtained from Equation 8 below as given by Bonilla in Reference 16.

$$T_W - T_{sat} = 49.8 (q'')^{0.0867} P^{-0.276} \quad (8)$$

Where  $T$  is in  $^{\circ}\text{F}$ ,  $q''$  in  $\text{Btu}/\text{Hr}\cdot\text{Ft}^2$ , and  $P$  in millimeters of mercury absolute (torrs).

The heat transfer coefficients obtained from Equations 7 and 8 were then combined using the interpolation formula suggested by Kutateladze (Reference 14), i.e.,

$$\frac{h_{NB}}{h_l} = \sqrt{1 + \left(\frac{h_{PB}}{h_l}\right)^2} \quad (9)$$

The results of this calculation for a 3/4-inch I.D. tube are shown in Figure 46. It was assumed in the construction of Figure 46 that the single phase Nusselt number was equal to seven, i.e., that the mass velocity was small.

Equation 8 is based on the pool boiling data of Bonillia (Reference 17). The data was obtained by boiling potassium on a horizontal nickel plate. The approximate range of the data is given below.

P(psia)	T <sub>sat</sub> (°F)	q" Btu/Hr-Ft <sup>2</sup>
0.0387 to 0.2322	690 to 840	up to 10 <sup>5</sup>
13.55 to 29.1	1380 to 1540	up to 10 <sup>5</sup>

Since both the surface conditions and the range of operating pressures in the current 100 KW facility are different from those in the pool boiling test, precise agreement between the predicted forced convective boiling heat transfer coefficient using this data and those obtained from the 100 KW Facility cannot be expected.

The following qualitative trends in the two-phase heat transfer coefficients result from the assumption of a boiling mechanism of vapor generation.

- a)  $h_{NB}$  is independent of quality (for all saturation temperatures)
- b)  $h_{NB}$  increases with increasing heat flux at a given saturation temperature.
- c)  $h_{NB}$  increases with increased saturation temperature (increased pressure) at a given heat flux.
- d)  $h_{NB}$  increases with increasing values of the single phase liquid heat transfer coefficient.

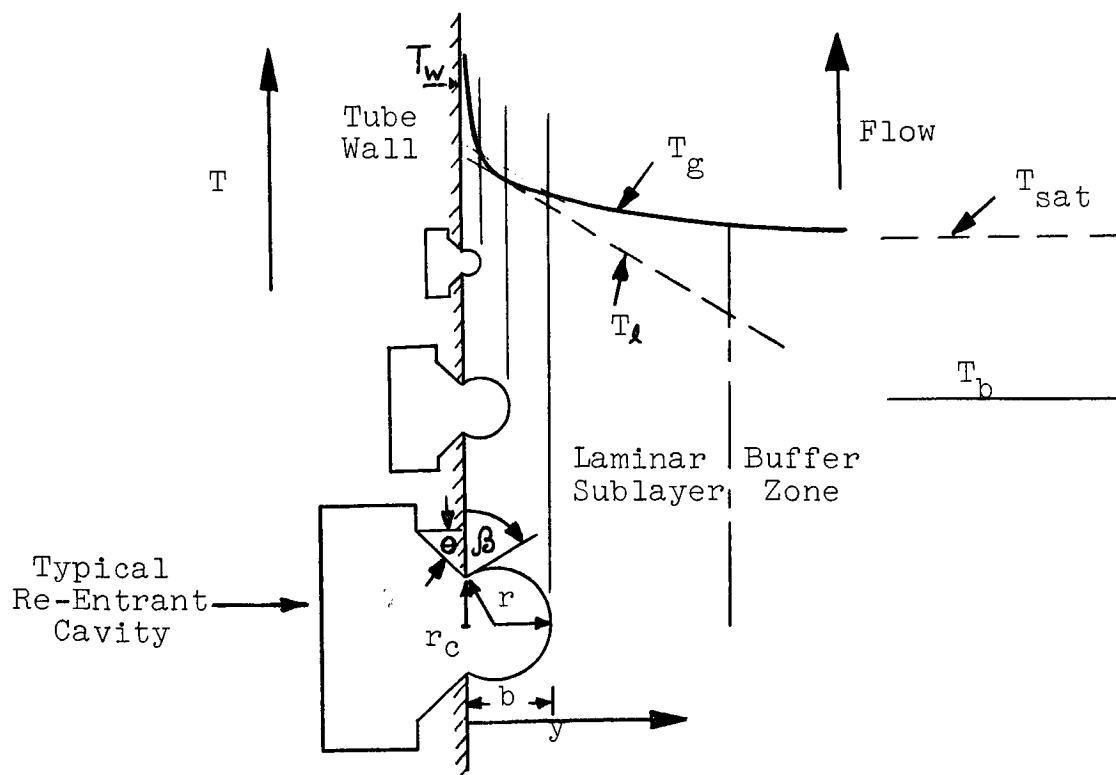
e)  $h_{PB}$  is independent of tube diameter.

It should also be noted that while it is possible to have total suppression of nucleation (i.e., heat transfer by film evaporation only); it is not possible to have boiling without some evaporation taking place. To the extent that film evaporation takes place, the effects mentioned in the preceding section will also be present during boiling.

### Suppression of Nucleation

The question as to which of the two preceding mechanisms of vapor generation will take place in a given situation will now be examined with the help of a model presented by Bergles and Rohsenow (Reference 18). In Reference 18 a graphical procedure was proposed which could be used to predict the conditions necessary for boiling inception.

The graphical procedure can best be understood by referring to Sketch B below:



Sketch B

The condition for bubble growth given in Reference 18 is that  $T_l \geq T_g$  for all values of  $y \leq b$ . For the limiting case of boiling inception, the following conditions apply.

$$(a) \quad T_l = T_g \text{ at } y = b$$

$$(b) \quad \frac{dT_l}{dy} = \frac{dT_g}{db} \text{ at } y = b$$

The liquid temperature near the wall is assumed to be linear and is determined from the equation:

$$T_l = T_w - q'' \frac{y}{K} \quad (10)$$

The temperature inside the vapor bubble is approximately the saturation temperature corresponding to the pressure inside the vapor bubble as given by the Helmholtz relations for the radius of curvature, i.e.,

$$P_g - P_l = \frac{2\sigma}{r} \quad (11)$$

The relationships between the height of the bubble ( $b$ ), the bubble radius ( $r$ ), and the cavity mouth radius ( $r_c$ ) are given by the following equations (obtained from Sketch B).

$$b = (1 + \cos \beta) r \quad (12)$$

$$r \sin \beta = r_c \quad (13)$$

where  $0^\circ < \beta \leq 90^\circ$

It might have been well to omit the consideration of contact angle in the following derivation since in general the relationships between cavity mouth radius, bubble height, and bubble radius at

boiling inception cannot be written down independent of the cavity shape. Since potassium is generally assumed to be a highly wetting fluid (i.e., small contact angle), it was assumed that all the non-re-entrant or conical type cavities would be "snuffed out" and that only those cavities which were not flooded by subcooled liquid (i.e., re-entrant cavities) would trap vapor. (Reference 19 contains a good discussion of re-entrant and conical type cavities). For the particular cavity shape shown in Sketch B, if it is assumed that  $\theta + \beta > 90^\circ$  then the conditions of equilibrium at the liquid vapor interface will require that the liquid be subcooled if the interface is within the cavity. Under these conditions the liquid vapor interface will retreat to the inside lip of the cavity as soon as some wall superheat is available, it will then, somehow, round the corner and hang on the outer lip of the cavity in the condition of equilibrium shown in Sketch B until boiling inception occurs. If it had been assumed that  $\theta + \beta < 90^\circ$  then the liquid would have been superheated within the cavity. The superheat required for boiling inception could then have been dependent on the cavity angle  $\theta$ . Since it was desired to include (in at least an approximate fashion) the effect of contact angle but not the effect of cavity angle, the above cavity configuration was chosen. In reality the solution to the boiling inception problems probably requires the solution to the fluid flow and heat transfer problem associated with the expansion of the initial volume of trapped vapor to the final state of boiling inception.

In Reference 18, the bubbles were assumed to be hemispherical ( $b = r = r_c$ ) and the above equations were solved graphically to obtain a boiling inception curve, i.e., the relationship between the heat flux and wall superheat at boiling inception. The actual

point of boiling inception is then determined by obtaining the point of intersection of the boiling inception curve with the usual single phase forced-convection or natural-convection heat transfer relationship between  $q''$  and  $T_w$  for a particular value of bulk fluid temperature.

Since the graphical procedure is somewhat tedious, an approximate solution to the above equations was obtained in the following manner. Assume that the vapor-temperature inside the bubble can be satisfactorily approximated for small superheats by the equation (Reference 20).

$$T_g = T_{sat} + \frac{2\sigma T_{sat} v_{fg}}{Jh_{fg} r} \quad (14)$$

where  $T_{sat}$  is the saturation temperature corresponding to the external liquid pressure. Equations 10, 12, 13 and 14 are then solved simultaneously to determine the relationship between  $q''$  and  $T_w - T_{sat}$  which will satisfy conditions (a) and (b) above. The resulting expression is of the form:

$$q'' = \frac{Jh_{fg} K (T_w - T_{sat})^2}{8\sigma (1 + \cos\beta) T_{sat} v_{fg}} \quad (15)$$

The critical cavity size (the cavity size that nucleates first) is given by the expression:

$$r_c = \frac{4\sigma v_{fg} T_{sat} \sin\beta}{Jh_{fg} (T_w - T_{sat})} \quad (16)$$

The accuracy of Equation 15 may be judged by referring to Figure 47, in which several graphical solutions have been compared with Equation 15. In each case it was assumed that  $\beta = 90^\circ$



(i.e.  $b = r = r_c$ ). The graphical solution for water is given in Reference 18, while that for Freon 113 was obtained from Reference 21. Preliminary comparison of Equation 15 with a graphical solution for potassium are also shown in Figure 47.

Equations 15 and 16 were used to generate the curves shown in Figure 48 for potassium. The wall superheat required for boiling inception at a given heat flux is shown as well as the critical cavity size. Equation 15 applies when an infinite range of cavity sizes are available on the heat transfer surface. If a maximum cavity size exist then

$$(T_w - T_{sat}) = \frac{26 T_{sat} v_{fg} \sin \theta}{J h_{fg} r_{max}} + \frac{q''}{K} \left( \frac{1 + \cos \theta}{\sin \theta} \right) r_{max} \quad (17)$$

where  $r_{max}$  is the maximum cavity size on the heat transfer surface. (The contact angle was assumed to be  $90^\circ$  in all calculations. It is recognized that this is probably a poor assumption for potassium. However, until contact angle data on potassium becomes available, and until the role of the contact angle in nucleation is somewhat better understood it was felt that the inclusion of this additional parameter in the ensuing calculations was not justified. The assumption of hemispherical bubbles has met with some success in the prediction of the boiling inception points for water (Reference 18) although the contact angle of water is known to differ from  $90^\circ$ ).

If it is assumed that Equation 17 correctly represents the effect of contact angle then a reduction in the wall superheat requirement for a given heat flux and cavity size would result. This does not necessarily imply a reduction in the wall superheat required for boiling inception since the "history" of the boiling surface must also be considered. This effect will subsequently be discussed in more detail.)

The existence of a limited range of cavity sizes acts to increase the superheat required for boiling inception at any heat flux. This behavior is shown in Figure 49. The nearly vertical lines represent the minimum wall superheat requirement as obtained from Equation 17 for the maximum cavity size shown on the curve. The asymptotic line was obtained from Equation 15. Also shown on Figure 49 are the usual single phase forced-convection lines obtained from Lyon's Equation (Reference 15).

$$N_{Nu} = 7 + .025 (N_{Re})^{.8} \quad (17)$$

Figure 49 illustrated the manner in which the boiling inception point is determined. If, for example, the test section heat flux is set at 20,000 Btu/Hr-Ft<sup>2</sup> then about 1°F of wall superheat is required for boiling inception if an infinite range of cavity sizes are available. Boiling would then commence when the bulk fluid was about 10°F subcooled. If on the other hand a maximum cavity size of 0.05 mils existed on the heat transfer surface then boiling would not begin until the bulk fluid was superheated about 30°F, i.e., due to the limited range of cavity sizes subcooled boiling would not take place at this heat flux.

Equations 15 and 17 will now be used to investigate the question of total suppression of nucleation in the region of net vapor generation. Many of the factors influencing nucleation are not clearly understood. In the following treatment it will be assumed that nucleation from the tube wall will take place if the following conditions exist.

- (a) Small cavities or pits are present on the tube wall.
- (b) These cavities contain entrapped vapor or gas.

- (c) The wall superheat is sufficient to activate the cavity, i.e., to cause the small vapor space present in the cavity to grow and produce bubbles.

Condition (a) is generally met by any commercial surface. Photographs of the heat transfer surface utilized in the 100 KW loop during the period 8/1/64 to 11/14/64 are shown in Figures 50a and 50b. The particular test section shown in these figures was removed from the loop on 11/14/64 after approximately 671 hours of operation at temperatures above 800°F. The approximate size of some of the more obvious pits or scratches have been designated in the photographs.

Condition (b) is probably the most difficult of the three conditions to treat adequately for alkali metals. In the 100 KW loop, for example, the potassium used as a working fluid is quite pure (less than 50 ppm  $O_2$ ) and considerable care is taken to exclude any gases from the test section. With the potassium fill line closed, the loop piping is evacuated down to approximately 25 microns with an auxiliary vacuum pump. The vacuum line is then closed and the loop is filled by pressurizing the dump tank with argon. If it is assumed that inerts are excluded from the test section, then each time subcooled liquid flows over the heat transfer surface all of the cavities are "snuffed out" except those of the smaller re-entrant type. This is due to the fact that potassium wets the surface. The net result of the above effects is that relatively high degrees of wall superheat would be required at the beginning of two-phase operation. Some verification of the above hypothesis is found in the relatively high value of wall superheat (about 200°F, at  $T_{sat} = 1800^\circ\text{F}$ ) reported at the beginning of two-phase operation (see Figures 32 and 33 of Reference 7). However, additional data will be required before any firm conclusion can be reached.

Condition (c) can be treated by using Equations 15 and 17 in conjunction with the previously derived film evaporation theory. It will be assumed that if the wall superheats calculated from the film evaporation model are sufficient to cause nucleation then nucleation will occur and the boiling mechanism will predominate. In view of the above discussion it is evident that this is a necessary but by no means sufficient conditions for boiling. However, the use of this assumption will at least permit a preliminary estimation to be made of the regions in which nucleate boiling and film evaporation will take place,

The steps necessary to construct such a map are illustrated by Figure 51. The wall superheats required are obtained from Equations 15 and 17. The maximum cavity size on the surface is taken as a parameter in the construction of these curves. The available wall superheat is then obtained from the film evaporation model using the Nusselt numbers from Figure 45. If the available superheat exceeds the required superheat it is assumed that nucleation will occur. The end results of this procedure for a 3/4-inch diameter tube are shown in Figures 52a and 52b.

In order to utilize Figure 52 some knowledge of the range of cavity sizes available on the heat transfer surface is required. For example, based on Figures 50a and 50b, a maximum cavity radius of  $\sim 0.1$  to  $.2$  mils may be estimated for the 100 KW loop. Based on this estimate Figure 52a would predict that the mechanism of vapor generation at  $q'' = 10^5$  Btu/Hr-Ft<sup>2</sup> and  $T_{\text{sat}} = 2100^\circ\text{F}$  would be vigorous nucleate boiling for qualities less than about 70%. For the same conditions at  $T_{\text{sat}} = 1500^\circ\text{F}$  no boiling would be predicted and the mechanism of vapor generation would be film evaporation.

It should be pointed out that Figure 52 applies only to a 3/4-inch I.D. tube. Since the film thickness increases when the tube size is increased (see Figure 44) the likelihood of boiling is greater for large diameter tubes and less for small diameter tubes if all other variables are the same.

The following qualitative trends are evidenced by Figure 52 .

- (a) At a given heat flux, saturation temperature, and maximum cavity size, nucleate boiling tends to be suppressed by increasing quality.
- (b) At a given heat flux, saturation temperature and quality, nucleate boiling tends to be suppressed for smaller values of the maximum cavity size (i.e., for smoother heat transfer surfaces).
- (c) At a given quality, saturation temperature, and maximum cavity size, nucleate boiling tends to be suppressed by lowering the heat flux.
- (d) At a given quality, heat flux, and maximum cavity size, nucleate boiling tends to be suppressed by lowering the pressure.

The highly preliminary nature of the mapping shown in Figure 52 should be stressed. Some of the more important sources of error are the following:

1. Inadequacies in the method used to calculate the film thickness

In this connection particular attention should be called to fact that in the method used an assumption was made that the film thickness is independent of the heat flux.

2. The assumption of a smooth interface

The assumption of a smooth interface (i.e., the assumed absence of waves on the liquid vapor interface) is known to be unrealistic. In general the presence of waves on the interface will probably increase the film evaporation heat transfer coefficient. Although there are many factors which influence the wave amplitude the effect of heat flux should be particularly noted. In Reference 22 N. Zuber suggested that the thrust exerted by the vapor on the liquid vapor interface would act to destabilize the interface. Since the vapor thrust is proportional to the square of the heat flux, waves of larger amplitude might be expected at higher heat flux levels. This would have the effect of extending the film evaporation region in Figure 52 at the higher heat fluxes, i.e., the transition lines would become more vertical for the higher heat fluxes.

3. Errors in the estimate of the maximum cavity size

4. The possible effect of contact angle on the wall superheat requirement. Some indication of this effect can be obtained by comparing Figures 52a and 52b.

Any of the factors listed above could quantitatively alter Figure 52. However, it is less probable that the qualitative trends evidenced by the map will be radically altered. It should also be pointed out that Figure 52 was constructed by assuming that the mechanism of vapor generation was film evaporation and calculating the conditions necessary for boiling to begin. In general, the location of the transition lines in Figure 52 would not be expected to be independent of the direction in which they are traversed. For this reason the map would be expected to be less reliable in predicting the point of boiling suppression than

the point of boiling inception.

### Vaporization of Potassium In A Tube Having A Uniform Heat Flux Imposed On The Tube Boundary

In this section the process of forced-convection vaporization of potassium inside a tube with a uniform heat flux imposed on the tube boundary will be discussed with the aid of data from the 100 KW loop. Before beginning the discussion, it would probably be well to point out the highly conjectural nature of much of what follows. This must necessarily be the case since in many instances data on which to base a firm conclusion is either absent or lacking in accuracy. During the course of the discussion frequent comparison will be made between the data and the previously derived analytical results. In this way the areas of agreement and disagreement can be assessed. Repeated reference to all the weaknesses in the analytical development will not be made when areas of disagreement with the data are found; only those weaknesses which appear to be the most likely cause of the discrepancy will be noted.

In Figure 53 several curves of temperature distribution along the 100 KW test section with the fluid in vertical upflow are shown. Some additional information on the runs shown in Figure 53 which is pertinent to the discussion is tabulated below:

<u>Table A</u>						
Run Desig.	$dT_b/d(L/D)$	$L/D$ To Sat.	$L/D$ To Spike	$T_b - T_{sat}$ At Spike (°F)	$T_w - T_{sat}$ At Spike (°F)	Two-Phase Pressure Drop (psia) (Calculated)
○	21.3°F	25.6	27.25	35.0	65	0.1747 ( $\Delta T_{sat} = 0.629^\circ\text{F}$ )
◊	19.9°F	27.9	30.00	41.8	62	0.16877 ( $\Delta T_{sat} = 0.608^\circ\text{F}$ )
△	16.3°F	32.8	35.50	44.0	58	0.15702 ( $\Delta T_{sat} = 0.565^\circ\text{F}$ )

Note: Since the inlet well is located about 3 L/D's upstream of the heated zone, it does not give an accurate indication of the inlet

liquid temperature. Due to the small specific heat of potassium and the relatively low flow rate any heat transferred to the fluid between the well location and the start of the heated zone could considerably alter the inlet liquid temperature. For this reason a great deal of confidence cannot be placed in the calculated values of the bulk liquid temperature in the test section.

Focusing attention on the curves, two distinct regions separated by a temperature spike are observed. Near the inlet of the tube both the wall and liquid temperatures are rising at about the same rate, since both temperatures are below the saturation temperature. No vaporization is taking place and the heat is transferred by ordinary single phase forced convection. The wall temperature then increases above the saturation temperature so that subcooled boiling becomes a possibility. However, the wall temperature continues to increase at about the same rate thus indicating no significant change in heat transfer coefficient and suggesting that no subcooled boiling takes place. The point of boiling inception should be predicted by Figure 49. If a maximum cavity size of 0.1 mils is assumed (based on Figure 50), boiling should occur according to Figure 49 when the bulk fluid is about 50°F subcooled for the higher heat flux run. In reality the situation is not this simple. Since the testing is generally conducted by lowering the point of first vapor generation in the tube by either increasing the heat flux or decreasing the flow starting from an initially subcooled condition, the larger cavities may have been "snuffed out" as discussed in the previous section. If this is true then nucleation must occur from the smaller re-entrant cavities. If, for example, the maximum re-entrant cavity size which contains vapor is taken as 0.01 mils then from Figure 49 the bulk fluid must be about 150°F superheated for the highest heat flux run in order to obtain the wall superheat necessary to



produce the first vapors. When this condition is present the boiling boundary (the point of first net vapor generation in the tube) is frequently unstable. The following is a quote from the 100 KW Log\* written at a time when the boiling boundary was experiencing this type of instability.

Time

1445: "Rubicon set on A-16, occasionally temperature variations of approximately 100°F, A-15 is very slightly active, A-17 is also very active similar to A-16" (A-15 -16 and 17 are thermocouples).

1515: "Reading taken"

The data taken at 1515 has been plotted in Figure 54. It should be noted that the temperatures were read from inlet to exit of the tube with about a 10 second delay between each reading. The resulting wall temperature profile is, therefore, not an instantaneous picture. The extent of the instability associated with the runs shown in Figure 53 is not known. However, it is felt that some instability is always associated with the boiling boundary when the first vapors are produced with the bulk fluid in a superheated condition. If subcooled boiling occurs the instability is probably minimized if not entirely absent for reasons discussed subsequently below.

A possible working hypothesis to explain this instability is the following. When the first bubbles are produced they grow very rapidly due to the fact that the liquid is superheated across the entire flow area of the tube. This produces a local pressure pulse which may increase the local wall temperature

\*100 KW Log, Vol. II, February 14, 1964, page 149

required for boiling to continue from the same size cavity which produced the first bubble. However, as the bulk liquid temperature drops toward saturation after the first bubble is produced, there is also an increase in the local value of  $T_w - T_b$  equal to the bulk fluid superheat. This latter effect causes the wall temperature to decrease. Therefore, after the first bubble is produced the system is faced with a situation where a higher wall temperature is required to continue boiling (due to the pressure pulse) but only a lower wall temperature is available (due to the cooling of the wall). Under these conditions the boiling action may cease unless larger cavities have been activated by the first vapors. If larger cavities have not become active the boiling action will cease, the vapors produced will be swept away and the liquid will begin to superheat again thus repeating the cycle. Other explanations of the instability such as a local flow oscillation are possible. At the present time there is insufficient data to draw any firm conclusion about the cause of the instability.

After vaporization has begun, the wall temperature in Figure 53 decreases rapidly at first and then reaches a relatively constant value. If the nature of the local instability at the boiling boundary is due to intermittent boiling as suggested above, then the mechanism of vapor generation in the low quality region is probably one of film evaporation. Thus, inspite of the fact that the local wall superheat is sufficient to produce boiling from the larger cavities, no boiling takes place since these cavities have been snuffed out. For the runs shown in Figure 53 boiling may not begin until sufficient vapor has been entrained in the film to activate the larger cavities present on the surface of the tube. In order for this to occur the following sequence of

events must take place.

1. Vapor must be entrained in the liquid film
2. The entrained vapor must displace the liquid from a nucleation site.
3. The "captured site" must itself be capable of serving as a site for further nucleation or as a site from which nucleation can spread to adjacent cavities.

Thus far it has been tacitly assumed that conical cavities are not sufficiently stable to serve as nucleation sites for liquid metals. However, it appears unlikely that the vapors would "capture" previously flooded re-entrant cavities, but rather the shallow conical cavities. Factors which might tend to make conical cavities stable are the high thermal conductivity and low specific heat of potassium, i.e., the liquid would heat up quite rapidly as it penetrated into the cavity. This might offset the effect of small contact angle. Obviously a dynamic analysis of cavity stability would be required to answer this question.

For the reasons given above the heat transfer coefficients in Figure 53 would be expected to increase with quality in accordance with the film evaporation theory until the larger cavities become active. At this point there should be a rather sudden increase in the heat transfer coefficient to about the pool boiling value, and very little change thereafter. Some confirmation of the suppression of nucleation in the low quality region downstream of the boiling boundary in Figure 53 is inferred from Figures 55a thru 55d, although the heat fluxes are somewhat lower than those of Figure 53.

In these runs some net quality was present of the inlet of the test section and, although the qualities were quite low, the heat transfer coefficients obtained were at or about the pool boiling value and showed little variation with quality.

In the preceding discussion some of the features which must be considered in connection with the vaporization of potassium in a plain tube have been presented. The phenomenon is complicated by the fact that, in the choice of a mechanism of vapor generation, the previous history of the boiling surface must be considered in addition to the wall superheat requirement as discussed in connection with Figure 52 .

The Nusselt numbers calculated from the data shown in Figure 53 have been compared with the values predicted by the film evaporation model. This comparison is shown in Figure 56 . The comparison at low qualities is a severe test of the film evaporation model, since it is in this region where the effects of both liquid entrainment and axial curvature of the interface would be expected to be the greatest. The latter effect was shown to be related to the parameter  $\frac{4q''}{Gh_{fg}}$  . This parameter was calculated for the curves of Figure 56 . In general the Nusselt number shows an increase with increasing values of this parameter. It is felt that a film evaporation theory which included the two effects mentioned above could adequately predict the Nusselt numbers in the low quality region. From a design standpoint the present model may provide a conservative estimate of the heat transfer coefficients in this region.

In Figures 57 thru 59 the relationship between heat flux and temperature difference has been plotted from data taken at the

tube exit, i.e., in a region well removed from the boiling boundary. From Figure 52 it can be estimated that for a 0.2 to 0.1 mil maximum cavity size all the data shown in Figure 57 ( $T_{\text{sat}} = 2100^{\circ}\text{F}$ ) should be boiling with the exception of the 2 points which fall to the right of the pool boiling line. The lack of any consistent detectable quality trend in the data (plots of the same data on  $h$  vs.  $x$  coordinate can be found in Figure 15c of Reference 7) together with the apparent heat flux effect tend to confirm the boiling mechanism. The two points which fall to the right of the pool boiling line should be remarked upon. The higher heat flux point is probably a DNB point. The lower heat flux point may also be a DNB point but this is less probable. This point will be discussed in more detail in connection with Figure 58.

From Figure 52a it can be estimated that for a .2 mil maximum cavity size no boiling should occur for qualities above about 40% at  $1990^{\circ}\text{F}$  and for a .1 mil maximum cavity size no boiling should occur above about 60% quality. However, both Figures 58 and 59 indicate that boiling persists at the lowest heat flux ( $q'' \approx 30,000 \text{ Btu/Hr-Ft}^2$ ) to quite high values of the quality. Further confirmation of the boiling mechanism at low heat fluxes is obtained from Figures 60a and 60b. From these Figures it can be seen that there is little or no variation in heat transfer coefficient with quality along the tube length. This strongly suggest that the tube is in nucleate boiling. The persistence of the boiling mechanism at the lower heat fluxes may be due to the fact that once boiling begins in the tube the presence of the bubbles in the film may alter the film thickness and temperature distribution in the film itself. If this takes place the tube might "hang" in boiling somewhat longer than would be expected. The assumption of a contact angle of  $90^{\circ}$  could also be the source of the discrepancy (the effect of contact angle on the map can be assessed by referring to Figure 52b). Whatever the reason,

the data definitely indicates that boiling persists up to about 35% quality at 1750°F. This is not true, however, of the higher heat flux data of Figure 58. At the higher heat fluxes the predicted boiling points fall to the right in the plot as would be expected. The remaining points trail off to the left but do not appear to line up along constant quality lines as would be predicted by the film evaporation model (the same data on  $h$  vs.  $x$  coordinates can be found in Figure 15b of Reference 7). This may be due simply to errors in the measurement of  $T_w - T_{sat}$  for these small values of  $\Delta T$ .

The data shown on Figure 58, therefore, pose the following questions:

1. Nucleate boiling appears to be present at the lowest heat flux for qualities up to about 72%. How then can boiling be suppressed at the higher heat fluxes at lower values of quality for which the thicker film would be expected to cause an even larger value of the wall superheat?
2. If boiling is suppressed at the higher heat fluxes why doesn't the data fall along constant quality lines as would be predicted by the film evaporation theory?

These questions will be examined in reverse order. The second question will be examined first by means of the error analysis which follows.

In an effort to ascertain if the lack of agreement between the data and the film evaporation model evidenced in Figure 58 could in part be attributed to experimental error in the measurement of small temperature differences, an error analysis

was carried out. The following sources of error were considered.

- a) Random errors in temperature measurement  
(as evidenced by multiple digital printouts  
of the temperature at a given station)
- b) Errors due to thermocouple drift  
(as evidenced by a change in the relative  
thermocouple calibrations before and after  
testing)
- c) Errors in the calculation of inside wall  
temperature due to the uncertainty in wall  
conductivity. (Taken as  $\pm 4\%$  probable error  
based on the results of Reference 23)
- d) Errors in heat flux (Estimated as  $\pm 3\%$   
probable error)

The details of the analysis are given in Appendix E . Two cases were considered. In the first case two wall thermocouples were analyzed, this is representative of the measuring station at the exit of the tube. In the second case only a single wall thermocouple was analyzed, this is representative of the remaining measuring stations along the length of the test section. The results are summarized in the table below.

Table B

$\frac{q''}{\text{Btu/Hr-Ft}^2}$	$P_{[T_{WI} - T_f]} (^{\circ}\text{F})$ (1 wall - 3 well)	$P_{[T_{WI} - T_f]} (^{\circ}\text{F})$ (2 wall - 3 well)
0	1.038 $^{\circ}\text{F}$	0.74753 $^{\circ}\text{F}$
$2.5 \times 10^4$	1.1676 $^{\circ}\text{F}$	0.91897 $^{\circ}\text{F}$
$5 \times 10^4$	1.4900 $^{\circ}\text{F}$	1.3045 $^{\circ}\text{F}$
$7.5 \times 10^4$	1.9102 $^{\circ}\text{F}$	1.7692 $^{\circ}\text{F}$
$1 \times 10^5$	2.3767 $^{\circ}\text{F}$	2.2649 $^{\circ}\text{F}$
$1.25 \times 10^5$	2.8671 $^{\circ}\text{F}$	2.7751 $^{\circ}\text{F}$
$1.5 \times 10^5$	3.3709 $^{\circ}\text{F}$	3.2930 $^{\circ}\text{F}$

These results can be conveniently represented in terms of percent probable error in  $\Delta T$ . This type of representation is shown in Figures 61a and 61b for the two cases considered. Note that the percentage error increases rapidly as  $\Delta T$  decreases or as the heat flux increases. The lack of agreement between the film evaporation model and the data evidenced at the higher heat fluxes in Figure 58 is easily explained in terms of the probable error. However, the low heat flux data cannot be easily explained in this fashion since the probable error is only about  $\pm 20\%$ . Therefore the error analysis tends to support the conclusion that boiling is present in the tube at the lower heat flux. The first question will now be examined. In discussing the limitations of the mapping shown in Figure 52 attention was called to the effect of heat flux both on the mean film thickness and on the amplitude of the interfacial waves. The presence of waves of relatively large amplitude at the higher heat fluxes might increase the film evaporation heat transfer coefficient sufficiently so that the wall superheat



developed could no longer support boiling at the higher heat fluxes. Note that it is being assumed that boiling is suppressed to some extent in Figure 59 as evidenced by the tendency of the points to trail off to the left. This could be due to an error in wall thermal conductivity or heat flux as indicated by the error analysis. If this were the case, however, it is difficult to see why the data in Figure 58 would not show a similar trend. The solution proposed above is not entirely satisfactory since the heat transfer coefficient would be expected to be higher than those obtained from the film evaporation theory, whereas, in actual fact, they are somewhat lower. If the above hypothesis is accepted this latter discrepancy must be attributed to experimental error. Another possible solution investigated was the effect of aging on the tube surface, i.e., the heat transfer surface might become smoother with time. However, little correlation with time could be found in the data shown in Figure 59.

The percentage probable error in  $\Delta T$  is approximately equal to the percentage probable error in heat transfer coefficient (equal to it if the relatively small percentage error due to heat flux is neglected). Figures 62a thru 62e show some of the runs used in the construction of Figure 59. If these runs are considered together with those shown in Figures 60a and 60b the increase in the scatter in heat transfer coefficient with increasing heat flux is evident. Although there appears to be a general trend toward increasing heat transfer coefficient with increasing heat flux over roughly the same quality range, the data is too scattered to form any conclusion as to the mechanism of vapor generation except at the lower heat fluxes.

## Conclusions

Based on the preceding discussion the following tentative conclusions may be drawn.

1. If boiling occurs in the tube, the forced-convection nucleate boiling heat transfer coefficients predicted by equation 9 appear to be somewhat conservative.
2. If vapor is generated by film evaporation, the two-phase heat transfer coefficients predicted by Equation 6 appear to be somewhat conservative in the low quality region (probably due to the neglect of liquid entrainment and axial curvature of the interface in the model chosen) but may over estimate the heat transfer coefficient in the high quality region.
3. The map presented in Figure 52 is useful in making a preliminary judgement as to the predominate mechanism of vapor generation in the tube if operation occurs entirely in a region well removed from the transition lines. However, the map does not predict the location of the transition lines with any great degree of accuracy.
4. The "history" of the boiling surface may be an important factor in determining the mechanism of vapor generation as well as in boiling inception.

For the range of the tube diameters, heat fluxes, operating pressures, and mass velocities currently being considered for boiler design; the two-phase heat transfer coefficient will be high at heat fluxes less than the critical (high relative to the single phase and transition boiling heat transfer coefficients)

regardless of the mechanism of vapor generation. For this reason an accurate method for predicting the mechanism of vapor generation is not required at the present time. It is important, however, to recognize that different mechanism of vapor generation may occur in the tube, since this could aid in the correlation and extrapolation of the data. For the reasons given above, it is felt that the present treatment is probably adequate for design purposes and a recommended design procedure for calculating two-phase heat transfer coefficient will be given below. Additional work is required, however, on the boiling inception problem and on the local instability associated with the boiling boundary. This work may aid in understanding the role played by the previous history of the boiling surface.

Recommended Design Procedure for Calculating Heat Transfer Coefficients at Heat Fluxes Less Than The Critical

The recommended design procedure is the following:

1. Utilizing Figure 43 together with Equation 6 calculate the film evaporation heat transfer coefficient.
2. Utilize equations 7, 8 and 9 to calculate the forced convection nucleate boiling heat transfer coefficients.
3. Utilizing a map similar to that shown in Figure 52 determine the mechanism of vapor generation.
4. Use the heat transfer coefficient applicable to the particular mode of vaporization expected. If additional conservatism is desired use the smaller of the two values irrespective of the regime.

## REFERENCES

1. "Alkali Metals Boiling and Condensing Investigations," Quarterly Reports No. 2 and 3, Contract NAS 3-2528, SPPS, RSD, General Electric Company, April 20, 1963
2. Gambill, W. R., R. D. Bundy and R. W. Wansbrough, "Heat Transfer, Burnout and Pressure Drop in Swirl Flow Through Tubes with Internal Twisted Tapes," Oak Ridge Report ORNL-2911, April 1960
3. Greene, N. D. (Convair Aircraft), "Confined-Vortex-Flow Heat Transfer," cited as private communication to W. R. Gambill and R. D. Bundy in "An Evaluation of the Present Status of Swirl-Flow Heat Transfer," Oak Ridge Report Central Files Number 61-4-61, April 1961
4. Rohsenow, W. M., and H. Y. Choi, Heat, Mass and Momentum Transfer, Prentice Hall, Inc., New Jersey, 1961
5. Zuber, N., "Stability of Boiling Heat Transfer," Trans. ASME, April 1958
6. Costello, C. P., and Adams, J. M., Paper No. 30, "1961 International Heat Transfer Conference," Boulder, Colorado, August 1961
7. "Alkali Metals Boiling and Condensing Investigations," Quarterly Report No. 11, NAS-CR-54405, Contract NAS 3-2528, SPPS, MSD, General Electric Company, April 23, 1965
8. Dukler, A. E., "Fluid Mechanics and Heat Transfer in Vertical Falling-Film Systems," Chem. Eng. Prog. Symposium Series, No. 30, Vol. 56, 1960
9. Lee, Jon, "Turbulent Film Condensation," AIChE Journal, pp. 540-544, July 19, 1964, Vol. 10, No. 4
10. Schrage, R. W., "A Theoretical Study of Interphase Mass Transfer," Columbia University Press, New York, 1953
11. Rohsenow, W. M., and Sukhatme, S. P., "Heat Transfer During Film Condensation of a Liquid Metal Vapor," Technical Report No. 9167-27, Department of Mechanical Engineering, MIT, April 1964
12. "Alkali Metals Boiling and Condensing Investigations," Quarterly Report No. 10, Contract NAS 3-2528, SPPS, RSD, General Electric Company, January 20, 1965

## REFERENCES (Continued)

13. Levy, S., "Steam Slip-Theoretical Prediction from Momentum Model," Journal of Heat Transfer, Vol. 82, p. 113, May 1960
14. S. S. Kutateladze, "Fundamentals of Heat Transfer," Academic Press, Inc., New York, 1963
15. Lyon, R. N., Chem. Eng. Progr., 47, 75 (1951).
16. "Alkali Metals Boiling and Condensing Investigations," Quarterly Report No. 8, NASA-CR-54138, Contract NAS 3-2528, SPSS, MSD, General Electric Company, July 20, 1964
17. Bonilla, C. F., Wiener, M. M., Bilfinger, H., "Pool Boiling of Potassium," Oak Ridge National Laboratory, September 5, 1963
18. Bergles, A. E., Rohsenow, W. M., "The Determination of Forced Convection Surface Boiling," ASME Paper 63-HT-22
19. Griffith, P., and Wallis, J. D., "The Role of Surface Conditions in Nucleate Boiling," Chem. Eng. Progr. Symposium Series, No. 30, Vol. 56, 1960
20. Rohsenow, W. M., editor, "Developments in Heat Transfer," MIT Press, 1964
21. Gouse, S. W., Jr., Coumou, K. G., "Heat Transfer and Fluid Flow Inside a Horizontal Tube Evaporator," Report DSR 9649-1, Engineering Project Laboratory, Department of Mechanical Engineering, MIT, June 1964
22. Staub, F. W., and Zuber, N., "A Program of Two-Phase Flow Investigation," Second Quarterly Report, July-September 1963, EURAEC 866
23. Deem, H. W., Matolick, J., Jr., "The Thermal Conductivity and Electrical Resistivity of Liquid Potassium and the Alloy Niobium-1 Zirconium," BATT-4676-T6, prepared for NASA, Contract NAS-5-584, April 30, 1963

#### REFERENCES (Continued)

24. Engelbrecht, J.C., "Heat Transfer Coefficients in the Boiling and Condensation of Liquid Metals: Potassium and Rubidium," M. Sc. Thesis, Dept. of Chem. Eng., Columbia University, October 1961.
25. Jamieson, D.T., "Condensation Coefficient of Water," Advances in Thermophysical Properties at Extreme Temperatures and Pressures, ASME, 1965, pp. 230-236.

TABLE 1  
CRITICAL HEAT FLUX AND TRANSITION BOILING  
DATA FROM 300 KW PROJECT

<u>3/4-inch Nominal Diameter Tube with P/D = 6 Helical Insert (0.67-inch I.D.)</u>											
Date <u>1964</u>	Time	G <sub>K</sub>	T <sub>K</sub> o <sub>F</sub> c	T <sub>K</sub> o <sub>F</sub> TB	X <sub>c</sub>	X <sub>TB</sub>	q" c	h <sub>TB</sub>	q" <sub>TB</sub>	ΔT <sub>TB</sub>	4√a
10/10	2150	38.6	1686.2	1669.6	.758	.879	298,900	842	97,200	115	2.84
10/11	0230	40.5	1686.7	1664.2	.736	.868	395,000	743	101,000	136	2.87
10/12	0800	34.1	1603.7	1582.4	.759	.880	261,400	1215	129,800	107	2.88
10/12	1200	38.1	1615.2	1576.4	.801	.901	287,100	678	94,400	139	3.09
10/12	1220	38.0	1618.6	1590.7	.731	.866	302,600	1326	138,600	104	2.94
10/12	1240	37.0	1615.7	1587.1	.709	.855	277,500	1690	161,800	96	2.86
10/17	0400	44.7	1655.0	1621.1	.696	.848	446,200	989	152,200	154	3.01
<u>3/4-inch Nominal Diameter Tube with No Insert, Counter Flow (0.67-inch I.D.)</u>											
Date <u>1964</u>	Time	G <sub>K</sub>	T <sub>K</sub> o <sub>F</sub> c	T <sub>K</sub> o <sub>F</sub> TB	X <sub>c</sub>	X <sub>TB</sub>	q" c	h <sub>TB</sub>	q" <sub>TB</sub>	ΔT <sub>TB</sub>	4√a
10/29	1130	31.7	1694.8	1691.1	.533	.648	187,000	1736	100,250	58	1.0
10/30	1330	36.0	1688.9	1685.3	.602	.659	193,200	1612	105,600	66	1.0
10/31	0300	50.6	1690.9	1685.4	.540	.617	269,800	2136	159,700	75	1.0
11/1	0030	31.7	1556.3	1550.0	.670	.745	221,950	1259	98,200	78	1.0
11/1	1730	38.0	1569.4	1551.9	.562	.652	427,000	385	59,700	155	1.0
11/1	2100	32.5	1576.6	1566.2	.556	.641	275,900	565	55,700	98.5	1.0
11/1	2330	31.7	1562.0	1551.0	.557	.683	341,700	612	68,800	112	1.0
11/2	0100	32.4	1555.5	1545.4	.548	.671	244,900	884	93,700	106	1.0
11/2	0230	32.1	1553.4	1543.0	.632	.713	280,700	471	66,800	142	1.0
11/14	1830	47.9	1702.7	1695.0	.505	.616	274,100	1695	151,900	90	1.0
11/15	2100	73.0	1597.2	1570.6	.486	.532	355,100	1952	234,100	120	1.0
11/16	0700	100.6	1643.2	1600.6	.398	.444	428,600	2394	304,600	127	1.0
11/17	0215	32.6	1566.8	1563.9	.708	.736	221,000	1034	101,200	98	1.0
11/17	0345	32.6	1558.9	1547.7	.607	.693	370,600	292	52,000	178	1.0
11/17	0900	49.3	1563.0	1557.5	.549	.576	295,000	474	74,800	158	1.0
11/17	0905	49.3	1554.1	1539.6	.524	.586	360,800	462	84,400	183	1.0
11/18	0215	33.3	1705.0	1703.5	.617	.688	191,100	2305	144,500	63	1.0
11/18	1000	50.8	1630.7	1618.4	.500	.591	377,700	608	104,500	172	1.0

TABLE 1 (Continued)

CRITICAL HEAT FLUX AND TRANSITION BOILING  
DATA FROM 300 KW PROJECT

<u>3/4-inch Nominal Diameter Tube with No Insert, Cocurrent Flow</u>											
<u>Date</u> <u>1964</u>	<u>Time</u>	<u>G<sub>K</sub></u>	<u>T<sub>K<sub>c</sub></sub></u> <u>O<sub>F</sub></u>	<u>T<sub>K<sub>TTB</sub></sub></u> <u>O<sub>F</sub></u>	<u>X<sub>c</sub></u>	<u>X<sub>TTB</sub></u>	<u>q<sup>"</sup><sub>c</sub></u>	<u>h<sub>TTB</sub></u>	<u>q<sup>"</sup><sub>TTB</sub></u>	<u>ΔT<sub>TTB</sub></u>	<u>4√a</u>
11/5	0930	29.9	1573.4	1557.2	.686	.784	178,600	1428	89,600	63	1.0
11/5	1030	35.6	1558.5	1540.0	.559	.661	200,300	1115	94,300	85	1.0
11/6	0515	32.8	1677.1	1673.7	.703	.800	210,400	750	82,100	109	1.0
11/7	1130	49.8	1703.5	1697.9	.687	.731	219,600	1957	129,950	66	1.0
11/8	0530	34.4	1563.5	1545.2	.597	.749	269,400	749	102,600	137	1.0
11/10	0100	48.8	1584.1	1559.1	.585	.673	287,500	849	115,700	136	1.0
11/12	0300	52.5	1583.1	1559.9	.576	.647	235,300	2183	181,800	83	1.0



Table 2 Critical Heat Flux Data From 100 KW Project

Date	Recorder Chart	Test Section I.D. Inch	Insert	T <sub>sat</sub> °F	G lb/sec-ft <sup>2</sup>	q" Btu/Hr-Ft <sup>2</sup>	x <sub>c</sub> %	L/D	Symbols Used In Figures 16,17,18	4 √a
10/22/64	CHF1C	0.767	None	2100	15.5	152,000	67	36.5	○	1.0
10/22/64	CHF2	0.767	None	2100	16	151,000	65	36.5	○	1.0
10/22/64	CHF3B	0.767	None	2100	15.5	152,000	66	36.5	○	1.0
10/23/64	CHF4	0.767	None	2100	22	129,000	91	36.5	△	1.0
	CHF5	0.740	P/D = 6	2100	22	150,000	93	37.8	△	1.76
	CHF6	0.740	P/D = 6	2100	16	150,000	84	37.8	○	1.42
2/27/65	CHF7	0.423	None	2105	61.6	157,000	81	66.3	◆	1.0
2/28/65	CHF8	0.423	None	2102	61.7	224,000	74	66.3	◆	1.0
3/17/65	CHF9	0.423	None	2100	31	101,000	66	66.3	■	1.0
3/27/65	CHF10	0.423	None	1838	41.2	171,000	57	66.3	✕	1.0
3/31/65	CHF11A	0.423	None	2104	47.6	95,000	88	66.3	◆	1.0
	CHF11B	0.423	None	2104	47.6	94,000	85	35.5	◆	1.0
3/31/65	CHF12A	0.423	None	2105	47.6	50,000	89	66.3	◆	1.0
	CHF12B	0.423	None	2105	47.6	50,000	90	35.5	◆	1.0
	CHF12C	0.423	None	2105	47.6	53,000	89	35.5	◆	1.0
	CHF12D	0.423	None	2105	47.6	50,000	87	66.3	◆	1.0
4/ 1/65	CHF13A	0.423	None	2105	46.7	211,000	59	66.3	◆	1.0
4/ 1/65	CHF13B	0.423	None	2106	46.5	214,000	61	66.3	◆	1.0

Table 3  
Film Boiling and Superheat Data - 100 KW Loop

Date	Test Section I.D. Inch	Insert	T <sub>sat</sub> °F	G lb/sec-ft <sup>2</sup>	q" Btu/hr-ft <sup>2</sup>	X <sub>FB</sub> %	h <sub>FB</sub> Btu/hr-ft <sup>2</sup> °F	h <sub>SH</sub> Btu/hr-ft <sup>2</sup> °F	(ΔT) <sub>SH</sub> °F
2/27/65	0.423	None	2105	61.6	157,000	87			
3/27/65	0.423	None	1838	41.2	171,000	57*			
3/31/65	0.423	None	2104	47.6	94,000	96	258		
3/31/65	0.423	None	2105	47.6	49,900	96	228		
	0.423	None	2105	47.6	49,900	95 - 99			
	0.423	None	2105	47.6	52,000	98 - 96			
	0.423	None	2105	47.6	53,000	95			
4/1/65	0.423	None	2105	46.7	211,000	59*			
4/1/65	0.423	None	2106	46.5	214,000	61*			
3/31/65	0.423	None	2105	47.6	49,900		194		25

\*X<sub>FB</sub> = X<sub>c</sub>  
 = Quality at which stable film boiling was established  
 X<sub>FB</sub> = Film Boiling Heat Transfer Coefficient  
 h<sub>FB</sub> = Superheated vapor heat transfer coefficient  
 h<sub>SH</sub> = Degrees of superheat (°F)  
 (ΔT)<sub>SH</sub>

# NOMENCLATURE FOR TABLE 4

<u>Symbol</u>	<u>Quantity</u>	<u>Units</u>
$\tau^*_{VT}$	Vapor shear stress at upper station	Dimensionless
$\tau^*_{VB}$	Vapor shear stress at bottom station	Dimensionless
$h_{VT}$	Vapor phase experimental heat transfer coefficient at upper station	Btu/hr-ft <sup>2</sup> °R
$h_{VB}$	Vapor phase experimental heat transfer coefficient at bottom station	Btu/hr-ft <sup>2</sup> °R
$\bar{h}_T$	Vapor phase theoretical heat transfer coefficient for $\sigma_c = \sigma_e = 1$ (upper station)	Btu/hr-ft <sup>2</sup> °R
$\sigma_{TE}$	Experimental condensation coefficient at upper station	Dimensionless
$\bar{h}_B$	Vapor phase theoretical heat transfer coefficient for $\sigma_c = \sigma_e = 1$ (bottom station)	Btu/hr-ft <sup>2</sup> °R
$\sigma_{BE}$	Experimental condensation coefficient at bottom station	Dimensionless

Table 4. Vapor Phase Heat Transfer Coefficients - 50 KW Project \*

A. Tubular Insert (Test Set No.5)

Run No.	$\gamma_{VT}^*$	$\gamma_{VB}^*$	$h_{VT}$	$h_{VB}$	$\bar{h}_T$	$\sigma_{TE}$	$\bar{h}_B$	$\sigma_{BE}$
1	7.1252+1	4.1314+0	2.0318+4	2.4445+4	7.0446+4	2.8842-1	7.2420+4	3.3755-1
2	5.4938+1	3.2319+0	2.0416+4	2.7149+4	8.6295+4	2.3659-1	8.7600+4	3.0992-1
3	3.3665+1	2.0042+0	2.5323+4	2.8226+4	1.1150+5	2.2710-1	1.1205+5	2.5191-1
4	2.1124+1	1.2640+0	3.8989+4	2.6678+4	1.4832+5	2.6287-1	1.4832+5	1.7987-1
5	6.2961+1	3.7079+0	2.0480+4	2.4701+4	1.4527+5	1.4098-1	1.4710+5	1.6792-1
6	8.9404+1	5.2055+0	1.9907+4	3.3584+4	1.1423+5	1.7427-1	1.1695+5	2.8715-1
7	1.4068+2	7.9103+0	1.9465+4	2.3404+4	8.4990+4	2.2903-1	8.9900+4	2.6033-1
8	1.7046+2	9.3146+0	1.8680+4	2.3457+4	7.0800+4	2.6385-1	7.6875+4	3.0513-1
9	2.2680+2	1.1896+1	1.8780+4	2.3795+4	7.0446+4	2.6659-1	7.9335+4	2.9993-1
10	1.7126+2	9.4385+0	1.8475+4	2.5060+4	8.7600+4	2.1090-1	9.4040+4	2.6648-1
11	1.3034+2	7.4741+0	2.2685+4	2.4741+4	1.1205+5	2.0245-1	1.1641+5	2.1253-1
12	7.1363+1	4.2273+0	2.6523+4	2.5357+4	1.7776+5	1.4921-1	1.7913+5	1.4156-1
13	4.1504+1	2.4727+0	3.1596+4	2.0627+4	2.6082+5	1.2114-1	2.6170+5	7.8820-2
14	5.1184+1	3.0493+0	3.0774+4	2.3293+4	2.5907+5	1.1878-1	2.5995+5	8.9605-2
15	9.5323+1	5.6220+0	2.3254+4	2.4118+4	1.8200+5	1.2777-1	1.8425+5	1.3090-1
16	1.4334+2	8.2705+0	1.9244+4	2.2857+4	1.3666+5	1.4082-1	1.4100+5	1.6210-1
17	1.7592+2	9.9284+0	1.6556+4	2.0862+4	1.1695+5	1.4156-1	1.2305+5	1.6954-1
18	3.1121+2	1.6345+1	1.8982+4	2.3448+4	1.0415+5	1.8225-1	1.1695+5	2.0049-1
19	2.1907+2	1.2370+1	2.1334+4	2.6040+4	1.4283+5	1.4936-1	1.4954+5	1.7413-1
20	1.7339+2	1.0095+1	2.2491+4	2.8590+4	1.7296+5	1.3003-1	1.7707+5	1.6146-1
21	9.8530+1	5.8480+0	2.4872+4	2.4754+4	2.5120+5	9.9013-2	2.5295+5	9.7862-2
22	1.4463+2	8.5816+0	2.3861+4	2.2567+4	2.5645+5	9.3045-2	2.5820+5	8.7403-2
23	2.4619+2	1.4163+1	2.4903+4	2.1989+4	1.7844+5	1.3956-1	1.8425+5	1.1934-1
24	2.6046+2	1.4185+1	2.3178+4	2.5187+4	1.7022+5	1.3616-1	1.8425+5	1.3670-1
25	3.2362+2	1.7904+1	1.8716+4	2.0455+4	1.4283+5	1.3103-1	1.5198+5	1.3459-1
26	4.2129+2	2.4439+1	1.9030+4	2.1812+4	1.1150+5	1.7066-1	1.1477+5	1.9004-1
27	4.3456+2	2.3993+1	2.2025+4	2.7694+4	1.4710+5	1.4973-1	1.5728+5	1.7608-1
28	3.6049+2	2.0528+1	2.1646+4	2.9587+4	1.7707+5	1.2224-1	1.8425+5	1.6058-1
29	2.0323+2	1.1956+1	2.2912+4	2.3023+4	2.6620+5	8.6072-2	2.6980+5	8.5335-2
30	2.7589+2	1.6017+1	1.8386+4	3.0092+4	2.6350+5	6.9774-2	2.6980+5	1.1153-1
31	4.7393+2	2.5644+1	1.8023+4	3.5614+4	1.7228+5	1.0461-1	1.8725+5	1.9020-1
32	5.9595+2	3.3890+1	2.6003+4	5.2001+4	1.6817+5	1.5463-1	1.7570+5	2.9595-1
33	6.0164+2	3.6916+1	2.0772+4	3.3257+4	1.5388+5	1.3499-1	1.5076+5	2.2060-1
34	7.4718+2	1.1333+2	1.9755+4	3.5948+3	1.2194+5	1.6201-1	5.4513+4	6.5943-2
35	7.6286+2	1.1036+2	1.8196+4	3.7926+3	9.4500+4	1.9255-1	4.3988+4	8.6220-2
36	9.2937+2	2.7962+2	1.7400+4	1.1917+3	6.6906+4	2.6006-1	1.6486+4	7.2283-2
37	3.6289+2	1.8519+1	1.8061+4	1.4942+4	9.0360+4	1.9988-1	1.0366+5	1.4415-1

Table 4. Vapor Phase Heat Transfer Coefficients - 50 KW Project (Continued)

## B. Helical Insert (Test Set No. 4)

Run No.	$T_{VT}^*$	$T_{VB}^*$	$h_{VT}$	$h_{VB}$	$\bar{h}_T$	$\sigma_{TE}$	$\bar{h}_B$	$\sigma_{BE}$
1	4.6371+1	2.8072+0	3.9153+4	1.5031+4	1.0464+5	3.7417-1	1.0366+5	1.4500-1
2	2.6963+1	1.6219+0	2.8877+4	1.2811+4	1.4161+5	2.0392-1	1.4100+5	9.0855-2
3	1.4483+2	8.8129+0	1.0818+5	1.6769+4	8.9900+4	1.2033+0	8.8520+4	1.8944-1
4	9.1672+1	5.5414+0	3.8207+4	2.2287+4	1.2527+5	3.0500-1	1.2416+5	1.7950-1
5	5.4022+1	3.2479+0	2.4980+4	2.3201+4	1.7296+5	1.4442-1	1.7228+5	1.3467-1
6	2.4144+1	1.4505+0	2.8548+4	1.8887+4	2.5645+5	1.1132-1	2.5557+5	7.3900-2
7	5.5621+1	3.3426+0	3.0249+4	2.0498+4	2.4945+5	1.2126-1	2.4857+5	8.2463-2
8	1.1716+2	7.0469+0	3.6672+4	2.2187+4	1.6340+5	2.2443-1	1.6272+5	1.3635-1
9	2.0038+2	1.2320+1	6.2533+4	2.1587+4	1.1641+5	5.3718-1	1.1368+5	1.8988-1
10	3.3459+2	2.4797+1	1.6203+5	2.4912+4	6.7968+4	2.3839+0	5.6820+4	4.3844-1
11	2.2221+2	1.4213+1	1.3012+5	2.2537+4	8.4990+4	1.5310+0	8.0205+4	2.8100-1
12	1.4494+2	8.8542+0	6.2098+4	2.5725+4	1.1423+5	5.4362-1	1.1205+5	2.2959-1
13	1.9226+2	1.1895+1	6.9080+4	2.4735+4	1.1805+5	5.8515-1	1.1477+5	2.1551-1
14	2.3216+2	1.5158+1	5.4198+4	2.6228+4	1.1314+5	4.7903-1	1.0464+5	2.5065-1
15	2.1629+2	1.4140+1	3.8593+4	3.0462+4	1.4466+5	2.6678-1	1.3418+5	2.2702-1
16	1.7590+2	1.0996+1	3.4686+4	3.1711+5	1.7091+5	2.0295-1	1.6476+5	1.9247-1
17	8.3589+1	5.0468+0	3.6478+4	3.5571+4	2.6350+5	1.3844-1	2.6170+5	1.3592-1
18	1.4370+2	8.7540+0	3.1911+4	3.5043+4	2.6170+5	1.2194-1	2.5820+5	1.3572-1
19	2.6196+2	1.7371+1	3.2685+4	2.9706+4	1.7091+5	1.9124-1	1.5660+5	1.8969-1
20	3.4740+2	2.5329+1	3.4935+4	2.5131+4	1.3604+5	2.5680-1	1.1477+5	2.1896-1
21	5.0251+2	6.0197+1	2.7452+4	2.4918+4	1.0170+5	2.6993-1	5.5831+4	4.4630-1
22	4.9724+2	5.0461+1	2.7032+4	4.2861+4	1.3480+5	2.0053-1	8.4990+4	5.0431-1
23	3.5891+2	2.6135+1	3.2375+4	6.4982+4	1.6885+5	1.9173-1	1.4344+5	4.5303-1
24	2.3266+2	1.4898+1	3.1505+4	1.8261+5	2.5470+5	1.2369-1	2.4080+5	7.5834-1
25	2.9009+2	1.9097+1	2.6758+4	1.5491+5	2.5032+5	1.0689-1	2.3145+5	6.6930-1
26	4.7873+2	4.0047+1	3.1494+4	6.1126+4	1.6544+5	1.9037-1	1.2471+5	4.9013-1
27	6.2971+2	6.9797+1	3.0836+4	3.6445+4	1.6612+5	1.8562-1	9.7780+4	3.7273-1
28	3.3729+2	2.2778+1	3.0304+4	2.0633+6	2.5207+5	1.2022-1	2.2805+5	9.0477+0
29	4.3028+2	3.2476+1	2.6935+4	8.3685+4	2.3655+5	1.1387-1	1.9550+5	4.2806-1
30	1.1364+2	7.5011+0	7.6701+4	6.7226+4	8.8520+4	8.6648-1	8.1075+4	8.2918-1
31	1.7027+2	1.1069+1	2.4208+5	9.7863+4	6.9738+4	3.4713+0	6.5136+4	1.5024+0
32	6.8991+2	4.3299+1	1.0756+5	7.3786+4	6.4782+4	1.6603+0	6.2340+4	1.1836+0
33	3.7086+2	2.2703+1	3.3434+4	4.8069+4	9.0360+4	3.7001-1	8.8520+4	5.4303-1

Table 5. Comparison of Experimental Data and Correlation  
- 50 KW Project

A. Tubular Insert (Test Set No. 5)  $\sigma_e = \sigma_c = 0.19$

<u>Run No.</u>	<u>% Error at Top Position</u>	<u>% Error at Bottom Position</u>
1	-48	-48
2	-22	-36
3	-17	-18
4	-31	- 3
5	23	6
6	8	-24
7	-19	-21
8	-36	-36
9	-38	-33
10	-10	-22
11	- 6	- 6
12	18	13
13	29	32
14	30	26
15	29	15
16	24	8
17	24	6
18	4	- 3
19	19	4
20	28	6
21	41	22
22	44	24
23	24	18
24	25	12
25	29	15
26	9	0
27	19	3
28	32	6
29	48	23
30	56	14
31	42	0
32	17	-14
33	27	- 6
34	14	59
35	- 1	50
36	-35	61
37	- 5	15

Table 5. Comparison of Experimental Data and Correlation  
- 50 KW Project (Continued)

B. Helical Insert (Test Set No. 4)  $\sigma_e = \sigma_c = 0.19$

<u>Run No.</u>	<u>% Error at Top Position</u>	<u>% Error at Bottom Position</u>
1	84	70
2	85	73
3	69	66
4	84	57
5	86	54
6	81	59
7	81	53
8	83	52
9	79	55
10	65	59
11	67	58
12	78	53
13	77	52
14	81	51
15	85	44
16	84	41
17	78	36
18	82	34
19	86	42
20	87	49
21	92	58
22	91	40
23	86	24
24	83	8
25	85	10
26	88	27
27	88	40
28	84	1
29	86	17
30	76	33
31	52	27
32	88	53
33	94	59

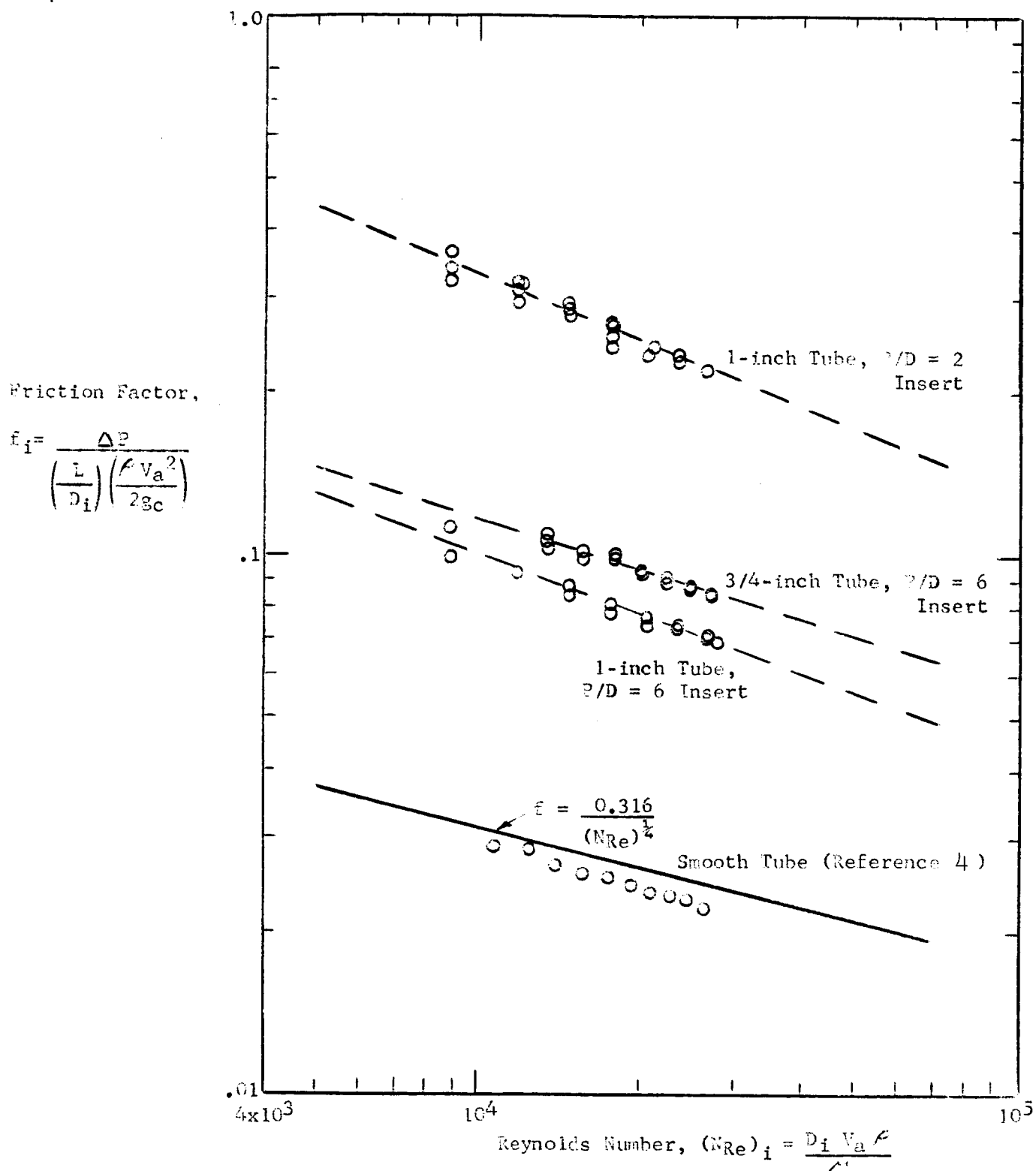


Figure 1 Experimental Single Phase Friction Factors for Water Flowing in Straight Tubes Containing Helical Inserts (300 KW Project)



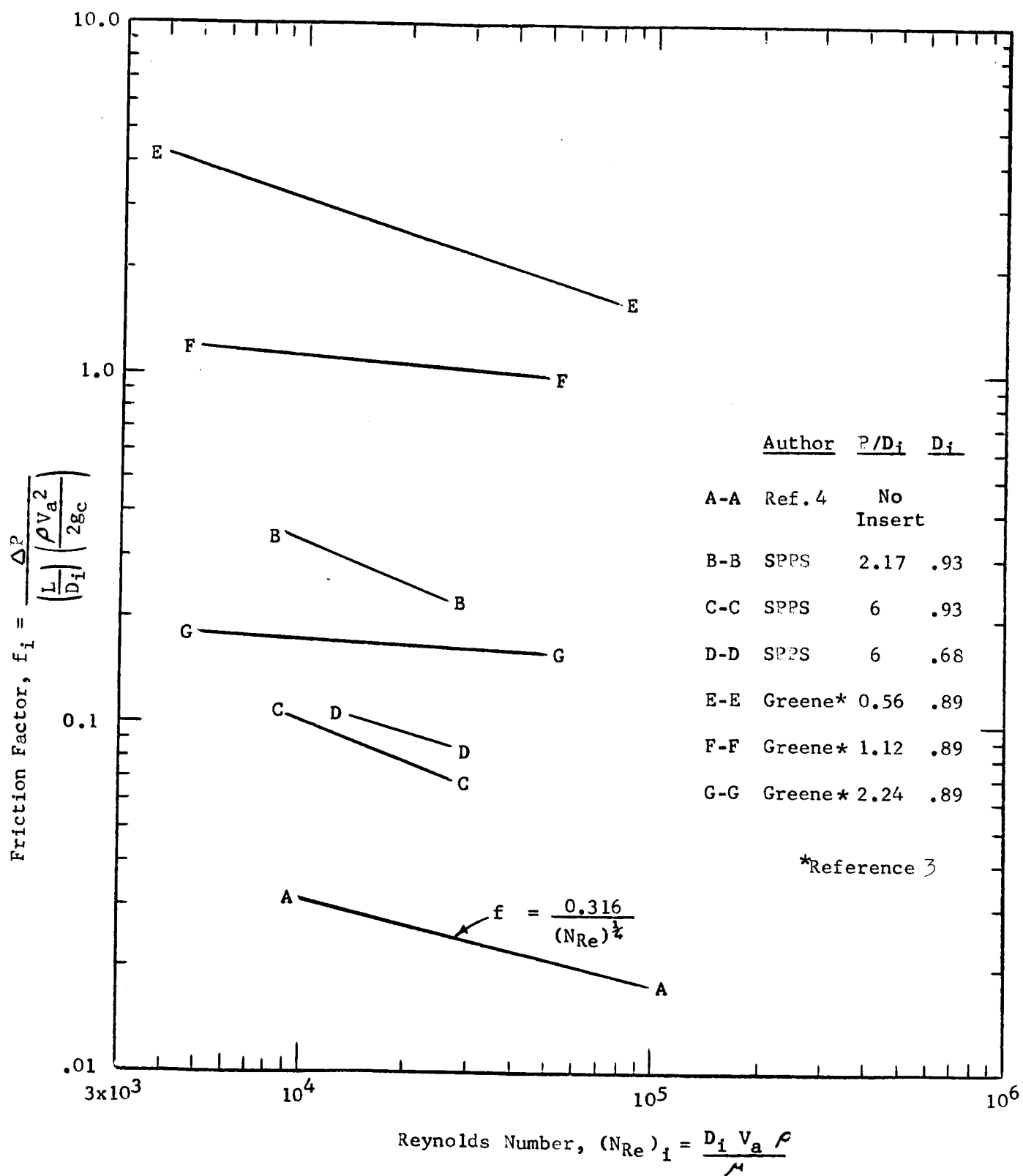


Figure 2 Summary of Single Phase Friction Factor Measurements from the Literature for Water Flowing in Straight Tubes Containing Helical Inserts

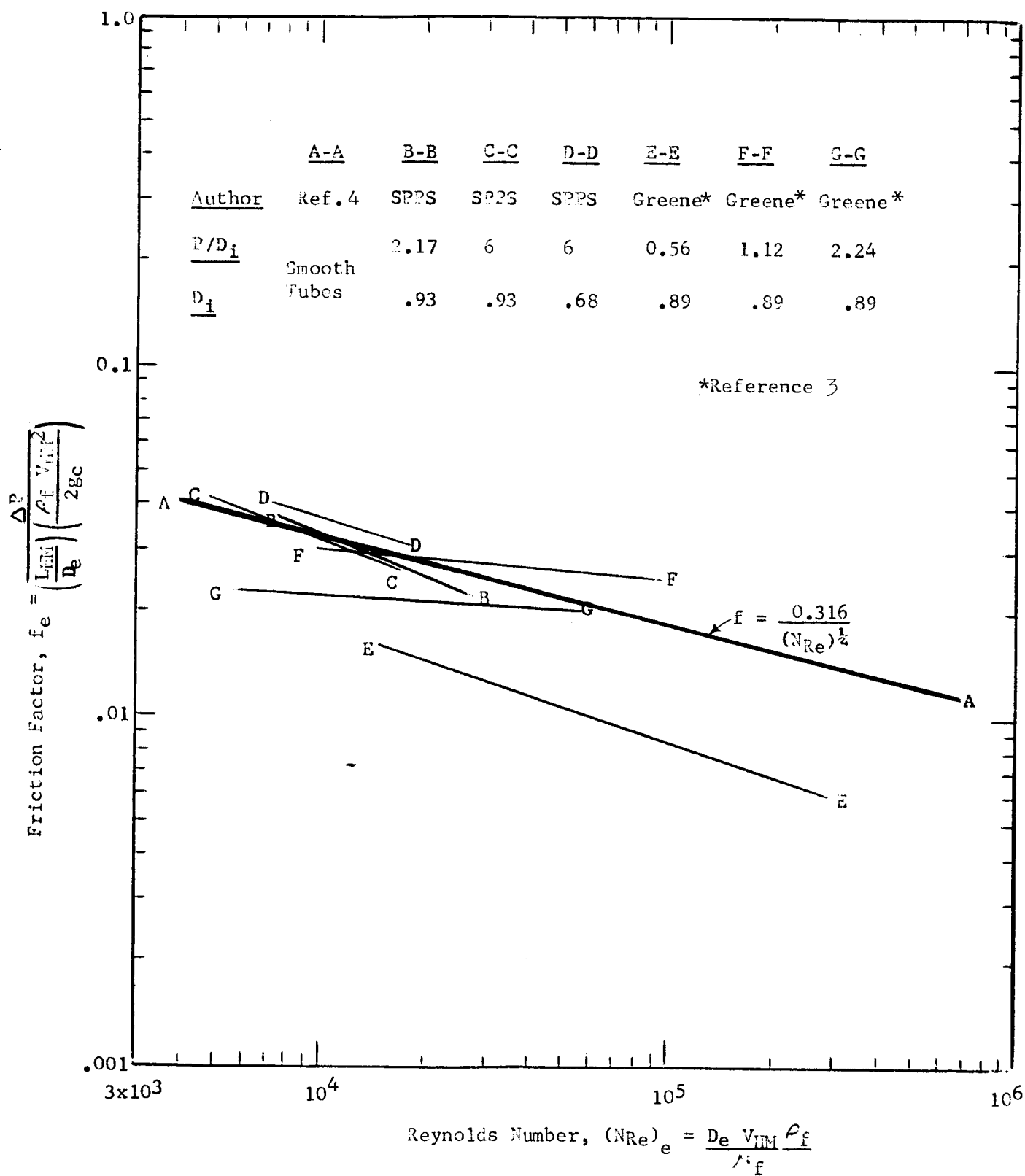


Figure 3 Relation of Helical Flow Friction Factors to the Helical Flow Reynolds Number

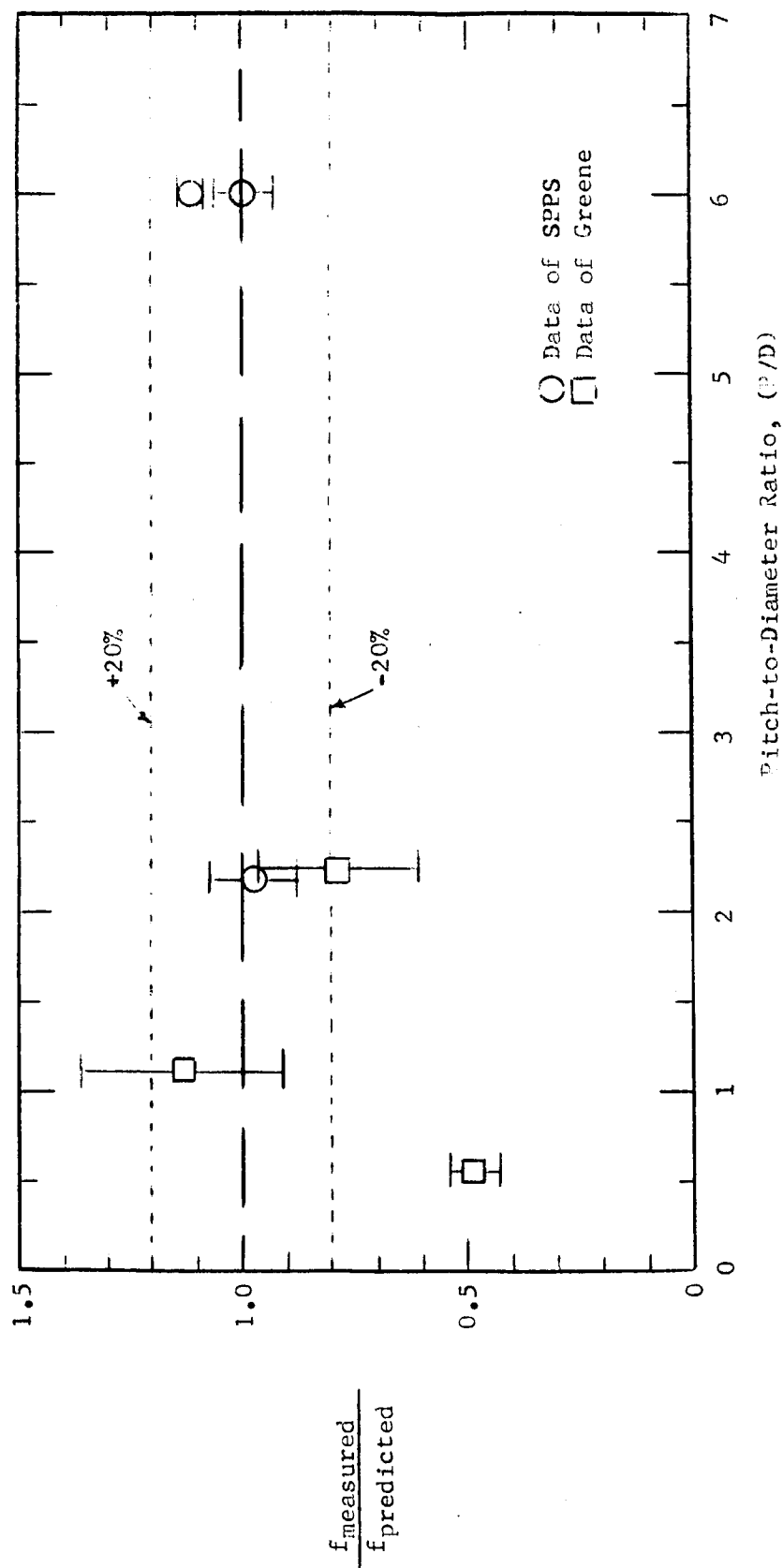


Figure 4 Comparison of Predicted and Measured Helical Single Phase Helical Flow Friction Factors

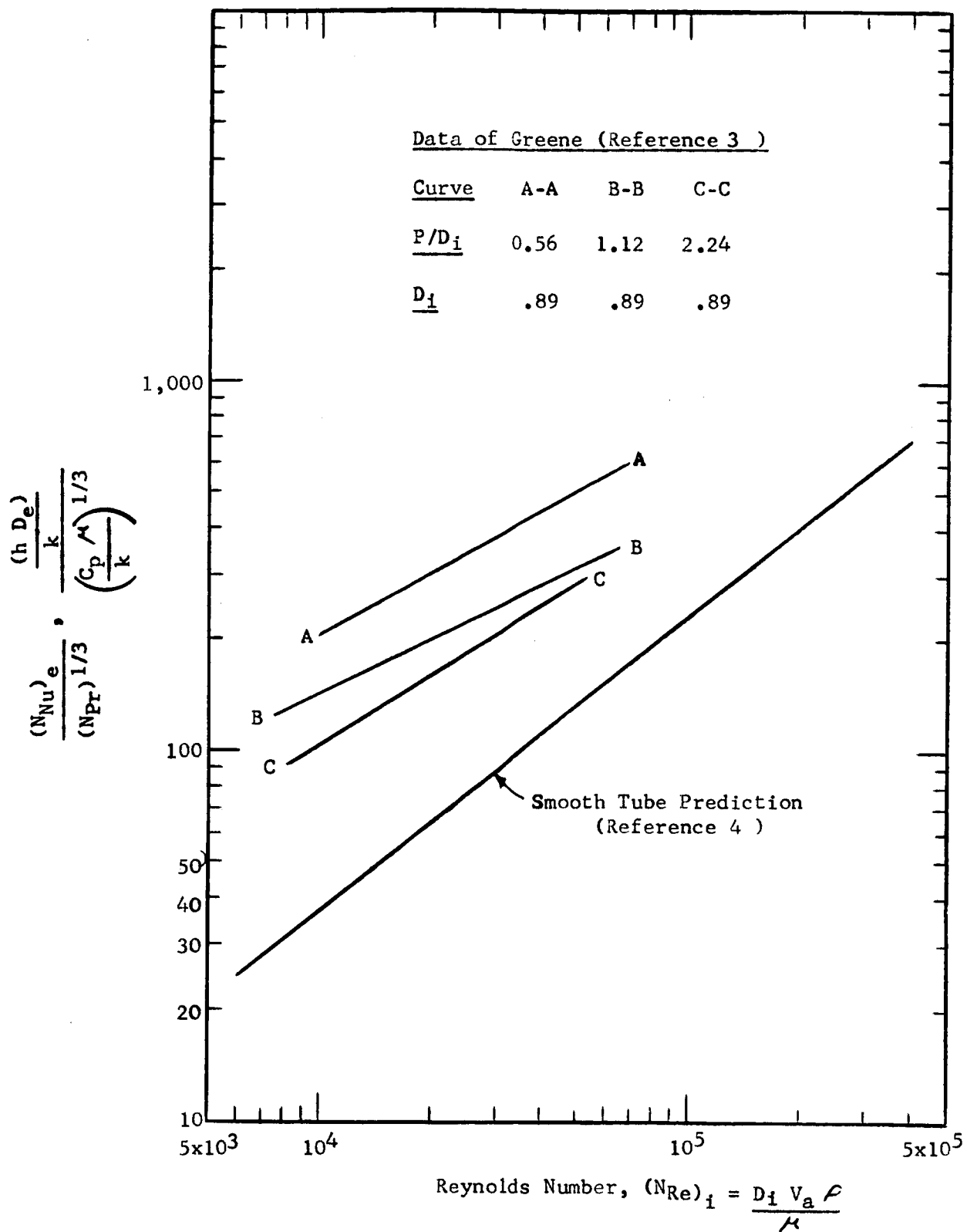


Figure 5 Summary of Heat Transfer Measurements for Water Flowing in Straight Tubes Containing Helical Inserts

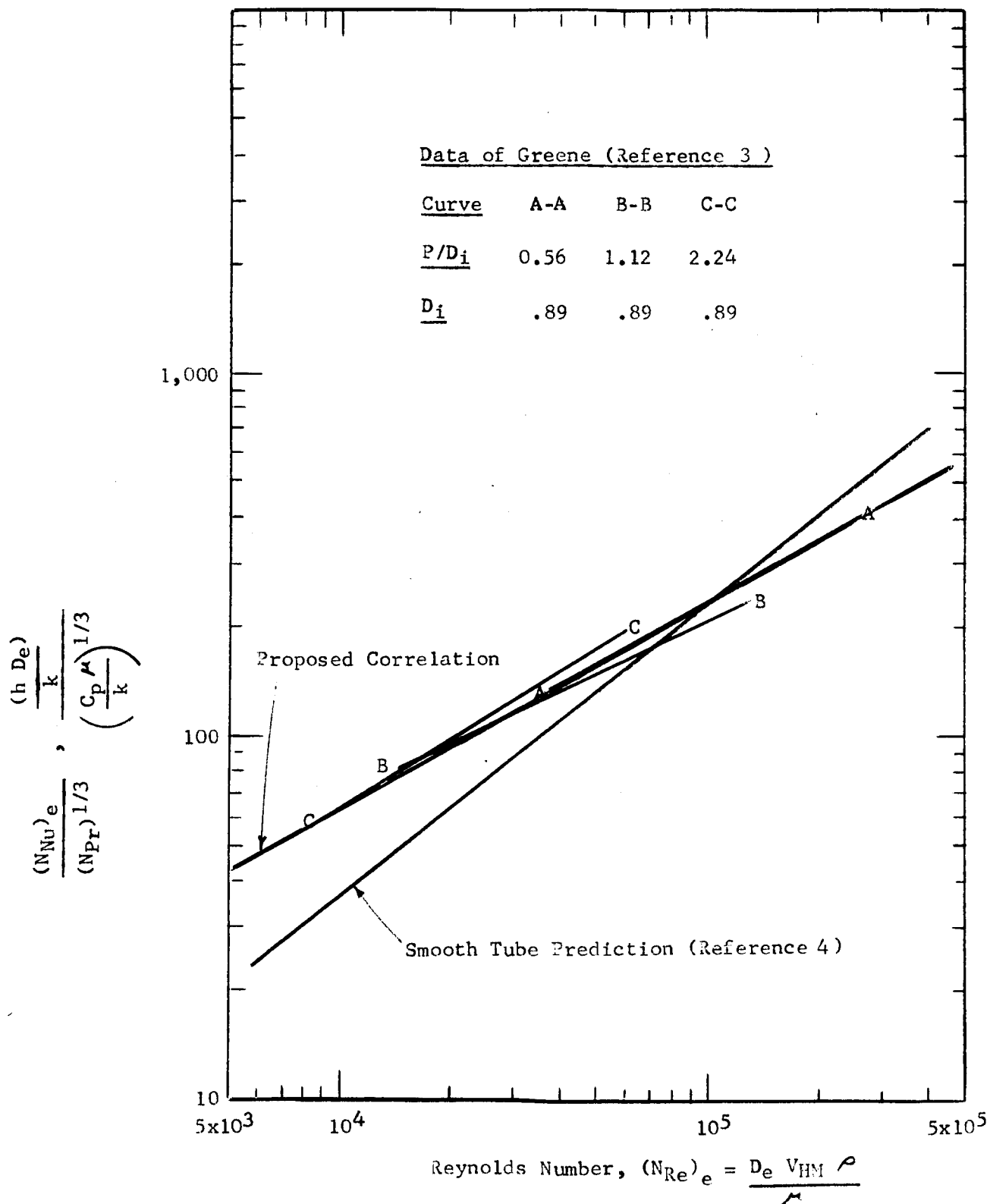


Figure 6 Correlation of Helical Flow Single Phase Heat Transfer Data

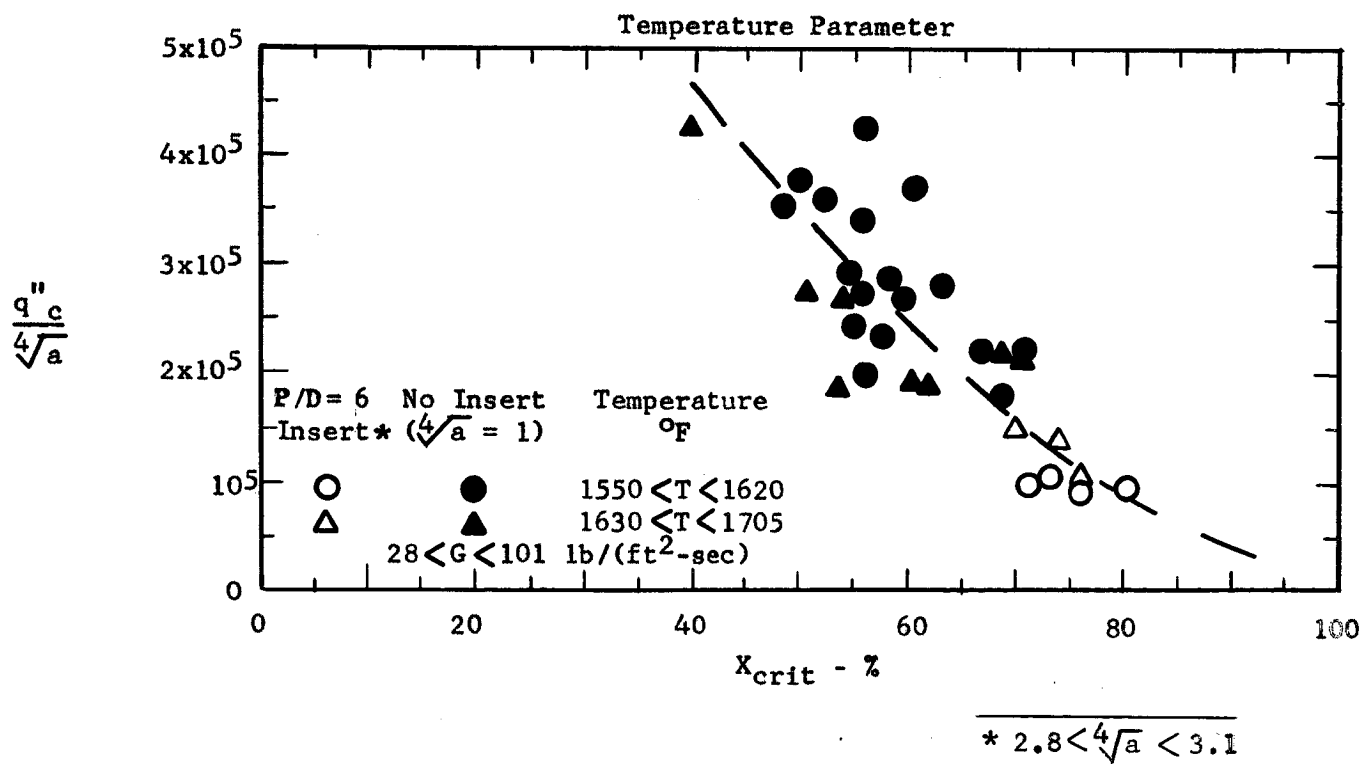
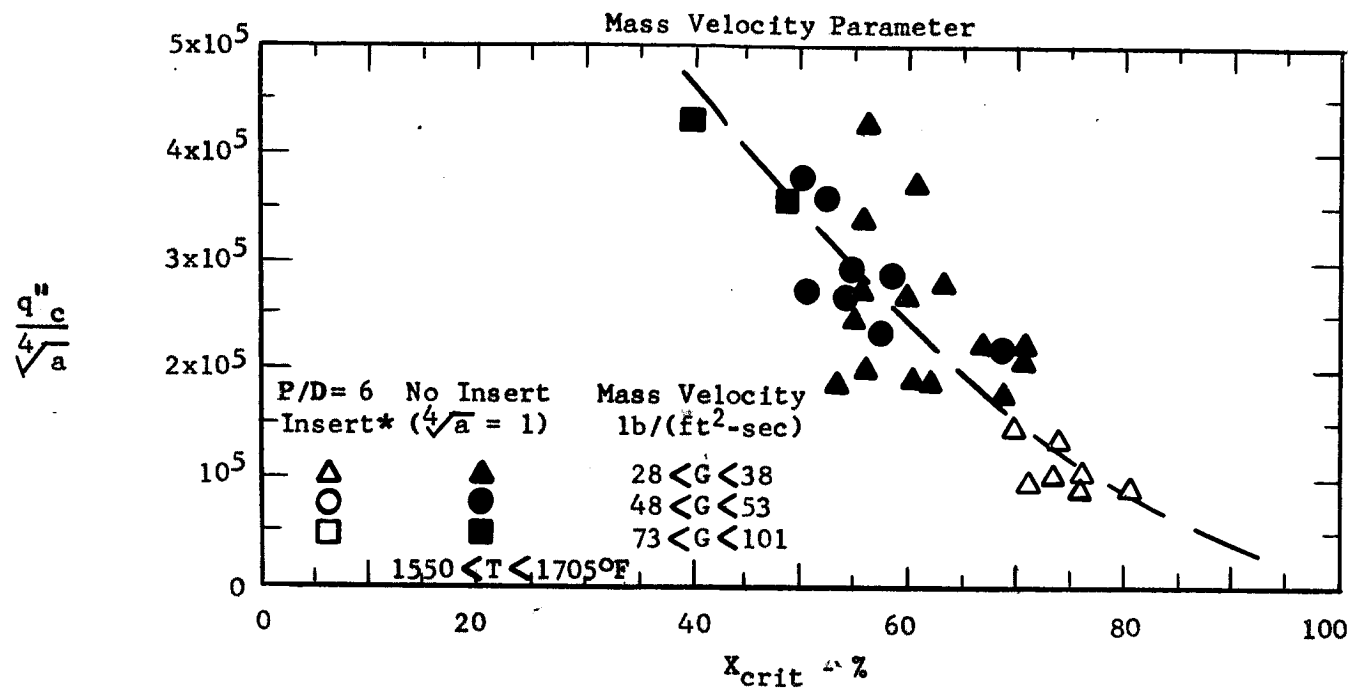


Figure 7 Critical Heat Flux Data Obtained in a 0.67-inch I.D. Tube (300 KW Facility)

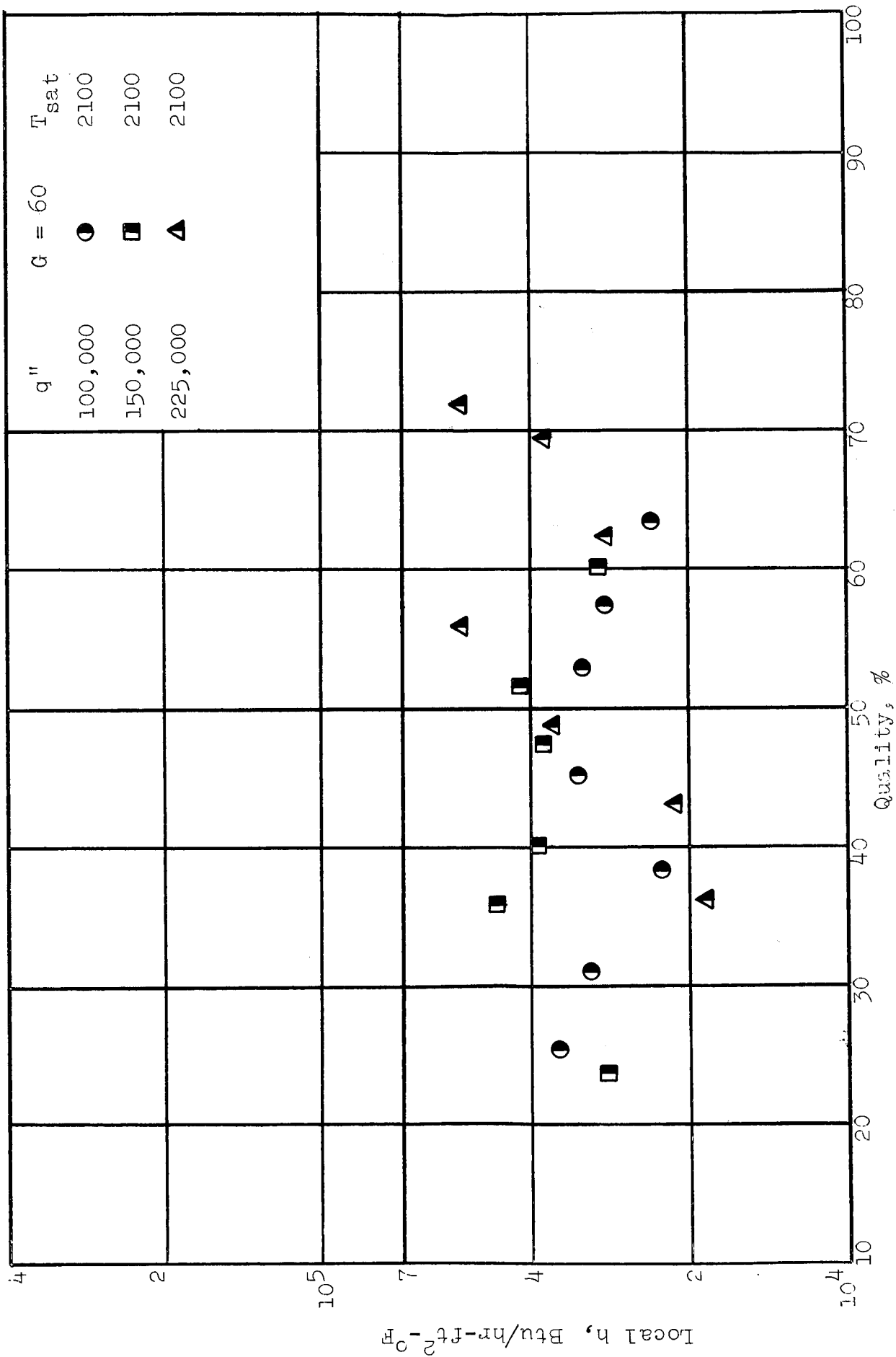


Figure 8a. Nucleate Boiling Results, 100 KW Loop  
(Test Section I.D. = 0.423 in., No Insert)  
 $T_{sat} = 2100^{\circ}F$ ,  $G = 60$  lbs/sec-ft<sup>2</sup>

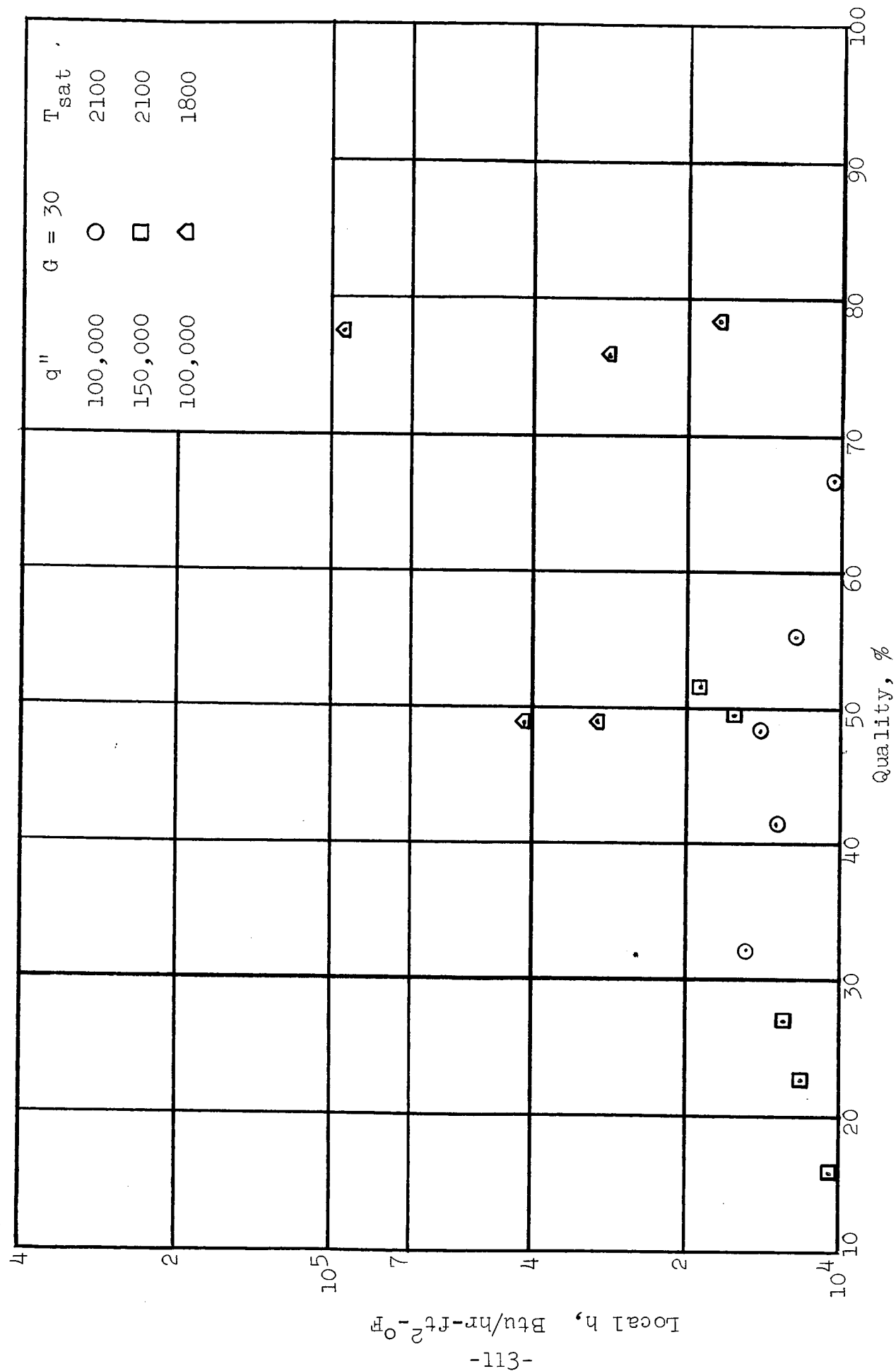


Figure 8b. Nucleate Boiling Results, 100 KW Loop  
(Test Section I.D. = 0.423 in., No Insert)  
 $T_{sat} = 1800^{\circ}\text{F}$  and  $2100^{\circ}\text{F}$ ,  $G = 30$  lbs/sec-ft<sup>2</sup>



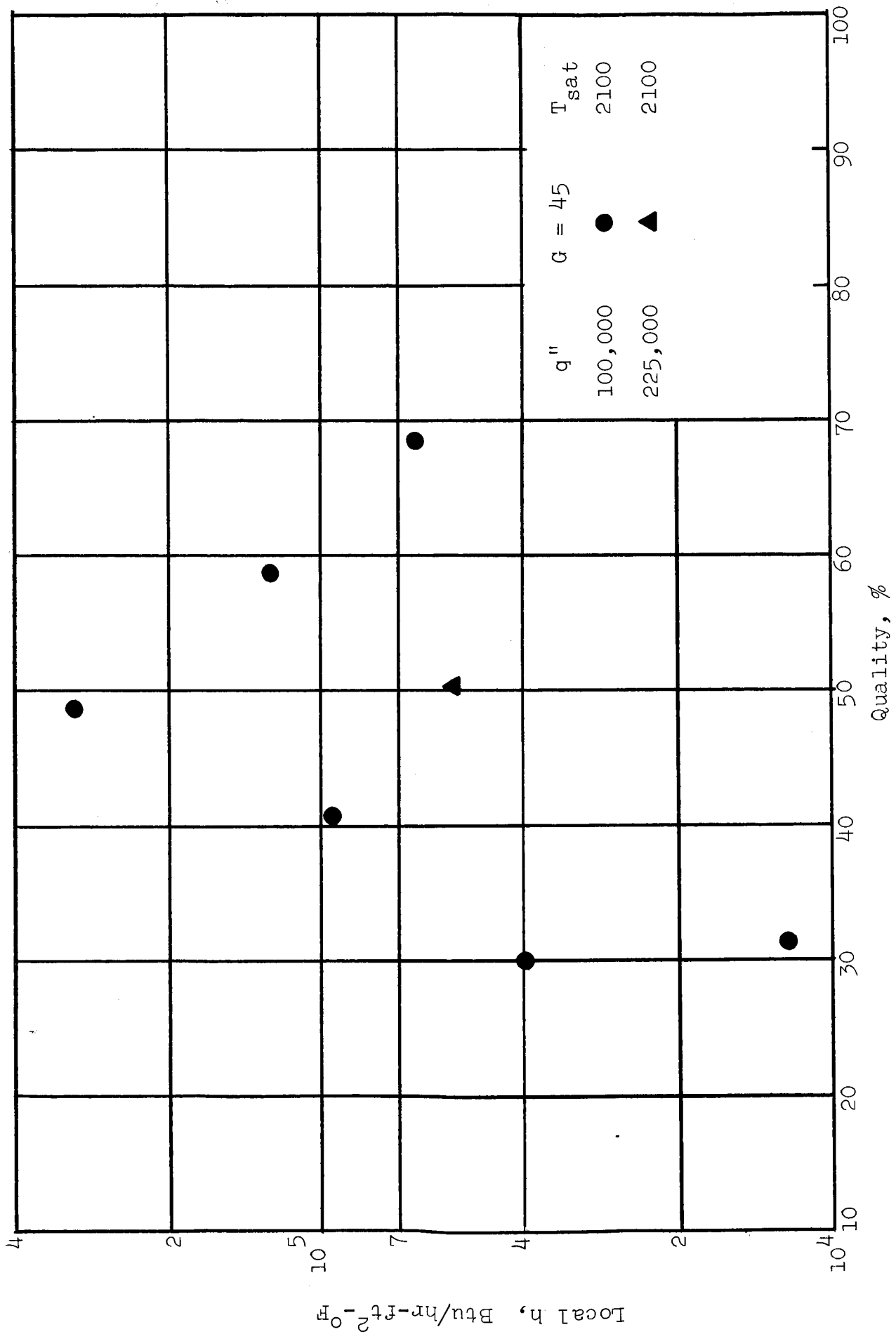


Figure 8c, Nucleate Boiling Results, 100 KW Loop  
 (Test Section I.D. = 0.423 in., No Insert)  
 $T_{sat} = 2100^{\circ}F$ ,  $G = 45$  lbs/sec-ft²

# Segment 1

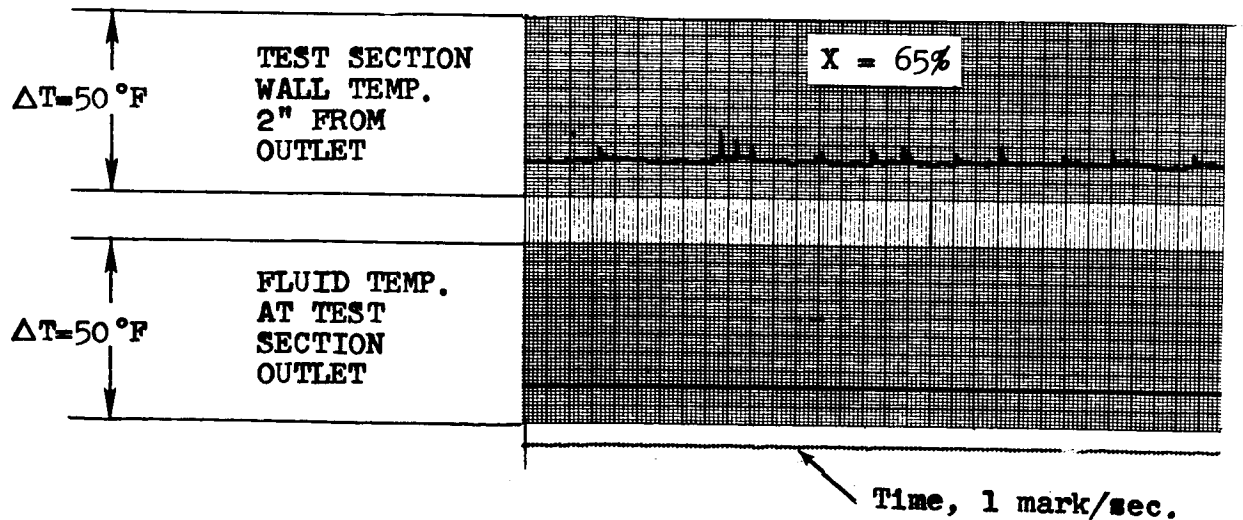
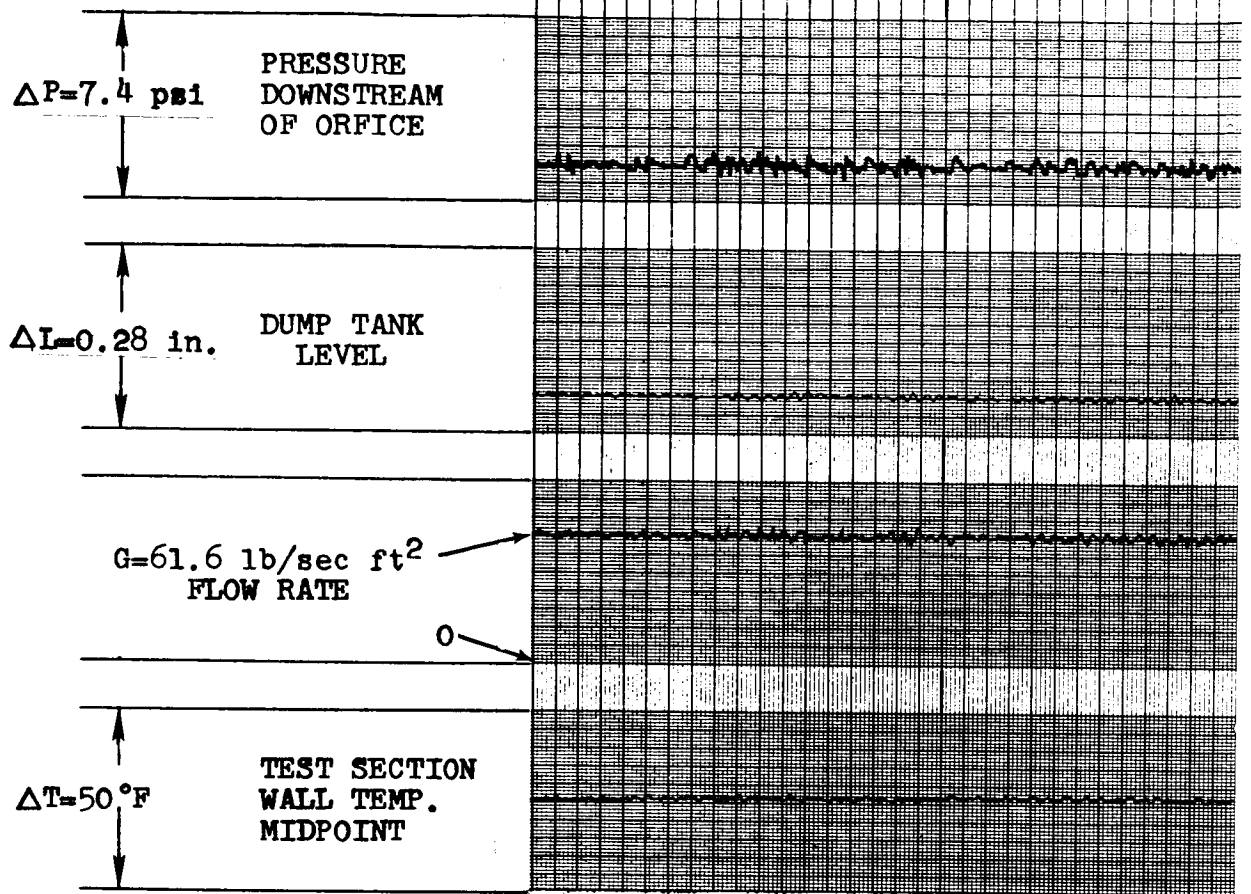
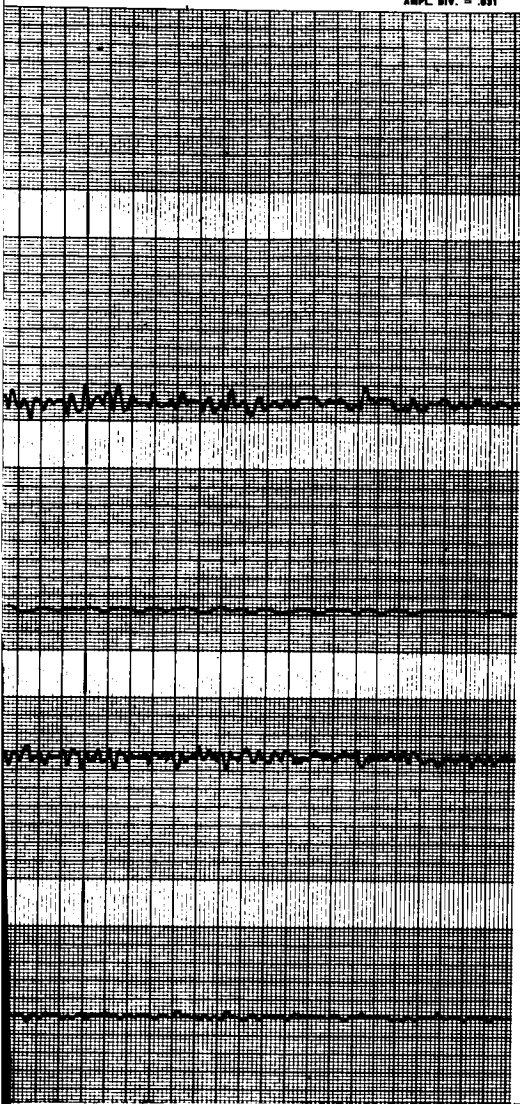


Figure 9. Recorder Chart Showing the Flux and Film Boiling Cond

AMPL. DIV. = .031



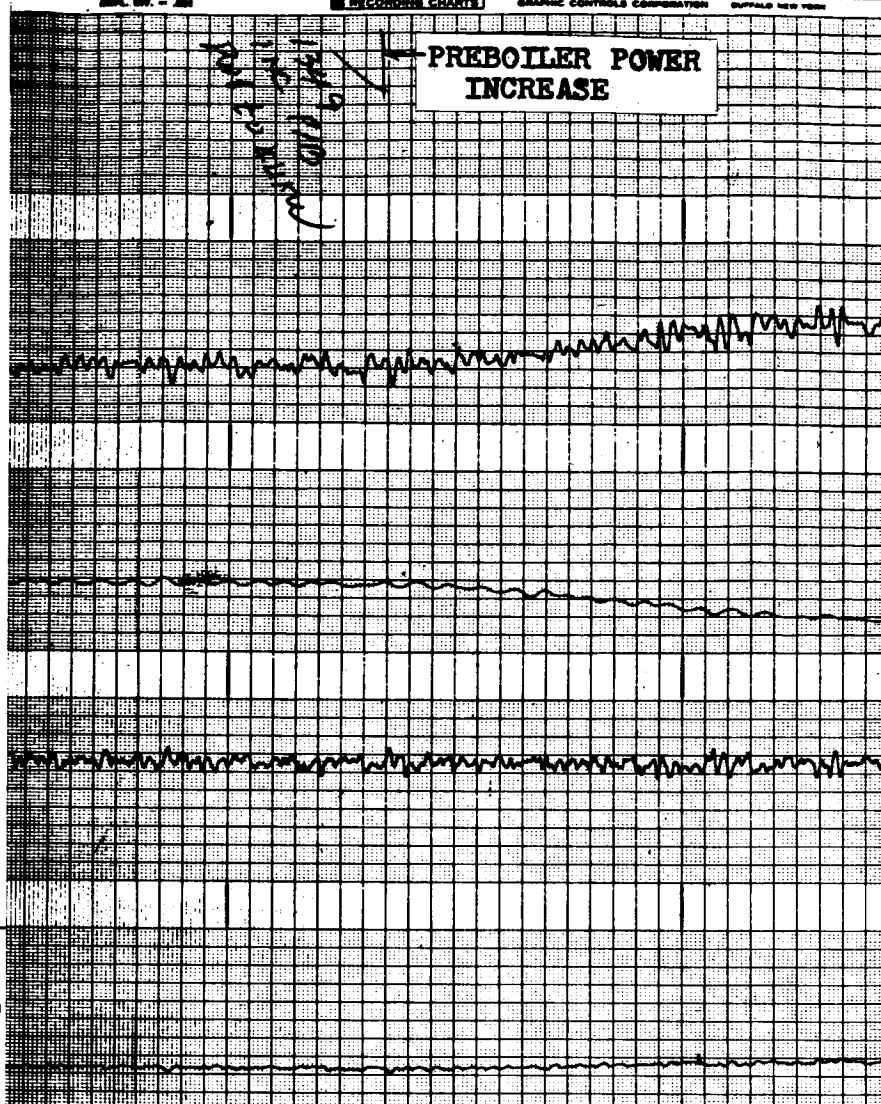
$\Delta T = 100^{\circ}F$

AMPL. DIV. = .031

RECORDING CHART

GRAPHIC CONTROLS CORPORATION

BUFFALO NEW YORK

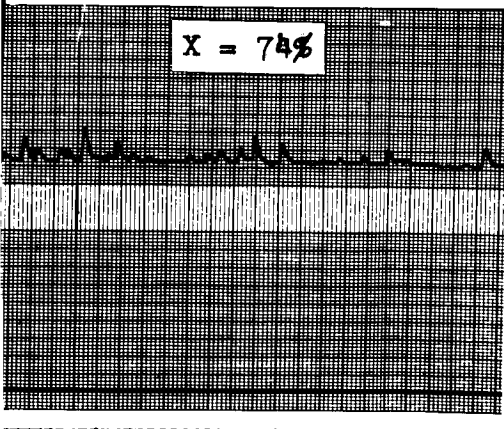


PREBOILER POWER INCREASE

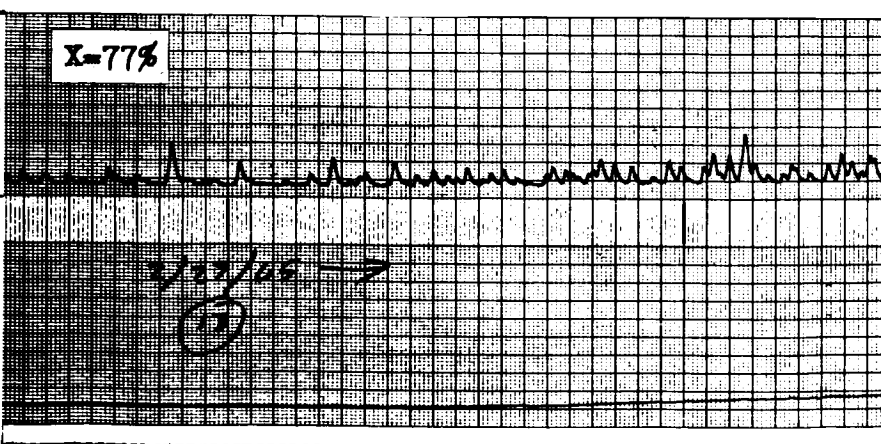
1/27/65  
100 KW

$\Delta T = 100^{\circ}F$

X = 74%

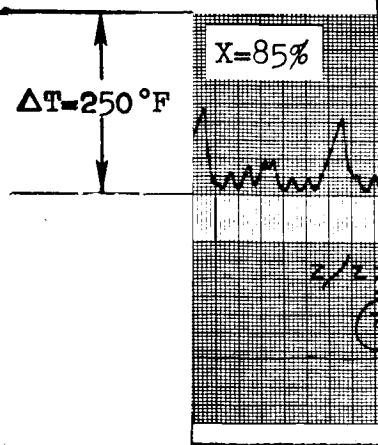
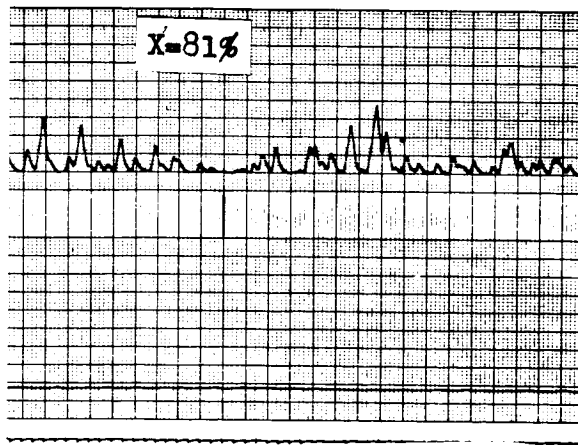
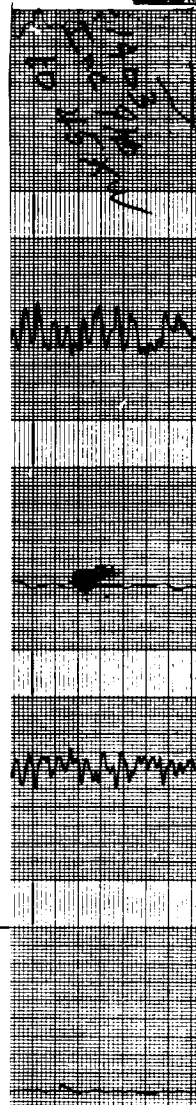
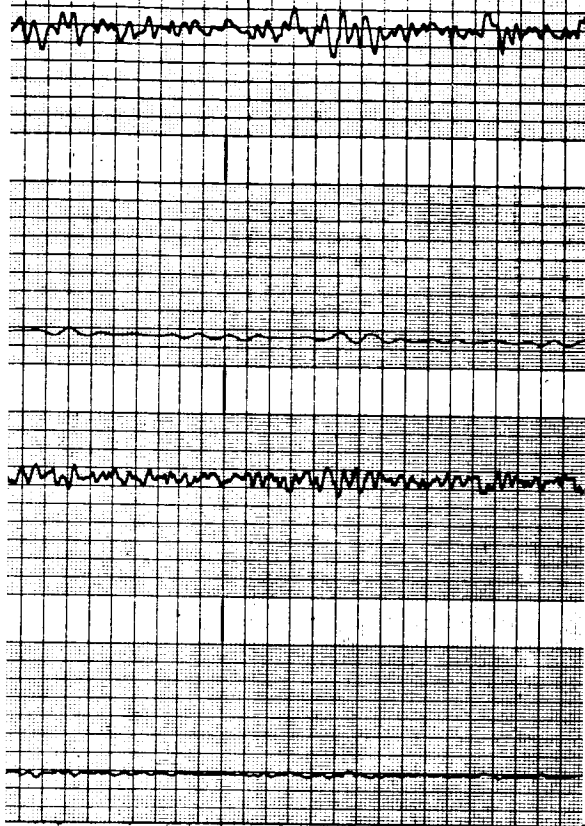


X=77%



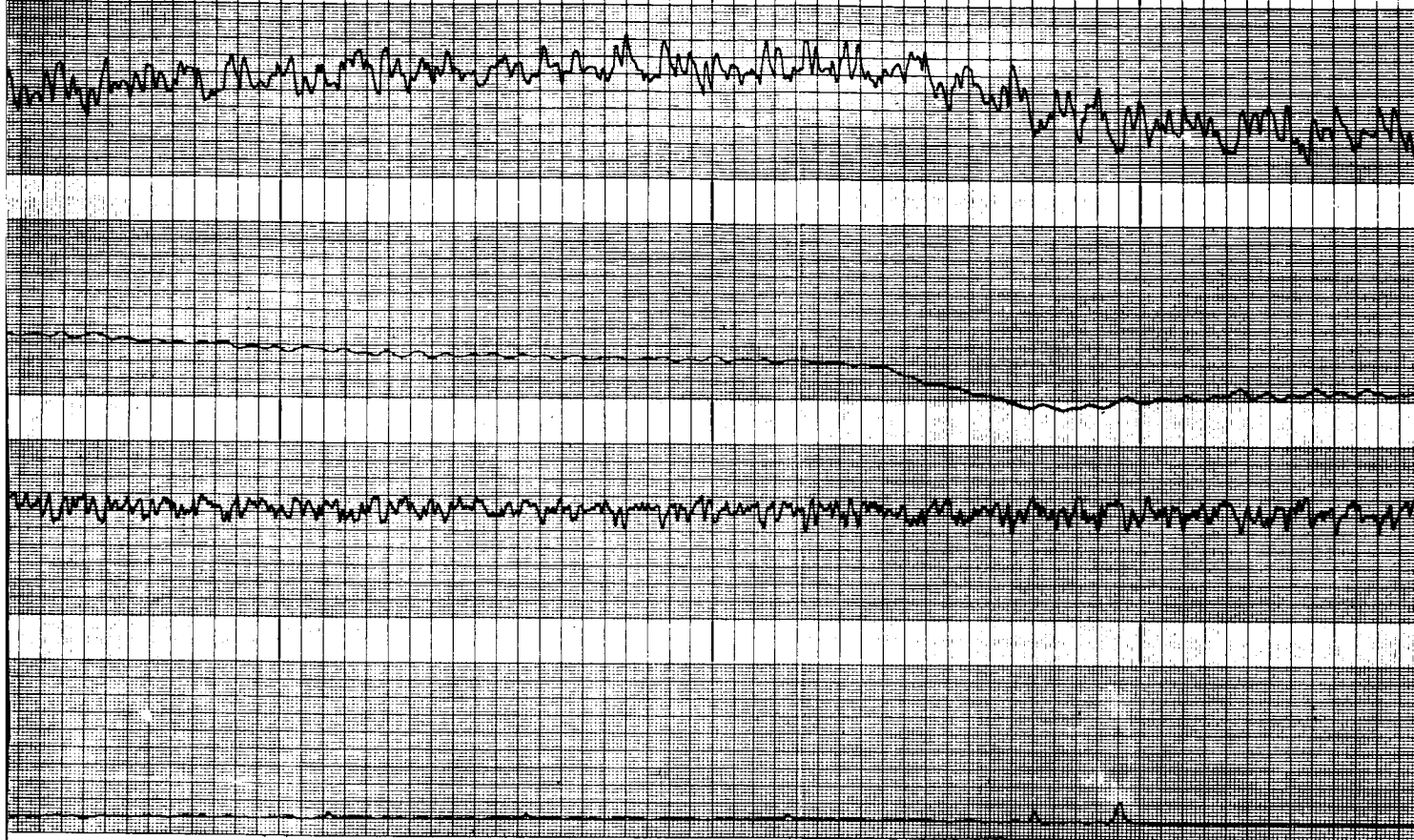
2/27/65  
(13)

Onset of the Critical Heat  
itions - 100KW Loop (2/27/65).

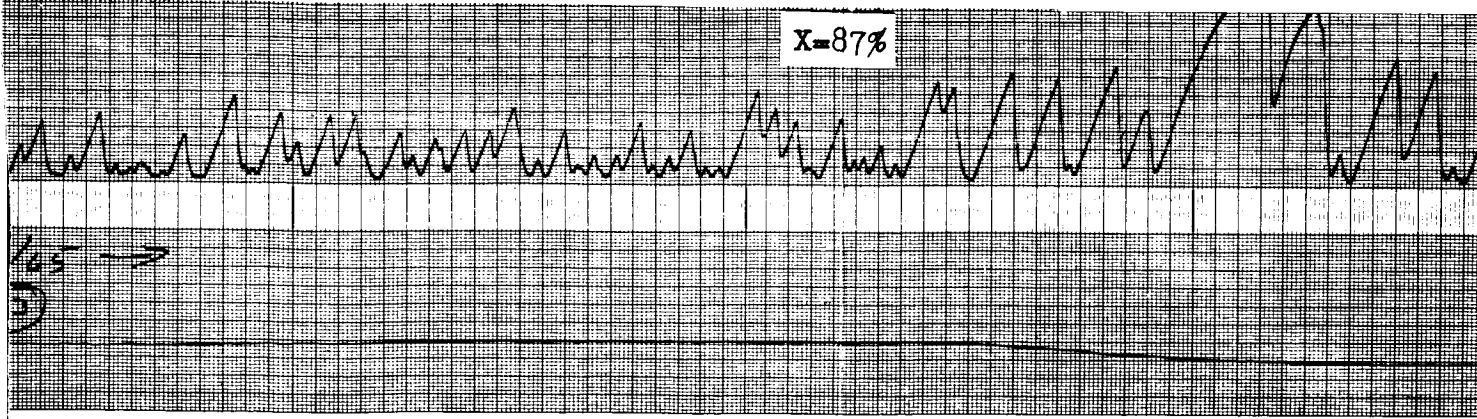


PREBOILER POWER  
INCREASE

Ref  
pt  
at  
100  
ft



X=87%



Test Section I.D. = 0.423 inch

$T_{sat} = 2105^{\circ}\text{F}$

$G = 61.6 \text{ lb/sec ft}^2$

$q'' = 157,000 \text{ Btu/hr ft}^2$



# Segment 1

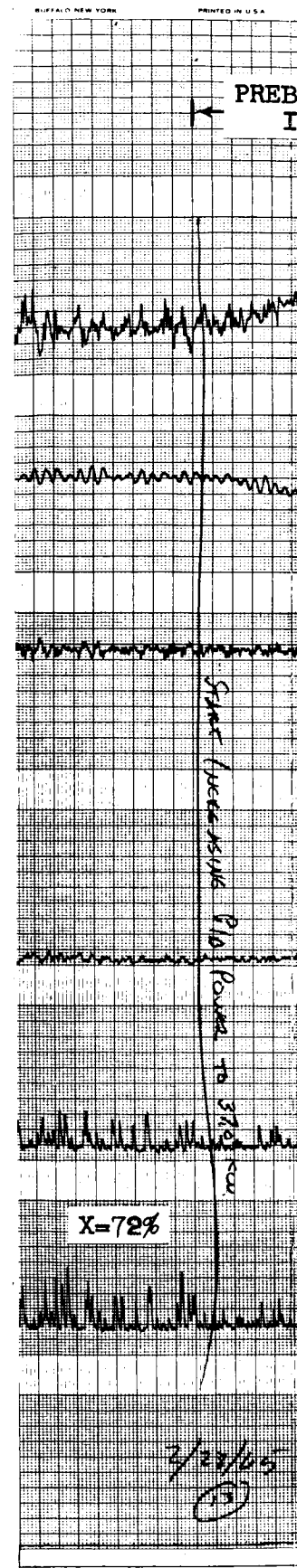
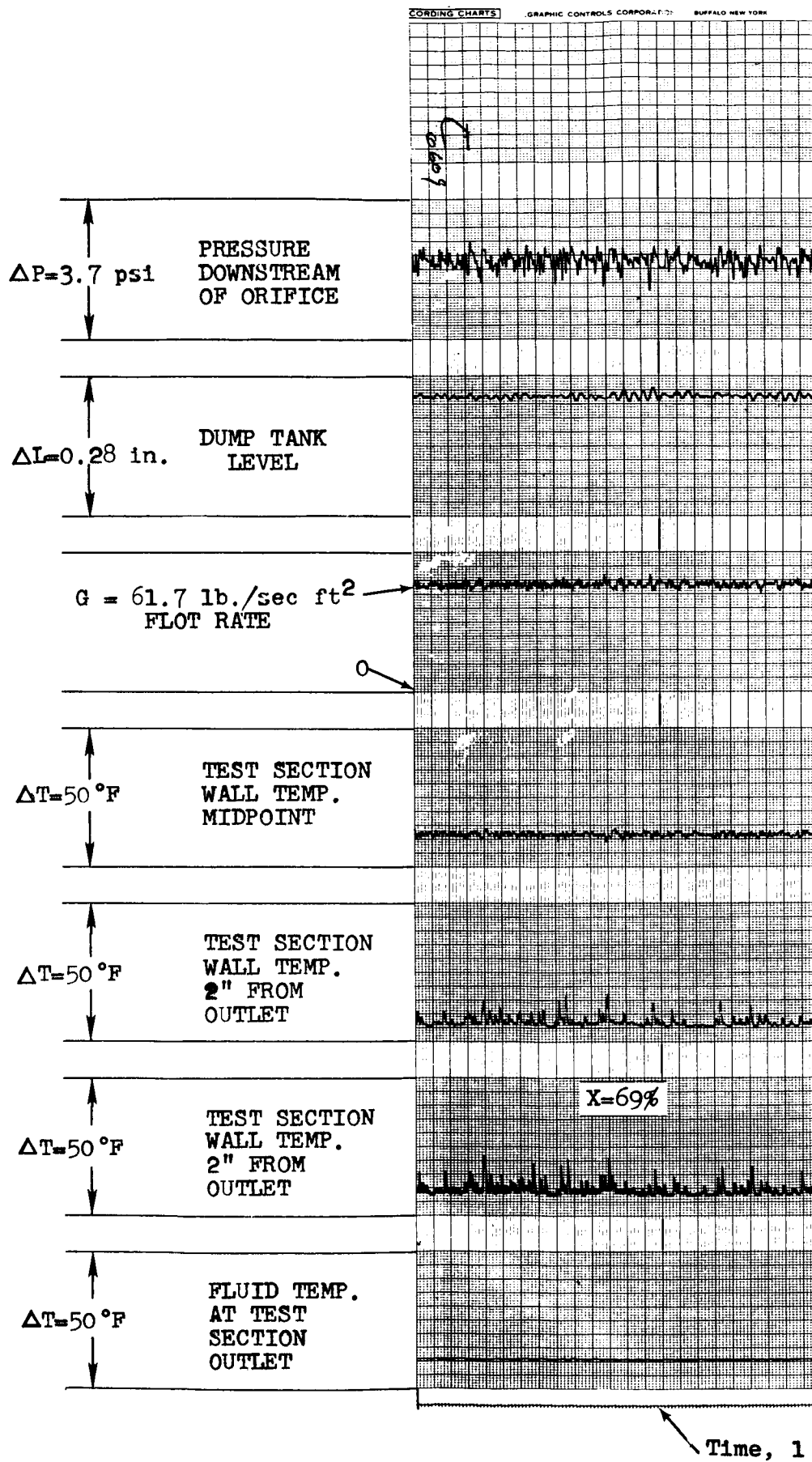


Figure 10. Recorder Chart Showing the C  
Flux Condition - 100KW Loop

# Segment 2

AMPL. DIV. .031

RECORDING CHARTS

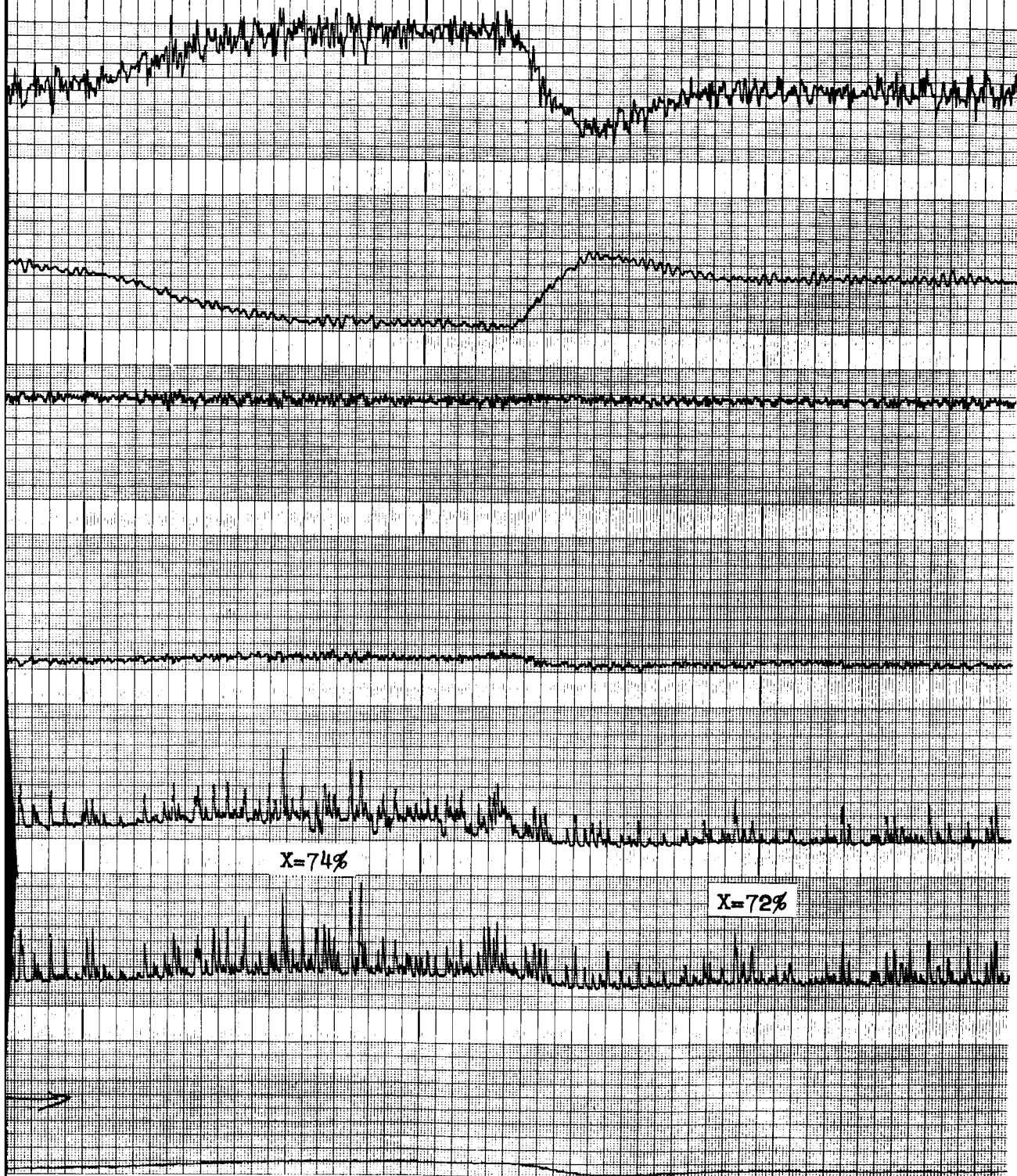
GRAPHIC CONTROLS CORPORATION

BUFFALO NEW YORK

PRINTED IN U.S.A.

OILER POWER  
INCREASE

PREBOILER POWER  
DECREASE



X=74%

X=72%

Test Section I.D. = 0.423 inch

$T_{sat} = 2102^{\circ}F$

$G = 61.7 \text{ lb./sec ft}^2$

$q'' = 224.000 \text{ Btu/hr ft}^2$

Onset of the Critical Heat  
(2/28/65).

$\Delta P = 3.7 \text{ psi}$

PRESSURE  
UPSTREAM  
OF ORIFICE

$\Delta P = 3.7 \text{ psi}$

PRESSURE  
DOWNSTREAM  
OF ORIFICE

$\Delta L = 0.28 \text{ psi}$

DUMP TANK  
LEVEL

FLOW RATE  
 $G = 31 \text{ lb/sec ft}^2$

$\Delta T = 50^\circ\text{F}$

TEST SECTION  
WALL TEMP.  
4" FROM  
INLET

$\Delta T = 50^\circ\text{F}$

TEST SECTION  
WALL TEMP.  
2" FROM  
OUTLET

$\Delta T = 50^\circ\text{F}$

TEST SECTION  
WALL TEMP.  
2" FROM  
OUTLET

$\Delta T = 50^\circ\text{F}$

FLUID TEMP  
AT TEST  
SECTION  
OUTLET



# Segment 1

# Segment 2

# Segment 3

101,000 Btu/Hr. ft<sup>2</sup>

$q'' = 101,000 \text{ Btu/Hr. ft}^2$

$q'' = 96,000 \text{ Btu/Hr.}$

$\Delta P = 18.6 \text{ psi}$

← 2 Minutes →

X=57%

X=66%

X=72%

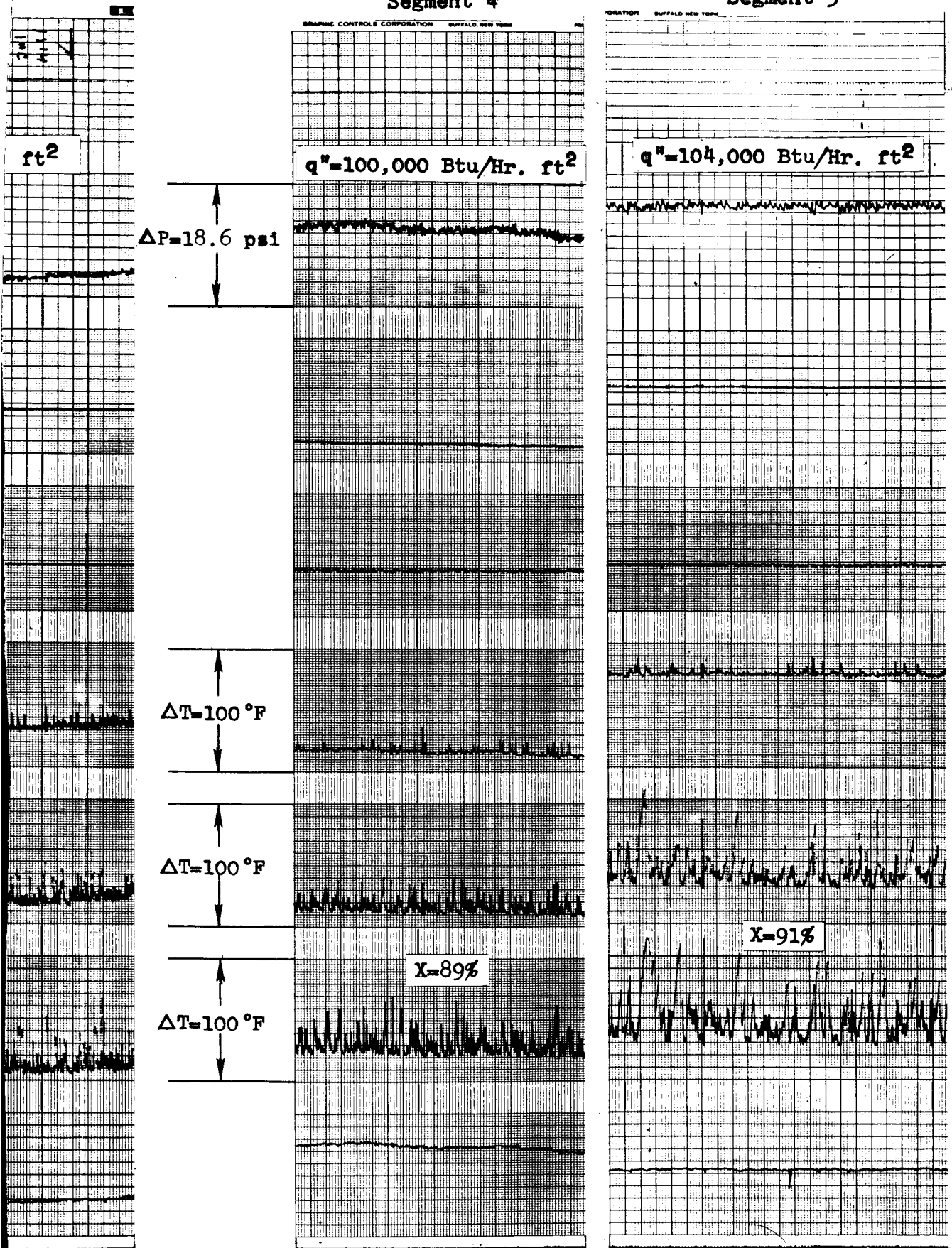
Time, 1 mark/sec.

Figure 11. Recorder Chart Showing the Onset of the Critical Heat Flux Condition - 100KW Loop (3/17/65).

3

Segment 4

Segment 5



Test Section I.D. = 0.423 inch

$T_{\text{sat}} = 2100^\circ\text{F}$

$G = 31$  lb./sec ft<sup>2</sup>

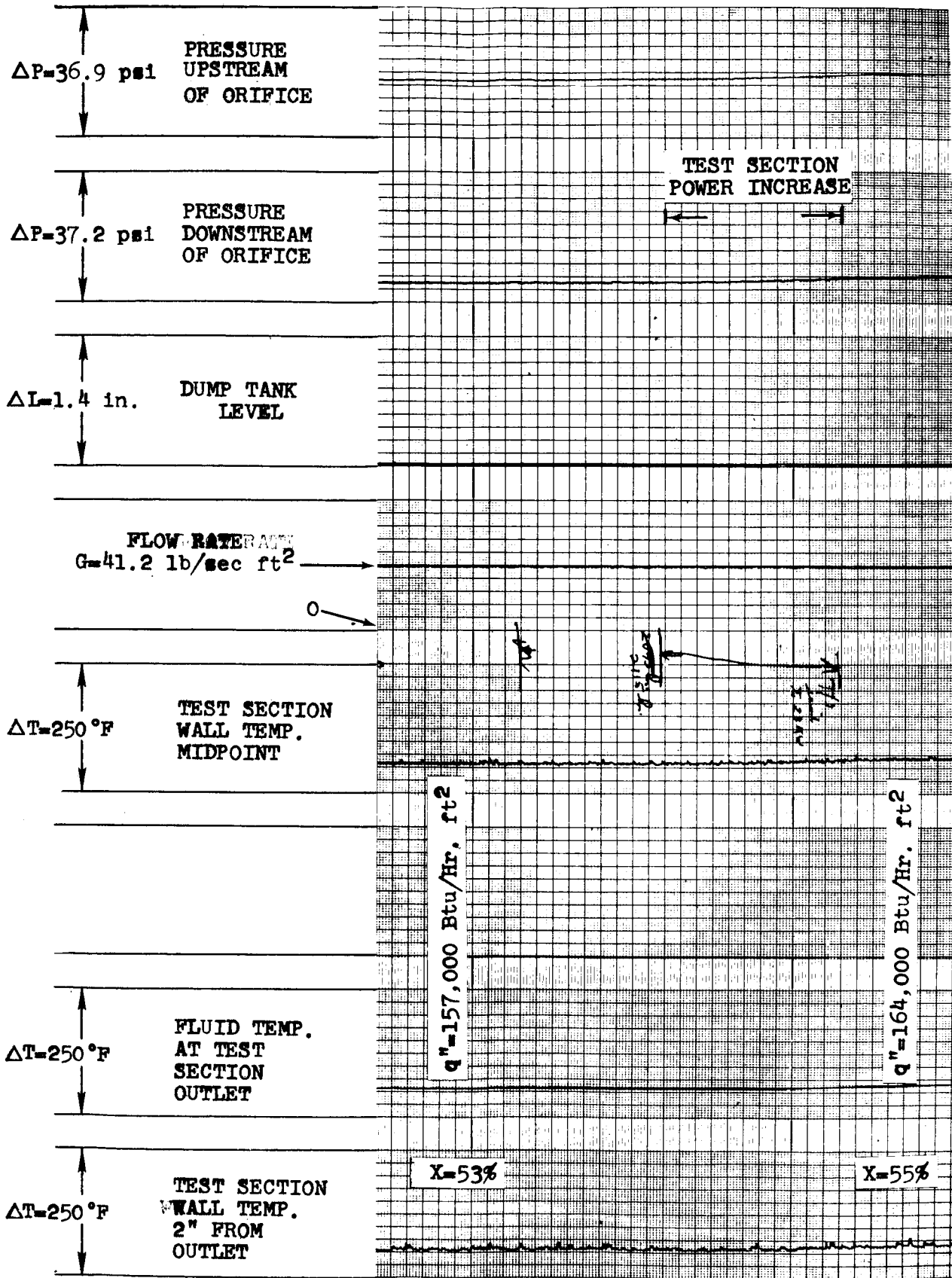


Figure 12. Recorder Chart Showing Flux Condition - 100K

# Segment 2

APPL. DIV. - 201

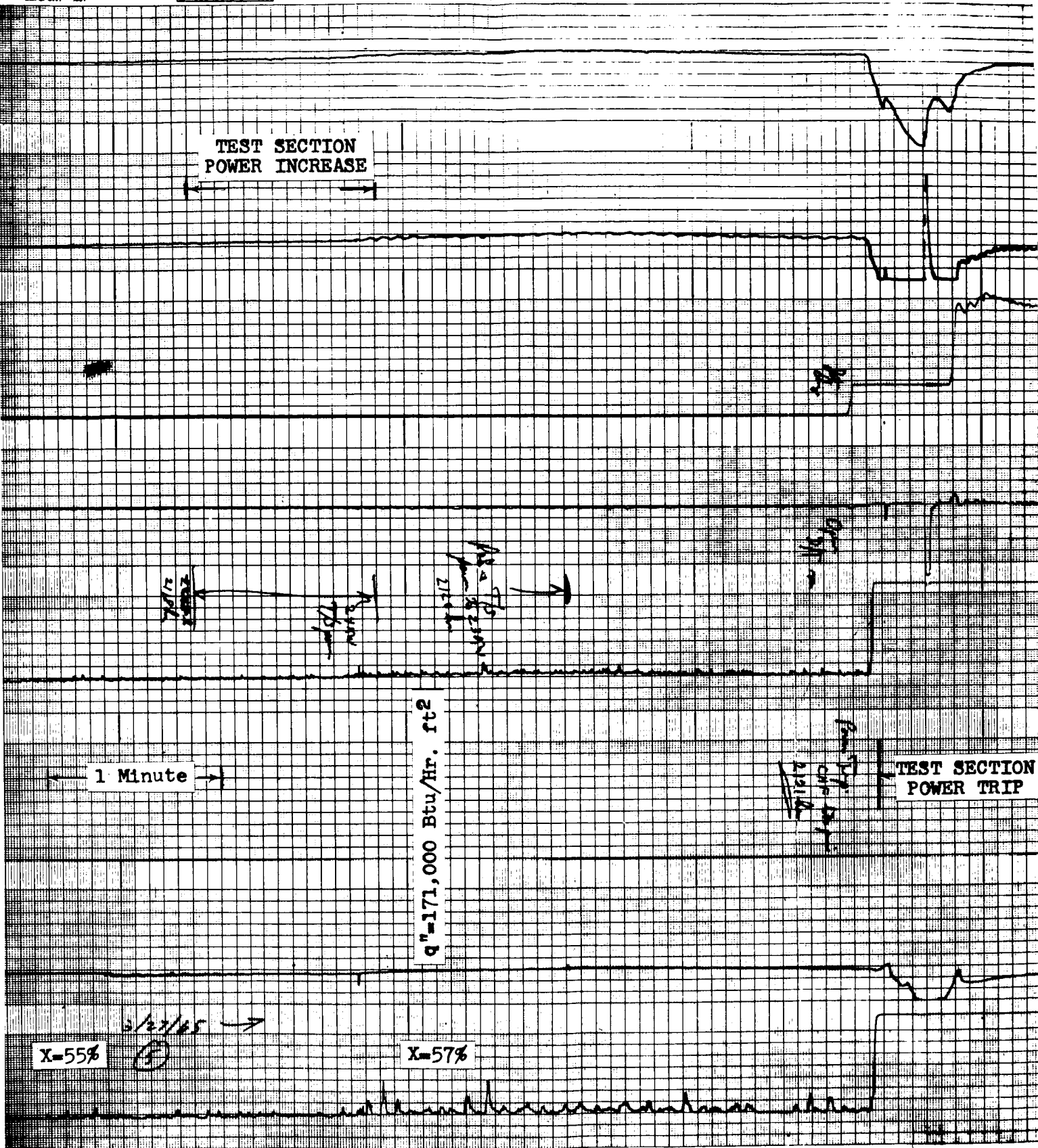
RECORDING CHARTS

GRAPHIC CONTROLS CORPORATION

BUFFALO NEW YORK

PRINTED IN U.S.A.

APPL. DIV. - 201



Test Section I.D. = 0.423 Inch

$T_{sat} = 1838^{\circ}F$

$G = 41.2 \text{ lb/sec ft}^2$

$q_c = 171,000 \text{ Btu/Hr. ft}^2$

$X_c = 57\%$

g the Onset of the Critical Heat  
W Loop (3/27/65).

PREBOILER POWER INCREASE

$\Delta P = 36.9 \text{ psi}$

PRESSURE  
UPSTREAM  
AT ORIFICE

$\Delta P = 37.2 \text{ psi}$

PRESSURE  
DOWNSTREAM  
AT ORIFICE

$\Delta L = 1.41 \text{ in.}$

DUMP TANK  
LEVEL

FLOW RATE  
 $G = 47.6 \text{ lb/sec ft}^2$

$\Delta T = 250^\circ \text{F}$

TEST SECTION  
WALL TEMP.  
MIDPOINT

$q'' = 97,000 \text{ Btu/hr. ft}^2$   
1143 Hrs. (3/31/65)

$\Delta T = 250^\circ \text{F}$

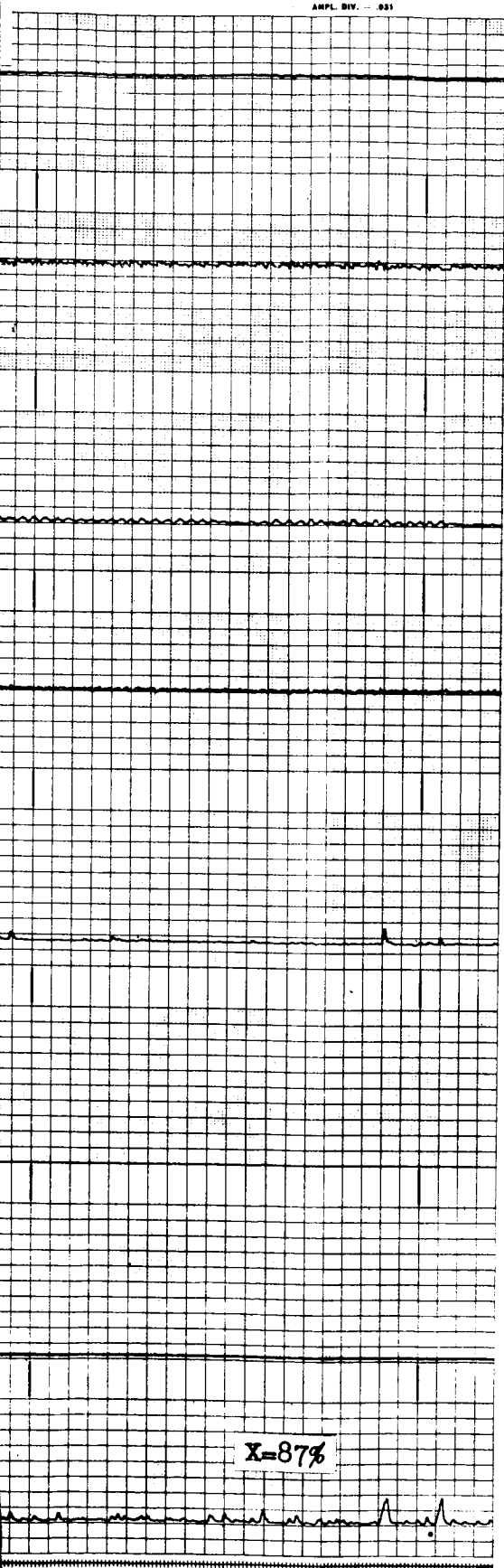
FLUID TEMP.  
AT TEST  
SECTION  
OUTLET

$\Delta T = 250^\circ \text{F}$

TEST SECTION  
WALL TEMP.  
2" FROM  
OUTLET

Time





1 mark/sec

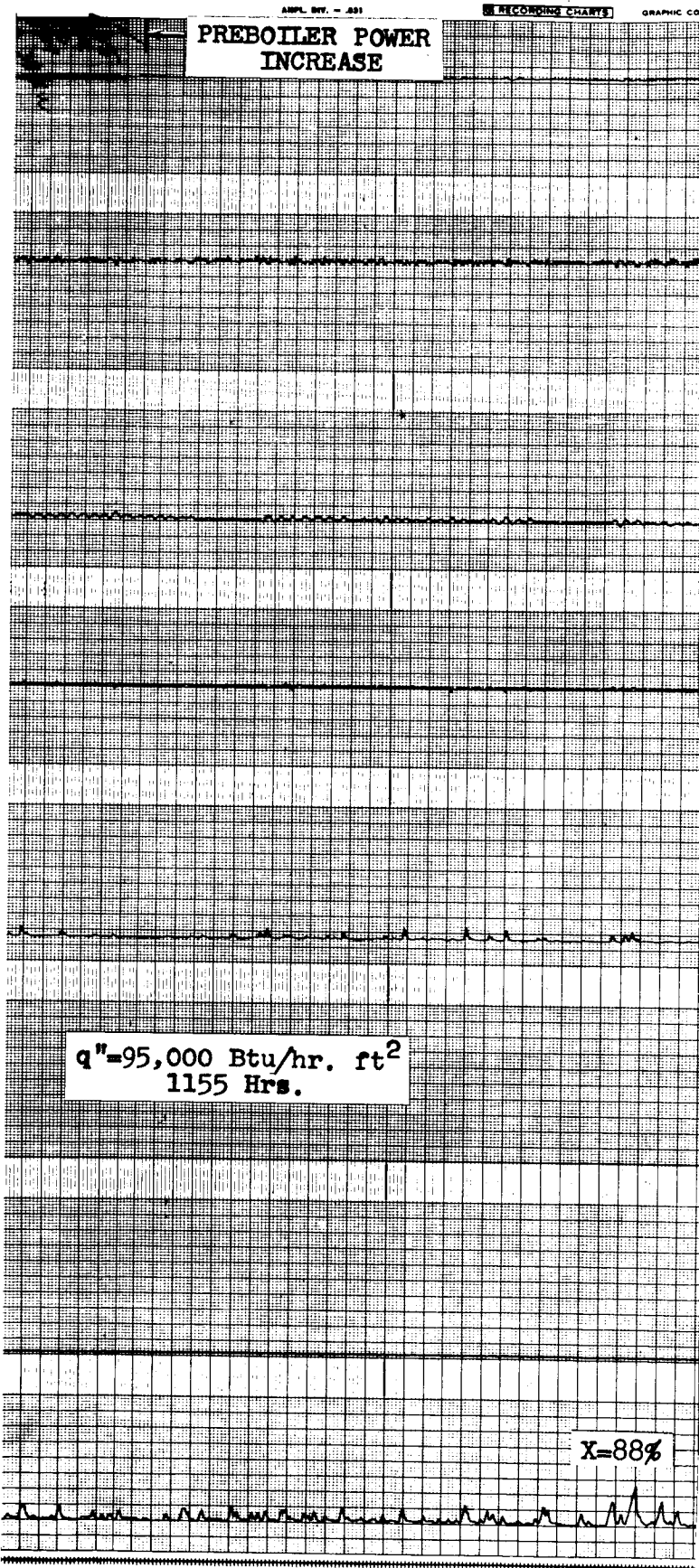
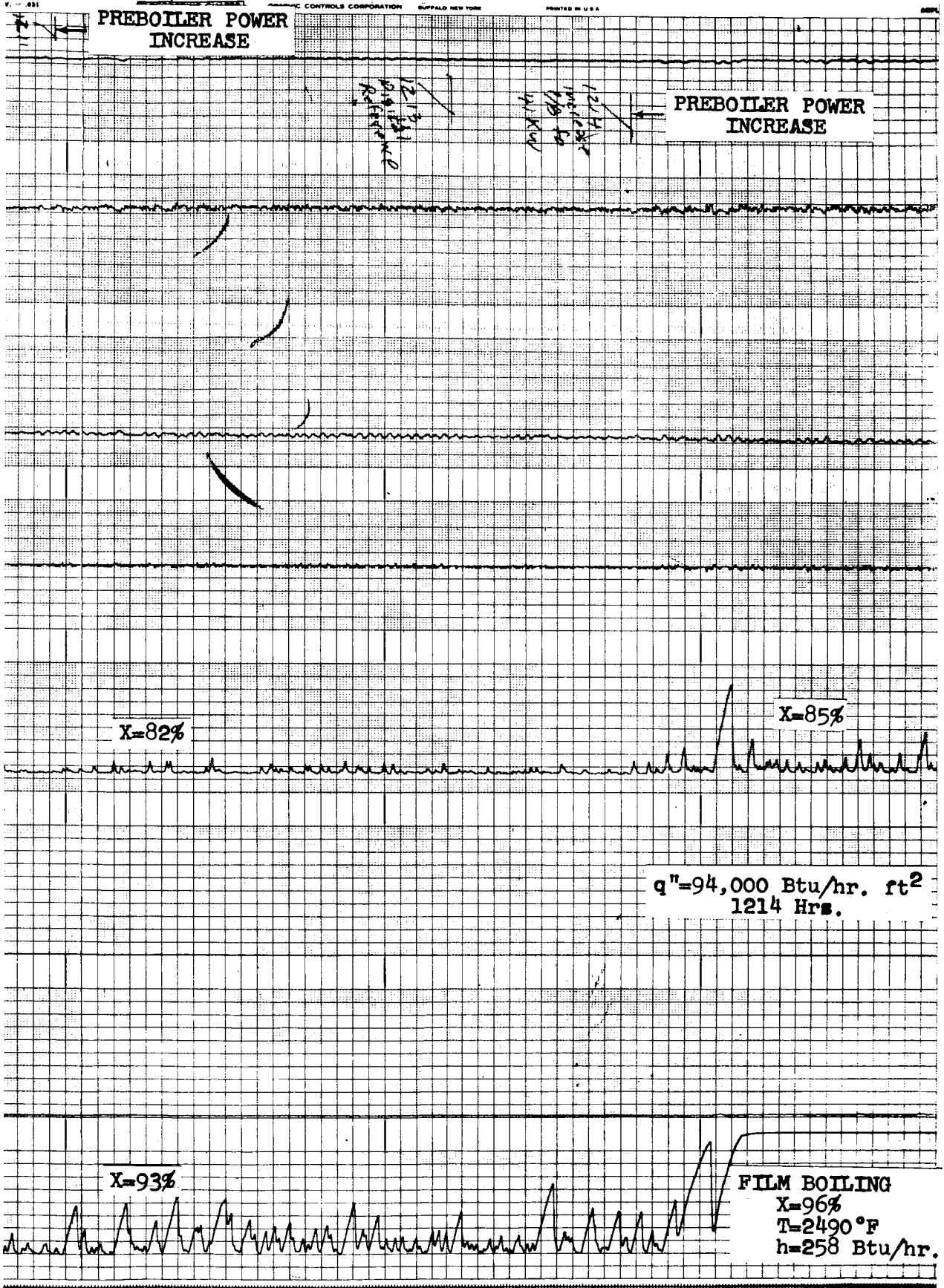


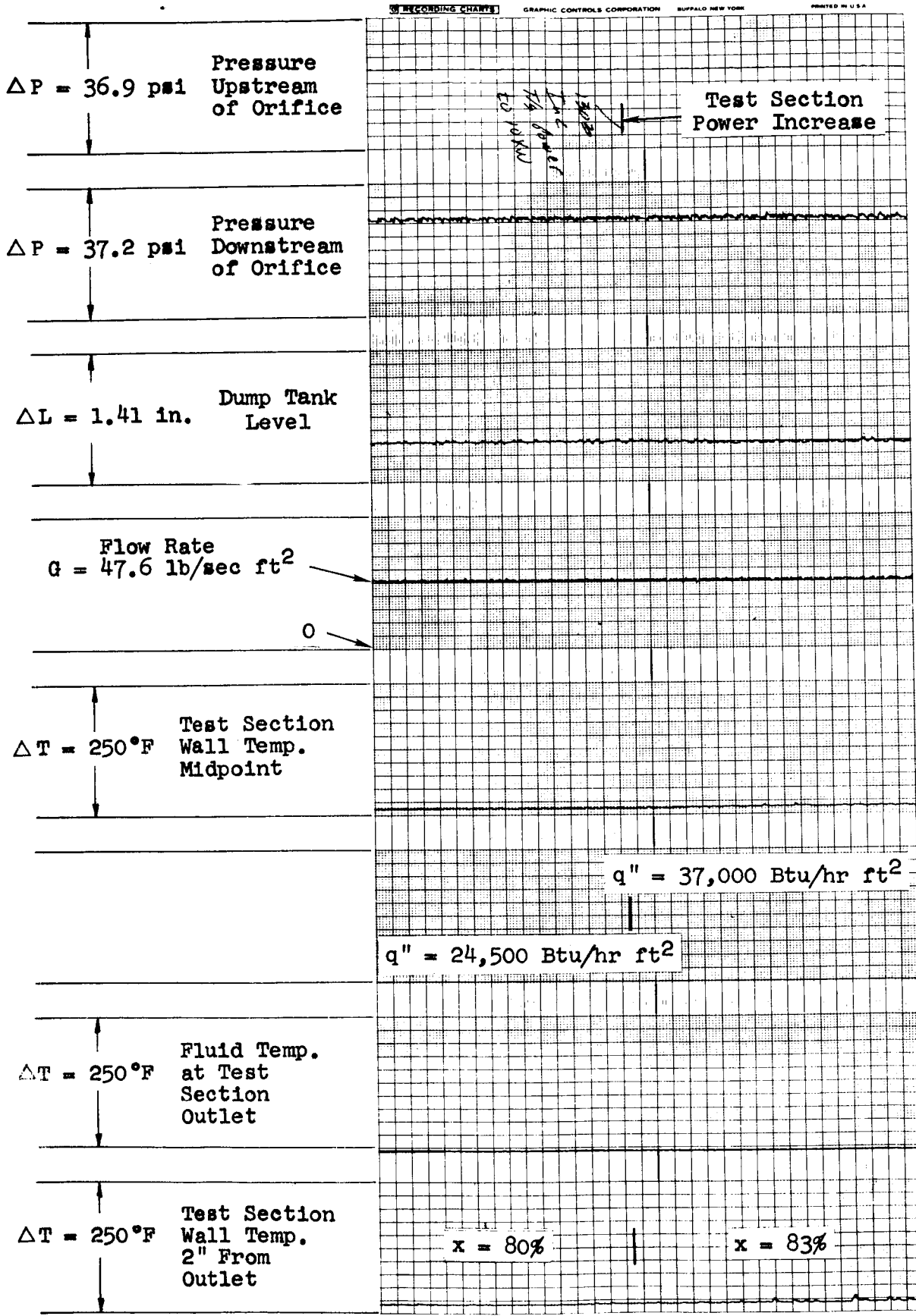
Figure 13. Recorder Chart Showing the Critical Transition Boiling and Film Boiling

3



Test Section I.D. = 0.423 inch  
T<sub>sat</sub> = 2104°F  
G=47.6 lb/sec ft.<sup>2</sup>

1 Heat Flux Condition,  
g - 100KW Loop (3/31/65).

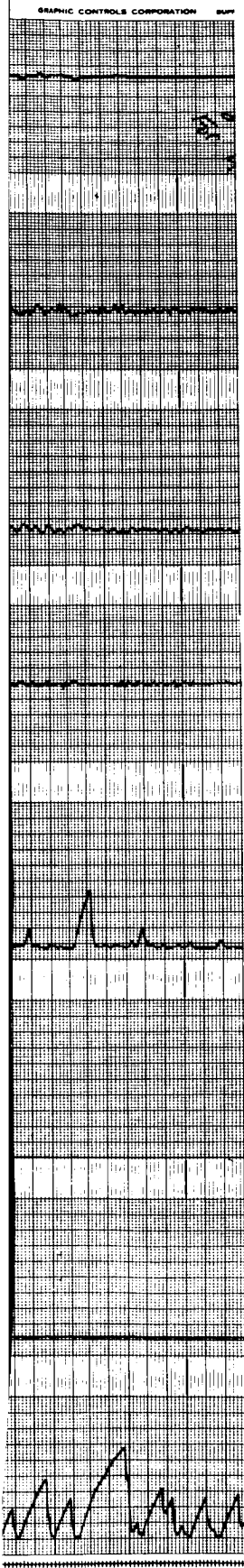


Test Section I.D. = .423 in. - No Insert  
 $T_{\text{sat}} = 2105^\circ\text{F}$   
 $G = 47.6 \text{ lb/sec ft}^2$





3



$\Delta P = 36.9 \text{ psi}$   
Pressure  
Upstream  
of Orifice

$\Delta P = 37.2 \text{ psi}$   
Pressure  
Downstream  
of Orifice

$\Delta L = 1.41 \text{ in.}$   
Dump Tank  
Level

Flow Rate  
 $G = 47.6 \text{ lb/sec ft}^2$

$\Delta T = 250^\circ\text{F}$   
Test Section  
Wall Temp.  
Midpoint

$\Delta T = 250^\circ\text{F}$   
Fluid Temp.  
at Test  
Section  
Outlet

$\Delta T = 250^\circ\text{F}$   
Test Section  
Wall Temp.  
2" From  
Outlet

*Inc 44  
2762  
2762*

Preboiler Power  
Increase

$x = 85\%$

$x = 90\%$

$q'' = 49,000 \text{ Btu/hr ft}^2$   
1342 Hrs

$x = 91\%$

$x = 96\%$

Test Section I.D. = 0.423 in. - No Insert  
 $T_{\text{sat}} = 2105^\circ\text{F}$   
 $G = 47.6 \text{ lb/sec ft}^2$

Time

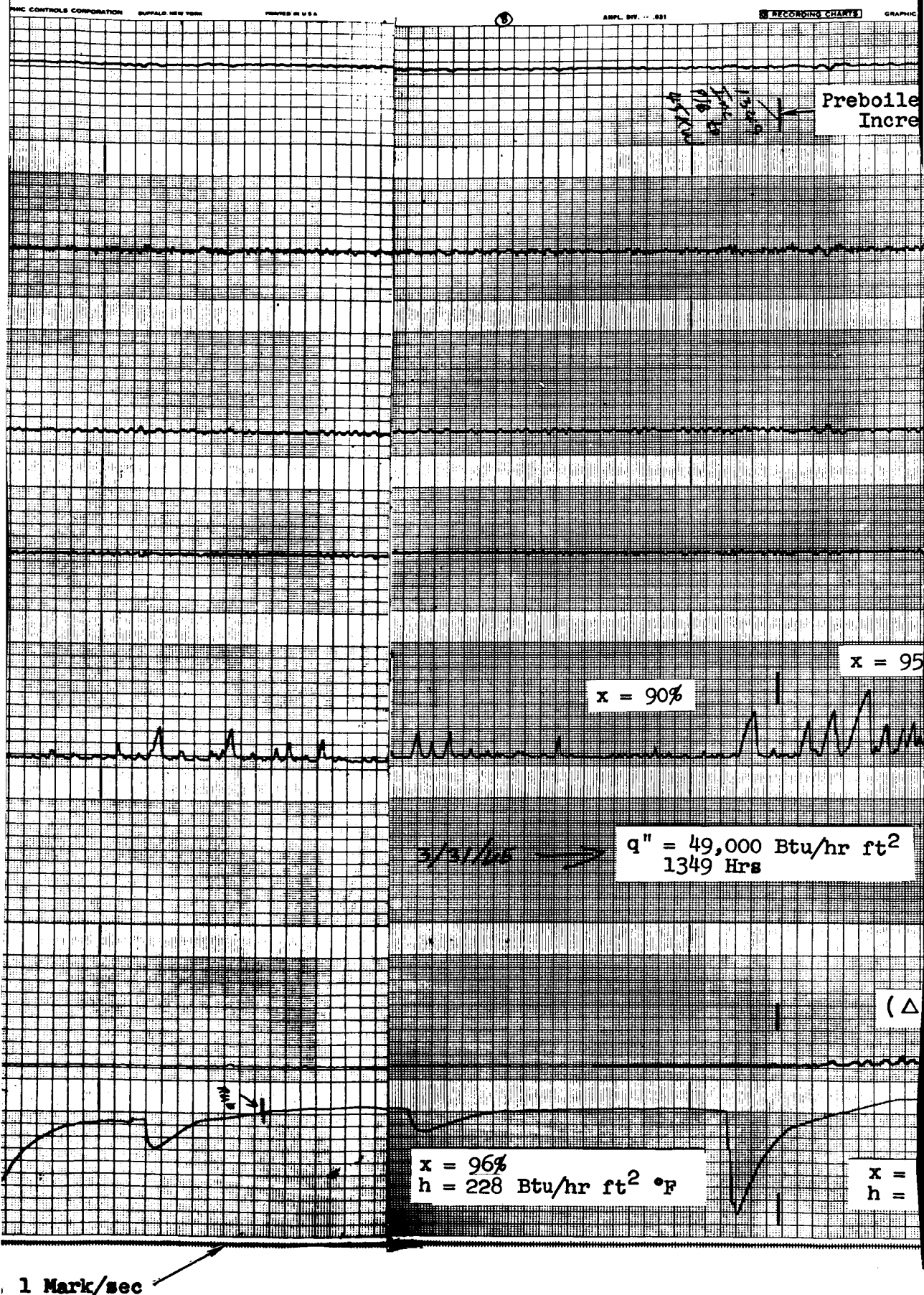


Figure 14b. Recorder Chart Showing Changes in Boiling Regime - 100KW Loop (continued)


$$T)_{SH} = 25^{\circ}F$$

101%  
194 Btu/hr ft<sup>2</sup> °F

$$\Delta T = 500^{\circ}\text{F}$$

**x = 99%**

$$x = 100\%$$
$$q'' = \frac{54,300 \text{ Btu/hr ft}^2}{1414 \text{ Hrs}}$$
$$(\Delta T)_{SH} = 120^{\circ}F$$
$$(\Delta T)_{SH} = 200^\circ F$$
$$\Delta T = 500^{\circ}\text{F}$$

**x = 105%**

$$x = 106\%$$

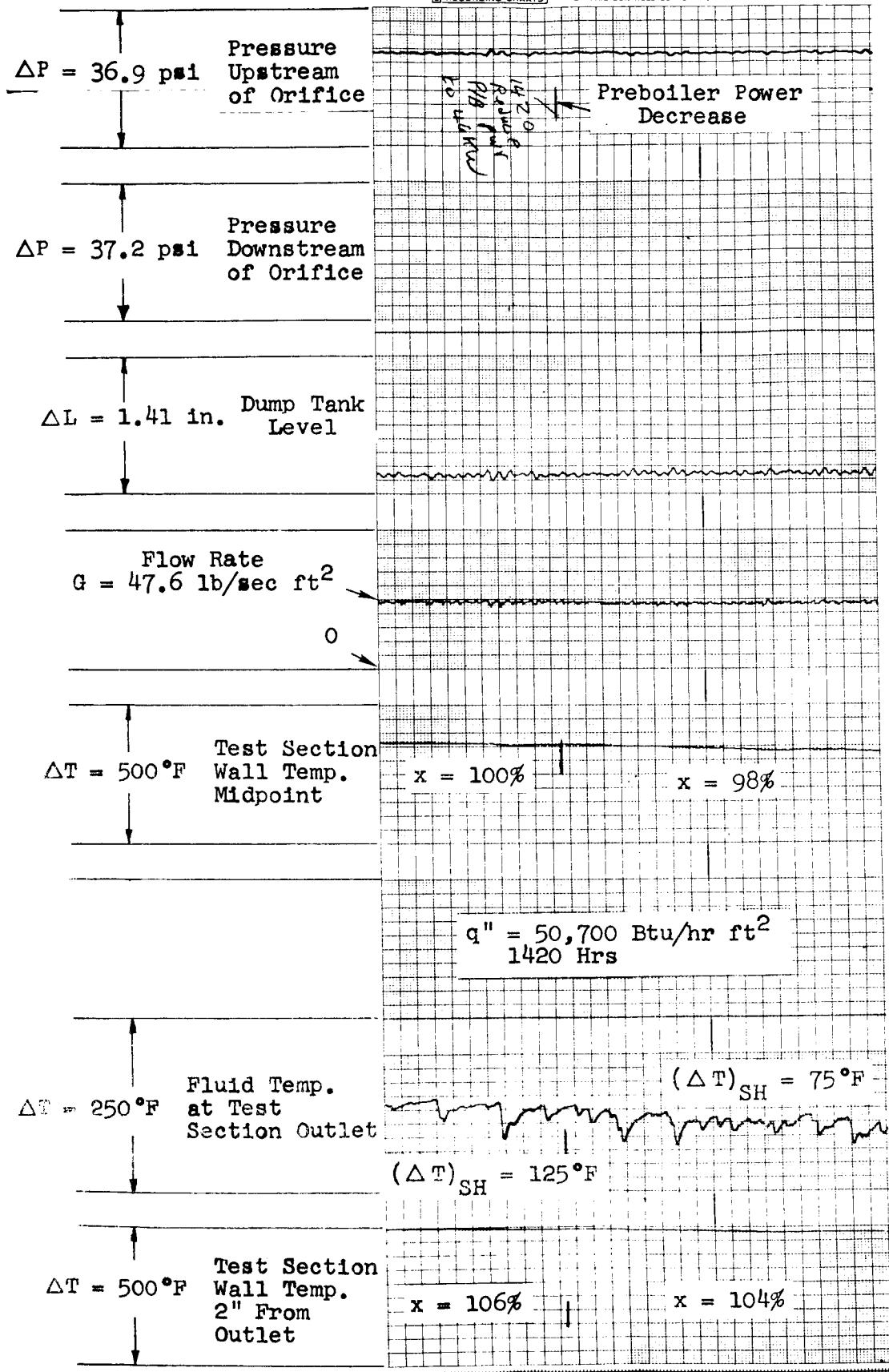
## Preboiler Power Increase

## Increase



RECORDING CHARTS

GRAPHIC CONTROLS CORPORATION BUFFALO NEW YORK



Test Section I.D. = 0.423 in. - No Insert  
 $T_{sat} = 2105^\circ\text{F}$   
 $G = 47.6 \text{ lb/sec ft}^2$

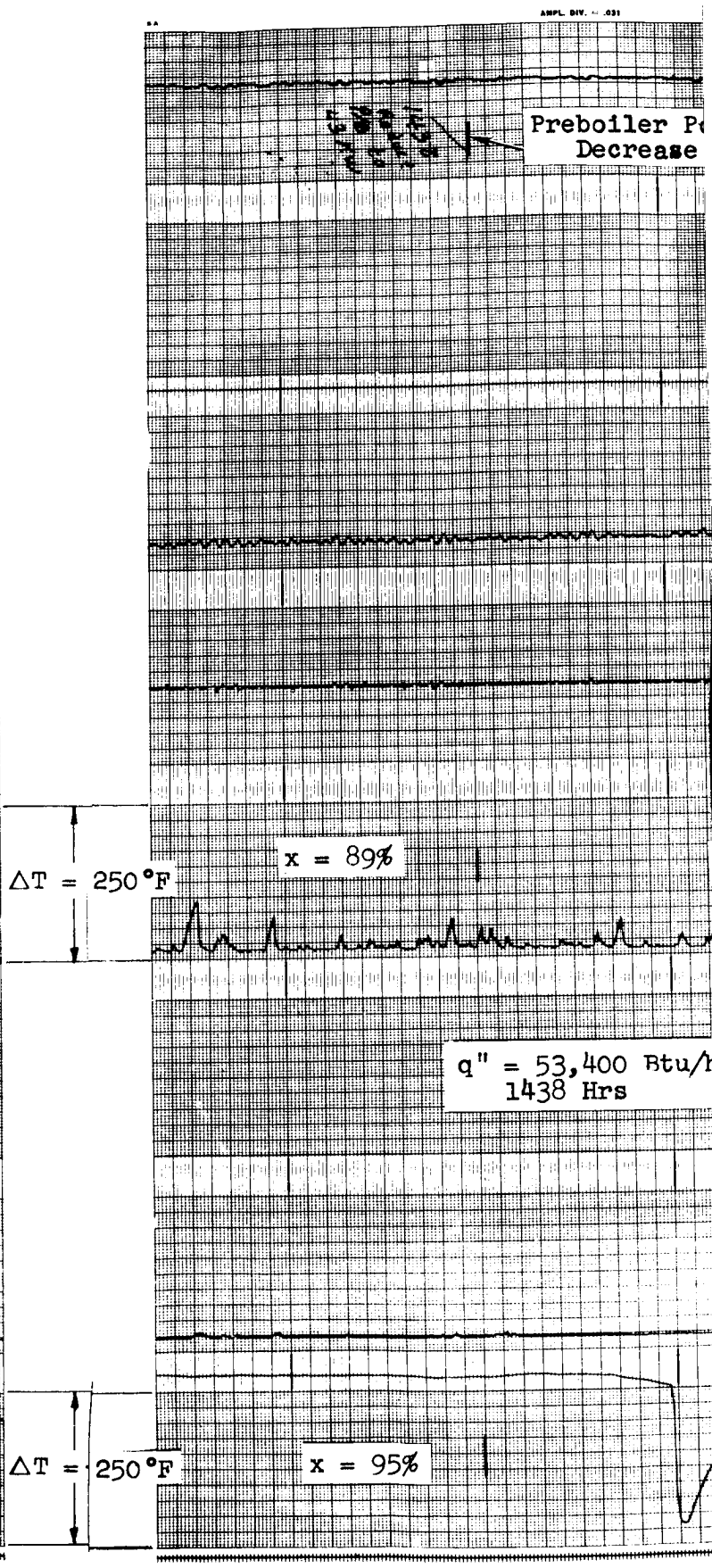
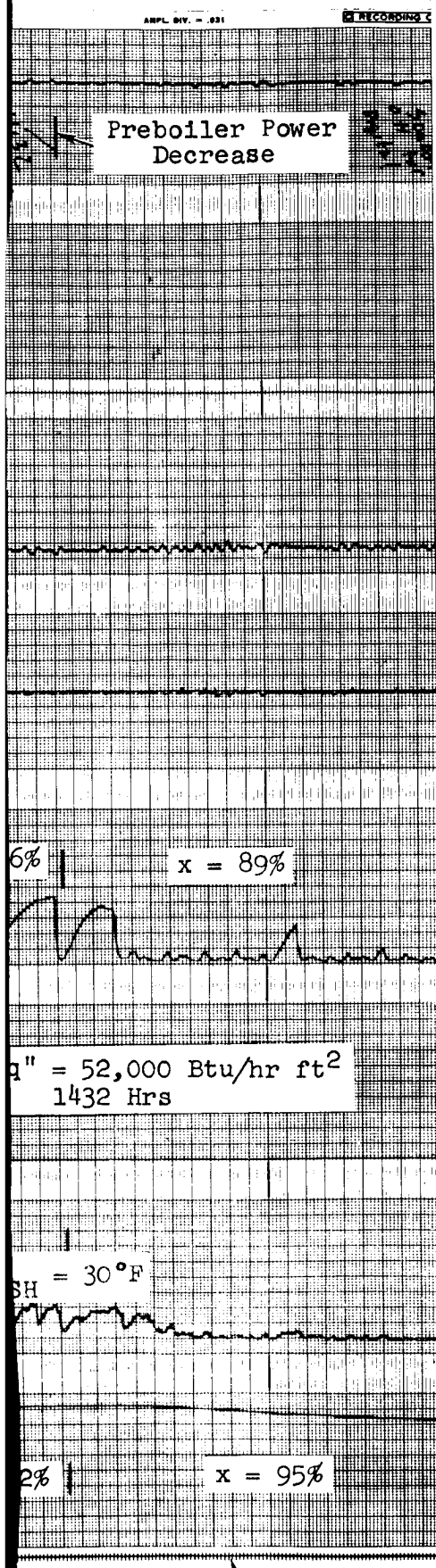
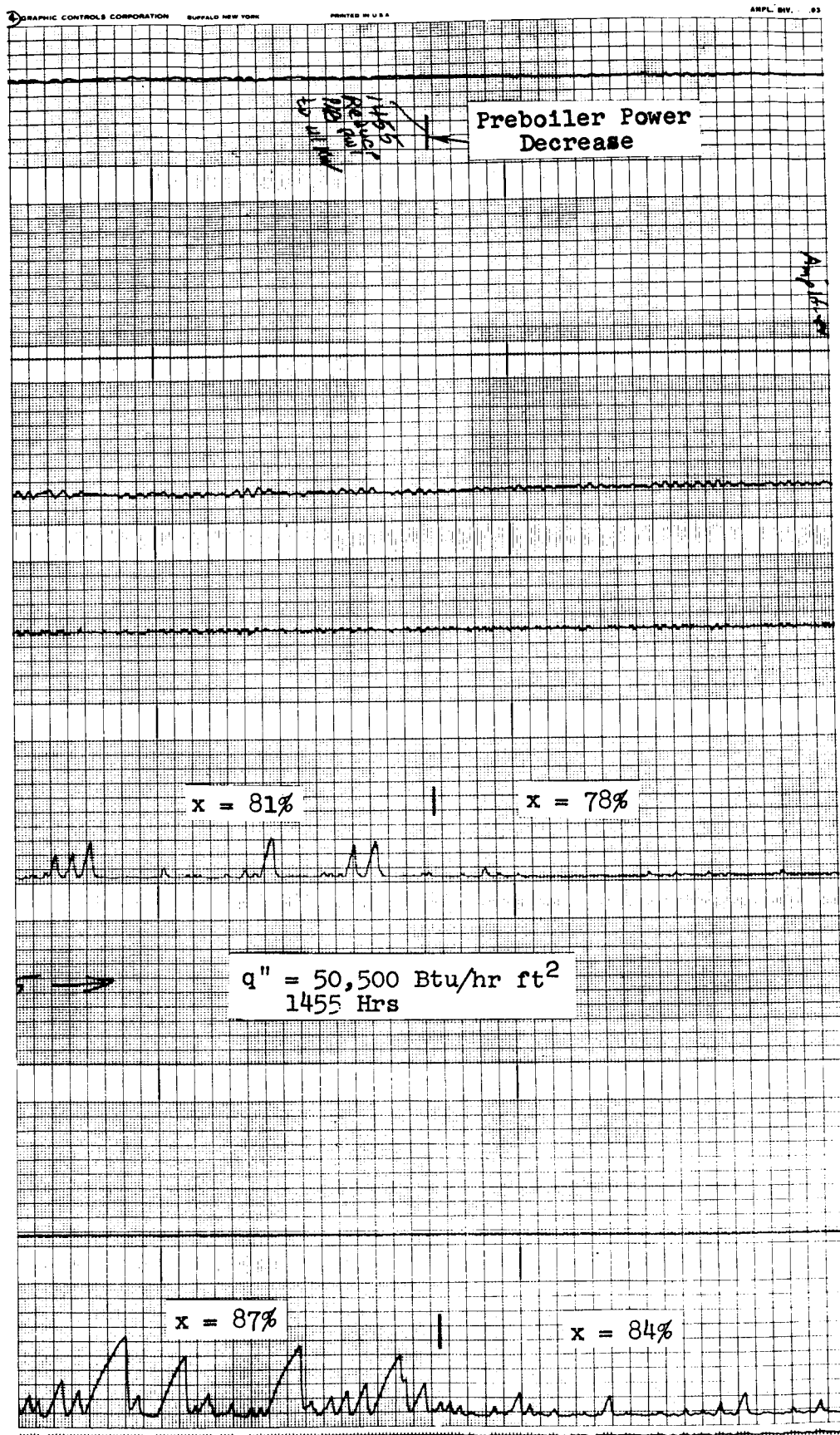
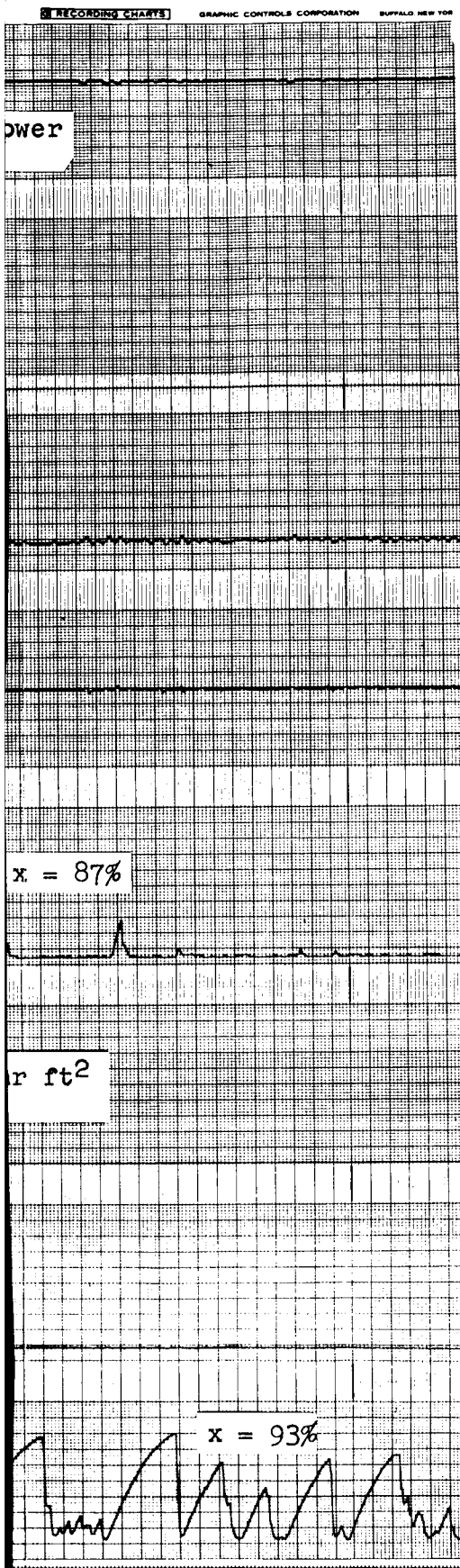


Figure 14c. Recorder Chart Showing Changes in Boiling  
100KW Loop (continued)





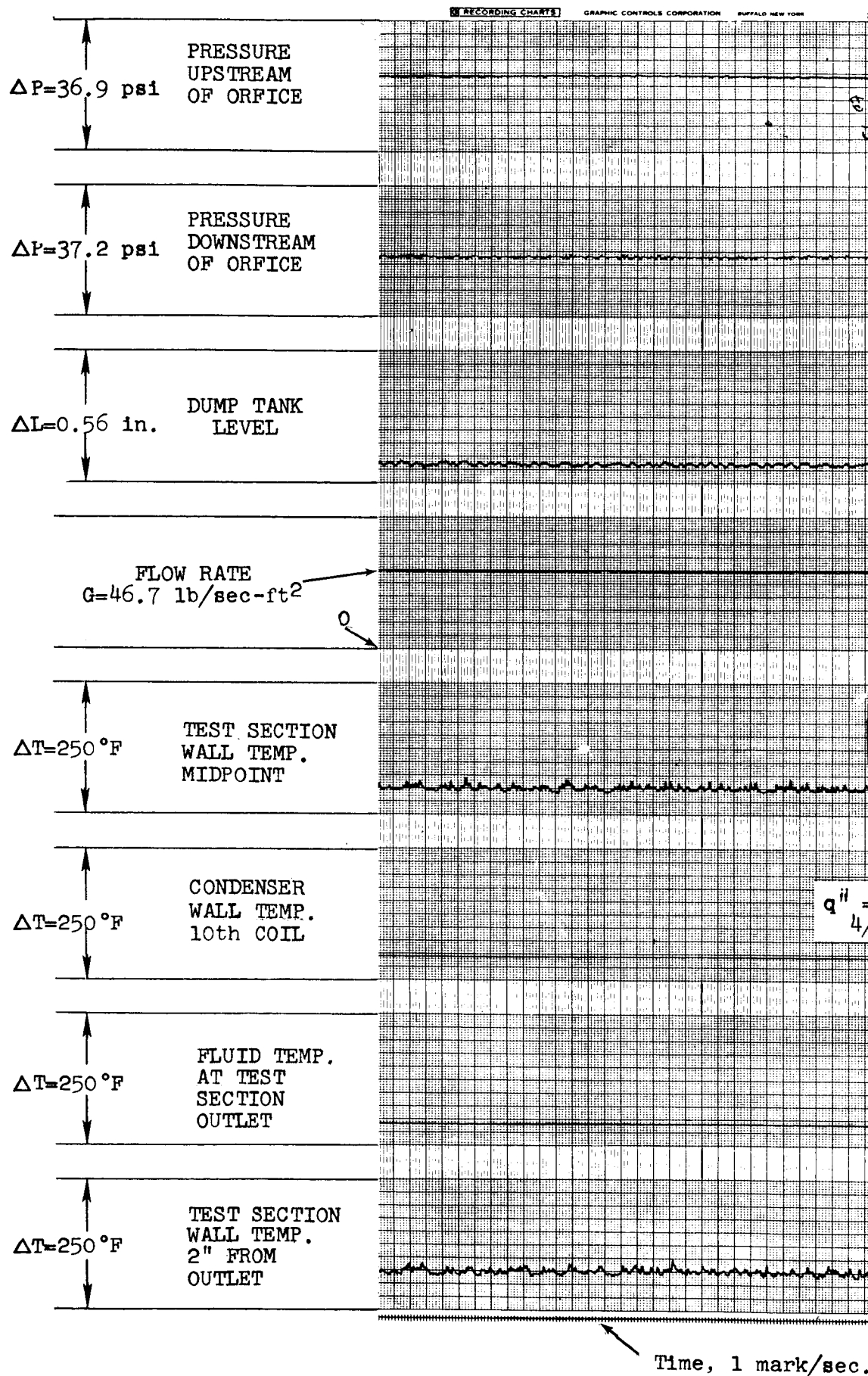
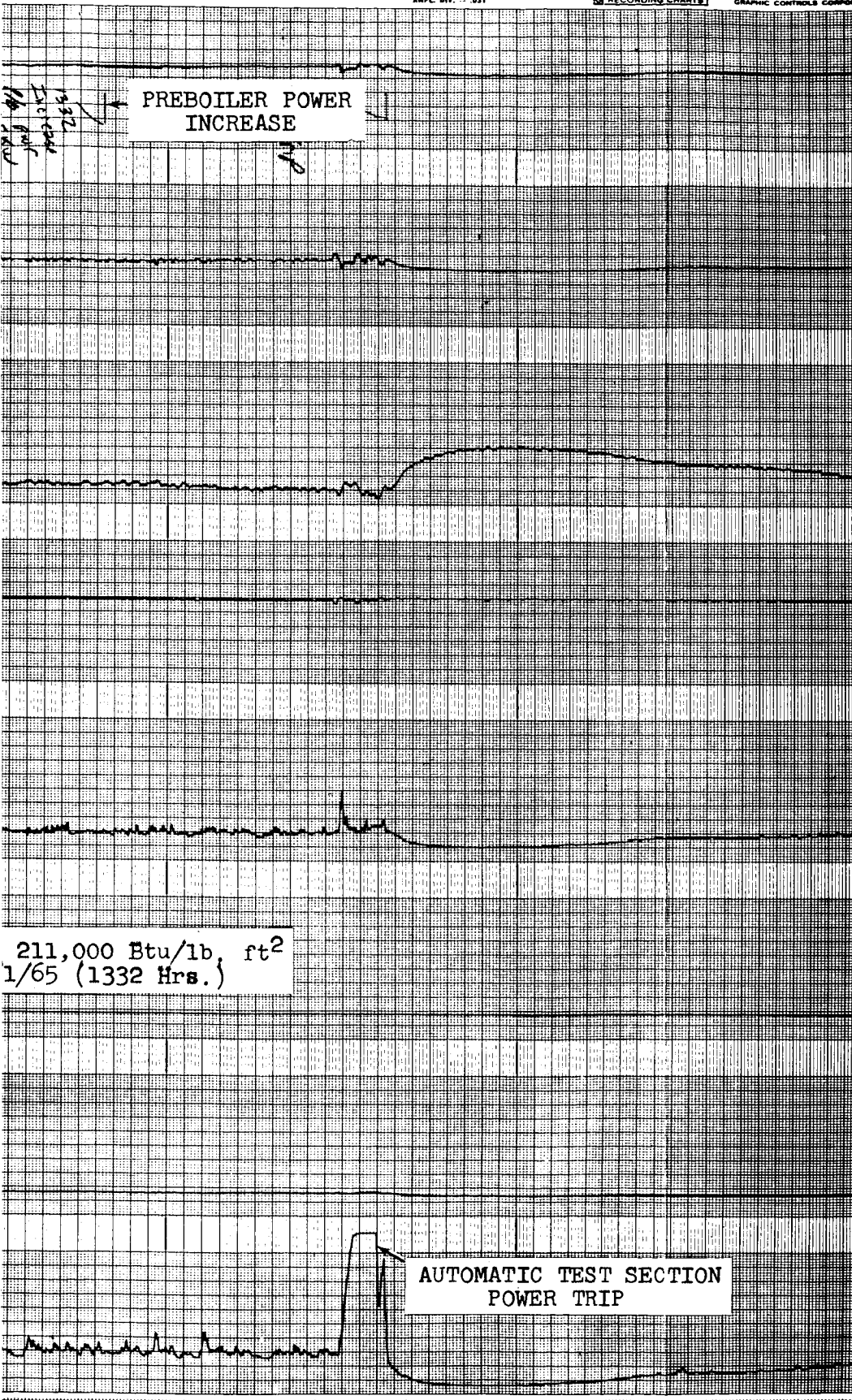


Figure 15a. Recorder Chart Showing the On Flux Condition - 100KW Loop (



set of the Critical Heat  
1/65).

Test Section I.D. = 0.423 in.  
 $T_{\text{sat}} = 2105^{\circ}\text{F}$   
 $G = 46.7 \text{ lb/sec. ft}^2$   
 $q_c'' = 211,000 \text{ Btu/hr. ft}^2$   
 $X_c = 59\%$

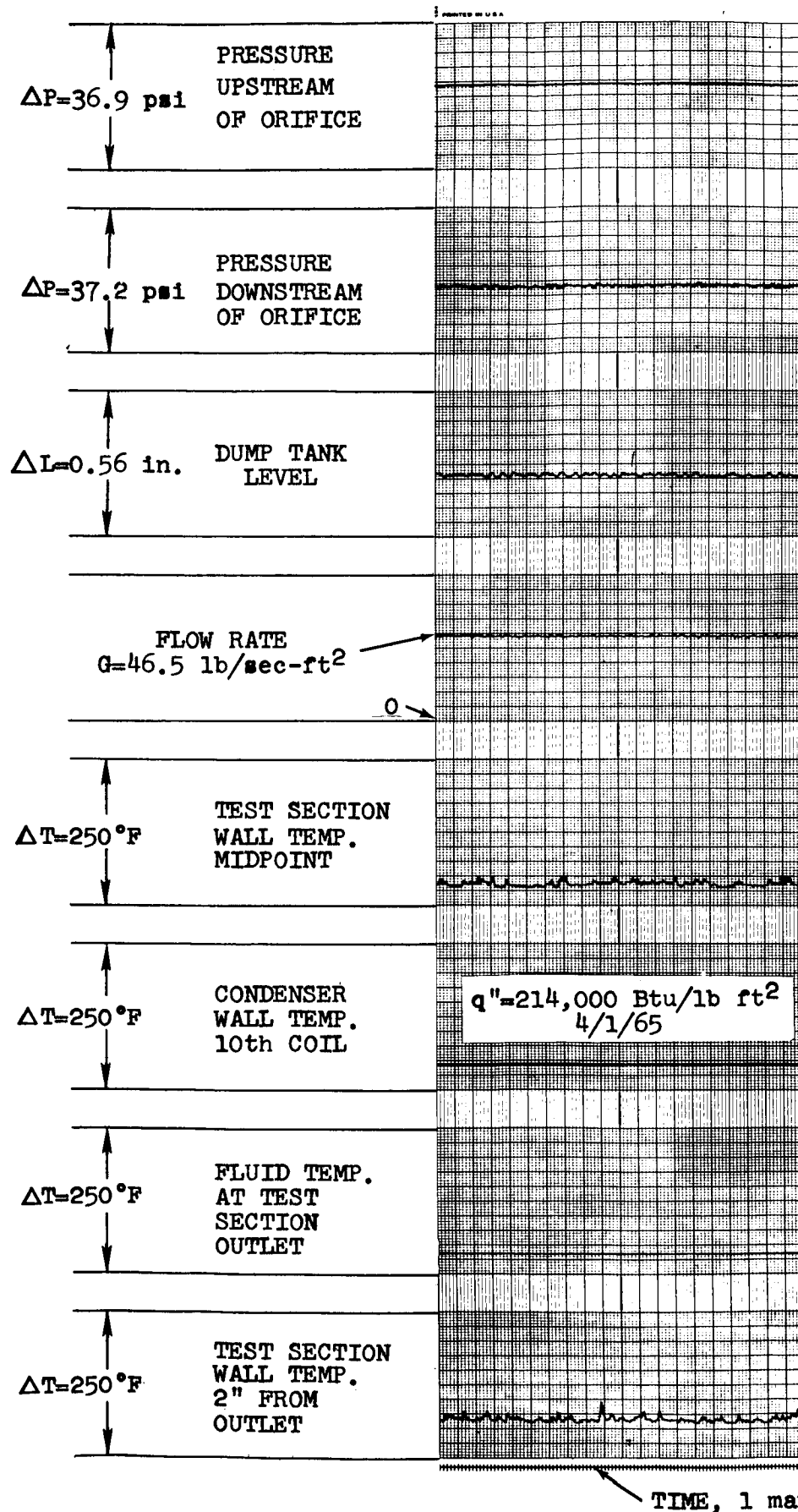
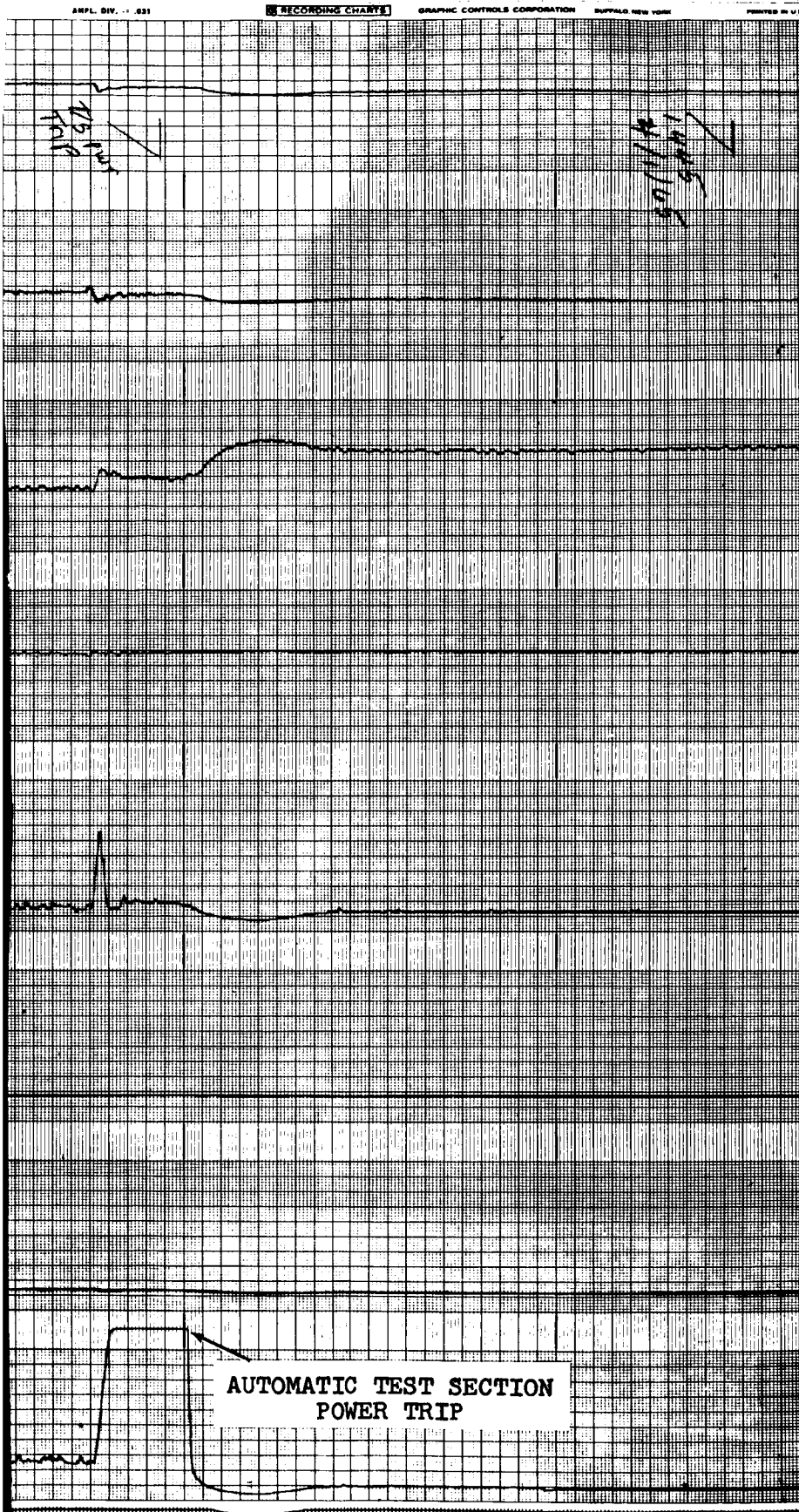


Figure 15b. Repeat of Critical Heat Flux Point 100KW Loop (4/1/65).



t/sec.

shown in Figure 15a -

TEST SECTION I.D. = 0.423 in.

$T_{sat} = 2106^{\circ}F$

$G = 46.5 \text{ lb/sec-ft}^2$

$q_c = 214,000 \text{ Btu/lb}$

$X_c = 61\%$

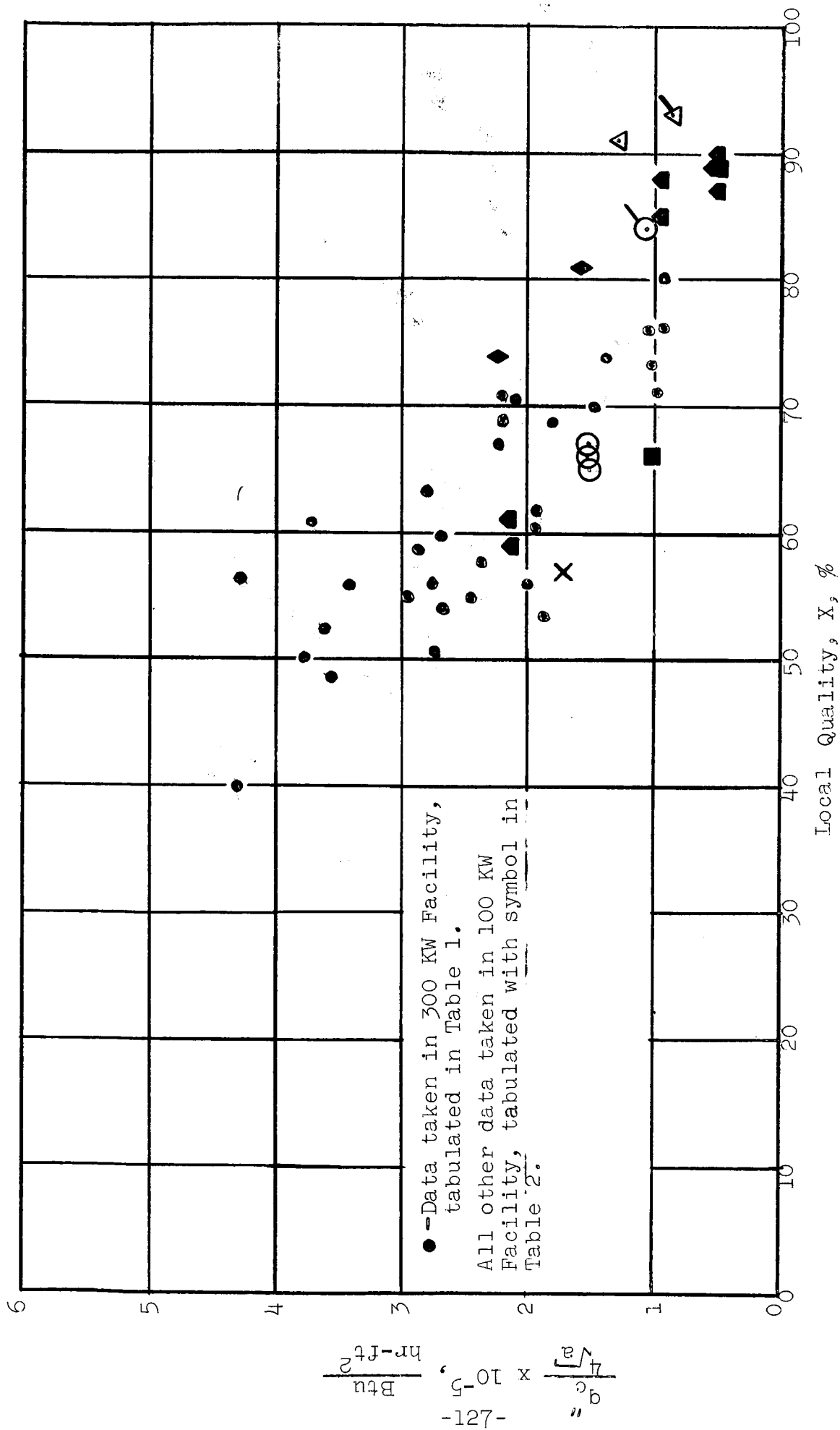


Figure 16. Comparison of Critical Heat Flux Data from the 100 KW and 300 KW Facilities

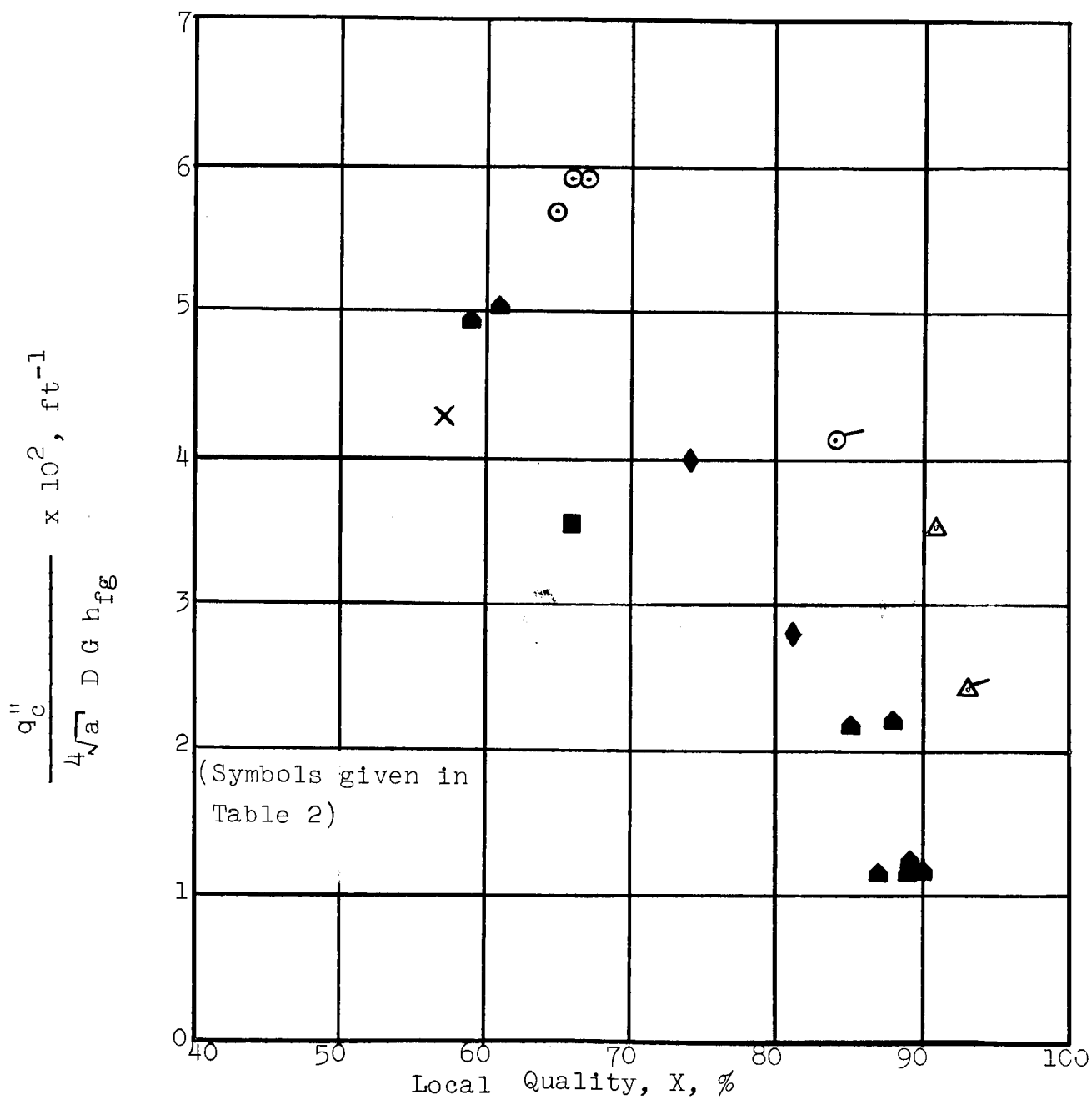


Figure 17. Critical Heat Flux Parameter  
As a Function of Quality -  
100 KW Loop

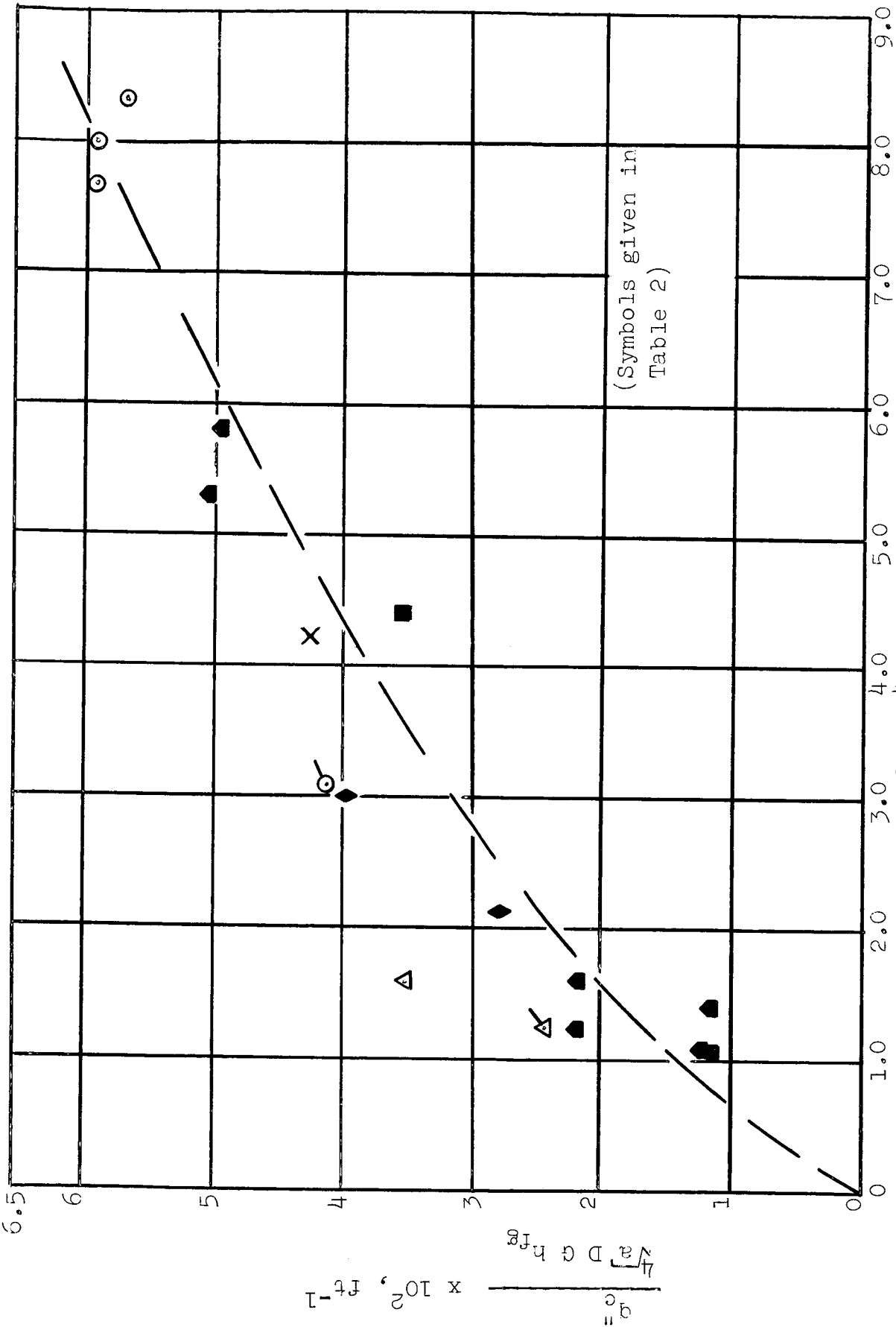


Figure 18. Critical Heat Flux Parameter as a Function of Liquid Film Thickness - 100 KW Loop

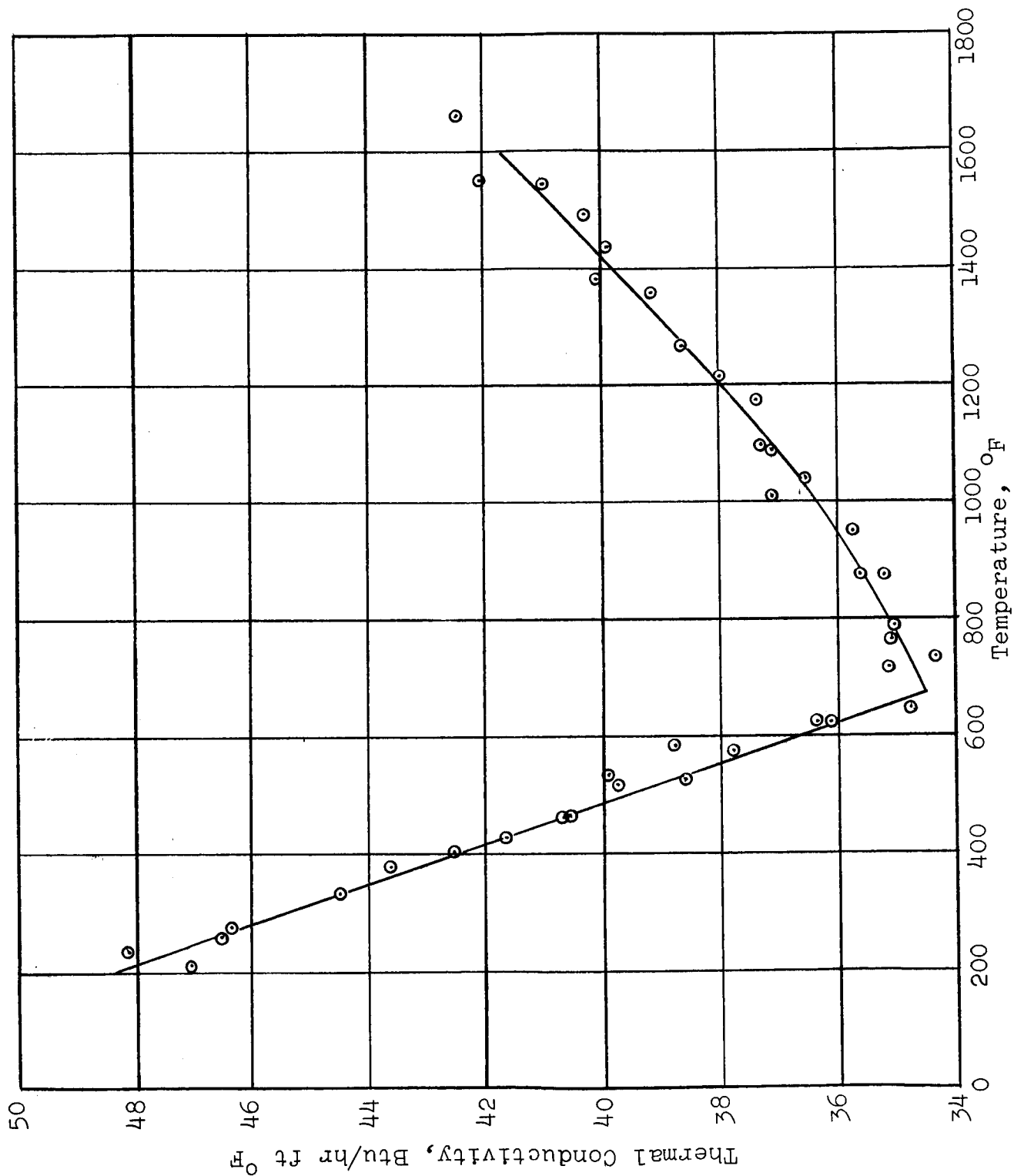


Figure 19 Thermal Conductivity of INCO Nickel 270 Material of 50 KW Loop Condenser Tube



2

Test Period: December 1964

Geometry: 5/8-inch I.D. with Tapered Pin Insert

Range of total G, lbs/sec-ft<sup>2</sup>: 3.7 to 19.3

Range of local T<sub>sat</sub>, °F: 1198 to 1435

Measuring Station:

L/D, from inlet

Top

Bottom

10

45

Approximate local X, %

86

26

Range of local q", 10<sup>5</sup> Btu/hr-ft<sup>2</sup> 0.50 to 2.3

0.64 to 3.0

Symbol in Figure 5:

0

●

Test Period: January 1965

Geometry: 3/8-inch ID plain Tube

Range of total G, lbs/sec-ft<sup>2</sup> 3.8 to 36.1

Range of local T<sub>sat</sub>, °F: 1143 to 1415

Measuring Station:

L/D, from inlet

Top

Bottom

21

75

Approximate local X, %

80

25

Range of local q", 10<sup>5</sup> Btu/hr-ft<sup>2</sup> 0.29 to 2.8

0.29 to 3.2

Symbol in Figure 5:

Δ

▲

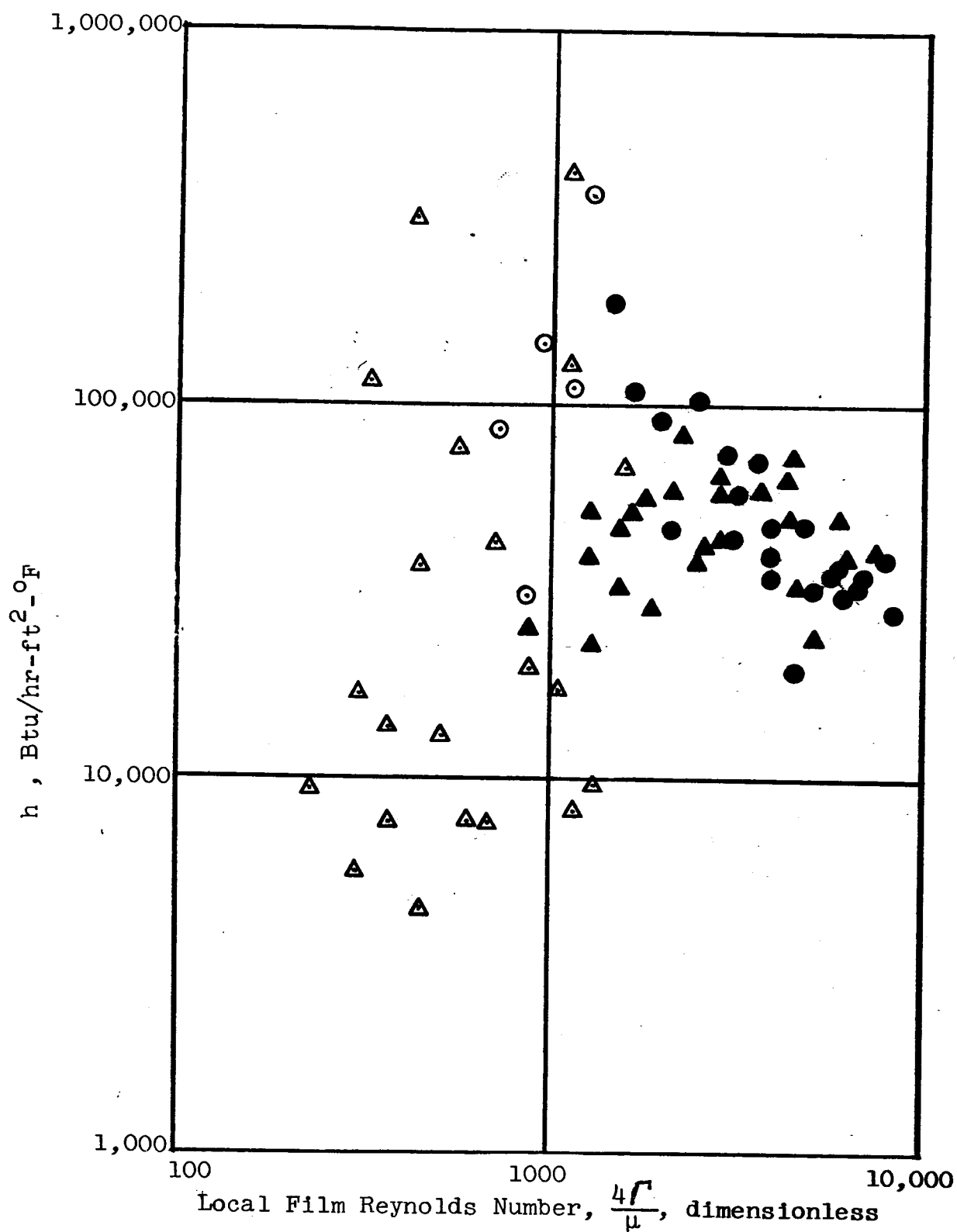


Figure 20. Local Condensing Heat Transfer Coefficients for Potassium Vapor (50 KW Facility, 5/8-inch Tube Tapered Pin Insert and 3/8-inch Tube Without Insert)

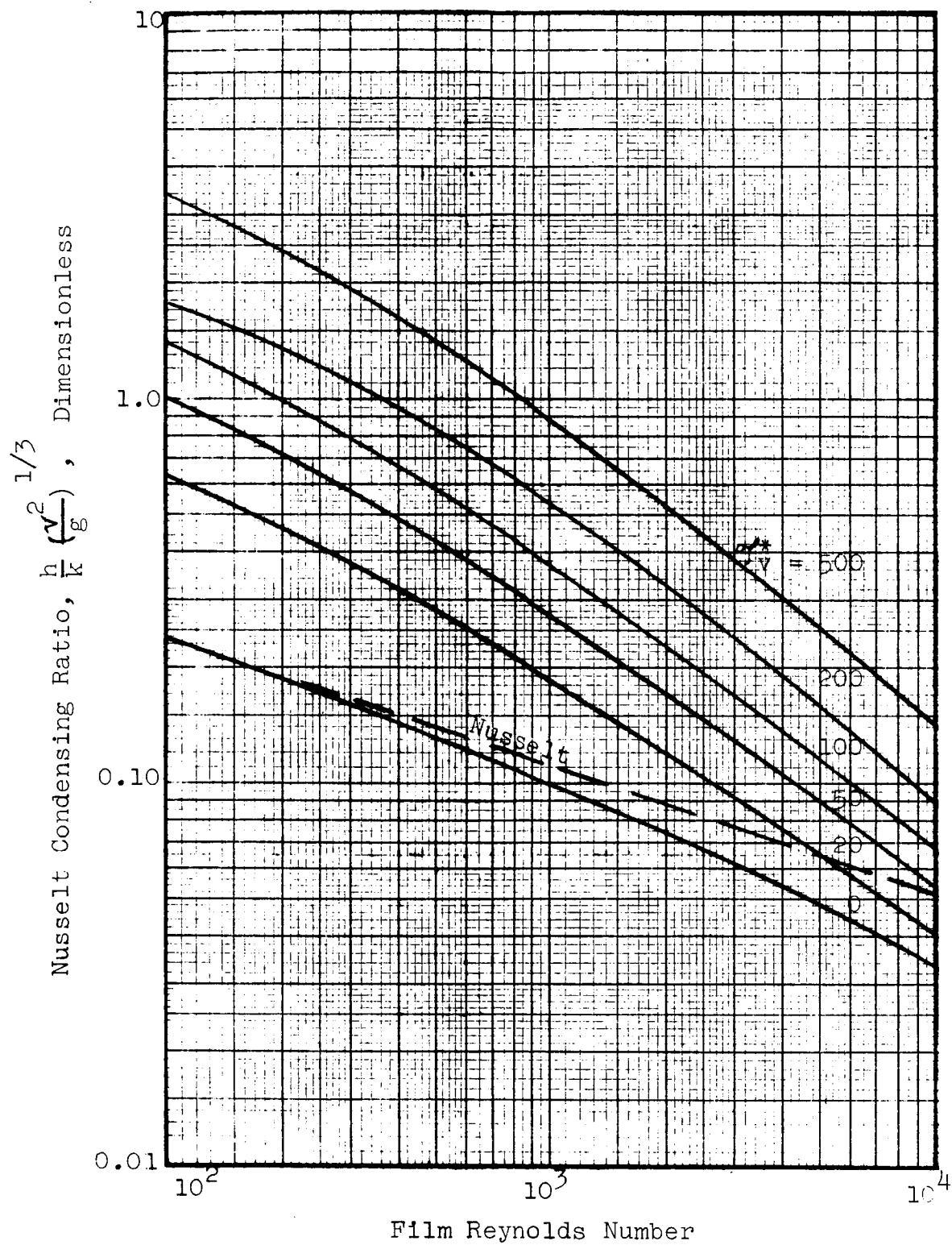


Figure 21. Predicted Nusselt Condensing Ratio from Dukler Film Thickness

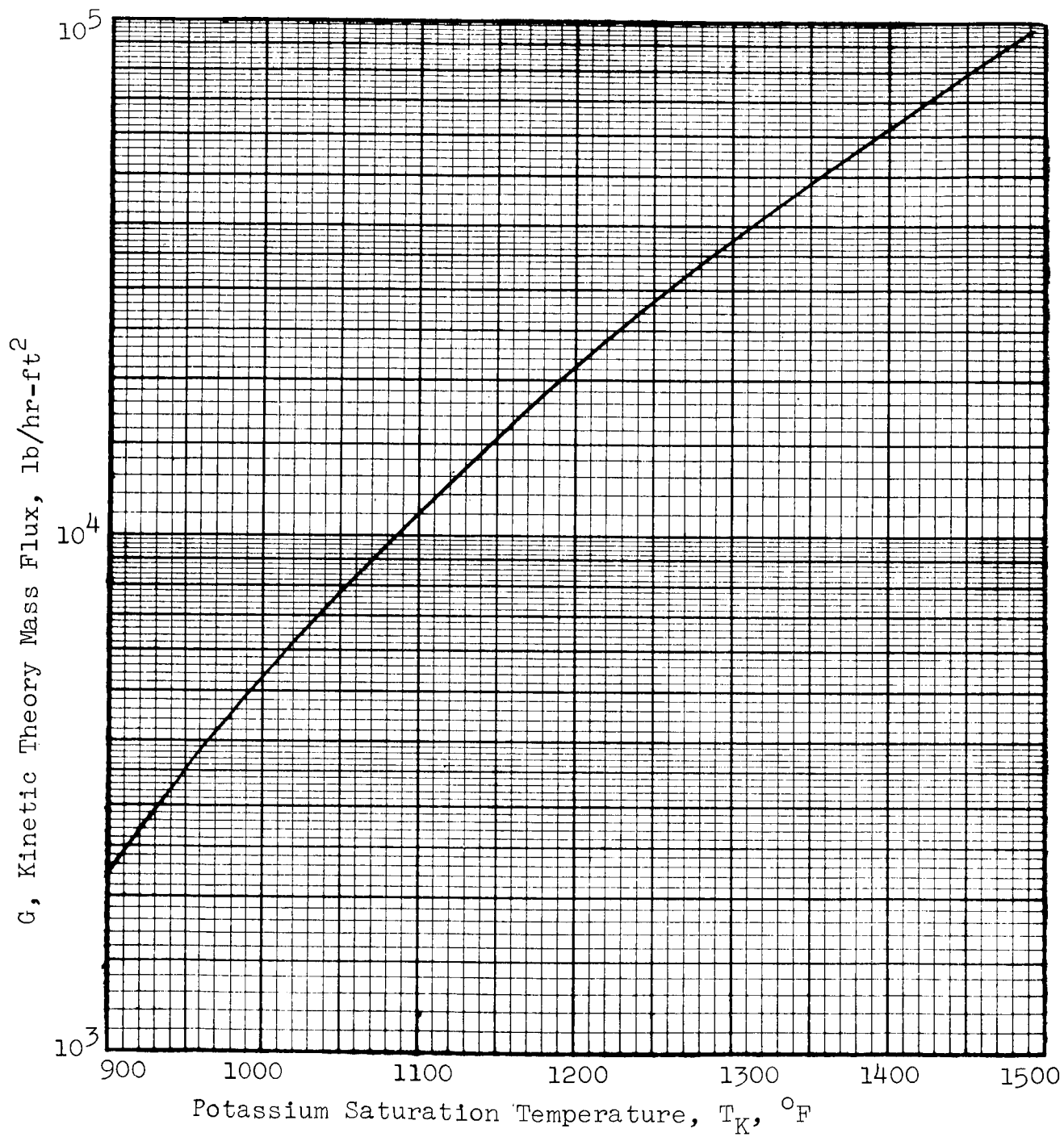


Figure 22 . Kinetic Theory Mass Flux

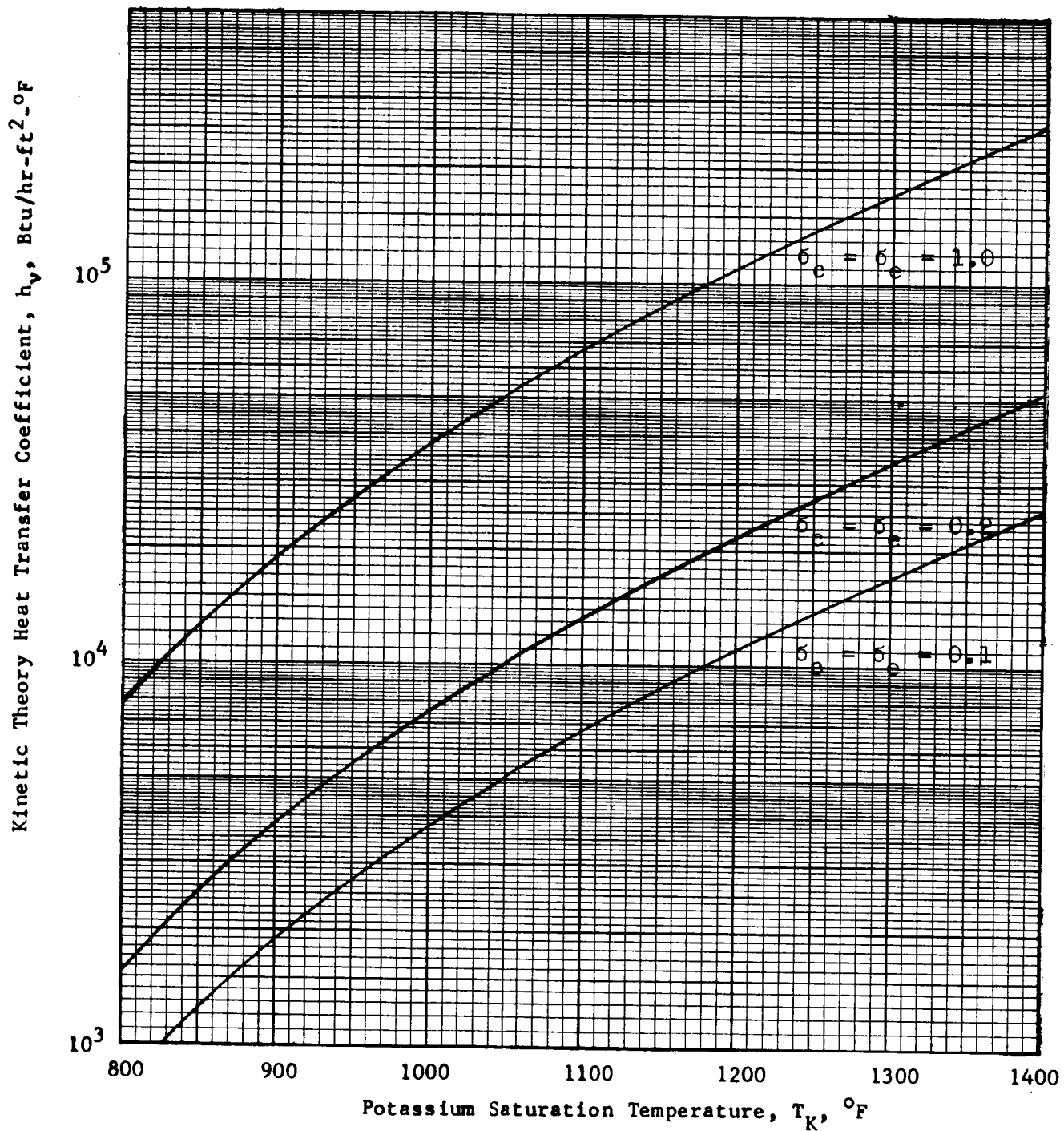


Figure 23. Kinetic Theory Heat Transfer Coefficient.

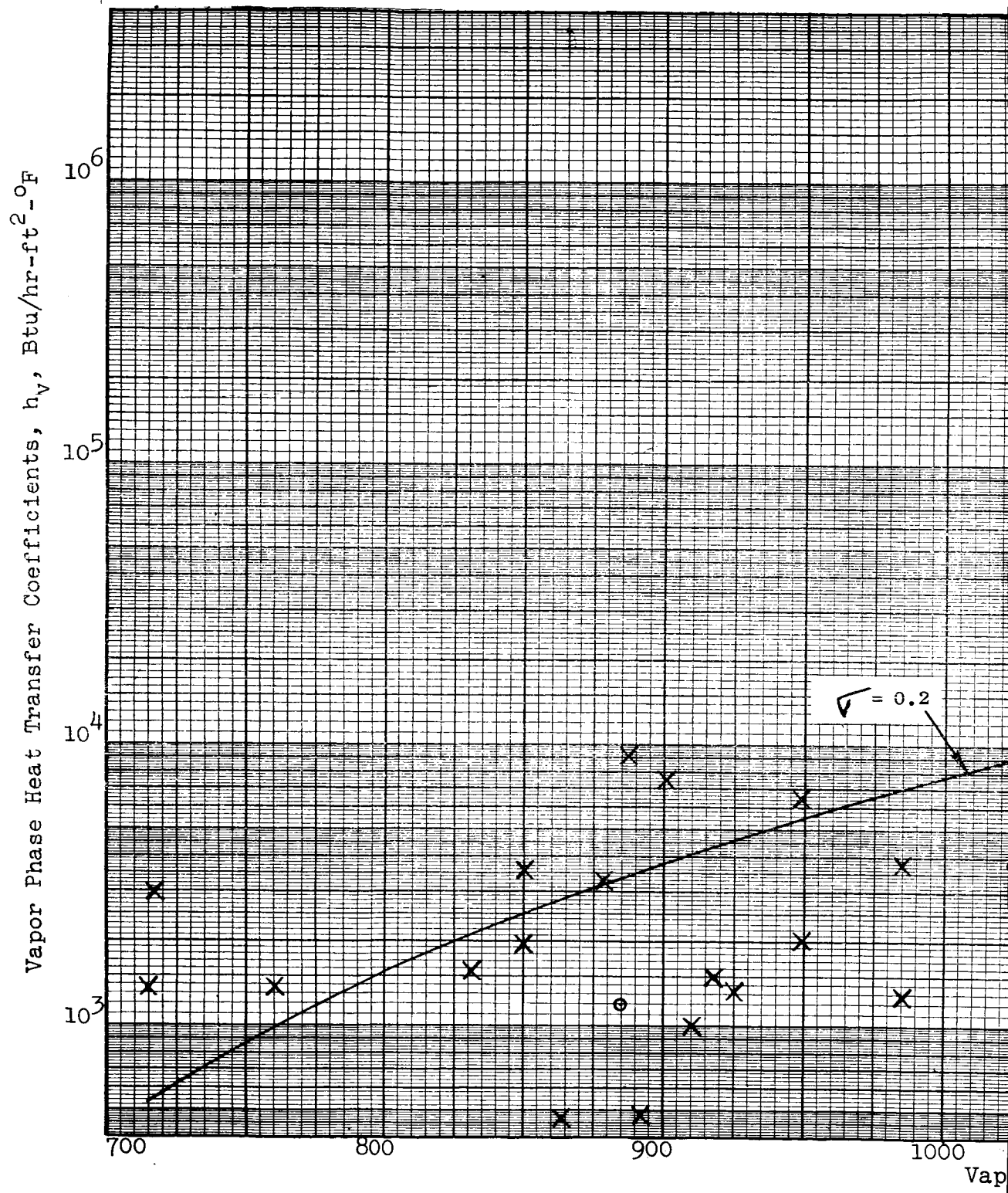
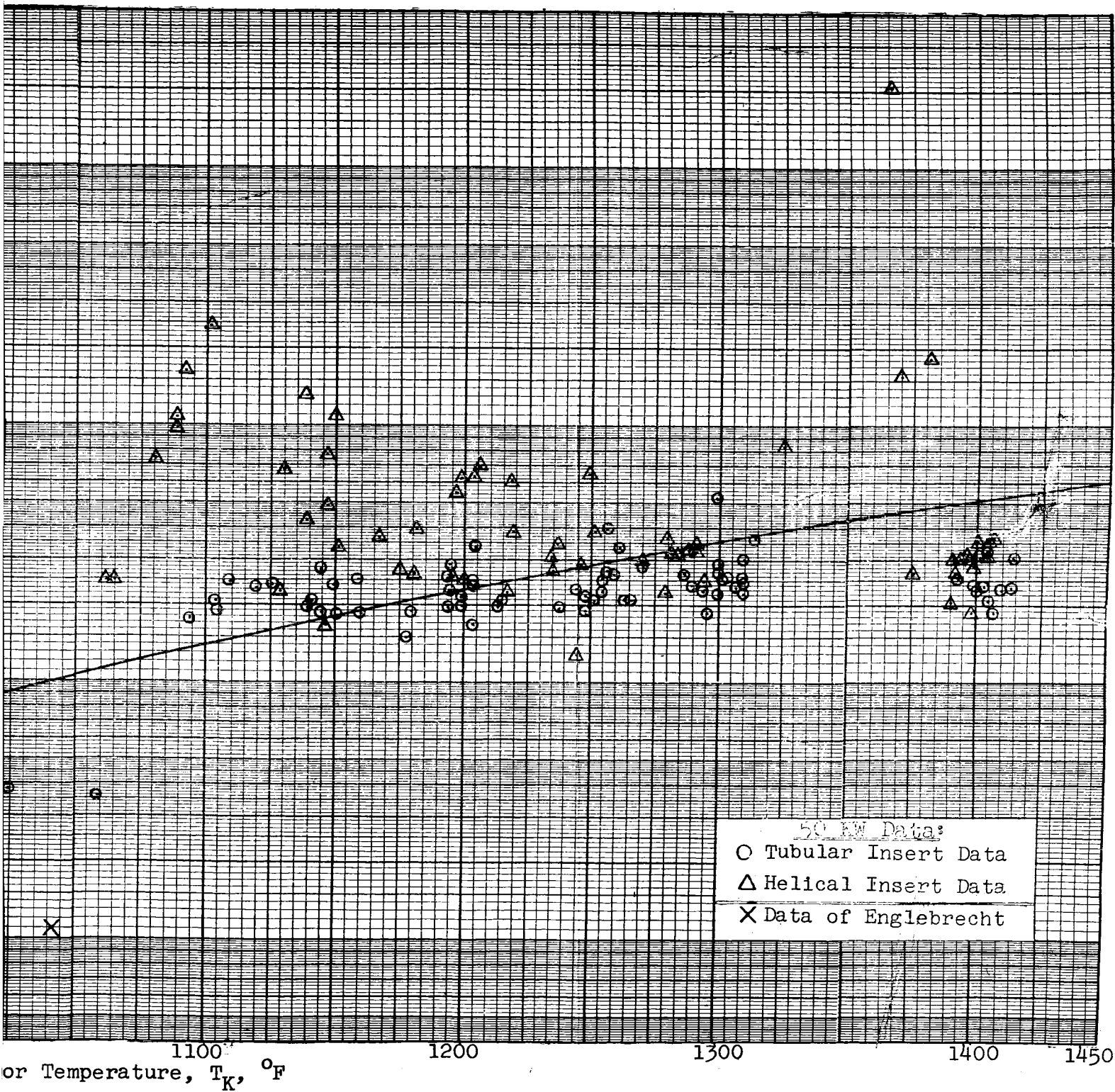


Figure 24. Comparison of Vapor Prediction (Potassi



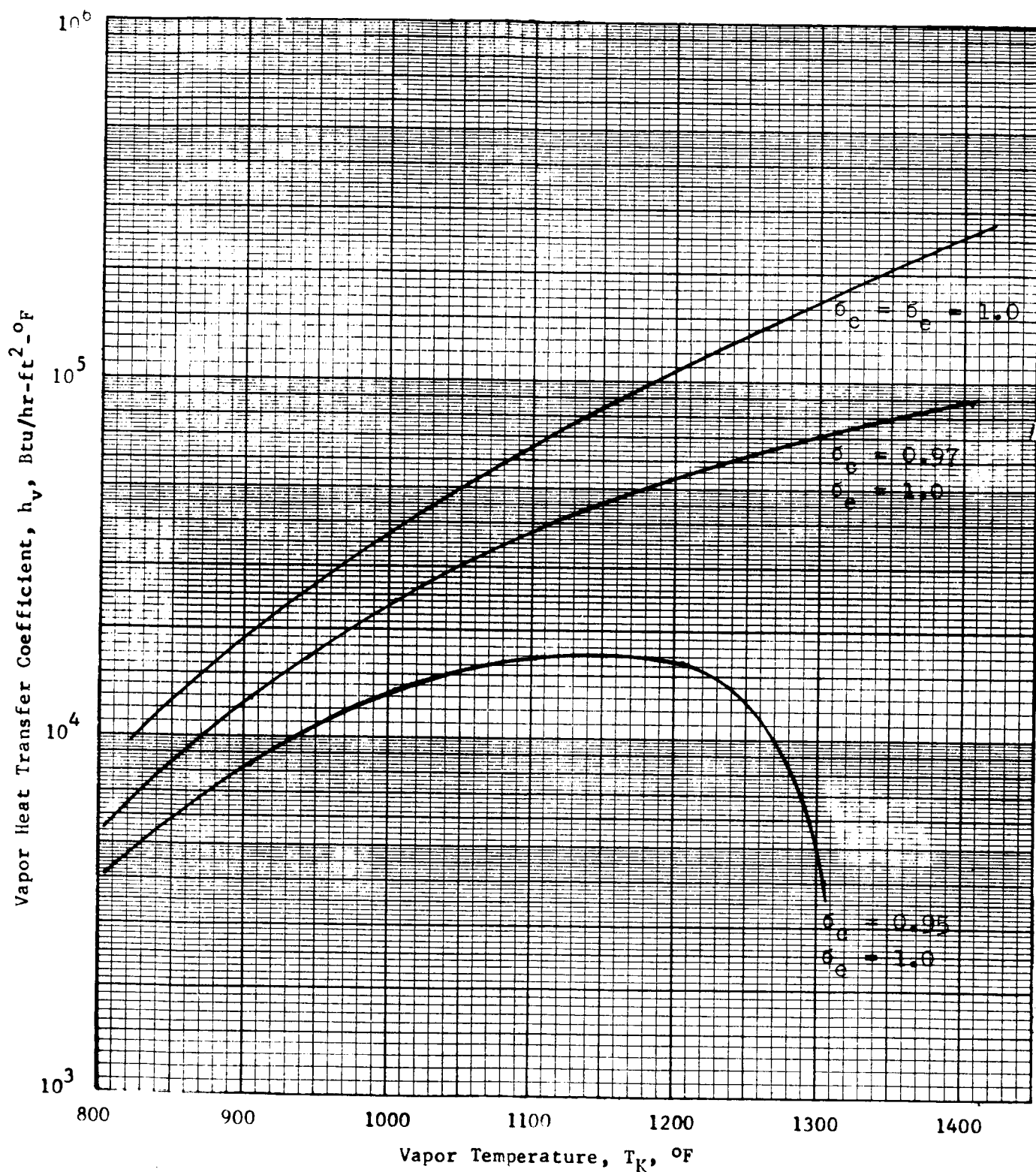


Figure 25. Kinetic Theory Heat Transfer Coefficient for  $\sigma_e = 1.0$ ,  $\sigma_c \neq 1.0$



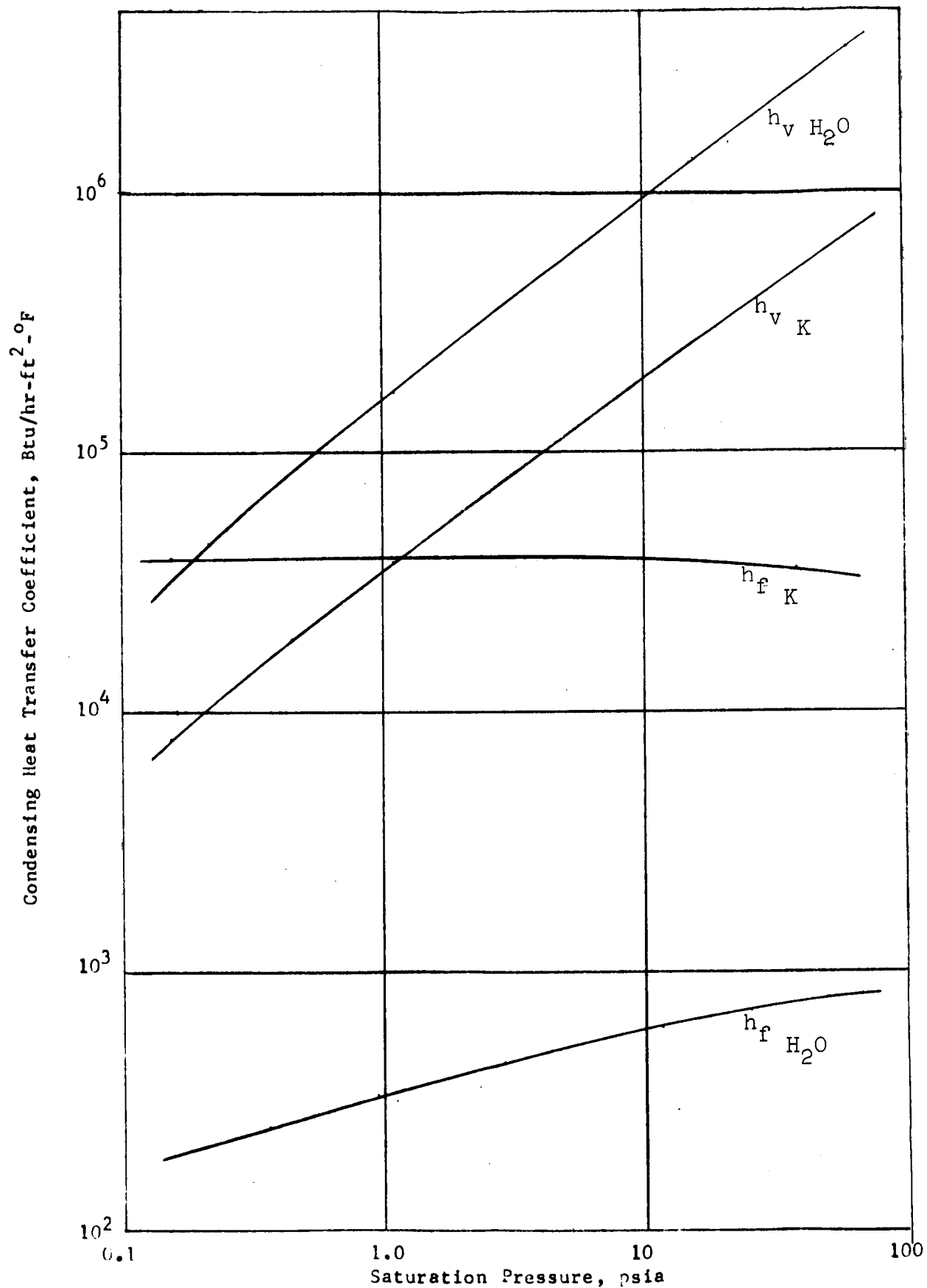
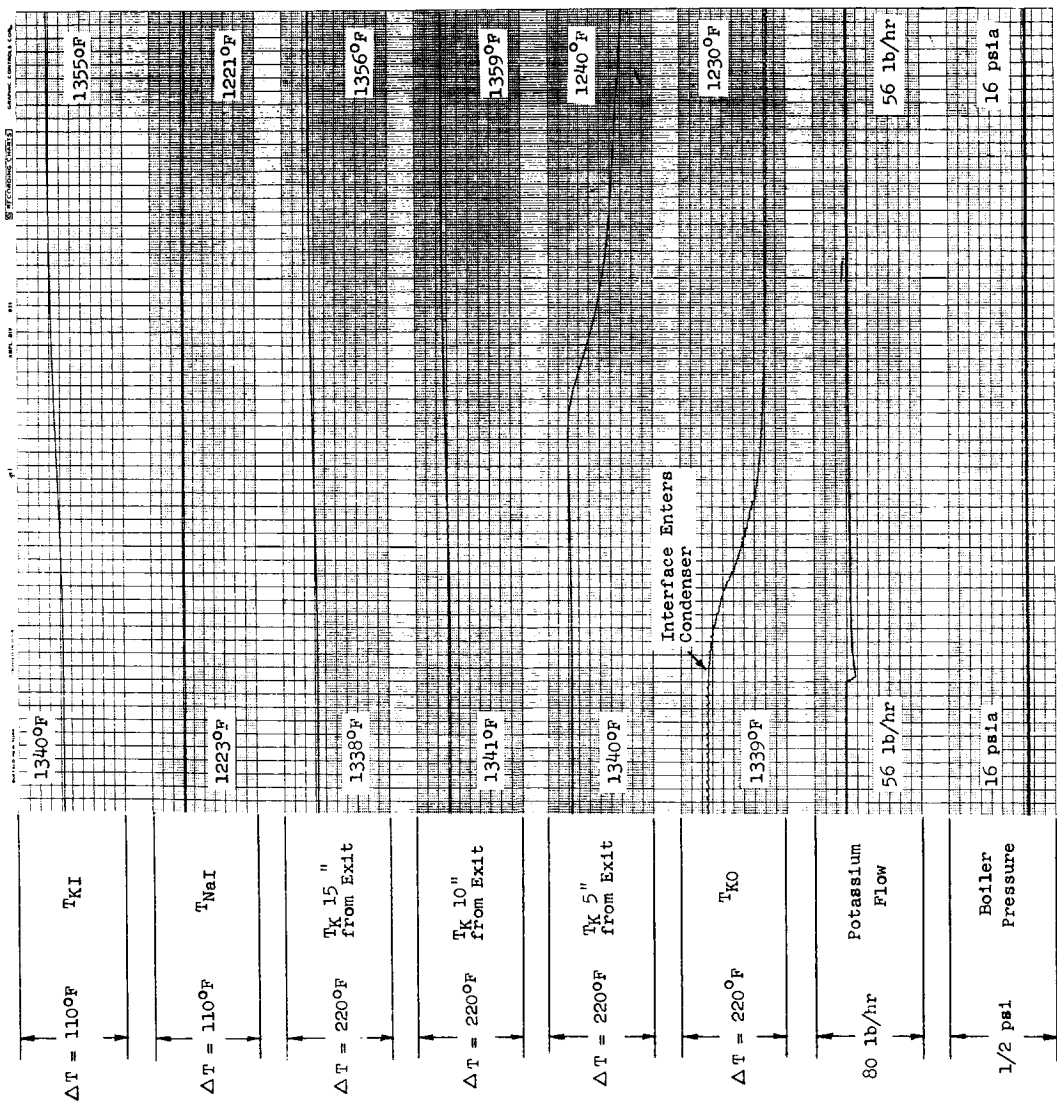


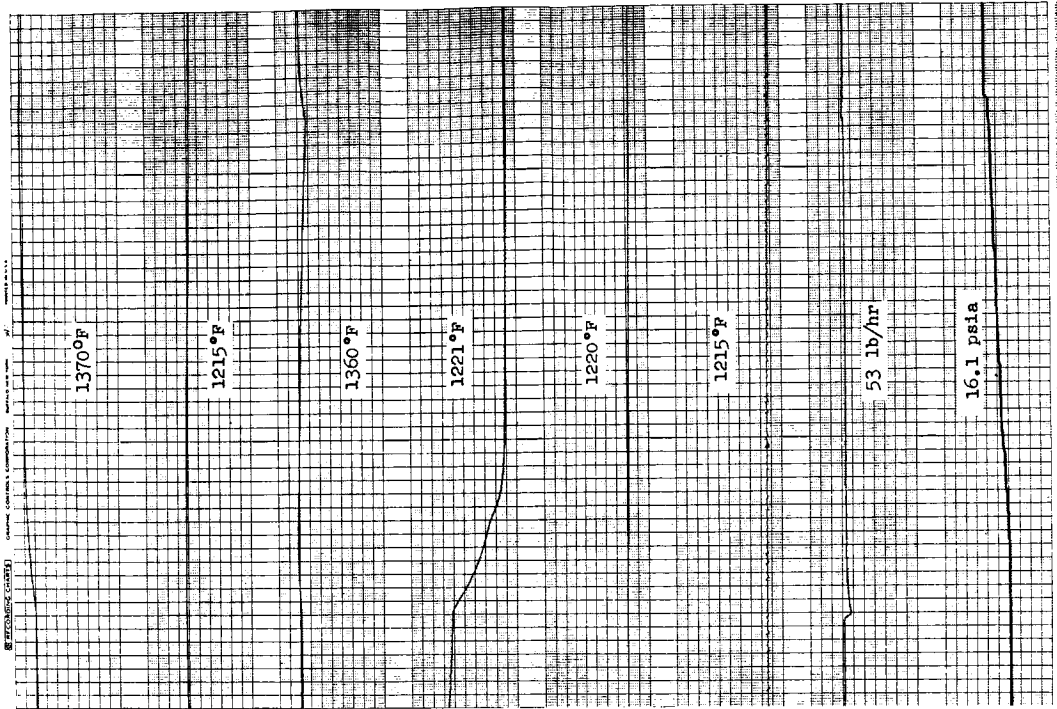
Figure 26. Comparison of Liquid Film and Vapor Heat Transfer Coefficients for Water and Potassium for  $\sigma_c = \sigma_e = 1$ .

Segment 1



Time, 1 Mark Per Second

Segment 2



Initial Conditions ( $q/A$ ) avg = 120,000 BTU/Hr.ft<sup>2</sup>  
 $W_K$  = 65 lb/hr  
 Test Section  $q$  = 20 KW

Constant Boiler Power of 25 KW

Figure 27. Liquid Vapor Interface Test (50 KW Facility, 5/8-Inch Tube with 1/4-Inch Tubular Insert).

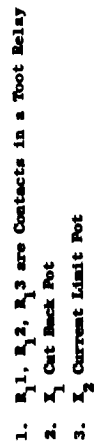


**Figure 28. Variable Automatic Power Cut Back Circuit - 100 KW Loop.**

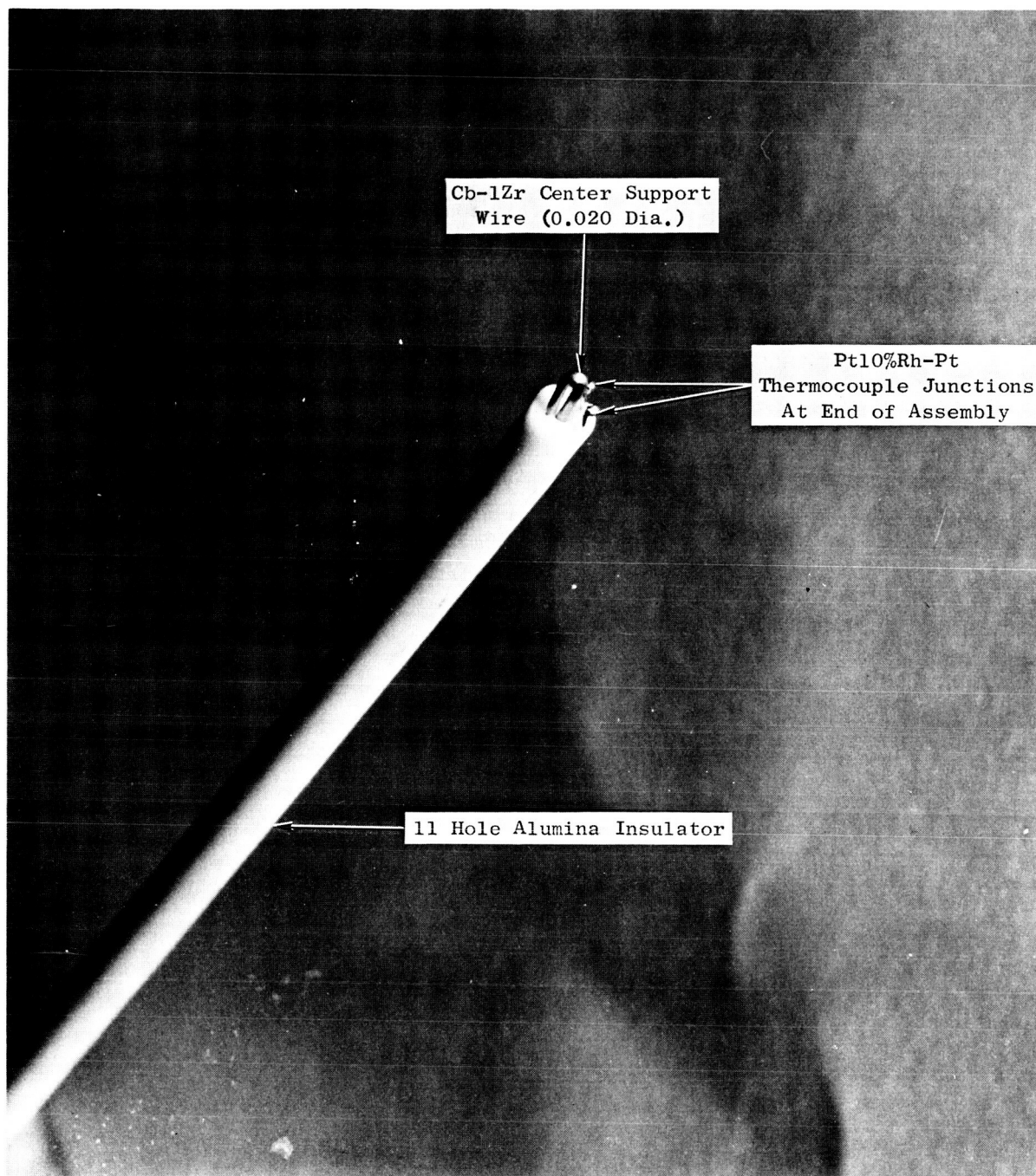


Figure 29. Thermocouple Junction at the End of an 11-Hole Insulator - 100 KW Facility.

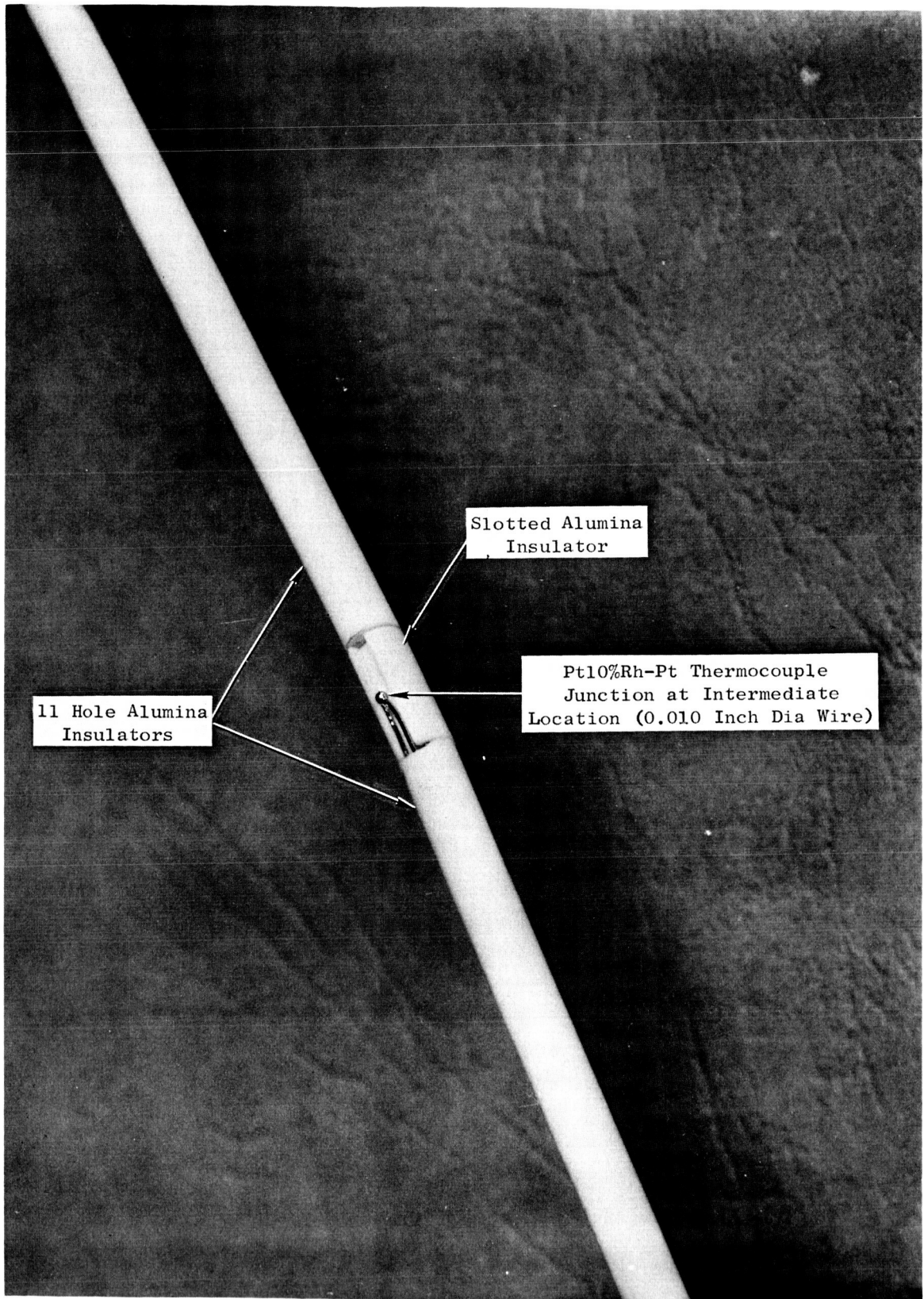


Figure 30. Thermocouple Junction in Slotted Insulator - 100 KW Facility.



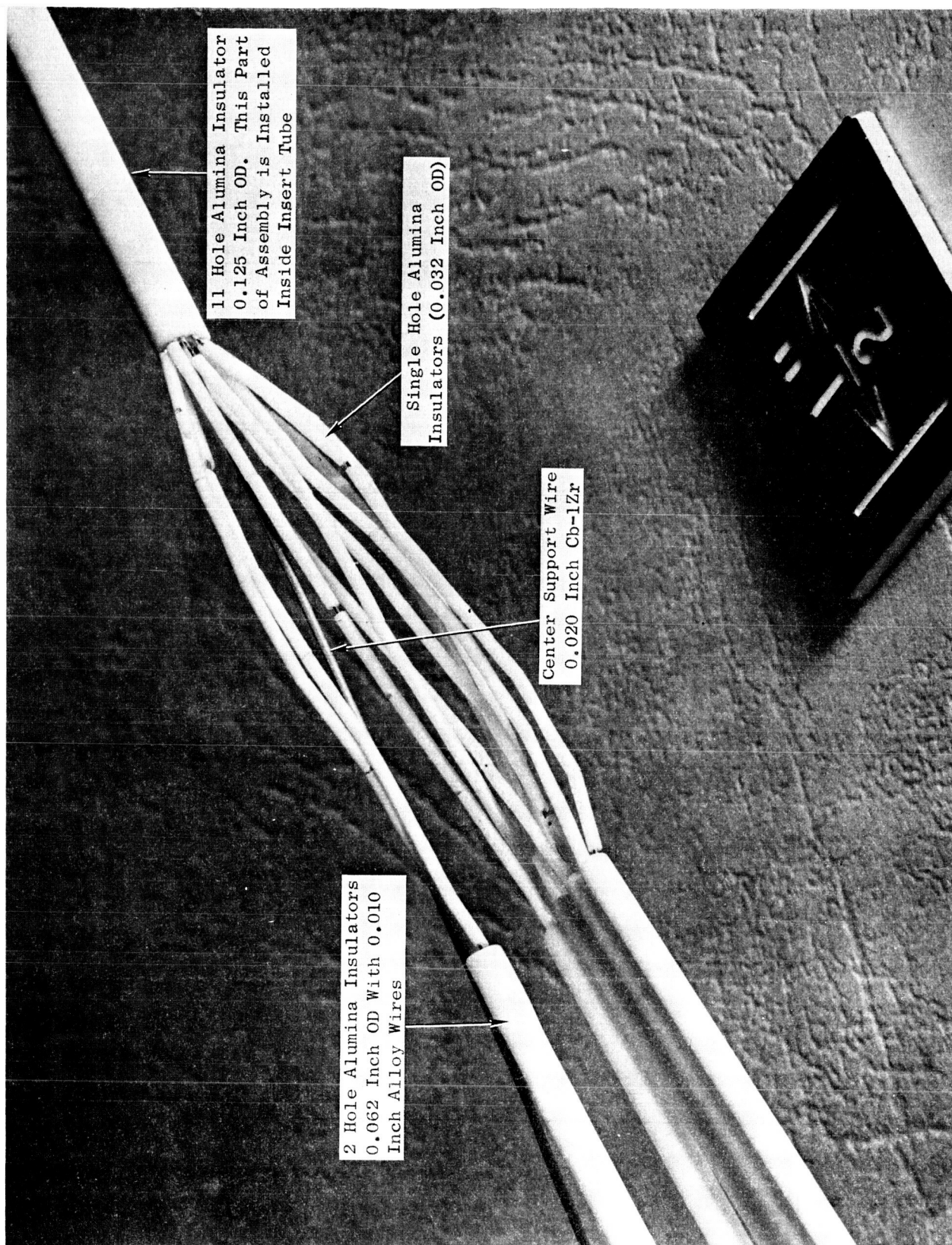


Figure 31. Transition Between 11-Hole Insulator and 2-Hole Insulator - 100 KW Facility.

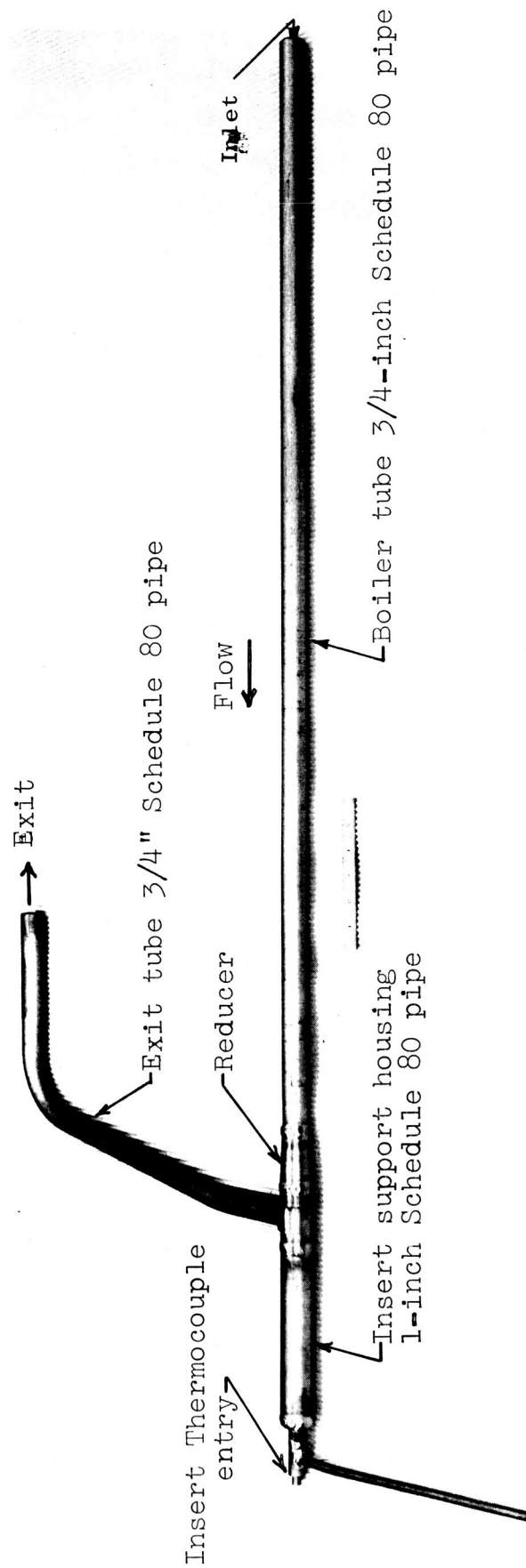


Figure 32. Cb-1Zr Test Section No. 4 for 100 KW Loop With Insert Installed.

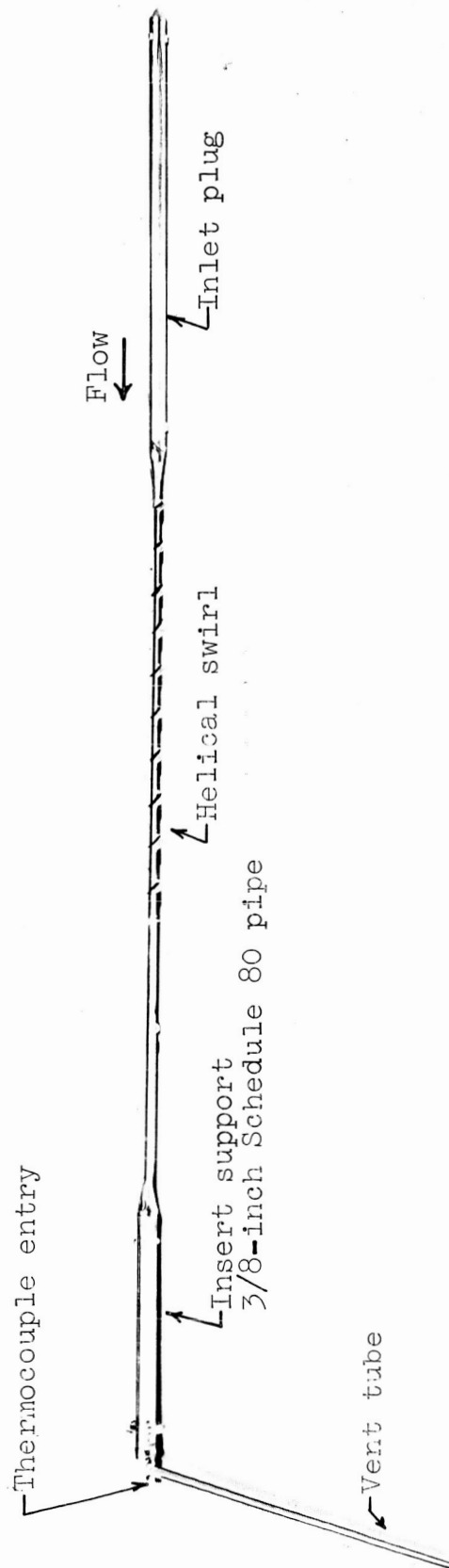


Figure 33. Cb-1Zr Helical-Plug Insert for Test Section No. 4, 100 KW Loop.



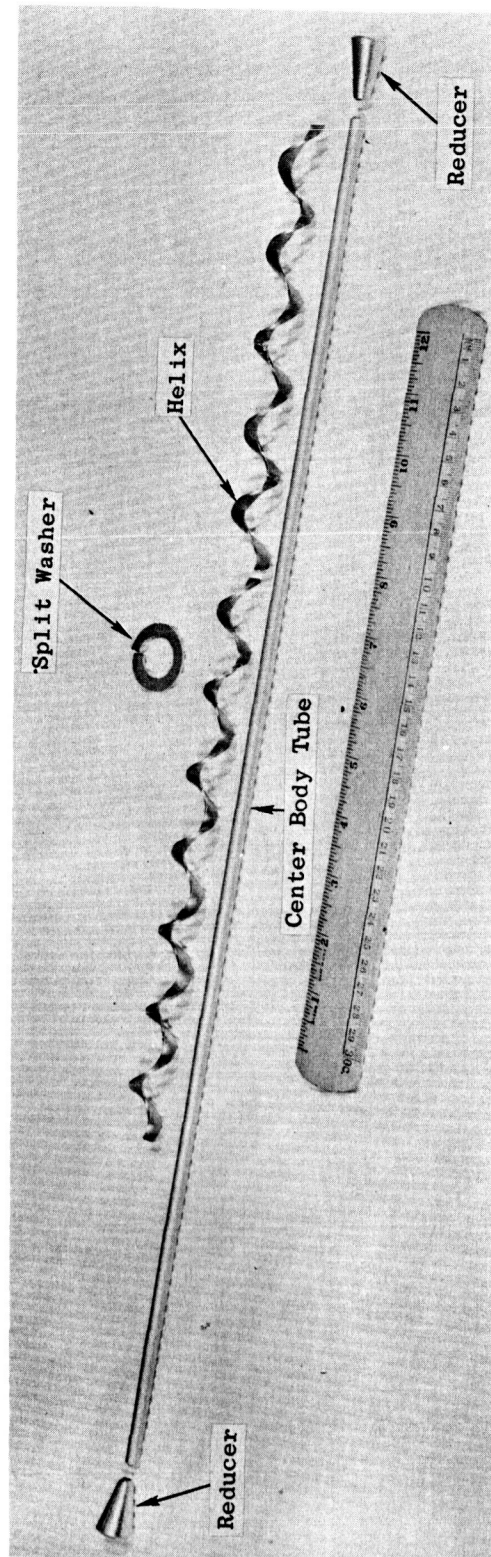


Figure 34. Component Parts of Helix (Test Section No. 4, 100 KW Facility).

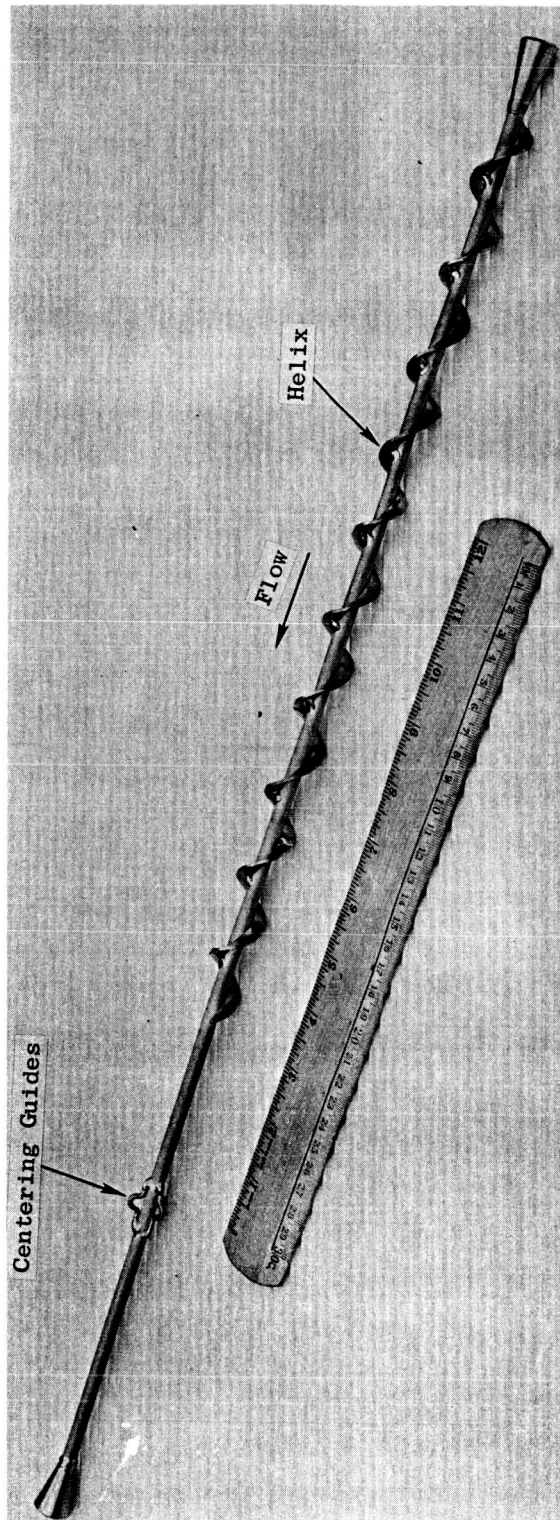


Figure 35. Helix Section of Insert (Test Section No. 4,  
100 KW Facility).

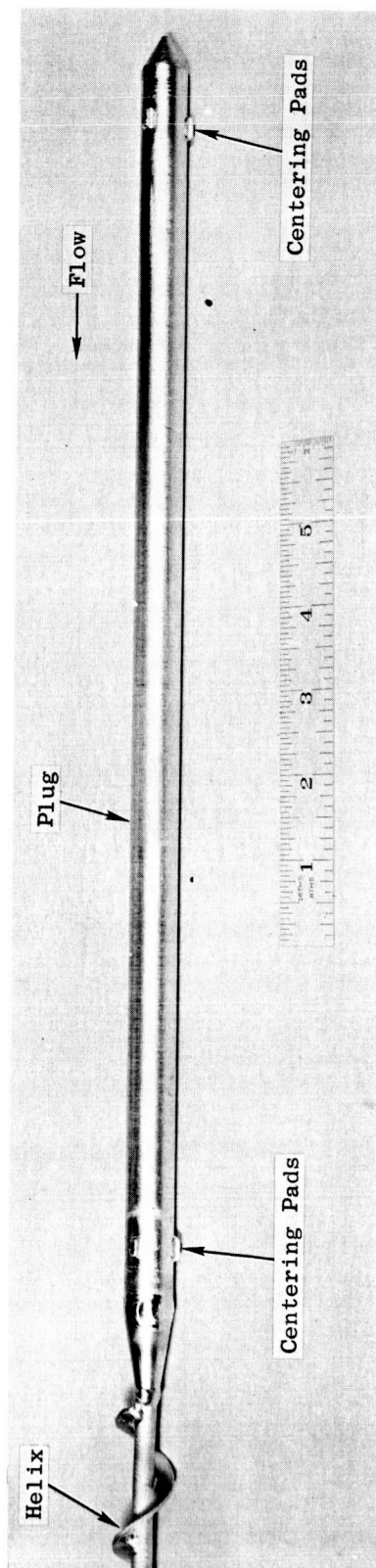


Figure 36. Insert Plug (Test Section No. 4, 100 KW Facility).

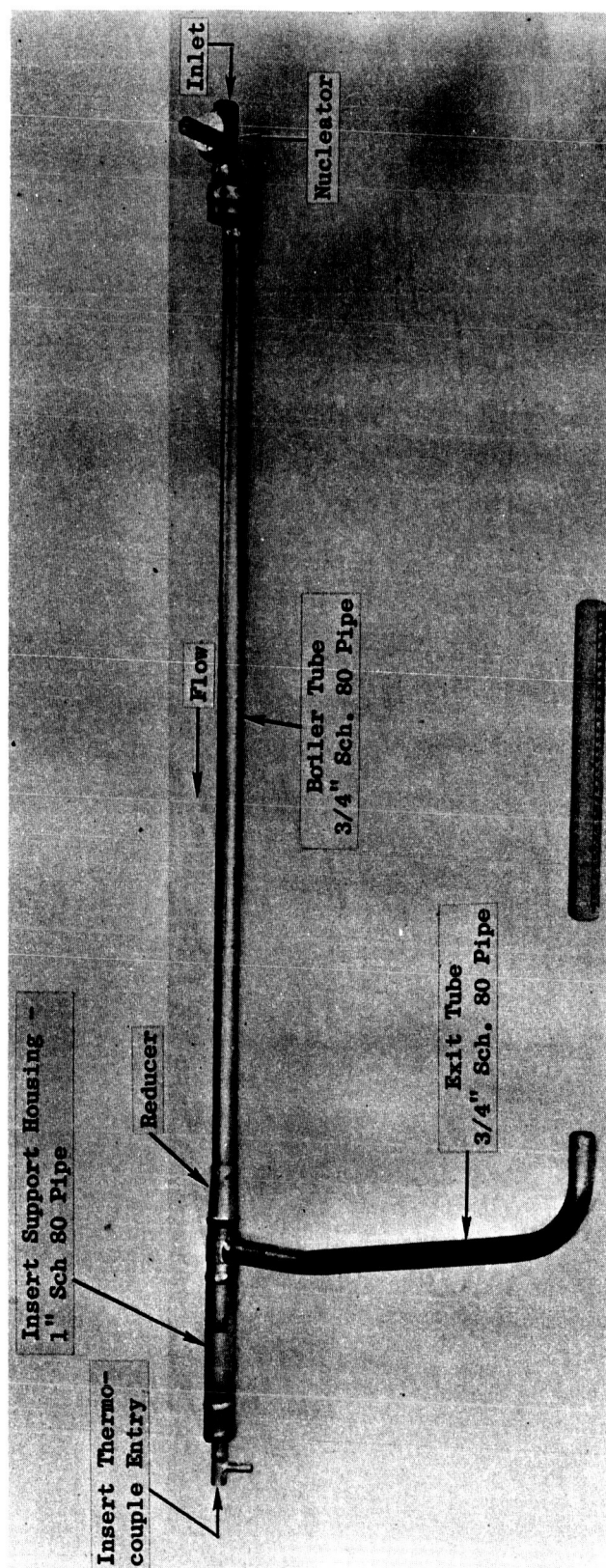


Figure 37. 100-KW Facility Test Section No. 5.

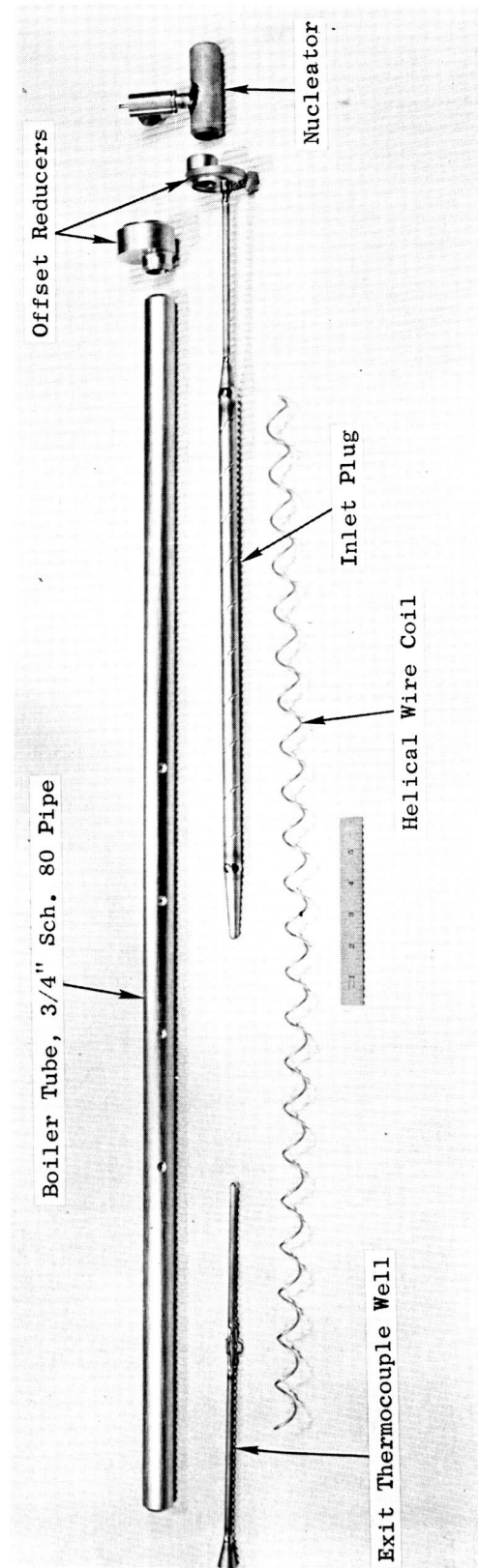


Figure 38. Test Section No. 5 Components, 100 KW Facility.



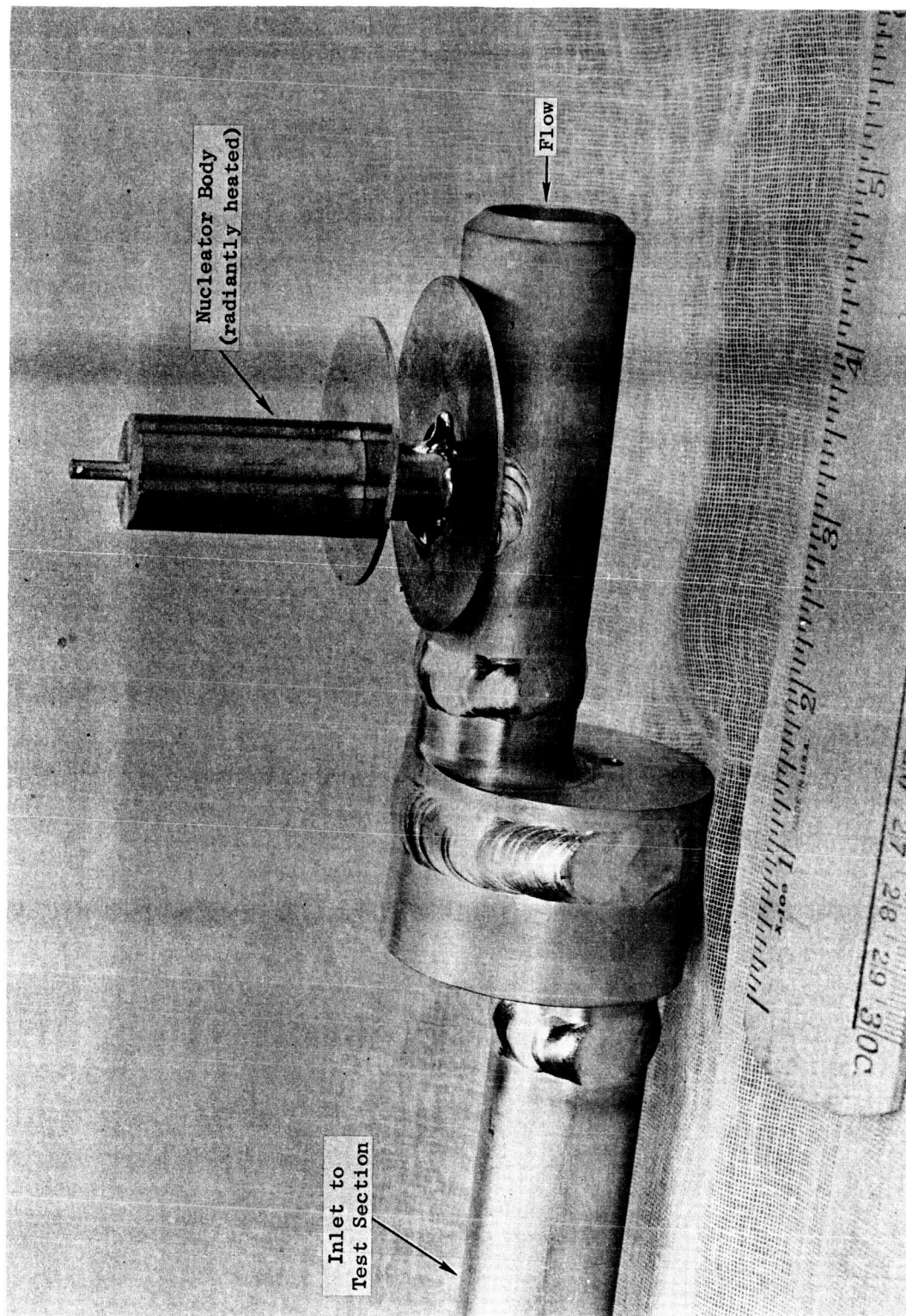


Figure 39. Boiling Nucleator (Test Section No. 5, 100 KW Facility).

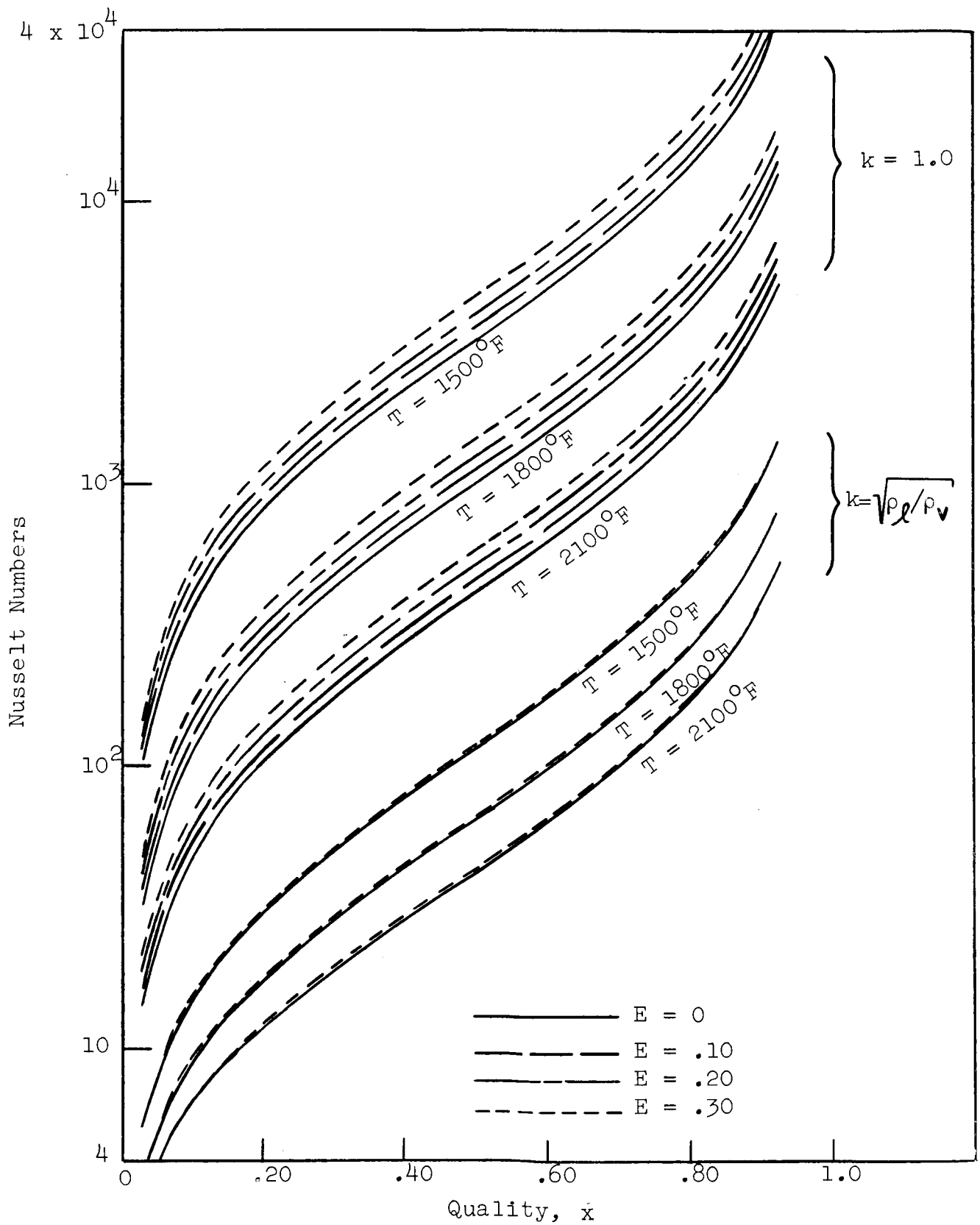


Figure 40. Effect of Liquid Entrainment on the Nusselt Numbers  
Calculated from the Film Evaporation Model

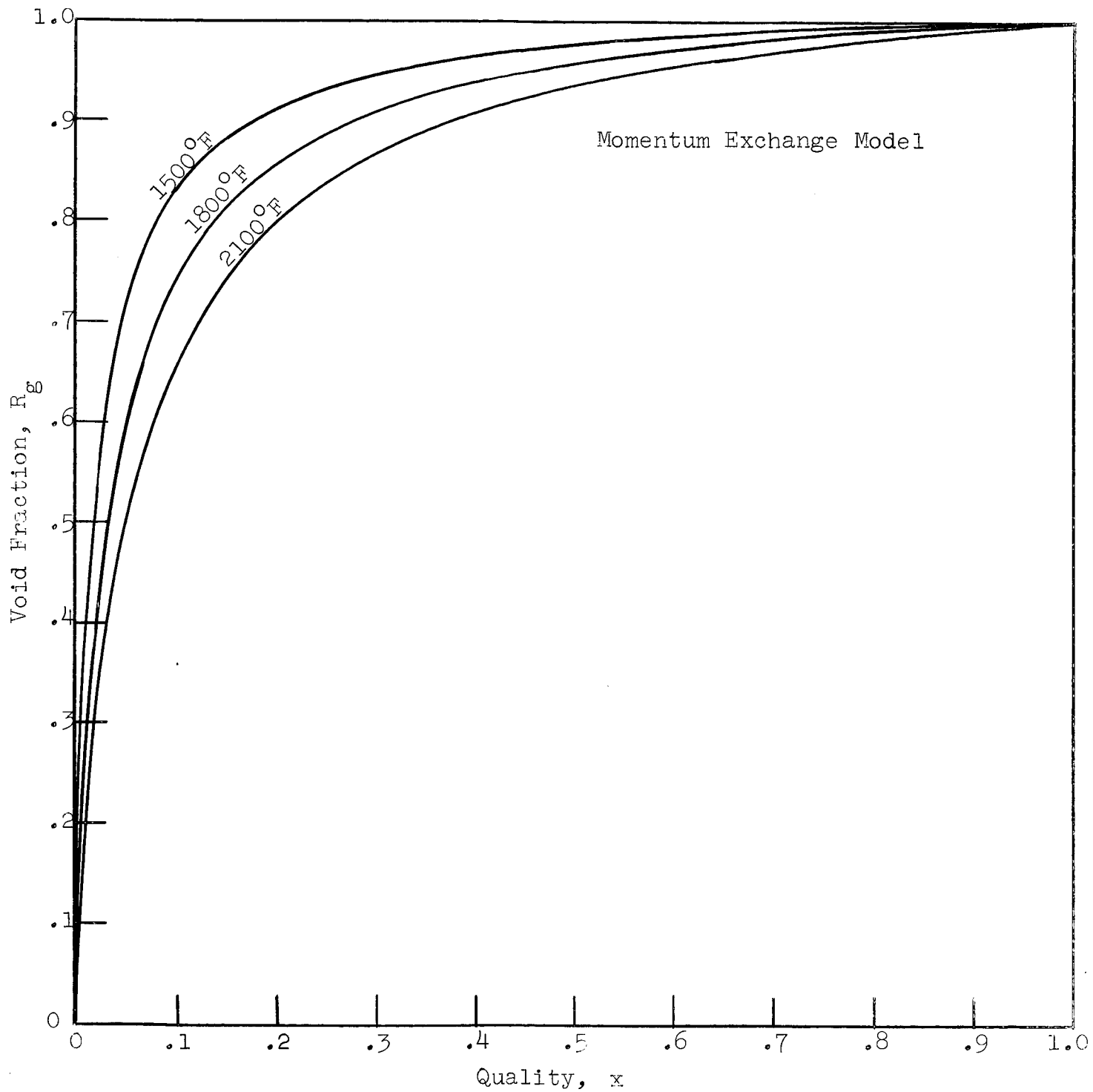


Figure 41. Void Fraction as a Function of Quality for Potassium



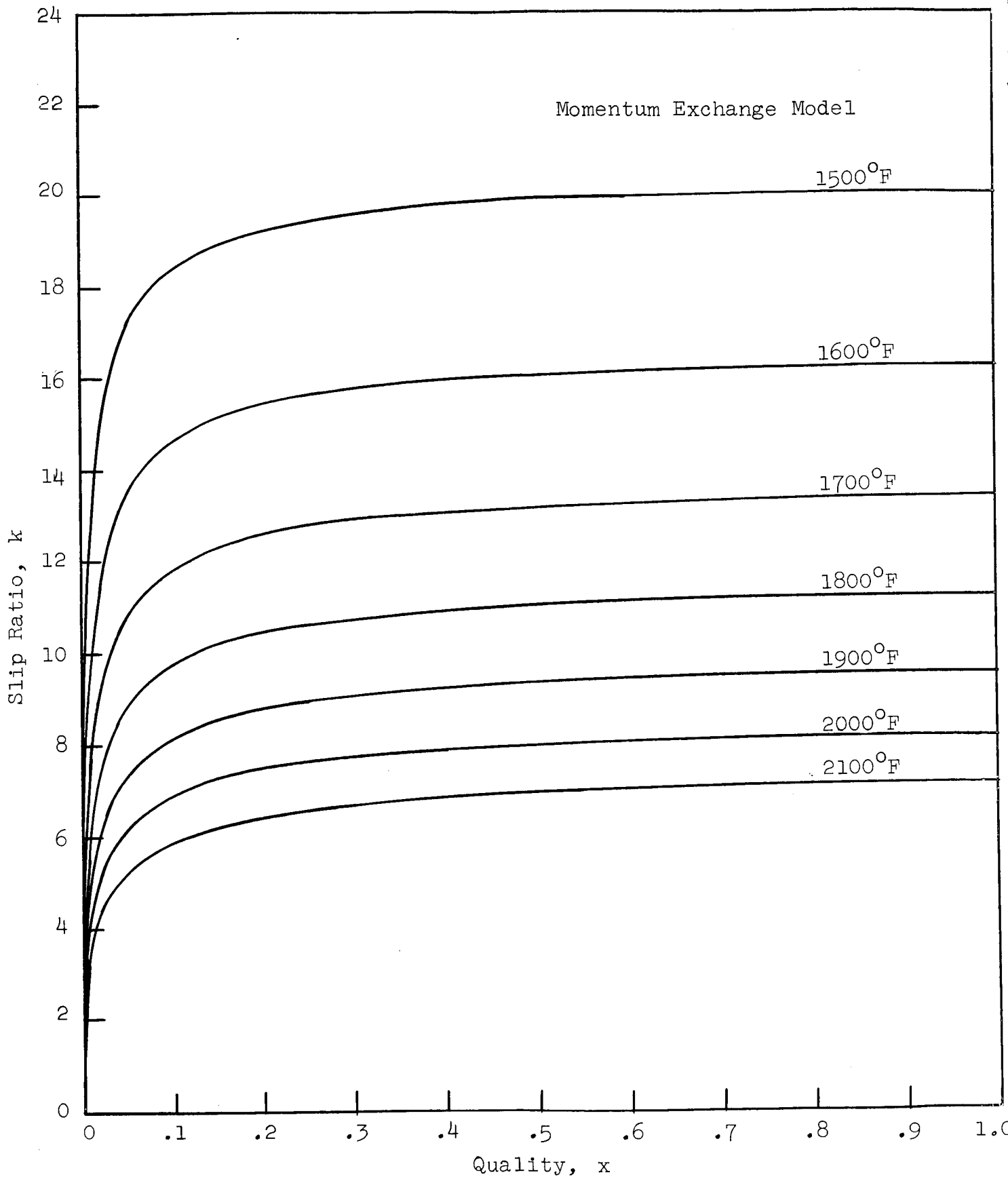


Figure 42. Slip Ratio as a Function of Quality for Potassium

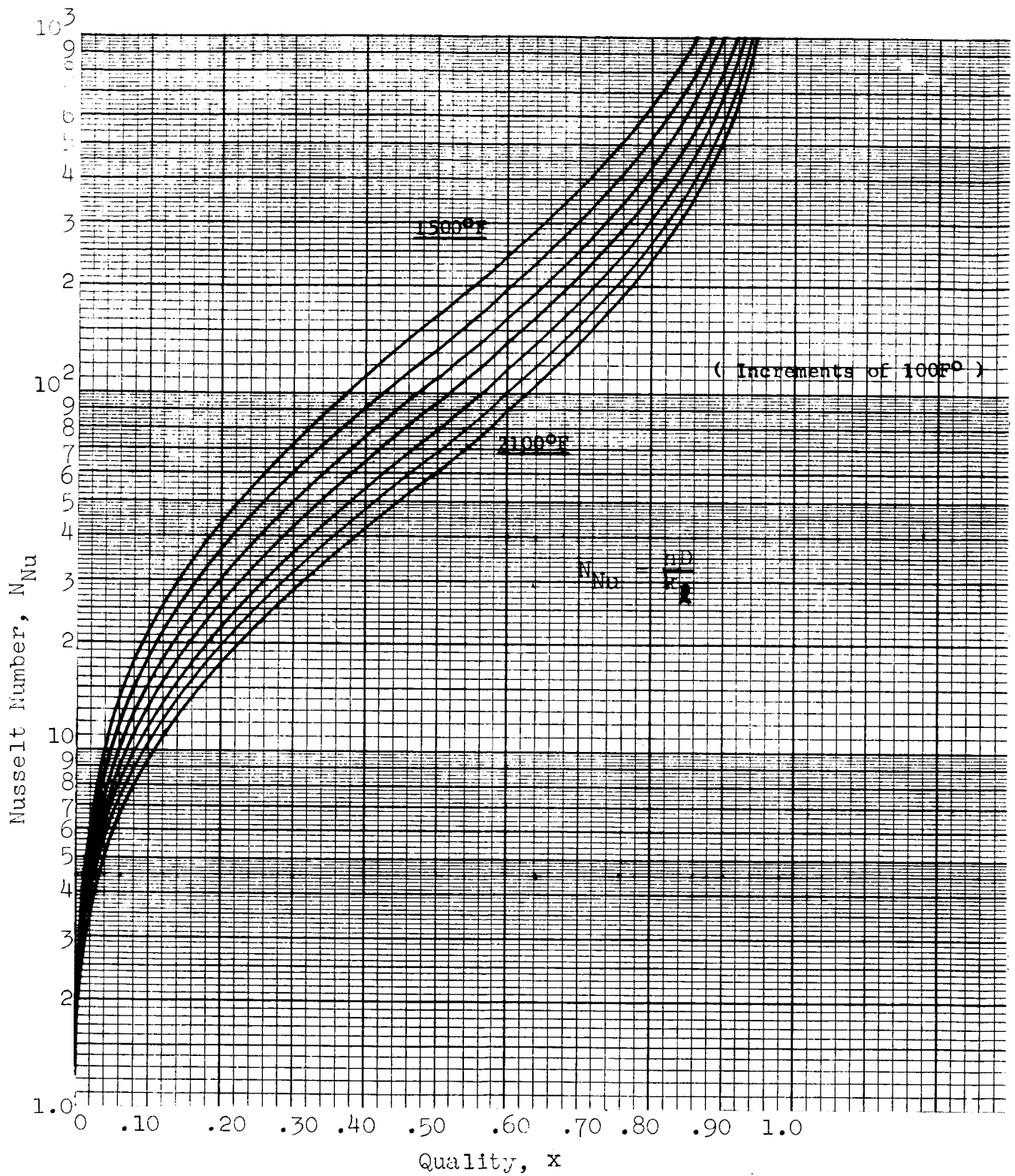


Figure 43. Nusselt Numbers from the Film Evaporation Model

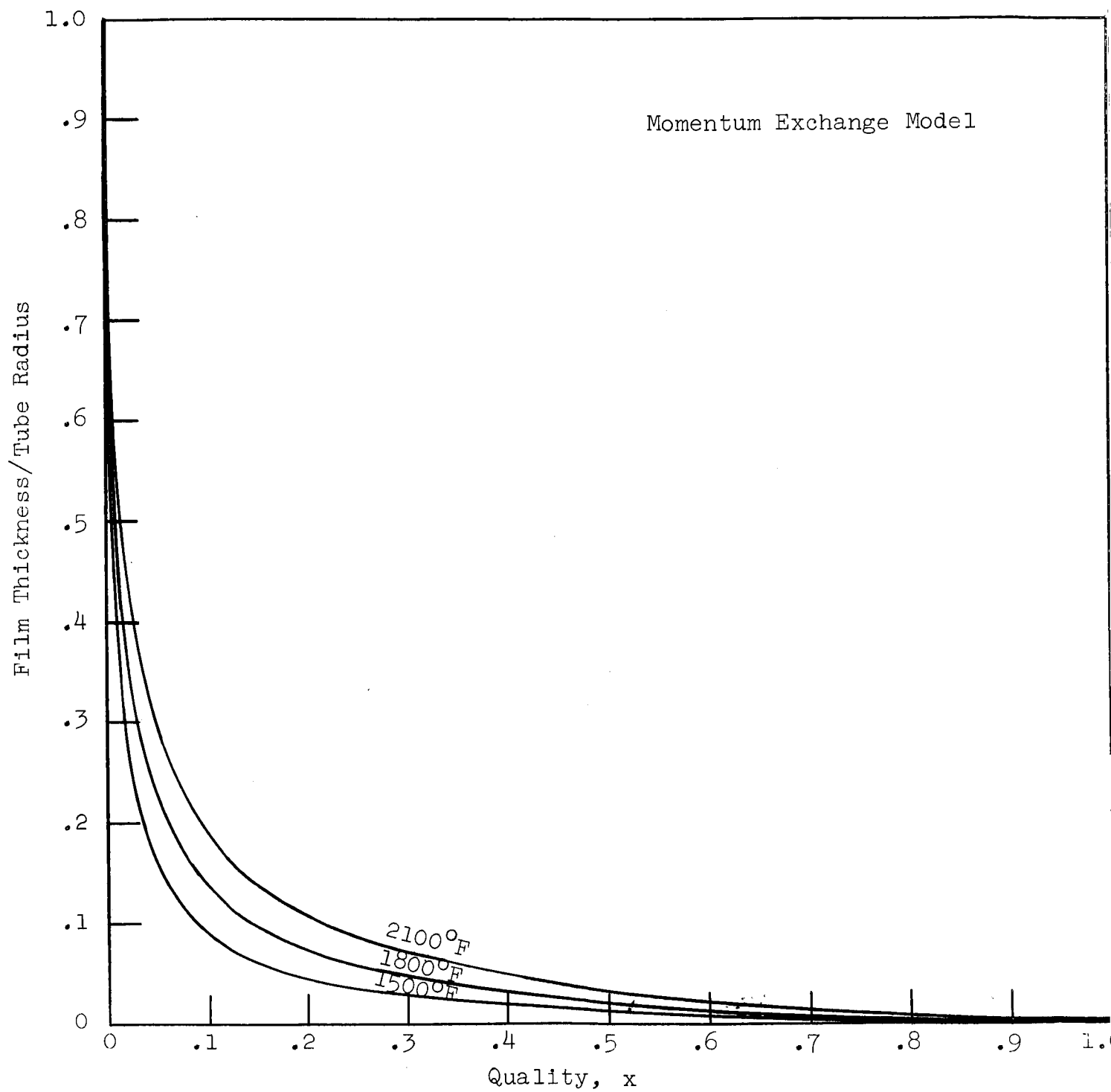


Figure 44. Film Thickness to Tube Radius Ratio as a Function of Quality

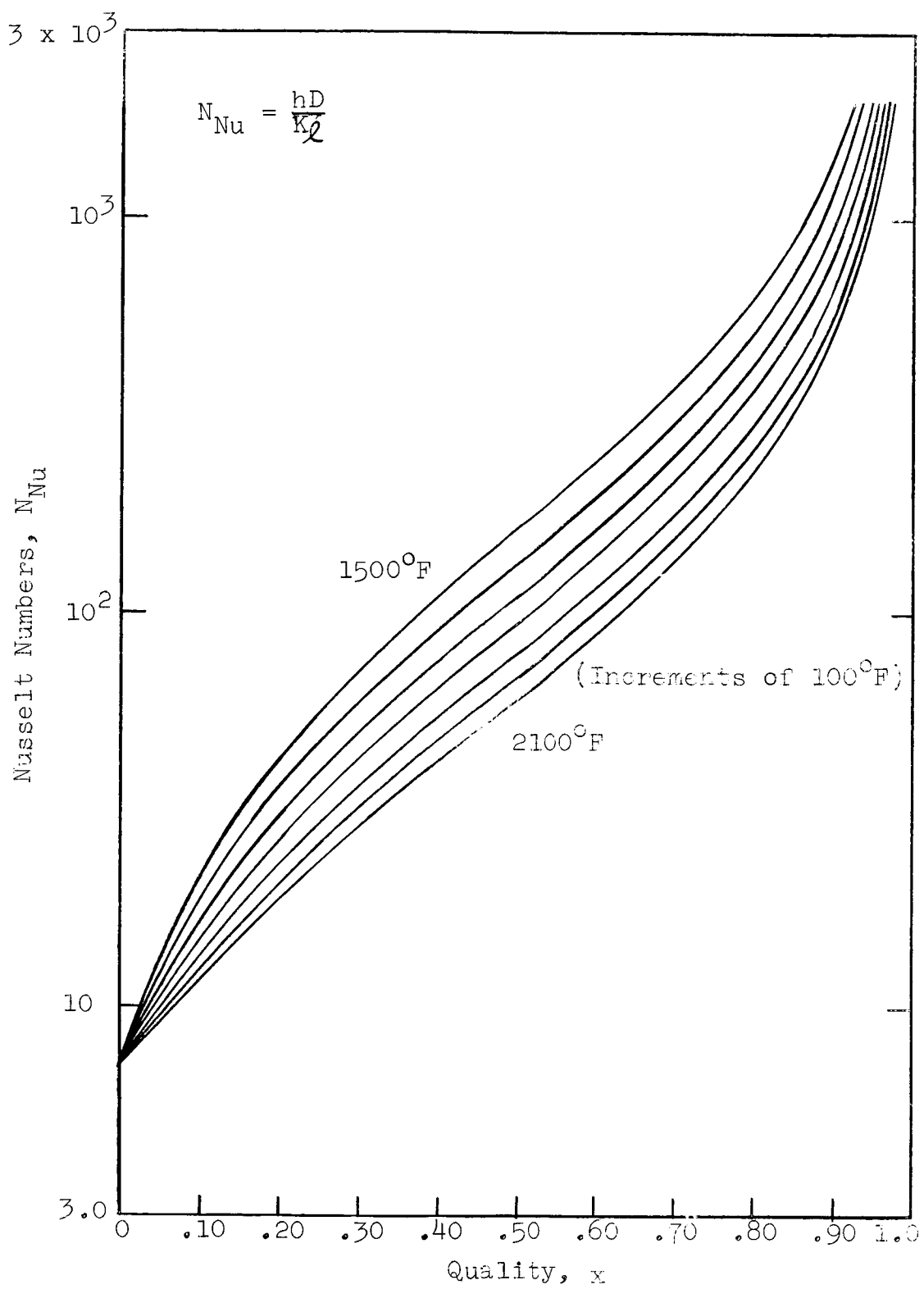


Figure 45. Modified Film Evaporation Nusselt Numbers

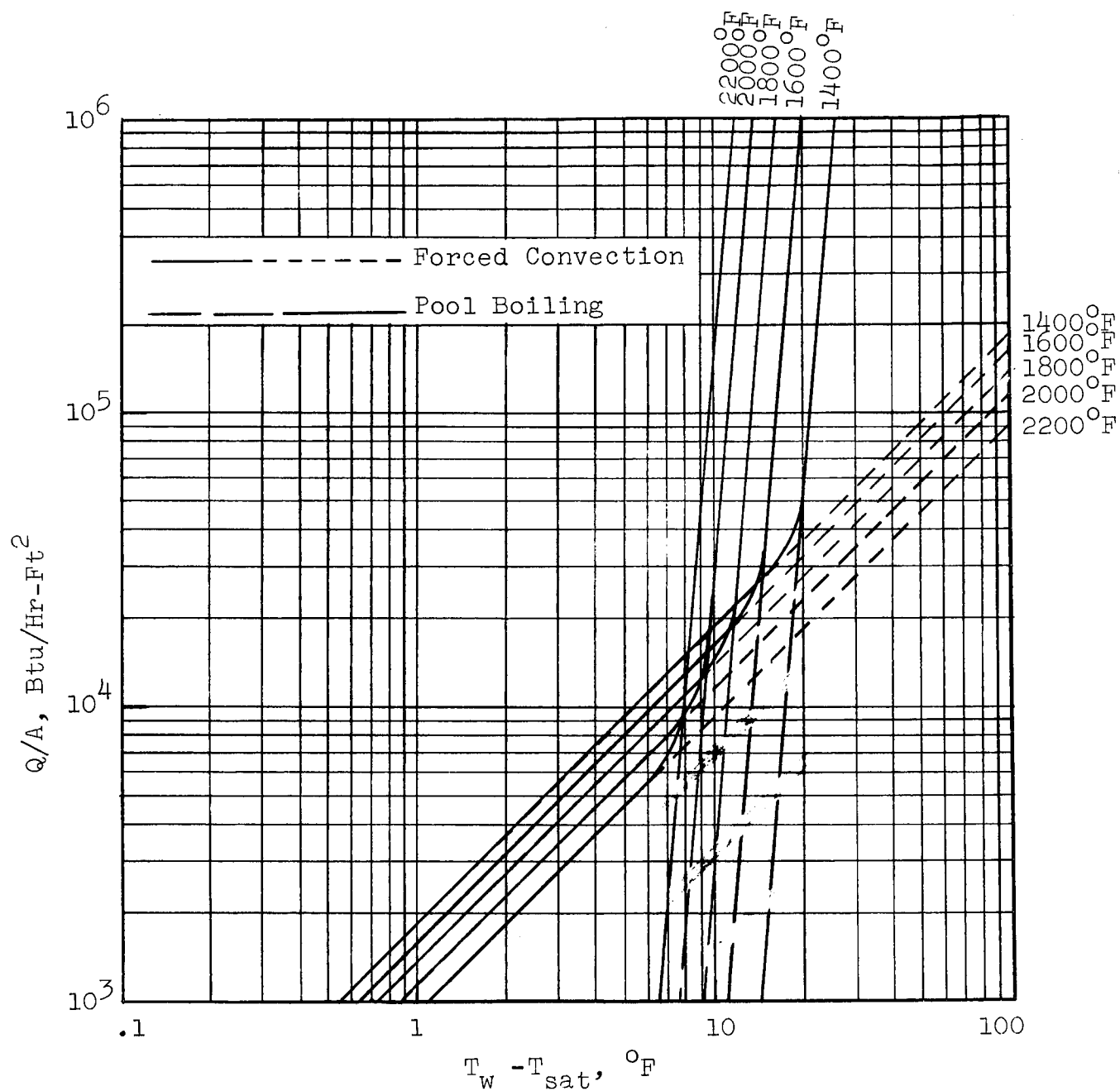


Figure 46. Heat Flux as a Function of  $T_w - T_{sat}$  for the Forced Convection Nucleate Boiling Model (Tube I.D. = .767 in.)

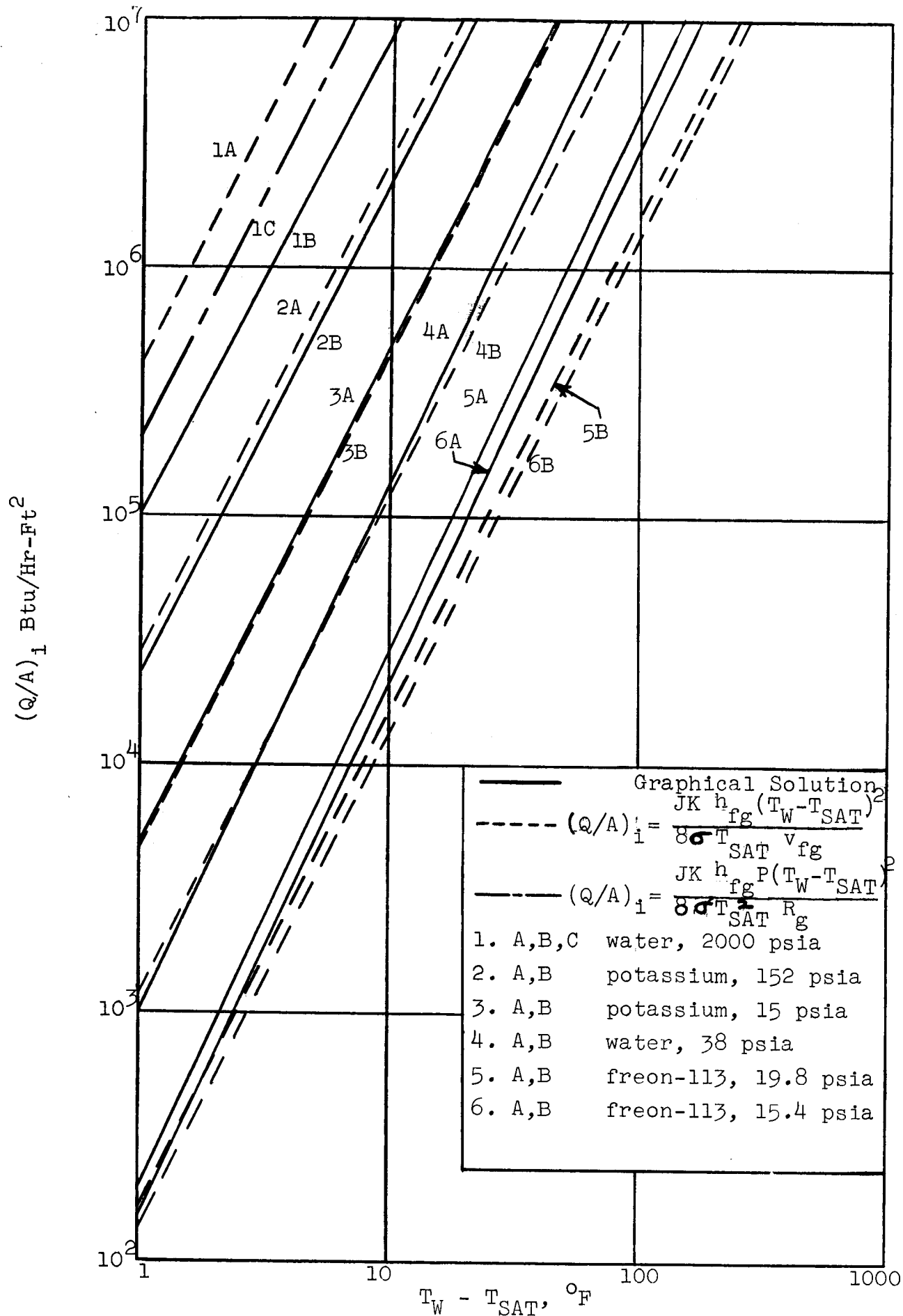


Figure 47. Superheat Requirements for Incipient Boiling Several Fluids

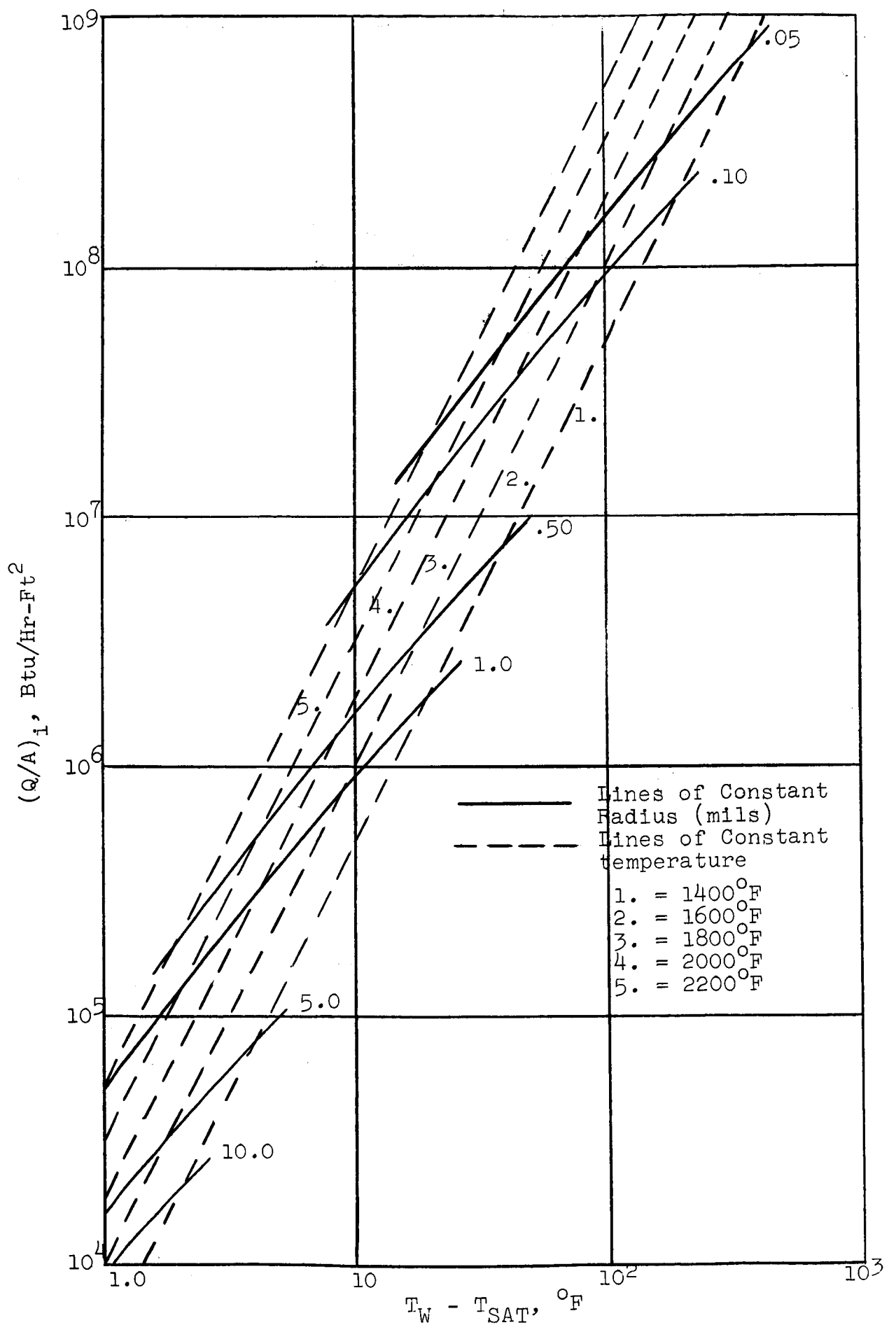


Figure 48. Superheat Requirements for Incipient Boiling of Potassium

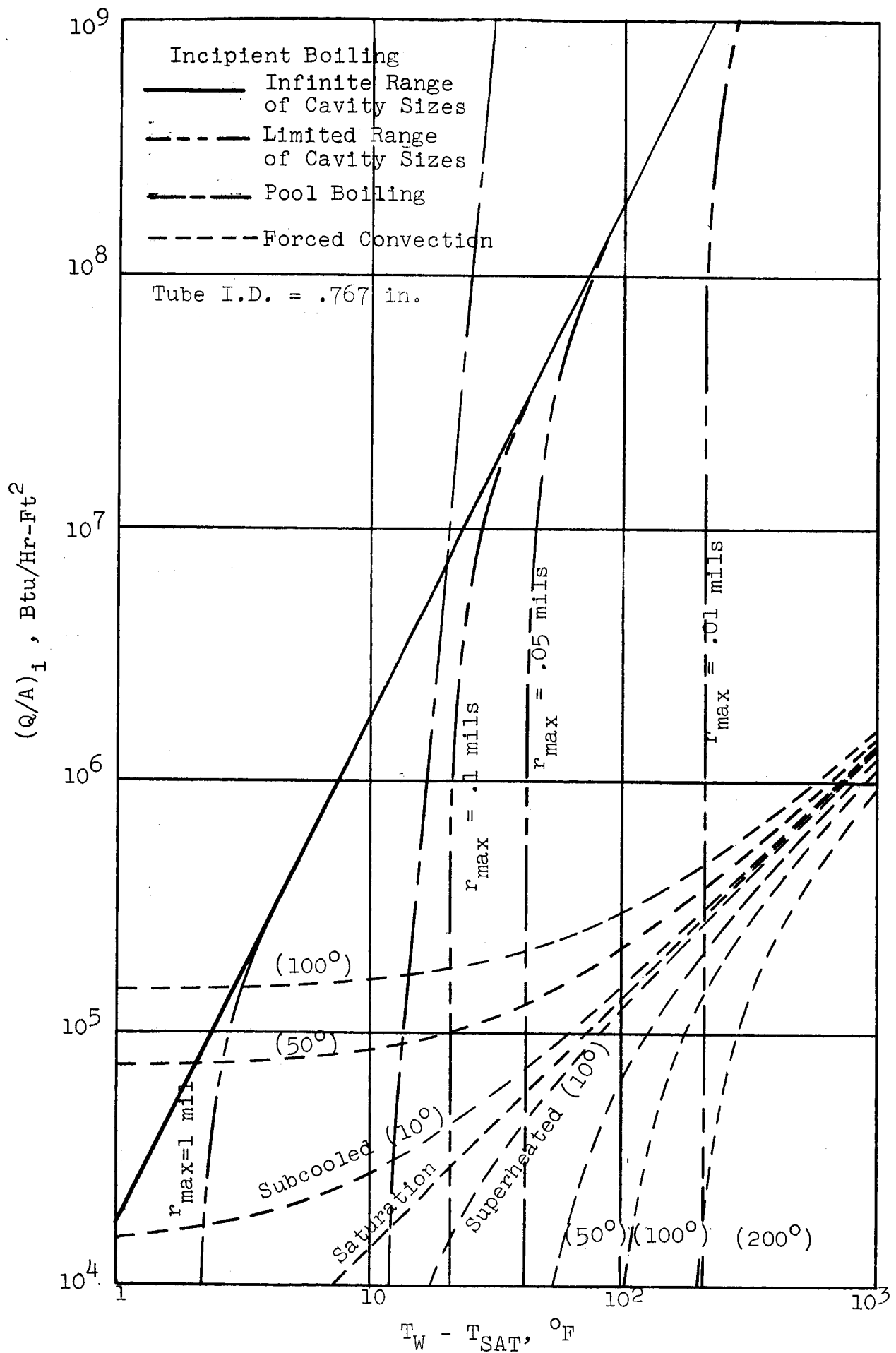


Figure 49. Effect of Cavity Size on Superheat Requirements for Incipient Boiling of Potassium ( $T_{sat} = 1800^\circ\text{F}$ )



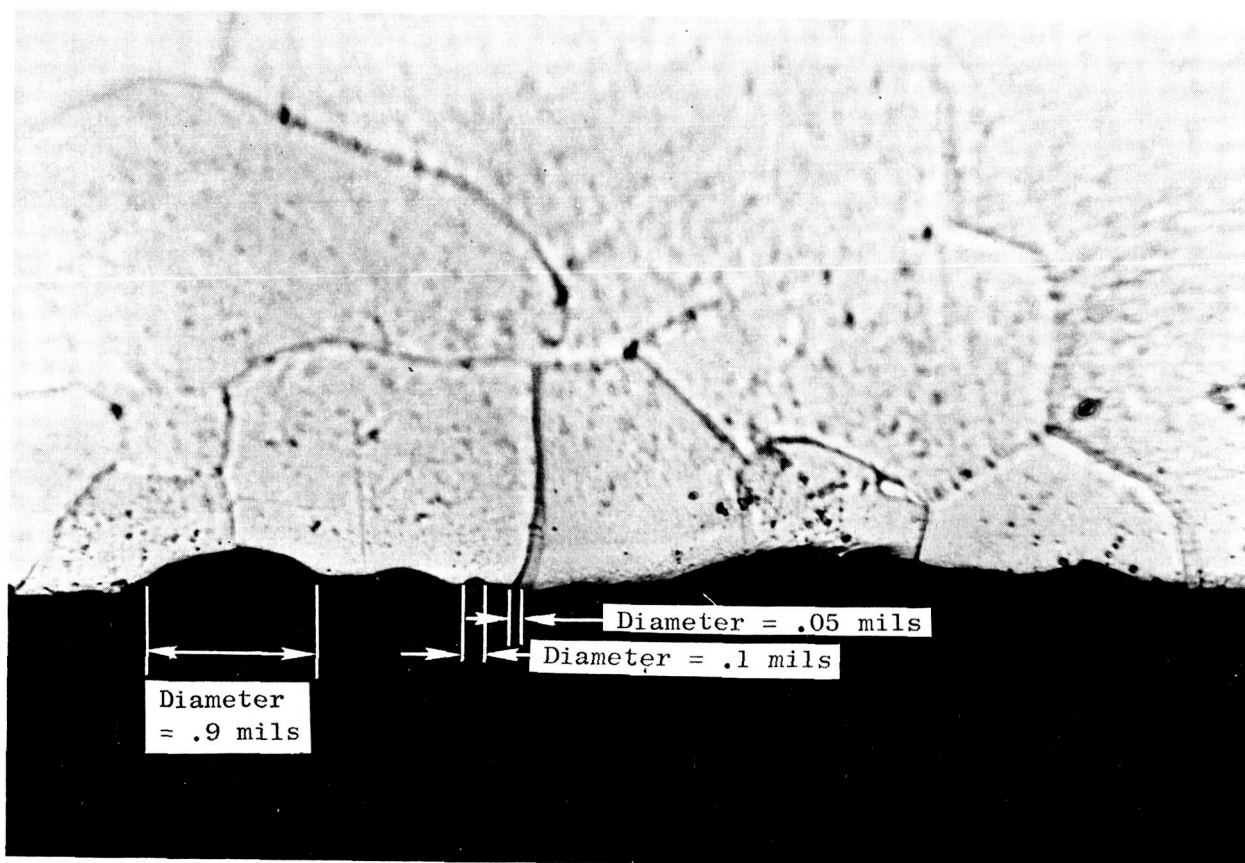


Figure 50a. Micrograph of 100 KW Boiling Surface (ID Transverse Magnified 1000 X - Polished But Not Etched) 3/4-Inch Sch. 80 Cb-1Zr Pipe (MCN-1209-1).

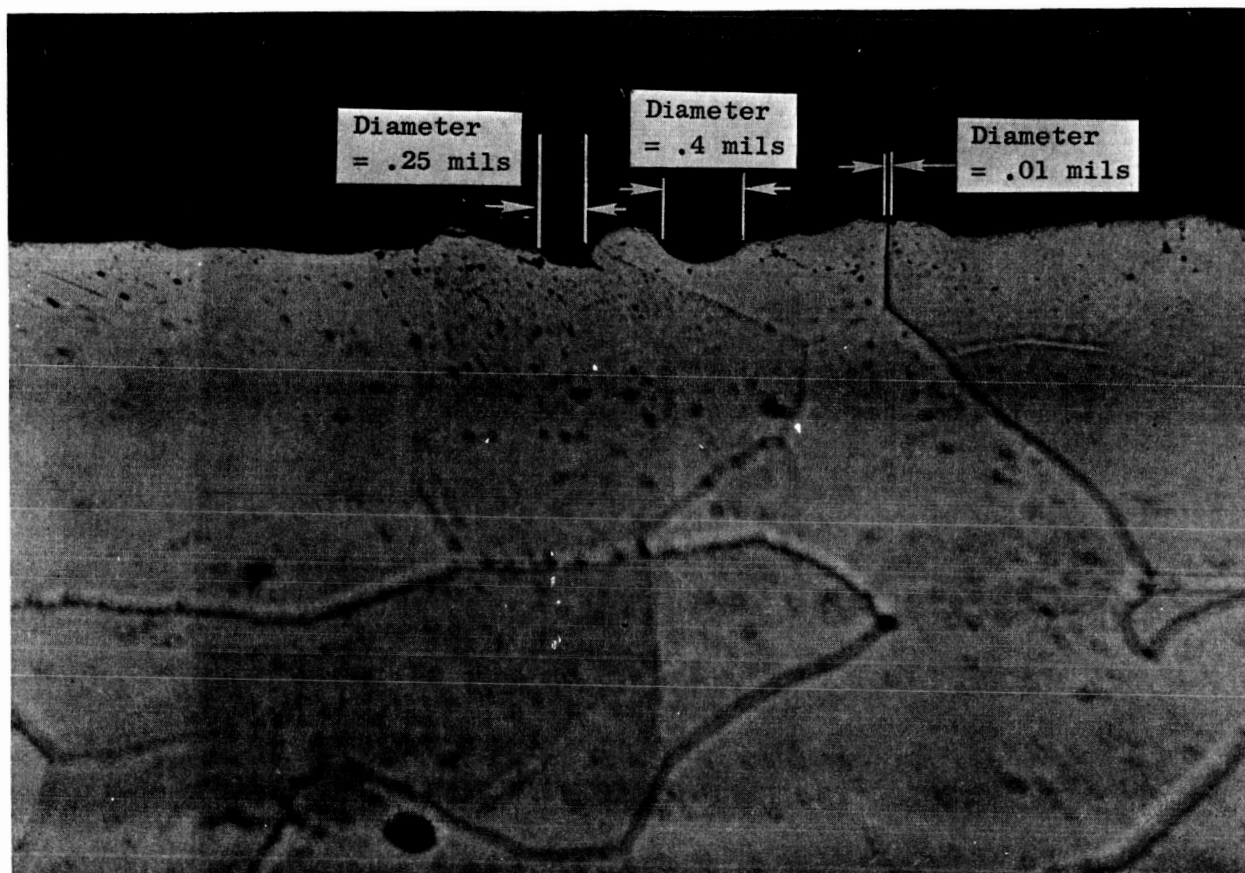


Figure 50b. Micrograph of 100 KW Boiling Surface (ID Longitudinal Magnified 1000 X - Polished But Not Etched) 3/4-Inch Sch. 80 Cb-1Zr Pipe (MCN-1209-1).

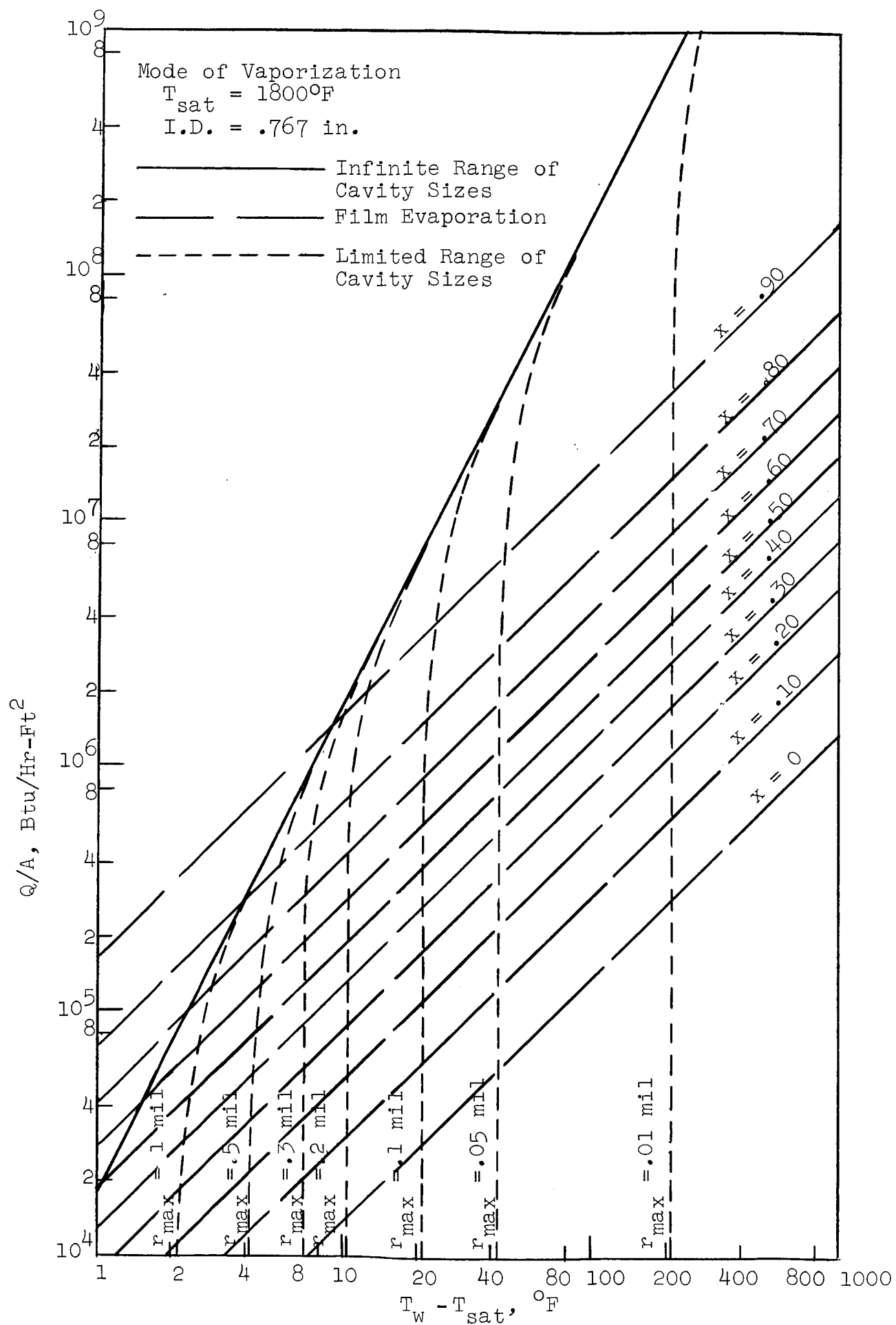


Figure 51. Quality Requirements for Boiling Suppression  
 $(T_{\text{sat}} = 1800^{\circ}\text{F})$

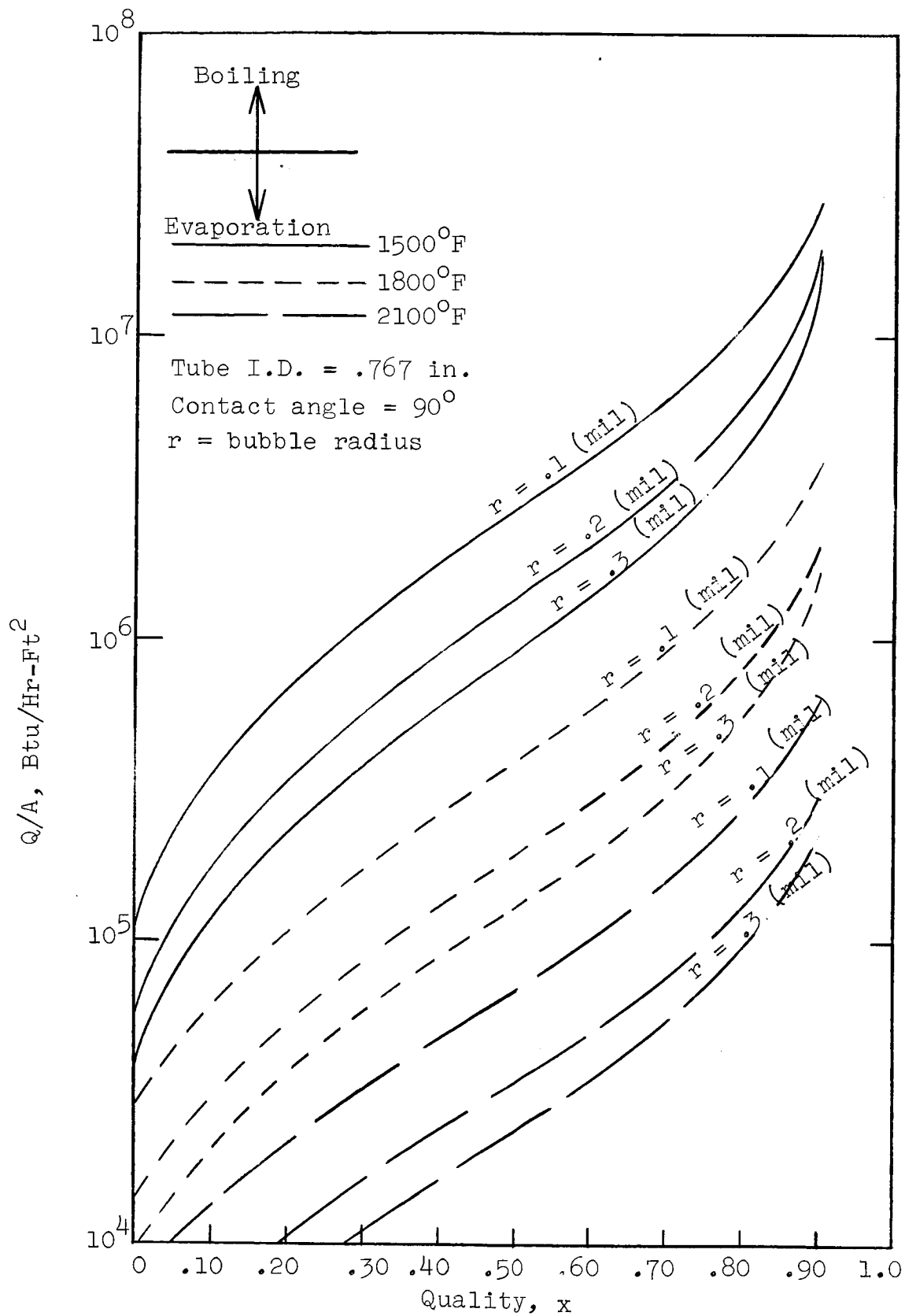


Figure 52a. Vaporization Regimes of Potassium (Heat Fluxes Less Than the Critical)

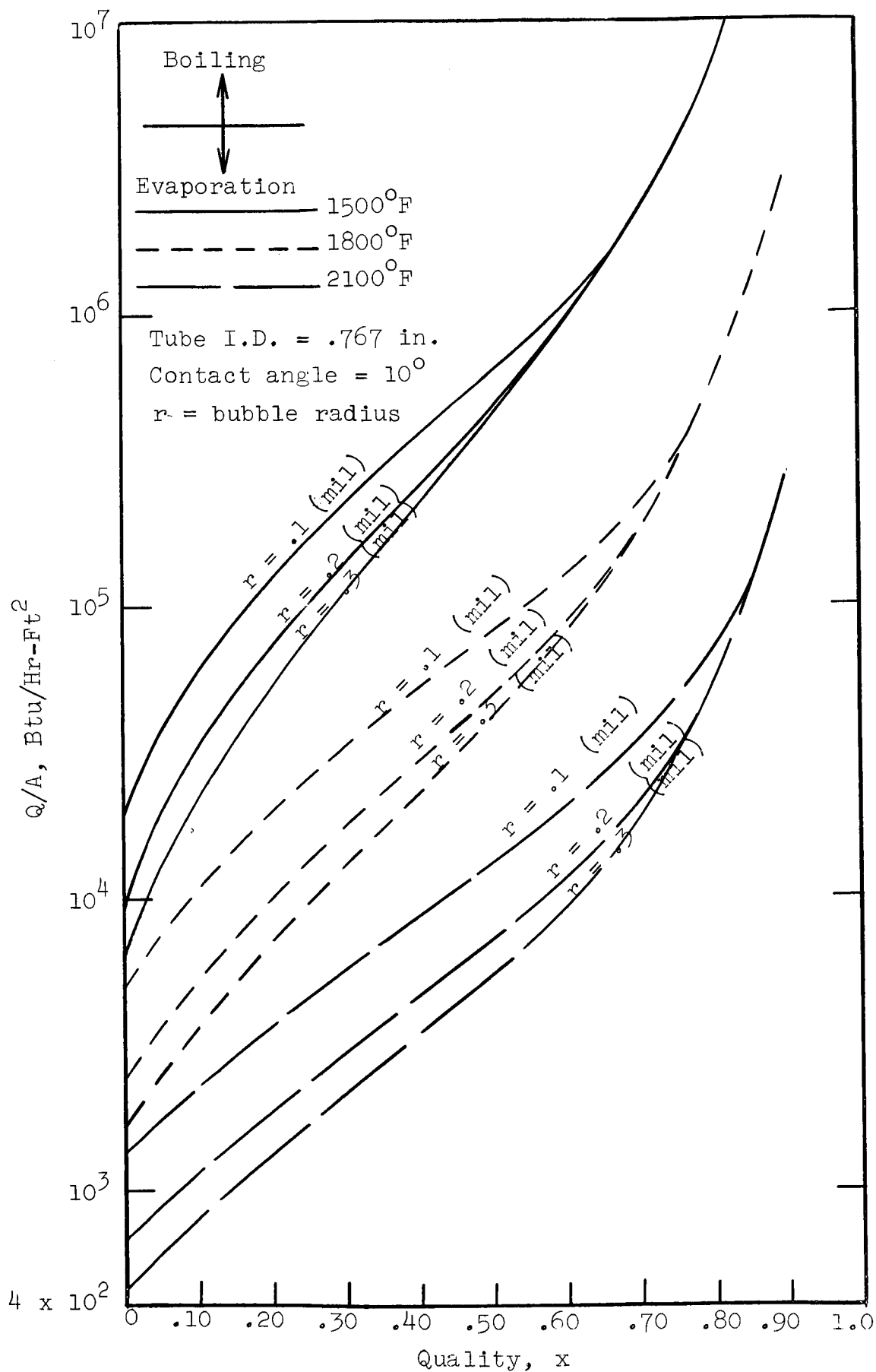


Figure 52b. Vaporization Regimes of Potassium (Heat Fluxes Less Than the Critical)

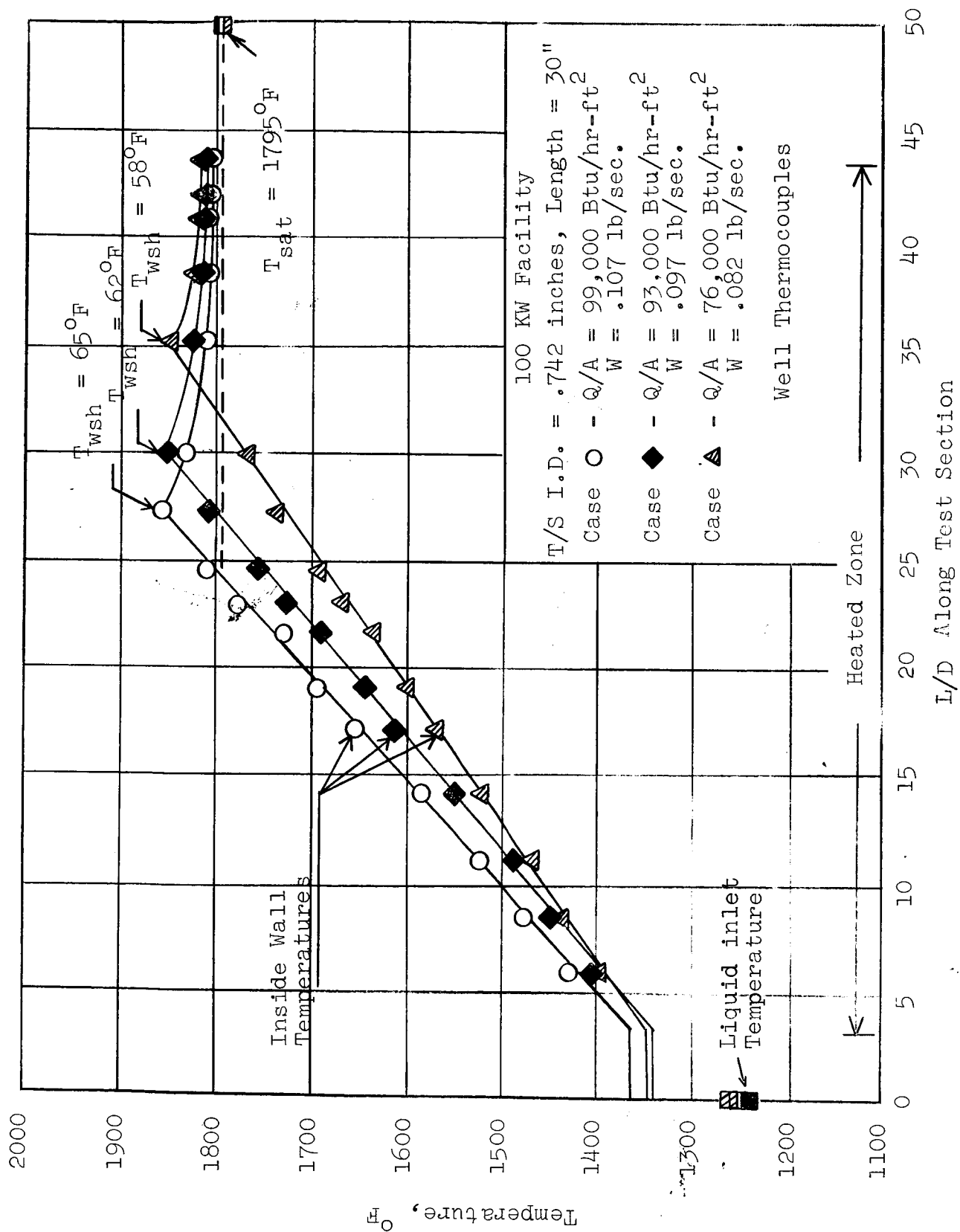


Figure 53a. Inside Wall Temperature as a Function of L/D (100 KW Test Section)

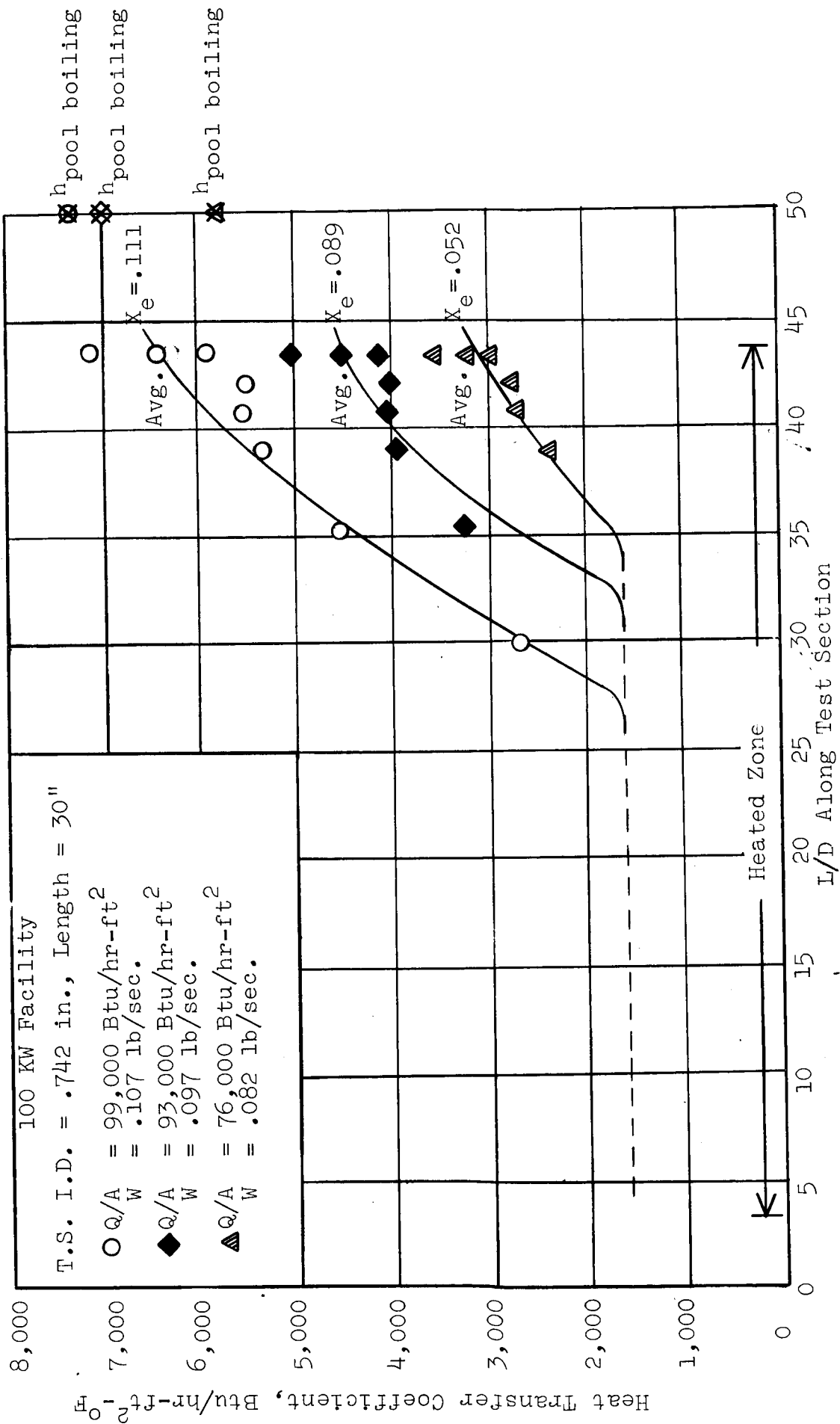


Figure 53b. Heat Transfer Coefficient as a Function of L/D (100 KW Test Section)

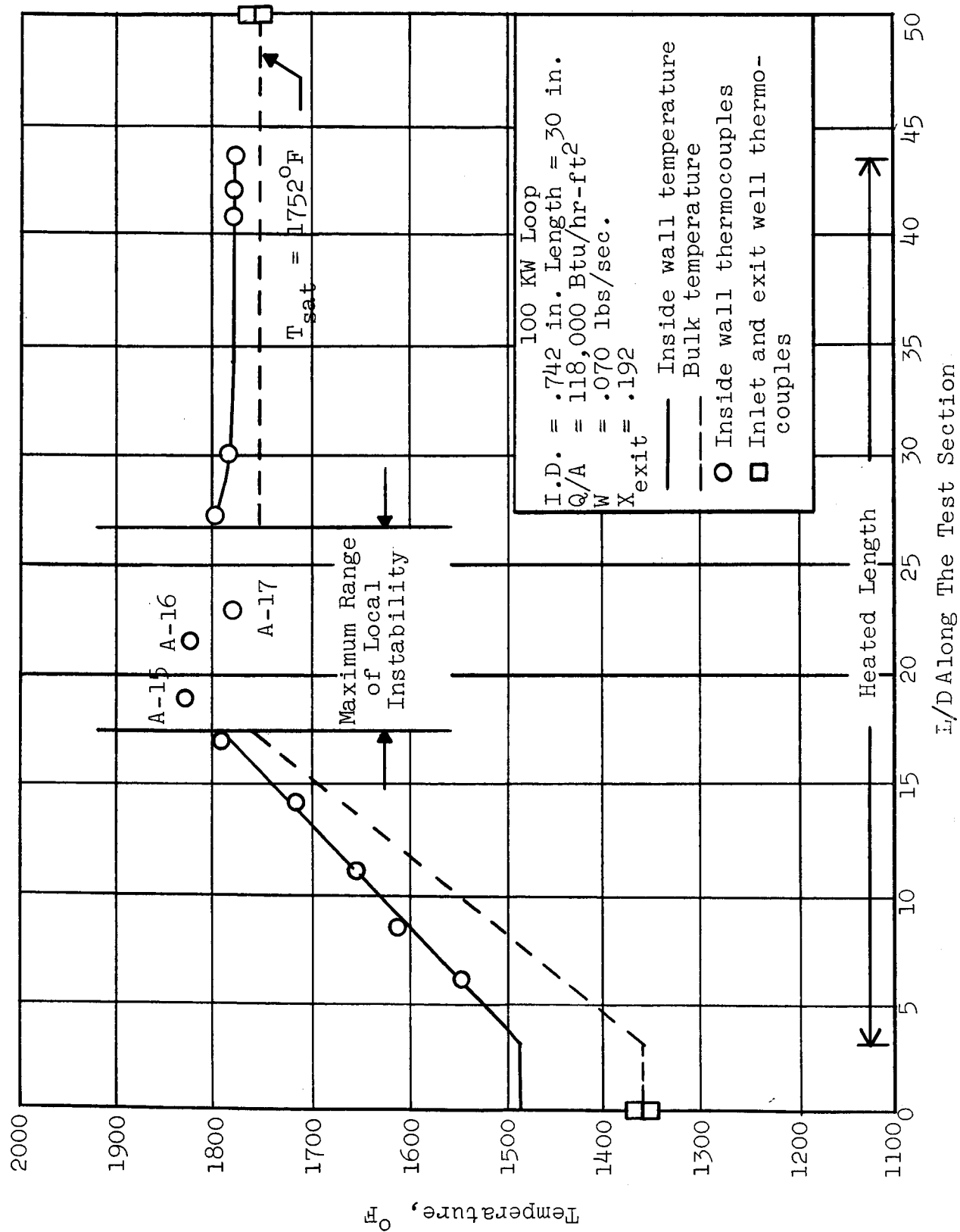


Figure 54. Inside Wall Temperature as a Function of L/D (100 KW Test Section)  
(Plot Shows the Local Instability Associated with the Boiling Boundary)



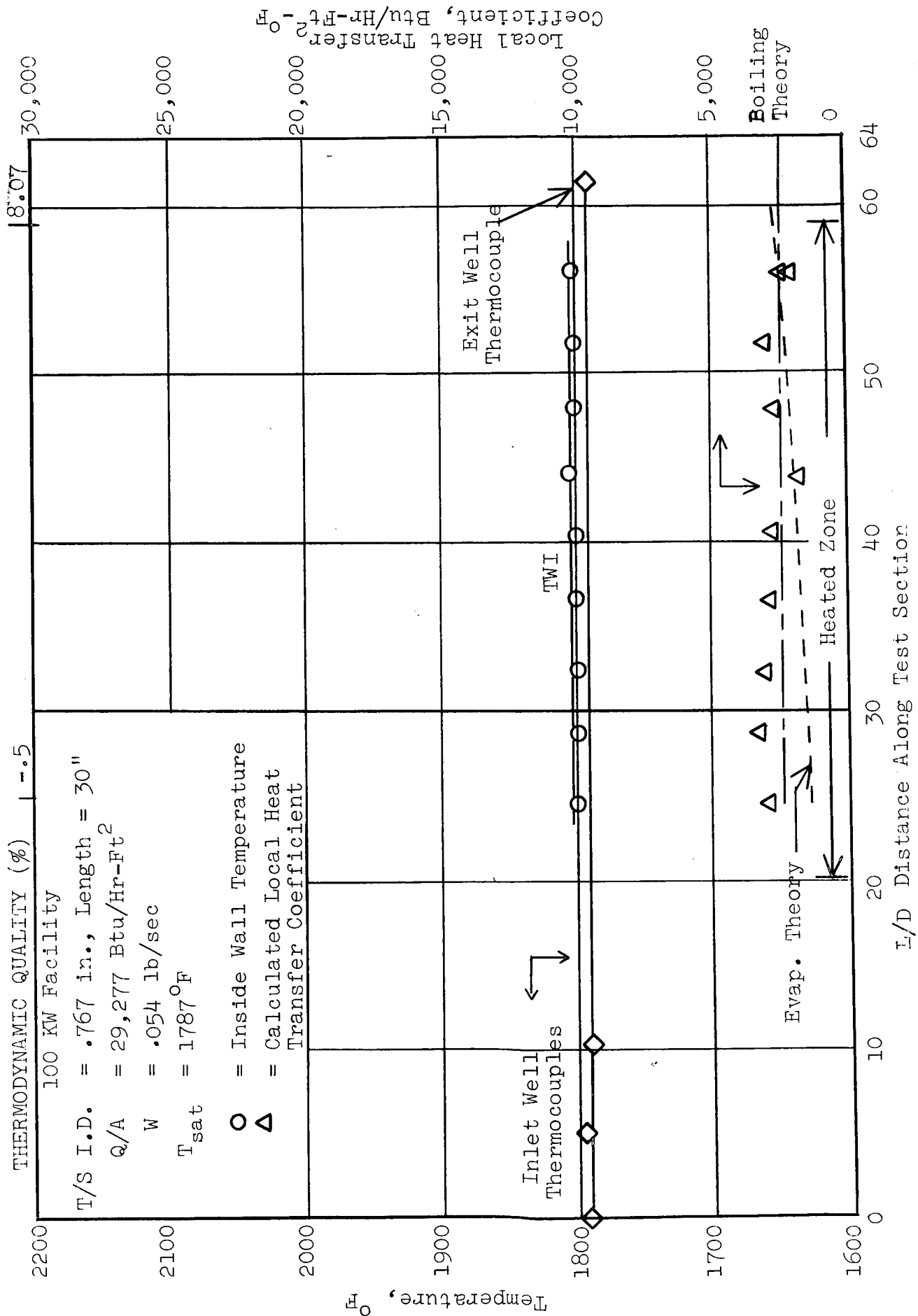


Figure 55a. Forced Convection Vaporization of Potassium at Low Vapor Qualities;  $q'' = 29,000$  Btu/hr-ft<sup>2</sup> (100 KW Data)

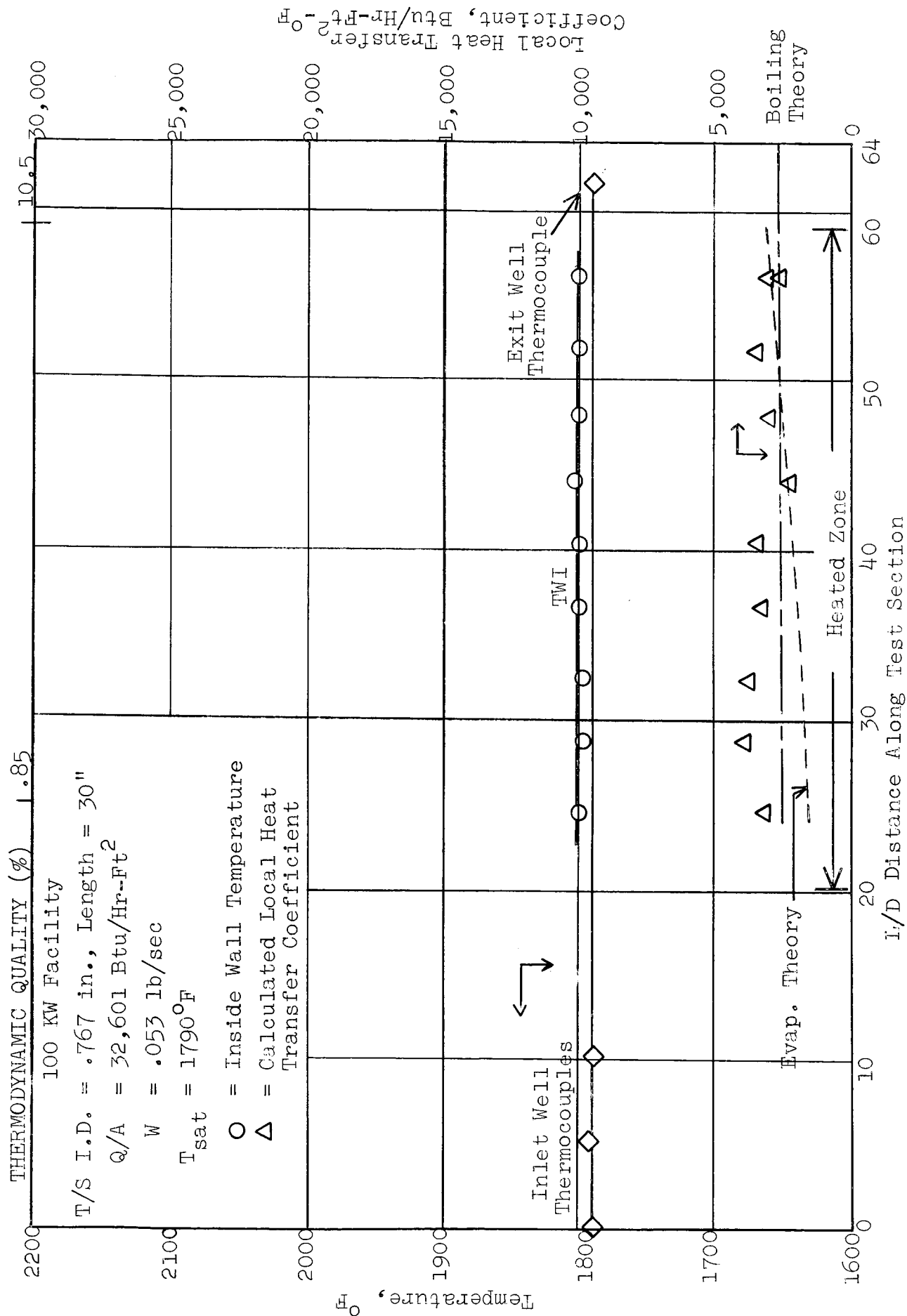


Figure 55b. Forced Convection Vaporization of Potassium at Low Vapor Qualities;  $q'' = 32,000 \text{ Btu/hr-ft}^2$  (100 KW Data)

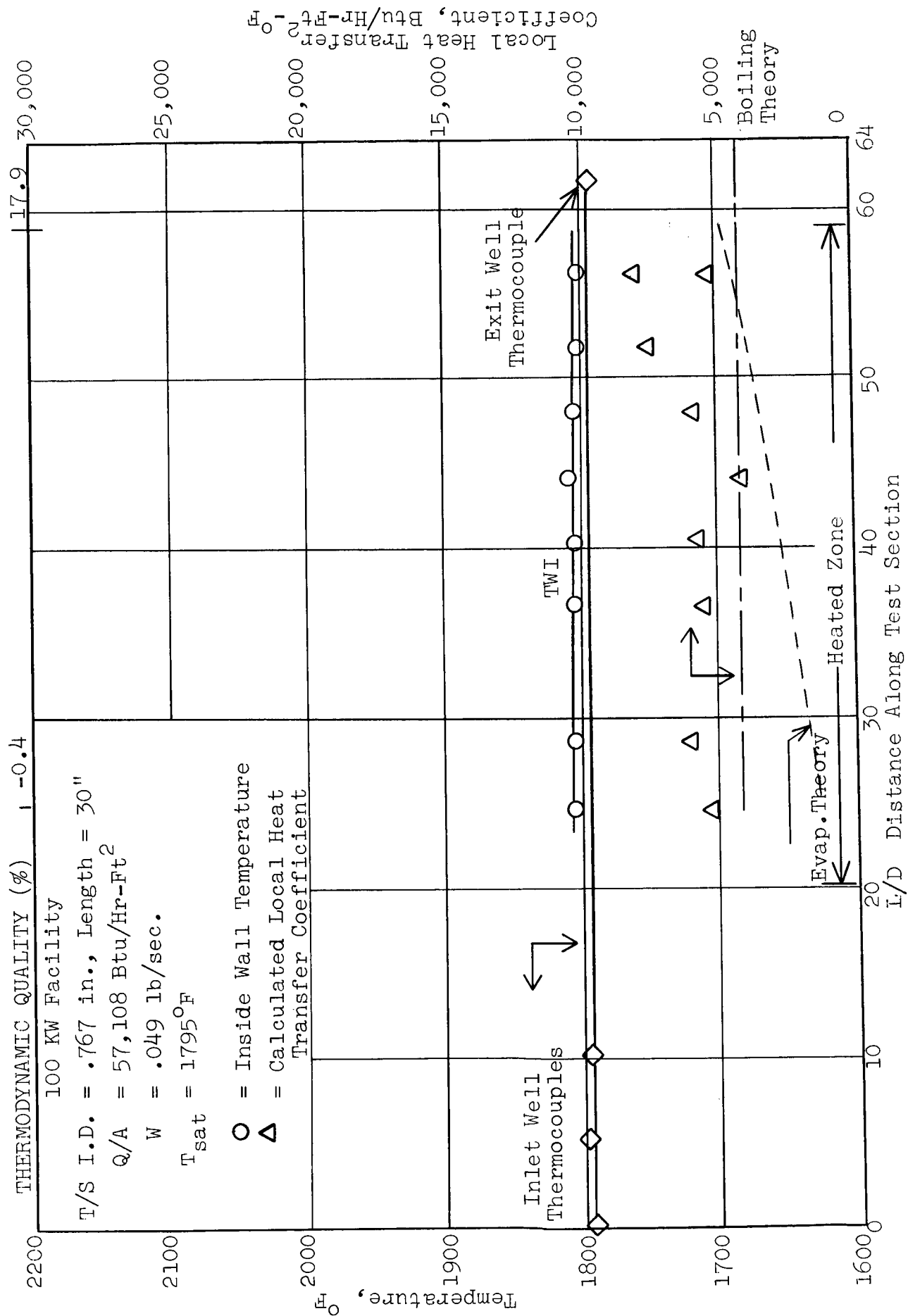


Figure 55c. Forced Convection Vaporization of Potassium at Low Vapor Qualities;  
 $q'' = 57,000 \text{ Btu/hr-ft}^2$  (100 KW Data)

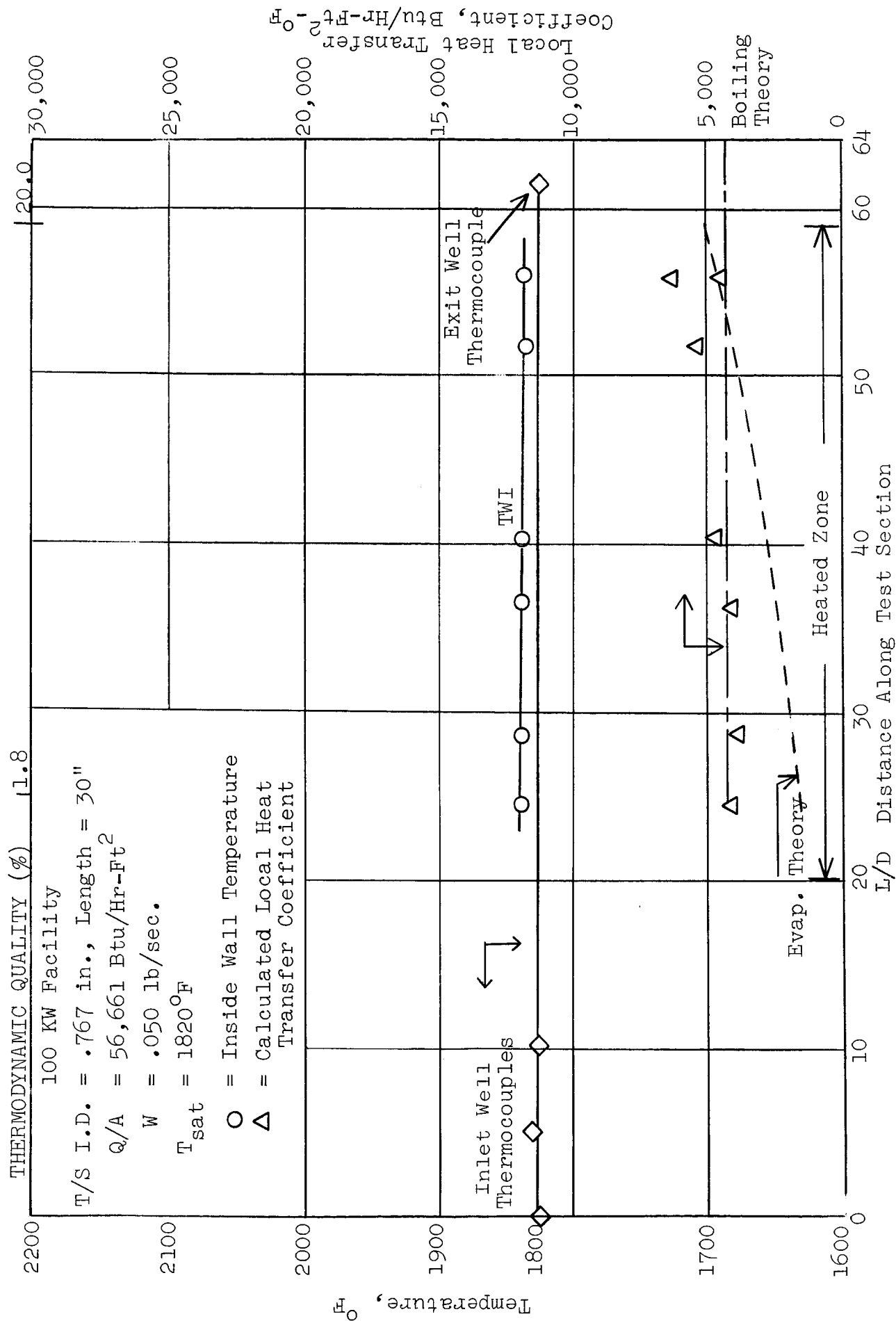


Figure 55d. Forced Convection Vaporization of Potassium at Low Vapor Qualities;  
 $q'' = 56,000 \text{ Btu/hr-ft}^2$  (100 KW Data)

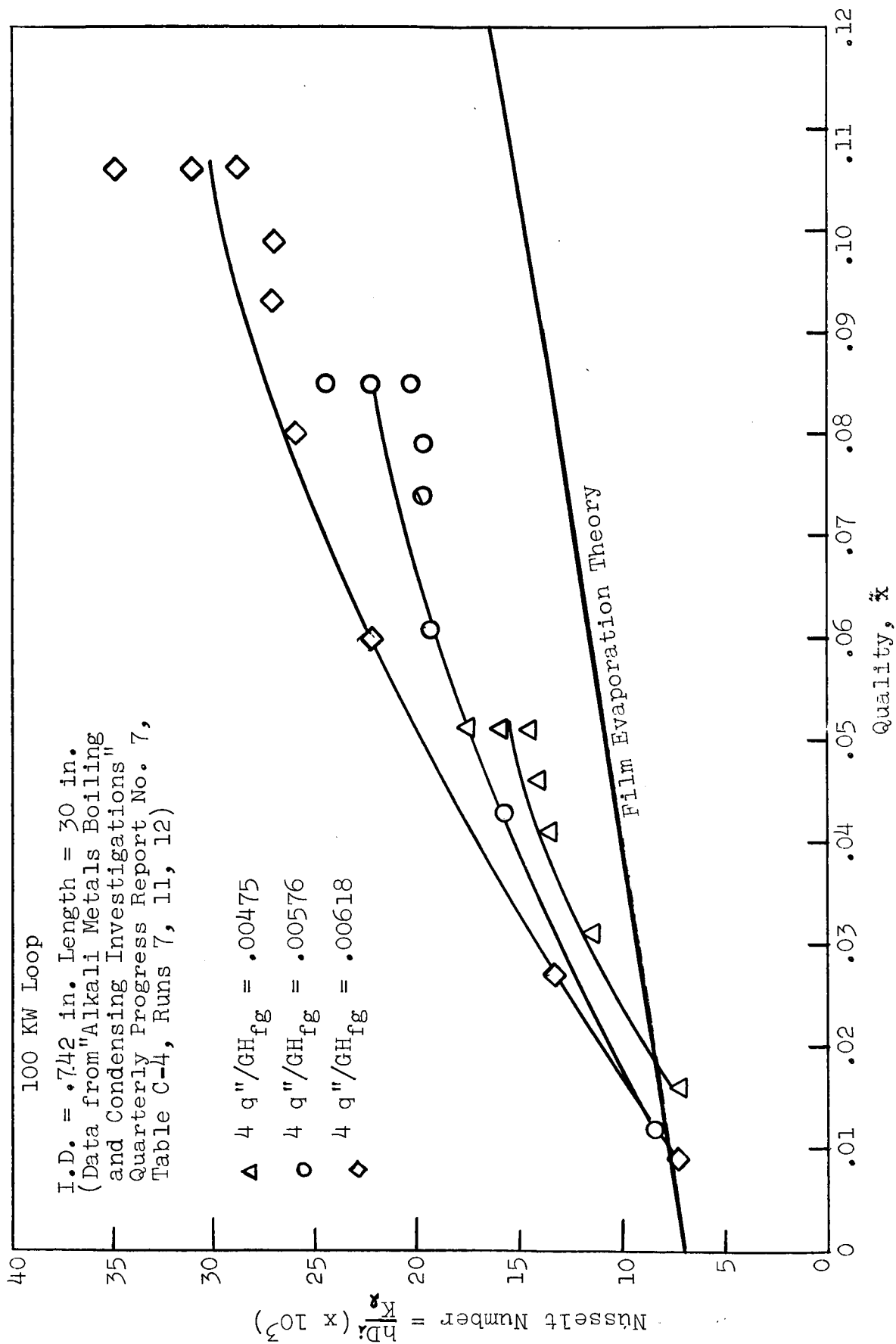
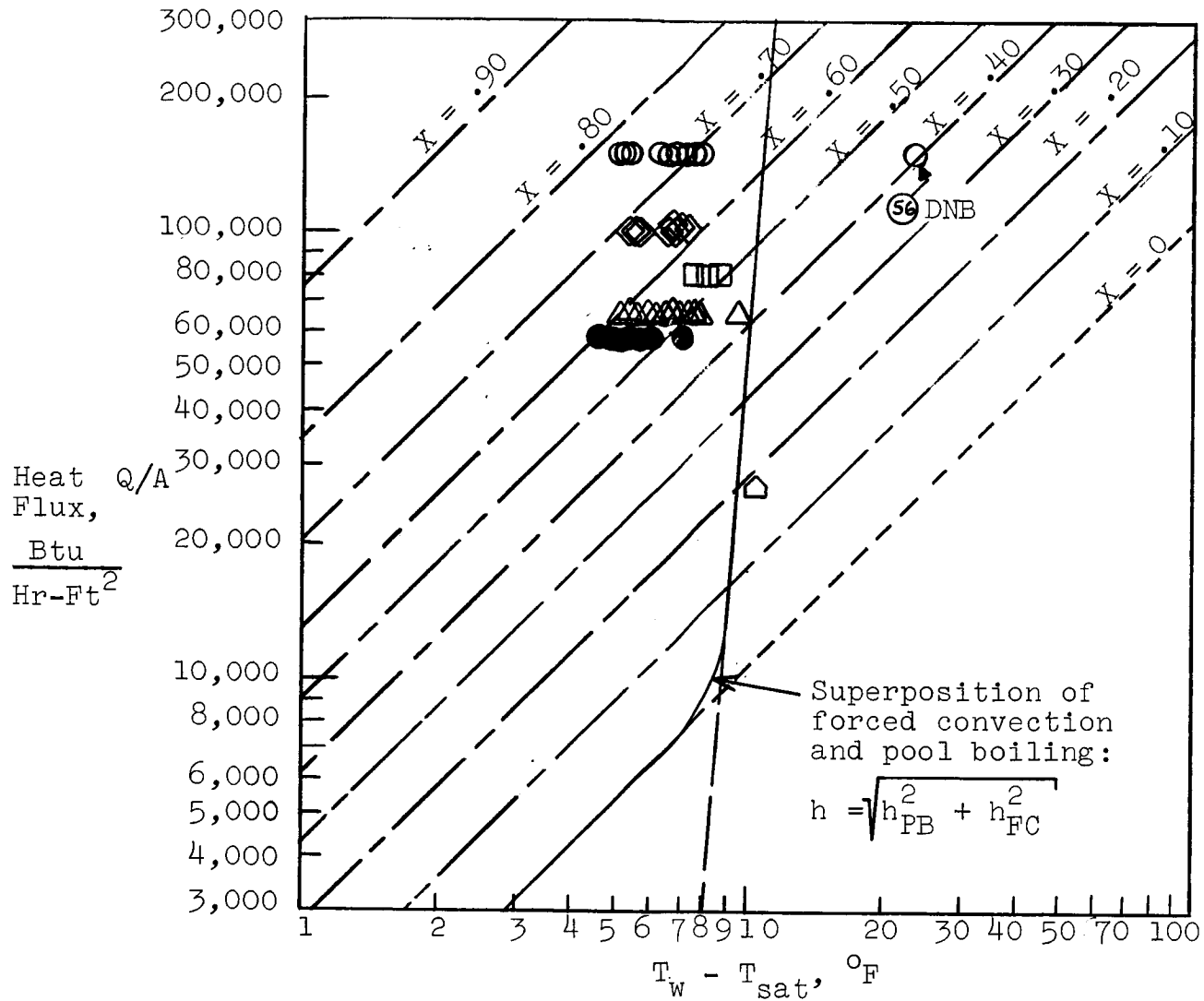


Figure 56. Nusselt Numbers as a Function of Vapor Quality (100 KW Data)

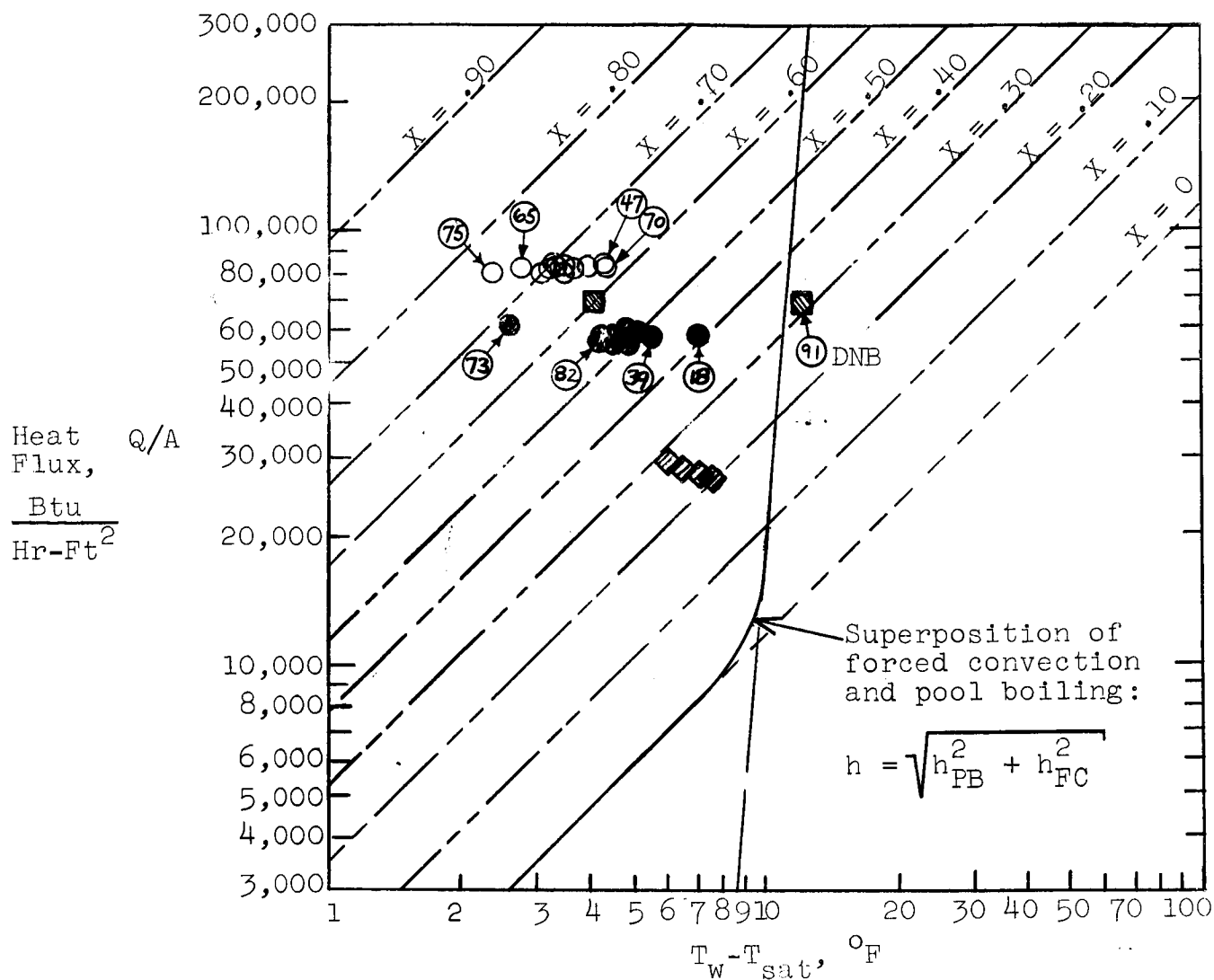


100 KW Data

$T_{sat} = 2100^\circ\text{F}$ , ID = .767 in., Length = 30 in.

	(N) →	= % Quality			
10 pts.	○	$Q/A = 150,000 \text{ Btu/Hr-Ft}^2$	$X = .30 - .56$	$G = 16 \text{ lb/sec-ft}^2$	
9 pts.	◇	$Q/A = 100,000 \text{ Btu/Hr-Ft}^2$	$X = .20 - .37$	$G = 16 \text{ lb/sec-ft}^2$	
3 pts.	□	$Q/A = 80,000 \text{ Btu/Hr-Ft}^2$	$X = .25 - .30$	$G = 16 \text{ lb/sec-ft}^2$	
7 pts.	●	$Q/A = 58,000 \text{ Btu/Hr-Ft}^2$	$X = .22 - .38$	$G = 16 \text{ lb/sec-ft}^2$	
1 pt.	△	$Q/A = 27,000 \text{ Btu/Hr-Ft}^2$	$X = .80$	$G = 16 \text{ lb/sec-ft}^2$	
			$T_{sat} = 2061^\circ\text{F}$		
14 pts.	△	$Q/A = 65,000 \text{ Btu/Hr-Ft}^2$	$X = .11 - .37$	$G = 22 \text{ lb/sec-ft}^2$	
				Pool Boiling	
				Forced Convection	
				Film Evaporation	

Figure 57. Heat Flux as a Function of Temperature Difference for  $T_{sat} = 2100^\circ\text{F}$  (100 KW Data) - Reference 7, Table C-3



100 KW Data

$T_{\text{sat}} = 1990^\circ\text{F}$ , Test Section I.D. = .767 in., Length = 30 in.

- 16 pts.  $\circ$   $Q/A = 80,000 \text{ Btu/hr-ft}^2$ ,  $X = .46 - .86$   $G = 16 \text{ lb/sec-ft}^2$   
 2 pts.  $\blacksquare$   $Q/A = 68,000 \text{ Btu/hr-ft}^2$ ,  $X = .82 - .91$   $G = 16 \text{ lb/sec-ft}^2$   
 13 pts.  $\bullet$   $Q/A = 58,000 \text{ Btu/hr-ft}^2$ ,  $X = .18 - .82$   $G = 16 \text{ lb/sec-ft}^2$   
 4 pts.  $\blacklozenge$   $Q/A = 28,000 \text{ Btu/hr-ft}^2$ ,  $X = .68 - .72$   $G = 16 \text{ lb/sec-ft}^2$

$\textcircled{N} = \% \text{ Quality}$

Pool Boiling  
 Forced Convection  
 Film Evaporation

Figure 58. Heat Flux as a Function of Temperature Difference for  $T_{\text{sat}} = 1990^\circ\text{F}$  (100 KW Data) - Reference 7, Table C-3

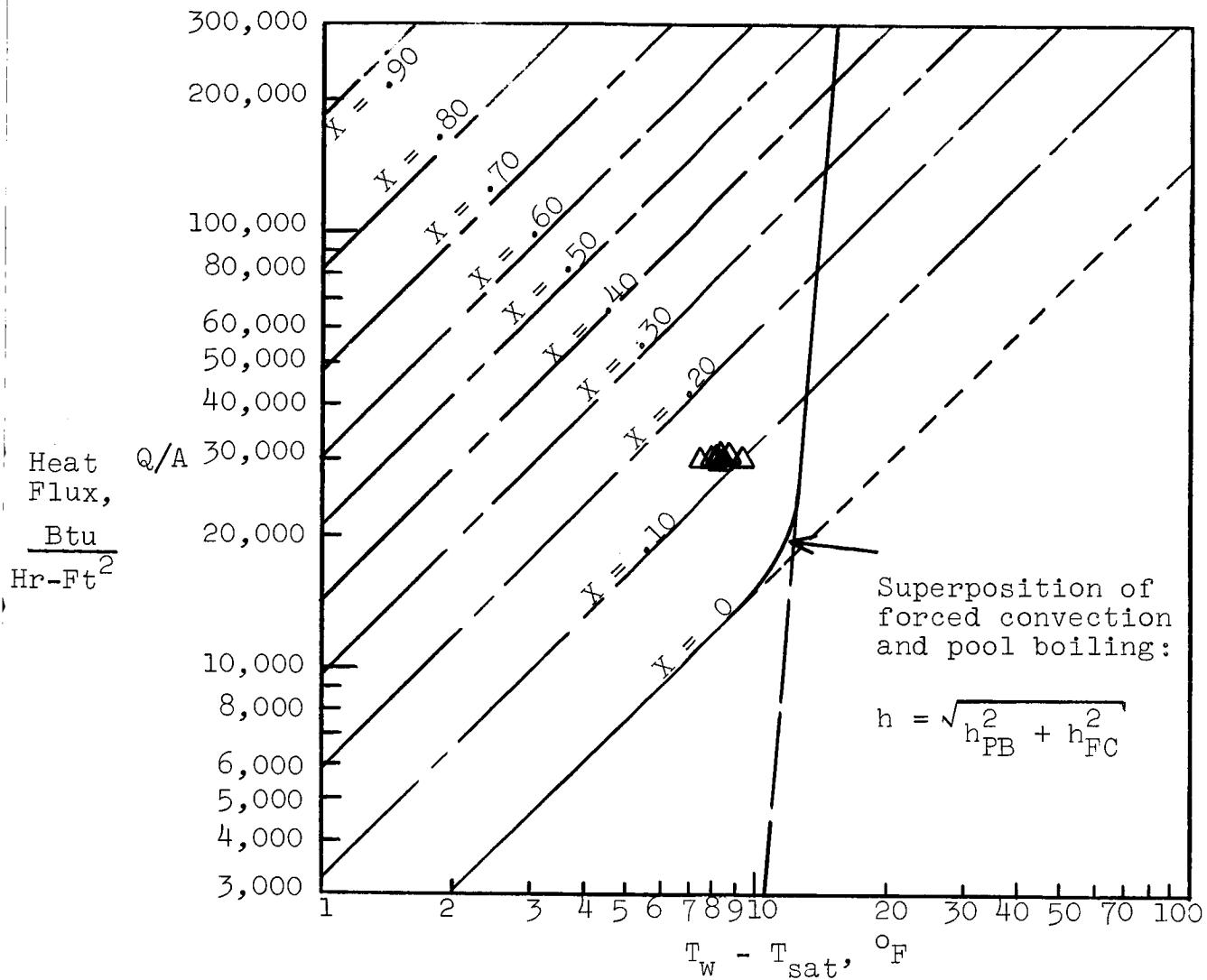


Figure 59. Heat Flux as a Function of Temperature Difference for  $T_{\text{sat}} = 1750^\circ\text{F}$  (100 KW Data) - Reference 7, Table C-3



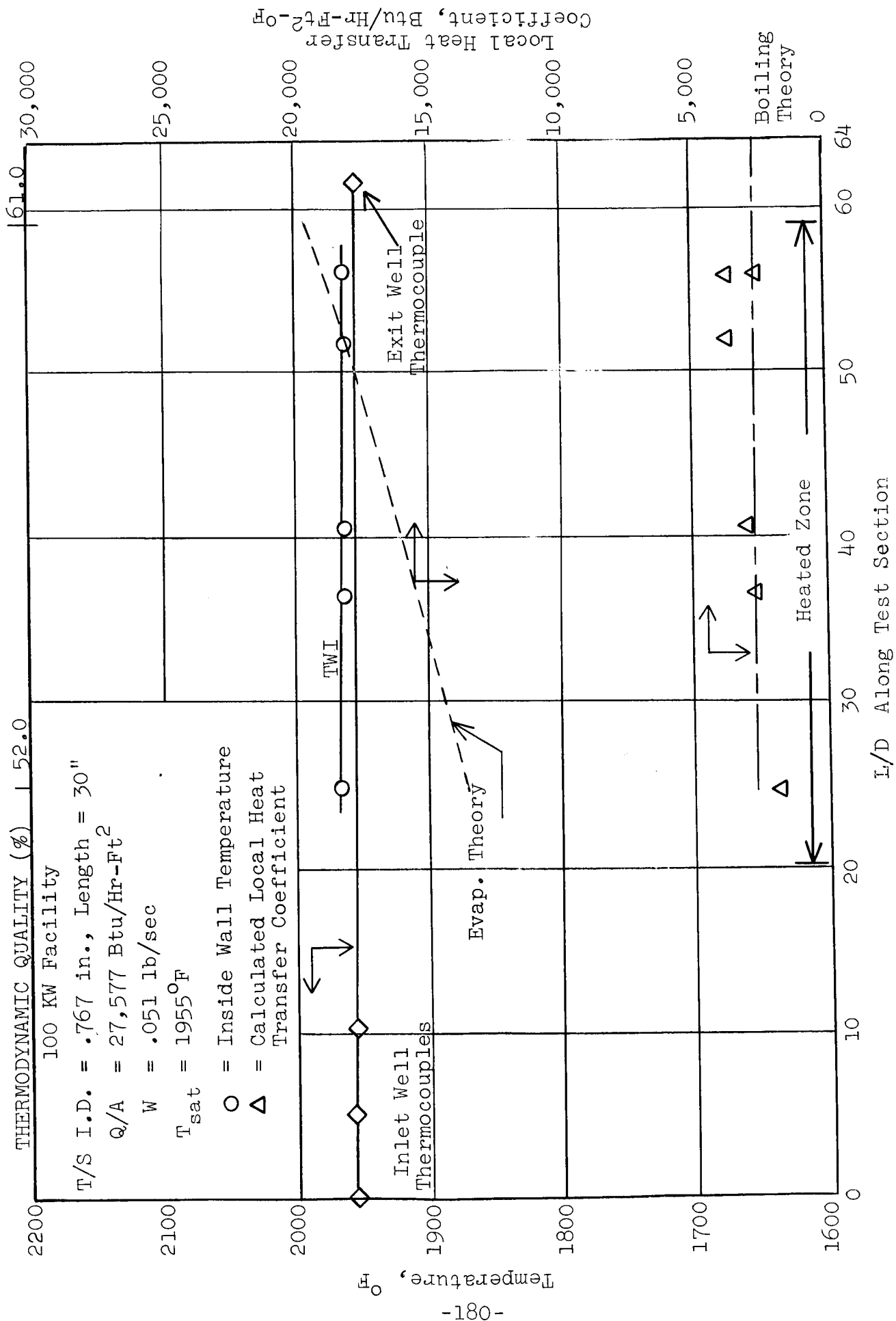


Figure 60a. Forced Convection Vaporization of Potassium at Intermediate Vapor Qualities;  $q'' = 27,000 \text{ Btu/hr-ft}^2$  (100 KW Data)

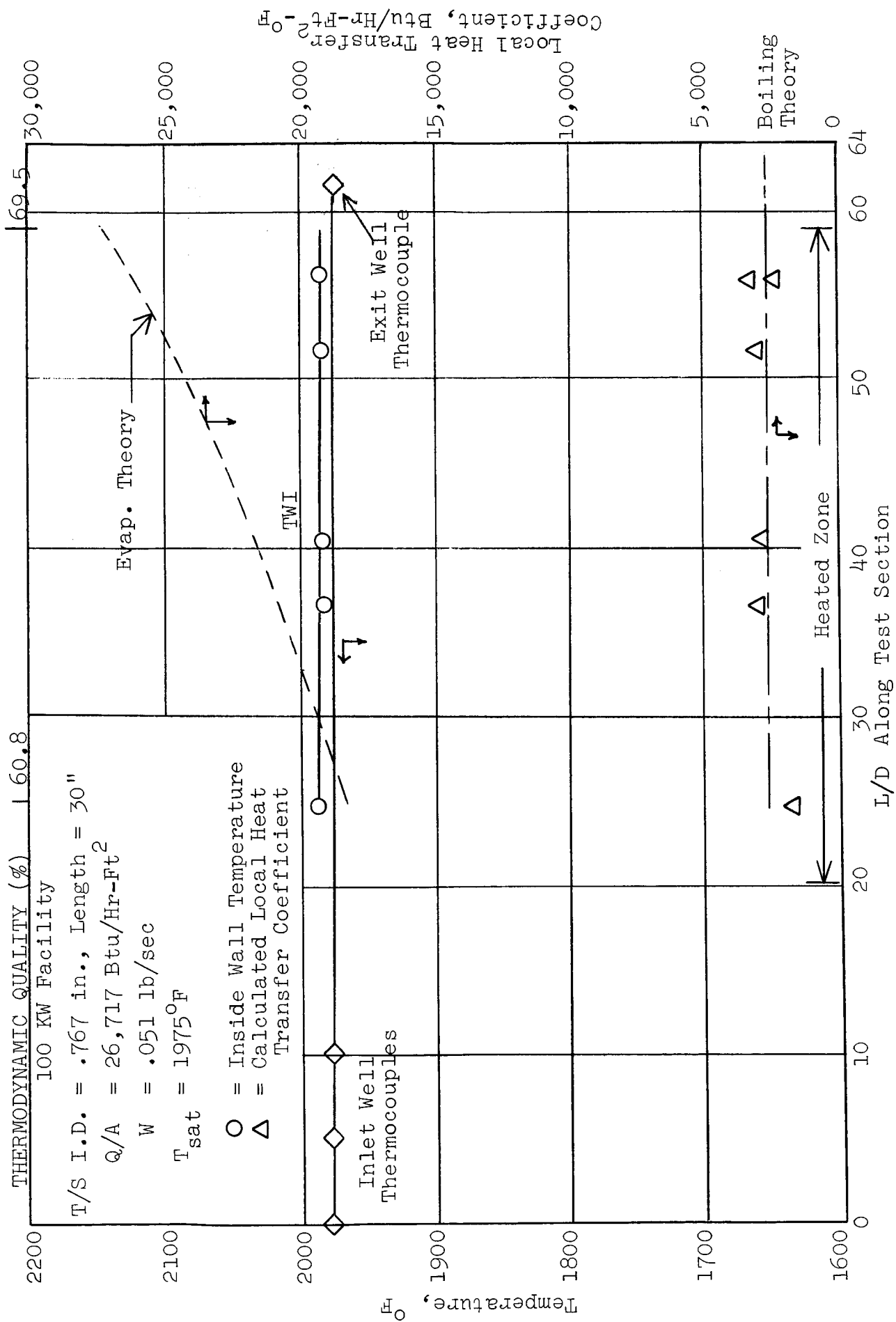


Figure 60b. Forced Convection Vaporization of Potassium at Intermediate Vapor Qualities;  
 $q'' \approx 27,000 \text{ Btu/hr-ft}^2$  (100 KW Data)

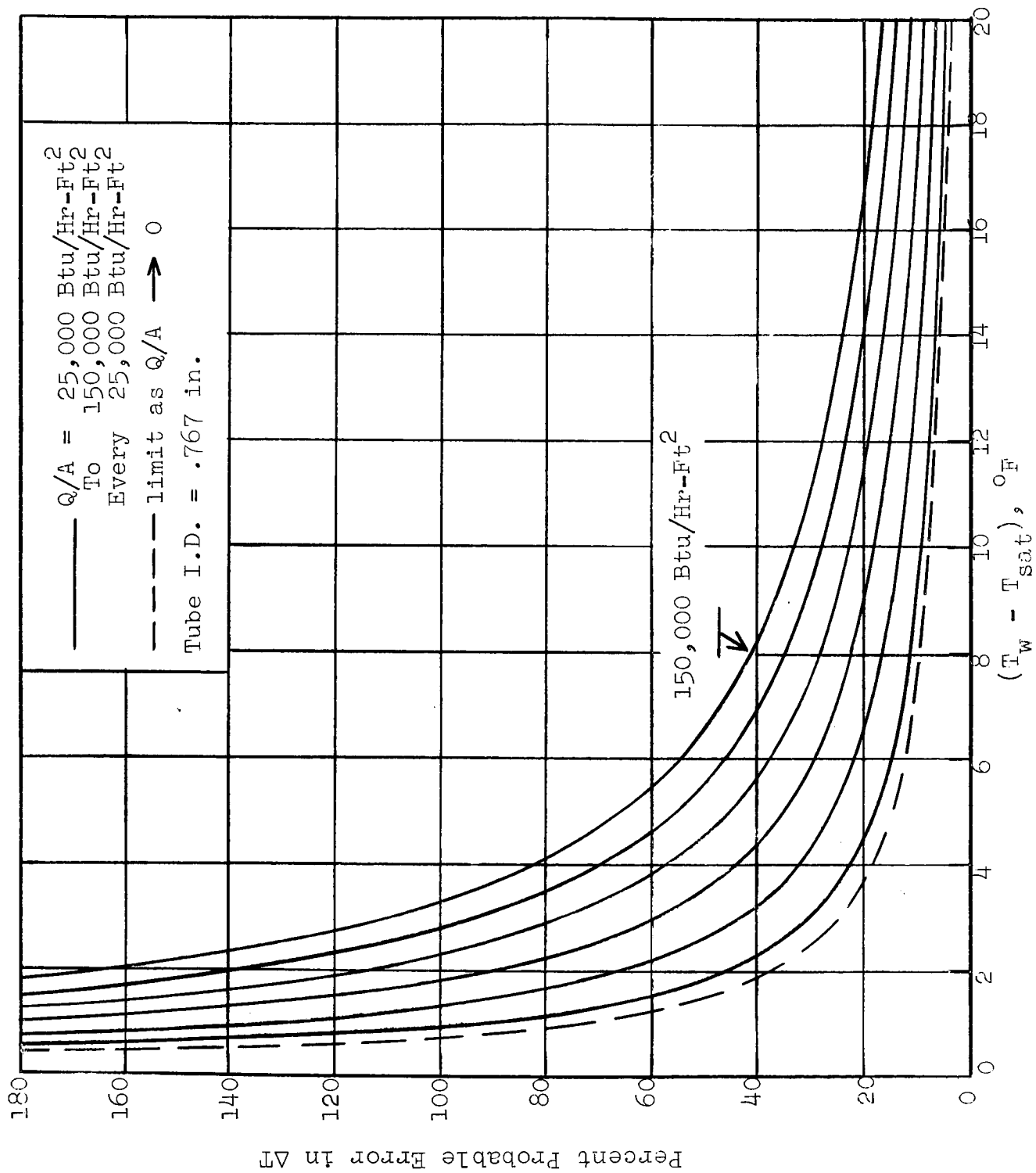


Figure 61a. Percent Probable Error in Inside Wall to Fluid Temperature Difference for the 100 KW Test Section (2 Wall and 3 Fluid Temperature Measurements at a Given Station

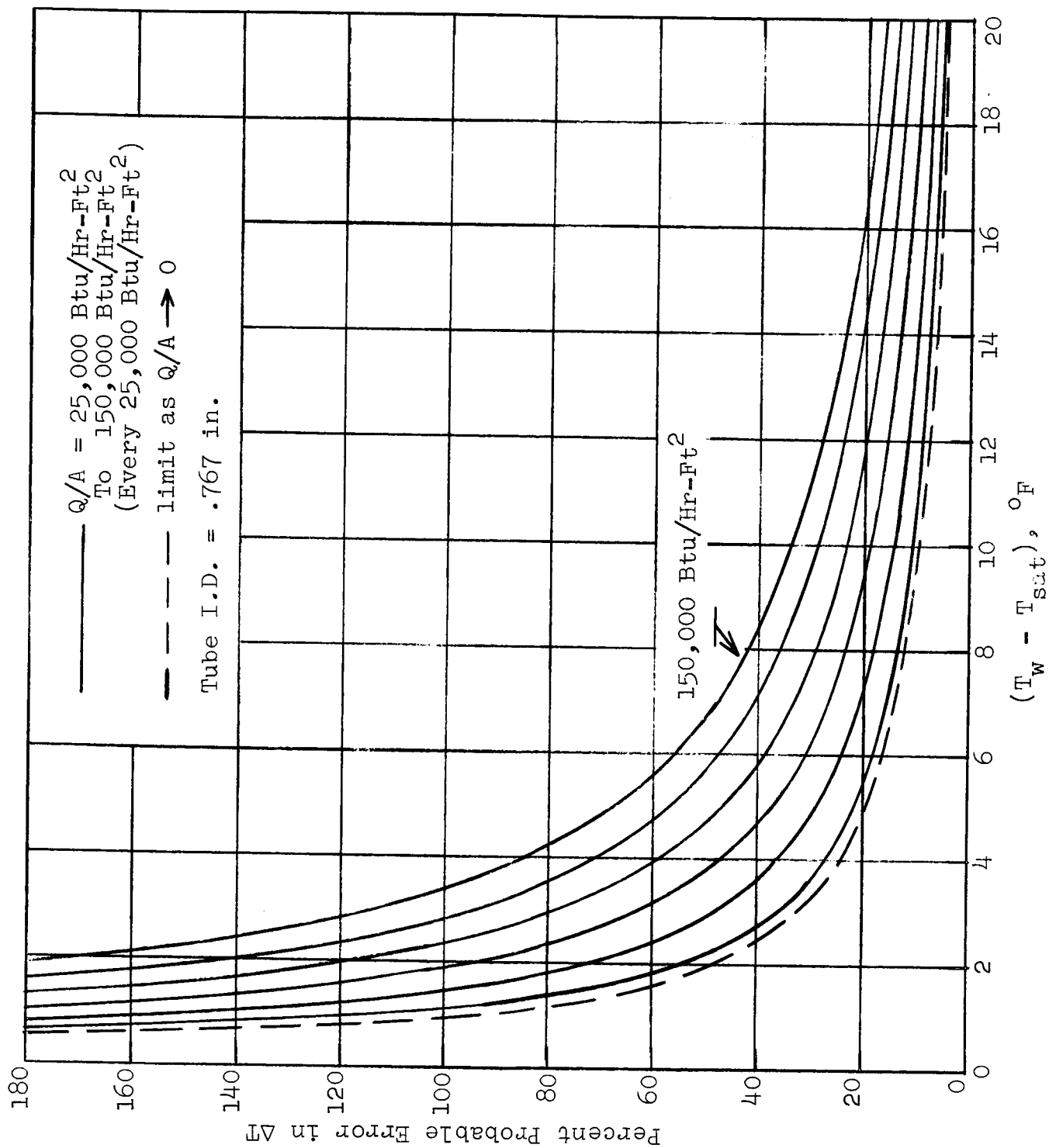


Figure 6lb. Percent Probable Error in Inside Wall to Fluid Temperature Difference for the 100 KW Test Section (1 Wall and 3 Fluid Temperature Measurements at a Given Station)

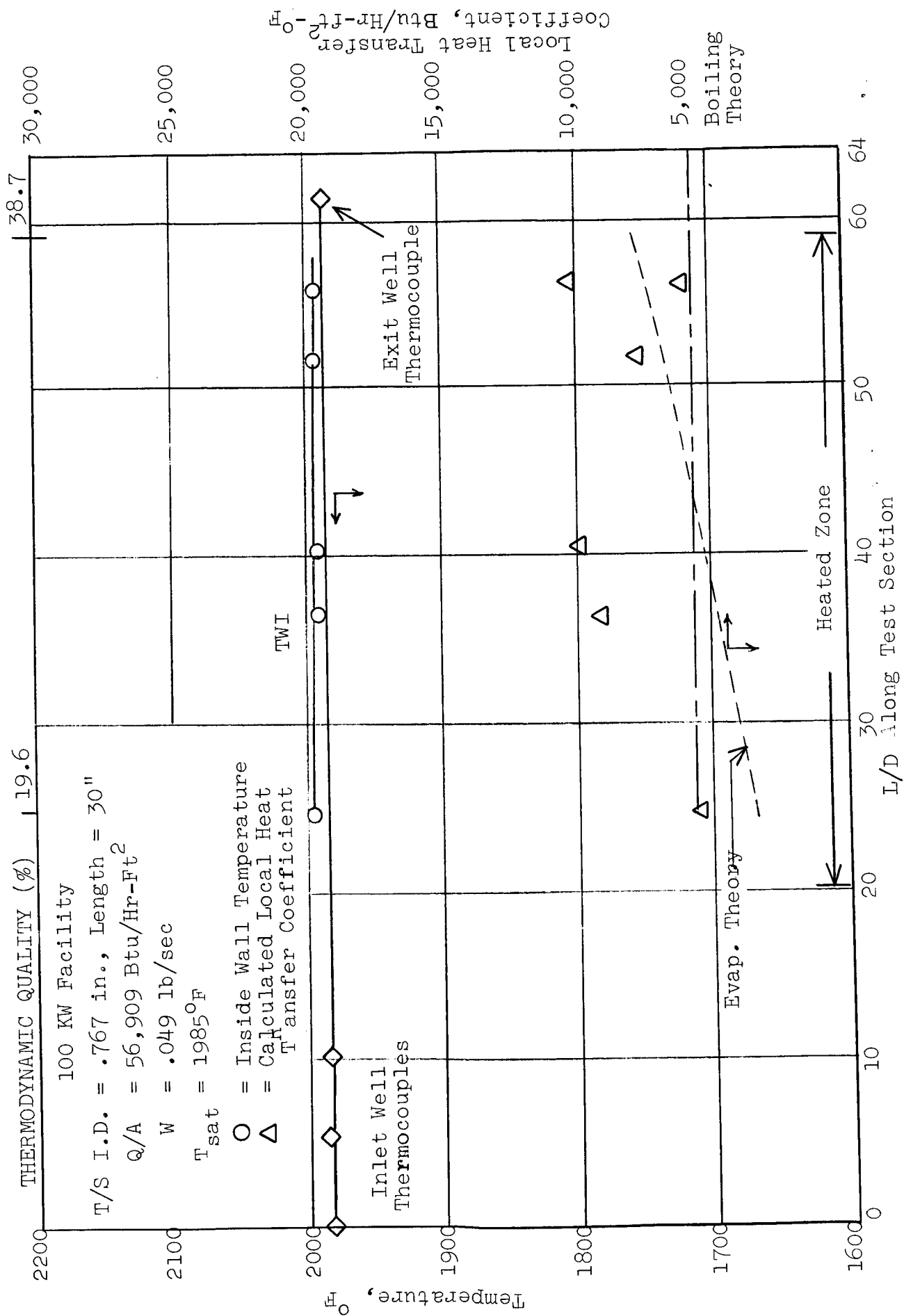


Figure 62a. Forced Convection Vaporization of Potassium at Intermediate Vapor Qualities;  
 $q'' = 57,000 \text{ Btu/hr-ft}^2$  (100 KW Data)

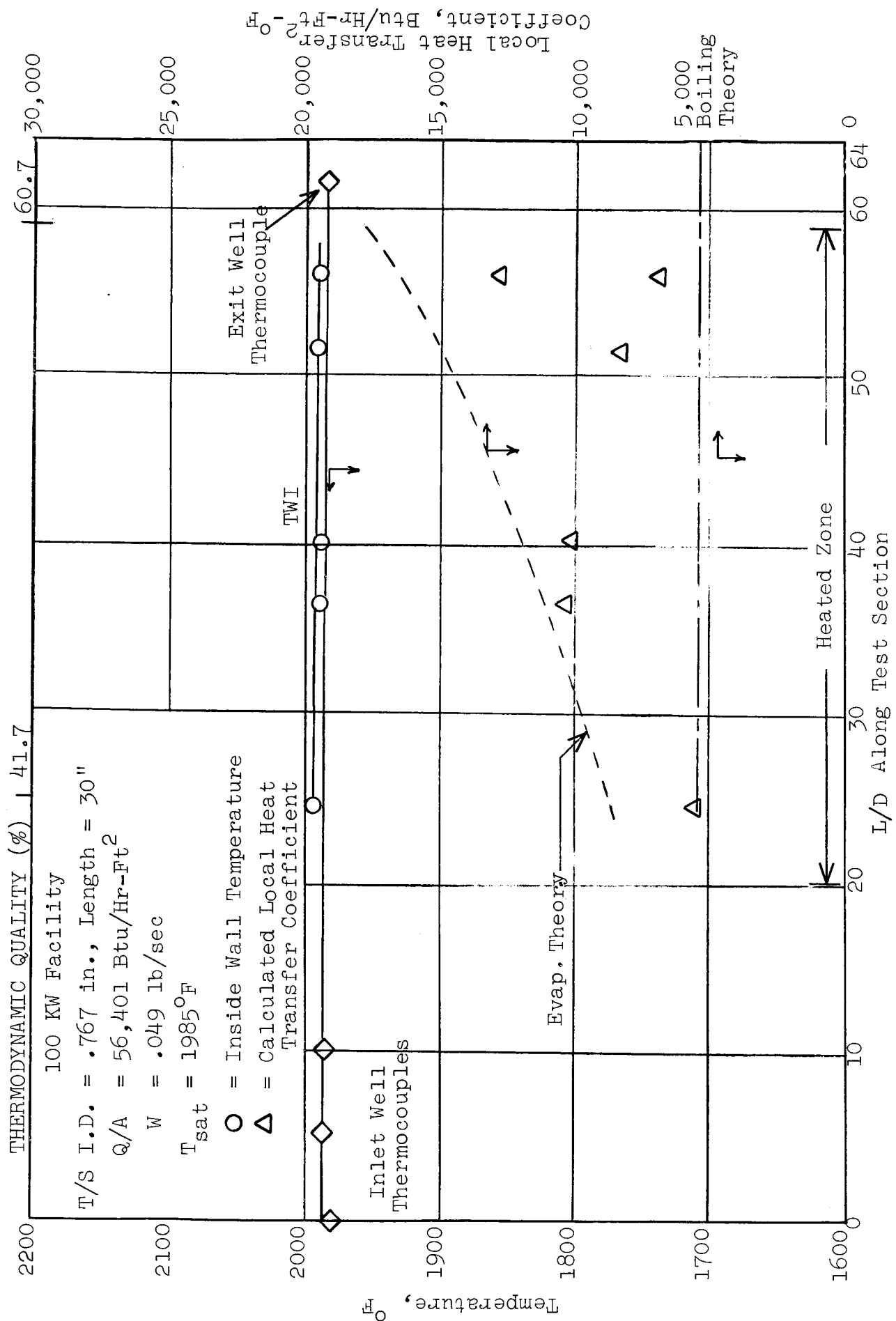


Figure 62b. Forced Convection Vaporization of Potassium at Intermediate Vapor Qualities;  
 $q'' \approx 56,000 \text{ Btu/hr-ft}^2$  (100 KW Data)

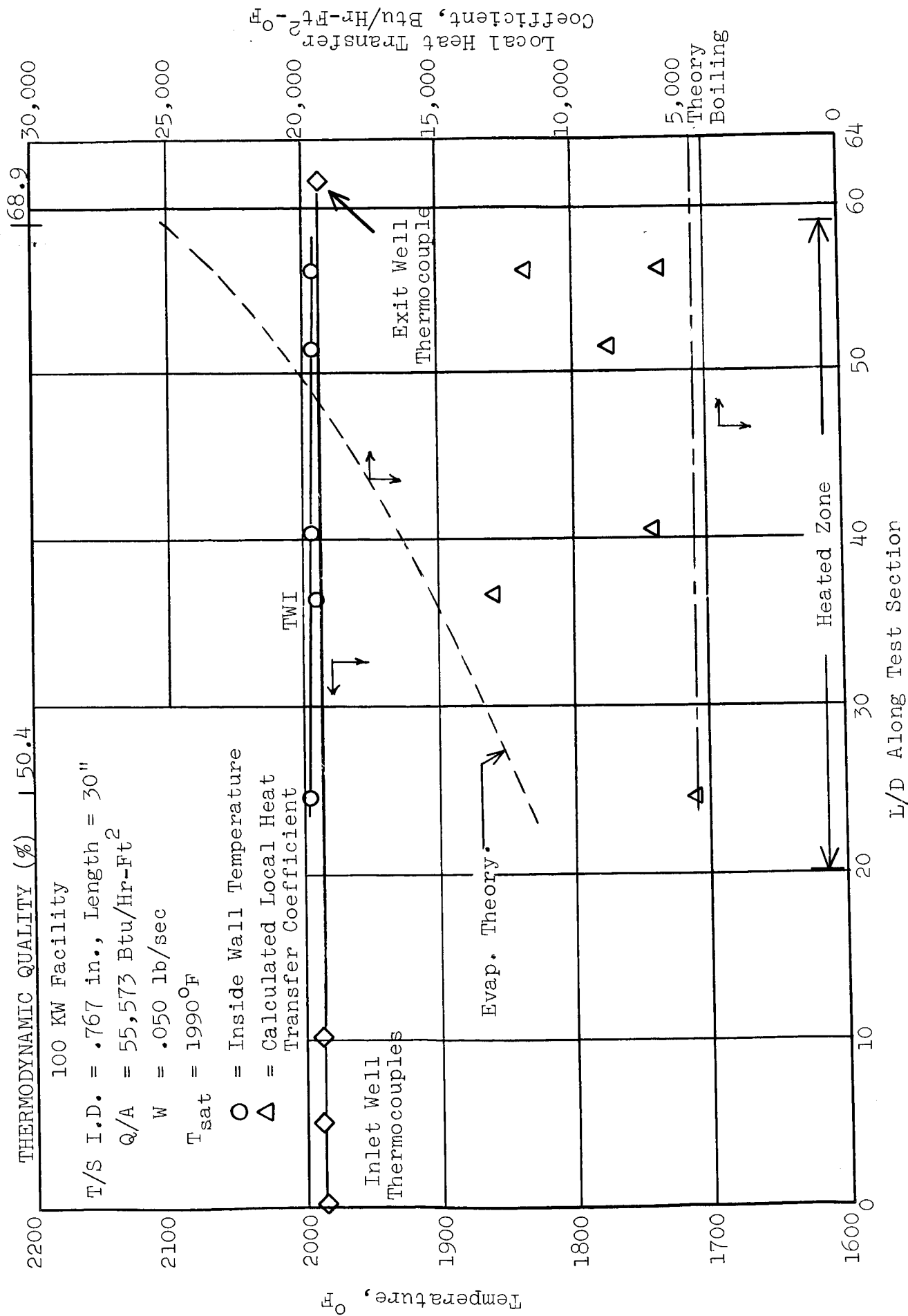


Figure 62c. Forced Convection Vaporization of Potassium at Intermediate Vapor Qualities;  
 $q'' = 55,000 \text{ Btu/hr-ft}^2$  (100 KW Data)

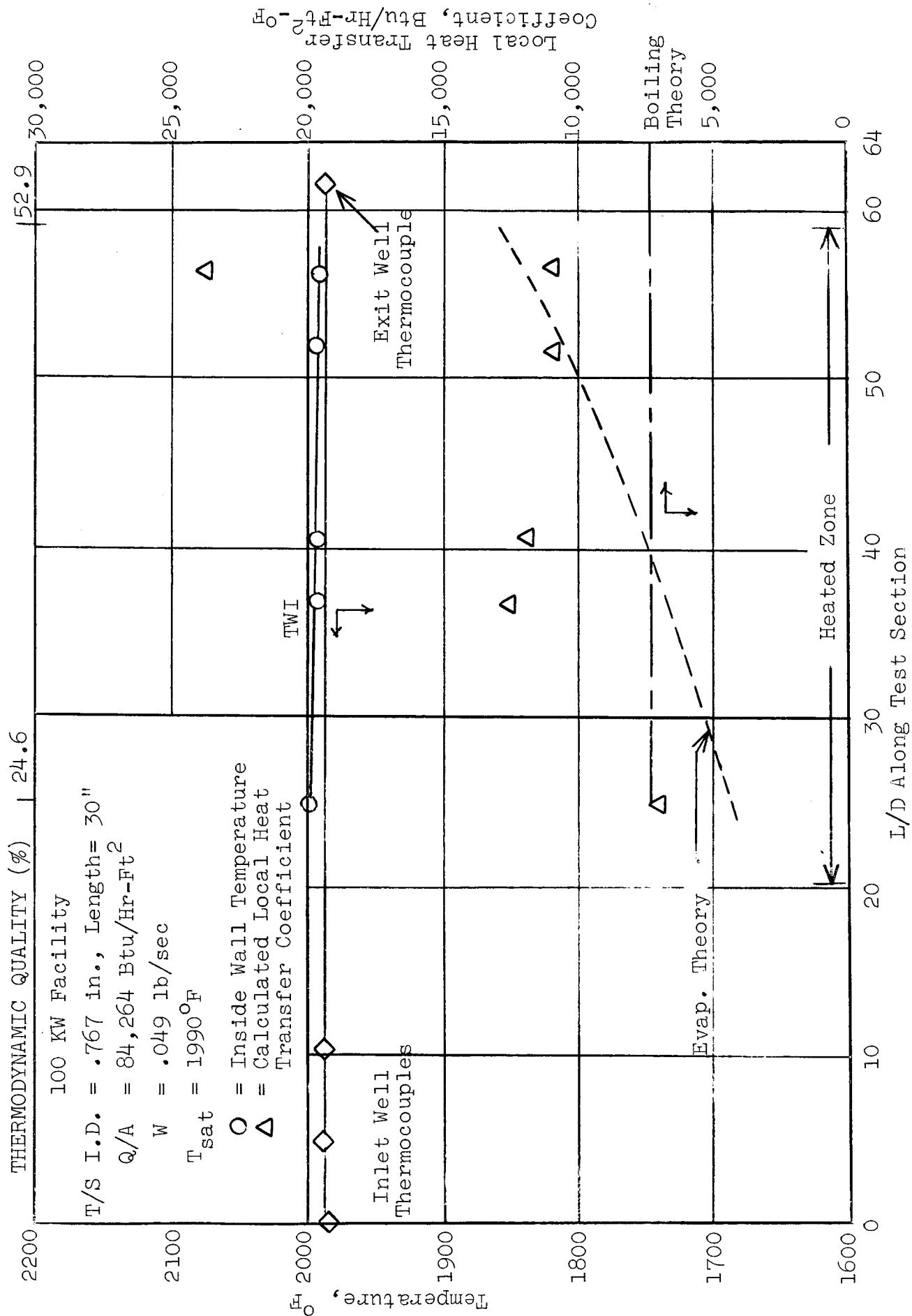


Figure 62d. Forced Convection Vaporization of Potassium at Intermediate Vapor Qualities;  
 $q'' = 84,000 \text{ Btu/hr-ft}^2$  (100 KW Data)



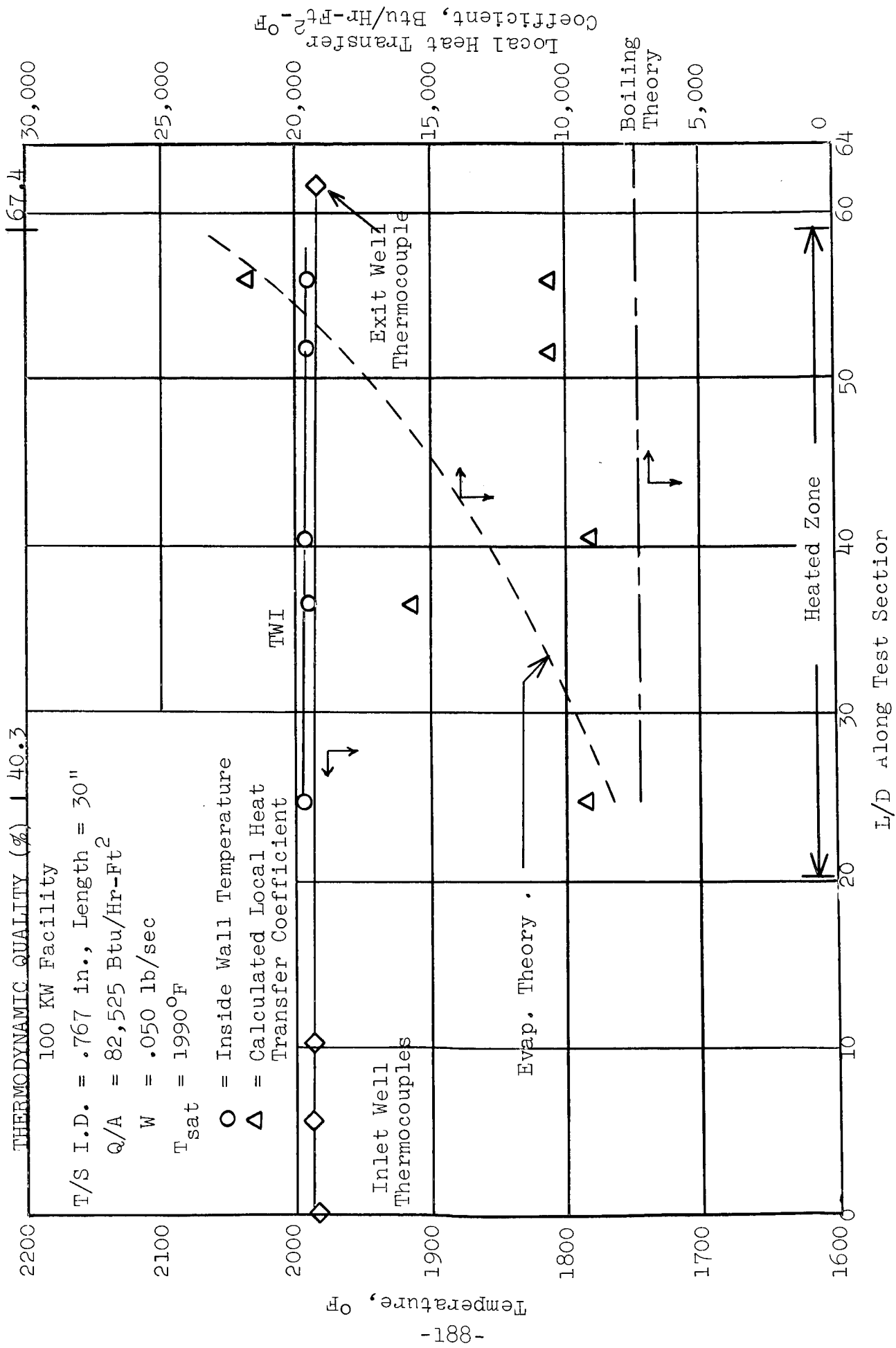


Figure 62e. Forced Convection Vaporization of Potassium at Intermediate Vapor Qualities;  
 $q'' = 82,000 \text{ Btu/hr-ft}^2$  (100 KW Data)

APPENDIX A  
DERIVATION OF HELIX EQUATIONS - 300 KW PROJECT

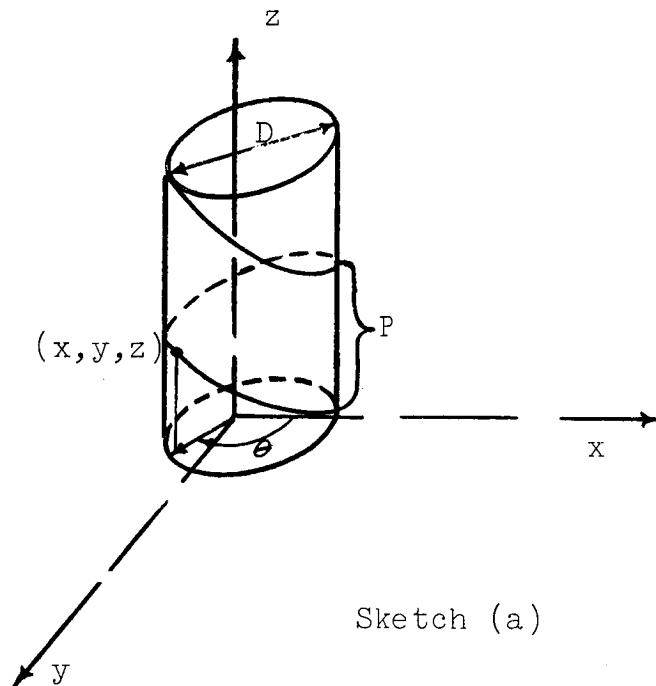
J. R. Peterson

APPENDIX A  
Derivation of Helix Equations

Definition of Helix

The cylindrical helix is the path of a point which moves around the surface of a right circular cylinder with a constant angular velocity  $w$  and at the same time moves parallel to the axis of the cylinder with a constant linear or axial velocity  $V_a$ . The pitch ( $P$ ) of the helix is the axial distance traveled for an angular displacement of  $2\pi$  radians.

Derivation of Helical Path Length and Helical Velocity:



Sketch (a)

Sketch (a) above illustrates the helical path. From the drawing, the co-ordinates  $x$ ,  $y$  and  $z$  are given as follows in terms of the angular displacement  $\theta$  the time  $t$  and the helix diameter  $D$ :

$$x = D/2 \cos \Theta \quad (1)$$

$$y = D/2 \sin \Theta \quad (2)$$

$$z = V_a t \quad (3)$$

$$\Theta = \omega t \quad (4)$$

From equations (3) + (4):

$$t = z/V_a = \Theta/\omega \quad (5)$$

The arc length  $s$  along a three dimensional curve is given as follows:

$$s = \int \sqrt{dx^2 + dy^2 + dz^2} \quad (6)$$

In terms of the parameter  $\Theta$  ,

$$s = \int \sqrt{\left(\frac{dx}{d\Theta}\right)^2 + \left(\frac{dy}{d\Theta}\right)^2 + \left(\frac{dz}{d\Theta}\right)^2} d\Theta \quad (7)$$

From equations (1) and (2):

$$\frac{dx}{d\Theta} = - D/2 \sin \Theta \quad (8)$$

$$\frac{dy}{d\Theta} = D/2 \cos \Theta \quad (9)$$

$$\left(\frac{dx}{d\Theta}\right)^2 + \left(\frac{dy}{d\Theta}\right)^2 = \frac{D^2}{4} (\sin^2 \Theta + \cos^2 \Theta) = D^2/4 \quad (10)$$

From equation (5)

$$z = \frac{V_a}{\omega} \Theta \quad (11)$$

In the time required for  $2\pi$  angular displacement, an axial length  $z = P$  is traveled, therefore from equation (5):

$$P = \frac{2\pi V_a}{w}, \text{ or } \frac{V_a}{w} = \frac{P}{2\pi} \quad (12)$$

From equations (11) and (12):

$$\frac{dz}{d\Theta} = P/2\pi \quad (13)$$

Combining equations (7), (8), (9) and (13) to obtain the helical path length  $L_H$ :

$$s = \int \sqrt{D^2/4 + \frac{P^2}{4\pi^2}} d\Theta = L_H \quad (14)$$

Upon integrating equation (14) over the angular displacement 0 to  $2\pi$  radians, and recognizing that the axial length  $L$  traversed for a  $2\pi$  angular displacement is  $P$ , we obtain:

$$\frac{L_H}{L} = \frac{L_H}{P} = \sqrt{1 + \left(\frac{\pi D}{P}\right)^2} \quad (15)$$

The helical velocity  $V_H$  is obtained by dividing the helical path length for  $2\pi$  revolutions by the time required by  $2\pi$  revolutions as follows; using equations (5) and (15):

$$V_H = \frac{\frac{L_H}{2\pi}}{\frac{P}{V_a}} = \frac{P \sqrt{1 + \left(\frac{\pi D}{P}\right)^2}}{(P/V_a)} \quad (16)$$

$$\frac{V_H}{V_a} = \sqrt{1 + \left(\frac{\pi D}{P}\right)^2} \quad (17)$$

Tangential Velocity:

In the time  $P/V_a$  required for  $2\pi$  revolutions, a circumferential distance of  $\pi D$  is traversed. The circumferential or tangential component of the helical velocity  $V_T$  is therefore given as follows:

$$V_T = \frac{\pi D}{P/V_a} \quad (18)$$

$$V_T/V_a = \frac{\pi D}{P} \quad (19)$$

Axial Flow Area and Equivalent Diameter:

The axial flow area  $A_F$  perpendicular to the axis of a tube containing a helical insert is given as follows, where  $D_i$  is the tube inside diameter,  $D_{cb}$  the helix centerbody diameter and  $\Delta$  is the thickness of the tape wound around the centerbody:

$$A_F = \frac{\pi}{4} \left[ D_i^2 - D_{cb}^2 \right] - \frac{[D_i - D_{cb}] \Delta}{2.0} \quad (20)$$

The wetted perimeter  $P_w$  encountered by the axial flow is as follows:

$$P_w = \pi (D_i + D_{cb}) + D_i - D_{cb} - 2\Delta \quad (21)$$

The equivalent diameter,  $D_e$ , of the tube containing helical insert from the flow area and wetted perimeter is given as follows:

$$D_e = \frac{4A_F}{P_w} = \frac{D_i \left[ 1 - \left(\frac{D_{cb}}{D_i}\right)^2 - \frac{2\Delta}{\pi} \left(\frac{1}{D_i} - \frac{D_{cb}}{D_i^2}\right) \right]}{1 + \frac{D_{cb}}{D_i} + \left(1 - \frac{D_{cb}}{D_i} - \frac{2\Delta}{D_i}\right) \frac{1}{\pi}} \quad (22)$$

Neglecting the tape width  $\Delta$ , equation (23) following is obtained:

$$D_e/D_i = \frac{1 - \left(\frac{D_{cb}}{D_i}\right)^2}{1 + \frac{D_{cb}}{D_i} + \frac{1}{\pi} \left(1 - \frac{D_{cb}}{D_i}\right)} \quad (23)$$

#### Radial Acceleration Developed by the Insert:

A parameter of interest in the analysis of the experimental boiling data is the radial acceleration developed by the insert in two phase flow in the thin liquid film at the tube wall. An expression for this radial acceleration  $a$ , expressed as a multiple of the standard gravitational acceleration  $g$ , is obtained as follows. Assuming that the liquid fraction in two phase potassium flow occupies a negligible fraction of the flow area, the axial vapor velocity  $V_{ag}$  is given by equation (24) in terms of the total mass flow rate  $W$ , or axial mass velocity  $G_a$ :

$$V_{ag} = \frac{XW}{\rho_g A_F} = \frac{XG_a}{\rho_g} \quad (24)$$

Using the ratio of vapor to liquid velocities  $K$  and equation (19), the tangential liquid velocity at the tube wall  $V_{fT}$  is obtained as follows:

$$V_{fT} = \frac{V_{ag}}{K} \frac{\pi D_i}{P} = \frac{XG_a}{\rho_g K} \frac{\pi D_i}{P} \quad (25)$$

The radial acceleration  $a$  in the liquid film at the tube wall is finally obtained as follows:

$$a = \frac{2V_{fT}^2}{D_i g} = \frac{2}{D_i g} \left( \frac{XG_a}{\rho_g K} \frac{\pi D_i}{P} \right)^2 \quad (26)$$

APPENDIX B

100 KW DATA



TABLE B-1

100 KW LOOP TEST SECTION INSTRUMENTATION FOR  
DATA TAKEN BETWEEN 2-25-65 AND 4-1-65

<u>T/C No.</u>	<u>Location</u>	<u>Distance Inches</u>
	Start of Heated Zone	15 1/4
20	Test Section Wall	20 7/16
21	Test Section Wall	20 1/2
22	Test Section Wall	30
23	Test Section Wall	30
24	Test Section Wall	41 5/8
25	Test Section Wall	41 5/8
26	Test Section Wall	43 3/4
27	Test Section Wall	43 5/8
31	Test Section Wall	43 9/16
32	Test Section Wall	43 5/8
	End of Heated Zone	45 1/4
33	Test Section Outlet Well	47
34	Test Section Outlet Well	47
35	Test Section Outlet Well	47

Test Section I.D. = 0.423 inches,  
No Insert

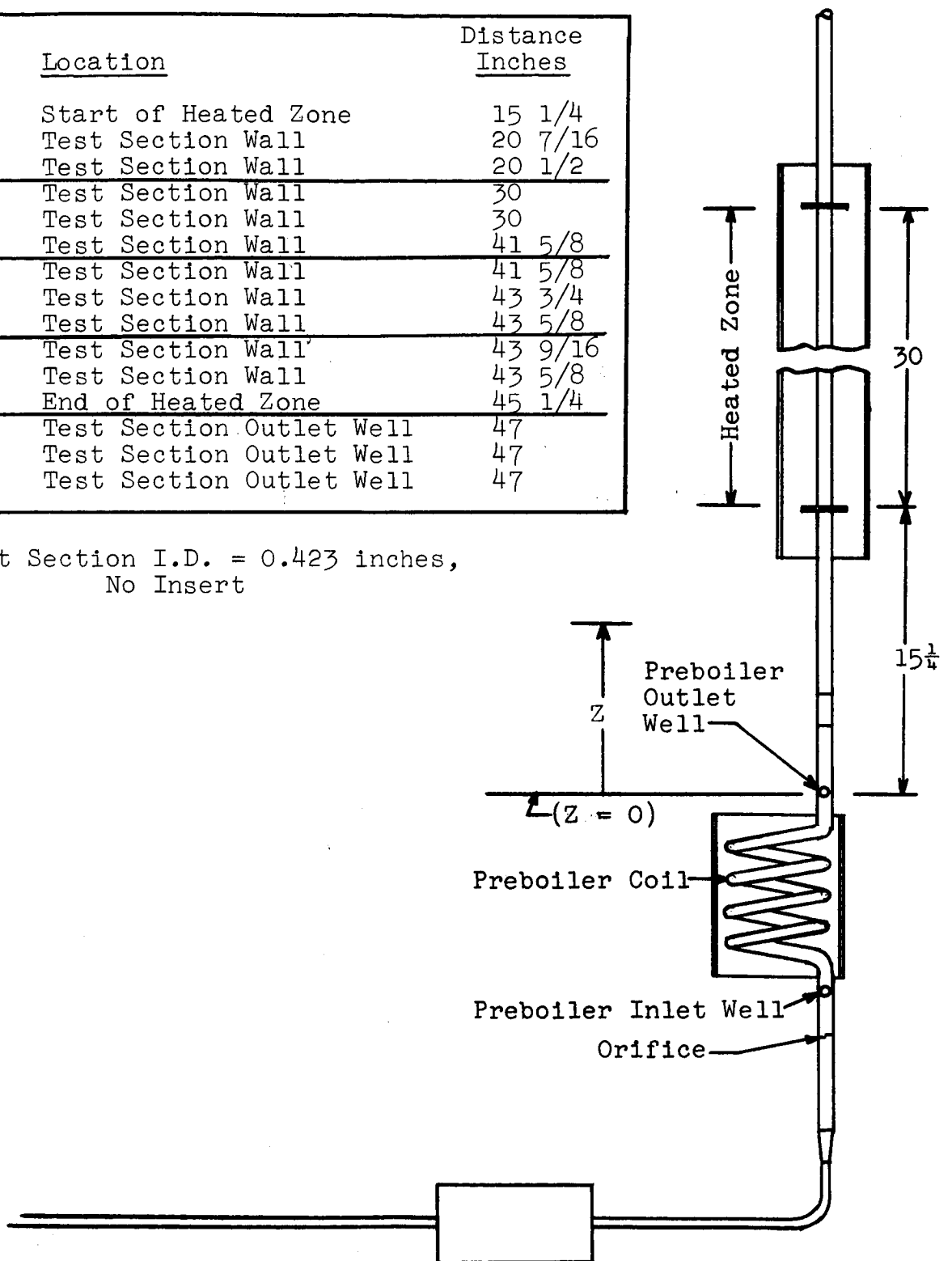


TABLE B-2

## NOMENCLATURE FOR TABULATED 100 KW BOILING DATA

(Key to Tables B-3a through B-3d)

<u>Col. No.</u>	<u>Heading</u>	<u>Description</u>
236	DATE	(e.g., 2.2550 + 03 = 2-25-65)
237	TIME	(e.g., 1.7240 + 03 = 1724)
274	TK FM	Fluid temperature at flowmeter, °F
282,290	TPB IN	Preboiler inlet temperature, °F
298-370	PBC N	Preboiler coil temperature, °F
380,389	TPBOUT	Preboiler outlet well temperature, °F
443-497	TWO N	Test Section Outside Pipe Wall temperature, °F
515,524	TTSOUT	Fluid temperature at test section outlet, °F
540	MAGNET	Flowmeter magnet temperature, °F
547-617	CND N	Condenser temperature at N, °F
624-659	PBRADS	Preboiler radiation shield temperature, °F
666-715	TSRADS	Test Section radiation shield temperature, °F
774	QN PB	Net preboiler power, KW
780	QN TS	Net test section power, KW
784	Q/A TS	T/S Heat Flux, Btu/hr-ft <sup>2</sup>
802	FLOW	Flow rate, lbs/sec
804	G	Mass velocity, lbs/sec-ft <sup>2</sup>
807	P SAT	Saturation pressure corresponding to fluid temperature at test section outlet, psi
816	X PB	Preboiler exit quality
823	X TS	Test section exit quality
825	ENTOUT	Mixture Enthalpy at T/S Outlet
828	VELOUT	Vapor velocity, ft/sec
1024-1066	TWI N	Inside wall temperature at N, °F
1067	DT 31	(TWI 31 - TTSOUT) Avg. at 31, °F
1068	H 31	$\frac{Q/A}{DT\ 31}$ , Btu/hr-ft <sup>2</sup> °F

TABLE B-3a

## 100 KW BOILING DATA .423-IN. TUBE, NO INSERT

	236	237	274	282	290	298
	DATE	TIME	TK FM	TPB IN	TPB IN	PBC 5
1	2.2550+03	1.7240+03	1.0407+03	1.0413+03	1.0418+03	1.8161+03
2	2.2550+03	1.9550+03	1.0622+03	1.0636+03	1.0649+03	1.9194+03
3	2.2550+03	2.1580+03	1.0906+03	1.0783+03	1.0948+03	2.0232+03
4	2.2650+03	5.0000+01	1.1002+03	1.0712+03	1.1051+03	2.1148+03
5	2.2650+03	2.5000+02	1.1321+03	1.1116+03	1.1364+03	2.1996+03
6	2.2650+03	5.0500+02	1.1571+03	1.1475+03	1.1607+03	2.1206+03
7	2.2650+03	8.3000+02	1.2065+03	1.2026+03	1.2068+03	2.1327+03
8	2.2650+03	1.2300+03	1.2166+03	1.2134+03	1.2165+03	2.1336+03
9	2.2650+03	2.0370+03	1.0165+03	1.0143+03	1.0131+03	1.6745+03
10	2.2650+03	2.3070+03	1.0357+03	1.0371+03	1.0363+03	1.8019+03
11	2.2750+03	1.5200+02	1.0390+03	1.0405+03	1.0382+03	1.9212+03
12	2.2750+03	4.3000+02	1.0641+03	1.0670+03	1.0648+03	1.9991+03
13	2.2750+03	6.3200+02	1.0832+03	1.0876+03	1.0860+03	2.0990+03
14	2.2750+03	9.3000+02	1.1163+03	1.1202+03	1.1187+03	2.1770+03
15	2.2750+03	1.2150+03	1.1424+03	1.1456+03	1.1464+03	2.1217+03
16	2.2750+03	1.8380+03	1.0480+03	1.0438+03	1.0433+03	1.6861+03
17	2.2750+03	2.0570+03	1.0588+03	1.0568+03	1.0556+03	1.8058+03
18	2.2750+03	2.3290+03	1.0824+03	1.0816+03	1.0805+03	1.8899+03
19	2.2850+03	2.2300+02	1.1079+03	1.1085+03	1.1084+03	2.0280+03
20	2.2850+03	4.3000+02	1.1318+03	1.1330+03	1.1309+03	2.1206+03
21	2.2850+03	6.2500+02	1.1648+03	1.1647+03	1.1643+03	2.1378+03
22	2.2850+03	9.0000+02	1.1913+03	1.1900+03	1.1894+03	2.1206+03

100 KW BOILING DATA .423-IN. TUBE, NO INSERT

	314	322	330	338	346	362
	PBC 7	PBC 8	PBC 9	PBC 10	PBC 11	PBC 13
1	2.0143+03	2.1001+03	2.1652+03	2.1090+03	2.1140+03	2.0957+03
2	2.1207+03	2.1240+03	2.1144+03	2.1094+03	2.1174+03	2.0996+03
3	2.1166+03	2.1229+03	2.1199+03	2.1147+03	2.1192+03	2.1019+03
4	2.1118+03	2.1228+03	2.1201+03	2.1133+03	2.1189+03	2.0991+03
5	2.1186+03	2.1351+03	2.1231+03	2.1172+03	2.1215+03	2.1020+03
6	2.1247+03	2.1338+03	2.1265+03	2.1211+03	2.1242+03	2.1035+03
7	2.1281+03	2.1353+03	2.1299+03	2.1241+03	2.1271+03	2.1062+03
8	2.1270+03	2.1361+03	2.1311+03	2.1247+03	2.1275+03	2.1050+03
9	1.8723+03	1.9531+03	2.0168+03	2.0704+03	2.1381+03	2.1027+03
10	2.0097+03	2.0928+03	2.1518+03	2.1165+03	2.1172+03	2.0988+03
11	2.1277+03	2.1191+03	2.1090+03	2.1069+03	2.1151+03	2.0964+03
12	2.1158+03	2.1156+03	2.1139+03	2.1118+03	2.1169+03	2.0984+03
13	2.1126+03	2.1236+03	2.1190+03	2.1140+03	2.1204+03	2.1011+03
14	2.1204+03	2.1369+03	2.1260+03	2.1207+03	2.1266+03	2.1075+03
15	2.1209+03	2.1337+03	2.1256+03	2.1198+03	2.1248+03	2.1057+03
16	1.8777+03	1.9545+03	2.0140+03	2.0669+03	2.1340+03	2.0968+03
17	2.0104+03	2.0937+03	2.1519+03	2.1072+03	2.1150+03	2.0963+03
18	2.0943+03	2.1364+03	2.1110+03	2.1069+03	2.1170+03	2.0984+03
19	2.1139+03	2.1212+03	2.1158+03	2.1137+03	2.1210+03	2.1023+03
20	2.1190+03	2.1323+03	2.1260+03	2.1220+03	2.1277+03	2.1070+03
21	2.1211+03	2.1376+03	2.1257+03	2.1204+03	2.1263+03	2.1072+03
22	2.1217+03	2.1345+03	2.1265+03	2.1217+03	2.1267+03	2.1069+03

100 KW BOILING DATA .423-IN. TUBE, NO INSERT

	370	380	389	443	452	497
	PBC 14	TPBOUT	TPBOUT	TWO 22	TWO 23	TWO 31
1	2.1009+03	2.1041+03	2.1190+03	2.1322+03	2.1691+03	2.1299+03
2	2.1045+03	2.1051+03	2.1199+03	2.1367+03	2.1737+03	2.1313+03
3	2.1047+03	2.1047+03	2.1194+03	2.1358+03	2.1729+03	2.1292+03
4	2.1031+03	2.1016+03	2.1165+03	2.1332+03	2.1760+03	2.1279+03
5	2.1060+03	2.1029+03	2.1174+03	2.1336+03	2.1787+03	2.1280+03
6	2.1081+03	2.1034+03	2.1171+03	2.1346+03	2.1770+03	2.1277+03
7	2.1088+03	2.1026+03	2.1169+03	2.1343+03	2.1716+03	2.1268+03
8	2.1076+03	2.1011+03	2.1146+03	2.1310+03	2.1682+03	2.1252+03
9	2.1060+03	2.1324+03	2.1463+03	2.1624+03	2.1973+03	2.1468+03
10	2.1027+03	2.1078+03	2.1226+03	2.1530+03	2.2003+03	2.1489+03
11	2.1013+03	2.1045+03	2.1185+03	2.1494+03	2.1970+03	2.1432+03
12	2.1015+03	2.1034+03	2.1176+03	2.1491+03	2.1991+03	2.1427+03
13	2.1047+03	2.1044+03	2.1191+03	2.1498+03	2.2003+03	2.1428+03
14	2.1106+03	2.1103+03	2.1230+03	2.1543+03	2.2051+03	2.1462+03
15		2.1069+03	2.1194+03	2.1512+03	2.2035+03	2.1437+03
16		2.1301+03	2.1437+03	2.1924+03	2.2558+03	2.1671+03
17		2.1075+03	2.1219+03	2.1842+03	2.2554+03	2.1688+03
18		2.1083+03	2.1219+03	2.1856+03	2.2548+03	2.1682+03
19	2.1052+03	2.1072+03	2.1223+03	2.1793+03	2.2431+03	2.1625+03
20	2.1108+03	2.1133+03	2.1260+03	2.1918+03	2.2612+03	2.1758+03
21	2.1103+03	2.1104+03	2.1238+03	2.1774+03	2.2394+03	2.1626+03
22	2.1096+03	2.1088+03	2.1218+03	2.1752+03	2.2345+03	2.1597+03

100 KW BOILING DATA .423-IN. TUBE, NO INSERT

	515	524	540	547	554	561
	TTSOUT	TTSOUT	MAGNET	CND 37	CND 38	CND 39
1	2.1047+03	2.1067+03	5.8953+02	2.0781+03	1.7806+03	9.2173+02
2	2.1042+03	2.1064+03	6.0621+02	2.0778+03	1.8892+03	9.3898+02
3	2.1022+03	2.1044+03	6.2348+02	2.0751+03	2.0397+03	9.5678+02
4	2.1000+03	2.1019+03	6.3519+02	2.0720+03	2.0383+03	
5	2.1013+03	2.1020+03	6.4999+02	2.0707+03	2.0360+03	
6	2.1007+03	2.1013+03	6.6182+02	2.0700+03	2.0351+03	
7	2.0990+03	2.0994+03	6.7186+02	2.0675+03	2.0316+03	
8	2.0953+03	2.0968+03	6.6749+02	2.0652+03	2.0297+03	
9	2.1079+03	2.1072+03	5.3274+02	2.0822+03	1.7250+03	
10	2.1079+03	2.0836+03	5.5399+02	2.0822+03	1.8230+03	
11	2.1049+03	2.1048+03	5.6387+02	2.0779+03	1.9686+03	
12	2.1036+03	2.1037+03	5.7589+02	2.0752+03	2.0383+03	
13	2.1031+03	2.1040+03	5.8965+02	2.0748+03	2.0407+03	
14	2.1051+03	2.1070+03	6.0529+02	2.0780+03	2.0422+03	
15	2.1009+03	2.1023+03	6.1844+02	2.0734+03	2.0378+03	
16	2.1035+03	2.1047+03	5.5065+02	2.0766+03	2.0028+03	
17	2.1053+03	2.1066+03	5.5810+02	2.0781+03	2.0458+03	
18	2.1061+03	2.1068+03	5.7052+02	2.0774+03	2.0444+03	
19	2.1049+03	2.1056+03	5.8798+02	2.0754+03	2.0415+03	
20	2.1174+03	2.1124+03	6.0031+02	2.0779+03	2.0441+03	
21	2.1028+03	2.1043+03	6.1507+02	2.0752+03	2.0401+03	
22	2.1016+03	2.1028+03	6.2639+02	2.0733+03	2.0381+03	

100 KW BOILING DATA .423-IN. TUBE, NO INSERT

	568	575	582	589	596	603
	CND 40	CND 41	CND 42	CND 43	CND 44	CND 45
1	1.1965+03	1.3009+03		1.2240+03	1.0600+03	1.1641+03
2	1.2327+03	1.3341+03		1.2533+03	1.0865+03	1.1897+03
3	1.2886+03	1.3845+03		1.2948+03	1.1183+03	1.2249+03
4		1.4295+03		1.3293+03		1.2528+03
5		1.4939+03		1.3802+03		1.2944+03
6		1.5703+03		1.4363+03		1.3375+03
7	1.5676+03	1.6835+03	1.5980+03	1.5200+03	1.2855+03	1.4036+03
8	1.7139+03	1.7996+03	1.6794+03	1.5809+03		1.4481+03
9	1.1998+03	1.2960+03	1.2501+03	1.2075+03		1.1420+03
10	1.2332+03	1.3278+03	1.2790+03	1.2344+03		1.1650+03
11		1.3554+03	1.3041+03	1.2557+03		1.1810+03
12		1.4067+03	1.3500+03	1.2972+03		1.2157+03
13		1.4608+03	1.3972+03	1.3385+03		1.2499+03
14	1.4381+03	1.5345+03	1.4634+03	1.3977+03		1.2988+03
15	1.5159+03	1.6131+03	1.5276+03	1.4524+03		1.3404+03
16	1.2735+03	1.3713+03	1.3165+03	1.2659+03		1.1891+03
17	1.3156+03	1.4134+03	1.3537+03	1.2993+03		1.2162+03
18	1.3702+03	1.4704+03	1.4044+03	1.3447+03		1.2539+03
19		1.5402+03	1.4648+03	1.3955+03		1.2931+03
20		1.6142+03	1.5240+03	1.4473+03		1.3343+03
21		1.7276+03	1.6174+03	1.5247+03	1.2631+03	1.3918+03
22	1.7356+03	1.8054+03	1.6848+03	1.5805+03	1.3056+03	1.4345+03

100 KW BOILING DATA .423-IN. TUBE, NO INSERT

	610	617	624	631	638	645
	CND 46	CND 47	PBRADS	PBRADS	PBRADS	PBRADS
1	1.1360+03	1.1145+03	9.2856+02	9.6455+02	8.9677+02	9.0768+02
2	1.1599+03	1.1370+03	9.6110+02	9.9403+02	9.2915+02	9.4100+02
3	1.1919+03	1.1671+03	9.9571+02	1.0265+03	9.6370+02	9.7514+02
4	1.2169+03	1.1889+03	1.0234+03	1.0519+03	9.9120+02	1.0015+03
5	1.2553+03	1.2248+03	1.0524+03	1.0780+03	1.0199+03	1.0287+03
6	1.2934+03	1.2592+03	1.0767+03	1.1005+03	1.0457+03	1.0528+03
7	1.3519+03	1.3124+03	1.1000+03	1.1213+03	1.0957+03	1.0982+03
8	1.3894+03	1.3448+03	1.1115+03	1.1301+03	1.0843+03	1.0864+03
9	1.1117+03	1.0880+03	8.5522+02	8.9551+02	8.2711+02	8.3164+02
10	1.1326+03	1.1081+03	8.9650+02	9.3341+02	8.6446+02	8.7540+02
11	1.1469+03	1.1207+03	9.2944+02	9.6251+02	8.9568+02	9.0987+02
12	1.1782+03	1.1501+03	9.5918+02	9.8932+02	9.2683+02	9.4083+02
13	1.2089+03	1.1773+03	9.9080+02	1.0185+03	9.5985+02	9.7266+02
14	1.2536+03	1.2188+03	1.0234+03	1.0485+03	9.9317+02	1.0034+03
15	1.2903+03	1.2521+03	1.0468+03	1.0694+03	1.0175+03	1.0260+03
16	1.1533+03	1.1267+03	8.6344+02	9.0247+02	8.3692+02	8.3433+02
17	1.1785+03	1.1494+03	9.0599+02	9.4133+02	8.7611+02	8.7932+02
18	1.2118+03	1.1797+03	9.3421+02	9.6665+02	9.0453+02	9.0851+02
19	1.2470+03	1.2118+03	9.7286+02	1.0014+03	9.4300+02	9.4891+02
20	1.2844+03	1.2459+03	1.0019+03	1.0284+03	9.7257+02	9.7744+02
21	1.3352+03	1.2913+03	1.0315+03	1.0550+03	1.0023+03	1.0046+03
22	1.3728+03	1.3260+03	1.0510+03	1.0727+03	1.0213+03	1.0219+03



100 KW BOILING DATA .423-IN. TUBE, NO INSERT

	652	659	666	673	680	687
	PBRADS	PBRADS	TSRADS	TSRADS	TSRADS	TSRADS
1	8.8772+02	9.5677+02	1.1517+03	1.1523+03	1.1716+03	1.1710+03
2	9.2077+02	9.8708+02	1.1581+03	1.1588+03	1.1787+03	1.1790+03
3	9.5436+02	1.0188+03	1.1620+03	1.1627+03	1.1835+03	1.1836+03
4	9.8063+02	1.0435+03	1.1732+03	1.1739+03	1.1934+03	1.1941+03
5	1.0077+03	1.0685+03	1.1762+03	1.1770+03	1.1966+03	1.1975+03
6	1.0326+03	1.0896+03	1.1752+03	1.1760+03	1.1973+03	1.1979+03
7	1.0743+03	1.1243+03	1.1845+03	1.1835+03	1.2001+03	1.1990+03
8	1.0688+03	1.1173+03	1.1752+03	1.1760+03	1.1976+03	1.1988+03
9	8.1730+02	8.8330+02	1.2097+03	1.2102+03	1.2333+03	1.2325+03
10	8.5861+02	9.2528+02	1.2112+03	1.2118+03	1.2345+03	1.2347+03
11	8.9159+02	9.5657+02	1.2151+03	1.2157+03	1.2394+03	1.2403+03
12	9.2294+02	9.8462+02	1.2150+03	1.2156+03	1.2388+03	1.2395+03
13	9.5583+02	1.0141+03	1.2205+03	1.2212+03	1.2441+03	1.2454+03
14	9.8787+02	1.0443+03	1.2306+03	1.2313+03	1.2550+03	1.2572+03
15	1.0110+03	1.0653+03	1.2351+03	1.2359+03	1.2594+03	1.2604+03
16	8.2250+02	8.8657+02	1.2762+03	1.2767+03	1.2998+03	1.3010+03
17	8.6538+02	9.2919+02	1.2915+03	1.2920+03	1.3013+03	1.3033+03
18	8.9216+02	9.5562+02	1.2900+03	1.2906+03	1.3014+03	1.3039+03
19	9.3389+02	9.9216+02	1.2782+03	1.2788+03	1.2888+03	1.2921+03
20	9.6273+02	1.0191+03	1.2760+03	1.2766+03	1.2868+03	1.2900+03
21	9.9083+02	1.0453+03	1.2775+03	1.2782+03	1.2880+03	1.2921+03
22	1.0087+03	1.0615+03	1.2724+03	1.2731+03	1.2830+03	1.2875+03

100 KW BOILING DATA .423-IN. TUBE, NO INSERT

	708	715	774	780	784	802
	TSRADS	TSRADS	QN PB	QN TS	Q/A TS	FLOW
1	1.1886+03	1.0813+03	1.5585+01	8.1248+00	1.0002+05	6.0212-02
2	1.1965+03	1.0888+03	1.7596+01	7.8935+00	9.7175+04	6.0756-02
3	1.2000+03	1.0892+03	2.0168+01	7.7631+00	9.5571+04	6.0961-02
4	1.2096+03	1.0966+03	2.2773+01	7.7167+00	9.5000+04	5.9569-02
5	1.2126+03	1.1003+03	2.5326+01	7.9532+00	9.7911+04	5.9772-02
6	1.2121+03	1.0994+03	2.8444+01	8.0502+00	9.9105+04	5.9914-02
7	1.2115+03	1.0971+03	3.0826+01	8.2008+00	1.0096+05	6.1605-02
8	1.2126+03	1.0961+03	3.3267+01	8.4140+00	1.0358+05	6.1597-02
9	1.2523+03	1.1112+03	1.3401+01	1.1662+01	1.4357+05	6.0200-02
10	1.2517+03	1.1128+03	1.5425+01	1.1486+01	1.4141+05	5.9980-02
11	1.2575+03	1.1188+03	1.7593+01	1.1984+01	1.4753+05	5.8626-02
12	1.2558+03	1.1188+03	1.9687+01	1.1995+01	1.4767+05	5.9571-02
13	1.2612+03	1.1240+03	2.2295+01	1.2032+01	1.4812+05	5.9027-02
14	1.2720+03	1.1359+03	2.4060+01	1.2406+01	1.5273+05	6.0026-02
15	1.2765+03	1.1409+03	2.7539+01	1.2567+01	1.5471+05	6.0214-02
16	1.3136+03	1.1703+03	1.2549+01	1.7521+01	2.1569+05	5.9342-02
17	1.3153+03	1.1710+03	1.5083+01	1.7892+01	2.2027+05	5.9307-02
18	1.3168+03	1.1728+03	1.7074+01	1.8889+01	2.3254+05	6.0555-02
19	1.3093+03	1.1673+03	1.9837+01	1.8102+01	2.2286+05	5.9021-02
20	1.3065+03	1.1666+03	2.2397+01	1.8144+01	2.2337+05	5.8929-02
21	1.3084+03	1.1704+03	2.4932+01	1.8104+01	2.2287+05	5.8664-02
22	1.3039+03	1.1668+03	2.6815+01	1.8201+01	2.2407+05	6.0332-02

100 KW BOILING DATA .423-IN. TUBE, NO INSERT

	804	807	816	823	825	828
	G	P SAT	X PB	X TS	ENTOUT	VELCUT
1	6.1567+01	2.0380+02	3.4004-02	2.1357-01	6.6312+02	3.7448+01
2	6.2123+01	2.0358+02	8.0295-02	2.5355-01	6.9180+02	4.4907+01
3	6.2332+01	2.0249+02	1.4065-01	3.1075-01	7.3261+02	5.5502+01
4	6.0909+01	2.0122+02	2.0978-01	3.8238-01	7.8380+02	6.7130+01
5	6.1116+01	2.0160+02	2.7367-01	4.5091-01	8.3324+02	7.9290+01
6	6.1262+01	2.0123+02	3.4908-01	5.2803-01	8.8867+02	9.3231+01
7	6.2991+01	2.0030+02	3.9668-01	5.7408-01	9.2162+02	1.0467+02
8	6.2982+01	1.9863+02	4.5226-01	6.3421-01	9.6459+02	1.1649+02
9	6.1554+01	2.0482+02	-2.9792-02	2.3556-01	6.7927+02	4.1103+01
10	6.1329+01	1.9849+02	2.9463-02	2.8701-01	7.1425+02	5.1364+01
11	5.9945+01	2.0332+02	8.7911-02	3.5912-01	7.6767+02	6.1448+01
12	6.0911+01	2.0267+02	1.3522-01	4.0233-01	7.9857+02	7.0160+01
13	6.0355+01	2.0263+02	2.0265-01	4.7325-01	8.4959+02	8.1789+01
14	6.1376+01	2.0400+02	2.4062-01	5.1566-01	8.8045+02	9.0056+01
15	6.1558+01	2.0155+02	3.2339-01	6.0087-01	9.4119+02	1.0645+02
16	6.0677+01	2.0294+02	-3.5961-02	3.6327-01	7.7054+02	6.3029+01
17	6.0641+01	2.0393+02	3.0960-02	4.3116-01	8.1965+02	7.4420+01
18	6.1917+01	2.0420+02	7.3819-02	4.8745-01	8.6021+02	8.5800+01
19	6.0349+01	2.0354+02	1.5268-01	5.5939-01	9.1179+02	9.6263+01
20	6.0254+01	2.0878+02	2.1581-01	6.2367-01	9.5914+02	1.0463+02
21	5.9984+01	2.0262+02	2.8462-01	6.9433-01	1.0087+03	1.1927+02
22	6.1689+01	2.0189+02	3.1755-01	7.1781-01	1.0255+03	1.2724+02

100 KW BOILING DATA .423-IN. TUBE, NO INSERT

	1024	1031	1066	1067	1068
	TWI 22	TWI 23	TWI 31	DT 31	H 31
1	2.1083+03	2.1453+03	2.1060+03	2.7899-01	3.5852+05
2	2.1135+03	2.1506+03	2.1081+03	2.7557+00	3.5264+04
3	2.1130+03	2.1502+03	2.1064+03	3.0928+00	3.0901+04
4	2.1105+03	2.1534+03	2.1052+03	4.2318+00	2.2449+04
5	2.1102+03	2.1554+03	2.1047+03	3.0129+00	3.2497+04
6	2.1110+03	2.1534+03	2.1041+03	3.1023+00	3.1946+04
7	2.1102+03	2.1476+03	2.1027+03	3.5066+00	2.8791+04
8	2.1063+03	2.1435+03	2.1005+03	4.4529+00	2.3262+04
9	2.1282+03	2.1632+03	2.1126+03	5.0034+00	2.8696+04
10	2.1193+03	2.1667+03	2.1152+03	1.9439+01	7.2744+03
11	2.1142+03	2.1619+03	2.1080+03	3.1903+00	4.6243+04
12	2.1139+03	2.1640+03	2.1075+03	3.8472+00	3.8384+04
13	2.1145+03	2.1650+03	2.1075+03	3.9099+00	3.7883+04
14	2.1178+03	2.1688+03	2.1098+03	3.6949+00	4.1337+04
15	2.1143+03	2.1667+03	2.1068+03	5.2168+00	2.9656+04
16	2.1411+03	2.2047+03	2.1158+03	1.1657+01	1.8504+04
17	2.1318+03	2.2033+03	2.1163+03	1.0382+01	2.1217+04
18	2.1303+03	2.1997+03	2.1129+03	6.4061+00	3.6300+04
19	2.1263+03	2.1903+03	2.1094+03	4.1394+00	5.3838+04
20	2.1386+03	2.2083+03	2.1226+03	7.7097+00	2.8973+04
21	2.1244+03	2.1866+03	2.1095+03	6.0039+00	3.7121+04
22	2.1219+03	2.1814+03	2.1063+03	4.1487+00	5.4009+04

TABLE B-3b

100 KW EGILING DATA .423-IN. TUBE, NO INSERT

	236	237	274	282	290	298
	DATE	TIME	TK FM	TPB IN	TPB IN	PBC 5
1	3.1250+03	1.4300+03	9.0676+02	8.9879+02	8.9885+02	1.6956+03
2	3.1250+03	1.6250+03	9.1789+02	9.1341+02	9.1264+02	1.8873+03
3	3.1250+03	1.9320+03	9.3387+02	9.3042+02	9.2865+02	2.0174+03
4	3.1250+03	2.2040+03	9.6197+02	9.5784+02	9.5624+02	2.1074+03
5	3.1350+03	2.1700+02	9.6313+02	9.6086+02	9.5820+02	
6	3.1650+03	1.3300+03	9.4296+02	9.3352+02	9.3365+02	1.7908+03
7	3.1650+03	1.6160+03	9.4690+02	9.3656+02	9.3689+02	1.7798+03
8	3.1850+03	4.3000+02	8.7249+02	8.4981+02	8.5763+02	
9	3.1850+03	6.5000+02	8.7747+02	8.5805+02	8.6417+02	
10	3.1850+03	1.0300+03	8.8421+02	8.6717+02	8.7221+02	

## 100 KW BOILING DATA .423-IN. TUBE, NO INSERT

	306	314	322	330	338	346
	PBC 6	PBC 7	PBC 8	PBC 9	PBC 10	PBC 11
1	1.8057+03	1.8738+03	1.9280+03	1.9946+03	2.0220+03	2.0628+03
2	2.0058+03	2.0750+03	2.1274+03	2.1212+03	2.1027+03	2.1080+03
3	2.1363+03	2.1248+03	2.1058+03	2.1151+03	2.1061+03	2.1071+03
4	2.1362+03	2.1213+03	2.1143+03	2.1178+03	2.1109+03	2.1099+03
5	2.1414+03	2.1314+03	2.1274+03	2.1248+03	2.1218+03	2.1164+03
6	1.8305+03	1.8927+03	1.9411+03	2.0079+03	2.0315+03	2.0677+03
7	1.8191+03	1.8808+03	1.9298+03	1.9961+03	2.0194+03	2.0565+03
8	8.5745+02	8.5485+02	8.4549+02	8.5138+02	8.4356+02	8.4252+02
9	1.0165+03	1.0305+03	1.0394+03	1.0663+03	1.0737+03	1.0951+03
10	1.1570+03	1.1865+03	1.2100+03	1.2530+03	1.2714+03	1.3084+03

100 KW BOILING DATA .423-IN. TUBE, NO INSERT

	362	370	380	389	425	434
	PBC 13	PBC 14	TPBOUT	TPBOUT	TWO 20	TWO 21
1	2.0379+03	2.0466+03	2.0548+03	2.0609+03		2.1445+03
2	2.0905+03	2.0981+03	2.1041+03	2.1088+03		2.1376+03
3	2.0889+03	2.0971+03	2.1023+03	2.1064+03		2.1336+03
4	2.0917+03	2.0991+03	2.1042+03	2.1072+03		2.1338+03
5	2.1003+03	2.1039+03	2.1080+03	2.1105+03		2.1377+03
6	2.0459+03	2.0531+03	2.0615+03	2.0626+03		2.1704+03
7	2.0270+03	2.0421+03	2.0512+03	2.0524+03		2.1246+03
8	8.4082+02	8.4044+02	8.5145+02	8.4210+02		1.3006+03
9	1.0875+03	1.0896+03	1.0912+03	1.0948+03		1.5605+03
10	1.2944+03	1.3007+03	1.2988+03	1.3081+03		1.7740+03

100 KW BOILING DATA .423-IN. TUBE, NO INSERT

	470	488	497	506	515	524
	TWO 25	TWO 27	TWO 31	TWO 32	TTSOUT	TTSOUT
1	2.1269+03	2.1319+03	2.1346+03	2.1351+03	2.1057+03	2.1048+03
2	2.1293+03	2.1353+03	2.1362+03	2.1369+03	2.1056+03	2.1049+03
3	2.1260+03	2.1340+03	2.1324+03	2.1333+03	2.1035+03	2.1032+03
4	2.1295+03	2.1324+03	2.1346+03	2.1362+03	2.1041+03	2.1043+03
5	2.1343+03	2.1384+03	2.1407+03	2.1394+03	2.1070+03	2.1070+03
6	2.1656+03	2.1625+03	2.1576+03	2.1643+03	2.1120+03	2.1133+03
7	2.1155+03	2.1140+03	2.1098+03	2.1113+03	2.0695+03	2.0603+03
8	2.1607+03	2.1588+03	2.1558+03	2.1595+03	2.1044+03	2.1061+03
9	2.1119+03	2.1479+03	2.1445+03	2.1477+03	2.0957+03	2.0974+03
10	2.1651+03	2.1534+03	2.1490+03	2.1533+03	2.1021+03	2.1026+03



100 KW BOILING DATA .423-IN. TUBE, NO INSERT

	540	547	561	568	575	582
	MAGNET	CND 37	CND 39	CND 40	CND 41	CND 42
1	4.5562+02	2.0806+03	1.1214+03	9.4253+02	9.9731+02	9.6342+02
2	4.7162+02	2.0805+03	1.0894+03	9.7657+02	1.0306+03	1.0029+03
3	4.8874+02	2.0786+03	1.1993+03	1.0001+03	1.0557+03	1.0167+03
4	5.0253+02	2.0787+03	1.2433+03	1.0290+03	1.0845+03	1.0449+03
5	5.1667+02	2.0808+03	1.2963+03	1.0641+03	1.1162+03	1.0738+03
6	4.7767+02	2.0913+03	7.9086+02	9.9752+02	1.0541+03	1.0147+03
7	4.7979+02	2.0392+03		1.0051+03	1.0626+03	1.0220+03
8	3.9634+02	2.0668+03	1.0641+03		9.4510+02	9.1243+02
9	4.0225+02	2.0781+03	1.0998+03		9.6196+02	9.2847+02
10	4.1840+02	2.0791+03	1.1142+03	9.1192+02	9.7834+02	9.4433+02

100 KW BOILING DATA .423-IN. TUBE, NO INSERT

	589	596	603	610	617	624
	CND 43	CND 44	CND 45	CND 46	CND 47	PBRADS
1	9.3262+02	8.8847+02	8.8231+02	8.5841+02	8.3944+02	7.5246+02
2	9.7055+02	9.2573+02	9.1626+02	8.9019+02	8.7017+02	8.1533+02
3	9.8213+02	9.3775+02	9.2860+02	9.0267+02	8.8220+02	8.4939+02
4	1.0082+03	9.6121+02	9.5067+02	9.2379+02	9.0298+02	8.7718+02
5	1.0337+03	9.8300+02	9.7238+02	9.4435+02	9.2210+02	9.0664+02
6	9.8004+02	9.3248+02	9.2558+02	8.9920+02	8.7632+02	7.6333+02
7	9.8588+02	9.3723+02	9.2996+02	9.0310+02	8.8228+02	7.6120+02
8	8.8218+02	8.3518+02	8.3325+02	8.0932+02	7.9072+02	4.5571+02
9	8.9737+02	8.5034+02	8.4719+02	8.2274+02	8.0372+02	5.1317+02
10	9.1316+02	8.6616+02	8.6244+02	8.3768+02	8.1846+02	5.6338+02

100 KW BOILING DATA .423-IN. TUBE, NO INSERT

	631	638	645	652	659	666
	PBRADS	PBRADS	PBRADS	PBRADS	PBRADS	TSRADS
1	7.8756+02	7.2399+02	7.4641+02	7.4096+02	7.8837+02	1.0697+03
2	8.4781+02	7.8334+02	8.1127+02	8.0061+02	8.5029+02	1.0760+03
3	8.7810+02	8.1714+02	8.4511+02	8.3441+02	8.8085+02	1.0782+03
4	9.0360+02	8.4275+02	8.7211+02	8.6123+02	9.0577+02	1.0838+03
5	9.3105+02	8.7211+02	9.0052+02	8.8846+02	9.3211+02	1.0969+03
6	8.0011+02	7.3274+02	7.5039+02	7.4135+02	7.9865+02	1.1885+03
7	7.9809+02	7.3087+02	7.4723+02	7.3922+02	7.9516+02	1.1908+03
8	4.7391+02	4.4690+02	3.9881+02	3.9647+02	4.4058+02	1.1302+03
9	5.4203+02	5.0414+02	4.6688+02	4.7078+02	5.1291+02	1.1465+03
10	5.9593+02	5.5213+02	5.2834+02	5.3349+02	5.7250+02	1.1505+03

## 100 KW BOILING DATA 423 IN TUBE, NO INSERT

	673	680	687	708	715	774
	TSRADS	TSRADS	TSRADS	TSRADS	TSRADS	QN PB
1	1.0651+03	1.0711+03	1.0665+03	1.0918+03	1.1066+03	7.5714+00
2	1.0729+03	1.0775+03	1.0743+03	1.0991+03	1.1151+03	9.5645+00
3	1.0775+03	1.0798+03	1.0791+03	1.1015+03	1.1183+03	1.1330+01
4	1.0843+03	1.0856+03	1.0860+03	1.1077+03	1.1251+03	1.3003+01
5	1.0990+03	1.0987+03	1.1008+03	1.1199+03	1.1379+03	1.4765+01
6	1.1960+03	1.1901+03	1.1976+03	1.2044+03	1.2297+03	7.4118+00
7	1.1994+03	1.1924+03	1.2010+03	1.2078+03	1.2339+03	7.4391+00
8	1.1294+03	1.1311+03	1.1302+03	1.1274+03	1.1461+03	-5.3292-01
9	1.1464+03	1.1474+03	1.1473+03	1.1407+03	1.1596+03	1.1570+00
10	1.1511+03	1.1514+03	1.1520+03	1.1440+03	1.1622+03	2.4412+00

100 KW BOILING DATA .423-IN. TUBE, NO INSERT

	780	784	802	804	807	816
	QN TS	Q/A TS	FLOW	G	P SAT	X PB
1	7.8582+00	9.6741+04	3.0655-02	3.1345+01	2.0354+02	-1.8965-03
2	8.0259+00	9.8805+04	3.0793-02	3.1486+01	2.0355+02	7.0953-02
3	7.6673+00	9.4391+04	3.0645-02	3.1334+01	2.0250+02	1.5361-01
4	7.7034+00	9.4836+04	3.1045-02	3.1743+01	2.0300+02	2.2491-01
5	8.1473+00	1.0030+05	3.0428-02	3.1113+01	2.0450+02	3.1222-01
6	1.2144+01	1.4951+05	3.1125-02	3.1826+01	2.0755+02	-6.0090-03
7	1.2479+01	1.5363+05	3.1289-02	3.1993+01	1.8268+02	-2.6860-03
8	1.2275+01	1.5112+05	3.0357-02	3.1040+01	2.0356+02	-1.7067-02
9	1.2087+01	1.4980+05	3.0418-02	3.1102+01	1.9892+02	-7.2699-03
10	1.2012+01	1.4788+05	3.0867-02	3.1561+01	2.0198+02	-8.5266-03

100 KW BOILING DATA .423-IN. TUBE, NO INSERT

	823	825	828	1017	1045	1059
	X TS	ENTOUT	VELOUT	TWI 21	TWI 25	TWI 27
1	3.2167-01	7.4079+02	2.8750+01	2.1215+03	2.1038+03	2.1088+03
2	4.1474-01	8.0774+02	3.7234+01	2.1140+03	2.1057+03	2.1117+03
3	4.8343-01	8.5688+02	4.3401+01	2.1110+03	2.1034+03	2.1115+03
4	5.5217-01	9.0647+02	5.0103+01	2.1111+03	2.1069+03	2.1098+03
5	6.6570-01	9.8846+02	5.8800+01	2.1138+03	2.1104+03	2.1145+03
6	4.9371-01	8.6556+02	4.3989+01	2.1348+03	2.1299+03	2.1269+03
7	5.1409-01	8.7398+02	5.1761+01	2.0879+03	2.0787+03	2.0773+03
8	1.5711-01	6.2242+02	1.3904+01	1.2625+03	2.1247+03	2.1227+03
9	2.2513-01	6.6979+02	2.0393+01	1.5236+03	2.0763+03	2.1124+03
10	2.6904-01	7.0243+02	2.4388+01	1.7379+03	2.1299+03	2.1182+03

100 KW BOILING DATA .423-IN. TUBE, NO INSERT

	1060	1061	1066	1067	1068	1073
	DT 27	H 27	TWI 31	DT 31	H 31	TWI 32
1	3.5739+00	2.7068+04	2.1116+03	6.3152+00	1.5319+04	2.1120+03
2	6.4211+00	1.5387+04	2.1126+03	7.3933+00	1.3364+04	2.1133+03
3	8.1380+00	1.1599+04	2.1099+03	6.5805+00	1.4344+04	2.1107+03
4	5.5382+00	1.7124+04	2.1120+03	7.7272+00	1.2273+04	2.1136+03
5	7.4520+00	1.3459+04	2.1167+03	9.7441+00	1.0293+04	2.1154+03
6	1.4245+01	1.0496+04	2.1219+03	9.2861+00	1.6100+04	2.1287+03
7	1.2413+01	1.2376+04	2.0731+03	8.1652+00	1.8815+04	2.0746+03
8	1.7473+01	8.6485+03	2.1198+03	1.4550+01	1.0386+04	2.1235+03
9	1.5832+01	9.3986+03	2.1090+03	1.2465+01	1.1938+04	2.1123+03
10	1.5802+01	9.3585+03	2.1138+03	1.1391+01	1.2982+04	2.1180+03

100 KW BCILING DATA .423-IN. TUBE, NO INSERT

1074

1075

DT 32

H 32

1	6.8064+00	1.4213+04
2	8.0741+00	1.2237+04
3	7.4044+00	1.2748+04
4	9.3569+00	1.0135+04
5	8.4218+00	1.1910+04
6	1.6066+01	9.3057+03
7	9.6809+00	1.5869+04
8	1.8259+01	8.2762+03
9	1.5678+01	9.4911+03
10	1.5670+01	9.4376+03



TABLE B-3c  
100 KW BOILING DATA .423-IN. TUBE, NO INSERT

	236	237	274	282	290	306
	DATE	TIME	TK FM	TPB IN	TPB IN	PBC 6
1	3.2550+03	7.3000+02	9.0010+02	8.9413+02	8.9329+02	1.8854+03
2	3.2550+03	1.3300+03	9.3945+02	1.1903+03	1.1932+03	1.8788+03
3	3.2650+03	3.0800+02	9.8670+02	9.8049+02	9.8097+02	1.8504+03
4	3.2650+03	3.5000+02	1.0021+03	9.9303+02	9.9455+02	1.8493+03
5	3.2650+03	4.3000+02	1.0104+03	1.0044+03	1.0041+03	1.8540+03

100 KW BCILING DATA .423-IN. TUBE, NO INSERT

	314	322	330	338	346	362
	PBC 7	PBC 8	PBC 9	PBC 10	PBC 11	PBC 13
1	1.8205+03	1.8095+03	1.8198+03	1.8075+03	1.8122+03	1.8001+03
2	1.8726+03	1.8596+03	1.8722+03	1.8602+03	1.8645+03	1.8511+03
3	1.8460+03	1.8484+03	1.8374+03	1.8300+03	1.8416+03	1.8138+03
4	1.8376+03	1.8428+03	1.8366+03	1.8255+03	1.8303+03	1.8203+03
5	1.8405+03	1.8369+03	1.8352+03	1.8274+03	1.8308+03	1.8157+03

100 KW BOILING DATA .423-IN. TUBE, NO INSERT

	370	380	389	443	461	470
	PBC 14	TPBOUT	TPBOUT	TWO 22	TWO 24	TWO 25
1	1.8026+03	1.8145+03	1.8086+03	1.8336+03	1.8318+03	1.8368+03
2	1.8546+03	1.8681+03	1.8623+03	1.8913+03	1.8904+03	1.8940+03
3	1.8099+03	1.8178+03	1.8147+03	1.8395+03	1.8375+03	1.8395+03
4	1.8128+03	1.8210+03	1.8163+03	1.8376+03	1.8369+03	1.8370+03
5	1.8141+03	1.8207+03	1.8173+03	1.8383+03	1.8373+03	1.8374+03

100 KW BOILING DATA .423-IN. TUBE, NO INSERT

	488	497	515	524	540	547
	TWO 27	TWO 31	TTSOUT	TTSOUT	MAGNET	CND 37
1	1.8313+03	1.8311+03	1.8044+03	1.8048+03	4.6135+02	1.7868+03
2	1.8886+03	1.8892+03	1.8622+03	1.8621+03	4.8519+02	1.8425+03
3	1.8339+03	1.8351+03	1.8066+03	1.8041+03	4.9294+02	1.7886+03
4	1.8321+03	1.8321+03	1.8041+03	1.8055+03	5.0733+02	1.7874+03
5	1.8352+03	1.8336+03	1.8057+03	1.8120+03	5.1138+02	1.7879+03

100 KW BOILING DATA .423-IN. TUBE, NO INSERT

	554	561	568	575	582	589
	CND 38	CND 39	CND 40	CND 41	CND 42	CND 43
1	1.8569+03	9.4684+02	9.8953+02	1.0585+03	1.0142+03	9.7561+02
2		6.3171+02	9.9109+02	1.0539+03	1.0120+03	9.7595+02
3	1.7913+03	1.7221+03	1.1999+03	1.2474+03	1.1598+03	1.1121+03
4	1.8051+03	1.8040+03		1.2522+03	1.1784+03	1.1200+03
5	1.8047+03	1.7191+03	1.2975+03	1.3518+03	1.2634+03	1.1938+03

100 KW BOILING DATA .423-IN. TUBE, NO INSERT

	596	603	610	617	624	631
	CND 44	CND 45	CND 46	CND 47	PBRADS	PBRADS
1	9.1806+02	9.1588+02	8.8743+02	8.6519+02	7.6053+02	7.9091+02
2	9.2018+02	9.1826+02	8.9081+02	8.6943+02	7.7769+02	8.0485+02
3	1.0326+03	1.0240+03	9.8553+02	9.5617+02	8.5494+02	8.8230+02
4	1.0413+03	1.0327+03	9.9335+02	9.6390+02	8.5504+02	8.8112+02
5	1.1051+03	1.0878+03	1.0376+03	9.8281+02	8.7545+02	9.0084+02

100 KW BOILING DATA .423-IN. TUBE, NO INSERT

	638	645	652	659	666	673
	PBRADS	PBRADS	PBRADS	PBRADS	TSRADS	TSRADS
1	7.3620+02	7.5007+02	7.4455+02	7.8755+02	1.0165+03	1.0183+03
2	7.5680+02	7.7214+02	7.7544+02	8.0425+02	1.0236+03	1.0256+03
3	8.4110+02	8.4567+02	8.5332+02	8.7450+02	1.0154+03	1.0158+03
4	8.4078+02	8.4402+02	8.5191+02	8.7302+02	1.0284+03	1.0321+03
5	8.6129+02	8.6308+02	8.7184+02	8.9010+02	1.0337+03	1.0341+03

100 KW BOILING DATA .423-IN. TUBE, NO INSERT

	680	687	708	715	774	780
	TSRADS	TSRADS	TSRADS	TSRADS	QN PB	QN TS
1	1.0180+03	1.0198+03	1.0238+03	1.0464+03	9.4861+00	8.0657+00
2	1.0257+03	1.0277+03	1.0304+03	1.0525+03	8.5455+00	7.9458+00
3	1.0373+03	1.0377+03	1.0405+03	1.0662+03	1.5666+01	8.0156+00
4	1.0301+03	1.0339+03	1.0371+03	1.0641+03	1.5583+01	7.9820+00
5	1.0355+03	1.0359+03	1.0427+03	1.0702+03	1.7471+01	7.9073+00



100 KW BOILING DATA .423-IN. TUBE, NO INSERT

	784	802	804	807	816	823
	Q/A TS	FLOW	G	P SAT	X PB	X TS
1	9.9295+04	2.9834-02	3.0505+01	8.2553+01	1.5275-01	4.8721-01
2	9.7820+04	3.0609-02	3.1297+01	9.9973+01	1.6468-01	4.8910-01
3	9.8678+04	2.9169-02	2.9825+01	8.2776+01	4.4252-01	7.8277-01
4	9.8265+04	2.9873-02	3.0545+01	8.2615+01	4.2614-01	7.5756-01
5	9.7346+04	3.1689-02	3.2402+01	8.3777+01	4.6526-01	7.7445-01

100 KW BOILING DATA .423-IN. TUBE, NO INSERT

	825	828	1024	1038	1045	1059
	ENTOUT	VELOUT	TWI 22	TWI 24	TWI 25	TWI 27
1	8.2046+02	9.7235+01	1.8094+03	1.8076+03	1.8127+03	1.8071+03
2	8.2930+02	8.3863+01	1.8675+03	1.8667+03	1.8703+03	1.8649+03
3	1.0481+03	1.5235+02	1.8155+03	1.8135+03	1.8154+03	1.8099+03
4	1.0287+03	1.5129+02	1.8137+03	1.8130+03	1.8131+03	1.8081+03
5	1.0420+03	1.6189+02	1.8146+03	1.8136+03	1.8137+03	1.8115+03

100 KW BOILING DATA .423-IN. TUBE, NO INSERT

	1060	1061	1066	1067	1068
	DT 27	H 27	TWI 31	DT 31	H 31
1	2.5481+00	3.8968+04	1.8069+03	2.3644+00	4.1995+04
2	2.7111+00	3.6081+04	1.8654+03	3.2824+00	2.9801+04
3	4.5633+00	2.1625+04	1.8111+03	5.7153+00	1.7266+04
4	3.3482+00	2.9349+04	1.8082+03	3.4279+00	2.8666+04
5	2.6808+00	3.6313+04	1.8099+03	1.0253+00	9.4941+04

TABLE B-3d

100 KW BOILING DATA .423-IN. TUBE, NO INSERT

	236	237	274	282	290	298
	DATE	TIME	TK FM	TPB IN	TPB IN	PBC 5
1	3.3050+03	1.9410+03	1.2737+03	1.2504+03	1.2568+03	2.0804+03
2	3.3050+03	2.2000+03	1.2968+03	1.2736+03	1.2799+03	2.1915+03
3	3.3150+03	1.4000+02	1.3171+03	1.2940+03	1.2992+03	2.3121+03
4	3.3150+03	3.3000+02	1.3466+03	1.3225+03	1.3275+03	2.4045+03
5	3.3150+03	5.1000+02	1.3641+03	1.3408+03	1.3454+03	
6	3.3150+03	7.4500+02	1.3849+03	1.3617+03	1.3658+03	2.4430+03
7	4.0150+03	5.4500+02	1.3461+03	1.3168+03	1.3249+03	

100 KW BOILING DATA .423-IN. TUBE, NO INSERT

	306	314	322	330	338	346
	PBC 6	PBC 7	PBC 8	PBC 9	PBC 10	PBC 11
1		2.0167+03	2.0566+03	2.1222+03	2.1401+03	2.1120+03
2		2.1315+03	2.1174+03	2.1177+03	2.1005+03	2.1075+03
3	2.1875+03	2.1181+03	2.1094+03	2.1173+03	2.1029+03	2.1061+03
4	2.1342+03	2.1232+03	2.1201+03	2.1194+03	2.1041+03	2.1109+03
5	2.1390+03	2.1307+03	2.1323+03	2.1287+03	2.1106+03	2.1150+03
6	2.1474+03	2.1354+03	2.1314+03	2.1251+03	2.1154+03	2.1163+03
7	1.9008+03	1.9480+03	1.9824+03	2.0447+03	2.0615+03	2.0971+03

100 KW BOILING DATA .423-IN. TUBE, NO INSERT

	362	370	380	389	461	470
	PBC 13	PBC 14	TPBOUT	TPBOUT	TWO 24	TWO 25
1	2.1519+03	2.1019+03	2.1037+03	2.1082+03	2.1373+03	2.1380+03
2	2.0927+03	2.0971+03	2.1064+03	2.1086+03	2.1368+03	2.1386+03
3	2.0914+03	2.0937+03	2.1026+03	2.1038+03	2.1333+03	2.1341+03
4	2.0949+03	2.0966+03	2.1049+03	2.1051+03	2.1328+03	2.1355+03
5	2.0980+03	2.0982+03	2.1062+03	2.1062+03	2.1339+03	2.1347+03
6	2.1004+03	2.1000+03	2.1074+03	2.1066+03	2.1330+03	2.1347+03
7	2.0719+03	2.0803+03	2.0932+03	2.0996+03	2.1614+03	2.2373+03

100 KW BOILING DATA .423-IN. TUBE, NO INSERT

	479	488	497	515	524	533
	TWO 26	TWO 27	TWO 31	TTSOUT	TTSOUT	TTSOUT
1	2.1354+03	2.1314+03	2.1317+03	2.0883+03	2.1058+03	2.1070+03
2	2.1349+03	2.1314+03	2.1312+03	2.0853+03	2.1057+03	2.1066+03
3	2.1295+03	2.1259+03	2.1267+03	2.1019+03	2.1016+03	2.1022+03
4	2.1309+03	2.1272+03	2.1273+03	2.1029+03	2.1039+03	2.1040+03
5	2.1304+03	2.1274+03	2.1274+03	2.1027+03	2.1030+03	2.1038+03
6	2.1300+03	2.1276+03	2.1277+03	2.1024+03	2.1023+03	2.1033+03
7	2.1660+03		2.1533+03	2.0967+03	2.0971+03	2.0971+03

100 KW BOILING DATA .423-IN. TUBE, NO INSERT

	540	547	561	568	575	582
	MAGNET	CND 37	CND 39	CND 40	CND 41	CND 42
1	5.0156+02	2.0855+03	1.2179+03	1.1044+03	1.0783+03	1.0483+03
2	5.1921+02	2.0848+03	1.2556+03	1.1313+03	1.1044+03	1.0733+03
3	5.3881+02	2.0797+03	1.3108+03	1.1696+03	1.1398+03	1.1065+03
4	5.5396+02	2.0784+03	1.3673+03	1.2070+03	1.1679+03	1.1368+03
5	5.7030+02	2.0776+03	1.4297+03	1.2471+03	1.2092+03	1.1691+03
6	5.8648+02	2.0757+03	1.5182+03	1.2990+03	1.2560+03	1.2100+03
7	5.3878+02	2.0709+03	1.3596+03	1.2027+03	1.1694+03	1.1336+03



100 KW BOILING DATA .423-IN. TUBE, NO INSERT

	589	596	603	610	617	624
	CND 43	CND 44	CND 45	CND 46	CND 47	PBRADS
1	1.0189+03	9.7161+02	9.7232+02	9.4763+02	9.3134+02	8.1535+02
2	1.0433+03	9.9395+02	9.9356+02	9.6788+02	9.5100+02	8.5503+02
3	1.0749+03	1.0237+03	1.0220+03	9.9615+02	9.7659+02	8.9955+02
4	1.1034+03	1.0505+03	1.0476+03	1.0197+03	9.9821+02	9.3488+02
5	1.1329+03	1.0780+03	1.0741+03	1.0446+03	1.0213+03	9.6721+02
6	1.1690+03	1.1104+03	1.1041+03	1.0724+03	1.0477+03	9.9897+02
7	1.1006+03	1.0491+03	1.0449+03	1.0174+03	9.9602+02	8.1476+02

100 KW BOILING DATA .423-IN. TUBE, NO INSERT

	631	638	645	652	659	666
	PBRADS	PBRADS	PBRADS	PBRADS	PBRADS	TSRADS
1	8.4840+02	7.7741+02	7.9204+02	7.6073+02	8.0853+02	1.0015+03
2	8.8352+02	8.2434+02	8.4681+02	8.3754+02	8.8684+02	1.0714+03
3	9.2334+02	8.6940+02	8.9163+02	8.8329+02	9.2710+02	1.0738+03
4	9.5588+02	9.0651+02	9.2659+02	9.1968+02	9.5932+02	1.0819+03
5	9.8737+02	9.4104+02	9.5943+02	9.5305+02	9.9006+02	1.0877+03
6	1.0177+03	9.7450+02	9.9148+02	9.8507+02	1.0204+03	1.0946+03
7	8.4794+02	7.8441+02	7.8979+02	7.8185+02	8.3934+02	1.2657+03

100 KW BOILING DATA .423-IN. TUBE, NO INSERT

	673	680	687	708	715	774
	TSRADS	TSRADS	TSRADS	TSRADS	TSRADS	QN PB
1	9.9507+02	9.7546+02	9.6906+02	1.0030+03	1.0097+03	8.9817+00
2	1.0719+03	1.0710+03	1.0736+03	1.0996+03	1.0998+03	1.0710+01
3	1.0743+03	1.0716+03	1.0762+03	1.1030+03	1.1032+03	1.3657+01
4	1.0825+03	1.0791+03	1.0849+03	1.1096+03	1.1098+03	1.6017+01
5	1.0883+03	1.0857+03	1.0910+03	1.1140+03	1.1142+03	1.8626+01
6	1.0953+03	1.0928+03	1.0990+03	1.1199+03	1.1201+03	2.1468+01
7	1.2662+03	1.2605+03	1.2716+03	1.2844+03	1.2846+03	7.1919+00

100 KW BOILING DATA .423-IN. TUBE, NO INSERT

	780	784	802	804	807	816
	QN TS	Q/A TS	FLOW	G	P SAT	X PB
1	9.6365+00	1.1863+05	4.4894-02	4.5904+01	2.0090+02	1.5223-02
2	8.1103+00	9.9845+04	4.4874-02	4.5884+01	2.0029+02	7.2054-02
3	8.0656+00	9.9294+04	4.4578-02	4.5581+01	2.0174+02	1.6794-01
4	7.9288+00	9.7610+04	4.4236-02	4.5231+01	2.0267+02	2.4892-01
5	7.9796+00	9.8236+04	4.3388-02	4.4364+01	2.0242+02	3.4231-01
6	8.0054+00	9.8553+04	4.3148-02	4.4119+01	2.0215+02	4.3793-01
7	1.7825+01	2.1944+05	4.5104-02	4.6118+01	1.9913+02	-1.6612-02

100 KW BOILING DATA .423-IN. TUBE, NO INSERT

	823	825	828	1038	1045	1052
	X TS	ENTOUT	VELOUT	TWI 24	TWI 25	TWI 26
1	2.9943-01	7.2397+02	3.9677+01	2.1090+03	2.1097+03	2.1071+03
2	3.1226-01	7.3302+02	4.1472+01	2.1130+03	2.1147+03	2.1110+03
3	4.0651-01	8.0131+02	5.3277+01	2.1096+03	2.1104+03	2.1058+03
4	4.8534-01	8.5830+02	6.2849+01	2.1095+03	2.1122+03	2.1076+03
5	5.8521-01	9.3011+02	7.4416+01	2.1105+03	2.1112+03	2.1070+03
6	6.8314-01	1.0005+03	8.6496+01	2.1095+03	2.1112+03	2.1065+03
7	5.0295-01	8.7009+02	6.7493+01	2.1091+03	2.1853+03	2.1137+03

100 KW BOILING DATA .423-IN. TUBE, NO INSERT

	1053	1054	1059	1060	1061	1066
	DT 26	H 26	TWI 27	DT 27	H 27	TWI 31
1	6.7175+00	1.7660+04	2.1031+03	2.7072+00	4.3822+04	2.1034+03
2	1.1838+01	8.4344+03	2.1075+03	8.3069+00	1.2019+04	2.1073+03
3	3.8430+00	2.5838+04	2.1022+03	2.9626-01	3.3515+05	2.1030+03
4	3.9748+00	2.4557+04	2.1039+03	2.9269-01	3.3349+05	2.1039+03
5	3.8236+00	2.5692+04	2.1039+03	7.4304-01	1.3221+05	2.1040+03
6	3.8220+00	2.5786+04	2.1040+03	1.3636+00	7.2277+04	2.1042+03
7	1.6742+01	1.3107+04				2.1010+03

100 KW BOILING DATA .423-IN. TUBE, NO INSERT

1067

1068

DT 31

H 31

1	3.0013+00	3.9528+04
2	8.1393+00	1.2267+04
3	1.0549+00	9.4124+04
4	3.2294-01	3.0226+05
5	7.8754-01	1.2474+05
6	1.5262+00	6.4572+04
7	4.0394+00	5.4324+04

APPENDIX C

CONDENSING TEST SECTION  
MECHANICAL DESIGN DESCRIPTION (50 KW PROJECT)



CONDENSING TEST SECTION  
MECHANICAL DESIGN DESCRIPTION (50 KW PROJECT)  
R.R. Oliver

A description of the condensing test section equipment used in the condensing tests under the 50 KW Project is summarized here for convenient reference.

The heat exchangers used in these experiments were single tube, parallel counter-current flow devices with the potassium condensation occurring inside the center tube and with the sodium cooling flow located in a surrounding concentric tube. Figure C1 shows the flow path arrangement in a schematic type drawing. Operation of this test equipment in the facility was with the condensing tube axis vertical and with the potassium in vertical down-flow.

The whole test section, but particularly the tubes where condensation occurs, are of a highly specialized design to suit the type and quantity of instrumentation required. The condensing tubes used were made of INCO Nickel 270 material which was selected because of its high purity and uniform heat conductivity in combination with its compatibility with the alkali metal environment of the test. Two different size tubes were used in the testing: both were 2-inch outside diameter by 38 inches long; one had a 5/8-inch inside diameter hole and the other a 3/8-inch inside diameter hole. The center holes were concentric with the outside diameter of the tube to within 0.003-inch.

Ten thermocouples were used to determine condensing tube wall temperatures. These thermocouples were located in holes which entered the bar, five from each end, and ran parallel to

the center hole or axis of the tube. These thermocouple holes were 0.050 inch in diameter by 9 inches deep and their location was held within 0.004 inch of the true location for their entire length. The holes were located at different radial locations: two as close as possible to the inside diameter; one at an intermediate radius; and two more near the outside diameter. The location of these thermocouple holes is indicated on Figure C1, and shows more clearly in Figure C2. Figure C2 is an enlarged photo (approximately 2x) of one end of the 3/8-inch inside diameter test piece. Figure C3 also shows these thermocouple holes and in addition shows one of the stainless steel pipes which were brazed into each end of the test pieces to allow the two-inch diameter test condensing section to be welded to the loop potassium piping.

In addition to the potassium pipes shown in Figure C3 each end of the nickel tube was also fitted with a two-inch diameter stainless steel tube which was welded to the outside diameter of the test section at each end and was used to join the nickel pipe to the surrounding, sodium containing shell. The space between these two concentric pipes, just described, formed an annulus open to the atmosphere through which the thermocouples could be installed and the thermocouple leads could be brought out. This permitted the leads to be brought out without crossing either the sodium or potassium flow passages and in that way avoiding the mechanical complexities and undesirable flow disturbances that would have been caused by attempting to get the thermocouples and their connections across either of the fluid paths. This annulus shows in the schematic diagram of Figure C1. The outer casing was con-

structed with two enlarged ends. These ends were made from stainless steel pipe reducers and flat plates and were internally baffled with perforated discs. These enlargements served as inlet and exit manifolds to assure uniform sodium distribution in the central annulus, which was the actual heat exchanger region. Concentricity of the condensing pipe in this heat exchanger annular region was maintained by small spacers which were attached to each end of the nickel test section. The needed flexibility to accommodate the lengthwise differential thermal expansion which could exist between the stainless steel shell and the nickel center tube was provided by a guided convoluted expansion joint located at one end of the outer casing.

All the features just described can be easily seen in Figure C1; and the external geometry of the completed 5/8-inch inside diameter test heat exchanger is shown in Figure C4, which is a photograph of the completed unit. Figure C4 also shows the 3/8 -inch inside diameter condensing tube which has its potassium end adapter pipes attached. The 3/8-inch test section is shown located adjacent to the casing so as to indicate the relative length and location of the condensing tube when it is installed in the outer casing.

Figure C5 is a photo of the detailed component parts made prior to the initial assembly.

In addition to the condensing tube wall temperature thermocouples mentioned earlier, other instrumentation located in the test section measured the bulk temperature of the sodium inlet and exit fluid. Figure C6 is a photo of the end of the completed test section which shows three thermocouple wells

located on one end in the enlarged section where the thermocouples for measuring bulk sodium temperature were installed, three more were similarly located at the opposite end. Figure C7 shows the entire unit installed in the facility just prior to application of the insulation. This figure shows the method of mounting the entire unit in a reinforcing frame so as to prevent distortions to the test section that might be caused by forces resulting from thermal expansion during loop operation.

Two complete outer casings were built to go with the two condensing tubes. This was done to allow a rapid change of test sections for different tests or for ready exchange of test sections due to failure of a test section.

The two test sections used for these tests had the following testing sequence.

1. 5/8-inch inside diameter with no insert.
2. 5/8-inch inside diameter with an uninstrumented tapered plug insert.
3. 3/8-inch inside diameter with no insert.
4. 5/8-inch inside diameter with an instrumented helical insert.
5. 5/8-inch inside diameter with an instrumented straight plug insert.

As can be seen from this list, the majority of testing

was done with the 5/8-inch inside diameter condensing tube as it was used both with and without inserts.

The first of the inserts used consisted of a non-instrumented long tapered pin which was as long as the condensing section, and which was used to simulate a tapered tube flow channel geometry. The installed insert was held concentric with the inside diameter of the condensing tube by wire prongs located at approximately nine inches from each end. This tapered pin was also secured in an axial direction by a hair pin shaped yoke which was attached to the upstream or small end and which was tack welded to the pipe inside diameter at the field weld location above the test section. Figure C9 is a photo of this tapered pin before installation and shows both the centering wires and the supporting yoke. When installed this insert formed a converging concentric annulus as the condensing section.

The second of the inserts used in the 5/8-inch inside diameter tube was an instrumented helical insert. This consisted of a single helix with a pitch to diameter ratio of 6 which was located around a 1/4-inch outside diameter tube. Multiple thermocouples were located inside this tube. The tube was brought out of the potassium inlet pipe wall at an enlarged section upstream of the test section installed specifically for this purpose. This enlargement consisted of two eccentric reducers welded back to back. This arrangement was used for two purposes, first to permit a gradual long radius bend in the insert tube which made insertion and removal of the thermocouples possible without danger of breaking the thermocouples, and second this provided a penetration location which had the proper angle and accessibility for a good weld where the tube came through

the wall. The helical insert and the attached enlarged section for the wall penetration are shown in Figure C9.

The third insert used was very similar to the one shown in Figure C9 but was without the helix. In this insert the 1/4-inch outside diameter center tube was held concentric with the test section with wire clips in the same fashion as had been used previously with the tapered insert shown in Figure C8. This straight tube insert also contained multiple thermocouples that were the same as had been used in the helical insert.

The key assembly drawings which define these previously discussed test sections are as follows:

The 5/8-inch diameter test section is described by GE drawing No. 263E544 - Group 1, Group 3, Group 4 and Group 5 (Figures C10a and C10b).

The 3/8-inch diameter test section is defined by GE drawing No. 941D572 - Group 1 (Figure C11).

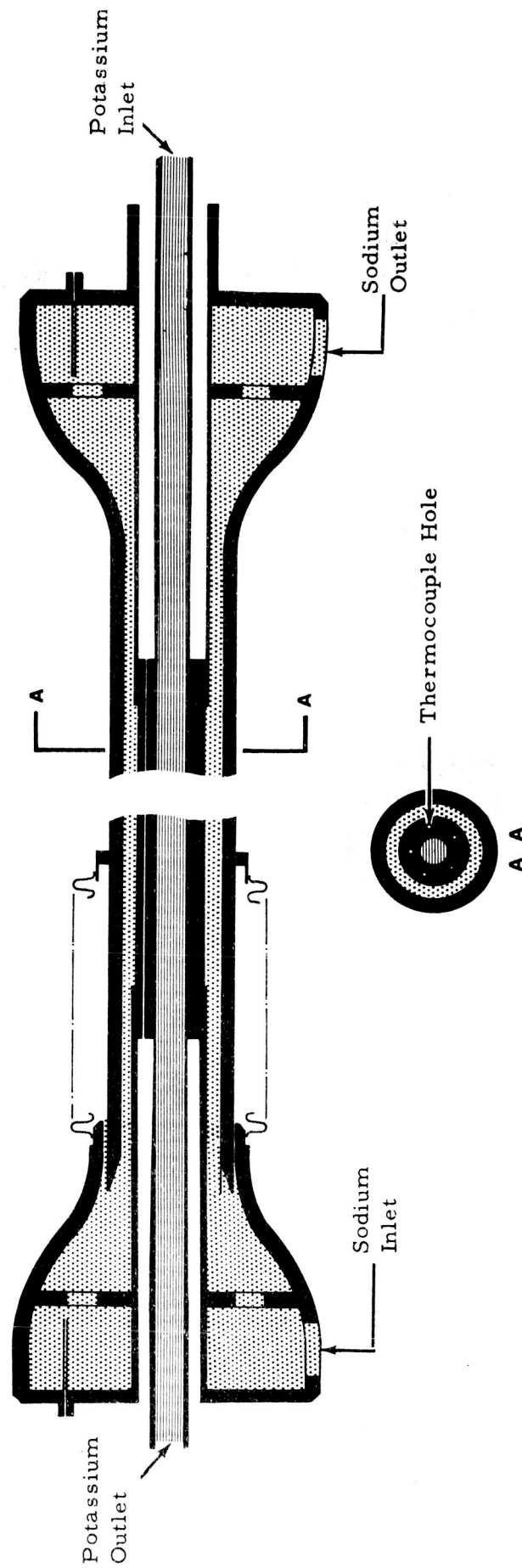


Figure C1. 50 KW Condenser Schematic Diagram.

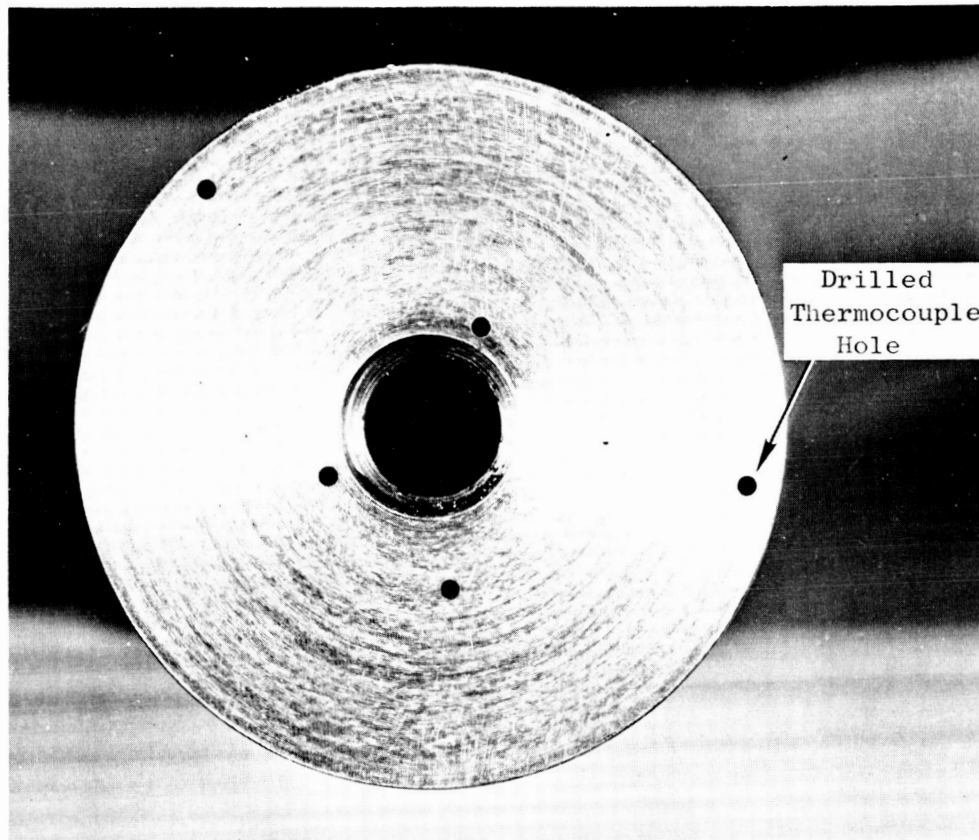


Figure C2. End View of 3/8-Inch ID Condensing Tube (Showing Drilled Thermocouple Holes).



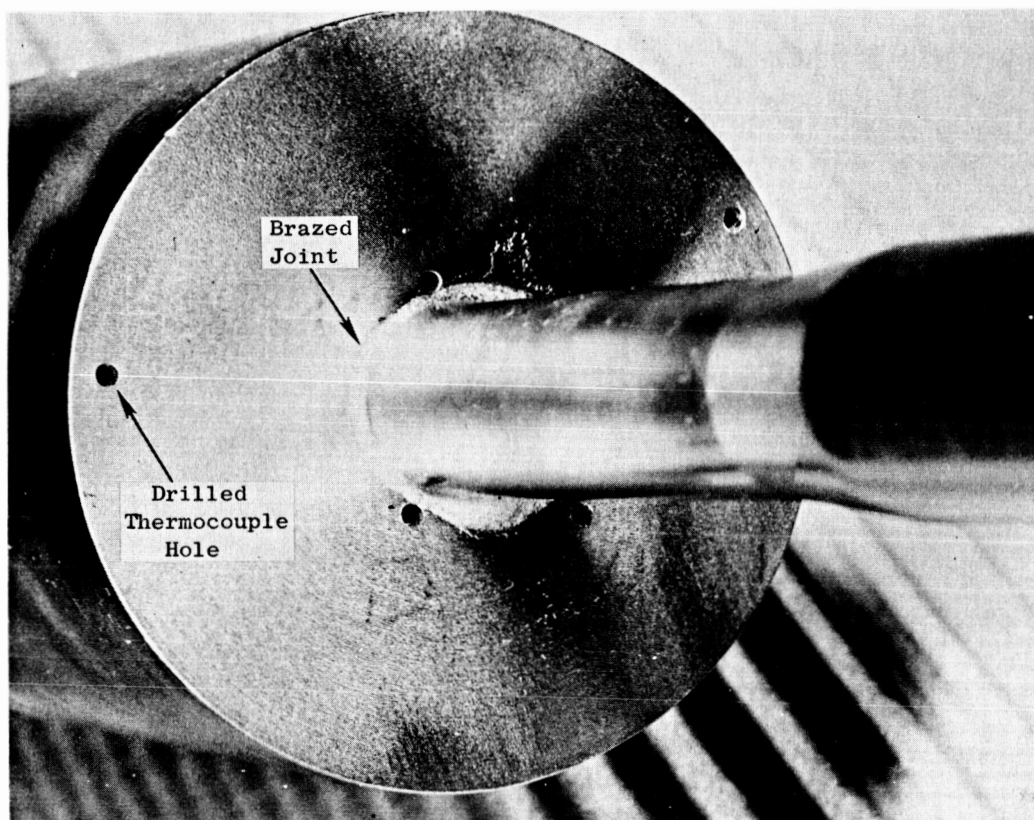


Figure C3. End View of 3/8-Inch ID Condensing Tube (Showing Adapter Pipe for Potassium).

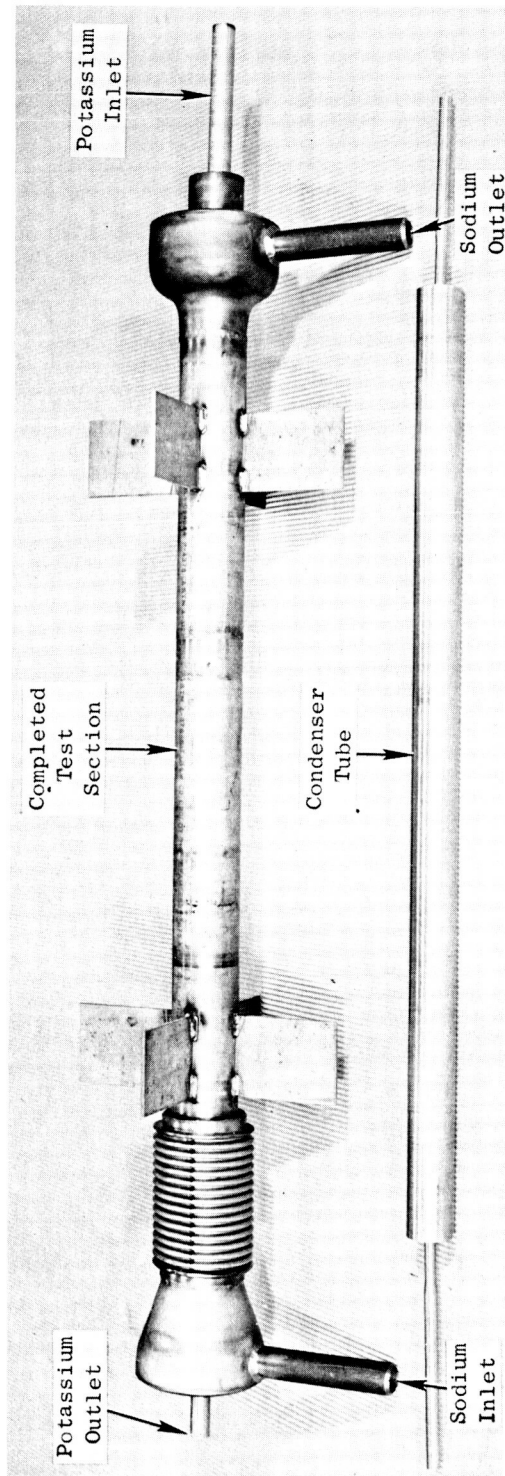


Figure C4. 5/8 Inch ID Test Condenser and 3/8-Inch ID Condenser Tube.

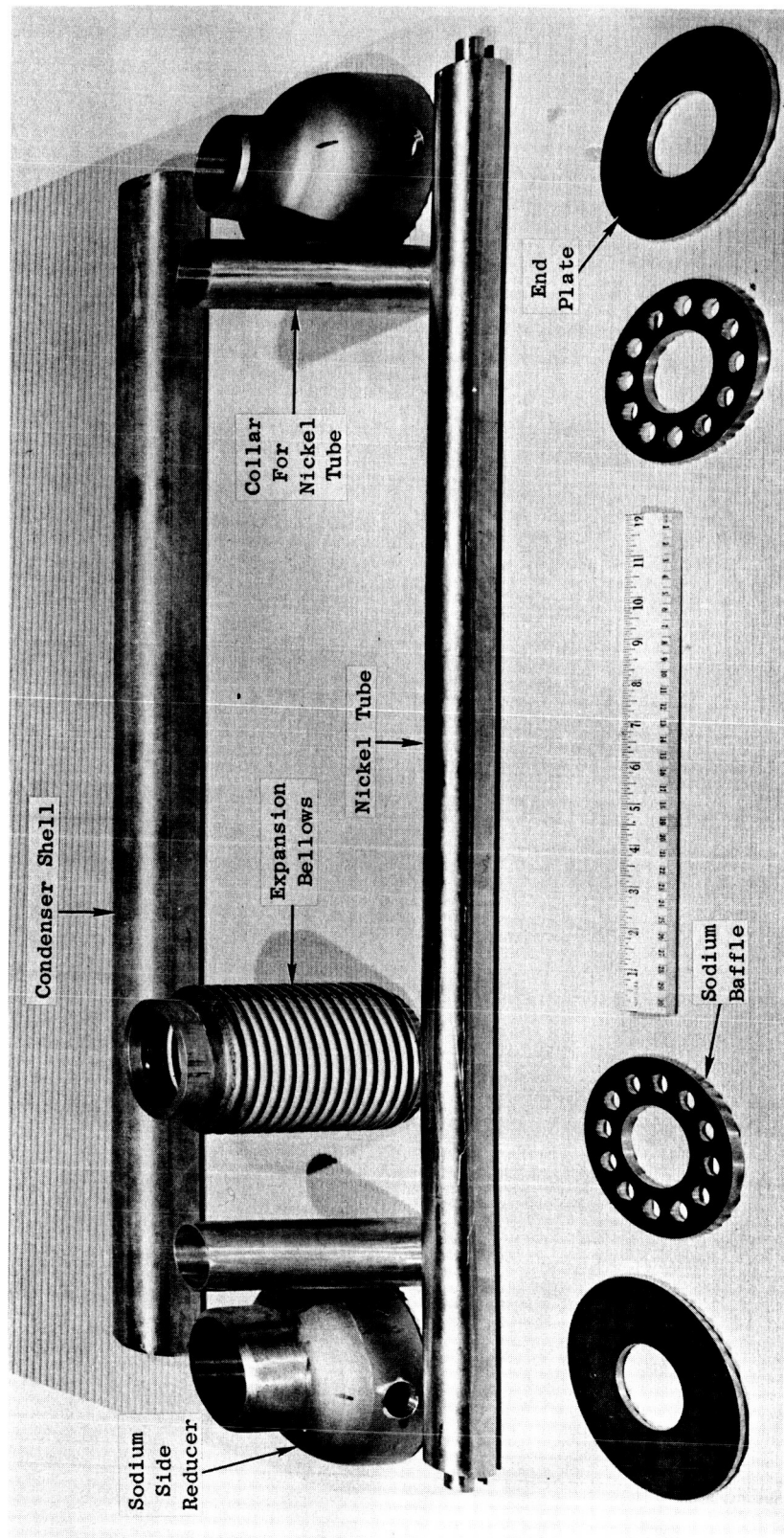


Figure C5. Test Condenser Detail Components.

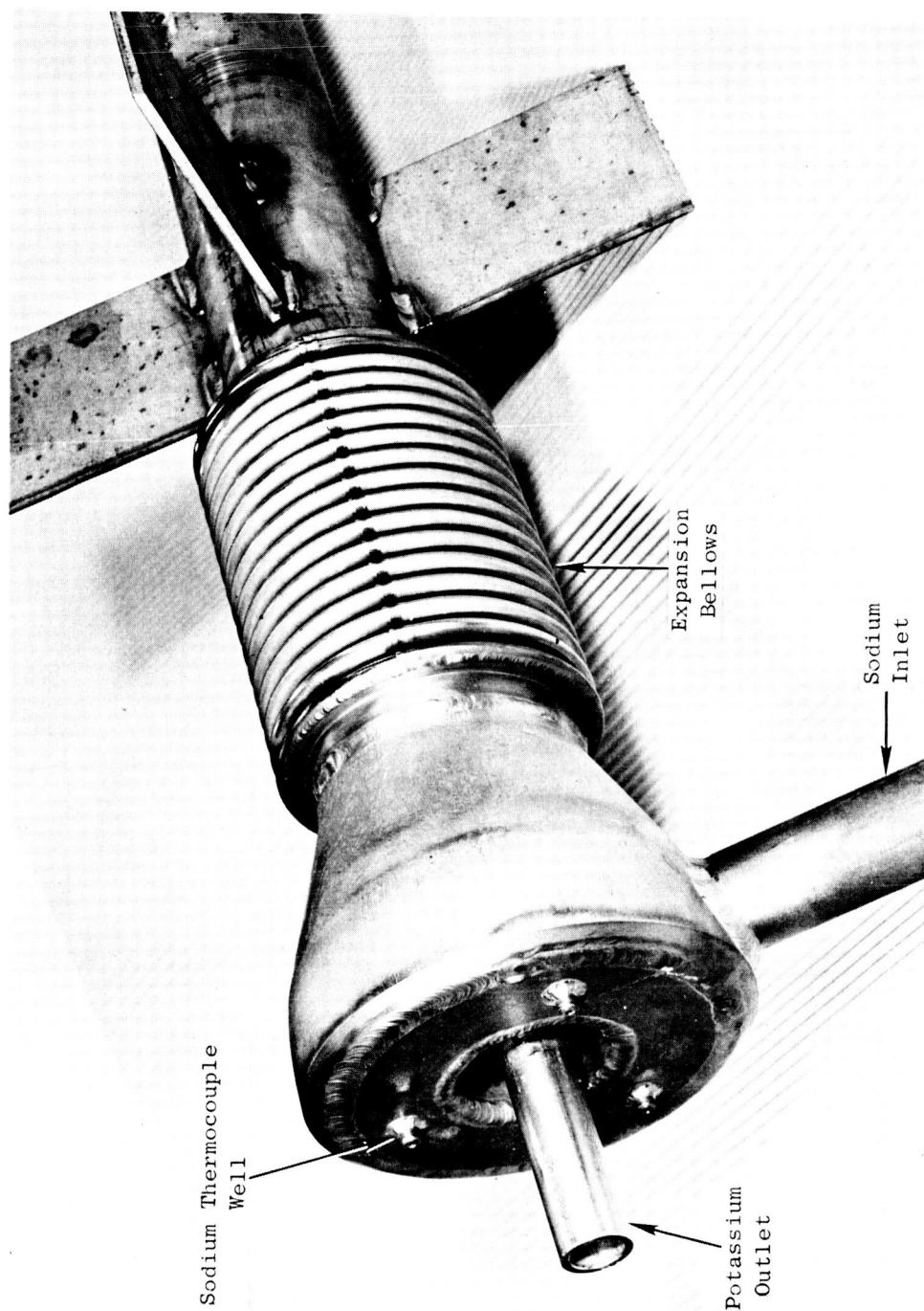


Figure C6. End View of Test Condenser Shell.

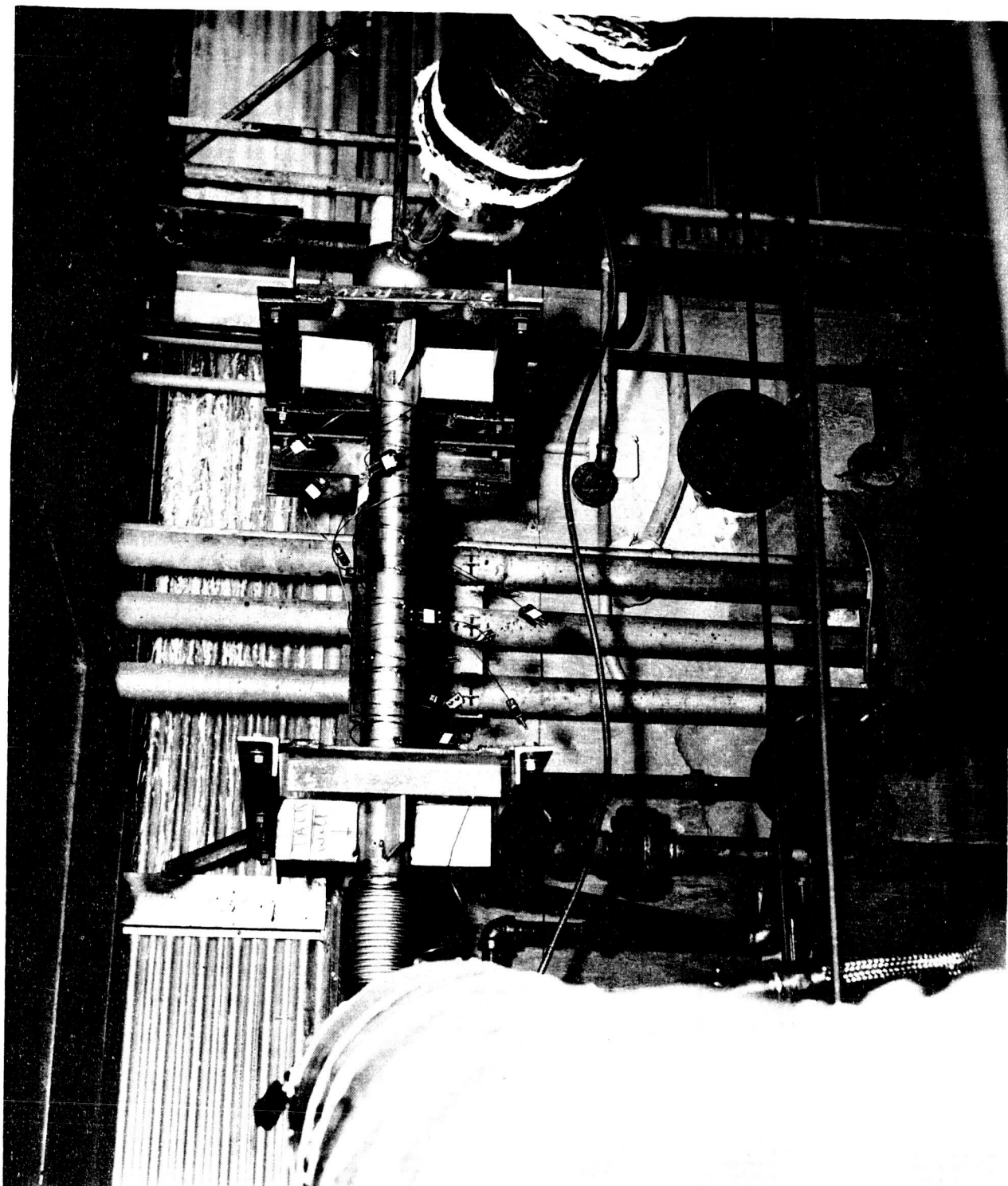
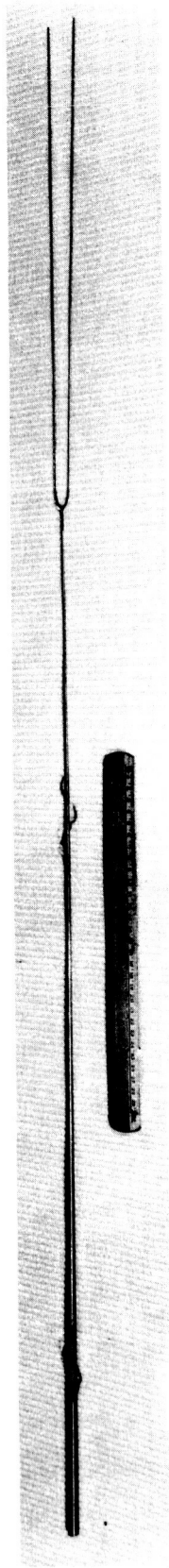


Figure C7. Condenser Installation.



**Figure C8. Tapered Pin Insert**



a) Insert

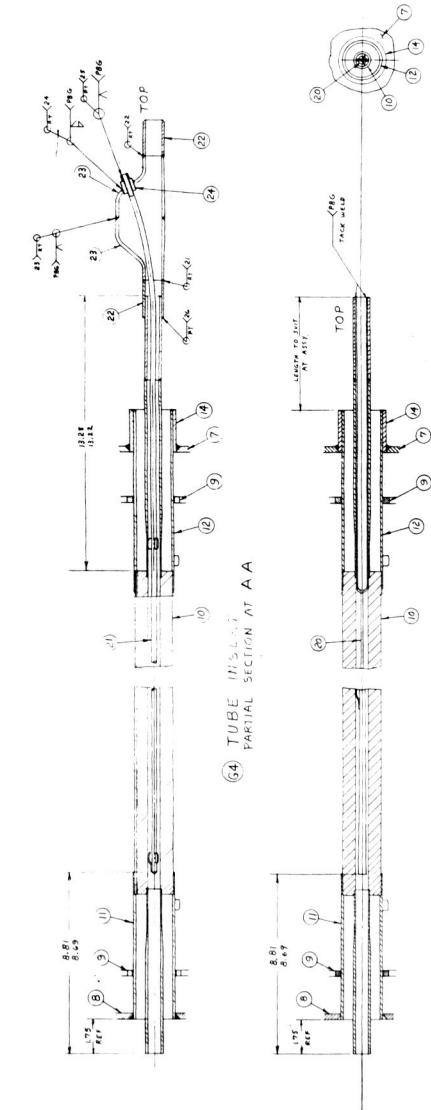


b) Penetration

Figure C9. Helical Insert.

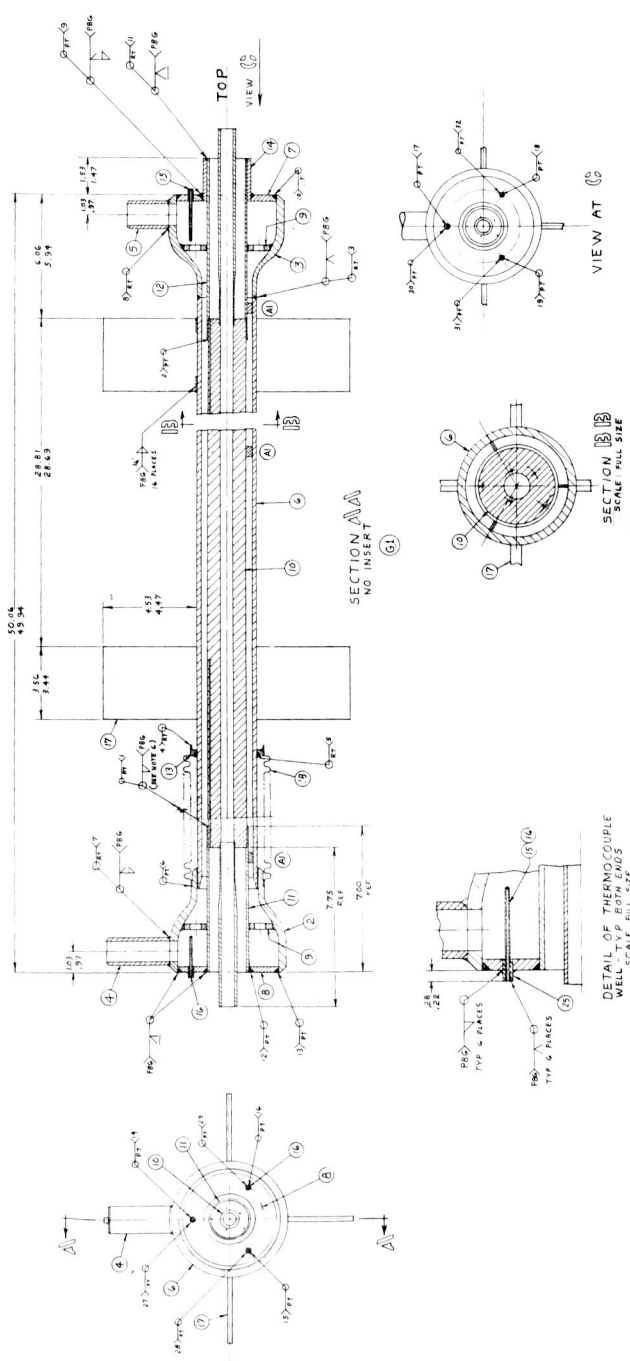


ITEM	DESCRIPTION OR NAME	QTY	UNIT
1	2.2175 IN. DIA. 1/2 IN. THICK 304 STAINLESS STEEL FLANGE	1	FLANGE
2	2.2175 IN. DIA. 1/2 IN. THICK 304 STAINLESS STEEL FLANGE	1	FLANGE
3	1/2 IN. DIA. 1/2 IN. THICK 304 STAINLESS STEEL FLANGE	1	FLANGE
4	1/2 IN. DIA. 1/2 IN. THICK 304 STAINLESS STEEL FLANGE	1	FLANGE
5	1/2 IN. DIA. 1/2 IN. THICK 304 STAINLESS STEEL FLANGE	1	FLANGE
6	1/2 IN. DIA. 1/2 IN. THICK 304 STAINLESS STEEL FLANGE	1	FLANGE
7	1/2 IN. DIA. 1/2 IN. THICK 304 STAINLESS STEEL FLANGE	1	FLANGE
8	1/2 IN. DIA. 1/2 IN. THICK 304 STAINLESS STEEL FLANGE	1	FLANGE
9	1/2 IN. DIA. 1/2 IN. THICK 304 STAINLESS STEEL FLANGE	1	FLANGE
10	1/2 IN. DIA. 1/2 IN. THICK 304 STAINLESS STEEL FLANGE	1	FLANGE
11	1/2 IN. DIA. 1/2 IN. THICK 304 STAINLESS STEEL FLANGE	1	FLANGE
12	1/2 IN. DIA. 1/2 IN. THICK 304 STAINLESS STEEL FLANGE	1	FLANGE
13	1/2 IN. DIA. 1/2 IN. THICK 304 STAINLESS STEEL FLANGE	1	FLANGE
14	1/2 IN. DIA. 1/2 IN. THICK 304 STAINLESS STEEL FLANGE	1	FLANGE
15	1/2 IN. DIA. 1/2 IN. THICK 304 STAINLESS STEEL FLANGE	1	FLANGE
16	1/2 IN. DIA. 1/2 IN. THICK 304 STAINLESS STEEL FLANGE	1	FLANGE
17	1/2 IN. DIA. 1/2 IN. THICK 304 STAINLESS STEEL FLANGE	1	FLANGE
18	1/2 IN. DIA. 1/2 IN. THICK 304 STAINLESS STEEL FLANGE	1	FLANGE
19	1/2 IN. DIA. 1/2 IN. THICK 304 STAINLESS STEEL FLANGE	1	FLANGE
20	1/2 IN. DIA. 1/2 IN. THICK 304 STAINLESS STEEL FLANGE	1	FLANGE
21	1/2 IN. DIA. 1/2 IN. THICK 304 STAINLESS STEEL FLANGE	1	FLANGE
22	1/2 IN. DIA. 1/2 IN. THICK 304 STAINLESS STEEL FLANGE	1	FLANGE
23	1/2 IN. DIA. 1/2 IN. THICK 304 STAINLESS STEEL FLANGE	1	FLANGE
24	1/2 IN. DIA. 1/2 IN. THICK 304 STAINLESS STEEL FLANGE	1	FLANGE
25	1/2 IN. DIA. 1/2 IN. THICK 304 STAINLESS STEEL FLANGE	1	FLANGE



(63) TAPER PLUG INSERT  
PARTIAL SECTION AT AA

(64) TUBE INSERT  
PARTIAL SECTION AT AA



DETAIL OF THERMOCOUPLE  
WELL TYP BOTH ENDS  
SCALE FULL SIZE

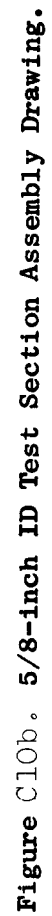
SECTION BB  
SCALE FULL SIZE

VIEW AT C

- NOTES:
1. FLEXONICS CORP. BARTLETT, ILL. OR EQUAL
  2. MATL. SPECS. ONE & PINE FITTINGS, 316 STN. STL. PER ASTM A192-67, A276-67 (304), AND A276-67 (316)
  3. ALL WELDS TO BE WELDED SPEC. EPR-41. THIS IS AN ALKALI METAL CONTAINING ASSY.
  4. SPECTROMETER LEAK TEST PER MIL STD 271C (304) SPECTROMETER LEAK TEST PER MIL STD 271C (316)
  5. UNLESS OTHERWISE SPECIFIED, SYMBOLS PER AWS A2.2-58
  6. PARTS 11 AND 12 ARE TO BE WELDED TO PART 10 USING AWS A2.2-58
  7. PARTS 11 AND 12 ARE TO BE WELDED TO PART 10 USING AWS A2.2-58
  8. PARTS 11 AND 12 ARE TO BE WELDED TO PART 10 USING AWS A2.2-58

Figure 0104, 5/8-inch ID Test Section Assembly Drawing.

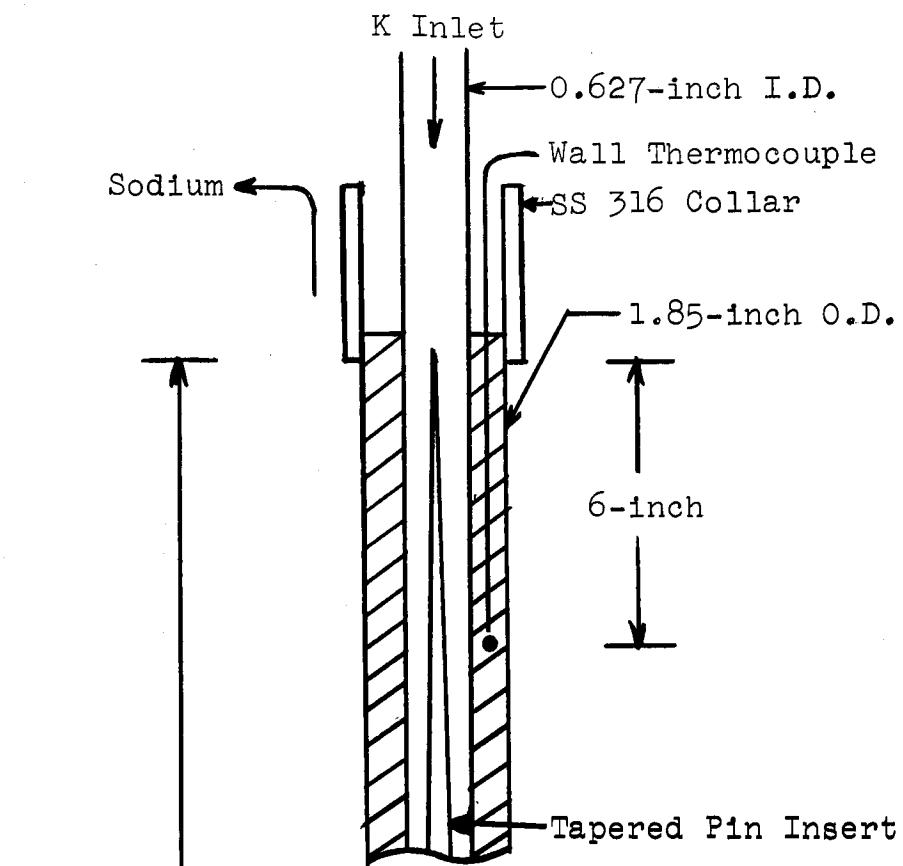




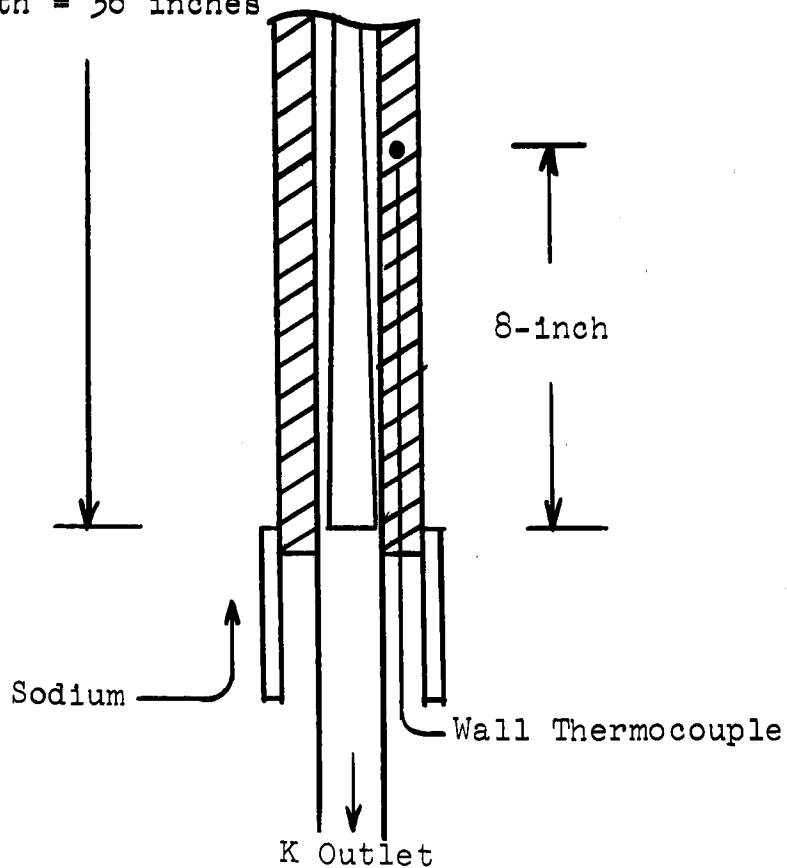


APPENDIX D

50 KW DATA



Active Condensing  
Length = 36 inches



50 KW Test Section Schematic

(5/8-inch I.D. tube with tapered pin insert, Test Set  
No. 2, December, 1964)

TABLE D-1. NOMENCLATURE FOR CONDENSING HEAT TRANSFER  
RESULTS FROM THE 50 KW FACILITY  
(Key to Table D-2)

Column	Symbol	Identification
131	DATE	(e.g., 1.2074 + 04 = 12/7/64)
132	TIME	(e.g., 1.000 + 03 = 1000)
<u>Fluid Thermocouples</u>		
	<u>TC Number</u>	
134	1	Potassium inlet
136	2	Potassium inlet
138	3	Potassium outlet
140	4	Potassium outlet
142	5	Sodium outlet
144	6	Sodium outlet
146	7	Sodium outlet
148	8	Sodium inlet
150	9	Sodium inlet
152	10	Sodium inlet
<u>Wall Thermocouples</u>		
	<u>TC Number</u>	<u>Radius Within Tube Wall - Inches</u> <u>Distance from Condense Inlet - Inches</u>
154	11	.409      6
156	12	.400      6
158	13	.539      6
160	14	.834      6
162	15	.832      6
164	16	.408      28
166	17	.411      28
168	18	.541      28
170	19	.837      28
172	20	.833      28

Column	Symbol	Identification
174	TKI	Inlet potassium temperature, $^{\circ}\text{F}$
176	TKO	Outlet potassium temperature, $^{\circ}\text{F}$
181-219	TKNC	Corrected temperature of thermocouple N, $^{\circ}\text{F}$
221	TKICC	Corrected inlet potassium temperature, $^{\circ}\text{F}$
223	TKOC	Corrected outlet potassium temperature, $^{\circ}\text{F}$
226	TNAO	Outlet Sodium temperature, $^{\circ}\text{F}$
229	TNAI	Inlet Sodium temperature, $^{\circ}\text{F}$
230	DTNA	Sodium temperature increase, $^{\circ}\text{F}$
235	WNA	Sodium Flow rate, lb/hr
237	TNAM	Sodium mean temperature, $^{\circ}\text{F}$
238	CPNA	Sodium specific heat, Btu/lb- $^{\circ}\text{F}$
240	QNA	Sodium heat gain, Btu/hr
243	DTQL	Temperature Difference, Test Section Shell - Ambient, $^{\circ}\text{F}$
246	QC	Condenser load, Btu/hr
247	Q/AA	Average heat flux, Btu/hr-ft $^2$
251	WK	Potassium flow rate, lb/hr
306	TWIT*	Inner wall temperature at top axial station, $^{\circ}\text{F}$
317	Q/AT*	Heat Flux at inner wall at top axial station, Btu/hr-ft $^2$
319	TWOT*	Outer wall temperature at top axial station, $^{\circ}\text{F}$
324	HCONT*	Condensing heat transfer coefficient at top axial station, Btu/hr-ft $^2$ $^{\circ}\text{F}$
326	NUCT*	Nusselt's condensing ratio at top axial station, dimensionless
354	TWIB*	Inner wall temperature at bottom axial station, $^{\circ}\text{F}$
365	Q/AB*	Heat flux at inner wall at bottom axial station, Btu/hr-ft $^2$
367	TWOB*	Outer wall temperature at bottom axial station, $^{\circ}\text{F}$
372	HCONB*	Condensing heat transfer coefficient at bottom axial station, Btu/hr-ft $^2$ $^{\circ}\text{F}$
374	NUCB*	Nusselt's condensing ratio at bottom axial station, dimensionless
450	PSI HD	Inlet vapor velocity head, psi
451	PI*	Inlet potassium vapor pressure, lb/in $^2$
452	PO*	Outlet potassium vapor pressure, lb/in $^2$
453	DPC*	Condensing pressure drop

\*These values were also calculated, accounting for the thermocouple standardizations obtained in the vapor standardization runs. The values of the parameters utilizing the thermocouple standardization are indicated in the columns in which the notation for the above parameters are followed by a C, e.g., TWITC is the Inner Wall Temperature at top axial station utilizing the standardized correction factor,  $^{\circ}\text{F}$ .

Column	Symbol	Identification
700	X B	Potassium Quality, Bottom Station, $L/D = 45$
495	WKL B	Local Potassium liquid flowrate at bottom station, lb/hr
701	X T	Potassium Quality, Top Station, $L/D = 10$
498	WKL T	Local Potassium liquid flowrate at top station, lb/hr
504	NREF T	Liquid film Reynolds number at top station, $L/D = 10$
507	NREF B	Liquid film Reynolds number at bottom station, $L/D = 45$

TABLE D-2

CONDENSING DATA REDUCTION (Test Set No. 2)

	131	132	134	136	138	140
	DATE	TIME	TC1	TC2	TC3	TC4
1	1.2074+04	1.0000+03	1.1982+03	1.1868+03	1.2060+03	1.1922+03
2	1.2074+04	1.0000+03	1.1982+03	1.1867+03	1.2059+03	1.1921+03
3	1.2074+04	1.0000+03	1.1982+03	1.1868+03	1.2061+03	1.1924+03
4	1.2074+04	1.3000+03	1.2921+03	1.2797+03	1.2463+03	1.2321+03
5	1.2074+04	1.3000+03	1.2921+03	1.2798+03	1.2482+03	1.2339+03
6	1.2074+04	1.3000+03	1.2921+03	1.2797+03	1.2535+03	1.2394+03
7	1.2074+04	1.9000+03	1.3981+03	1.3851+03	1.3075+03	1.2929+03
8	1.2074+04	1.9000+03	1.3981+03	1.3850+03	1.3082+03	1.2935+03
9	1.2074+04	1.9000+03	1.3978+03	1.3847+03	1.3083+03	1.2937+03
10	1.2084+04	7.4500+02	1.2989+03	1.2875+03	1.3046+03	1.2896+03
11	1.2084+04	7.4500+02	1.2990+03	1.2876+03	1.3045+03	1.2895+03
12	1.2084+04	7.4500+02	1.2990+03	1.2875+03	1.3044+03	1.2894+03
13	1.2084+04	1.3000+03	1.1984+03	1.1876+03	1.2127+03	1.1985+03
14	1.2084+04	1.3000+03	1.1984+03	1.1875+03	1.2127+03	1.1986+03
15	1.2084+04	1.3000+03	1.1984+03	1.1876+03	1.2127+03	1.1985+03
16	1.2084+04	1.8300+03	1.1975+03	1.1866+03	1.2148+03	1.2006+03
17	1.2084+04	1.8300+03	1.1975+03	1.1865+03	1.2107+03	1.1974+03
18	1.2084+04	1.8300+03	1.1978+03	1.1870+03	1.2144+03	1.2000+03
19	1.2084+04	2.2150+03	1.2919+03	1.2806+03	1.3001+03	1.2851+03
20	1.2084+04	2.2150+03	1.2918+03	1.2804+03	1.2999+03	1.2852+03
21	1.2084+04	2.2150+03	1.2922+03	1.2806+03	1.2997+03	1.2848+03
22	1.2094+04	2.4500+02	1.4191+03	1.4066+03	1.4219+03	1.4054+03
23	1.2094+04	2.4500+02	1.4191+03	1.4066+03	1.4219+03	1.4054+03
24	1.2094+04	2.4500+02	1.4190+03	1.4066+03	1.4219+03	1.4056+03
25	1.2094+04	1.9300+03	1.3933+03	1.3816+03	1.3970+03	1.3809+03
26	1.2094+04	1.9300+03	1.3932+03	1.3816+03	1.3971+03	1.3811+03
27	1.2094+04	1.9300+03	1.3932+03	1.3815+03	1.3970+03	1.3810+03
28	1.2104+04	2.0000+01	1.2635+03	1.2530+03	1.2768+03	1.2620+03
29	1.2104+04	2.0000+01	1.2638+03	1.2534+03	1.2771+03	1.2623+03
30	1.2104+04	2.0000+01	1.2639+03	1.2533+03	1.2776+03	1.2628+03



# CONDENSING DATA REDUCTION

	131	132	134	136	138	140
	DATE	TIME	TC1	TC2	TC3	TC4
31	1.2104+04	5.0000+02	1.1924+03	1.1835+03	1.2021+03	1.1881+03
32	1.2104+04	5.0000+02	1.1917+03	1.1829+03	1.2029+03	1.1889+03
33	1.2104+04	5.0000+02	1.1916+03	1.1828+03	1.2030+03	1.1890+03
34	1.2104+04	1.1300+03	1.2884+03	1.2781+03	1.3006+03	1.2849+03
35	1.2104+04	1.1300+03	1.2883+03	1.2781+03	1.3003+03	1.2845+03
36	1.2104+04	1.1300+03	1.2887+03	1.2784+03	1.3007+03	1.2849+03
37	1.2104+04	1.7150+03	1.3995+03	1.3883+03	1.4046+03	1.3888+03
38	1.2104+04	1.7150+03	1.3998+03	1.3887+03	1.4049+03	1.3892+03
39	1.2104+04	1.7150+03	1.3998+03	1.3887+03	1.4051+03	1.3894+03
40	1.2104+04	2.2000+03	1.3971+03	1.3861+03	1.4027+03	1.3871+03
41	1.2104+04	2.2000+03	1.3969+03	1.3859+03	1.4025+03	1.3869+03
42	1.2104+04	2.2000+03	1.3971+03	1.3861+03	1.4027+03	1.3871+03
43	1.2114+04	2.2000+02	1.3392+03	1.3289+03	1.3488+03	1.3339+03
44	1.2114+04	2.2000+02	1.3381+03	1.3279+03	1.3481+03	1.3332+03
45	1.2114+04	2.2000+02	1.3372+03	1.3271+03	1.3475+03	1.3328+03
46	1.2114+04	1.0300+03	1.2582+03	1.2488+03	1.2742+03	1.2600+03
47	1.2114+04	1.0300+03	1.2579+03	1.2487+03	1.2745+03	1.2602+03
48	1.2114+04	1.0300+03	1.2583+03	1.2491+03	1.2741+03	1.2598+03
49	1.2114+04	1.5400+03	1.2488+03	1.2375+03	1.2625+03	1.2482+03
50	1.2114+04	1.5400+03	1.2490+03	1.2377+03	1.2626+03	1.2483+03
51	1.2114+04	1.5400+03	1.2488+03	1.2375+03	1.2625+03	1.2482+03
52	1.2114+04	1.6450+03	1.2368+03	1.2270+03	1.2481+03	1.2351+03
53	1.2114+04	1.6450+03	1.2364+03	1.2265+03	1.2471+03	1.2342+03
54	1.2114+04	1.6450+03	1.2366+03	1.2267+03	1.2480+03	1.2350+03
55	1.2114+04	1.8150+03	1.2288+03	1.2189+03	1.2377+03	1.2249+03
56	1.2114+04	1.8150+03	1.2291+03	1.2191+03	1.2379+03	1.2251+03
57	1.2114+04	1.8150+03	1.2289+03	1.2190+03	1.2377+03	1.2249+03
58	1.2114+04	1.9200+03	1.2275+03	1.2176+03	1.2343+03	1.2217+03
59	1.2114+04	1.9200+03	1.2277+03	1.2178+03	1.2344+03	1.2218+03
60	1.2114+04	1.9200+03	1.2277+03	1.2178+03	1.2344+03	1.2218+03

# CONDENSING DATA REDUCTION

	131	132	134	136	138	140
	DATE	TIME	TC1	TC2	TC3	TC4
61	1.2114+04	2.0200+03	1.2286+03	1.2186+03	1.2335+03	1.2210+03
62	1.2114+04	2.0200+03	1.2283+03	1.2183+03	1.2334+03	1.2209+03
63	1.2114+04	2.0200+03	1.2284+03	1.2184+03	1.2334+03	1.2209+03
64	1.2114+04	2.1000+03	1.2145+03	1.2046+03	1.2196+03	1.2073+03
65	1.2114+04	2.1000+03	1.2147+03	1.2047+03	1.2197+03	1.2073+03
66	1.2114+04	2.1000+03	1.2147+03	1.2048+03	1.2198+03	1.2075+03
67	1.2124+04	1.4300+03	1.4079+03	1.3981+03	1.4189+03	1.4024+03
68	1.2124+04	1.4300+03	1.4083+03	1.3985+03	1.4197+03	1.4043+03
69	1.2124+04	1.4300+03	1.4079+03	1.3985+03	1.4200+03	1.4048+03
70	1.2124+04	1.1000+03	1.4318+03	1.4218+03	1.4384+03	1.4229+03
71	1.2124+04	1.1000+03	1.4282+03	1.4184+03	1.4367+03	1.4211+03
72	1.2124+04	1.1000+03	1.4267+03	1.4168+03	1.4343+03	1.4193+03

# CONDENSING DATA REDUCTION

	142	144	146	148	150	152
	TC5	TC6	TC7	TC8	TC9	TC10
1	1.1498+03	1.1464+03	1.1311+03	1.1267+03	1.1269+03	1.1285+03
2	1.1497+03	1.1466+03	1.1311+03	1.1267+03	1.1269+03	1.1286+03
3	1.1500+03	1.1466+03	1.1313+03	1.1269+03	1.1271+03	1.1286+03
4	1.2374+03	1.2338+03	1.2172+03	1.2120+03	1.2121+03	1.2137+03
5	1.2372+03	1.2341+03	1.2171+03	1.2121+03	1.2122+03	1.2138+03
6	1.2373+03	1.2333+03	1.2171+03	1.2119+03	1.2121+03	1.2137+03
7	1.3284+03	1.3232+03	1.3060+03	1.2970+03	1.2970+03	1.2990+03
8	1.3285+03	1.3232+03	1.3059+03	1.2968+03	1.2970+03	1.2988+03
9	1.3283+03	1.3234+03	1.3060+03	1.2970+03	1.2970+03	1.2988+03
10	1.2326+03	1.2266+03	1.2109+03	1.1994+03	1.1991+03	1.2010+03
11	1.2324+03	1.2268+03	1.2107+03	1.1993+03	1.1991+03	1.2011+03
12	1.2323+03	1.2265+03	1.2107+03	1.1993+03	1.1991+03	1.2012+03
13	1.1341+03	1.1279+03	1.1129+03	1.0981+03	1.0977+03	1.0999+03
14	1.1344+03	1.1281+03	1.1132+03	1.0982+03	1.0978+03	1.1001+03
15	1.1343+03	1.1279+03	1.1133+03	1.0982+03	1.0978+03	1.1000+03
16	1.1188+03	1.1107+03	1.0962+03	1.0708+03	1.0699+03	1.0733+03
17	1.1188+03	1.1106+03	1.0957+03	1.0711+03	1.0700+03	1.0734+03
18	1.1186+03	1.1111+03	1.0960+03	1.0709+03	1.0700+03	1.0734+03
19	1.2115+03	1.2038+03	1.1879+03	1.1650+03	1.1640+03	1.1671+03
20	1.2114+03	1.2035+03	1.1879+03	1.1652+03	1.1643+03	1.1674+03
21	1.2117+03	1.2034+03	1.1879+03	1.1649+03	1.1640+03	1.1671+03
22	1.3412+03	1.3341+03	1.3168+03	1.2992+03	1.2986+03	1.3011+03
23	1.3409+03	1.3341+03	1.3169+03	1.2991+03	1.2985+03	1.3012+03
24	1.3411+03	1.3342+03	1.3169+03	1.2994+03	1.2987+03	1.3012+03
25	1.2933+03	1.2841+03	1.2676+03	1.2389+03	1.2378+03	1.2411+03
26	1.2929+03	1.2835+03	1.2677+03	1.2390+03	1.2378+03	1.2410+03
27	1.2930+03	1.2842+03	1.2679+03	1.2389+03	1.2376+03	1.2410+03
28	1.1652+03	1.1551+03	1.1405+03	1.1076+03	1.1063+03	1.1101+03
29	1.1651+03	1.1553+03	1.1408+03	1.1077+03	1.1063+03	1.1103+03
30	1.1653+03	1.1547+03	1.1406+03	1.1076+03	1.1062+03	1.1103+03

# CONDENSING DATA REDUCTION

	142	144	146	148	150	152
	TC5	TC6	TC7	TC8	TC9	TC10
31	1.0842+03	1.0753+03	1.0623+03	1.0278+03	1.0255+03	1.0299+03
32	1.0843+03	1.0755+03	1.0624+03	1.0280+03	1.0256+03	1.0300+03
33	1.0847+03	1.0760+03	1.0629+03	1.0282+03	1.0258+03	1.0302+03
34	1.1667+03	1.1544+03	1.1403+03	1.0962+03	1.0944+03	1.0988+03
35	1.1668+03	1.1538+03	1.1401+03	1.0964+03	1.0945+03	1.0989+03
36	1.1669+03	1.1543+03	1.1403+03	1.0965+03	1.0945+03	1.0990+03
37	1.2781+03	1.2670+03	1.2507+03	1.2112+03	1.2096+03	1.2132+03
38	1.2784+03	1.2669+03	1.2507+03	1.2111+03	1.2094+03	1.2130+03
39	1.2781+03	1.2666+03	1.2510+03	1.2110+03	1.2094+03	1.2129+03
40	1.2616+03	1.2479+03	1.2325+03	1.1848+03	1.1832+03	1.1871+03
41	1.2616+03	1.2478+03	1.2328+03	1.1852+03	1.1835+03	1.1875+03
42	1.2618+03	1.2479+03	1.2332+03	1.1853+03	1.1838+03	1.1875+03
43	1.2030+03	1.1890+03	1.1746+03	1.1241+03	1.1226+03	1.1265+03
44	1.2026+03	1.1884+03	1.1743+03	1.1243+03	1.1228+03	1.1267+03
45	1.2026+03	1.1891+03	1.1743+03	1.1244+03	1.1229+03	1.1268+03
46	1.1366+03	1.1241+03	1.1109+03	1.0660+03	1.0643+03	1.0679+03
47	1.1365+03	1.1244+03	1.1108+03	1.0653+03	1.0639+03	1.0675+03
48	1.1364+03	1.1244+03	1.1109+03	1.0662+03	1.0646+03	1.0684+03
49	1.1623+03	1.1549+03	1.1408+03	1.1158+03	1.1144+03	1.1171+03
50	1.1623+03	1.1549+03	1.1409+03	1.1157+03	1.1144+03	1.1172+03
51	1.1625+03	1.1553+03	1.1410+03	1.1159+03	1.1146+03	1.1173+03
52	1.1622+03	1.1568+03	1.1428+03	1.1246+03	1.1237+03	1.1258+03
53	1.1617+03	1.1564+03	1.1422+03	1.1246+03	1.1236+03	1.1258+03
54	1.1621+03	1.1567+03	1.1427+03	1.1246+03	1.1236+03	1.1259+03
55	1.1677+03	1.1644+03	1.1498+03	1.1396+03	1.1389+03	1.1407+03
56	1.1679+03	1.1643+03	1.1499+03	1.1398+03	1.1391+03	1.1408+03
57	1.1677+03	1.1642+03	1.1498+03	1.1397+03	1.1390+03	1.1408+03
58	1.1753+03	1.1728+03	1.1581+03	1.1536+03	1.1531+03	1.1546+03
59	1.1755+03	1.1729+03	1.1582+03	1.1537+03	1.1532+03	1.1546+03
60	1.1754+03	1.1728+03	1.1583+03	1.1538+03	1.1532+03	1.1547+03

# CONDENSING DATA REDUCTION

	142	144	146	148	150	152
	TC5	TC6	TC7	TC8	TC9	TC10
61	1.1827+03	1.1809+03	1.1661+03	1.1656+03	1.1651+03	1.1665+03
62	1.1826+03	1.1808+03	1.1660+03	1.1656+03	1.1652+03	1.1665+03
63	1.1827+03	1.1808+03	1.1660+03	1.1656+03	1.1652+03	1.1664+03
64	1.1717+03	1.1702+03	1.1554+03	1.1566+03	1.1562+03	1.1575+03
65	1.1720+03	1.1704+03	1.1557+03	1.1568+03	1.1565+03	1.1577+03
66	1.1721+03	1.1706+03	1.1559+03	1.1574+03	1.1569+03	1.1582+03
67	1.2401+03	1.2230+03	1.2084+03	1.1458+03	1.1439+03	1.1485+03
68	1.2391+03	1.2235+03	1.2080+03	1.1464+03	1.1444+03	1.1489+03
69	1.2416+03	1.2245+03	1.2097+03	1.1456+03	1.1436+03	1.1479+03
70	1.2717+03	1.2565+03	1.2406+03	1.1809+03	1.1788+03	1.1832+03
71	1.2718+03	1.2559+03	1.2403+03	1.1803+03	1.1785+03	1.1830+03
72	1.2714+03	1.2556+03	1.2403+03	1.1809+03	1.1786+03	1.1833+03

# CONDENSING DATA REDUCTION

	154	156	158	160	162	164
	TC11	TC12	TC13	TC14	TC15	TC16
1	1.1694+03	1.1911+03	1.1781+03	1.1556+03	1.1388+03	1.1725+03
2	1.1696+03	1.1913+03	1.1782+03	1.1558+03	1.1389+03	1.1727+03
3	1.1697+03	1.1913+03	1.1782+03	1.1555+03	1.1388+03	1.1724+03
4	1.2591+03	1.2823+03	1.2680+03	1.2432+03	1.2258+03	1.2613+03
5	1.2591+03	1.2825+03	1.2682+03	1.2435+03	1.2258+03	1.2612+03
6	1.2588+03	1.2823+03	1.2679+03	1.2433+03	1.2258+03	1.2613+03
7	1.3590+03	1.3847+03	1.3670+03	1.3367+03	1.3171+03	1.3589+03
8	1.3590+03	1.3847+03	1.3670+03	1.3367+03	1.3172+03	1.3592+03
9	1.3587+03	1.3844+03	1.3667+03	1.3365+03	1.3169+03	1.3588+03
10	1.2639+03	1.2871+03	1.2699+03	1.2400+03	1.2212+03	1.2634+03
11	1.2639+03	1.2871+03	1.2699+03	1.2403+03	1.2214+03	1.2635+03
12	1.2639+03	1.2871+03	1.2700+03	1.2404+03	1.2215+03	1.2636+03
13	1.1687+03	1.1895+03	1.1721+03	1.1420+03	1.1235+03	1.1693+03
14	1.1688+03	1.1896+03	1.1723+03	1.1422+03	1.1237+03	1.1693+03
15	1.1688+03	1.1897+03	1.1723+03	1.1421+03	1.1236+03	1.1694+03
16	1.1643+03	1.1853+03	1.1646+03	1.1281+03	1.1086+03	1.1627+03
17	1.1638+03	1.1848+03	1.1641+03	1.1278+03	1.1082+03	1.1621+03
18	1.1641+03	1.1852+03	1.1645+03	1.1282+03	1.1086+03	1.1625+03
19	1.2544+03	1.2771+03	1.2567+03	1.2207+03	1.2005+03	1.2510+03
20	1.2546+03	1.2772+03	1.2567+03	1.2206+03	1.2003+03	1.2510+03
21	1.2541+03	1.2766+03	1.2566+03	1.2206+03	1.2005+03	1.2506+03
22	1.3778+03	1.4031+03	1.3838+03	1.3497+03	1.3291+03	1.3754+03
23	1.3779+03	1.4033+03	1.3839+03	1.3498+03	1.3291+03	1.3756+03
24	1.3780+03	1.4034+03	1.3841+03	1.3499+03	1.3291+03	1.3754+03
25	1.3482+03	1.3725+03	1.3479+03	1.3044+03	1.2835+03	1.3412+03
26	1.3481+03	1.3725+03	1.3478+03	1.3044+03	1.2834+03	1.3409+03
27	1.3480+03	1.3724+03	1.3476+03	1.3043+03	1.2832+03	1.3408+03
28	1.2251+03	1.2468+03	1.2214+03	1.1761+03	1.1565+03	1.2182+03
29	1.2254+03	1.2471+03	1.2216+03	1.1761+03	1.1566+03	1.2185+03
30	1.2258+03	1.2475+03	1.2219+03	1.1764+03	1.1568+03	1.2190+03

# CONDENSING DATA REDUCTION

	154	156	158	160	162	164
	TC11	TC12	TC13	TC14	TC15	TC16
31	1.1489+03	1.1694+03	1.1421+03	1.0955+03	1.0777+03	1.1400+03
32	1.1497+03	1.1701+03	1.1428+03	1.0963+03	1.0784+03	1.1408+03
33	1.1497+03	1.1700+03	1.1428+03	1.0962+03	1.0785+03	1.1403+03
34	1.2453+03	1.2674+03	1.2356+03	1.1801+03	1.1593+03	1.2321+03
35	1.2445+03	1.2667+03	1.2349+03	1.1797+03	1.1591+03	1.2319+03
36	1.2450+03	1.2668+03	1.2355+03	1.1801+03	1.1595+03	1.2318+03
37	1.3495+03	1.3735+03	1.3436+03	1.2914+03	1.2697+03	1.3391+03
38	1.3497+03	1.3737+03	1.3437+03	1.2912+03	1.2695+03	1.3392+03
39	1.3496+03	1.3735+03	1.3437+03	1.2912+03	1.2696+03	1.3389+03
40	1.3448+03	1.3685+03	1.3348+03	1.2758+03	1.2539+03	1.3313+03
41	1.3447+03	1.3684+03	1.3349+03	1.2756+03	1.2543+03	1.3315+03
42	1.3443+03	1.3679+03	1.3347+03	1.2765+03	1.2539+03	1.3308+03
43	1.2897+03	1.3118+03	1.2779+03	1.2172+03	1.1962+03	1.2751+03
44	1.2883+03	1.3105+03	1.2767+03	1.2169+03	1.1952+03	1.2742+03
45	1.2885+03	1.3107+03	1.2766+03	1.2161+03	1.1952+03	1.2745+03
46	1.2181+03	1.2391+03	1.2063+03	1.1495+03	1.1302+03	1.2045+03
47	1.2179+03	1.2389+03	1.2065+03	1.1497+03	1.1303+03	1.2045+03
48	1.2174+03	1.2384+03	1.2061+03	1.1496+03	1.1303+03	1.2045+03
49	1.2139+03	1.2347+03	1.2108+03	1.1718+03	1.1538+03	1.2092+03
50	1.2140+03	1.2348+03	1.2108+03	1.1719+03	1.1538+03	1.2095+03
51	1.2138+03	1.2345+03	1.2107+03	1.1719+03	1.1538+03	1.2092+03
52	1.2034+03	1.2243+03	1.2042+03	1.1704+03	1.1541+03	1.2028+03
53	1.2028+03	1.2238+03	1.2036+03	1.1698+03	1.1537+03	1.2024+03
54	1.2035+03	1.2246+03	1.2043+03	1.1705+03	1.1543+03	1.2033+03
55	1.1983+03	1.2194+03	1.2025+03	1.1748+03	1.1592+03	1.2004+03
56	1.1983+03	1.2194+03	1.2026+03	1.1749+03	1.1593+03	1.2004+03
57	1.1983+03	1.2194+03	1.2025+03	1.1747+03	1.1592+03	1.2004+03
58	1.1982+03	1.2193+03	1.2048+03	1.1814+03	1.1661+03	1.2018+03
59	1.1983+03	1.2194+03	1.2048+03	1.1814+03	1.1662+03	1.2018+03
60	1.1983+03	1.2194+03	1.2050+03	1.1814+03	1.1662+03	1.2018+03

# CONDENSING DATA REDUCTION

	154	156	158	160	162	164
	TC11	TC12	TC13	TC14	TC15	TC16
61	1.2000+03	1.2212+03	1.2085+03	1.1880+03	1.1729+03	1.2046+03
62	1.2000+03	1.2211+03	1.2083+03	1.1880+03	1.1729+03	1.2046+03
63	1.1999+03	1.2211+03	1.2083+03	1.1879+03	1.1728+03	1.2046+03
64	1.1871+03	1.2079+03	1.1959+03	1.1767+03	1.1620+03	1.1922+03
65	1.1872+03	1.2080+03	1.1961+03	1.1769+03	1.1621+03	1.1924+03
66	1.1873+03	1.2081+03	1.1962+03	1.1772+03	1.1624+03	1.1926+03
67	1.3414+03	1.3634+03	1.3269+03	1.2583+03	1.2338+03	1.3207+03
68	1.3492+03	1.3729+03	1.3314+03	1.2597+03	1.2360+03	1.3325+03
69	1.3503+03	1.3743+03	1.3324+03	1.2605+03	1.2361+03	1.3336+03
70	1.3739+03	1.3980+03	1.3586+03	1.2903+03	1.2657+03	1.3566+03
71	1.3710+03	1.3954+03	1.3563+03	1.2897+03	1.2643+03	1.3550+03
72	1.3707+03	1.3950+03	1.3557+03	1.2883+03	1.2640+03	1.3546+03



# CONDENSING DATA REDUCTION

	166	168	170	172	174	176
	TC17	TC18	TC19	TC20	TKI	TKO
1	1.1886+03	1.1733+03	1.1468+03	1.1437+03	1.1925+03	1.1991+03
2	1.1887+03	1.1733+03	1.1467+03	1.1435+03	1.1924+03	1.1990+03
3	1.1885+03	1.1733+03	1.1467+03	1.1436+03	1.1925+03	1.1993+03
4	1.2781+03	1.2622+03	1.2338+03	1.2302+03	1.2859+03	1.2392+03
5	1.2780+03	1.2621+03	1.2336+03	1.2301+03	1.2860+03	1.2410+03
6	1.2779+03	1.2621+03	1.2339+03	1.2303+03	1.2859+03	1.2464+03
7	1.3781+03	1.3584+03	1.3221+03	1.3186+03	1.3916+03	1.3002+03
8	1.3784+03	1.3585+03	1.3221+03	1.3186+03	1.3915+03	1.3008+03
9	1.3781+03	1.3584+03	1.3224+03	1.3187+03	1.3912+03	1.3010+03
10	1.2823+03	1.2626+03	1.2259+03	1.2222+03	1.2932+03	1.2971+03
11	1.2823+03	1.2627+03	1.2260+03	1.2225+03	1.2933+03	1.2970+03
12	1.2824+03	1.2626+03	1.2259+03	1.2224+03	1.2932+03	1.2969+03
13	1.1884+03	1.1661+03	1.1266+03	1.1232+03	1.1930+03	1.2056+03
14	1.1885+03	1.1661+03	1.1264+03	1.1232+03	1.1929+03	1.2057+03
15	1.1884+03	1.1661+03	1.1264+03	1.1232+03	1.1930+03	1.2056+03
16	1.1838+03	1.1556+03	1.1063+03	1.1030+03	1.1921+03	1.2077+03
17	1.1833+03	1.1553+03	1.1064+03	1.1030+03	1.1920+03	1.2040+03
18	1.1836+03	1.1555+03	1.1064+03	1.1031+03	1.1924+03	1.2072+03
19	1.2719+03	1.2462+03	1.1997+03	1.1959+03	1.2863+03	1.2926+03
20	1.2718+03	1.2461+03	1.1997+03	1.1959+03	1.2861+03	1.2925+03
21	1.2714+03	1.2459+03	1.1995+03	1.1956+03	1.2864+03	1.2923+03
22	1.3963+03	1.3738+03	1.3318+03	1.3274+03	1.4129+03	1.4137+03
23	1.3965+03	1.3739+03	1.3318+03	1.3272+03	1.4128+03	1.4137+03
24	1.3964+03	1.3738+03	1.3316+03	1.3271+03	1.4128+03	1.4137+03
25	1.3640+03	1.3342+03	1.2792+03	1.2748+03	1.3874+03	1.3890+03
26	1.3637+03	1.3340+03	1.2791+03	1.2748+03	1.3874+03	1.3891+03
27	1.3635+03	1.3338+03	1.2790+03	1.2747+03	1.3874+03	1.3890+03
28	1.2413+03	1.2083+03	1.1489+03	1.1456+03	1.2583+03	1.2694+03
29	1.2417+03	1.2084+03	1.1489+03	1.1456+03	1.2586+03	1.2697+03
30	1.2421+03	1.2088+03	1.1490+03	1.1458+03	1.2586+03	1.2702+03

# CONDENSING DATA REDUCTION

	166	168	170	172	174	176
	TC17	TC18	TC19	TC20	TKI	TKO
31	1.1629+03	1.1281+03	1.0681+03	1.0657+03	1.1879+03	1.1951+03
32	1.1638+03	1.1289+03	1.0684+03	1.0663+03	1.1873+03	1.1959+03
33	1.1632+03	1.1284+03	1.0683+03	1.0663+03	1.1872+03	1.1960+03
34	1.2574+03	1.2177+03	1.1457+03	1.1423+03	1.2832+03	1.2927+03
35	1.2572+03	1.2176+03	1.1461+03	1.1422+03	1.2832+03	1.2924+03
36	1.2573+03	1.2175+03	1.1458+03	1.1422+03	1.2835+03	1.2928+03
37	1.3636+03	1.3271+03	1.2591+03	1.2554+03	1.3939+03	1.3967+03
38	1.3637+03	1.3272+03	1.2589+03	1.2556+03	1.3943+03	1.3971+03
39	1.3634+03	1.3269+03	1.2591+03	1.2553+03	1.3943+03	1.3972+03
40	1.3573+03	1.3158+03	1.2391+03	1.2350+03	1.3916+03	1.3949+03
41	1.3574+03	1.3159+03	1.2396+03	1.2352+03	1.3914+03	1.3947+03
42	1.3568+03	1.3154+03	1.2391+03	1.2350+03	1.3916+03	1.3949+03
43	1.3011+03	1.2582+03	1.1795+03	1.1751+03	1.3341+03	1.3413+03
44	1.3003+03	1.2576+03	1.1791+03	1.1752+03	1.3330+03	1.3407+03
45	1.3006+03	1.2577+03	1.1791+03	1.1753+03	1.3322+03	1.3401+03
46	1.2297+03	1.1886+03	1.1151+03	1.1120+03	1.2535+03	1.2671+03
47	1.2297+03	1.1887+03	1.1152+03	1.1119+03	1.2533+03	1.2674+03
48	1.2296+03	1.1886+03	1.1153+03	1.1122+03	1.2537+03	1.2669+03
49	1.2307+03	1.2028+03	1.1505+03	1.1464+03	1.2432+03	1.2553+03
50	1.2310+03	1.2029+03	1.1504+03	1.1464+03	1.2434+03	1.2554+03
51	1.2308+03	1.2028+03	1.1505+03	1.1465+03	1.2432+03	1.2554+03
52	1.2214+03	1.1975+03	1.1535+03	1.1514+03	1.2319+03	1.2416+03
53	1.2210+03	1.1971+03	1.1532+03	1.1510+03	1.2314+03	1.2407+03
54	1.2221+03	1.1978+03	1.1536+03	1.1515+03	1.2316+03	1.2415+03
55	1.2171+03	1.1984+03	1.1627+03	1.1608+03	1.2239+03	1.2313+03
56	1.2171+03	1.1985+03	1.1629+03	1.1607+03	1.2241+03	1.2315+03
57	1.2171+03	1.1984+03	1.1628+03	1.1608+03	1.2240+03	1.2313+03
58	1.2170+03	1.2021+03	1.1726+03	1.1708+03	1.2226+03	1.2280+03
59	1.2171+03	1.2022+03	1.1727+03	1.1708+03	1.2227+03	1.2281+03
60	1.2171+03	1.2023+03	1.1726+03	1.1709+03	1.2228+03	1.2281+03

# CONDENSING DATA REDUCTION

	166	168	170	172	174	176
	TC17	TC18	TC19	TC20	TKI	TKO
61	1.2188+03	1.2069+03	1.1816+03	1.1799+03	1.2236+03	1.2273+03
62	1.2188+03	1.2068+03	1.1816+03	1.1798+03	1.2233+03	1.2272+03
63	1.2187+03	1.2069+03	1.1816+03	1.1797+03	1.2234+03	1.2272+03
64	1.2059+03	1.1950+03	1.1715+03	1.1695+03	1.2096+03	1.2134+03
65	1.2060+03	1.1952+03	1.1715+03	1.1698+03	1.2097+03	1.2135+03
66	1.2062+03	1.1954+03	1.1719+03	1.1703+03	1.2097+03	1.2136+03
67	1.3479+03	1.3017+03	1.2116+03	1.2069+03	1.4030+03	1.4107+03
68	1.3615+03	1.3091+03	1.2135+03	1.2094+03	1.4034+03	1.4120+03
69	1.3631+03	1.3098+03	1.2131+03	1.2092+03	1.4032+03	1.4124+03
70	1.3850+03	1.3355+03	1.2447+03	1.2411+03	1.4268+03	1.4306+03
71	1.3834+03	1.3340+03	1.2440+03	1.2399+03	1.4233+03	1.4289+03
72	1.3829+03	1.3337+03	1.2438+03	1.2400+03	1.4217+03	1.4268+03

# CONDENSING DATA REDUCTION

	181	183	185	187	189	191
	TC1C	TC2C	TC3C	TC4C	TC5C	TC6C
1	1.1982+03	1.1954+03	1.2043+03	1.1999+03	1.1546+03	1.1489+03
2	1.1982+03	1.1952+03	1.2042+03	1.1998+03	1.1546+03	1.1491+03
3	1.1982+03	1.1954+03	1.2045+03	1.2001+03	1.1549+03	1.1490+03
4	1.2921+03	1.2904+03	1.2447+03	1.2412+03	1.2427+03	1.2364+03
5	1.2921+03	1.2904+03	1.2466+03	1.2430+03	1.2426+03	1.2367+03
6	1.2921+03	1.2903+03	1.2519+03	1.2487+03	1.2426+03	1.2359+03
7	1.3981+03	1.3981+03	1.3060+03	1.3041+03	1.3343+03	1.3260+03
8	1.3981+03	1.3980+03	1.3067+03	1.3048+03	1.3345+03	1.3260+03
9	1.3978+03	1.3977+03	1.3069+03	1.3049+03	1.3342+03	1.3262+03
10	1.2989+03	1.2983+03	1.3031+03	1.3007+03	1.2379+03	1.2292+03
11	1.2990+03	1.2984+03	1.3030+03	1.3006+03	1.2377+03	1.2293+03
12	1.2990+03	1.2983+03	1.3029+03	1.3006+03	1.2376+03	1.2291+03
13	1.1984+03	1.1962+03	1.2111+03	1.2064+03	1.1388+03	1.1303+03
14	1.1984+03	1.1961+03	1.2111+03	1.2065+03	1.1392+03	1.1305+03
15	1.1984+03	1.1962+03	1.2111+03	1.2064+03	1.1390+03	1.1303+03
16	1.1975+03	1.1952+03	1.2131+03	1.2085+03	1.1234+03	1.1131+03
17	1.1975+03	1.1951+03	1.2091+03	1.2052+03	1.1234+03	1.1129+03
18	1.1978+03	1.1955+03	1.2128+03	1.2080+03	1.1232+03	1.1135+03
19	1.2919+03	1.2913+03	1.2986+03	1.2961+03	1.2167+03	1.2064+03
20	1.2918+03	1.2910+03	1.2984+03	1.2961+03	1.2166+03	1.2061+03
21	1.2922+03	1.2913+03	1.2982+03	1.2958+03	1.2169+03	1.2059+03
22	1.4191+03	1.4201+03	1.4206+03	1.4207+03	1.3472+03	1.3368+03
23	1.4191+03	1.4200+03	1.4206+03	1.4207+03	1.3469+03	1.3369+03
24	1.4190+03	1.4200+03	1.4206+03	1.4208+03	1.3471+03	1.3370+03
25	1.3933+03	1.3945+03	1.3957+03	1.3953+03	1.2990+03	1.2868+03
26	1.3932+03	1.3945+03	1.3958+03	1.3954+03	1.2986+03	1.2862+03
27	1.3932+03	1.3944+03	1.3957+03	1.3954+03	1.2988+03	1.2869+03
28	1.2635+03	1.2631+03	1.2752+03	1.2721+03	1.1701+03	1.1576+03
29	1.2638+03	1.2634+03	1.2756+03	1.2724+03	1.1700+03	1.1578+03
30	1.2639+03	1.2634+03	1.2760+03	1.2730+03	1.1702+03	1.1572+03

# CONDENSING DATA REDUCTION

	181	183	185	187	189	191
	TC1C	TC2C	TC3C	TC4C	TC5C	TC6C
31	1.1924+03	1.1921+03	1.2004+03	1.1956+03	1.0886+03	1.0776+03
32	1.1917+03	1.1914+03	1.2013+03	1.1964+03	1.0887+03	1.0778+03
33	1.1916+03	1.1913+03	1.2014+03	1.1966+03	1.0891+03	1.0783+03
34	1.2884+03	1.2887+03	1.2991+03	1.2958+03	1.1716+03	1.1569+03
35	1.2883+03	1.2887+03	1.2988+03	1.2954+03	1.1717+03	1.1563+03
36	1.2887+03	1.2890+03	1.2992+03	1.2958+03	1.1718+03	1.1567+03
37	1.3995+03	1.4013+03	1.4032+03	1.4035+03	1.2838+03	1.2697+03
38	1.3998+03	1.4018+03	1.4036+03	1.4039+03	1.2840+03	1.2695+03
39	1.3998+03	1.4018+03	1.4038+03	1.4040+03	1.2838+03	1.2692+03
40	1.3971+03	1.3991+03	1.4014+03	1.4016+03	1.2671+03	1.2506+03
41	1.3969+03	1.3989+03	1.4012+03	1.4014+03	1.2672+03	1.2504+03
42	1.3971+03	1.3991+03	1.4014+03	1.4017+03	1.2674+03	1.2506+03
43	1.3392+03	1.3407+03	1.3473+03	1.3466+03	1.2081+03	1.1915+03
44	1.3381+03	1.3396+03	1.3467+03	1.3459+03	1.2078+03	1.1909+03
45	1.3372+03	1.3388+03	1.3461+03	1.3454+03	1.2077+03	1.1916+03
46	1.2582+03	1.2588+03	1.2727+03	1.2701+03	1.1413+03	1.1265+03
47	1.2579+03	1.2587+03	1.2730+03	1.2703+03	1.1412+03	1.1268+03
48	1.2583+03	1.2591+03	1.2726+03	1.2698+03	1.1411+03	1.1269+03
49	1.2488+03	1.2472+03	1.2610+03	1.2578+03	1.1672+03	1.1573+03
50	1.2490+03	1.2474+03	1.2610+03	1.2579+03	1.1672+03	1.1574+03
51	1.2488+03	1.2472+03	1.2610+03	1.2579+03	1.1674+03	1.1578+03
52	1.2368+03	1.2364+03	1.2465+03	1.2443+03	1.1671+03	1.1593+03
53	1.2364+03	1.2359+03	1.2456+03	1.2434+03	1.1666+03	1.1589+03
54	1.2366+03	1.2362+03	1.2465+03	1.2442+03	1.1669+03	1.1591+03
55	1.2288+03	1.2282+03	1.2361+03	1.2337+03	1.1726+03	1.1668+03
56	1.2291+03	1.2284+03	1.2363+03	1.2340+03	1.1728+03	1.1668+03
57	1.2289+03	1.2283+03	1.2361+03	1.2337+03	1.1727+03	1.1667+03
58	1.2275+03	1.2269+03	1.2327+03	1.2304+03	1.1803+03	1.1753+03
59	1.2277+03	1.2270+03	1.2328+03	1.2305+03	1.1804+03	1.1754+03
60	1.2277+03	1.2270+03	1.2328+03	1.2306+03	1.1804+03	1.1753+03

# CONDENSING DATA REDUCTION

	181	183	185	187	189	191
	TC1C	TC2C	TC3C	TC4C	TC5C	TC6C
61	1.2286+03	1.2279+03	1.2319+03	1.2297+03	1.1878+03	1.1834+03
62	1.2283+03	1.2276+03	1.2318+03	1.2296+03	1.1877+03	1.1833+03
63	1.2284+03	1.2277+03	1.2318+03	1.2296+03	1.1877+03	1.1833+03
64	1.2145+03	1.2136+03	1.2180+03	1.2155+03	1.1766+03	1.1727+03
65	1.2147+03	1.2137+03	1.2180+03	1.2155+03	1.1770+03	1.1729+03
66	1.2147+03	1.2138+03	1.2182+03	1.2157+03	1.1771+03	1.1731+03
67	1.4079+03	1.4113+03	1.4176+03	1.4176+03	1.2455+03	1.2256+03
68	1.4083+03	1.4118+03	1.4184+03	1.4195+03	1.2445+03	1.2261+03
69	1.4079+03	1.4118+03	1.4187+03	1.4200+03	1.2470+03	1.2271+03
70	1.4318+03	1.4356+03	1.4371+03	1.4387+03	1.2773+03	1.2592+03
71	1.4282+03	1.4321+03	1.4354+03	1.4369+03	1.2774+03	1.2585+03
72	1.4267+03	1.4305+03	1.4330+03	1.4350+03	1.2770+03	1.2582+03

# CONDENSING DATA REDUCTION

	193	195	197	199	201	203
	TC7C	TC8C	TC9C	TC10C	TC11C	TC12C
1	1.1479+03	1.1267+03	1.1266+03	1.1277+03	1.1872+03	1.1900+03
2	1.1479+03	1.1267+03	1.1267+03	1.1278+03	1.1873+03	1.1902+03
3	1.1481+03	1.1269+03	1.1268+03	1.1277+03	1.1874+03	1.1902+03
4	1.2350+03	1.2120+03	1.2117+03	1.2128+03	1.2792+03	1.2807+03
5	1.2349+03	1.2121+03	1.2118+03	1.2130+03	1.2793+03	1.2809+03
6	1.2349+03	1.2119+03	1.2117+03	1.2128+03	1.2790+03	1.2807+03
7	1.3248+03	1.2970+03	1.2965+03	1.2980+03	1.3819+03	1.3824+03
8	1.3247+03	1.2968+03	1.2965+03	1.2979+03	1.3819+03	1.3825+03
9	1.3248+03	1.2970+03	1.2965+03	1.2978+03	1.3816+03	1.3821+03
10	1.2287+03	1.1994+03	1.1987+03	1.2001+03	1.2842+03	1.2854+03
11	1.2285+03	1.1993+03	1.1987+03	1.2002+03	1.2842+03	1.2855+03
12	1.2285+03	1.1993+03	1.1988+03	1.2003+03	1.2842+03	1.2855+03
13	1.1296+03	1.0981+03	1.0974+03	1.0991+03	1.1864+03	1.1885+03
14	1.1298+03	1.0982+03	1.0976+03	1.0993+03	1.1865+03	1.1886+03
15	1.1299+03	1.0982+03	1.0976+03	1.0992+03	1.1865+03	1.1886+03
16	1.1126+03	1.0708+03	1.0697+03	1.0725+03	1.1819+03	1.1843+03
17	1.1121+03	1.0711+03	1.0698+03	1.0726+03	1.1813+03	1.1838+03
18	1.1124+03	1.0709+03	1.0697+03	1.0726+03	1.1817+03	1.1842+03
19	1.2054+03	1.1650+03	1.1637+03	1.1663+03	1.2744+03	1.2755+03
20	1.2053+03	1.1652+03	1.1640+03	1.1666+03	1.2746+03	1.2757+03
21	1.2053+03	1.1649+03	1.1637+03	1.1663+03	1.2741+03	1.2751+03
22	1.3358+03	1.2992+03	1.2981+03	1.3002+03	1.4012+03	1.4008+03
23	1.3358+03	1.2991+03	1.2981+03	1.3002+03	1.4013+03	1.4009+03
24	1.3358+03	1.2994+03	1.2982+03	1.3002+03	1.4014+03	1.4011+03
25	1.2860+03	1.2389+03	1.2374+03	1.2402+03	1.3708+03	1.3704+03
26	1.2861+03	1.2390+03	1.2374+03	1.2401+03	1.3707+03	1.3704+03
27	1.2863+03	1.2389+03	1.2373+03	1.2401+03	1.3706+03	1.3702+03
28	1.1574+03	1.1076+03	1.1061+03	1.1093+03	1.2444+03	1.2455+03
29	1.1577+03	1.1077+03	1.1061+03	1.1095+03	1.2447+03	1.2457+03
30	1.1575+03	1.1076+03	1.1059+03	1.1094+03	1.2451+03	1.2461+03

# CONDENSING DATA REDUCTION

	193	195	197	199	201	203
	TC7C	TC8C	TC9C	TC10C	TC11C	TC12C
31	1.0784+03	1.0278+03	1.0253+03	1.0291+03	1.1661+03	1.1685+03
32	1.0784+03	1.0280+03	1.0254+03	1.0292+03	1.1668+03	1.1692+03
33	1.0790+03	1.0282+03	1.0257+03	1.0295+03	1.1668+03	1.1690+03
34	1.1572+03	1.0962+03	1.0942+03	1.0980+03	1.2651+03	1.2659+03
35	1.1571+03	1.0964+03	1.0943+03	1.0981+03	1.2643+03	1.2652+03
36	1.1572+03	1.0965+03	1.0942+03	1.0982+03	1.2648+03	1.2653+03
37	1.2689+03	1.2112+03	1.2092+03	1.2124+03	1.3722+03	1.3714+03
38	1.2689+03	1.2111+03	1.2090+03	1.2122+03	1.3724+03	1.3716+03
39	1.2692+03	1.2110+03	1.2091+03	1.2121+03	1.3723+03	1.3714+03
40	1.2505+03	1.1848+03	1.1828+03	1.1862+03	1.3673+03	1.3664+03
41	1.2508+03	1.1852+03	1.1831+03	1.1866+03	1.3672+03	1.3663+03
42	1.2512+03	1.1853+03	1.1835+03	1.1866+03	1.3668+03	1.3658+03
43	1.1919+03	1.1241+03	1.1224+03	1.1257+03	1.3107+03	1.3100+03
44	1.1916+03	1.1243+03	1.1225+03	1.1259+03	1.3093+03	1.3087+03
45	1.1916+03	1.1244+03	1.1226+03	1.1260+03	1.3095+03	1.3090+03
46	1.1275+03	1.0660+03	1.0641+03	1.0672+03	1.2371+03	1.2378+03
47	1.1274+03	1.0653+03	1.0637+03	1.0667+03	1.2370+03	1.2376+03
48	1.1275+03	1.0662+03	1.0644+03	1.0676+03	1.2364+03	1.2371+03
49	1.1577+03	1.1158+03	1.1141+03	1.1163+03	1.2328+03	1.2334+03
50	1.1578+03	1.1157+03	1.1142+03	1.1163+03	1.2329+03	1.2335+03
51	1.1579+03	1.1159+03	1.1143+03	1.1165+03	1.2327+03	1.2332+03
52	1.1597+03	1.1246+03	1.1234+03	1.1250+03	1.2220+03	1.2231+03
53	1.1592+03	1.1246+03	1.1234+03	1.1250+03	1.2214+03	1.2225+03
54	1.1597+03	1.1246+03	1.1234+03	1.1251+03	1.2222+03	1.2233+03
55	1.1669+03	1.1396+03	1.1386+03	1.1398+03	1.2169+03	1.2182+03
56	1.1669+03	1.1398+03	1.1388+03	1.1400+03	1.2169+03	1.2182+03
57	1.1669+03	1.1397+03	1.1387+03	1.1399+03	1.2169+03	1.2182+03
58	1.1753+03	1.1536+03	1.1528+03	1.1538+03	1.2168+03	1.2181+03
59	1.1754+03	1.1537+03	1.1529+03	1.1538+03	1.2168+03	1.2182+03
60	1.1755+03	1.1538+03	1.1529+03	1.1539+03	1.2169+03	1.2182+03



# CONDENSING DATA REDUCTION

	193	195	197	199	201	203
	TC7C	TC8C	TC9C	TC10C	TC11C	TC12C
61	1.1833+03	1.1656+03	1.1648+03	1.1656+03	1.2186+03	1.2199+03
62	1.1832+03	1.1656+03	1.1649+03	1.1656+03	1.2186+03	1.2199+03
63	1.1832+03	1.1656+03	1.1649+03	1.1656+03	1.2185+03	1.2199+03
64	1.1725+03	1.1566+03	1.1559+03	1.1566+03	1.2053+03	1.2068+03
65	1.1728+03	1.1568+03	1.1561+03	1.1569+03	1.2054+03	1.2069+03
66	1.1730+03	1.1574+03	1.1566+03	1.1573+03	1.2055+03	1.2070+03
67	1.2261+03	1.1458+03	1.1436+03	1.1476+03	1.3638+03	1.3613+03
68	1.2257+03	1.1464+03	1.1442+03	1.1481+03	1.3719+03	1.3708+03
69	1.2274+03	1.1456+03	1.1433+03	1.1471+03	1.3730+03	1.3721+03
70	1.2586+03	1.1809+03	1.1785+03	1.1824+03	1.3972+03	1.3957+03
71	1.2584+03	1.1803+03	1.1782+03	1.1822+03	1.3943+03	1.3931+03
72	1.2583+03	1.1809+03	1.1783+03	1.1824+03	1.3939+03	1.3928+03

# CONDENSING DATA REDUCTION

	205	207	209	211	213	215
	TC13C	TC14C	TC15C	TC16C	TC17C	TC18C
1	1.1798+03	1.1610+03	1.1558+03	1.1807+03	1.1889+03	1.1713+03
2	1.1799+03	1.1611+03	1.1560+03	1.1809+03	1.1889+03	1.1713+03
3	1.1799+03	1.1608+03	1.1559+03	1.1806+03	1.1888+03	1.1713+03
4	1.2697+03	1.2490+03	1.2450+03	1.2715+03	1.2785+03	1.2608+03
5	1.2698+03	1.2492+03	1.2449+03	1.2714+03	1.2784+03	1.2607+03
6	1.2696+03	1.2490+03	1.2450+03	1.2715+03	1.2784+03	1.2607+03
7	1.3687+03	1.3428+03	1.3385+03	1.3713+03	1.3787+03	1.3577+03
8	1.3687+03	1.3428+03	1.3386+03	1.3716+03	1.3790+03	1.3579+03
9	1.3683+03	1.3426+03	1.3383+03	1.3712+03	1.3787+03	1.3577+03
10	1.2716+03	1.2457+03	1.2403+03	1.2736+03	1.2827+03	1.2612+03
11	1.2716+03	1.2460+03	1.2404+03	1.2737+03	1.2827+03	1.2613+03
12	1.2717+03	1.2461+03	1.2406+03	1.2738+03	1.2828+03	1.2613+03
13	1.1738+03	1.1473+03	1.1402+03	1.1774+03	1.1886+03	1.1640+03
14	1.1740+03	1.1475+03	1.1404+03	1.1774+03	1.1887+03	1.1640+03
15	1.1739+03	1.1474+03	1.1404+03	1.1775+03	1.1886+03	1.1640+03
16	1.1663+03	1.1333+03	1.1249+03	1.1707+03	1.1840+03	1.1534+03
17	1.1658+03	1.1330+03	1.1246+03	1.1701+03	1.1835+03	1.1531+03
18	1.1662+03	1.1334+03	1.1249+03	1.1704+03	1.1838+03	1.1533+03
19	1.2583+03	1.2263+03	1.2190+03	1.2610+03	1.2723+03	1.2447+03
20	1.2584+03	1.2262+03	1.2189+03	1.2609+03	1.2722+03	1.2446+03
21	1.2583+03	1.2262+03	1.2191+03	1.2605+03	1.2718+03	1.2444+03
22	1.3855+03	1.3558+03	1.3508+03	1.3881+03	1.3970+03	1.3732+03
23	1.3856+03	1.3560+03	1.3508+03	1.3883+03	1.3971+03	1.3733+03
24	1.3857+03	1.3560+03	1.3508+03	1.3881+03	1.3971+03	1.3733+03
25	1.3495+03	1.3104+03	1.3040+03	1.3532+03	1.3646+03	1.3333+03
26	1.3494+03	1.3104+03	1.3039+03	1.3529+03	1.3644+03	1.3331+03
27	1.3493+03	1.3102+03	1.3037+03	1.3527+03	1.3641+03	1.3330+03
28	1.2230+03	1.1815+03	1.1740+03	1.2274+03	1.2416+03	1.2065+03
29	1.2232+03	1.1815+03	1.1741+03	1.2278+03	1.2420+03	1.2066+03
30	1.2236+03	1.1818+03	1.1743+03	1.2282+03	1.2425+03	1.2071+03

# CONDENSING DATA REDUCTION

	205	207	209	211	213	215
	TC13C	TC14C	TC15C	TC16C	TC17C	TC18C
31	1.1438+03	1.1006+03	1.0933+03	1.1475+03	1.1630+03	1.1257+03
32	1.1445+03	1.1014+03	1.0940+03	1.1482+03	1.1639+03	1.1265+03
33	1.1445+03	1.1013+03	1.0941+03	1.1478+03	1.1633+03	1.1260+03
34	1.2373+03	1.1855+03	1.1769+03	1.2416+03	1.2578+03	1.2160+03
35	1.2365+03	1.1851+03	1.1767+03	1.2414+03	1.2576+03	1.2159+03
36	1.2371+03	1.1856+03	1.1771+03	1.2414+03	1.2576+03	1.2158+03
37	1.3453+03	1.2973+03	1.2899+03	1.3511+03	1.3642+03	1.3261+03
38	1.3453+03	1.2971+03	1.2897+03	1.3511+03	1.3644+03	1.3263+03
39	1.3454+03	1.2971+03	1.2898+03	1.3508+03	1.3640+03	1.3260+03
40	1.3364+03	1.2816+03	1.2737+03	1.3431+03	1.3579+03	1.3148+03
41	1.3365+03	1.2815+03	1.2742+03	1.3432+03	1.3580+03	1.3149+03
42	1.3363+03	1.2823+03	1.2737+03	1.3425+03	1.3574+03	1.3144+03
43	1.2796+03	1.2228+03	1.2146+03	1.2856+03	1.3015+03	1.2568+03
44	1.2784+03	1.2225+03	1.2137+03	1.2846+03	1.3007+03	1.2562+03
45	1.2782+03	1.2217+03	1.2136+03	1.2850+03	1.3010+03	1.2563+03
46	1.2080+03	1.1549+03	1.1470+03	1.2134+03	1.2301+03	1.1867+03
47	1.2082+03	1.1550+03	1.1472+03	1.2134+03	1.2300+03	1.1867+03
48	1.2077+03	1.1549+03	1.1472+03	1.2134+03	1.2299+03	1.1867+03
49	1.2124+03	1.1773+03	1.1713+03	1.2182+03	1.2310+03	1.2010+03
50	1.2124+03	1.1773+03	1.1712+03	1.2185+03	1.2313+03	1.2011+03
51	1.2124+03	1.1773+03	1.1712+03	1.2182+03	1.2311+03	1.2010+03
52	1.2059+03	1.1758+03	1.1715+03	1.2116+03	1.2217+03	1.1956+03
53	1.2053+03	1.1752+03	1.1712+03	1.2113+03	1.2213+03	1.1953+03
54	1.2060+03	1.1759+03	1.1717+03	1.2122+03	1.2223+03	1.1959+03
55	1.2041+03	1.1802+03	1.1768+03	1.2092+03	1.2174+03	1.1965+03
56	1.2042+03	1.1803+03	1.1768+03	1.2092+03	1.2174+03	1.1966+03
57	1.2041+03	1.1802+03	1.1768+03	1.2092+03	1.2174+03	1.1965+03
58	1.2065+03	1.1868+03	1.1838+03	1.2106+03	1.2173+03	1.2003+03
59	1.2065+03	1.1868+03	1.1839+03	1.2106+03	1.2173+03	1.2004+03
60	1.2066+03	1.1869+03	1.1840+03	1.2107+03	1.2174+03	1.2004+03

# CONDENSING DATA REDUCTION

	205	207	209	211	213	215
	TC13C	TC14C	TC15C	TC16C	TC17C	TC18C
61	1.2101+03	1.1935+03	1.1908+03	1.2135+03	1.2191+03	1.2051+03
62	1.2100+03	1.1935+03	1.1908+03	1.2135+03	1.2191+03	1.2050+03
63	1.2100+03	1.1934+03	1.1907+03	1.2135+03	1.2190+03	1.2051+03
64	1.1976+03	1.1821+03	1.1796+03	1.2009+03	1.2062+03	1.1932+03
65	1.1977+03	1.1824+03	1.1797+03	1.2010+03	1.2063+03	1.1933+03
66	1.1979+03	1.1826+03	1.1800+03	1.2012+03	1.2064+03	1.1935+03
67	1.3286+03	1.2641+03	1.2532+03	1.3322+03	1.3484+03	1.3006+03
68	1.3330+03	1.2655+03	1.2555+03	1.3443+03	1.3621+03	1.3080+03
69	1.3340+03	1.2663+03	1.2555+03	1.3454+03	1.3637+03	1.3088+03
70	1.3602+03	1.2962+03	1.2859+03	1.3689+03	1.3857+03	1.3347+03
71	1.3579+03	1.2956+03	1.2844+03	1.3672+03	1.3841+03	1.3331+03
72	1.3573+03	1.2942+03	1.2841+03	1.3668+03	1.3836+03	1.3329+03

# CONDENSING DATA REDUCTION

	217	219	221	223	226	229
	TC19C	TC20C	TKICC	TKOC	TNAO	TNAI
1	1.1479+03	1.1454+03	1.1978+03	1.2021+03	1.1505+03	1.1270+03
2	1.1478+03	1.1452+03	1.1977+03	1.2020+03	1.1505+03	1.1271+03
3	1.1478+03	1.1453+03	1.1979+03	1.2023+03	1.1507+03	1.1271+03
4	1.2348+03	1.2325+03	1.2917+03	1.2430+03	1.2380+03	1.2122+03
5	1.2346+03	1.2324+03	1.2917+03	1.2448+03	1.2381+03	1.2123+03
6	1.2349+03	1.2326+03	1.2916+03	1.2503+03	1.2378+03	1.2121+03
7	1.3231+03	1.3217+03	1.3984+03	1.3051+03	1.3284+03	1.2972+03
8	1.3230+03	1.3217+03	1.3983+03	1.3057+03	1.3284+03	1.2971+03
9	1.3233+03	1.3218+03	1.3980+03	1.3059+03	1.3284+03	1.2971+03
10	1.2269+03	1.2245+03	1.2994+03	1.3019+03	1.2319+03	1.1994+03
11	1.2270+03	1.2248+03	1.2995+03	1.3018+03	1.2318+03	1.1994+03
12	1.2269+03	1.2247+03	1.2994+03	1.3017+03	1.2317+03	1.1995+03
13	1.1277+03	1.1248+03	1.1996+03	1.2088+03	1.1329+03	1.0982+03
14	1.1276+03	1.1247+03	1.1996+03	1.2088+03	1.1331+03	1.0983+03
15	1.1276+03	1.1247+03	1.1996+03	1.2087+03	1.1331+03	1.0983+03
16	1.1074+03	1.1043+03	1.2001+03	1.2108+03	1.1164+03	1.0710+03
17	1.1075+03	1.1044+03	1.2000+03	1.2071+03	1.1161+03	1.0712+03
18	1.1075+03	1.1045+03	1.2004+03	1.2104+03	1.1164+03	1.0711+03
19	1.2008+03	1.1980+03	1.2930+03	1.2973+03	1.2095+03	1.1650+03
20	1.2008+03	1.1980+03	1.2928+03	1.2973+03	1.2094+03	1.1652+03
21	1.2006+03	1.1977+03	1.2931+03	1.2970+03	1.2094+03	1.1649+03
22	1.3327+03	1.3305+03	1.4200+03	1.4206+03	1.3399+03	1.2992+03
23	1.3328+03	1.3303+03	1.4199+03	1.4206+03	1.3399+03	1.2991+03
24	1.3325+03	1.3303+03	1.4199+03	1.4207+03	1.3400+03	1.2993+03
25	1.2802+03	1.2775+03	1.3947+03	1.3955+03	1.2906+03	1.2388+03
26	1.2800+03	1.2775+03	1.3947+03	1.3956+03	1.2903+03	1.2388+03
27	1.2799+03	1.2775+03	1.3947+03	1.3955+03	1.2906+03	1.2388+03
28	1.1500+03	1.1473+03	1.2664+03	1.2737+03	1.1617+03	1.1077+03
29	1.1500+03	1.1473+03	1.2667+03	1.2740+03	1.1619+03	1.1078+03
30	1.1501+03	1.1475+03	1.2667+03	1.2745+03	1.1616+03	1.1077+03

# CONDENSING DATA REDUCTION

	217	219	221	223	226	229
	TC19C	TC20C	TKICC	TKOC	TNAO	TNAI
31	1.0693+03	1.0668+03	1.1986+03	1.1980+03	1.0815+03	1.0274+03
32	1.0696+03	1.0674+03	1.1980+03	1.1989+03	1.0816+03	1.0275+03
33	1.0695+03	1.0674+03	1.1980+03	1.1990+03	1.0822+03	1.0278+03
34	1.1468+03	1.1440+03	1.2922+03	1.2975+03	1.1619+03	1.0961+03
35	1.1472+03	1.1439+03	1.2921+03	1.2971+03	1.1617+03	1.0963+03
36	1.1470+03	1.1439+03	1.2925+03	1.2975+03	1.1619+03	1.0963+03
37	1.2601+03	1.2579+03	1.4016+03	1.4034+03	1.2741+03	1.2109+03
38	1.2599+03	1.2582+03	1.4020+03	1.4037+03	1.2742+03	1.2108+03
39	1.2601+03	1.2579+03	1.4020+03	1.4039+03	1.2741+03	1.2107+03
40	1.2401+03	1.2374+03	1.3997+03	1.4015+03	1.2561+03	1.1846+03
41	1.2406+03	1.2376+03	1.3995+03	1.4013+03	1.2561+03	1.1850+03
42	1.2401+03	1.2374+03	1.3997+03	1.4015+03	1.2564+03	1.1851+03
43	1.1806+03	1.1770+03	1.3427+03	1.3470+03	1.1972+03	1.1241+03
44	1.1801+03	1.1771+03	1.3416+03	1.3463+03	1.1968+03	1.1243+03
45	1.1802+03	1.1773+03	1.3408+03	1.3458+03	1.1970+03	1.1243+03
46	1.1163+03	1.1135+03	1.2632+03	1.2714+03	1.1318+03	1.0658+03
47	1.1163+03	1.1134+03	1.2631+03	1.2716+03	1.1318+03	1.0653+03
48	1.1165+03	1.1137+03	1.2634+03	1.2712+03	1.1318+03	1.0661+03
49	1.1516+03	1.1482+03	1.2503+03	1.2594+03	1.1608+03	1.1154+03
50	1.1515+03	1.1481+03	1.2505+03	1.2595+03	1.1608+03	1.1154+03
51	1.1516+03	1.1482+03	1.2504+03	1.2594+03	1.1610+03	1.1156+03
52	1.1546+03	1.1531+03	1.2383+03	1.2454+03	1.1620+03	1.1243+03
53	1.1543+03	1.1528+03	1.2378+03	1.2445+03	1.1616+03	1.1243+03
54	1.1547+03	1.1532+03	1.2381+03	1.2453+03	1.1619+03	1.1244+03
55	1.1638+03	1.1626+03	1.2296+03	1.2349+03	1.1688+03	1.1393+03
56	1.1640+03	1.1626+03	1.2298+03	1.2351+03	1.1689+03	1.1395+03
57	1.1639+03	1.1626+03	1.2296+03	1.2349+03	1.1688+03	1.1394+03
58	1.1736+03	1.1727+03	1.2278+03	1.2315+03	1.1769+03	1.1534+03
59	1.1738+03	1.1727+03	1.2280+03	1.2316+03	1.1771+03	1.1534+03
60	1.1737+03	1.1728+03	1.2280+03	1.2317+03	1.1771+03	1.1535+03

CONDENSING DATA REDUCTION

	217	219	221	223	226	229
	TC19C	TC20C	TKICC	TKOC	TNAO	TNAI
61	1.1827+03	1.1818+03	1.2286+03	1.2308+03	1.1848+03	1.1653+03
62	1.1826+03	1.1818+03	1.2284+03	1.2307+03	1.1847+03	1.1653+03
63	1.1827+03	1.1817+03	1.2284+03	1.2307+03	1.1848+03	1.1653+03
64	1.1726+03	1.1714+03	1.2144+03	1.2167+03	1.1739+03	1.1564+03
65	1.1726+03	1.1717+03	1.2146+03	1.2168+03	1.1742+03	1.1566+03
66	1.1730+03	1.1722+03	1.2146+03	1.2169+03	1.1744+03	1.1571+03
67	1.2127+03	1.2091+03	1.4118+03	1.4176+03	1.2324+03	1.1457+03
68	1.2145+03	1.2116+03	1.4122+03	1.4189+03	1.2321+03	1.1462+03
69	1.2142+03	1.2114+03	1.4121+03	1.4193+03	1.2338+03	1.1453+03
70	1.2457+03	1.2435+03	1.4353+03	1.4379+03	1.2650+03	1.1806+03
71	1.2450+03	1.2424+03	1.4318+03	1.4361+03	1.2648+03	1.1802+03
72	1.2448+03	1.2424+03	1.4303+03	1.4340+03	1.2645+03	1.1805+03

# CONDENSING DATA REDUCTION

	230	235	237	238	240	243
	DTNA	WNA	TNAM	CPNA	QNA	DTQL
1	2.3498+01	4.7695+03	1.1387+03	3.0000-01	3.3622+04	1.0597+03
2	2.3455+01	4.7695+03	1.1388+03	3.0000-01	3.3561+04	1.0598+03
3	2.3527+01	4.7695+03	1.1389+03	3.0000-01	3.3664+04	1.0599+03
4	2.5879+01	4.6131+03	1.2251+03	3.0013-01	3.5829+04	1.1470+03
5	2.5779+01	4.6131+03	1.2252+03	3.0013-01	3.5691+04	1.1466+03
6	2.5679+01	4.6131+03	1.2250+03	3.0012-01	3.5552+04	1.1468+03
7	3.1170+01	4.6254+03	1.3128+03	3.0069-01	4.3352+04	1.2347+03
8	3.1313+01	4.6254+03	1.3127+03	3.0069-01	4.3551+04	1.2346+03
9	3.1298+01	4.6254+03	1.3128+03	3.0069-01	4.3531+04	1.2347+03
10	3.2543+01	4.7176+03	1.2157+03	3.0008-01	4.6069+04	1.1313+03
11	3.2442+01	4.7176+03	1.2156+03	3.0008-01	4.5926+04	1.1313+03
12	3.2242+01	4.7176+03	1.2156+03	3.0008-01	4.5643+04	1.1312+03
13	3.4683+01	4.6515+03	1.1155+03	3.0000-01	4.8398+04	1.0307+03
14	3.4798+01	4.6515+03	1.1157+03	3.0000-01	4.8560+04	1.0314+03
15	3.4770+01	4.6515+03	1.1157+03	3.0000-01	4.8520+04	1.0313+03
16	4.5372+01	4.4159+03	1.0937+03	3.0005-01	6.0117+04	1.0111+03
17	4.4977+01	4.4159+03	1.0937+03	3.0005-01	5.9594+04	1.0111+03
18	4.5301+01	4.4159+03	1.0937+03	3.0005-01	6.0024+04	1.0116+03
19	4.4528+01	4.4353+03	1.1872+03	3.0000-01	5.9249+04	1.1020+03
20	4.4114+01	4.4353+03	1.1873+03	3.0000-01	5.8699+04	1.1020+03
21	4.4442+01	4.4353+03	1.1872+03	3.0000-01	5.9135+04	1.1019+03
22	4.0776+01	4.3160+03	1.3195+03	3.0079-01	5.2937+04	1.2294+03
23	4.0733+01	4.3160+03	1.3195+03	3.0079-01	5.2881+04	1.2289+03
24	4.0719+01	4.3160+03	1.3196+03	3.0079-01	5.2863+04	1.2294+03
25	5.1790+01	4.6033+03	1.2647+03	3.0032-01	7.1599+04	1.1768+03
26	5.1447+01	4.6033+03	1.2646+03	3.0032-01	7.1125+04	1.1766+03
27	5.1876+01	4.6033+03	1.2647+03	3.0032-01	7.1718+04	1.1763+03
28	5.4055+01	4.6114+03	1.1347+03	3.0000-01	7.4780+04	1.0508+03
29	5.4113+01	4.6114+03	1.1348+03	3.0000-01	7.4860+04	1.0509+03
30	5.3955+01	4.6114+03	1.1346+03	3.0000-01	7.4642+04	1.0512+03



# CONDENSING DATA REDUCTION

	230	235	237	238	240	243
	DTNA	WNA	TNAM	CPNA	QNA	DTQL
31	5.4123+01	4.6244+03	1.0545+03	3.0036-01	7.5177+04	9.6295+02
32	5.4108+01	4.6244+03	1.0546+03	3.0036-01	7.5156+04	9.6307+02
33	5.4376+01	4.6244+03	1.0550+03	3.0036-01	7.5527+04	9.6345+02
34	6.5788+01	4.6258+03	1.1290+03	3.0000-01	9.1296+04	1.0460+03
35	6.5420+01	4.6258+03	1.1290+03	3.0000-01	9.0786+04	1.0464+03
36	6.5620+01	4.6258+03	1.1291+03	3.0000-01	9.1064+04	1.0461+03
37	6.3163+01	4.5665+03	1.2425+03	3.0021-01	8.6591+04	1.1599+03
38	6.3391+01	4.5665+03	1.2425+03	3.0021-01	8.6904+04	1.1599+03
39	6.3349+01	4.5665+03	1.2424+03	3.0021-01	8.6846+04	1.1598+03
40	7.1436+01	4.5676+03	1.2203+03	3.0010-01	9.7922+04	1.1386+03
41	7.1153+01	4.5676+03	1.2205+03	3.0010-01	9.7534+04	1.1389+03
42	7.1269+01	4.5676+03	1.2207+03	3.0010-01	9.7693+04	1.1391+03
43	7.3139+01	4.5693+03	1.1606+03	3.0000-01	1.0026+05	1.0821+03
44	7.2512+01	4.5693+03	1.1605+03	3.0000-01	9.9398+04	1.0819+03
45	7.2656+01	4.5693+03	1.1607+03	3.0000-01	9.9595+04	1.0821+03
46	6.6008+01	4.6431+03	1.0988+03	3.0001-01	9.1947+04	1.9411+02
47	6.6540+01	4.6431+03	1.0985+03	3.0001-01	9.2688+04	1.9387+02
48	6.5742+01	4.6431+03	1.0989+03	3.0001-01	9.1576+04	1.9428+02
49	4.5359+01	4.6942+03	1.1381+03	3.0000-01	6.3876+04	2.3342+02
50	4.5388+01	4.6942+03	1.1381+03	3.0000-01	6.3917+04	2.3345+02
51	4.5461+01	4.6942+03	1.1383+03	3.0000-01	6.4020+04	2.3363+02
52	3.7722+01	4.6776+03	1.1432+03	3.0000-01	5.2935+04	2.3852+02
53	3.7236+01	4.6776+03	1.1429+03	3.0000-01	5.2253+04	2.3828+02
54	3.7565+01	4.6776+03	1.1431+03	3.0000-01	5.2715+04	2.3847+02
55	2.9449+01	4.6791+03	1.1541+03	3.0000-01	4.1338+04	2.4939+02
56	2.9323+01	4.6791+03	1.1542+03	3.0000-01	4.1162+04	2.4953+02
57	2.9308+01	4.6791+03	1.1541+03	3.0000-01	4.1140+04	2.4944+02
58	2.3543+01	4.6799+03	1.1652+03	3.0000-01	3.3054+04	2.6050+02
59	2.3644+01	4.6799+03	1.1653+03	3.0000-01	3.3195+04	2.6061+02
60	2.3530+01	4.6799+03	1.1653+03	3.0000-01	3.3036+04	2.6064+02

# CONDENSING DATA REDUCTION

	230	235	237	238	240	243
	DTNA	WNA	TNAM	CPNA	QNA	DTQL
61	1.9484+01	4.6834+03	1.1751+03	3.0000-01	2.7376+04	2.7040+02
62	1.9398+01	4.6834+03	1.1750+03	3.0000-01	2.7255+04	2.7038+02
63	1.9413+01	4.6834+03	1.1750+03	3.0000-01	2.7275+04	2.7038+02
64	1.7543+01	4.6988+03	1.1652+03	3.0000-01	2.4729+04	2.6051+02
65	1.7630+01	4.6988+03	1.1654+03	3.0000-01	2.4853+04	2.6076+02
66	1.7304+01	4.6988+03	1.1657+03	3.0000-01	2.4393+04	2.6109+02
67	8.6698+01	4.6445+03	1.1890+03	3.0000-01	1.2080+05	7.3367+01
68	8.5888+01	4.6445+03	1.1892+03	3.0000-01	1.1967+05	7.3484+01
69	8.8499+01	4.6445+03	1.1896+03	3.0000-01	1.2331+05	7.3901+01
70	8.4440+01	4.5836+03	1.2228+03	3.0011-01	1.1616+05	1.0714+02
71	8.4524+01	4.5836+03	1.2225+03	3.0011-01	1.1627+05	1.0683+02
72	8.3982+01	4.5836+03	1.2225+03	3.0011-01	1.1553+05	1.0684+02

# CONDENSING DATA REDUCTION

	246	247	251	306	317	319
	QC	Q/AA	WK	TWI T	Q/A T	TWO T
1	3.6168+04	7.3453+04	4.1734+01	1.1951+03	6.8350+04	1.1438+03
2	3.6108+04	7.3331+04	4.1664+01	1.1953+03	6.8483+04	1.1439+03
3	3.6212+04	7.3541+04	4.1785+01	1.1954+03	6.8911+04	1.1437+03
4	3.8723+04	7.8641+04	4.5167+01	1.2868+03	7.6247+04	1.2308+03
5	3.8583+04	7.8356+04	4.5010+01	1.2870+03	7.6299+04	1.2309+03
6	3.8444+04	7.8076+04	4.4868+01	1.2866+03	7.5899+04	1.2309+03
7	4.6611+04	9.4661+04	5.5157+01	1.3915+03	9.6579+04	1.3221+03
8	4.6809+04	9.5062+04	5.5394+01	1.3915+03	9.6533+04	1.3221+03
9	4.6789+04	9.5023+04	5.5371+01	1.3911+03	9.6381+04	1.3218+03
10	4.8899+04	9.9307+04	5.7344+01	1.2948+03	9.4060+04	1.2257+03
11	4.8756+04	9.9017+04	5.7177+01	1.2947+03	9.3655+04	1.2259+03
12	4.8473+04	9.8442+04	5.6844+01	1.2948+03	9.3529+04	1.2261+03
13	5.0834+04	1.0324+05	5.8696+01	1.1987+03	9.4783+04	1.1275+03
14	5.0998+04	1.0357+05	5.8885+01	1.1988+03	9.4623+04	1.1277+03
15	5.0958+04	1.0349+05	5.8839+01	1.1989+03	9.4788+04	1.1277+03
16	6.2478+04	1.2688+05	7.2156+01	1.1982+03	1.1483+05	1.1118+03
17	6.1955+04	1.2582+05	7.1530+01	1.1976+03	1.1451+05	1.1114+03
18	6.2387+04	1.2670+05	7.2050+01	1.1980+03	1.1443+05	1.1118+03
19	6.1961+04	1.2584+05	7.2598+01	1.2888+03	1.1470+05	1.2043+03
20	6.1411+04	1.2472+05	7.1952+01	1.2891+03	1.1535+05	1.2041+03
21	6.1847+04	1.2560+05	7.2463+01	1.2884+03	1.1411+05	1.2043+03
22	5.6173+04	1.1408+05	6.7309+01	1.4124+03	1.0982+05	1.3338+03
23	5.6114+04	1.1396+05	6.7239+01	1.4125+03	1.0991+05	1.3339+03
24	5.6099+04	1.1393+05	6.7221+01	1.4127+03	1.1015+05	1.3338+03
25	7.4615+04	1.5153+05	8.8982+01	1.3877+03	1.4069+05	1.2861+03
26	7.4140+04	1.5057+05	8.8416+01	1.3877+03	1.4068+05	1.2861+03
27	7.4731+04	1.5177+05	8.9121+01	1.3876+03	1.4081+05	1.2859+03
28	7.7292+04	1.5697+05	9.0193+01	1.2643+03	1.4315+05	1.1579+03
29	7.7373+04	1.5713+05	9.0292+01	1.2646+03	1.4345+05	1.1580+03
30	7.7156+04	1.5669+05	9.0042+01	1.2651+03	1.4394+05	1.1581+03

# CONDENSING DATA REDUCTION

	246	247	251	306	317	319
	QC	Q/AA	WK	TWI T	Q/A T	TWO T
31	7.7359+04	1.5711+05	8.9242+01	1.1881+03	1.4586+05	1.0777+03
32	7.7339+04	1.5706+05	8.9221+01	1.1888+03	1.4594+05	1.0784+03
33	7.7711+04	1.5782+05	8.9651+01	1.1887+03	1.4577+05	1.0784+03
34	9.3790+04	1.9048+05	1.0988+02	1.2908+03	1.7783+05	1.1590+03
35	9.3281+04	1.8944+05	1.0928+02	1.2898+03	1.7692+05	1.1587+03
36	9.3558+04	1.9001+05	1.0962+02	1.2902+03	1.7671+05	1.1592+03
37	8.9537+04	1.8184+05	1.0692+02	1.3942+03	1.7081+05	1.2707+03
38	8.9850+04	1.8247+05	1.0730+02	1.3945+03	1.7157+05	1.2704+03
39	8.9792+04	1.8236+05	1.0724+02	1.3943+03	1.7118+05	1.2705+03
40	1.0078+05	2.0467+05	1.2031+02	1.3932+03	1.9278+05	1.2535+03
41	1.0039+05	2.0389+05	1.1984+02	1.3930+03	1.9222+05	1.2537+03
42	1.0055+05	2.0421+05	1.2004+02	1.3923+03	1.9092+05	1.2539+03
43	1.0289+05	2.0896+05	1.2161+02	1.3380+03	1.9475+05	1.1950+03
44	1.0203+05	2.0721+05	1.2057+02	1.3364+03	1.9320+05	1.1944+03
45	1.0223+05	2.0761+05	1.2079+02	1.3368+03	1.9452+05	1.1939+03
46	9.2112+04	1.8707+05	1.0744+02	1.2636+03	1.8072+05	1.1287+03
47	9.2852+04	1.8857+05	1.0830+02	1.2633+03	1.8011+05	1.1289+03
48	9.1741+04	1.8631+05	1.0701+02	1.2626+03	1.7906+05	1.1290+03
49	6.4098+04	1.3018+05	7.4615+01	1.2491+03	1.2584+05	1.1554+03
50	6.4139+04	1.3026+05	7.4664+01	1.2492+03	1.2600+05	1.1554+03
51	6.4242+04	1.3047+05	7.4783+01	1.2489+03	1.2553+05	1.1554+03
52	5.3165+04	1.0797+05	6.1759+01	1.2352+03	1.0591+05	1.1562+03
53	5.2482+04	1.0658+05	6.0959+01	1.2346+03	1.0575+05	1.1557+03
54	5.2944+04	1.0752+05	6.1501+01	1.2354+03	1.0611+05	1.1563+03
55	4.1585+04	8.4454+04	4.8233+01	1.2266+03	8.6327+04	1.1622+03
56	4.1409+04	8.4096+04	4.8030+01	1.2266+03	8.6163+04	1.1623+03
57	4.1387+04	8.4051+04	4.8003+01	1.2266+03	8.6327+04	1.1622+03
58	3.3319+04	6.7666+04	3.8629+01	1.2240+03	7.2561+04	1.1699+03
59	3.3461+04	6.7954+04	3.8794+01	1.2241+03	7.2683+04	1.1699+03
60	3.3301+04	6.7630+04	3.8609+01	1.2242+03	7.2661+04	1.1700+03

# CONDENSING DATA REDUCTION

	246	247	251	306	317	319
	QC	Q/AA	WK	TWI T	Q/A T	TWO T
61	2.7657+04	5.6168+04	3.2065+01	1.2241+03	6.2822+04	1.1773+03
62	2.7536+04	5.5922+04	3.1924+01	1.2240+03	6.2721+04	1.1773+03
63	2.7556+04	5.5963+04	3.1947+01	1.2240+03	6.2730+04	1.1773+03
64	2.4994+04	5.0760+04	2.8912+01	1.2102+03	5.8613+04	1.1665+03
65	2.5118+04	5.1012+04	2.9056+01	1.2104+03	5.8534+04	1.1666+03
66	2.4659+04	5.0078+04	2.8525+01	1.2104+03	5.8152+04	1.1670+03
67	1.2083+05	2.4540+05	1.4463+02	1.3946+03	2.2238+05	1.2329+03
68	1.1971+05	2.4311+05	1.4331+02	1.4053+03	2.3673+05	1.2335+03
69	1.2334+05	2.5050+05	1.4767+02	1.4068+03	2.3841+05	1.2338+03
70	1.1622+05	2.3603+05	1.3970+02	1.4284+03	2.2746+05	1.2644+03
71	1.1633+05	2.3626+05	1.3977+02	1.4250+03	2.2373+05	1.2636+03
72	1.1559+05	2.3475+05	1.3882+02	1.4248+03	2.2465+05	1.2627+03

# CONDENSING DATA REDUCTION

	324	326	354	365	367	372
	HCON T	NUC T	TWI B	Q/A B	TWO B	HCON B
1	-4.6108+04	-1.2943-01	1.1955+03	7.2451+04	1.1412+03	3.4481+04
2	-3.8299+04	-1.0751-01	1.1958+03	7.3007+04	1.1410+03	4.1188+04
3	-3.9274+04	-1.1025-01	1.1955+03	7.2508+04	1.1411+03	3.1652+04
4	-8.7739+03	-2.4989-02	1.2858+03	7.9005+04	1.2277+03	-2.1853+03
5	-8.9851+03	-2.5592-02	1.2857+03	7.9046+04	1.2275+03	-2.2827+03
6	-1.0346+04	-2.9472-02	1.2856+03	7.8604+04	1.2278+03	-2.5846+03
7	-6.4017+03	-1.8542-02	1.3888+03	1.0294+05	1.3148+03	-1.5066+03
8	-6.4167+03	-1.8586-02	1.3893+03	1.0367+05	1.3147+03	-1.5183+03
9	-6.4801+03	-1.8769-02	1.3887+03	1.0253+05	1.3150+03	-1.5153+03
10	-9.8935+04	-2.8255-01	1.2934+03	1.0204+05	1.2184+03	3.6315+04
11	-1.1448+05	-3.2695-01	1.2935+03	1.0182+05	1.2186+03	3.7262+04
12	-1.0037+05	-2.8666-01	1.2936+03	1.0216+05	1.2184+03	4.0904+04
13	-2.6202+04	-7.3565-02	1.2013+03	1.1017+05	1.1184+03	6.9538+04
14	-2.5217+04	-7.0801-02	1.2013+03	1.1042+05	1.1183+03	7.3910+04
15	-2.5278+04	-7.0971-02	1.2014+03	1.1043+05	1.1183+03	7.5488+04
16	-3.2555+04	-9.1397-02	1.2014+03	1.3949+05	1.0962+03	4.8969+04
17	-3.1693+04	-8.8974-02	1.2006+03	1.3832+05	1.0963+03	1.8928+05
18	-3.6918+04	-1.0365-01	1.2010+03	1.3884+05	1.0963+03	4.7804+04
19	-7.5043+04	-2.1407-01	1.2878+03	1.3222+05	1.1902+03	3.9209+04
20	-5.8725+04	-1.6752-01	1.2877+03	1.3216+05	1.1901+03	3.8968+04
21	-1.0971+05	-3.1296-01	1.2873+03	1.3183+05	1.1899+03	3.6169+04
22	1.7160+05	5.0081-01	1.4096+03	1.2072+05	1.3230+03	3.0602+04
23	2.4494+05	7.1485-01	1.4098+03	1.2117+05	1.3229+03	3.2900+04
24	4.2474+05	1.2396+00	1.4097+03	1.2128+05	1.3228+03	3.1834+04
25	-2.6889+06	-7.8031+00	1.3839+03	1.6022+05	1.2678+03	3.3521+04
26	-8.2027+06	-2.3804+01	1.3835+03	1.5985+05	1.2678+03	3.0940+04
27	2.4887+06	7.2221+00	1.3833+03	1.5958+05	1.2677+03	2.9808+04
28	-3.4391+04	-9.7638-02	1.2635+03	1.6966+05	1.1370+03	5.0063+04
29	-3.4412+04	-9.7703-02	1.2640+03	1.7035+05	1.1370+03	5.2287+04
30	-3.1413+04	-8.9190-02	1.2646+03	1.7103+05	1.1371+03	5.6135+04

# CONDENSING DATA REDUCTION

	324	326	354	365	367	372
	HCON T	NUC T	TWI B	Q/A B	TWO B	HCON B
31	1.3874+05	3.8930-01	1.1857+03	1.7049+05	1.0562+03	2.1856+04
32	-2.2310+06	-6.2598+00	1.1867+03	1.7127+05	1.0566+03	2.3352+04
33	-2.9476+06	-8.2705+00	1.1859+03	1.7029+05	1.0566+03	2.0979+04
34	-2.9808+04	-8.4995-02	1.2858+03	2.0741+05	1.1314+03	4.2821+04
35	-3.4472+04	-9.8292-02	1.2854+03	2.0667+05	1.1316+03	4.2034+04
36	-3.4672+04	-9.8867-02	1.2855+03	2.0692+05	1.1314+03	3.9375+04
37	9.8223+05	2.8536+00	1.3899+03	1.9877+05	1.2456+03	3.2343+04
38	7.2109+05	2.0951+00	1.3901+03	1.9901+05	1.2456+03	3.1406+04
39	3.6542+05	1.0617+00	1.3896+03	1.9841+05	1.2456+03	2.8649+04
40	-1.8694+05	-5.4292-01	1.3881+03	2.2577+05	1.2237+03	3.7076+04
41	-1.8045+05	-5.2404-01	1.3881+03	2.2527+05	1.2240+03	3.8303+04
42	-1.1101+06	-3.2240+00	1.3873+03	2.2458+05	1.2237+03	3.2771+04
43	-7.0474+04	-2.0270-01	1.3332+03	2.3003+05	1.1634+03	3.5014+04
44	-9.2718+04	-2.6664-01	1.3320+03	2.2864+05	1.1633+03	3.3042+04
45	-5.8246+04	-1.6748-01	1.3324+03	2.2906+05	1.1634+03	3.8362+04
46	-2.3176+04	-6.5748-02	1.2591+03	2.1160+05	1.1005+03	4.2272+04
47	-2.3471+04	-6.6583-02	1.2591+03	2.1161+05	1.1005+03	4.1056+04
48	-2.6935+04	-7.6414-02	1.2589+03	2.1112+05	1.1007+03	4.1562+04
49	-3.2571+04	-9.2227-02	1.2496+03	1.4709+05	1.1398+03	4.8167+04
50	-3.3129+04	-9.3812-02	1.2500+03	1.4782+05	1.1397+03	5.3476+04
51	-3.4196+04	-9.6830-02	1.2496+03	1.4708+05	1.1398+03	4.8130+04
52	-6.2773+04	-1.7738-01	1.2368+03	1.2267+05	1.1452+03	4.5552+04
53	-6.7041+04	-1.8942-01	1.2364+03	1.2254+05	1.1448+03	5.3964+04
54	-5.0312+04	-1.4216-01	1.2375+03	1.2358+05	1.1452+03	6.7332+04
55	-5.7358+04	-1.6184-01	1.2285+03	9.6819+04	1.1562+03	8.1527+04
56	-6.6548+04	-1.8777-01	1.2285+03	9.6695+04	1.1563+03	7.0215+04
57	-6.0963+04	-1.7201-01	1.2285+03	9.6816+04	1.1562+03	8.0971+04
58	-1.3521+05	-3.8140-01	1.2255+03	7.7923+04	1.1674+03	6.0015+04
59	-1.5249+05	-4.3014-01	1.2255+03	7.7840+04	1.1675+03	5.7539+04
60	-1.4193+05	-4.0035-01	1.2256+03	7.8018+04	1.1675+03	5.8908+04

# CONDENSING DATA REDUCTION

	324	326	354	365	367	372
	HCON T	NUC T	TWI B	Q/A B	TWO B	HCON B
61	5.1496+05	1.4528+00	1.2252+03	6.4267+04	1.1774+03	5.2210+04
62	-2.1331+06	-6.0174+00	1.2252+03	6.4266+04	1.1773+03	5.7780+04
63	1.7215+06	4.8565+00	1.2252+03	6.4319+04	1.1773+03	5.8488+04
64	-1.8248+06	-5.1353+00	1.2117+03	5.9212+04	1.1675+03	6.4630+04
65	-2.2971+07	-6.4643+01	1.2118+03	5.9168+04	1.1676+03	6.9379+04
66	2.9048+06	8.1746+00	1.2119+03	5.8652+04	1.1681+03	6.3872+04
67	2.2944+04	6.6799-02	1.3855+03	2.6219+05	1.1937+03	1.1162+04
68	-4.8091+05	-1.4004+00	1.4018+03	2.8427+05	1.1943+03	3.4274+04
69	-1.1427+05	-3.3274-01	1.4038+03	2.8780+05	1.1937+03	4.3857+04
70	-2.2915+05	-6.7146-01	1.4227+03	2.7014+05	1.2267+03	3.8037+04
71	-2.8220+05	-8.2618-01	1.4207+03	2.6852+05	1.2259+03	3.8684+04
72	-1.0048+05	-2.9404-01	1.4201+03	2.6774+05	1.2259+03	4.8677+04



# CONDENSING DATA REDUCTION

	374	389	399	401	405	406
	NUC B	TWI TC	Q/A TC	TWO TC	TKC-TW	HCONTC
1	9.6834-02	1.2001+03	6.0943+04	1.1545+03	-1.5657+00	-3.8924+04
2	1.1567-01	1.2003+03	6.1076+04	1.1546+03	-1.8768+00	-3.2543+04
3	8.8892-02	1.2004+03	6.1508+04	1.1544+03	-1.8371+00	-3.3482+04
4	-6.1928-03	1.2924+03	6.7861+04	1.2426+03	-8.7959+00	-7.7151+03
5	-6.4703-03	1.2925+03	6.7912+04	1.2427+03	-8.5947+00	-7.9016+03
6	-7.3316-03	1.2922+03	6.7507+04	1.2427+03	-7.4225+00	-9.0949+03
7	-4.3226-03	1.3976+03	8.7264+04	1.3351+03	-1.4805+01	-5.8941+03
8	-4.3564-03	1.3976+03	8.7214+04	1.3351+03	-1.4759+01	-5.9092+03
9	-4.3479-03	1.3972+03	8.7065+04	1.3348+03	-1.4587+01	-5.9685+03
10	1.0376-01	1.3005+03	8.5936+04	1.2374+03	-6.5471-01	-1.3126+05
11	1.0646-01	1.3004+03	8.5524+04	1.2377+03	-5.2490-01	-1.6293+05
12	1.1686-01	1.3004+03	8.5395+04	1.2378+03	-6.4775-01	-1.3183+05
13	1.9543-01	1.2038+03	8.7865+04	1.1380+03	2.7017+00	-3.2522+04
14	2.0772-01	1.2039+03	8.7702+04	1.1382+03	-2.8216+00	-3.1082+04
15	2.1215-01	1.2040+03	8.7868+04	1.1381+03	-2.8237+00	-3.1118+04
16	1.3766-01	1.2034+03	1.0830+05	1.1220+03	-1.4399+00	-7.5217+04
17	5.3182-01	1.2028+03	1.0798+05	1.1216+03	-1.5931+00	-6.7782+04
18	1.3437-01	1.2031+03	1.0791+05	1.1220+03	-1.0316+00	-1.0460+05
19	1.1193-01	1.2945+03	1.0707+05	1.2157+03	-7.9288-01	-1.3504+05
20	1.1124-01	1.2948+03	1.0773+05	1.2155+03	-1.2559+00	-8.5779+04
21	1.0325-01	1.2941+03	1.0648+05	1.2157+03	-3.0940-01	-3.4414+05
22	8.9326-02	1.4187+03	1.0051+05	1.3469+03	1.3898+00	7.2319+04
23	9.6032-02	1.4188+03	1.0060+05	1.3470+03	1.1966+00	8.4075+04
24	9.2921-02	1.4190+03	1.0085+05	1.3470+03	1.0064+00	1.0020+05
25	9.7294-02	1.3940+03	1.3233+05	1.2986+03	8.5715-01	1.5438+05
26	8.9802-02	1.3939+03	1.3232+05	1.2986+03	8.8387-01	1.4971+05
27	8.6515-02	1.3938+03	1.3245+05	1.2984+03	9.6922-01	1.3666+05
28	1.4230-01	1.2699+03	1.3637+05	1.1687+03	-2.3058+00	-5.9142+04
29	1.4863-01	1.2702+03	1.3668+05	1.1688+03	-2.3125+00	-5.9105+04
30	1.5958-01	1.2707+03	1.3717+05	1.1690+03	-2.7446+00	-4.9978+04

# CONDENSING DATA REDUCTION

	374	389	399	401	405	406
	NUC B	TWI TC	Q/A TC	TWO TC	TKC-TW	HCONTC
31	6.1352-02	1.1933+03	1.4004+05	1.0874+03	5.2753+00	2.6546+04
32	6.5556-02	1.1940+03	1.4011+05	1.0881+03	4.1898+00	3.3440+04
33	5.8896-02	1.1939+03	1.3994+05	1.0882+03	4.2719+00	3.2758+04
34	1.2222-01	1.2966+03	1.7141+05	1.1698+03	-3.5116+00	-4.8812+04
35	1.1997-01	1.2957+03	1.7048+05	1.1695+03	-2.7059+00	-6.3004+04
36	1.1239-01	1.2960+03	1.7027+05	1.1700+03	-2.6602+00	-6.4006+04
37	9.3990-02	1.4005+03	1.6298+05	1.2830+03	1.3616+00	1.1970+05
38	9.1274-02	1.4009+03	1.6374+05	1.2827+03	1.4324+00	1.1431+05
39	8.3263-02	1.4007+03	1.6335+05	1.2828+03	1.6629+00	9.8235+04
40	1.0771-01	1.3996+03	1.8539+05	1.2655+03	4.1582-01	4.4585+05
41	1.1127-01	1.3994+03	1.8482+05	1.2657+03	3.7315-01	4.9530+05
42	9.5205-02	1.3987+03	1.8352+05	1.2660+03	1.2742+00	1.4402+05
43	1.0079-01	1.3442+03	1.8807+05	1.2063+03	-7.2658-01	-2.5885+05
44	9.5099-02	1.3425+03	1.8652+05	1.2057+03	-6.6818-02	-2.7914+06
45	1.1040-01	1.3429+03	1.8786+05	1.2052+03	-1.3064+00	-1.4380+05
46	1.2010-01	1.2692+03	1.7468+05	1.1391+03	-4.6596+00	-3.7487+04
47	1.1664-01	1.2690+03	1.7406+05	1.1394+03	-4.4557+00	-3.9065+04
48	1.1808-01	1.2683+03	1.7300+05	1.1394+03	-3.5427+00	-4.8831+04
49	1.3657-01	1.2545+03	1.1891+05	1.1662+03	-2.6921+00	-4.4169+04
50	1.5162-01	1.2547+03	1.1907+05	1.1662+03	-2.6318+00	-4.5243+04
51	1.3647-01	1.2544+03	1.1860+05	1.1662+03	-2.4878+00	-4.7671+04
52	1.2885-01	1.2405+03	9.8742+04	1.1670+03	-1.0351+00	-9.5390+04
53	1.5263-01	1.2399+03	9.8588+04	1.1665+03	-9.6381-01	-1.0229+05
54	1.9046-01	1.2407+03	9.8947+04	1.1671+03	-1.4708+00	-6.7274+04
55	2.3022-01	1.2319+03	7.8883+04	1.1731+03	-1.4133+00	-5.5813+04
56	1.9828-01	1.2319+03	7.8715+04	1.1733+03	-1.2108+00	-6.5013+04
57	2.2865-01	1.2319+03	7.8882+04	1.1731+03	-1.3342+00	-5.9122+04
58	1.6939-01	1.2292+03	6.4881+04	1.1809+03	-7.7228-01	-8.4013+04
59	1.6240-01	1.2293+03	6.5003+04	1.1809+03	-7.0610-01	-9.2059+04
60	1.6627-01	1.2294+03	6.4980+04	1.1810+03	-7.4727-01	-8.6956+04

# CONDENSING DATA REDUCTION

	374	389	399	401	405	406
	NUC B	TWI TC	Q/A TC	TWO TC	TKC-TW	HCONTC
61	1.4735-01	1.2293+03	5.4952+04	1.1884+03	-2.7708-01	-1.9832+05
62	1.6306-01	1.2292+03	5.4851+04	1.1884+03	-4.3402-01	-1.2638+05
63	1.6506-01	1.2291+03	5.4859+04	1.1884+03	-3.6635-01	-1.4975+05
64	1.8195-01	1.2153+03	5.0831+04	1.1774+03	-5.5008-01	-9.2407+04
65	1.9533-01	1.2154+03	5.0749+04	1.1776+03	-5.1651-01	-9.8254+04
66	1.7982-01	1.2155+03	5.0360+04	1.1779+03	-5.0574-01	-9.9577+04
67	3.2540-02	1.4011+03	2.1561+05	1.2447+03	1.1692+01	1.8440+04
68	9.9948-02	1.4119+03	2.3007+05	1.2453+03	1.3981+00	1.6456+05
69	1.2790-01	1.4134+03	2.3176+05	1.2456+03	-8.1116-02	-2.8572+06
70	1.1153-01	1.4351+03	2.2033+05	1.2766+03	6.5974-01	3.3396+05
71	1.1336-01	1.4317+03	2.1657+05	1.2758+03	8.9500-01	2.4197+05
72	1.4256-01	1.4315+03	2.1751+05	1.2749+03	-5.6947-01	-3.8194+05

# CONDENSING DATA REDUCTION

	408	424	434	436	439	440
	NUC TC	TWI BC	Q/A BC	TWO BC	TK-TWI	HCONBC
1	-1.0932-01	1.1994+03	7.7356+04	1.1414+03	1.7383+00	4.4501+04
2	-9.1398-02	1.1997+03	7.7918+04	1.1412+03	1.4041+00	5.5492+04
3	-9.4037-02	1.1994+03	7.7412+04	1.1413+03	1.9329+00	4.0050+04
4	-2.1994-02	1.2910+03	8.5673+04	1.2280+03	-3.7201+01	-2.3029+03
5	-2.2527-02	1.2909+03	8.5711+04	1.2279+03	-3.5651+01	-2.4042+03
6	-2.5933-02	1.2908+03	8.5270+04	1.2282+03	-3.1357+01	-2.7193+03
7	-1.7090-02	1.3956+03	1.1169+05	1.3153+03	-6.9788+01	-1.6005+03
8	-1.7134-02	1.3960+03	1.1243+05	1.3152+03	-6.9736+01	-1.6122+03
9	-1.7306-02	1.3955+03	1.1128+05	1.3155+03	-6.9112+01	-1.6101+03
10	-3.7525-01	1.2987+03	1.0883+05	1.2187+03	2.6277+00	4.1416+04
11	-4.6582-01	1.2988+03	1.0861+05	1.2189+03	2.5465+00	4.2652+04
12	-3.7690-01	1.2989+03	1.0896+05	1.2188+03	2.3067+00	4.7235+04
13	-9.1373-02	1.2051+03	1.1514+05	1.1186+03	1.6247+00	7.0867+04
14	-8.7326-02	1.2052+03	1.1540+05	1.1185+03	1.5385+00	7.5008+04
15	-8.7429-02	1.2052+03	1.1541+05	1.1185+03	1.5050+00	7.6685+04
16	-2.1136-01	1.2051+03	1.4443+05	1.0962+03	3.3239+00	4.3453+04
17	-1.9044-01	1.2044+03	1.4324+05	1.0964+03	1.1518+00	1.2437+05
18	-2.9394-01	1.2048+03	1.4378+05	1.0964+03	3.3708+00	4.2654+04
19	-3.8564-01	1.2929+03	1.3887+05	1.1904+03	3.4232+00	4.0566+04
20	-2.4496-01	1.2928+03	1.3881+05	1.1904+03	3.4377+00	4.0378+04
21	-9.8282-01	1.2925+03	1.3847+05	1.1902+03	3.6964+00	3.7461+04
22	2.1148-01	1.4166+03	1.2988+05	1.3235+03	3.9170+00	3.3158+04
23	2.4585-01	1.4168+03	1.3034+05	1.3234+03	3.6521+00	3.5690+04
24	2.9301-01	1.4167+03	1.3044+05	1.3233+03	3.7830+00	3.4482+04
25	4.4856-01	1.3904+03	1.6881+05	1.2682+03	4.9469+00	3.4125+04
26	4.3497-01	1.3901+03	1.6843+05	1.2681+03	5.3371+00	3.1559+04
27	3.9706-01	1.3898+03	1.6815+05	1.2681+03	5.5294+00	3.0410+04
28	-1.6813-01	1.2682+03	1.7578+05	1.1372+03	3.8873+00	4.5219+04
29	-1.6803-01	1.2686+03	1.7648+05	1.1371+03	3.7557+00	4.6989+04
30	-1.4209-01	1.2692+03	1.7717+05	1.1372+03	3.5411+00	5.0033+04

# CONDENSING DATA REDUCTION

	408	424	434	436	439	440
	NUC TC	TWI BC	Q/A BC	TWO BC	TK-TWI	HCONBC
31	7.4556-02	1.1891+03	1.7510+05	1.0562+03	9.0118+00	1.9430+04
32	9.3917-02	1.1901+03	1.7589+05	1.0566+03	8.5538+00	2.0563+04
33	9.2000-02	1.1894+03	1.7491+05	1.0566+03	9.3636+00	1.8679+04
34	-1.3939-01	1.2907+03	2.1394+05	1.1315+03	5.6404+00	3.7929+04
35	-1.7991-01	1.2903+03	2.1319+05	1.1317+03	5.7015+00	3.7392+04
36	-1.8278-01	1.2903+03	2.1344+05	1.1315+03	6.0493+00	3.5283+04
37	3.4826-01	1.3964+03	2.0745+05	1.2459+03	6.5347+00	3.1746+04
38	3.3262-01	1.3966+03	2.0769+05	1.2459+03	6.7323+00	3.0849+04
39	2.8585-01	1.3961+03	2.0708+05	1.2459+03	7.3278+00	2.8260+04
40	1.2965+00	1.3945+03	2.3438+05	1.2239+03	6.6399+00	3.5299+04
41	1.4403+00	1.3945+03	2.3389+05	1.2243+03	6.4231+00	3.6413+04
42	4.1881-01	1.3937+03	2.3318+05	1.2240+03	7.4108+00	3.1464+04
43	-7.4556-01	1.3387+03	2.3750+05	1.1635+03	7.3322+00	3.2388+04
44	-8.0386+00	1.3376+03	2.3608+05	1.1634+03	7.6791+00	3.0743+04
45	-4.1405-01	1.3379+03	2.3651+05	1.1635+03	6.7254+00	3.5167+04
46	-1.0651-01	1.2635+03	2.1760+05	1.1005+03	6.0292+00	3.6091+04
47	-1.1099-01	1.2635+03	2.1761+05	1.1005+03	6.2009+00	3.5094+04
48	-1.3875-01	1.2634+03	2.1711+05	1.1008+03	6.0889+00	3.5657+04
49	-1.2522-01	1.2541+03	1.5296+05	1.1400+03	3.2987+00	4.6370+04
50	-1.2826-01	1.2545+03	1.5370+05	1.1398+03	3.0064+00	5.1124+04
51	-1.3515-01	1.2541+03	1.5295+05	1.1400+03	3.3047+00	4.6283+04
52	-2.6983-01	1.2411+03	1.2833+05	1.1453+03	2.7051+00	4.7440+04
53	-2.8932-01	1.2407+03	1.2818+05	1.1450+03	2.2649+00	5.6595+04
54	-1.9029-01	1.2419+03	1.2925+05	1.1454+03	1.8340+00	7.0477+04
55	-1.5763-01	1.2328+03	1.0234+05	1.1564+03	9.3718-01	1.0920+05
56	-1.8362-01	1.2328+03	1.0222+05	1.1565+03	1.1265+00	9.0742+04
57	-1.6698-01	1.2328+03	1.0234+05	1.1565+03	9.4205-01	1.0863+05
58	-2.3719-01	1.2298+03	8.3406+04	1.1677+03	8.9490-01	9.3202+04
59	-2.5991-01	1.2299+03	8.3325+04	1.1678+03	9.5073-01	8.7643+04
60	-2.4550-01	1.2300+03	8.3503+04	1.1677+03	9.2130-01	9.0637+04

# CONDENSING DATA REDUCTION

	408	424	434	436	439	440
	NUC TC	TWI BC	Q/A BC	TWO BC	TK-TWI	HCONBC
61	-5.5996-01	1.2296+03	6.9759+04	1.1777+03	7.3232-01	9.5259+04
62	-3.5682-01	1.2296+03	6.9758+04	1.1777+03	6.1153-01	1.1407+05
63	-4.2279-01	1.2296+03	6.9812+04	1.1776+03	5.9781-01	1.1678+05
64	-2.6025-01	1.2158+03	6.4448+04	1.1677+03	3.6780-01	1.7523+05
65	-2.7673-01	1.2160+03	6.4406+04	1.1679+03	3.0412-01	2.1178+05
66	-2.8046-01	1.2160+03	6.3891+04	1.1684+03	3.6621-01	1.7447+05
67	5.3815-02	1.3917+03	2.7070+05	1.1939+03	2.4562+01	1.1021+04
68	4.8030-01	1.4082+03	2.9310+05	1.1944+03	9.1939+00	3.1880+04
69	-8.3396+00	1.4103+03	2.9666+05	1.1938+03	7.4822+00	3.9649+04
70	9.8082-01	1.4295+03	2.7944+05	1.2269+03	7.8583+00	3.5559+04
71	7.1004-01	1.4275+03	2.7777+05	1.2261+03	7.7020+00	3.6065+04
72	-1.1203+00	1.4269+03	2.7698+05	1.2261+03	6.2357+00	4.4419+04

# CONDENSING DATA REDUCTION

	442	450	451	452	453	610
	NUC BC	PSI HD	PI	PO	DPC	PIC
1	1.2503-01	2.9424-01	4.5680+00	4.7677+00	-1.9966-01	4.7291+00
2	1.5591-01	2.9341-01	4.5654+00	4.7644+00	-1.9902-01	4.7264+00
3	1.1253-01	2.9491-01	4.5686+00	4.7728+00	-2.0418-01	4.7298+00
4	-6.5309-03	2.0230-01	8.1339+00	6.1448+00	1.9890+00	8.4109+00
5	-6.8197-03	2.0086-01	8.1359+00	6.2142+00	1.9217+00	8.4128+00
6	-7.7193-03	1.9969-01	8.1319+00	6.4235+00	1.7084+00	8.4084+00
7	-4.5960-03	1.7614-01	1.4535+01	8.8329+00	5.7026+00	1.5051+01
8	-4.6299-03	1.7771-01	1.4531+01	8.8650+00	5.6656+00	1.5046+01
9	-4.6241-03	1.7779-01	1.4509+01	8.8739+00	5.6353+00	1.5025+01
10	1.1844-01	3.1302-01	8.4865+00	8.6780+00	-1.9144-01	8.7912+00
11	1.2197-01	3.1106-01	8.4907+00	8.6748+00	-1.8404-01	8.7952+00
12	1.3507-01	3.0761-01	8.4865+00	8.6695+00	-1.8298-01	8.7904+00
13	1.9931-01	5.7588-01	4.5835+00	4.9746+00	3.9107-01	4.7834+00
14	2.1095-01	5.7975-01	4.5816+00	4.9753+00	-3.9369-01	4.7820+00
15	2.1567-01	5.7865-01	4.5835+00	4.9739+00	-3.9039-01	4.7838+00
16	1.2224-01	8.6766-01	4.5551+00	5.0393+00	-4.8420-01	4.7990+00
17	3.4970-01	8.5329-01	4.5538+00	4.9235+00	-3.6972-01	4.7953+00
18	1.1999-01	8.6354-01	4.5648+00	5.0257+00	-4.6088-01	4.8085+00
19	1.1590-01	5.1902-01	8.1500+00	8.4558+00	-3.0580-01	8.4744+00
20	1.1537-01	5.1038-01	8.1420+00	8.4527+00	-3.1070-01	8.4645+00
21	1.0703-01	5.1670-01	8.1571+00	8.4400+00	-2.8286-01	8.4814+00
22	9.6975-02	2.3704-01	1.6207+01	1.6273+01	-6.6423-02	1.6792+01
23	1.0438-01	2.3660-01	1.6203+01	1.6273+01	-7.0014-02	1.6788+01
24	1.0085-01	2.3652-01	1.6200+01	1.6279+01	-7.8989-02	1.6785+01
25	9.9157-02	4.6639-01	1.4225+01	1.4340+01	-1.1516-01	1.4773+01
26	9.1701-02	4.6059-01	1.4221+01	1.4348+01	-1.2621-01	1.4769+01
27	8.8364-02	4.6794-01	1.4221+01	1.4343+01	-1.2147-01	1.4770+01
28	1.2865-01	9.2588-01	6.9032+00	7.3756+00	-4.7247-01	7.2468+00
29	1.3369-01	9.2637-01	6.9154+00	7.3903+00	-4.7492-01	7.2597+00
30	1.4236-01	9.2125-01	6.9163+00	7.4119+00	-4.9557-01	7.2598+00

# CONDENSING DATA REDUCTION

	442	450	451	452	453	610
	NUC BC	PSI HD	PI	PO	DPC	PIC
31	5.4569-02	1.3390+00	4.4336+00	4.6455+00	-2.1195-01	4.7536+00
32	5.7754-02	1.3431+00	4.4152+00	4.6714+00	-2.5617-01	4.7354+00
33	5.2464-02	1.3563+00	4.4121+00	4.6746+00	-2.6247-01	4.7346+00
34	1.0837-01	1.1940+00	8.0076+00	8.4622+00	-4.5456-01	8.4368+00
35	1.0683-01	1.1816+00	8.0046+00	8.4442+00	-4.3961-01	8.4315+00
36	1.0081-01	1.1865+00	8.0208+00	8.4643+00	-4.4354-01	8.4492+00
37	9.2393-02	6.5177-01	1.4710+01	1.4925+01	-2.1508-01	1.5304+01
38	8.9794-02	6.5518-01	1.4739+01	1.4953+01	-2.1355-01	1.5335+01
39	8.2258-02	6.5435-01	1.4739+01	1.4964+01	-2.2511-01	1.5335+01
40	1.0268-01	8.3266-01	1.4537+01	1.4788+01	-2.5062-01	1.5155+01
41	1.0592-01	8.2716-01	1.4519+01	1.4771+01	-2.5219-01	1.5136+01
42	9.1527-02	8.2894-01	1.4537+01	1.4788+01	-2.5061-01	1.5154+01
43	9.3329-02	1.1244+00	1.0690+01	1.1125+01	-4.3518-01	1.1209+01
44	8.8576-02	1.1115+00	1.0628+01	1.1082+01	-4.5490-01	1.1143+01
45	1.0131-01	1.1203+00	1.0577+01	1.1051+01	-4.7381-01	1.1091+01
46	1.0263-01	1.3368+00	6.7071+00	7.2792+00	-5.7209-01	7.1119+00
47	9.9802-02	1.3591+00	6.7001+00	7.2893+00	-5.8920-01	7.1085+00
48	1.0140-01	1.3247+00	6.7167+00	7.2718+00	-5.5511-01	7.1198+00
49	1.3158-01	6.9306-01	6.2976+00	6.7824+00	-4.8476-01	6.5777+00
50	1.4508-01	6.9320-01	6.3051+00	6.7867+00	-4.8163-01	6.5856+00
51	1.3134-01	6.9613-01	6.2976+00	6.7841+00	-4.8651-01	6.5781+00
52	1.3430-01	5.0834-01	5.8711+00	6.2367+00	-3.6563-01	6.1099+00
53	1.6019-01	4.9659-01	5.8553+00	6.2001+00	-3.4482-01	6.0923+00
54	1.9951-01	5.0476-01	5.8632+00	6.2334+00	-3.7023-01	6.1014+00
55	3.0859-01	3.2607-01	5.5856+00	5.8505+00	-2.6493-01	5.7863+00
56	2.5643-01	3.2296-01	5.5931+00	5.8576+00	-2.6453-01	5.7934+00
57	3.0699-01	3.2280-01	5.5893+00	5.8505+00	-2.6116-01	5.7896+00
58	2.6324-01	2.1123-01	5.5395+00	5.7312+00	-1.9164-01	5.7249+00
59	2.4754-01	2.1282-01	5.5456+00	5.7334+00	-1.8787-01	5.7312+00
60	2.5600-01	2.1078-01	5.5463+00	5.7365+00	-1.9013-01	5.7317+00



# CONDENSING DATA REDUCTION

	442	450	451	452	453	610
	NUC BC	PSI HD	PI	PO	DPC	PIC
61	2.6903-01	1.4486-01	5.5765+00	5.7063+00	-1.2977-01	5.7541+00
62	3.2215-01	1.4382-01	5.5667+00	5.7018+00	-1.3505-01	5.7440+00
63	3.2980-01	1.4399-01	5.5682+00	5.7018+00	-1.3354-01	5.7456+00
64	4.9363-01	1.2796-01	5.0992+00	5.2289+00	-1.2972-01	5.2606+00
65	5.9660-01	1.2910-01	5.1046+00	5.2304+00	-1.2570-01	5.2665+00
66	4.9151-01	1.2442-01	5.1053+00	5.2354+00	-1.3004-01	5.2667+00
67	3.2195-02	1.1369+00	1.5411+01	1.6024+01	-6.1216-01	1.6117+01
68	9.3157-02	1.1141+00	1.5446+01	1.6135+01	-6.8912-01	1.6149+01
69	1.1587-01	1.1830+00	1.5432+01	1.6167+01	-7.3524-01	1.6147+01
70	1.0448-01	9.5114-01	1.7380+01	1.7711+01	-3.3072-01	1.8132+01
71	1.0590-01	9.6750-01	1.7078+01	1.7559+01	-4.8167-01	1.7819+01
72	1.3036-01	9.6140-01	1.6945+01	1.7376+01	-4.3127-01	1.7679+01

# CONDENSING DATA REDUCTION

	611	613	700	495	701	498
	POC	DPCC	X B	WKL B	X T	WKL T
1	4.8621+00	-1.3301-01	2.7124-01	3.0414+01	8.6918-01	5.4598+00
2	4.8586+00	-1.3225-01	2.7124-01	3.0363+01	8.6918-01	5.4505+00
3	4.8677+00	-1.3784-01	2.7191-01	3.0423+01	8.6964-01	5.4470+00
4	6.2897+00	2.1212+00	2.6209-01	3.3329+01	8.6931-01	5.9027+00
5	6.3618+00	2.0511+00	2.5581-01	3.3496+01	8.6333-01	6.1516+00
6	6.5755+00	1.8329+00	2.3969-01	3.4114+01	8.4848-01	6.7986+00
7	9.0857+00	5.9652+00	5.0672-01	2.7208+01	1.1861+00	-1.0262+01
8	9.1184+00	5.9277+00	4.9366-01	2.8048+01	1.1642+00	-9.0941+00
9	9.1274+00	5.8971+00	4.9010-01	2.8234+01	1.1586+00	-8.7833+00
10	8.9208+00	-1.2967-01	2.6260-01	4.2285+01	8.6312-01	7.8491+00
11	8.9174+00	-1.2227-01	2.6212-01	4.2190+01	8.6279-01	7.8454+00
12	8.9118+00	-1.2142-01	2.6190-01	4.1956+01	8.6264-01	7.8082+00
13	5.0742+00	-2.9079-01	2.7970-01	4.2279+01	8.7500-01	7.3371+00
14	5.0749+00	-2.9288-01	2.8015-01	4.2388+01	8.7530-01	7.3429+00
15	5.0735+00	-2.8971-01	2.7981-01	4.2376+01	8.7507-01	7.3510+00
16	5.1415+00	-3.4250-01	2.7931-01	5.2002+01	8.7466-01	9.0439+00
17	5.0224+00	-2.2713-01	2.7256-01	5.2034+01	8.6999-01	9.2996+00
18	5.1269+00	-3.1839-01	2.7777-01	5.2036+01	8.7360-01	9.1069+00
19	8.6901+00	-2.1577-01	2.6766-01	5.3166+01	8.6657-01	9.6865+00
20	8.6870+00	-2.2249-01	2.6763-01	5.2695+01	8.6656-01	9.6010+00
21	8.6740+00	-1.9260-01	2.6669-01	5.3137+01	8.6590-01	9.7174+00
22	1.6851+01	-5.8569-02	2.6020-01	4.9795+01	8.6136-01	9.3317+00
23	1.6851+01	-6.2259-02	2.6024-01	4.9741+01	8.6139-01	9.3201+00
24	1.6856+01	-7.1657-02	2.6047-01	4.9711+01	8.6155-01	9.3065+00
25	1.4833+01	-6.0229-02	2.5934-01	6.5906+01	8.6077-01	1.2389+01
26	1.4842+01	-7.2808-02	2.5927-01	6.5493+01	8.6073-01	1.2314+01
27	1.4837+01	-6.6699-02	2.5952-01	6.5993+01	8.6090-01	1.2397+01
28	7.5683+00	-3.2159-01	2.6925-01	6.5909+01	8.6773-01	1.1930+01
29	7.5840+00	-3.2430-01	2.6929-01	6.5978+01	8.6775-01	1.1941+01
30	7.6066+00	-3.4687-01	2.6982-01	6.5748+01	8.6813-01	1.1874+01

# CONDENSING DATA REDUCTION

	611	613	700	495	701	498
	POC	DPCC	X B	WKL B	X T	WKL T
31	4.7342+00	1.9427-02	2.5537-01	6.6453+01	8.5800-01	1.2673+01
32	4.7605+00	-2.5054-02	2.5726-01	6.6268+01	8.5935-01	1.2549+01
33	4.7638+00	-2.9213-02	2.5771-01	6.6547+01	8.5966-01	1.2582+01
34	8.6963+00	-2.5945-01	2.6431-01	8.0841+01	8.6428-01	1.4914+01
35	8.6780+00	-2.4641-01	2.6383-01	8.0452+01	8.6395-01	1.4869+01
36	8.6984+00	-2.4919-01	2.6395-01	8.0683+01	8.6403-01	1.4905+01
37	1.5443+01	-1.3899-01	2.6005-01	7.9118+01	8.6128-01	1.4832+01
38	1.5473+01	-1.3714-01	2.6004-01	7.9400+01	8.6128-01	1.4886+01
39	1.5485+01	-1.4950-01	2.6017-01	7.9336+01	8.6137-01	1.4866+01
40	1.5298+01	-1.4298-01	2.6001-01	8.9027+01	8.6125-01	1.6693+01
41	1.5280+01	-1.4456-01	2.5999-01	8.8683+01	8.6123-01	1.6630+01
42	1.5298+01	-1.4363-01	2.6002-01	8.8825+01	8.6126-01	1.6654+01
43	1.1474+01	-2.6418-01	2.6264-01	8.9670+01	8.6311-01	1.6647+01
44	1.1431+01	-2.8803-01	2.6291-01	8.8873+01	8.6330-01	1.6482+01
45	1.1398+01	-3.0706-01	2.6352-01	8.8961+01	8.6372-01	1.6461+01
46	7.4655+00	-3.5362-01	2.6730-01	7.8720+01	8.6640-01	1.4354+01
47	7.4763+00	-3.6776-01	2.6792-01	7.9288+01	8.6682-01	1.4424+01
48	7.4576+00	-3.3780-01	2.6675-01	7.8463+01	8.6601-01	1.4337+01
49	6.9482+00	-3.7051-01	2.7338-01	5.4217+01	8.7065-01	9.6516+00
50	6.9526+00	-3.6708-01	2.7318-01	5.4267+01	8.7051-01	9.6681+00
51	6.9500+00	-3.7184-01	2.7361-01	5.4321+01	8.7080-01	9.6618+00
52	6.3851+00	-2.7520-01	2.7164-01	4.4983+01	8.6946-01	8.0618+00
53	6.3478+00	-2.5554-01	2.7032-01	4.4480+01	8.6856-01	8.0127+00
54	6.3818+00	-2.8031-01	2.7187-01	4.4781+01	8.6963-01	8.0180+00
55	5.9847+00	-1.9843-01	2.7027-01	3.5197+01	8.6853-01	6.3411+00
56	5.9920+00	-1.9855-01	2.7005-01	3.5059+01	8.6839-01	6.3212+00
57	5.9847+00	-1.9508-01	2.6982-01	3.5051+01	8.6823-01	6.3255+00
58	5.8595+00	-1.3464-01	2.6677-01	2.8324+01	8.6612-01	5.1715+00
59	5.8619+00	-1.3076-01	2.6653-01	2.8454+01	8.6595-01	5.2005+00
60	5.8652+00	-1.3350-01	2.6659-01	2.8317+01	8.6600-01	5.1738+00

# CONDENSING DATA REDUCTION

	611	613	700	495	701	498
	POC	DPCC	X B	WKL B	X T	WKL T
61	5.8329+00	-7.8801-02	2.6216-01	2.3659+01	8.6290-01	4.3962+00
62	5.8280+00	-8.4012-02	2.6274-01	2.3536+01	8.6331-01	4.3637+00
63	5.8280+00	-8.2441-02	2.6258-01	2.3559+01	8.6320-01	4.3705+00
64	5.3392+00	-7.8562-02	2.6272-01	2.1316+01	8.6332-01	3.9516+00
65	5.3406+00	-7.4113-02	2.6246-01	2.1430+01	8.6313-01	3.9770+00
66	5.3458+00	-7.9046-02	2.6267-01	2.1032+01	8.6329-01	3.8997+00
67	1.6594+01	-4.7740-01	2.6190-01	1.0675+02	8.6262-01	1.9870+01
68	1.6709+01	-5.5966-01	2.6230-01	1.0572+02	8.6292-01	1.9645+01
69	1.6742+01	-5.9467-01	2.6383-01	1.0871+02	8.6396-01	2.0088+01
70	1.8361+01	-2.2950-01	2.6026-01	1.0334+02	8.6143-01	1.9358+01
71	1.8203+01	-3.8432-01	2.6234-01	1.0310+02	8.6289-01	1.9164+01
72	1.8010+01	-3.3061-01	2.6191-01	1.0246+02	8.6258-01	1.9077+01

# CONDENSING DATA REDUCTION

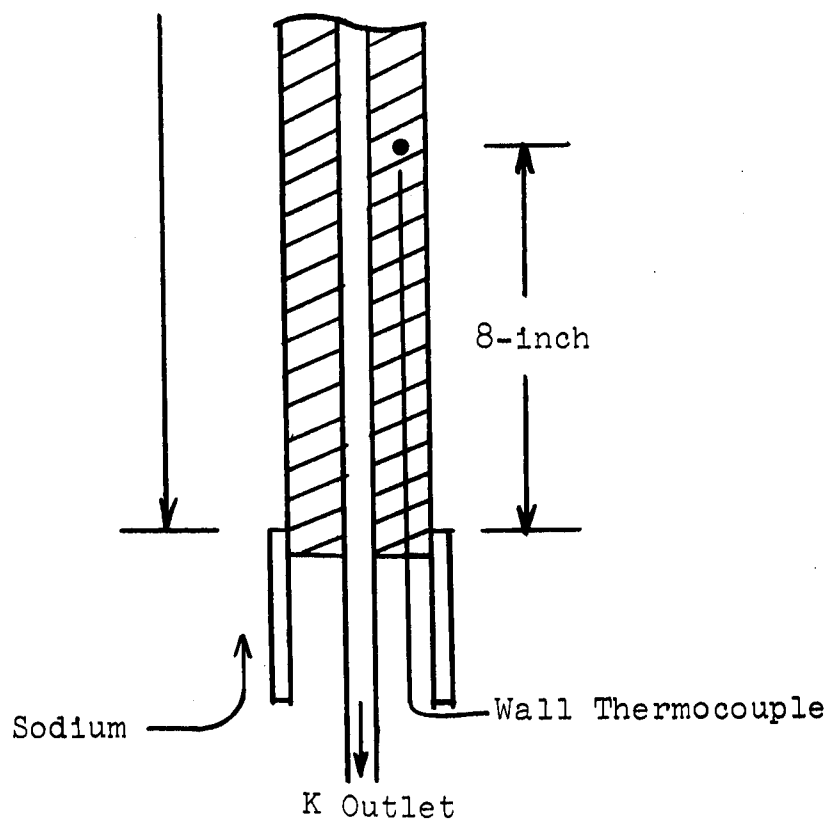
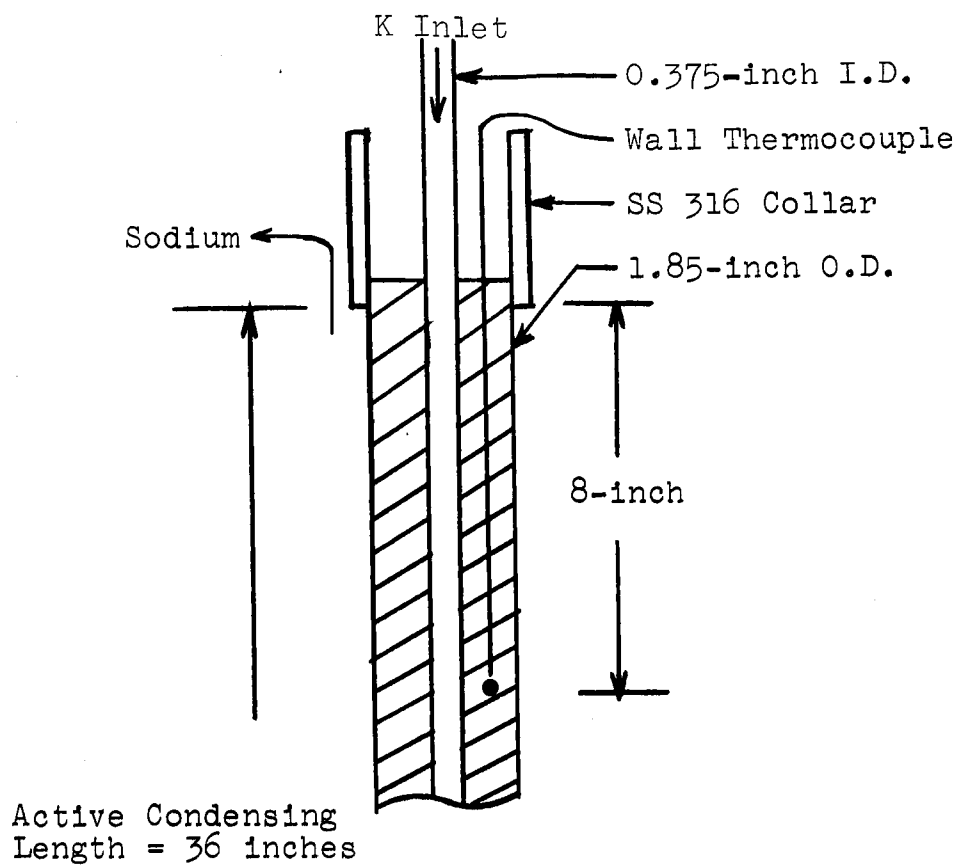
	504	507
	NREF T	NREF B
1	3.7293+02	2.0809+03
2	3.7227+02	2.0772+03
3	3.7207+02	2.0817+03
4	4.2392+02	2.3529+03
5	4.4187+02	2.3667+03
6	4.8855+02	2.4163+03
7	-7.7675+02	2.0005+03
8	-6.8835+02	2.0628+03
9	-6.6476+02	2.0765+03
10	5.6845+02	3.0652+03
11	5.6821+02	3.0582+03
12	5.6548+02	3.0411+03
13	5.0198+02	2.9028+03
14	5.0236+02	2.9104+03
15	5.0293+02	2.9095+03
16	6.1906+02	3.5743+03
17	6.3627+02	3.5699+03
18	6.2344+02	3.5761+03
19	6.9931+02	3.8436+03
20	6.9308+02	3.8094+03
21	7.0157+02	3.8411+03
22	7.1977+02	3.8415+03
23	7.1886+02	3.8373+03
24	7.1781+02	3.8351+03
25	9.4389+02	5.0226+03
26	9.3814+02	4.9913+03
27	9.4451+02	5.0293+03
28	8.4900+02	4.7026+03
29	8.4991+02	4.7085+03
30	8.4518+02	4.6932+03

# CONDENSING DATA REDUCTION

	504	507
	NREF T	NREF B
31	8.6559+02	4.5379+03
32	8.5696+02	4.5268+03
33	8.5917+02	4.5461+03
34	1.0763+03	5.8441+03
35	1.0730+03	5.8151+03
36	1.0758+03	5.8330+03
37	1.1343+03	6.0534+03
38	1.1385+03	6.0761+03
39	1.1371+03	6.0715+03
40	1.2754+03	6.8056+03
41	1.2704+03	6.7786+03
42	1.2725+03	6.7901+03
43	1.2355+03	6.6643+03
44	1.2226+03	6.6023+03
45	1.2205+03	6.6068+03
46	1.0197+03	5.6087+03
47	1.0247+03	5.6497+03
48	1.0186+03	5.5900+03
49	6.8060+02	3.8355+03
50	6.8184+02	3.8393+03
51	6.8133+02	3.8430+03
52	5.6446+02	3.1574+03
53	5.6084+02	3.1206+03
54	5.6133+02	3.1431+03
55	4.4169+02	2.4562+03
56	4.4035+02	2.4469+03
57	4.4062+02	2.4461+03
58	3.5981+02	1.9732+03
59	3.6185+02	1.9824+03
60	3.6000+02	1.9729+03

# CONDENSING DATA REDUCTION

	504	507
	NREF T	NREF B
61	3.0596+02	1.6479+03
62	3.0366+02	1.6392+03
63	3.0414+02	1.6407+03
64	2.7270+02	1.4724+03
65	2.7448+02	1.4803+03
66	2.6915+02	1.4530+03
67	1.5273+03	8.2194+03
68	1.5104+03	8.1441+03
69	1.5445+03	8.3756+03
70	1.5034+03	8.0312+03
71	1.4862+03	8.0049+03
72	1.4784+03	7.9483+03



50 KW Test Section Schematic  
(3/8-inch ID plain tube, Test Set No. 3, January, 1965)



TABLE D-3. NOMENCLATURE FOR CONDENSING HEAT TRANSFER  
RESULTS FROM THE 50 KW FACILITY  
(Key to Table D-4)

Column	Symbol	Identification
131	DATE	{e.g., 1.1050 + 03 = 1/10/65) (e.g., 1.200 + 03 = 1200)
132	TIME	
<u>Fluid Thermocouples</u>		
	<u>TC Number</u>	
134	1	Potassium inlet
136	2	Potassium inlet
138	3	Potassium outlet
140	4	Potassium outlet
142	5	Sodium outlet
144	6	Sodium outlet
146	7	Sodium outlet
148	8	Sodium inlet
150	9	Sodium inlet
152	10	Sodium inlet
<u>Wall Thermocouples</u>		
	<u>TC Number</u>	<u>Radius Within Tube Wall - Inches</u> <u>Distance from Condenser Inlet - Inches</u>
154	11	.293      8
156	12	.288      8
158	13	.412      8
160	14	.834      8
162	15	.822      8
164	16	.291      28
166	17	.293      28
168	18	.410      28
170	19	.830      28
172	20	.828      28

Column	Symbol	Identification
174	TKI	Inlet potassium temperature, °F
176	TKO	Outlet potassium temperature, °F
181-219	TKNC	Corrected temperature of thermocouple N, °F
221	TKICC	Corrected inlet potassium temperature, °F
223	TKOC	Corrected outlet potassium temperature, °F
226	TNAO	Outlet Sodium temperature, °F
229	TNAI	Inlet Sodium temperature, °F
230	DTNA	Sodium temperature increase, °F
235	WNA	Sodium Flow rate, lb/hr
237	TNAM	Sodium mean temperature, °F
238	CPNA	Sodium specific heat, Btu/lb-°F
240	QNA	Sodium heat gain, Btu/hr
243	DTQL	Temperature Difference, Test Section Shell - Ambient, °F
246	QC	Condenser load, Btu/hr
247	Q/AA	Average heat flux, Btu/hr-ft <sup>2</sup>
251	WK	Potassium flow rate, lb/hr
306	TWIT*	Inner wall temperature at top axial station, °F
317	Q/AT*	Heat Flux at inner wall at top axial station, Btu/hr-ft <sup>2</sup>
319	TWOT*	Outer wall temperature at top axial station, °F
323	TK-TWI*	Potassium - Inner wall temperature
324	HCONT*	Condensing heat transfer coefficient at top axial station, Btu/hr-ft <sup>2</sup> °F
326	NUCT*	Nusselt's condensing ratio at top axial station, dimensionless
354	TWIB*	Inner wall temperature at bottom axial station, °F
365	Q/AB*	Heat Flux at inner wall at bottom axial station, Btu/hr-ft <sup>2</sup>
367	TWOB*	Outer wall temperature at bottom axial station, °F
372	HCONB*	Condensing heat transfer coefficient at bottom axial station, Btu/hr-ft <sup>2</sup> -°F
374	NUCB*	Nusselt's condensing ratio at bottom axial station, dimensionless
450	PSI HD	Inlet vapor velocity head, psi
451	PI*	Inlet potassium vapor pressure, lb/in <sup>2</sup>
452	PO*	Outlet potassium vapor pressure, lb/in <sup>2</sup>
453	DPC*	Condensing pressure drop

\*These values were also calculated, accounting for the thermocouple standardizations obtained in the vapor standardization runs. The values of the parameters utilizing the thermocouple standardization are indicated in the columns in which the notation for the above parameters are followed by a C, e.g., TWITC is the Inner Wall Temperature at top axial station utilizing the standardized correction factor, °F.

Column	Symbol	Identification
700	X B	Potassium Quality, Bottom Station, $L/D = 75$
495	WKL B	Local Potassium liquid flowrate at bottom station, lb/hr
701	X T	Potassium Quality, Top Station, $L/D = 21$
498	WKL T	Local Potassium liquid flowrate at top station, lb/hr
504	NREF T	Liquid film Reynolds number at top station, $L/D = 21$
507	NREF B	Liquid film Reynolds number at bottom station, $L/D = 75$

TABLE D-4

CONDENSING DATA REDUCTION (Test Set No. 3)

	131	132	134	138	140	142
	DATE	TIME	TC1	TC3	TC4	TC5
1	1.1050+03	1.2000+03	1.1865+03	1.2006+03	1.1916+03	1.1412+03
2	1.1050+03	1.2000+03	1.1867+03	1.2006+03	1.1916+03	1.1413+03
3	1.1050+03	1.2000+03	1.1867+03	1.2006+03	1.1916+03	1.1411+03
*4	1.1050+03	1.5000+03	1.1877+03	1.1973+03	1.1882+03	1.1196+03
*5	1.1050+03	1.5000+03	1.1878+03	1.1971+03	1.1879+03	1.1195+03
*6	1.1050+03	1.5000+03	1.1877+03	1.1971+03	1.1880+03	1.1193+03
7	1.1050+03	1.8000+03	1.2408+03	1.2541+03	1.2449+03	1.1945+03
8	1.1050+03	1.8000+03	1.2412+03	1.2543+03	1.2453+03	1.1949+03
9	1.1050+03	1.8000+03	1.2412+03	1.2543+03	1.2452+03	1.1950+03
10	1.1050+03	2.0000+03	1.3013+03	1.3109+03	1.3012+03	1.2555+03
11	1.1050+03	2.0000+03	1.3016+03	1.3110+03	1.3013+03	1.2555+03
12	1.1050+03	2.0000+03	1.3016+03	1.3111+03	1.3013+03	1.2556+03
13	1.1150+03	2.3000+02	1.3972+03	1.4037+03	1.3922+03	1.3468+03
14	1.1150+03	2.3000+02	1.3974+03	1.4039+03	1.3924+03	1.3471+03
15	1.1150+03	2.3000+02	1.3976+03	1.4039+03	1.3922+03	1.3474+03
16	1.1150+03	9.0000+02	1.2404+03	1.2585+03	1.2487+03	1.1788+03
17	1.1150+03	9.0000+02	1.2404+03	1.2583+03	1.2484+03	1.1788+03
18	1.1150+03	9.0000+02	1.2405+03	1.2584+03	1.2486+03	1.1788+03
*19	1.1150+03	1.5300+03	1.2076+03	1.1964+03	1.1866+03	1.1012+03
*20	1.1150+03	1.5300+03	1.2080+03	1.1964+03	1.1866+03	1.1010+03
*21	1.1150+03	1.5300+03	1.2077+03	1.1964+03	1.1867+03	1.1010+03
*22	1.1150+03	2.0450+03	1.2469+03	1.1868+03	1.1787+03	1.0727+03
*23	1.1150+03	2.0450+03	1.2466+03	1.1870+03	1.1788+03	1.0729+03
*24	1.1150+03	2.0450+03	1.2468+03	1.1873+03	1.1791+03	1.0732+03
25	1.1250+03	2.0000+02	1.2985+03	1.3159+03	1.3057+03	1.2261+03
26	1.1250+03	2.0000+02	1.2987+03	1.3159+03	1.3058+03	1.2261+03
27	1.1250+03	2.0000+02	1.2985+03	1.3159+03	1.3057+03	1.2260+03
28	1.1250+03	4.3000+02	1.3919+03	1.4027+03	1.3910+03	1.3105+03
29	1.1250+03	4.3000+02	1.3919+03	1.4027+03	1.3910+03	1.3105+03
30	1.1250+03	4.3000+02	1.3920+03	1.4029+03	1.3912+03	1.3106+03

\*Subcooled liquid at test section outlet, therefore calculational procedure not valid. Not plotted in Figure 20.

## CONDENSING DATA REDUCTION

	144	146	148	150	152	154
	TC6	TC7	TC8	TC9	TC10	TC11
1	1.1422+03	1.1286+03	1.1317+03	1.1330+03	1.1326+03	1.1529+03
2	1.1422+03	1.1286+03	1.1317+03	1.1328+03	1.1324+03	1.1528+03
3	1.1421+03	1.1285+03	1.1316+03	1.1328+03	1.1325+03	1.1528+03
4	1.1203+03	1.1069+03	1.1067+03	1.1078+03	1.1074+03	1.1349+03
5	1.1204+03	1.1069+03	1.1066+03	1.1077+03	1.1074+03	1.1350+03
6	1.1203+03	1.1068+03	1.1066+03	1.1077+03	1.1074+03	1.1349+03
7	1.1956+03	1.1814+03	1.1838+03	1.1851+03	1.1849+03	1.2109+03
8	1.1959+03	1.1817+03	1.1840+03	1.1853+03	1.1850+03	1.2110+03
9	1.1958+03	1.1817+03	1.1842+03	1.1856+03	1.1853+03	1.2112+03
10	1.2566+03	1.2418+03	1.2448+03	1.2462+03	1.2460+03	1.2724+03
11	1.2567+03	1.2420+03	1.2450+03	1.2464+03	1.2462+03	1.2726+03
12	1.2567+03	1.2420+03	1.2450+03	1.2464+03	1.2462+03	1.2727+03
13	1.3482+03	1.3326+03	1.3359+03	1.3374+03	1.3372+03	1.3657+03
14	1.3486+03	1.3328+03	1.3363+03	1.3378+03	1.3376+03	1.3658+03
15	1.3488+03	1.3332+03	1.3365+03	1.3376+03	1.3377+03	1.3659+03
16	1.1798+03	1.1660+03	1.1634+03	1.1645+03	1.1644+03	1.2041+03
17	1.1798+03	1.1660+03	1.1633+03	1.1646+03	1.1644+03	1.2042+03
18	1.1797+03	1.1660+03	1.1632+03	1.1644+03	1.1643+03	1.2041+03
19	1.1019+03	1.0891+03	1.0852+03	1.0863+03	1.0863+03	1.1231+03
20	1.1017+03	1.0889+03	1.0850+03	1.0861+03	1.0861+03	1.1231+03
21	1.1018+03	1.0889+03	1.0850+03	1.0861+03	1.0862+03	1.1231+03
22	1.0732+03	1.0608+03	1.0514+03	1.0524+03	1.0526+03	1.1144+03
23	1.0734+03	1.0611+03	1.0518+03	1.0528+03	1.0529+03	1.1146+03
24	1.0737+03	1.0612+03	1.0518+03	1.0528+03	1.0529+03	1.1147+03
25	1.2267+03	1.2127+03	1.2056+03	1.2069+03	1.2068+03	1.2621+03
26	1.2267+03	1.2127+03	1.2056+03	1.2069+03	1.2068+03	1.2622+03
27	1.2265+03	1.2126+03	1.2055+03	1.2068+03	1.2068+03	1.2621+03
28	1.3114+03	1.2966+03	1.2874+03	1.2888+03	1.2888+03	1.3532+03
29	1.3112+03	1.2967+03	1.2875+03	1.2891+03	1.2889+03	1.3533+03
30	1.3113+03	1.2967+03	1.2875+03	1.2891+03	1.2889+03	1.3532+03

## CONDENSING DATA REDUCTION

	156	158	160	162	164	166
	TC12	TC13	TC14	TC15	TC16	TC17
1	1.1729+03	1.1628+03	1.1447+03	1.1294+03	1.1710+03	1.1763+03
2	1.1729+03	1.1627+03	1.1445+03	1.1292+03	1.1709+03	1.1762+03
3	1.1728+03	1.1626+03	1.1445+03	1.1292+03	1.1709+03	1.1763+03
4	1.1547+03	1.1434+03	1.1233+03	1.1077+03	1.1601+03	1.1643+03
5	1.1547+03	1.1435+03	1.1234+03	1.1078+03	1.1601+03	1.1642+03
6	1.1546+03	1.1433+03	1.1235+03	1.1077+03	1.1602+03	1.1642+03
7	1.2319+03	1.2200+03	1.1989+03	1.1830+03	1.2253+03	1.2306+03
8	1.2321+03	1.2201+03	1.1988+03	1.1830+03	1.2252+03	1.2306+03
9	1.2322+03	1.2203+03	1.1992+03	1.1833+03	1.2255+03	1.2309+03
10	1.2944+03	1.2819+03	1.2596+03	1.2434+03	1.2835+03	1.2893+03
11	1.2947+03	1.2822+03	1.2598+03	1.2435+03	1.2835+03	1.2893+03
12	1.2947+03	1.2822+03	1.2599+03	1.2437+03	1.2838+03	1.2897+03
13	1.3900+03	1.3759+03	1.3516+03	1.3347+03	1.3748+03	1.3814+03
14	1.3901+03	1.3762+03	1.3519+03	1.3351+03	1.3750+03	1.3816+03
15	1.3903+03	1.3764+03	1.3523+03	1.3355+03	1.3752+03	1.3818+03
16	1.2249+03	1.2103+03	1.1845+03	1.1686+03	1.2226+03	1.2267+03
17	1.2250+03	1.2103+03	1.1844+03	1.1686+03	1.2226+03	1.2265+03
18	1.2248+03	1.2102+03	1.1843+03	1.1684+03	1.2224+03	1.2264+03
19	1.1422+03	1.1288+03	1.1056+03	1.0904+03	1.1510+03	1.1546+03
20	1.1421+03	1.1287+03	1.1056+03	1.0904+03	1.1510+03	1.1546+03
21	1.1422+03	1.1289+03	1.1056+03	1.0905+03	1.1512+03	1.1546+03
22	1.1327+03	1.1135+03	1.0791+03	1.0633+03	1.1253+03	1.1277+03
23	1.1329+03	1.1137+03	1.0793+03	1.0636+03	1.1253+03	1.1278+03
24	1.1330+03	1.1138+03	1.0794+03	1.0637+03	1.1256+03	1.1280+03
25	1.2838+03	1.2656+03	1.2333+03	1.2160+03	1.2767+03	1.2804+03
26	1.2839+03	1.2657+03	1.2334+03	1.2161+03	1.2766+03	1.2803+03
27	1.2838+03	1.2656+03	1.2333+03	1.2161+03	1.2768+03	1.2805+03
28	1.3769+03	1.3560+03	1.3190+03	1.3006+03	1.3626+03	1.3668+03
29	1.3770+03	1.3561+03	1.3191+03	1.3009+03	1.3628+03	1.3669+03
30	1.3769+03	1.3560+03	1.3190+03	1.3007+03	1.3628+03	1.3669+03

## CONDENSING DATA REDUCTION

	168	170	172	174	176	181
	TC18	TC19	TC20	TKI	TKO	TC1C
1	1.1694+03	1.1439+03	1.1417+03	1.1865+03	1.1961+03	1.1865+03
2	1.1693+03	1.1437+03	1.1416+03	1.1867+03	1.1961+03	1.1867+03
3	1.1694+03	1.1438+03	1.1417+03	1.1867+03	1.1961+03	1.1867+03
4	1.1549+03	1.1223+03	1.1200+03	1.1877+03	1.1927+03	1.1877+03
5	1.1550+03	1.1224+03	1.1200+03	1.1878+03	1.1925+03	1.1878+03
6	1.1548+03	1.1223+03	1.1200+03	1.1877+03	1.1926+03	1.1877+03
7	1.2236+03	1.1969+03	1.1946+03	1.2408+03	1.2495+03	1.2408+03
8	1.2236+03	1.1968+03	1.1945+03	1.2412+03	1.2498+03	1.2412+03
9	1.2239+03	1.1972+03	1.1949+03	1.2412+03	1.2498+03	1.2412+03
10	1.2829+03	1.2571+03	1.2548+03	1.3013+03	1.3061+03	1.3013+03
11	1.2830+03	1.2573+03	1.2549+03	1.3016+03	1.3062+03	1.3016+03
12	1.2833+03	1.2575+03	1.2551+03	1.3016+03	1.3062+03	1.3016+03
13	1.3753+03	1.3487+03	1.3459+03	1.3972+03	1.3980+03	1.3972+03
14	1.3755+03	1.3492+03	1.3464+03	1.3974+03	1.3981+03	1.3974+03
15	1.3757+03	1.3494+03	1.3466+03	1.3976+03	1.3981+03	1.3976+03
16	1.2165+03	1.1811+03	1.1783+03	1.2404+03	1.2536+03	1.2404+03
17	1.2163+03	1.1808+03	1.1781+03	1.2404+03	1.2534+03	1.2404+03
18	1.2163+03	1.1807+03	1.1780+03	1.2405+03	1.2535+03	1.2405+03
19	1.1430+03	1.1043+03	1.1015+03	1.2076+03	1.1915+03	1.2076+03
20	1.1430+03	1.1043+03	1.1015+03	1.2080+03	1.1915+03	1.2080+03
21	1.1430+03	1.1042+03	1.1014+03	1.2077+03	1.1916+03	1.2077+03
22	1.1146+03	1.0729+03	1.0704+03	1.2469+03	1.1827+03	1.2469+03
23	1.1147+03	1.0730+03	1.0705+03	1.2466+03	1.1829+03	1.2466+03
24	1.1150+03	1.0733+03	1.0708+03	1.2468+03	1.1832+03	1.2468+03
25	1.2683+03	1.2265+03	1.2235+03	1.2985+03	1.3108+03	1.2985+03
26	1.2682+03	1.2265+03	1.2234+03	1.2987+03	1.3109+03	1.2987+03
27	1.2683+03	1.2265+03	1.2235+03	1.2985+03	1.3108+03	1.2985+03
28	1.3541+03	1.3099+03	1.3066+03	1.3919+03	1.3969+03	1.3919+03
29	1.3541+03	1.3099+03	1.3065+03	1.3919+03	1.3969+03	1.3919+03
30	1.3542+03	1.3100+03	1.3068+03	1.3920+03	1.3970+03	1.3920+03

## CONDENSING DATA REDUCTION

	185	187	189	191	193	195
	TC3C	TC4C	TC5C	TC6C	TC7C	TC8C
1	1.1966+03	1.1954+03	1.1441+03	1.1440+03	1.1434+03	1.1317+03
2	1.1967+03	1.1954+03	1.1442+03	1.1441+03	1.1435+03	1.1317+03
3	1.1967+03	1.1954+03	1.1441+03	1.1439+03	1.1433+03	1.1316+03
4	1.1933+03	1.1919+03	1.1225+03	1.1221+03	1.1215+03	1.1067+03
5	1.1931+03	1.1917+03	1.1224+03	1.1222+03	1.1216+03	1.1066+03
6	1.1931+03	1.1918+03	1.1222+03	1.1221+03	1.1214+03	1.1066+03
7	1.2501+03	1.2492+03	1.1976+03	1.1975+03	1.1969+03	1.1838+03
8	1.2504+03	1.2496+03	1.1979+03	1.1978+03	1.1972+03	1.1840+03
9	1.2504+03	1.2495+03	1.1980+03	1.1977+03	1.1972+03	1.1842+03
10	1.3070+03	1.3061+03	1.2587+03	1.2586+03	1.2580+03	1.2448+03
11	1.3071+03	1.3062+03	1.2587+03	1.2587+03	1.2582+03	1.2450+03
12	1.3072+03	1.3062+03	1.2588+03	1.2587+03	1.2582+03	1.2450+03
13	1.3998+03	1.3980+03	1.3502+03	1.3504+03	1.3499+03	1.3359+03
14	1.4000+03	1.3981+03	1.3506+03	1.3508+03	1.3501+03	1.3363+03
15	1.4000+03	1.3980+03	1.3508+03	1.3510+03	1.3505+03	1.3365+03
16	1.2546+03	1.2531+03	1.1818+03	1.1817+03	1.1813+03	1.1634+03
17	1.2543+03	1.2528+03	1.1818+03	1.1817+03	1.1813+03	1.1633+03
18	1.2544+03	1.2530+03	1.1818+03	1.1816+03	1.1813+03	1.1632+03
19	1.1924+03	1.1904+03	1.1040+03	1.1037+03	1.1035+03	1.0852+03
20	1.1924+03	1.1903+03	1.1038+03	1.1035+03	1.1033+03	1.0850+03
21	1.1924+03	1.1904+03	1.1038+03	1.1035+03	1.1033+03	1.0850+03
22	1.1828+03	1.1823+03	1.0755+03	1.0749+03	1.0749+03	1.0514+03
23	1.1830+03	1.1825+03	1.0756+03	1.0751+03	1.0751+03	1.0518+03
24	1.1833+03	1.1828+03	1.0760+03	1.0754+03	1.0753+03	1.0518+03
25	1.3120+03	1.3106+03	1.2292+03	1.2287+03	1.2286+03	1.2056+03
26	1.3120+03	1.3107+03	1.2292+03	1.2287+03	1.2286+03	1.2056+03
27	1.3119+03	1.3106+03	1.2291+03	1.2285+03	1.2285+03	1.2055+03
28	1.3988+03	1.3967+03	1.3138+03	1.3136+03	1.3135+03	1.2874+03
29	1.3988+03	1.3968+03	1.3138+03	1.3134+03	1.3135+03	1.2875+03
30	1.3990+03	1.3969+03	1.3139+03	1.3134+03	1.3136+03	1.2875+03



# CONDENSING DATA REDUCTION

	197	199	201	203	205	207
	TC9C	TC10C	TC11C	TC12C	TC13C	TC14C
1	1.1323+03	1.1319+03	1.1682+03	1.1688+03	1.1606+03	1.1455+03
2	1.1321+03	1.1317+03	1.1681+03	1.1688+03	1.1605+03	1.1453+03
3	1.1321+03	1.1318+03	1.1681+03	1.1686+03	1.1604+03	1.1453+03
4	1.1071+03	1.1067+03	1.1499+03	1.1506+03	1.1412+03	1.1240+03
5	1.1070+03	1.1067+03	1.1500+03	1.1506+03	1.1413+03	1.1241+03
6	1.1070+03	1.1067+03	1.1499+03	1.1505+03	1.1411+03	1.1241+03
7	1.1845+03	1.1843+03	1.2272+03	1.2276+03	1.2180+03	1.2001+03
8	1.1846+03	1.1844+03	1.2274+03	1.2278+03	1.2181+03	1.2000+03
9	1.1849+03	1.1847+03	1.2275+03	1.2280+03	1.2183+03	1.2004+03
10	1.2456+03	1.2454+03	1.2898+03	1.2901+03	1.2800+03	1.2612+03
11	1.2458+03	1.2456+03	1.2901+03	1.2904+03	1.2803+03	1.2614+03
12	1.2457+03	1.2456+03	1.2902+03	1.2904+03	1.2803+03	1.2615+03
13	1.3368+03	1.3367+03	1.3849+03	1.3855+03	1.3743+03	1.3538+03
14	1.3372+03	1.3371+03	1.3850+03	1.3855+03	1.3745+03	1.3542+03
15	1.3370+03	1.3372+03	1.3851+03	1.3857+03	1.3747+03	1.3545+03
16	1.1638+03	1.1637+03	1.2203+03	1.2207+03	1.2082+03	1.1856+03
17	1.1639+03	1.1638+03	1.2205+03	1.2207+03	1.2083+03	1.1855+03
18	1.1638+03	1.1636+03	1.2203+03	1.2205+03	1.2082+03	1.1853+03
19	1.0855+03	1.0856+03	1.1379+03	1.1381+03	1.1266+03	1.1061+03
20	1.0854+03	1.0854+03	1.1378+03	1.1380+03	1.1265+03	1.1061+03
21	1.0854+03	1.0854+03	1.1379+03	1.1381+03	1.1266+03	1.1061+03
22	1.0516+03	1.0518+03	1.1290+03	1.1286+03	1.1112+03	1.0794+03
23	1.0520+03	1.0521+03	1.1292+03	1.1289+03	1.1114+03	1.0796+03
24	1.0520+03	1.0521+03	1.1293+03	1.1289+03	1.1115+03	1.0798+03
25	1.2062+03	1.2062+03	1.2794+03	1.2795+03	1.2637+03	1.2347+03
26	1.2063+03	1.2062+03	1.2795+03	1.2796+03	1.2638+03	1.2348+03
27	1.2062+03	1.2061+03	1.2794+03	1.2794+03	1.2636+03	1.2347+03
28	1.2882+03	1.2882+03	1.3721+03	1.3724+03	1.3543+03	1.3210+03
29	1.2884+03	1.2884+03	1.3722+03	1.3725+03	1.3544+03	1.3211+03
30	1.2884+03	1.2884+03	1.3721+03	1.3724+03	1.3543+03	1.3210+03

## CONDENSING DATA REDUCTION

	209	211	213	215	217	219
	TC15C	TC16C	TC17C	TC18C	TC19C	TC20C
1	1.1426+03	1.1787+03	1.1750+03	1.1669+03	1.1428+03	1.1416+03
2	1.1424+03	1.1786+03	1.1748+03	1.1668+03	1.1427+03	1.1416+03
3	1.1425+03	1.1786+03	1.1750+03	1.1668+03	1.1427+03	1.1417+03
4	1.1205+03	1.1677+03	1.1630+03	1.1524+03	1.1211+03	1.1197+03
5	1.1206+03	1.1677+03	1.1629+03	1.1525+03	1.1212+03	1.1197+03
6	1.1206+03	1.1678+03	1.1629+03	1.1523+03	1.1211+03	1.1196+03
7	1.1972+03	1.2332+03	1.2294+03	1.2211+03	1.1962+03	1.1952+03
8	1.1972+03	1.2332+03	1.2294+03	1.2211+03	1.1961+03	1.1951+03
9	1.1975+03	1.2335+03	1.2297+03	1.2214+03	1.1965+03	1.1955+03
10	1.2585+03	1.2917+03	1.2883+03	1.2803+03	1.2568+03	1.2562+03
11	1.2587+03	1.2918+03	1.2883+03	1.2804+03	1.2570+03	1.2563+03
12	1.2588+03	1.2921+03	1.2887+03	1.2807+03	1.2572+03	1.2565+03
13	1.3514+03	1.3836+03	1.3807+03	1.3725+03	1.3490+03	1.3484+03
14	1.3518+03	1.3837+03	1.3809+03	1.3728+03	1.3495+03	1.3489+03
15	1.3522+03	1.3840+03	1.3811+03	1.3730+03	1.3497+03	1.3491+03
16	1.1825+03	1.2306+03	1.2255+03	1.2139+03	1.1802+03	1.1787+03
17	1.1825+03	1.2305+03	1.2253+03	1.2137+03	1.1799+03	1.1785+03
18	1.1823+03	1.2304+03	1.2252+03	1.2137+03	1.1799+03	1.1784+03
19	1.1030+03	1.1586+03	1.1532+03	1.1405+03	1.1030+03	1.1010+03
20	1.1030+03	1.1586+03	1.1532+03	1.1405+03	1.1029+03	1.1010+03
21	1.1030+03	1.1588+03	1.1532+03	1.1405+03	1.1029+03	1.1009+03
22	1.0754+03	1.1328+03	1.1262+03	1.1122+03	1.0714+03	1.0695+03
23	1.0757+03	1.1328+03	1.1263+03	1.1122+03	1.0715+03	1.0696+03
24	1.0758+03	1.1331+03	1.1265+03	1.1126+03	1.0717+03	1.0699+03
25	1.2307+03	1.2849+03	1.2794+03	1.2657+03	1.2260+03	1.2244+03
26	1.2308+03	1.2849+03	1.2793+03	1.2656+03	1.2260+03	1.2244+03
27	1.2308+03	1.2850+03	1.2795+03	1.2657+03	1.2260+03	1.2245+03
28	1.3167+03	1.3713+03	1.3660+03	1.3514+03	1.3099+03	1.3086+03
29	1.3170+03	1.3715+03	1.3662+03	1.3514+03	1.3100+03	1.3085+03
30	1.3168+03	1.3714+03	1.3662+03	1.3515+03	1.3100+03	1.3088+03

# CONDENSING DATA REDUCTION

	221	223	226	229	230	235
	TKICC	TKOC	TNAO	TNAI	DTNA	WNA
1	1.1901+03	1.1960+03	1.1438+03	1.1320+03	1.1893+01	4.6438+03
2	1.1903+03	1.1960+03	1.1439+03	1.1318+03	1.2120+01	4.6438+03
3	1.1903+03	1.1960+03	1.1438+03	1.1318+03	1.1964+01	4.6438+03
4	1.1932+03	1.1926+03	1.1220+03	1.1068+03	1.5193+01	4.6422+03
5	1.1933+03	1.1924+03	1.1220+03	1.1068+03	1.5278+01	4.6422+03
6	1.1931+03	1.1925+03	1.1219+03	1.1068+03	1.5122+01	4.6422+03
7	1.2432+03	1.2497+03	1.1973+03	1.1842+03	1.3148+01	4.6238+03
8	1.2437+03	1.2500+03	1.1976+03	1.1843+03	1.3292+01	4.6238+03
9	1.2435+03	1.2499+03	1.1977+03	1.1846+03	1.3078+01	4.6238+03
10	1.3027+03	1.3065+03	1.2584+03	1.2453+03	1.3172+01	4.6008+03
11	1.3030+03	1.3066+03	1.2585+03	1.2455+03	1.3088+01	4.6008+03
12	1.3030+03	1.3067+03	1.2585+03	1.2454+03	1.3102+01	4.6008+03
13	1.3979+03	1.3989+03	1.3502+03	1.3365+03	1.3687+01	4.5160+03
14	1.3980+03	1.3991+03	1.3505+03	1.3369+03	1.3617+01	4.5160+03
15	1.3983+03	1.3990+03	1.3508+03	1.3369+03	1.3875+01	4.5160+03
16	1.2449+03	1.2538+03	1.1816+03	1.1637+03	1.7961+01	4.7026+03
17	1.2449+03	1.2536+03	1.1816+03	1.1637+03	1.7947+01	4.7026+03
18	1.2450+03	1.2537+03	1.1816+03	1.1635+03	1.8047+01	4.7026+03
19	1.2139+03	1.1914+03	1.1037+03	1.0854+03	1.8310+01	4.6759+03
20	1.2143+03	1.1914+03	1.1035+03	1.0852+03	1.8279+01	4.6759+03
21	1.2140+03	1.1914+03	1.1036+03	1.0853+03	1.8266+01	4.6759+03
22	1.2536+03	1.1826+03	1.0751+03	1.0516+03	2.3460+01	4.6752+03
23	1.2533+03	1.1828+03	1.0753+03	1.0520+03	2.3335+01	4.6752+03
24	1.2536+03	1.1831+03	1.0756+03	1.0520+03	2.3574+01	4.6752+03
25	1.3024+03	1.3113+03	1.2288+03	1.2060+03	2.2835+01	4.6054+03
26	1.3026+03	1.3113+03	1.2288+03	1.2060+03	2.2835+01	4.6054+03
27	1.3024+03	1.3113+03	1.2287+03	1.2059+03	2.2778+01	4.6054+03
28	1.3939+03	1.3978+03	1.3136+03	1.2879+03	2.5668+01	4.5219+03
29	1.3939+03	1.3978+03	1.3136+03	1.2881+03	2.5468+01	4.5219+03
30	1.3941+03	1.3979+03	1.3136+03	1.2881+03	2.5526+01	4.5219+03

## CONDENSING DATA REDUCTION

	237	238	240	243	246	247
	TNAM	CPNA	QNA	DTQL	QC	Q/AA
1	1.1379+03	3.0000-01	1.6569+04	1.0486+03	1.9073+04	6.4764+04
2	1.1379+03	3.0000-01	1.6885+04	1.0490+03	1.9390+04	6.5841+04
3	1.1378+03	3.0000-01	1.6667+04	1.0490+03	1.9172+04	6.5100+04
4	1.1144+03	3.0000-01	2.1159+04	1.0220+03	2.3561+04	8.0002+04
5	1.1144+03	3.0000-01	2.1277+04	1.0220+03	2.3679+04	8.0405+04
6	1.1143+03	3.0000-01	2.1060+04	1.0224+03	2.3463+04	7.9670+04
7	1.1908+03	3.0000-01	1.8238+04	1.1166+03	2.1009+04	7.1338+04
8	1.1910+03	3.0000-01	1.8438+04	1.1169+03	2.1210+04	7.2020+04
9	1.1911+03	3.0000-01	1.8142+04	1.1170+03	2.0914+04	7.1015+04
10	1.2518+03	3.0026-01	1.8197+04	1.1822+03	2.1235+04	7.2104+04
11	1.2520+03	3.0026-01	1.8080+04	1.1828+03	2.1120+04	7.1716+04
12	1.2520+03	3.0026-01	1.8099+04	1.1824+03	2.1138+04	7.1776+04
13	1.3433+03	3.0115-01	1.8614+04	1.2710+03	2.2028+04	7.4799+04
14	1.3437+03	3.0116-01	1.8519+04	1.2714+03	2.1935+04	7.4483+04
15	1.3438+03	3.0116-01	1.8871+04	1.2715+03	2.2287+04	7.5679+04
16	1.1726+03	3.0000-01	2.5340+04	1.1008+03	2.8047+04	9.5236+04
17	1.1726+03	3.0000-01	2.5319+04	1.1012+03	2.8029+04	9.5174+04
18	1.1726+03	3.0000-01	2.5460+04	1.1011+03	2.8169+04	9.5650+04
19	1.0946+03	3.0004-01	2.5688+04	1.0160+03	2.8068+04	9.5306+04
20	1.0944+03	3.0004-01	2.5646+04	1.0158+03	2.8025+04	9.5160+04
21	1.0944+03	3.0004-01	2.5627+04	1.0159+03	2.8006+04	9.5096+04
22	1.0634+03	3.0029-01	3.2935+04	9.8880+02	3.5213+04	1.1957+05
23	1.0636+03	3.0029-01	3.2760+04	9.8908+02	3.5038+04	1.1898+05
24	1.0638+03	3.0029-01	3.3095+04	9.8922+02	3.5374+04	1.2012+05
25	1.2174+03	3.0009-01	3.1559+04	1.1442+03	3.4441+04	1.1695+05
26	1.2174+03	3.0009-01	3.1559+04	1.1442+03	3.4441+04	1.1695+05
27	1.2173+03	3.0009-01	3.1479+04	1.1445+03	3.4363+04	1.1668+05
28	1.3008+03	3.0051-01	3.4880+04	1.2262+03	3.8103+04	1.2938+05
29	1.3008+03	3.0051-01	3.4609+04	1.2263+03	3.7832+04	1.2846+05
30	1.3009+03	3.0051-01	3.4687+04	1.2263+03	3.7910+04	1.2873+05

# CONDENSING DATA REDUCTION

	251	306	317	319	324	326
	WK	TWI T	Q/A T	TWO T	HCON T	NUC T
1	2.1986+01	1.1764+03	6.2065+04	1.1352+03	5.0751+03	1.4240-02
2	2.2352+01	1.1765+03	6.2349+04	1.1351+03	5.0497+03	1.4169-02
3	2.2101+01	1.1763+03	6.2092+04	1.1351+03	4.9719+03	1.3950-02
4	2.7159+01	1.1597+03	6.9605+04	1.1133+03	2.3919+03	6.7114-03
5	2.7295+01	1.1598+03	6.9465+04	1.1134+03	2.3873+03	6.6986-03
6	2.7046+01	1.1596+03	6.9235+04	1.1134+03	2.3736+03	6.6600-03
7	2.4423+01	1.2369+03	7.3515+04	1.1887+03	1.2672+04	3.5866-02
8	2.4658+01	1.2371+03	7.3913+04	1.1887+03	1.2290+04	3.4787-02
9	2.4314+01	1.2372+03	7.3514+04	1.1891+03	1.2570+04	3.5579-02
10	2.4920+01	1.2997+03	7.8178+04	1.2491+03	2.8774+04	8.2298-02
11	2.4786+01	1.3000+03	7.8444+04	1.2493+03	2.9956+04	8.5682-02
12	2.4807+01	1.3000+03	7.8242+04	1.2494+03	2.9584+04	8.4618-02
13	2.6286+01	1.3955+03	8.6905+04	1.3406+03	4.5325+04	1.3175-01
14	2.6175+01	1.3955+03	8.6196+04	1.3410+03	4.0750+04	1.1845-01
15	2.6596+01	1.3955+03	8.5685+04	1.3414+03	3.8798+04	1.1278-01
16	3.2620+01	1.2331+03	9.0772+04	1.1735+03	8.8377+03	2.5017-02
17	3.2598+01	1.2332+03	9.1018+04	1.1734+03	9.0279+03	2.5555-02
18	3.2762+01	1.2331+03	9.1072+04	1.1733+03	8.8589+03	2.5077-02
19	3.2401+01	1.1496+03	8.1331+04	1.0952+03	1.4949+03	4.2022-03
20	3.2352+01	1.1495+03	8.1084+04	1.0952+03	1.4783+03	4.1556-03
21	3.2330+01	1.1496+03	8.1295+04	1.0952+03	1.4922+03	4.1947-03
22	4.0749+01	1.1478+03	1.2107+05	1.0665+03	1.4270+03	4.0318-03
23	4.0547+01	1.1480+03	1.2100+05	1.0667+03	1.4328+03	4.0481-03
24	4.0938+01	1.1481+03	1.2100+05	1.0668+03	1.4306+03	4.0420-03
25	4.0434+01	1.2960+03	1.1620+05	1.2206+03	2.1835+04	6.2439-02
26	4.0435+01	1.2960+03	1.1626+05	1.2206+03	2.1795+04	6.2327-02
27	4.0342+01	1.2959+03	1.1609+05	1.2206+03	2.1782+04	6.2288-02
28	4.5446+01	1.3912+03	1.3560+05	1.3050+03	7.5498+04	2.1929-01
29	4.5123+01	1.3912+03	1.3539+05	1.3052+03	7.7232+04	2.2433-01
30	4.5217+01	1.3911+03	1.3549+05	1.3050+03	6.9404+04	2.0159-01

## CONDENSING DATA REDUCTION

	354	365	367	372	374	389
	TWI B	Q/A B	TWO B	HCON B	NUC B	TWI TC
1	1.1886+03	7.3113+04	1.1402+03	1.3704+04	3.8470-02	1.1788+03
2	1.1884+03	7.2968+04	1.1401+03	1.3034+04	3.6591-02	1.1788+03
3	1.1885+03	7.2965+04	1.1402+03	1.3271+04	3.7257-02	1.1786+03
4	1.1816+03	9.6303+04	1.1175+03	9.5904+03	2.6917-02	1.1620+03
5	1.1815+03	9.6024+04	1.1176+03	9.6245+03	2.7012-02	1.1620+03
6	1.1815+03	9.6276+04	1.1175+03	9.6829+03	2.7176-02	1.1619+03
7	1.2436+03	7.7186+04	1.1931+03	1.9371+04	5.4873-02	1.2395+03
8	1.2436+03	7.7245+04	1.1930+03	1.7859+04	5.0594-02	1.2397+03
9	1.2438+03	7.7048+04	1.1934+03	1.9023+04	5.3889-02	1.2398+03
10	1.3014+03	7.4060+04	1.2535+03	2.0214+04	5.7840-02	1.3025+03
11	1.3013+03	7.3857+04	1.2536+03	1.9282+04	5.5175-02	1.3029+03
12	1.3017+03	7.4119+04	1.2539+03	2.1216+04	6.0710-02	1.3029+03
13	1.3935+03	7.6907+04	1.3449+03	1.7669+04	5.1363-02	1.3987+03
14	1.3935+03	7.6066+04	1.3454+03	1.6892+04	4.9106-02	1.3987+03
15	1.3937+03	7.6137+04	1.3456+03	1.7940+04	5.2152-02	1.3988+03
16	1.2458+03	1.0688+05	1.1757+03	2.1779+04	6.1729-02	1.2357+03
17	1.2457+03	1.0711+05	1.1754+03	2.2361+04	6.3378-02	1.2358+03
18	1.2456+03	1.0709+05	1.1754+03	2.1418+04	6.0705-02	1.2357+03
19	1.1760+03	1.1637+05	1.0984+03	6.1074+03	1.7147-02	1.1519+03
20	1.1761+03	1.1644+05	1.0984+03	6.1019+03	1.7132-02	1.1517+03
21	1.1762+03	1.1676+05	1.0983+03	6.1541+03	1.7279-02	1.1519+03
22	1.1517+03	1.2670+05	1.0666+03	2.7946+03	7.8477-03	1.1501+03
23	1.1517+03	1.2664+05	1.0667+03	2.7911+03	7.8380-03	1.1503+03
24	1.1520+03	1.2664+05	1.0670+03	2.7925+03	7.8420-03	1.1504+03
25	1.3036+03	1.2864+05	1.2202+03	2.8527+04	8.1671-02	1.2989+03
26	1.3035+03	1.2847+05	1.2202+03	2.7475+04	7.8662-02	1.2990+03
27	1.3037+03	1.2874+05	1.2202+03	2.9348+04	8.4021-02	1.2988+03
28	1.3911+03	1.3829+05	1.3032+03	2.9819+04	8.6652-02	1.3945+03
29	1.3914+03	1.3879+05	1.3031+03	3.1595+04	9.1814-02	1.3945+03
30	1.3913+03	1.3832+05	1.3033+03	2.9893+04	8.6870-02	1.3945+03

# CONDENSING DATA REDUCTION

	399	401	405	406	408	424
	Q/A TC	TWO TC	TKC-TW	HCONTC	NUC TC	TWI BC
1	5.6217+04	1.1415+03	1.2612+01	4.4574+03	1.2510-02	1.1920+03
2	5.6504+04	1.1413+03	1.2822+01	4.4067+03	1.2368-02	1.1918+03
3	5.6246+04	1.1414+03	1.2897+01	4.3613+03	1.2241-02	1.1919+03
*4	6.4091+04	1.1193+03	3.1042+01	2.0646+03	5.7955-03	1.1850+03
*5	6.3949+04	1.1194+03	3.1081+01	2.0575+03	5.7756-03	1.1849+03
*6	6.3718+04	1.1194+03	3.1076+01	2.0504+03	5.7555-03	1.1850+03
7	6.7071+04	1.1956+03	5.1246+00	1.3088+04	3.7056-02	1.2469+03
8	6.7472+04	1.1956+03	5.3654+00	1.2575+04	3.5608-02	1.2469+03
9	6.7066+04	1.1959+03	5.1449+00	1.3036+04	3.6910-02	1.2472+03
10	7.0981+04	1.2567+03	1.0125+00	7.0107+04	2.0056-01	1.3047+03
11	7.1247+04	1.2569+03	8.9740-01	7.9393+04	2.2713-01	1.3047+03
12	7.1042+04	1.2570+03	9.2558-01	7.6754+04	2.1958-01	1.3050+03
13	7.8536+04	1.3492+03	-6.4943-01	-1.2093+05	-3.5155-01	1.3968+03
14	7.7816+04	1.3496+03	-4.5531-01	-1.7091+05	-4.9685-01	1.3968+03
15	7.7295+04	1.3500+03	-3.4555-01	-2.2369+05	-6.5030-01	1.3970+03
16	8.4657+04	1.1802+03	1.1208+01	7.5530+03	2.1394-02	1.2492+03
17	8.4905+04	1.1801+03	1.1012+01	7.7100+03	2.1838-02	1.2491+03
18	8.4962+04	1.1800+03	1.1247+01	7.5542+03	2.1397-02	1.2490+03
*19	7.6133+04	1.1010+03	5.7049+01	1.3345+03	3.7546-03	1.1795+03
*20	7.5884+04	1.1010+03	5.7459+01	1.3207+03	3.7158-03	1.1795+03
*21	7.6095+04	1.1010+03	5.7095+01	1.3328+03	3.7497-03	1.1797+03
*22	1.1652+05	1.0719+03	8.7710+01	1.3284+03	3.7567-03	1.1552+03
*23	1.1644+05	1.0722+03	8.7277+01	1.3341+03	3.7726-03	1.1552+03
*24	1.1643+05	1.0723+03	8.7500+01	1.3307+03	3.7631-03	1.1555+03
25	1.0968+05	1.2278+03	5.5507+00	1.9759+04	5.6534-02	1.3070+03
26	1.0973+05	1.2279+03	5.5588+00	1.9740+04	5.6481-02	1.3069+03
27	1.0956+05	1.2278+03	5.5453+00	1.9758+04	5.6530-02	1.3071+03
28	1.2811+05	1.3132+03	3.0226-01	4.2385+05	1.2315+00	1.3945+03
29	1.2790+05	1.3134+03	2.3526-01	5.4366+05	1.5796+00	1.3948+03
30	1.2801+05	1.3132+03	4.3967-01	2.9114+05	8.4592-01	1.3947+03

\*Subcooled liquid at test section outlet, therefore calculational procedure not valid. Not plotted in Figure 20.

## CONDENSING DATA REDUCTION

	434	436	439	440	442	450
	Q/A BC	TWO BC	TK-TWI	HCONBC	NUC BC	PSI HD
1	8.0450+04	1.1387+03	2.6751+00	3.0073+04	8.4431-02	6.6014-01
2	8.0305+04	1.1386+03	2.9648+00	2.7086+04	7.6045-02	6.8108-01
3	8.0300+04	1.1387+03	2.8450+00	2.8225+04	7.9241-02	6.6620-01
*4	1.0401+05	1.1158+03	7.7417+00	1.3436+04	3.7713-02	9.8805-01
*5	1.0373+05	1.1159+03	7.6886+00	1.3492+04	3.7871-02	9.9715-01
*6	1.0399+05	1.1158+03	7.6319+00	1.3626+04	3.8246-02	9.8036-01
7	8.3844+04	1.1921+03	1.3064+00	6.4180+04	1.8183-01	5.9613-01
8	8.3903+04	1.1920+03	1.6564+00	5.0655+04	1.4352-01	6.0589-01
9	8.3700+04	1.1924+03	1.3662+00	6.1266+04	1.7358-01	5.8962-01
10	7.9889+04	1.2531+03	1.0043+00	7.9545+04	2.2764-01	4.4788-01
11	7.9684+04	1.2532+03	1.1674+00	6.8260+04	1.9535-01	4.4243-01
12	7.9943+04	1.2534+03	8.3080-01	9.6225+04	2.7538-01	4.4317-01
13	8.1473+04	1.3453+03	1.9262+00	4.2298+04	1.2298-01	3.0919-01
14	8.0621+04	1.3458+03	2.0773+00	3.8810+04	1.1284-01	3.0636-01
15	8.0689+04	1.3461+03	1.8225+00	4.4274+04	1.2872-01	3.1593-01
16	1.1388+05	1.1745+03	2.6413+00	4.3116+04	1.2223-01	1.0529+00
17	1.1411+05	1.1743+03	2.5205+00	4.5274+04	1.2834-01	1.0515+00
18	1.1409+05	1.1742+03	2.7417+00	4.1614+04	1.1797-01	1.0616+00
*19	1.2440+05	1.0965+03	1.6895+01	7.3633+03	2.0676-02	1.2425+00
*20	1.2447+05	1.0965+03	1.6912+01	7.3597+03	2.0666-02	1.2362+00
*21	1.2479+05	1.0964+03	1.6805+01	7.4260+03	2.0852-02	1.2367+00
*22	1.3516+05	1.0644+03	4.3195+01	3.1291+03	8.7883-03	1.5646+00
*23	1.3511+05	1.0645+03	4.3222+01	3.1259+03	8.7792-03	1.5522+00
*24	1.3511+05	1.0648+03	4.3229+01	3.1253+03	8.7780-03	1.5793+00
25	1.3512+05	1.2194+03	2.3108+00	5.8473+04	1.6744-01	1.1806+00
26	1.3495+05	1.2194+03	2.4767+00	5.4490+04	1.5604-01	1.1798+00
27	1.3522+05	1.2195+03	2.1841+00	6.1912+04	1.7729-01	1.1756+00
28	1.4367+05	1.3032+03	2.3954+00	5.9975+04	1.7432-01	9.4154-01
29	1.4417+05	1.3032+03	2.1424+00	6.7293+04	1.9559-01	9.2834-01
30	1.4370+05	1.3034+03	2.3801+00	6.0375+04	1.7548-01	9.3161-01

\*Subcooled liquid at test section outlet, therefore calculational procedure not valid. Not plotted in Figure 20.



# CONDENSING DATA REDUCTION

	451	452	453	610	611	613
	PI	PO	DPC	PIC	POC	DPCC
1	4.3932+00	4.6766+00	-2.8340-01	4.4939+00	4.6739+00	-1.7998-01
2	4.3981+00	4.6778+00	-2.7979-01	4.5027+00	4.6752+00	-1.7247-01
3	4.3981+00	4.6778+00	-2.7979-01	4.5001+00	4.6752+00	-1.7512-01
4	4.4275+00	4.5745+00	-1.4700-01	4.5889+00	4.5713+00	1.7556-02
5	4.4299+00	4.5680+00	-1.3809-01	4.5930+00	4.5648+00	2.8248-02
6	4.4262+00	4.5699+00	-1.4370-01	4.5862+00	4.5668+00	1.9420-02
7	6.2034+00	6.5435+00	-3.4009-01	6.2976+00	6.5506+00	-2.5296-01
8	6.2217+00	6.5552+00	-3.3342-01	6.3174+00	6.5623+00	-2.4491-01
9	6.2184+00	6.5543+00	-3.3592-01	6.3113+00	6.5615+00	-2.5016-01
10	8.8905+00	9.1363+00	-2.4586-01	8.9603+00	9.1605+00	-2.0010-01
11	8.9060+00	9.1419+00	-2.3589-01	8.9749+00	9.1660+00	-1.9116-01
12	8.9060+00	9.1441+00	-2.3811-01	8.9750+00	9.1682+00	-1.9326-01
13	1.4966+01	1.5023+01	-5.7085-02	1.5013+01	1.5094+01	-8.0385-02
14	1.4979+01	1.5035+01	-5.5501-02	1.5026+01	1.5105+01	-7.9352-02
15	1.4995+01	1.5030+01	-3.4143-02	1.5044+01	1.5100+01	-5.6413-02
16	6.1901+00	6.7123+00	-5.2225-01	6.3659+00	6.7206+00	-3.5467-01
17	6.1901+00	6.7009+00	-5.1087-01	6.3656+00	6.7091+00	-3.4348-01
18	6.1917+00	6.7071+00	-5.1533-01	6.3691+00	6.7153+00	-3.4618-01
19	5.0372+00	4.5383+00	4.9895-01	5.2459+00	4.5349+00	7.1098-01
20	5.0495+00	4.5370+00	5.1250-01	5.2572+00	4.5336+00	7.2364-01
21	5.0400+00	4.5396+00	5.0039-01	5.2475+00	4.5362+00	7.1136-01
22	6.4418+00	4.2841+00	2.1577+00	6.7114+00	4.2797+00	2.4317+00
23	6.4301+00	4.2896+00	2.1405+00	6.6972+00	4.2853+00	2.4119+00
24	6.4385+00	4.2976+00	2.1409+00	6.7109+00	4.2933+00	2.4176+00
25	8.7499+00	9.3841+00	-6.3425-01	8.9487+00	9.4106+00	-4.6194-01
26	8.7562+00	9.3864+00	-6.3022-01	8.9550+00	9.4129+00	-4.5790-01
27	8.7478+00	9.3818+00	-6.3405-01	8.9456+00	9.4083+00	-4.6273-01
28	1.4555+01	1.4937+01	-3.8205-01	1.4715+01	1.5007+01	-2.9234-01
29	1.4555+01	1.4937+01	-3.8204-01	1.4713+01	1.5007+01	-2.9474-01
30	1.4565+01	1.4949+01	-3.8373-01	1.4723+01	1.5019+01	-2.9599-01

## CONDENSING DATA REDUCTION

	700	495	701	498	504	507
	X B	WKL B	X T	WKL T	NREF T	NREF B
1	2.6578-01	1.6143+01	8.1878-01	3.9843+00	4.5304+02	1.8393+03
2	2.6470-01	1.6436+01	8.1778-01	4.0731+00	4.6320+02	1.8728+03
3	2.6489-01	1.6247+01	8.1797-01	4.0231+00	4.5750+02	1.8513+03
4	2.3800-01	2.0695+01	7.9302-01	5.6214+00	6.3986+02	2.3552+03
5	2.3734-01	2.0817+01	7.9239-01	5.6668+00	6.4505+02	2.3688+03
6	2.3779-01	2.0615+01	7.9282-01	5.6033+00	6.3776+02	2.3458+03
7	2.6963-01	1.7838+01	8.2216-01	4.3433+00	5.1003+02	2.0990+03
8	2.6867-01	1.8033+01	8.2128-01	4.4068+00	5.1762+02	2.1224+03
9	2.6923-01	1.7768+01	8.2180-01	4.3326+00	5.0887+02	2.0911+03
10	2.5966-01	1.8449+01	8.1303-01	4.6593+00	5.6552+02	2.2421+03
11	2.5872-01	1.8374+01	8.1218-01	4.6555+00	5.6514+02	2.2331+03
12	2.5890-01	1.8384+01	8.1234-01	4.6552+00	5.6511+02	2.2345+03
13	2.4788-01	1.9770+01	8.0219-01	5.1995+00	6.6361+02	2.5240+03
14	2.4782-01	1.9688+01	8.0213-01	5.1792+00	6.6108+02	2.5139+03
15	2.4723-01	2.0021+01	8.0157-01	5.2773+00	6.7367+02	2.5563+03
16	2.6933-01	2.3834+01	8.2190-01	5.8095+00	6.8311+02	2.8106+03
17	2.6844-01	2.3848+01	8.2109-01	5.8321+00	6.8573+02	2.8118+03
18	2.6863-01	2.3961+01	8.2126-01	5.8558+00	6.8856+02	2.8254+03
19	2.2300-01	2.5175+01	7.7856-01	7.1748+00	8.2491+02	2.8717+03
20	2.2316-01	2.5132+01	7.7872-01	7.1588+00	8.2320+02	2.8668+03
21	2.2302-01	2.5120+01	7.7858-01	7.1584+00	8.2305+02	2.8654+03
22	2.7489-01	2.9548+01	8.3356-01	6.7825+00	7.9336+02	3.3746+03
23	2.7438-01	2.9422+01	8.3299-01	6.7717+00	7.9199+02	3.3603+03
24	2.7340-01	2.9746+01	8.3194-01	6.8802+00	8.0482+02	3.3979+03
25	2.6649-01	2.9659+01	8.1921-01	7.3100+00	8.8772+02	3.6123+03
26	2.6623-01	2.9670+01	8.1897-01	7.3198+00	8.8896+02	3.6138+03
27	2.6646-01	2.9592+01	8.1919-01	7.2943+00	8.8577+02	3.6041+03
28	2.5415-01	3.3896+01	8.0791-01	8.7298+00	1.1122+03	4.3234+03
29	2.5405-01	3.3659+01	8.0782-01	8.6715+00	1.1047+03	4.2932+03
30	2.5410-01	3.3727+01	8.0787-01	8.6875+00	1.1069+03	4.3022+03

# CONDENSING DATA REDUCTION

	131	132	134	138	140	142
	DATE	TIME	TC1	TC3	TC4	TC5
1	1.1250+03	8.0000+02	1.4016+03	1.4161+03	1.4042+03	1.2941+03
2	1.1250+03	8.0000+02	1.4016+03	1.4161+03	1.4043+03	1.2941+03
3	1.1250+03	8.0000+02	1.4015+03	1.4159+03	1.4039+03	1.2941+03
4	1.1250+03	1.4450+03	1.3020+03	1.3221+03	1.3111+03	1.2146+03
5	1.1250+03	1.4450+03	1.3023+03	1.3222+03	1.3110+03	1.2147+03
6	1.1250+03	1.4450+03	1.3015+03	1.3224+03	1.3113+03	1.2147+03
7	1.1250+03	1.6300+03	1.3026+03	1.3194+03	1.3089+03	1.1951+03
8	1.1250+03	1.6300+03	1.3030+03	1.3193+03	1.3087+03	1.1950+03
9	1.1250+03	1.6300+03	1.3028+03	1.3194+03	1.3088+03	1.1950+03
*10	1.1250+03	2.0300+03	1.3103+03	1.2409+03	1.2311+03	1.0873+03
*11	1.1250+03	2.0300+03	1.3102+03	1.2402+03	1.2305+03	1.0866+03
*12	1.1250+03	2.0300+03	1.3102+03	1.2399+03	1.2302+03	1.0863+03
13	1.1350+03	2.4000+02	1.4084+03	1.4245+03	1.4123+03	1.2726+03
14	1.1350+03	2.4000+02	1.4087+03	1.4244+03	1.4121+03	1.2728+03
15	1.1350+03	2.4000+02	1.4085+03	1.4246+03	1.4122+03	1.2729+03
*16	1.1350+03	4.4500+02	1.4053+03	1.4079+03	1.3958+03	1.2081+03
*17	1.1350+03	4.4500+02	1.4053+03	1.4077+03	1.3956+03	1.2079+03
*18	1.1350+03	4.4500+02	1.4051+03	1.4073+03	1.3953+03	1.2075+03
19	1.1350+03	1.6000+03	1.3549+03	1.3733+03	1.3614+03	1.2388+03
20	1.1350+03	1.6000+03	1.3547+03	1.3732+03	1.3615+03	1.2385+03
21	1.1350+03	1.6000+03	1.3547+03	1.3733+03	1.3614+03	1.2385+03
22	1.1350+03	2.0000+03	1.3551+03	1.3697+03	1.3587+03	1.2711+03
23	1.1350+03	2.0000+03	1.3550+03	1.3697+03	1.3587+03	1.2708+03
24	1.1350+03	2.0000+03	1.3550+03	1.3697+03	1.3587+03	1.2709+03
25	1.1350+03	2.2450+03	1.3556+03	1.3641+03	1.3531+03	1.2988+03
26	1.1350+03	2.2450+03	1.3559+03	1.3641+03	1.3531+03	1.2990+03
27	1.1350+03	2.2450+03	1.3558+03	1.3644+03	1.3534+03	1.2991+03
28	1.1450+03	3.0000+01	1.3012+03	1.3135+03	1.3033+03	1.2447+03
29	1.1450+03	3.0000+01	1.3016+03	1.3134+03	1.3033+03	1.2448+03
30	1.1450+03	3.0000+01	1.3014+03	1.3133+03	1.3032+03	1.2446+03

\* Subcooled liquid at test section outlet, therefore calculational procedure not valid. Not plotted in Figure 20.

## CONDENSING DATA REDUCTION

	144	146	148	150	152	154
	TC6	TC7	TC8	TC9	TC10	TC11
1	1.2947+03	1.2806+03	1.2615+03	1.2633+03	1.2626+03	1.3578+03
2	1.2946+03	1.2805+03	1.2614+03	1.2632+03	1.2626+03	1.3577+03
3	1.2945+03	1.2804+03	1.2614+03	1.2635+03	1.2626+03	1.3573+03
4	1.2150+03	1.2017+03	1.1891+03	1.1903+03	1.1903+03	1.2615+03
5	1.2150+03	1.2017+03	1.1889+03	1.1902+03	1.1902+03	1.2615+03
6	1.2150+03	1.2018+03	1.1889+03	1.1904+03	1.1903+03	1.2616+03
7	1.1954+03	1.1823+03	1.1650+03	1.1664+03	1.1664+03	1.2515+03
8	1.1954+03	1.1821+03	1.1649+03	1.1662+03	1.1664+03	1.2515+03
9	1.1952+03	1.1822+03	1.1649+03	1.1662+03	1.1661+03	1.2514+03
10	1.0875+03	1.0758+03	1.0518+03	1.0530+03	1.0531+03	1.1697+03
11	1.0866+03	1.0750+03	1.0512+03	1.0525+03	1.0527+03	1.1693+03
12	1.0865+03	1.0747+03	1.0509+03	1.0521+03	1.0522+03	1.1685+03
13	1.2728+03	1.2593+03	1.2297+03	1.2315+03	1.2313+03	1.3584+03
14	1.2729+03	1.2594+03	1.2295+03	1.2311+03	1.2310+03	1.3584+03
15	1.2728+03	1.2593+03	1.2295+03	1.2311+03	1.2310+03	1.3583+03
16	1.2075+03	1.1952+03	1.1509+03	1.1526+03	1.1525+03	1.3229+03
17	1.2074+03	1.1950+03	1.1504+03	1.1523+03	1.1522+03	1.3206+03
18	1.2069+03	1.1944+03	1.1506+03	1.1521+03	1.1524+03	1.3217+03
19	1.2388+03	1.2257+03	1.2029+03	1.2044+03	1.2044+03	1.3095+03
20	1.2386+03	1.2256+03	1.2026+03	1.2041+03	1.2042+03	1.3096+03
21	1.2385+03	1.2253+03	1.2027+03	1.2042+03	1.2042+03	1.3093+03
22	1.2712+03	1.2574+03	1.2459+03	1.2475+03	1.2476+03	1.3172+03
23	1.2710+03	1.2576+03	1.2463+03	1.2476+03	1.2478+03	1.3172+03
24	1.2712+03	1.2576+03	1.2463+03	1.2476+03	1.2478+03	1.3174+03
25	1.2996+03	1.2856+03	1.2851+03	1.2864+03	1.2865+03	1.3239+03
26	1.2998+03	1.2856+03	1.2851+03	1.2868+03	1.2868+03	1.3240+03
27	1.3000+03	1.2859+03	1.2855+03	1.2867+03	1.2869+03	1.3240+03
28	1.2455+03	1.2318+03	1.2300+03	1.2313+03	1.2314+03	1.2702+03
29	1.2455+03	1.2318+03	1.2300+03	1.2312+03	1.2313+03	1.2703+03
30	1.2453+03	1.2318+03	1.2298+03	1.2311+03	1.2313+03	1.2702+03

## CONDENSING DATA REDUCTION

	156	158	160	162	164	166
	TC12	TC13	TC14	TC15	TC16	TC17
1	1.3820+03	1.3542+03	1.3057+03	1.2862+03	1.3656+03	1.3677+03
2	1.3819+03	1.3541+03	1.3056+03	1.2862+03	1.3657+03	1.3678+03
3	1.3819+03	1.3541+03	1.3055+03	1.2862+03	1.3656+03	1.3679+03
4	1.2832+03	1.2616+03	1.2239+03	1.2061+03	1.2762+03	1.2797+03
5	1.2832+03	1.2616+03	1.2240+03	1.2062+03	1.2764+03	1.2799+03
6	1.2833+03	1.2617+03	1.2239+03	1.2061+03	1.2761+03	1.2797+03
7	1.2729+03	1.2486+03	1.2056+03	1.1873+03	1.2669+03	1.2683+03
8	1.2731+03	1.2486+03	1.2057+03	1.1874+03	1.2670+03	1.2683+03
9	1.2728+03	1.2484+03	1.2055+03	1.1872+03	1.2668+03	1.2682+03
10	1.1899+03	1.1570+03	1.0995+03	1.0813+03	1.1636+03	1.1638+03
11	1.1893+03	1.1565+03	1.0990+03	1.0810+03	1.1630+03	1.1632+03
12	1.1887+03	1.1560+03	1.0986+03	1.0805+03	1.1625+03	1.1626+03
13	1.3819+03	1.3479+03	1.2875+03	1.2669+03	1.3637+03	1.3641+03
14	1.3819+03	1.3480+03	1.2876+03	1.2669+03	1.3636+03	1.3640+03
15	1.3817+03	1.3478+03	1.2874+03	1.2668+03	1.3636+03	1.3641+03
16	1.3450+03	1.3019+03	1.2261+03	1.2040+03	1.3282+03	1.3258+03
17	1.3426+03	1.3006+03	1.2255+03	1.2033+03	1.3270+03	1.3247+03
18	1.3438+03	1.3009+03	1.2253+03	1.2032+03	1.3275+03	1.3252+03
19	1.3322+03	1.3029+03	1.2515+03	1.2320+03	1.3182+03	1.3194+03
20	1.3324+03	1.3029+03	1.2514+03	1.2319+03	1.3182+03	1.3193+03
21	1.3321+03	1.3027+03	1.2512+03	1.2316+03	1.3182+03	1.3191+03
22	1.3399+03	1.3181+03	1.2800+03	1.2619+03	1.3277+03	1.3315+03
23	1.3399+03	1.3181+03	1.2801+03	1.2619+03	1.3276+03	1.3313+03
24	1.3401+03	1.3182+03	1.2801+03	1.2620+03	1.3277+03	1.3314+03
25	1.3466+03	1.3315+03	1.3051+03	1.2882+03	1.3330+03	1.3391+03
26	1.3465+03	1.3317+03	1.3052+03	1.2883+03	1.3330+03	1.3391+03
27	1.3467+03	1.3316+03	1.3052+03	1.2883+03	1.3330+03	1.3391+03
28	1.2917+03	1.2769+03	1.2508+03	1.2343+03	1.2813+03	1.2868+03
29	1.2917+03	1.2770+03	1.2507+03	1.2343+03	1.2812+03	1.2867+03
30	1.2917+03	1.2770+03	1.2509+03	1.2344+03	1.2812+03	1.2866+03

## CONDENSING DATA REDUCTION

	168	170	172	174	176	181
	TC18	TC19	TC20	TKI	TKO	TC1C
1	1.3499+03	1.2914+03	1.2873+03	1.4016+03	1.4101+03	1.4016+03
2	1.3499+03	1.2912+03	1.2873+03	1.4016+03	1.4102+03	1.4016+03
3	1.3499+03	1.2912+03	1.2874+03	1.4015+03	1.4099+03	1.4015+03
4	1.2646+03	1.2144+03	1.2109+03	1.3020+03	1.3166+03	1.3020+03
5	1.2647+03	1.2145+03	1.2110+03	1.3023+03	1.3166+03	1.3023+03
6	1.2647+03	1.2144+03	1.2110+03	1.3015+03	1.3169+03	1.3015+03
7	1.2509+03	1.1938+03	1.1902+03	1.3026+03	1.3142+03	1.3026+03
8	1.2509+03	1.1938+03	1.1902+03	1.3030+03	1.3140+03	1.3030+03
9	1.2507+03	1.1937+03	1.1900+03	1.3028+03	1.3141+03	1.3028+03
10	1.1442+03	1.0834+03	1.0795+03	1.3103+03	1.2360+03	1.3103+03
11	1.1437+03	1.0829+03	1.0793+03	1.3102+03	1.2353+03	1.3102+03
12	1.1430+03	1.0825+03	1.0786+03	1.3102+03	1.2350+03	1.3102+03
13	1.3406+03	1.2676+03	1.2632+03	1.4084+03	1.4184+03	1.4084+03
14	1.3405+03	1.2676+03	1.2630+03	1.4087+03	1.4183+03	1.4087+03
15	1.3406+03	1.2676+03	1.2633+03	1.4085+03	1.4184+03	1.4085+03
16	1.2947+03	1.2001+03	1.1950+03	1.4053+03	1.4018+03	1.4053+03
17	1.2938+03	1.1999+03	1.1945+03	1.4053+03	1.4016+03	1.4053+03
18	1.2941+03	1.1999+03	1.1946+03	1.4051+03	1.4013+03	1.4051+03
19	1.2994+03	1.2359+03	1.2318+03	1.3549+03	1.3673+03	1.3549+03
20	1.2994+03	1.2354+03	1.2315+03	1.3547+03	1.3673+03	1.3547+03
21	1.2991+03	1.2354+03	1.2317+03	1.3547+03	1.3673+03	1.3547+03
22	1.3172+03	1.2703+03	1.2670+03	1.3551+03	1.3642+03	1.3551+03
23	1.3171+03	1.2702+03	1.2669+03	1.3550+03	1.3642+03	1.3550+03
24	1.3172+03	1.2700+03	1.2668+03	1.3550+03	1.3642+03	1.3550+03
25	1.3308+03	1.3005+03	1.2977+03	1.3556+03	1.3586+03	1.3556+03
26	1.3309+03	1.3007+03	1.2979+03	1.3559+03	1.3586+03	1.3559+03
27	1.3309+03	1.3006+03	1.2979+03	1.3558+03	1.3589+03	1.3558+03
28	1.2778+03	1.2460+03	1.2433+03	1.3012+03	1.3084+03	1.3012+03
29	1.2777+03	1.2459+03	1.2433+03	1.3016+03	1.3084+03	1.3016+03
30	1.2776+03	1.2459+03	1.2432+03	1.3014+03	1.3082+03	1.3014+03

# CONDENSING DATA REDUCTION

	185	187	189	191	193	195
	TC3C	TC4C	TC5C	TC6C	TC7C	TC8C
1	1.4122+03	1.4101+03	1.2974+03	1.2968+03	1.2973+03	1.2615+03
2	1.4122+03	1.4101+03	1.2974+03	1.2967+03	1.2972+03	1.2614+03
3	1.4120+03	1.4098+03	1.2974+03	1.2966+03	1.2970+03	1.2614+03
4	1.3182+03	1.3161+03	1.2177+03	1.2169+03	1.2174+03	1.1891+03
5	1.3183+03	1.3159+03	1.2178+03	1.2170+03	1.2174+03	1.1889+03
6	1.3185+03	1.3163+03	1.2179+03	1.2170+03	1.2175+03	1.1889+03
7	1.3155+03	1.3138+03	1.1981+03	1.1974+03	1.1978+03	1.1650+03
8	1.3153+03	1.3137+03	1.1981+03	1.1974+03	1.1976+03	1.1649+03
9	1.3155+03	1.3137+03	1.1981+03	1.1971+03	1.1977+03	1.1649+03
10	1.2369+03	1.2352+03	1.0901+03	1.0892+03	1.0900+03	1.0518+03
11	1.2363+03	1.2346+03	1.0894+03	1.0883+03	1.0892+03	1.0512+03
12	1.2360+03	1.2343+03	1.0891+03	1.0882+03	1.0889+03	1.0509+03
13	1.4206+03	1.4182+03	1.2759+03	1.2749+03	1.2757+03	1.2297+03
14	1.4205+03	1.4181+03	1.2760+03	1.2750+03	1.2759+03	1.2295+03
15	1.4207+03	1.4182+03	1.2761+03	1.2748+03	1.2757+03	1.2295+03
16	1.4040+03	1.4016+03	1.2112+03	1.2095+03	1.2108+03	1.1509+03
17	1.4037+03	1.4014+03	1.2110+03	1.2093+03	1.2106+03	1.1504+03
18	1.4034+03	1.4011+03	1.2106+03	1.2089+03	1.2101+03	1.1506+03
19	1.3694+03	1.3669+03	1.2419+03	1.2409+03	1.2417+03	1.2029+03
20	1.3693+03	1.3669+03	1.2417+03	1.2406+03	1.2416+03	1.2026+03
21	1.3694+03	1.3669+03	1.2417+03	1.2405+03	1.2414+03	1.2027+03
22	1.3657+03	1.3641+03	1.2743+03	1.2732+03	1.2738+03	1.2459+03
23	1.3657+03	1.3641+03	1.2741+03	1.2731+03	1.2740+03	1.2463+03
24	1.3658+03	1.3641+03	1.2741+03	1.2733+03	1.2740+03	1.2463+03
25	1.3601+03	1.3585+03	1.3021+03	1.3017+03	1.3023+03	1.2851+03
26	1.3602+03	1.3585+03	1.3023+03	1.3019+03	1.3023+03	1.2851+03
27	1.3605+03	1.3588+03	1.3024+03	1.3022+03	1.3026+03	1.2855+03
28	1.3095+03	1.3082+03	1.2479+03	1.2475+03	1.2479+03	1.2300+03
29	1.3095+03	1.3082+03	1.2480+03	1.2475+03	1.2479+03	1.2300+03
30	1.3094+03	1.3080+03	1.2478+03	1.2473+03	1.2478+03	1.2298+03

## CONDENSING DATA REDUCTION

	197	199	201	203	205	207
	TC9C	TC10C	TC11C	TC12C	TC13C	TC14C
1	1.2627+03	1.2620+03	1.3768+03	1.3774+03	1.3525+03	1.3076+03
2	1.2625+03	1.2620+03	1.3767+03	1.3773+03	1.3524+03	1.3075+03
3	1.2628+03	1.2621+03	1.3763+03	1.3773+03	1.3523+03	1.3074+03
4	1.1897+03	1.1896+03	1.2787+03	1.2788+03	1.2596+03	1.2253+03
5	1.1895+03	1.1895+03	1.2787+03	1.2788+03	1.2597+03	1.2254+03
6	1.1897+03	1.1896+03	1.2789+03	1.2790+03	1.2597+03	1.2253+03
7	1.1657+03	1.1657+03	1.2686+03	1.2686+03	1.2466+03	1.2069+03
8	1.1656+03	1.1657+03	1.2686+03	1.2687+03	1.2467+03	1.2069+03
9	1.1655+03	1.1655+03	1.2685+03	1.2685+03	1.2464+03	1.2067+03
10	1.0523+03	1.0523+03	1.1853+03	1.1857+03	1.1548+03	1.0999+03
11	1.0517+03	1.0519+03	1.1849+03	1.1851+03	1.1543+03	1.0995+03
12	1.0514+03	1.0515+03	1.1841+03	1.1845+03	1.1538+03	1.0991+03
13	1.2308+03	1.2307+03	1.3774+03	1.3773+03	1.3462+03	1.2893+03
14	1.2305+03	1.2304+03	1.3775+03	1.3774+03	1.3463+03	1.2893+03
15	1.2305+03	1.2304+03	1.3773+03	1.3772+03	1.3460+03	1.2892+03
16	1.1519+03	1.1519+03	1.3413+03	1.3405+03	1.3001+03	1.2274+03
17	1.1516+03	1.1516+03	1.3390+03	1.3382+03	1.2987+03	1.2269+03
18	1.1514+03	1.1517+03	1.3400+03	1.3394+03	1.2990+03	1.2267+03
19	1.2037+03	1.2038+03	1.3276+03	1.3277+03	1.3010+03	1.2530+03
20	1.2034+03	1.2036+03	1.3277+03	1.3279+03	1.3011+03	1.2529+03
21	1.2035+03	1.2036+03	1.3275+03	1.3276+03	1.3009+03	1.2527+03
22	1.2469+03	1.2471+03	1.3355+03	1.3354+03	1.3163+03	1.2818+03
23	1.2470+03	1.2472+03	1.3355+03	1.3354+03	1.3163+03	1.2819+03
24	1.2470+03	1.2472+03	1.3356+03	1.3356+03	1.3164+03	1.2818+03
25	1.2858+03	1.2860+03	1.3423+03	1.3421+03	1.3297+03	1.3070+03
26	1.2861+03	1.2863+03	1.3424+03	1.3420+03	1.3299+03	1.3071+03
27	1.2861+03	1.2863+03	1.3424+03	1.3422+03	1.3298+03	1.3071+03
28	1.2306+03	1.2308+03	1.2877+03	1.2873+03	1.2750+03	1.2523+03
29	1.2305+03	1.2307+03	1.2877+03	1.2873+03	1.2751+03	1.2523+03
30	1.2305+03	1.2307+03	1.2876+03	1.2873+03	1.2751+03	1.2524+03



# CONDENSING DATA REDUCTION

	209	211	213	215	217	219
	TC15C	TC16C	TC17C	TC18C	TC19C	TC20C
1	1.3021+03	1.3743+03	1.3670+03	1.3472+03	1.2913+03	1.2890+03
2	1.3021+03	1.3744+03	1.3670+03	1.3472+03	1.2911+03	1.2890+03
3	1.3021+03	1.3743+03	1.3672+03	1.3472+03	1.2911+03	1.2891+03
4	1.2206+03	1.2844+03	1.2787+03	1.2620+03	1.2138+03	1.2117+03
5	1.2207+03	1.2847+03	1.2789+03	1.2621+03	1.2139+03	1.2118+03
6	1.2206+03	1.2844+03	1.2787+03	1.2620+03	1.2138+03	1.2118+03
7	1.2015+03	1.2751+03	1.2673+03	1.2483+03	1.1930+03	1.1908+03
8	1.2016+03	1.2752+03	1.2673+03	1.2483+03	1.1931+03	1.1907+03
9	1.2014+03	1.2750+03	1.2672+03	1.2481+03	1.1929+03	1.1906+03
10	1.0938+03	1.1713+03	1.1624+03	1.1417+03	1.0819+03	1.0787+03
11	1.0934+03	1.1707+03	1.1619+03	1.1412+03	1.0814+03	1.0785+03
12	1.0930+03	1.1701+03	1.1613+03	1.1405+03	1.0810+03	1.0778+03
13	1.2825+03	1.3724+03	1.3633+03	1.3379+03	1.2674+03	1.2647+03
14	1.2825+03	1.3723+03	1.3633+03	1.3378+03	1.2674+03	1.2645+03
15	1.2824+03	1.3723+03	1.3633+03	1.3379+03	1.2674+03	1.2647+03
16	1.2185+03	1.3367+03	1.3249+03	1.2920+03	1.1994+03	1.1956+03
17	1.2178+03	1.3355+03	1.3238+03	1.2912+03	1.1992+03	1.1951+03
18	1.2177+03	1.3360+03	1.3243+03	1.2914+03	1.1992+03	1.1952+03
19	1.2470+03	1.3267+03	1.3185+03	1.2968+03	1.2354+03	1.2328+03
20	1.2468+03	1.3267+03	1.3184+03	1.2967+03	1.2350+03	1.2325+03
21	1.2465+03	1.3266+03	1.3182+03	1.2965+03	1.2349+03	1.2327+03
22	1.2774+03	1.3362+03	1.3306+03	1.3146+03	1.2701+03	1.2685+03
23	1.2774+03	1.3361+03	1.3305+03	1.3145+03	1.2700+03	1.2684+03
24	1.2774+03	1.3362+03	1.3305+03	1.3145+03	1.2698+03	1.2683+03
25	1.3042+03	1.3415+03	1.3383+03	1.3281+03	1.3004+03	1.2996+03
26	1.3042+03	1.3416+03	1.3383+03	1.3283+03	1.3007+03	1.2998+03
27	1.3042+03	1.3416+03	1.3383+03	1.3283+03	1.3006+03	1.2998+03
28	1.2493+03	1.2895+03	1.2858+03	1.2752+03	1.2456+03	1.2445+03
29	1.2493+03	1.2894+03	1.2857+03	1.2751+03	1.2456+03	1.2445+03
30	1.2494+03	1.2894+03	1.2856+03	1.2749+03	1.2455+03	1.2444+03

## CONDENSING DATA REDUCTION

	221	223	226	229	230	235
	TKICC	TKOC	TNAO	TNAI	DTNA	WNA
1	1.4052+03	1.4111+03	1.2972+03	1.2621+03	3.5110+01	4.5509+03
2	1.4052+03	1.4112+03	1.2971+03	1.2620+03	3.5138+01	4.5509+03
3	1.4051+03	1.4109+03	1.2970+03	1.2621+03	3.4924+01	4.5509+03
4	1.3074+03	1.3171+03	1.2173+03	1.1895+03	2.7898+01	4.5446+03
5	1.3078+03	1.3171+03	1.2174+03	1.1893+03	2.8069+01	4.5446+03
6	1.3070+03	1.3174+03	1.2174+03	1.1894+03	2.8026+01	4.5446+03
7	1.3099+03	1.3147+03	1.1978+03	1.1655+03	3.2292+01	4.5808+03
8	1.3103+03	1.3145+03	1.1977+03	1.1654+03	3.2306+01	4.5808+03
9	1.3101+03	1.3146+03	1.1976+03	1.1653+03	3.2334+01	4.5808+03
10	1.3197+03	1.2361+03	1.0898+03	1.0521+03	3.7642+01	4.6822+03
11	1.3194+03	1.2355+03	1.0890+03	1.0516+03	3.7358+01	4.6822+03
12	1.3195+03	1.2351+03	1.0887+03	1.0512+03	3.7511+01	4.6822+03
13	1.4139+03	1.4194+03	1.2755+03	1.2304+03	4.5082+01	4.4975+03
14	1.4142+03	1.4193+03	1.2756+03	1.2301+03	4.5496+01	4.4975+03
15	1.4140+03	1.4194+03	1.2756+03	1.2301+03	4.5438+01	4.4975+03
16	1.4150+03	1.4028+03	1.2105+03	1.1515+03	5.8963+01	4.5523+03
17	1.4150+03	1.4026+03	1.2103+03	1.1512+03	5.9119+01	4.5523+03
18	1.4147+03	1.4022+03	1.2099+03	1.1512+03	5.8618+01	4.5523+03
19	1.3612+03	1.3681+03	1.2415+03	1.2035+03	3.8005+01	4.5886+03
20	1.3611+03	1.3681+03	1.2413+03	1.2032+03	3.8118+01	4.5886+03
21	1.3610+03	1.3681+03	1.2412+03	1.2033+03	3.7890+01	4.5886+03
22	1.3584+03	1.3649+03	1.2738+03	1.2466+03	2.7158+01	4.5624+03
23	1.3582+03	1.3649+03	1.2737+03	1.2468+03	2.6859+01	4.5624+03
24	1.3582+03	1.3650+03	1.2738+03	1.2468+03	2.6988+01	4.5624+03
25	1.3568+03	1.3593+03	1.3020+03	1.2856+03	1.6392+01	4.6013+03
26	1.3571+03	1.3593+03	1.3022+03	1.2858+03	1.6364+01	4.6013+03
27	1.3570+03	1.3596+03	1.3024+03	1.2860+03	1.6408+01	4.6013+03
28	1.3034+03	1.3089+03	1.2478+03	1.2305+03	1.7299+01	4.5745+03
29	1.3038+03	1.3089+03	1.2478+03	1.2304+03	1.7384+01	4.5745+03
30	1.3036+03	1.3087+03	1.2477+03	1.2303+03	1.7312+01	4.5745+03

## CONDENSING DATA REDUCTION

	237	238	240	243	246	247
	TNAM	CPNA	QNA	DTQL	QC	Q/AA
1	1.2796+03	3.0040-01	4.7998+04	1.2010+03	5.1115+04	1.7356+05
2	1.2795+03	3.0040-01	4.8037+04	1.2010+03	5.1153+04	1.7369+05
3	1.2796+03	3.0040-01	4.7744+04	1.2010+03	5.0860+04	1.7270+05
4	1.2034+03	3.0002-01	3.8037+04	1.1181+03	4.0814+04	1.3859+05
5	1.2034+03	3.0002-01	3.8271+04	1.1181+03	4.1047+04	1.3938+05
6	1.2034+03	3.0002-01	3.8213+04	1.1182+03	4.0990+04	1.3918+05
7	1.1816+03	3.0000-01	4.4377+04	1.0972+03	4.7071+04	1.5983+05
8	1.1815+03	3.0000-01	4.4396+04	1.0972+03	4.7089+04	1.5990+05
9	1.1814+03	3.0000-01	4.4435+04	1.0971+03	4.7128+04	1.6003+05
10	1.0709+03	3.0023-01	5.2916+04	9.8790+02	5.5190+04	1.8740+05
11	1.0703+03	3.0024-01	5.2518+04	9.8725+02	5.4789+04	1.8604+05
12	1.0700+03	3.0024-01	5.2733+04	9.8695+02	5.5003+04	1.8677+05
13	1.2530+03	3.0026-01	6.0881+04	1.1739+03	6.3885+04	2.1693+05
14	1.2529+03	3.0026-01	6.1440+04	1.1734+03	6.4441+04	2.1882+05
15	1.2528+03	3.0026-01	6.1362+04	1.1734+03	6.4364+04	2.1855+05
16	1.1810+03	3.0000-01	8.0526+04	1.1011+03	8.3235+04	2.8263+05
17	1.1807+03	3.0000-01	8.0738+04	1.1004+03	8.3445+04	2.8334+05
18	1.1806+03	3.0000-01	8.0054+04	1.1006+03	8.2761+04	2.8102+05
19	1.2225+03	3.0011-01	5.2337+04	1.1462+03	5.5227+04	1.8753+05
20	1.2222+03	3.0011-01	5.2492+04	1.1464+03	5.5383+04	1.8806+05
21	1.2222+03	3.0011-01	5.2177+04	1.1463+03	5.5068+04	1.8699+05
22	1.2602+03	3.0030-01	3.7209+04	1.1883+03	4.0272+04	1.3675+05
23	1.2603+03	3.0030-01	3.6799+04	1.1884+03	3.9863+04	1.3536+05
24	1.2603+03	3.0030-01	3.6975+04	1.1884+03	4.0039+04	1.3596+05
25	1.2938+03	3.0047-01	2.2663+04	1.2193+03	2.5856+04	8.7796+04
26	1.2940+03	3.0047-01	2.2624+04	1.2199+03	2.5820+04	8.7673+04
27	1.2942+03	3.0047-01	2.2685+04	1.2201+03	2.5881+04	8.7882+04
28	1.2391+03	3.0020-01	2.3755+04	1.1699+03	2.6743+04	9.0808+04
29	1.2391+03	3.0020-01	2.3873+04	1.1699+03	2.6860+04	9.1205+04
30	1.2390+03	3.0019-01	2.3774+04	1.1698+03	2.6761+04	9.0869+04

# CONDENSING DATA REDUCTION

	251	306	317	319	324	326
	WK	TWI T	Q/A T	TWO T	HCON T	NUC T
1	6.1105+01	1.4037+03	1.8001+05	1.2892+03	-9.5482+05	-2.7793+00
2	6.1152+01	1.4035+03	1.7992+05	1.2891+03	-8.7929+06	-2.5595+01
3	6.0799+01	1.4033+03	1.7967+05	1.2891+03	5.4845+06	1.5964+01
4	4.7962+01	1.2989+03	1.3710+05	1.2099+03	2.1831+04	6.2470-02
5	4.8237+01	1.2989+03	1.3691+05	1.2100+03	2.0830+04	5.9609-02
6	4.8167+01	1.2992+03	1.3750+05	1.2099+03	2.3961+04	6.8563-02
7	5.5314+01	1.2923+03	1.5632+05	1.1905+03	1.2163+04	3.4806-02
8	5.5337+01	1.2924+03	1.5641+05	1.1905+03	1.1998+04	3.4336-02
9	5.5382+01	1.2922+03	1.5635+05	1.1903+03	1.1918+04	3.4105-02
10	6.4484+01	1.2194+03	2.0675+05	1.0818+03	2.7791+03	7.9368-03
11	6.4011+01	1.2188+03	2.0650+05	1.0814+03	2.7630+03	7.8906-03
12	6.4260+01	1.2181+03	2.0590+05	1.0810+03	2.7301+03	7.7964-03
13	7.6496+01	1.4118+03	2.2496+05	1.2684+03	-1.9640+05	-5.7284-01
14	7.7164+01	1.4119+03	2.2503+05	1.2684+03	-2.1069+05	-6.1452-01
15	7.7071+01	1.4116+03	2.2484+05	1.2683+03	-2.5064+05	-7.3104-01
16	9.9518+01	1.3861+03	2.8338+05	1.2034+03	1.5319+04	4.4604-02
17	9.9767+01	1.3832+03	2.7942+05	1.2030+03	1.3107+04	3.8164-02
18	9.8943+01	1.3847+03	2.8231+05	1.2026+03	1.4433+04	4.2020-02
19	6.5504+01	1.3566+03	1.8986+05	1.2343+03	1.7307+05	4.9971-01
20	6.5689+01	1.3568+03	1.9036+05	1.2342+03	2.5389+05	7.3303-01
21	6.5314+01	1.3565+03	1.9038+05	1.2340+03	2.0528+05	5.9267-01
22	4.7741+01	1.3555+03	1.3971+05	1.2659+03	8.2763+04	2.3894-01
23	4.7255+01	1.3554+03	1.3945+05	1.2659+03	8.2683+04	2.3870-01
24	4.7464+01	1.3556+03	1.3992+05	1.2659+03	9.9640+04	2.8765-01
25	3.0632+01	1.3543+03	9.4949+04	1.2936+03	4.8838+04	1.4097-01
26	3.0590+01	1.3544+03	9.4914+04	1.2937+03	4.4846+04	1.2946-01
27	3.0663+01	1.3544+03	9.5018+04	1.2937+03	4.5833+04	1.3231-01
28	3.1392+01	1.2998+03	9.3258+04	1.2395+03	3.1200+04	8.9244-02
29	3.1531+01	1.2999+03	9.3527+04	1.2394+03	2.9625+04	8.4744-02
30	3.1413+01	1.2998+03	9.3129+04	1.2396+03	3.0090+04	8.6070-02

# CONDENSING DATA REDUCTION

	354	365	367	372	374	389
	TWI B	Q/A B	TWO B	HCON B	NUC B	TWI TC
1	1.4022+03	1.8849+05	1.2822+03	3.1201+04	9.0940-02	1.4071+03
2	1.4023+03	1.8885+05	1.2820+03	3.1680+04	9.2338-02	1.4070+03
3	1.4023+03	1.8878+05	1.2821+03	3.3094+04	9.6451-02	1.4068+03
4	1.3082+03	1.5627+05	1.2067+03	3.0162+04	8.6431-02	1.3019+03
5	1.3084+03	1.5658+05	1.2068+03	3.1399+04	8.9976-02	1.3019+03
6	1.3081+03	1.5616+05	1.2068+03	2.9321+04	8.4023-02	1.3021+03
7	1.3022+03	1.7999+05	1.1849+03	1.9144+04	5.4840-02	1.2953+03
8	1.3023+03	1.8007+05	1.1850+03	1.9367+04	5.5480-02	1.2954+03
9	1.3021+03	1.8007+05	1.1848+03	1.9002+04	5.4436-02	1.2952+03
10	1.2010+03	1.9068+05	1.0737+03	3.7014+03	1.0494-02	1.2222+03
11	1.2003+03	1.9015+05	1.0733+03	3.6769+03	1.0424-02	1.2216+03
12	1.1997+03	1.9006+05	1.0727+03	3.6499+03	1.0347-02	1.2208+03
13	1.4085+03	2.3859+05	1.2561+03	3.1039+04	9.0668-02	1.4154+03
14	1.4084+03	2.3863+05	1.2560+03	3.0888+04	9.0226-02	1.4154+03
15	1.4084+03	2.3840+05	1.2561+03	3.0523+04	8.9162-02	1.4152+03
16	1.3851+03	3.0951+05	1.1850+03	1.7687+04	5.1470-02	1.3897+03
17	1.3836+03	3.0749+05	1.1848+03	1.6324+04	4.7501-02	1.3867+03
18	1.3843+03	3.0869+05	1.1848+03	1.7309+04	5.0365-02	1.3883+03
19	1.3575+03	2.0420+05	1.2259+03	2.8797+04	8.3242-02	1.3599+03
20	1.3577+03	2.0512+05	1.2254+03	2.9768+04	8.6048-02	1.3601+03
21	1.3574+03	2.0452+05	1.2255+03	2.8542+04	8.2505-02	1.3598+03
22	1.3579+03	1.4777+05	1.2631+03	3.4250+04	9.8964-02	1.3586+03
23	1.3577+03	1.4767+05	1.2630+03	3.3391+04	9.6481-02	1.3585+03
24	1.3579+03	1.4825+05	1.2628+03	3.4941+04	1.0096-01	1.3588+03
25	1.3539+03	9.0689+04	1.2960+03	2.2637+04	6.5362-02	1.3574+03
26	1.3538+03	9.0193+04	1.2962+03	2.1661+04	6.2543-02	1.3575+03
27	1.3539+03	9.0399+04	1.2962+03	2.1008+04	6.0662-02	1.3575+03
28	1.3028+03	9.5168+04	1.2413+03	2.3906+04	6.8426-02	1.3027+03
29	1.3027+03	9.5014+04	1.2412+03	2.2710+04	6.5005-02	1.3028+03
30	1.3026+03	9.4986+04	1.2412+03	2.3130+04	6.6205-02	1.3027+03

# CONDENSING DATA REDUCTION

	399	401	405	406	408	424
	Q/A TC	TWO TC	TKC-TW	HCONTC	NUC TC	TWI BC
1	1.7308+05	1.2972+03	-6.3651-01	-2.7192+05	-7.9218-01	1.4057+03
2	1.7300+05	1.2971+03	-4.6411-01	-3.7275+05	-1.0859+00	1.4058+03
3	1.7274+05	1.2971+03	-4.3932-01	-3.9321+05	-1.1455+00	1.4059+03
4	1.3088+05	1.2170+03	7.6431+00	1.7124+04	4.9039-02	1.3117+03
5	1.3069+05	1.2171+03	7.9736+00	1.6390+04	4.6938-02	1.3119+03
6	1.3128+05	1.2170+03	7.1566+00	1.8344+04	5.2529-02	1.3116+03
7	1.5050+05	1.1974+03	1.5649+01	9.6172+03	2.7547-02	1.3058+03
8	1.5059+05	1.1974+03	1.5816+01	9.5214+03	2.7274-02	1.3058+03
9	1.5053+05	1.1972+03	1.5920+01	9.4553+03	2.7084-02	1.3057+03
*10	2.0267+05	1.0874+03	7.8920+01	2.5680+03	7.3433-03	1.2046+03
*11	2.0242+05	1.0870+03	7.9158+01	2.5572+03	7.3120-03	1.2039+03
*12	2.0182+05	1.0866+03	7.9907+01	2.5257+03	7.2220-03	1.2033+03
13	2.1868+05	1.2762+03	-2.6643-01	-8.2077+05	-2.3968+00	1.4121+03
14	2.1875+05	1.2762+03	-1.1940-01	-1.8321+06	-5.3504+00	1.4121+03
15	2.1856+05	1.2761+03	4.6463-02	4.7039+06	1.3737+01	1.4120+03
*16	2.7840+05	1.2104+03	2.2642+01	1.2296+04	3.5878-02	1.3889+03
*17	2.7441+05	1.2100+03	2.5521+01	1.0752+04	3.1375-02	1.3874+03
*18	2.7732+05	1.2096+03	2.3636+01	1.1733+04	3.4233-02	1.3881+03
19	1.8373+05	1.2417+03	2.8918+00	6.3534+04	1.8360-01	1.3611+03
20	1.8424+05	1.2416+03	2.5800+00	7.1410+04	2.0635-01	1.3612+03
21	1.8426+05	1.2413+03	2.7027+00	6.8176+04	1.9700-01	1.3610+03
22	1.3279+05	1.2736+03	1.1771+00	1.1281+05	3.2583-01	1.3613+03
23	1.3252+05	1.2737+03	1.1250+00	1.1780+05	3.4023-01	1.3612+03
24	1.3300+05	1.2737+03	8.6440-01	1.5387+05	4.4440-01	1.3614+03
25	8.7299+04	1.3017+03	-2.8976-02	-3.0127+06	-8.6981+00	1.3572+03
26	8.7264+04	1.3018+03	1.3713-01	6.3636+05	1.8373+00	1.3572+03
27	8.7367+04	1.3018+03	1.0054-01	8.6898+05	2.5089+00	1.3572+03
28	8.6312+04	1.2469+03	1.9290+00	4.4744+04	1.2802-01	1.3062+03
29	8.6584+04	1.2469+03	2.1057+00	4.1118+04	1.1766-01	1.3061+03
30	8.6180+04	1.2470+03	2.0352+00	4.2345+04	1.2116-01	1.3060+03

\*Subcooled liquid at test section outlet, therefore calculational procedure not valid. Not plotted in Figure 20.

# CONDENSING DATA REDUCTION

	434	436	439	440	442	450
	Q/A BC	TWO BC	TK-TWI	HCONBC	NUC BC	PSI HD
1	1.9435+05	1.2820+03	4.0742+00	4.7703+04	1.3910-01	1.6141+00
2	1.9471+05	1.2819+03	3.9947+00	4.8741+04	1.4213-01	1.6162+00
3	1.9464+05	1.2819+03	3.7279+00	5.2212+04	1.5224-01	1.5986+00
4	1.6303+05	1.2059+03	3.2801+00	4.9703+04	1.4247-01	1.6183+00
5	1.6335+05	1.2059+03	3.0956+00	5.2766+04	1.5125-01	1.6337+00
6	1.6292+05	1.2059+03	3.4425+00	4.7326+04	1.3565-01	1.6356+00
7	1.8713+05	1.1839+03	7.8470+00	2.3847+04	6.8337-02	2.1248+00
8	1.8721+05	1.1839+03	7.7369+00	2.4197+04	6.9341-02	2.1220+00
9	1.8722+05	1.1837+03	7.9217+00	2.3633+04	6.7726-02	2.1276+00
*10	1.9929+05	1.0716+03	5.0038+01	3.9828+03	1.1297-02	2.7440+00
*11	1.9876+05	1.0712+03	5.0205+01	3.9590+03	1.1228-02	2.7070+00
*12	1.9868+05	1.0706+03	5.0578+01	3.9282+03	1.1140-02	2.7276+00
13	2.4499+05	1.2557+03	6.0513+00	4.0485+04	1.1833-01	2.4283+00
14	2.4504+05	1.2556+03	6.1097+00	4.0107+04	1.1722-01	2.4674+00
15	2.4480+05	1.2557+03	6.1935+00	3.9525+04	1.1552-01	2.4630+00
*16	3.1712+05	1.1840+03	1.6564+01	1.9146+04	5.5761-02	4.0879+00
*17	3.1510+05	1.1838+03	1.7917+01	1.7587+04	5.1219-02	4.1082+00
*18	3.1631+05	1.1837+03	1.6877+01	1.8742+04	5.4578-02	4.0476+00
19	2.1088+05	1.2252+03	5.5031+00	3.8320+04	1.1081-01	2.2934+00
20	2.1181+05	1.2247+03	5.3115+00	3.9878+04	1.1531-01	2.3078+00
21	2.1120+05	1.2248+03	5.5715+00	3.7908+04	1.0961-01	2.2834+00
22	1.5374+05	1.2627+03	2.1601+00	7.1172+04	2.0569-01	1.2356+00
23	1.5364+05	1.2627+03	2.2536+00	6.8176+04	1.9703-01	1.2118+00
24	1.5422+05	1.2625+03	2.0795+00	7.4161+04	2.1433-01	1.2223+00
25	9.5995+04	1.2959+03	1.5169+00	6.3283+04	1.8275-01	5.1258-01
26	9.5493+04	1.2962+03	1.6745+00	5.7028+04	1.6469-01	5.1043-01
27	9.5701+04	1.2961+03	1.8159+00	5.2703+04	1.5220-01	5.1309-01
28	1.0124+05	1.2407+03	1.4751+00	6.8634+04	1.9648-01	7.0796-01
29	1.0109+05	1.2407+03	1.6810+00	6.0136+04	1.7216-01	7.1271-01
30	1.0106+05	1.2406+03	1.6001+00	6.3158+04	1.8080-01	7.0828-01

\*Subcooled liquid at test section outlet, therefore calculational procedure not valid. Not plotted in Figure 20.

# CONDENSING DATA REDUCTION

	451	452	453	610	611	613
	PI	PO	DPC	PIC	POC	DPCC
1	1.5300+01	1.5981+01	-6.8016-01	1.5585+01	1.6062+01	-4.7688-01
2	1.5304+01	1.5984+01	-6.8030-01	1.5589+01	1.6066+01	-4.7670-01
3	1.5297+01	1.5961+01	-6.6421-01	1.5579+01	1.6042+01	-4.6337-01
4	8.9237+00	9.6992+00	-7.7556-01	9.2044+00	9.7272+00	-5.2280-01
5	8.9414+00	9.6981+00	-7.5668-01	9.2246+00	9.7260+00	-5.0137-01
6	8.8993+00	9.7132+00	-8.1383-01	9.1838+00	9.7412+00	-5.5732-01
7	8.9569+00	9.5660+00	-6.0910-01	9.3341+00	9.5934+00	-2.5929-01
8	8.9791+00	9.5567+00	-5.7769-01	9.3557+00	9.5841+00	-2.2830-01
9	8.9680+00	9.5625+00	-5.9455-01	9.3456+00	9.5899+00	-2.4424-01
10	9.3563+00	6.0235+00	3.3329+00	9.8638+00	6.0276+00	3.8362+00
11	9.3517+00	6.0004+00	3.3512+00	9.8517+00	6.0045+00	3.8473+00
12	9.3494+00	5.9893+00	3.3600+00	9.8537+00	5.9933+00	3.8604+00
13	1.5846+01	1.6663+01	-8.1717-01	1.6289+01	1.6747+01	-4.5820-01
14	1.5863+01	1.6654+01	-7.9094-01	1.6315+01	1.6738+01	-4.2378-01
15	1.5852+01	1.6663+01	-8.1027-01	1.6303+01	1.6747+01	-4.4423-01
16	1.5601+01	1.5321+01	2.7975-01	1.6384+01	1.5396+01	9.8851-01
17	1.5597+01	1.5305+01	2.9177-01	1.6385+01	1.5380+01	1.0049+00
18	1.5580+01	1.5280+01	3.0031-01	1.6355+01	1.5354+01	1.0005+00
19	1.1977+01	1.2801+01	-8.2345-01	1.2389+01	1.2853+01	-4.6380-01
20	1.1966+01	1.2801+01	-8.3459-01	1.2381+01	1.2853+01	-4.7225-01
21	1.1961+01	1.2801+01	-8.4015-01	1.2370+01	1.2853+01	-4.8285-01
22	1.1991+01	1.2588+01	-5.9613-01	1.2200+01	1.2638+01	-4.3814-01
23	1.1983+01	1.2588+01	-6.0448-01	1.2188+01	1.2638+01	-4.5074-01
24	1.1983+01	1.2589+01	-6.0594-01	1.2190+01	1.2640+01	-4.5027-01
25	1.2019+01	1.2214+01	-1.9482-01	1.2100+01	1.2261+01	-1.6088-01
26	1.2039+01	1.2217+01	-1.7812-01	1.2119+01	1.2264+01	-1.4465-01
27	1.2033+01	1.2235+01	-2.0178-01	1.2114+01	1.2282+01	-1.6791-01
28	8.8838+00	9.2570+00	-3.7322-01	8.9986+00	9.2817+00	-2.8311-01
29	8.9038+00	9.2559+00	-3.5218-01	9.0192+00	9.2806+00	-2.6139-01
30	8.8927+00	9.2493+00	-3.5661-01	9.0075+00	9.2739+00	-2.6647-01



# CONDENSING DATA REDUCTION

	700	495	701	498	504	507
	X B	WKL B	X T	WKL T	NREF T	NREF B
1	2.5573-01	4.5479+01	8.0935-01	1.1650+01	1.4930+03	5.8374+03
2	2.5572-01	4.5514+01	8.0933-01	1.1660+01	1.4943+03	5.8421+03
3	2.5536-01	4.5273+01	8.0901-01	1.1612+01	1.4880+03	5.8105+03
4	2.6422-01	3.5289+01	8.1715-01	8.7698+00	1.0683+03	4.3126+03
5	2.6334-01	3.5535+01	8.1634-01	8.8593+00	1.0793+03	4.3427+03
6	2.6587-01	3.5361+01	8.1864-01	8.7356+00	1.0639+03	4.3216+03
7	2.5129-01	4.1414+01	8.0535-01	1.0767+01	1.3126+03	5.0570+03
8	2.5034-01	4.1484+01	8.0447-01	1.0820+01	1.3193+03	5.0653+03
9	2.5081-01	4.1492+01	8.0491-01	1.0805+01	1.3173+03	5.0664+03
10	2.4523-01	4.8670+01	8.0176-01	1.2783+01	1.5493+03	5.7485+03
11	2.4608-01	4.8259+01	8.0265-01	1.2633+01	1.5308+03	5.6982+03
12	2.4615-01	4.8443+01	8.0273-01	1.2677+01	1.5361+03	5.7191+03
13	2.5331-01	5.7118+01	8.0713-01	1.4754+01	1.8985+03	7.3606+03
14	2.5299-01	5.7642+01	8.0682-01	1.4906+01	1.9183+03	7.4280+03
15	2.5327-01	5.7551+01	8.0708-01	1.4869+01	1.9134+03	7.4165+03
16	2.3656-01	7.5976+01	7.9158-01	2.0741+01	2.6654+03	9.7321+03
17	2.3648-01	7.6174+01	7.9151-01	2.0801+01	2.6730+03	9.7568+03
18	2.3633-01	7.5560+01	7.9136-01	2.0643+01	2.6523+03	9.6766+03
19	2.5563-01	4.8759+01	8.0927-01	1.2493+01	1.5663+03	6.1238+03
20	2.5585-01	4.8882+01	8.0947-01	1.2515+01	1.5690+03	6.1393+03
21	2.5596-01	4.8596+01	8.0958-01	1.2437+01	1.5591+03	6.1032+03
22	2.5930-01	3.5361+01	8.1263-01	8.9453+00	1.1200+03	4.4348+03
23	2.5954-01	3.4990+01	8.1285-01	8.8437+00	1.1072+03	4.3882+03
24	2.5964-01	3.5140+01	8.1294-01	8.8786+00	1.1115+03	4.4070+03
25	2.5248-01	2.2898+01	8.0642-01	5.9297+00	7.4142+02	2.8652+03
26	2.5162-01	2.2893+01	8.0563-01	5.9456+00	7.4351+02	2.8647+03
27	2.5290-01	2.2908+01	8.0680-01	5.9240+00	7.4081+02	2.8670+03
28	2.6240-01	2.3155+01	8.1548-01	5.7924+00	7.0350+02	2.8173+03
29	2.6087-01	2.3305+01	8.1409-01	5.8617+00	7.1206+02	2.8357+03
30	2.6117-01	2.3209+01	8.1437-01	5.8314+00	7.0829+02	2.8238+03

## CONDENSING DATA REDUCTION

	131	132	134	138	140	142
	DATE	TIME	TC1	TC3	TC4	TC5
1	1.1450+03	4.4000+02	1.2981+03	1.3044+03	1.2945+03	1.2632+03
2	1.1450+03	4.4000+02	1.2979+03	1.3042+03	1.2943+03	1.2631+03
3	1.1450+03	4.4000+02	1.2977+03	1.3043+03	1.2944+03	1.2631+03
4	1.1450+03	6.3000+02	1.2572+03	1.2669+03	1.2574+03	1.2181+03
5	1.1450+03	6.3000+02	1.2571+03	1.2666+03	1.2571+03	1.2182+03
6	1.1450+03	6.3000+02	1.2572+03	1.2668+03	1.2573+03	1.2182+03
7	1.1450+03	7.3000+02	1.2497+03	1.2569+03	1.2478+03	1.2216+03
8	1.1450+03	7.3000+02	1.2497+03	1.2568+03	1.2476+03	1.2217+03
9	1.1450+03	7.3000+02	1.2496+03	1.2566+03	1.2476+03	1.2216+03
10	1.1450+03	9.0000+02	1.1964+03	1.2058+03	1.1972+03	1.1677+03
11	1.1450+03	9.0000+02	1.1963+03	1.2058+03	1.1972+03	1.1677+03
12	1.1450+03	9.0000+02	1.1964+03	1.2058+03	1.1972+03	1.1677+03
13	1.1450+03	1.3000+03	1.2036+03	1.2153+03	1.2065+03	1.1686+03
14	1.1450+03	1.3000+03	1.2035+03	1.2153+03	1.2066+03	1.1687+03
15	1.1450+03	1.3000+03	1.2037+03	1.2153+03	1.2065+03	1.1686+03
16	1.1450+03	1.4300+03	1.1497+03	1.1631+03	1.1549+03	1.1176+03
17	1.1450+03	1.4300+03	1.1498+03	1.1632+03	1.1550+03	1.1176+03
18	1.1450+03	1.4300+03	1.1497+03	1.1629+03	1.1546+03	1.1173+03
19	1.1450+03	1.7150+03	1.1416+03	1.1481+03	1.1403+03	1.1198+03
20	1.1450+03	1.7150+03	1.1419+03	1.1482+03	1.1403+03	1.1198+03
21	1.1450+03	1.7150+03	1.1418+03	1.1481+03	1.1403+03	1.1200+03
22	1.1450+03	1.9300+03	1.1829+03	1.1947+03	1.1865+03	1.1469+03
23	1.1450+03	1.9300+03	1.1831+03	1.1948+03	1.1866+03	1.1470+03
24	1.1450+03	1.9300+03	1.1832+03	1.1949+03	1.1866+03	1.1470+03
25	1.1450+03	2.1300+03	1.2316+03	1.2462+03	1.2373+03	1.1758+03
26	1.1450+03	2.1300+03	1.2315+03	1.2465+03	1.2376+03	1.1760+03
27	1.1450+03	2.1300+03	1.2325+03	1.2467+03	1.2379+03	1.1762+03
28	1.1550+03	8.3000+02	1.2885+03	1.3059+03	1.2963+03	1.1905+03
29	1.1550+03	8.3000+02	1.2888+03	1.3056+03	1.2961+03	1.1904+03
30	1.1550+03	8.3000+02	1.2884+03	1.3056+03	1.2961+03	1.1902+03

# CONDENSING DATA REDUCTION

	144	146	148	150	152	154
	TC6	TC7	TC8	TC9	TC10	TC11
1	1.2644+03	1.2503+03	1.2569+03	1.2580+03	1.2582+03	1.2720+03
2	1.2644+03	1.2503+03	1.2570+03	1.2582+03	1.2583+03	1.2721+03
3	1.2643+03	1.2502+03	1.2568+03	1.2580+03	1.2582+03	1.2720+03
4	1.2192+03	1.2054+03	1.2098+03	1.2109+03	1.2112+03	1.2308+03
5	1.2192+03	1.2056+03	1.2099+03	1.2112+03	1.2113+03	1.2307+03
6	1.2192+03	1.2056+03	1.2100+03	1.2110+03	1.2113+03	1.2308+03
7	1.2229+03	1.2091+03	1.2174+03	1.2186+03	1.2184+03	1.2263+03
8	1.2228+03	1.2091+03	1.2172+03	1.2186+03	1.2183+03	1.2262+03
9	1.2227+03	1.2091+03	1.2174+03	1.2187+03	1.2183+03	1.2262+03
10	1.1687+03	1.1556+03	1.1628+03	1.1640+03	1.1638+03	1.1729+03
11	1.1687+03	1.1555+03	1.1627+03	1.1638+03	1.1637+03	1.1729+03
12	1.1686+03	1.1554+03	1.1626+03	1.1639+03	1.1637+03	1.1729+03
13	1.1695+03	1.1564+03	1.1615+03	1.1626+03	1.1626+03	1.1781+03
14	1.1697+03	1.1565+03	1.1615+03	1.1626+03	1.1625+03	1.1780+03
15	1.1695+03	1.1564+03	1.1617+03	1.1625+03	1.1626+03	1.1783+03
16	1.1185+03	1.1060+03	1.1117+03	1.1128+03	1.1127+03	1.1240+03
17	1.1185+03	1.1059+03	1.1115+03	1.1126+03	1.1125+03	1.1239+03
18	1.1185+03	1.1058+03	1.1116+03	1.1126+03	1.1128+03	1.1239+03
19	1.1210+03	1.1082+03	1.1178+03	1.1186+03	1.1189+03	1.1201+03
20	1.1209+03	1.1082+03	1.1176+03	1.1185+03	1.1189+03	1.1200+03
21	1.1210+03	1.1083+03	1.1177+03	1.1186+03	1.1189+03	1.1200+03
22	1.1480+03	1.1351+03	1.1402+03	1.1410+03	1.1414+03	1.1562+03
23	1.1480+03	1.1352+03	1.1401+03	1.1410+03	1.1413+03	1.1561+03
24	1.1479+03	1.1350+03	1.1400+03	1.1409+03	1.1412+03	1.1561+03
25	1.1763+03	1.1632+03	1.1626+03	1.1637+03	1.1640+03	1.1972+03
26	1.1765+03	1.1635+03	1.1627+03	1.1638+03	1.1641+03	1.1974+03
27	1.1767+03	1.1637+03	1.1630+03	1.1641+03	1.1644+03	1.1978+03
28	1.1906+03	1.1778+03	1.1627+03	1.1642+03	1.1644+03	1.2401+03
29	1.1904+03	1.1776+03	1.1626+03	1.1641+03	1.1643+03	1.2399+03
30	1.1903+03	1.1775+03	1.1630+03	1.1646+03	1.1647+03	1.2399+03

## CONDENSING DATA REDUCTION

	156	158	160	162	164	166
	TC12	TC13	TC14	TC15	TC16	TC17
1	1.2939+03	1.2840+03	1.2670+03	1.2516+03	1.2812+03	1.2886+03
2	1.2939+03	1.2839+03	1.2668+03	1.2514+03	1.2811+03	1.2884+03
3	1.2939+03	1.2841+03	1.2669+03	1.2515+03	1.2812+03	1.2884+03
4	1.2518+03	1.2411+03	1.2223+03	1.2070+03	1.2411+03	1.2477+03
5	1.2518+03	1.2410+03	1.2223+03	1.2070+03	1.2412+03	1.2478+03
6	1.2518+03	1.2411+03	1.2224+03	1.2071+03	1.2411+03	1.2478+03
7	1.2474+03	1.2390+03	1.2246+03	1.2098+03	1.2356+03	1.2431+03
8	1.2474+03	1.2390+03	1.2246+03	1.2098+03	1.2356+03	1.2432+03
9	1.2475+03	1.2389+03	1.2245+03	1.2097+03	1.2355+03	1.2431+03
10	1.1929+03	1.1847+03	1.1704+03	1.1562+03	1.1833+03	1.1906+03
11	1.1929+03	1.1847+03	1.1705+03	1.1563+03	1.1834+03	1.1906+03
12	1.1929+03	1.1847+03	1.1705+03	1.1563+03	1.1835+03	1.1904+03
13	1.1983+03	1.1887+03	1.1723+03	1.1576+03	1.1902+03	1.1967+03
14	1.1982+03	1.1886+03	1.1722+03	1.1575+03	1.1901+03	1.1968+03
15	1.1984+03	1.1889+03	1.1722+03	1.1575+03	1.1902+03	1.1967+03
16	1.1430+03	1.1348+03	1.1206+03	1.1066+03	1.1376+03	1.1442+03
17	1.1429+03	1.1348+03	1.1207+03	1.1067+03	1.1376+03	1.1442+03
18	1.1428+03	1.1347+03	1.1205+03	1.1065+03	1.1375+03	1.1441+03
19	1.1388+03	1.1326+03	1.1218+03	1.1085+03	1.1292+03	1.1367+03
20	1.1389+03	1.1328+03	1.1220+03	1.1087+03	1.1292+03	1.1368+03
21	1.1388+03	1.1327+03	1.1219+03	1.1086+03	1.1294+03	1.1369+03
22	1.1758+03	1.1666+03	1.1504+03	1.1361+03	1.1693+03	1.1756+03
23	1.1757+03	1.1665+03	1.1504+03	1.1361+03	1.1693+03	1.1757+03
24	1.1757+03	1.1665+03	1.1505+03	1.1360+03	1.1694+03	1.1759+03
25	1.2176+03	1.2042+03	1.1811+03	1.1654+03	1.2134+03	1.2183+03
26	1.2178+03	1.2045+03	1.1815+03	1.1658+03	1.2138+03	1.2187+03
27	1.2182+03	1.2048+03	1.1815+03	1.1659+03	1.2137+03	1.2190+03
28	1.2607+03	1.2389+03	1.2003+03	1.1823+03	1.2577+03	1.2601+03
29	1.2604+03	1.2387+03	1.2001+03	1.1821+03	1.2576+03	1.2600+03
30	1.2603+03	1.2385+03	1.2004+03	1.1821+03	1.2576+03	1.2599+03

# CONDENSING DATA REDUCTION

	168	170	172	174	176	181
	TC18	TC19	TC20	TKI	TKO	TC1C
1	1.2844+03	1.2659+03	1.2638+03	1.2981+03	1.2995+03	1.2981+03
2	1.2842+03	1.2659+03	1.2637+03	1.2979+03	1.2993+03	1.2979+03
3	1.2842+03	1.2658+03	1.2637+03	1.2977+03	1.2993+03	1.2977+03
4	1.2421+03	1.2204+03	1.2182+03	1.2572+03	1.2621+03	1.2572+03
5	1.2422+03	1.2206+03	1.2184+03	1.2571+03	1.2619+03	1.2571+03
6	1.2421+03	1.2206+03	1.2183+03	1.2572+03	1.2620+03	1.2572+03
7	1.2398+03	1.2246+03	1.2226+03	1.2497+03	1.2524+03	1.2497+03
8	1.2398+03	1.2246+03	1.2225+03	1.2497+03	1.2522+03	1.2497+03
9	1.2398+03	1.2247+03	1.2226+03	1.2496+03	1.2521+03	1.2496+03
10	1.1867+03	1.1705+03	1.1686+03	1.1964+03	1.2015+03	1.1964+03
11	1.1867+03	1.1706+03	1.1686+03	1.1963+03	1.2015+03	1.1963+03
12	1.1865+03	1.1703+03	1.1685+03	1.1964+03	1.2015+03	1.1964+03
13	1.1913+03	1.1712+03	1.1692+03	1.2036+03	1.2109+03	1.2036+03
14	1.1915+03	1.1714+03	1.1694+03	1.2035+03	1.2109+03	1.2035+03
15	1.1912+03	1.1711+03	1.1693+03	1.2037+03	1.2109+03	1.2037+03
16	1.1390+03	1.1206+03	1.1187+03	1.1497+03	1.1590+03	1.1497+03
17	1.1389+03	1.1206+03	1.1186+03	1.1498+03	1.1591+03	1.1498+03
18	1.1389+03	1.1204+03	1.1184+03	1.1497+03	1.1588+03	1.1497+03
19	1.1342+03	1.1231+03	1.1215+03	1.1416+03	1.1442+03	1.1416+03
20	1.1342+03	1.1230+03	1.1215+03	1.1419+03	1.1442+03	1.1419+03
21	1.1344+03	1.1233+03	1.1217+03	1.1418+03	1.1442+03	1.1418+03
22	1.1701+03	1.1499+03	1.1480+03	1.1829+03	1.1906+03	1.1829+03
23	1.1702+03	1.1500+03	1.1481+03	1.1831+03	1.1907+03	1.1831+03
24	1.1703+03	1.1499+03	1.1481+03	1.1832+03	1.1908+03	1.1832+03
25	1.2092+03	1.1780+03	1.1757+03	1.2316+03	1.2418+03	1.2316+03
26	1.2095+03	1.1783+03	1.1759+03	1.2315+03	1.2421+03	1.2315+03
27	1.2097+03	1.1785+03	1.1762+03	1.2325+03	1.2423+03	1.2325+03
28	1.2435+03	1.1902+03	1.1868+03	1.2885+03	1.3011+03	1.2885+03
29	1.2435+03	1.1900+03	1.1866+03	1.2888+03	1.3009+03	1.2888+03
30	1.2435+03	1.1902+03	1.1868+03	1.2884+03	1.3009+03	1.2884+03

## CONDENSING DATA REDUCTION

	185	187	189	191	193	195
	TC3C	TC4C	TC5C	TC6C	TC7C	TC8C
1	1.3005+03	1.2993+03	1.2664+03	1.2665+03	1.2666+03	1.2569+03
2	1.3003+03	1.2991+03	1.2663+03	1.2664+03	1.2666+03	1.2570+03
3	1.3004+03	1.2992+03	1.2663+03	1.2664+03	1.2665+03	1.2568+03
4	1.2629+03	1.2618+03	1.2212+03	1.2212+03	1.2212+03	1.2098+03
5	1.2626+03	1.2616+03	1.2214+03	1.2212+03	1.2214+03	1.2099+03
6	1.2629+03	1.2617+03	1.2213+03	1.2212+03	1.2214+03	1.2100+03
7	1.2530+03	1.2522+03	1.2248+03	1.2248+03	1.2249+03	1.2174+03
8	1.2528+03	1.2519+03	1.2248+03	1.2248+03	1.2249+03	1.2172+03
9	1.2526+03	1.2519+03	1.2247+03	1.2247+03	1.2249+03	1.2174+03
10	1.2018+03	1.2010+03	1.1707+03	1.1706+03	1.1708+03	1.1628+03
11	1.2019+03	1.2010+03	1.1707+03	1.1706+03	1.1707+03	1.1627+03
12	1.2019+03	1.2011+03	1.1707+03	1.1705+03	1.1706+03	1.1626+03
13	1.2113+03	1.2104+03	1.1716+03	1.1714+03	1.1716+03	1.1615+03
14	1.2113+03	1.2105+03	1.1717+03	1.1715+03	1.1716+03	1.1615+03
15	1.2113+03	1.2104+03	1.1716+03	1.1714+03	1.1716+03	1.1617+03
16	1.1591+03	1.1583+03	1.1205+03	1.1203+03	1.1206+03	1.1117+03
17	1.1592+03	1.1584+03	1.1205+03	1.1203+03	1.1205+03	1.1115+03
18	1.1589+03	1.1580+03	1.1202+03	1.1203+03	1.1204+03	1.1116+03
19	1.1441+03	1.1435+03	1.1227+03	1.1228+03	1.1228+03	1.1178+03
20	1.1442+03	1.1436+03	1.1227+03	1.1227+03	1.1228+03	1.1176+03
21	1.1442+03	1.1436+03	1.1228+03	1.1228+03	1.1230+03	1.1177+03
22	1.1908+03	1.1902+03	1.1499+03	1.1498+03	1.1501+03	1.1402+03
23	1.1909+03	1.1904+03	1.1499+03	1.1498+03	1.1501+03	1.1401+03
24	1.1910+03	1.1904+03	1.1500+03	1.1498+03	1.1499+03	1.1400+03
25	1.2422+03	1.2415+03	1.1788+03	1.1782+03	1.1785+03	1.1626+03
26	1.2426+03	1.2418+03	1.1790+03	1.1784+03	1.1788+03	1.1627+03
27	1.2427+03	1.2421+03	1.1792+03	1.1786+03	1.1790+03	1.1630+03
28	1.3020+03	1.3011+03	1.1936+03	1.1925+03	1.1932+03	1.1627+03
29	1.3017+03	1.3009+03	1.1935+03	1.1923+03	1.1931+03	1.1626+03
30	1.3017+03	1.3009+03	1.1932+03	1.1922+03	1.1929+03	1.1630+03

# CONDENSING DATA REDUCTION

	197	199	201	203	205	207
	TC9C	TC10C	TC11C	TC12C	TC13C	TC14C
1	1.2574+03	1.2576+03	1.2894+03	1.2895+03	1.2821+03	1.2686+03
2	1.2575+03	1.2578+03	1.2895+03	1.2895+03	1.2820+03	1.2684+03
3	1.2574+03	1.2577+03	1.2895+03	1.2895+03	1.2822+03	1.2686+03
4	1.2103+03	1.2106+03	1.2475+03	1.2475+03	1.2391+03	1.2236+03
5	1.2105+03	1.2107+03	1.2475+03	1.2474+03	1.2390+03	1.2236+03
6	1.2104+03	1.2107+03	1.2475+03	1.2475+03	1.2391+03	1.2238+03
7	1.2180+03	1.2178+03	1.2429+03	1.2431+03	1.2370+03	1.2259+03
8	1.2179+03	1.2177+03	1.2429+03	1.2431+03	1.2370+03	1.2259+03
9	1.2181+03	1.2177+03	1.2428+03	1.2432+03	1.2369+03	1.2258+03
10	1.1633+03	1.1631+03	1.1886+03	1.1888+03	1.1825+03	1.1714+03
11	1.1632+03	1.1630+03	1.1885+03	1.1887+03	1.1825+03	1.1715+03
12	1.1632+03	1.1631+03	1.1885+03	1.1888+03	1.1826+03	1.1715+03
13	1.1619+03	1.1619+03	1.1939+03	1.1941+03	1.1866+03	1.1733+03
14	1.1619+03	1.1618+03	1.1938+03	1.1941+03	1.1865+03	1.1732+03
15	1.1618+03	1.1620+03	1.1941+03	1.1942+03	1.1868+03	1.1732+03
16	1.1121+03	1.1120+03	1.1388+03	1.1389+03	1.1326+03	1.1212+03
17	1.1119+03	1.1118+03	1.1387+03	1.1388+03	1.1326+03	1.1213+03
18	1.1119+03	1.1120+03	1.1386+03	1.1388+03	1.1324+03	1.1211+03
19	1.1179+03	1.1182+03	1.1348+03	1.1347+03	1.1304+03	1.1224+03
20	1.1178+03	1.1182+03	1.1347+03	1.1348+03	1.1305+03	1.1226+03
21	1.1179+03	1.1182+03	1.1347+03	1.1347+03	1.1304+03	1.1226+03
22	1.1403+03	1.1407+03	1.1716+03	1.1717+03	1.1645+03	1.1513+03
23	1.1403+03	1.1406+03	1.1715+03	1.1715+03	1.1643+03	1.1512+03
24	1.1402+03	1.1406+03	1.1715+03	1.1716+03	1.1643+03	1.1513+03
25	1.1630+03	1.1634+03	1.2133+03	1.2133+03	1.2021+03	1.1822+03
26	1.1631+03	1.1634+03	1.2136+03	1.2135+03	1.2025+03	1.1826+03
27	1.1634+03	1.1638+03	1.2140+03	1.2139+03	1.2028+03	1.1826+03
28	1.1635+03	1.1638+03	1.2570+03	1.2564+03	1.2369+03	1.2015+03
29	1.1634+03	1.1636+03	1.2568+03	1.2561+03	1.2367+03	1.2013+03
30	1.1639+03	1.1640+03	1.2568+03	1.2560+03	1.2365+03	1.2016+03

## CONDENSING DATA REDUCTION

	209	211	213	215	217	219
	TC15C	TC16C	TC17C	TC18C	TC19C	TC20C
1	1.2669+03	1.2895+03	1.2876+03	1.2817+03	1.2657+03	1.2652+03
2	1.2667+03	1.2893+03	1.2874+03	1.2816+03	1.2656+03	1.2652+03
3	1.2668+03	1.2894+03	1.2874+03	1.2816+03	1.2656+03	1.2651+03
4	1.2216+03	1.2491+03	1.2466+03	1.2395+03	1.2198+03	1.2190+03
5	1.2215+03	1.2492+03	1.2467+03	1.2396+03	1.2201+03	1.2193+03
6	1.2216+03	1.2492+03	1.2467+03	1.2395+03	1.2200+03	1.2192+03
7	1.2244+03	1.2436+03	1.2420+03	1.2372+03	1.2240+03	1.2235+03
8	1.2244+03	1.2437+03	1.2420+03	1.2372+03	1.2240+03	1.2235+03
9	1.2243+03	1.2435+03	1.2420+03	1.2372+03	1.2241+03	1.2235+03
10	1.1698+03	1.1911+03	1.1893+03	1.1841+03	1.1696+03	1.1689+03
11	1.1700+03	1.1912+03	1.1894+03	1.1841+03	1.1697+03	1.1689+03
12	1.1700+03	1.1912+03	1.1892+03	1.1840+03	1.1695+03	1.1687+03
13	1.1713+03	1.1980+03	1.1955+03	1.1888+03	1.1703+03	1.1695+03
14	1.1712+03	1.1979+03	1.1955+03	1.1890+03	1.1705+03	1.1696+03
15	1.1712+03	1.1980+03	1.1955+03	1.1887+03	1.1702+03	1.1696+03
16	1.1195+03	1.1451+03	1.1428+03	1.1365+03	1.1194+03	1.1184+03
17	1.1195+03	1.1451+03	1.1427+03	1.1364+03	1.1193+03	1.1183+03
18	1.1193+03	1.1450+03	1.1427+03	1.1364+03	1.1192+03	1.1180+03
19	1.1214+03	1.1366+03	1.1353+03	1.1318+03	1.1219+03	1.1212+03
20	1.1216+03	1.1367+03	1.1353+03	1.1317+03	1.1218+03	1.1212+03
21	1.1215+03	1.1369+03	1.1355+03	1.1319+03	1.1221+03	1.1214+03
22	1.1495+03	1.1770+03	1.1743+03	1.1676+03	1.1489+03	1.1480+03
23	1.1495+03	1.1770+03	1.1744+03	1.1677+03	1.1490+03	1.1481+03
24	1.1494+03	1.1771+03	1.1745+03	1.1678+03	1.1489+03	1.1481+03
25	1.1793+03	1.2213+03	1.2171+03	1.2067+03	1.1772+03	1.1760+03
26	1.1797+03	1.2217+03	1.2175+03	1.2069+03	1.1775+03	1.1763+03
27	1.1797+03	1.2216+03	1.2178+03	1.2071+03	1.1776+03	1.1765+03
28	1.1964+03	1.2659+03	1.2590+03	1.2409+03	1.1894+03	1.1873+03
29	1.1962+03	1.2658+03	1.2590+03	1.2409+03	1.1892+03	1.1871+03
30	1.1963+03	1.2658+03	1.2588+03	1.2410+03	1.1895+03	1.1873+03



# CONDENSING DATA REDUCTION

	221	223	226	229	230	235
	TKICC	TKOC	TNAO	TNAI	DTNA	WNA
1	1.2988+03	1.2999+03	1.2665+03	1.2573+03	9.1796+00	4.5242+03
2	1.2986+03	1.2997+03	1.2664+03	1.2574+03	8.9941+00	4.5242+03
3	1.2984+03	1.2998+03	1.2664+03	1.2573+03	9.0935+00	4.5242+03
4	1.2586+03	1.2624+03	1.2212+03	1.2102+03	1.0956+01	4.4773+03
5	1.2585+03	1.2621+03	1.2213+03	1.2104+03	1.0942+01	4.4773+03
6	1.2586+03	1.2623+03	1.2213+03	1.2103+03	1.0942+01	4.4773+03
7	1.2504+03	1.2526+03	1.2248+03	1.2177+03	7.1255+00	4.5367+03
8	1.2504+03	1.2524+03	1.2248+03	1.2176+03	7.1968+00	4.5367+03
9	1.2503+03	1.2523+03	1.2248+03	1.2177+03	7.0399+00	4.5367+03
10	1.1977+03	1.2014+03	1.1707+03	1.1631+03	7.5911+00	4.5392+03
11	1.1977+03	1.2014+03	1.1706+03	1.1630+03	7.6762+00	4.5392+03
12	1.1978+03	1.2015+03	1.1706+03	1.1630+03	7.6331+00	4.5392+03
13	1.2056+03	1.2108+03	1.1715+03	1.1618+03	9.7615+00	4.5009+03
14	1.2055+03	1.2109+03	1.1716+03	1.1618+03	9.8758+00	4.5009+03
15	1.2056+03	1.2108+03	1.1715+03	1.1618+03	9.6758+00	4.5009+03
16	1.1525+03	1.1587+03	1.1205+03	1.1119+03	8.5744+00	4.5301+03
17	1.1526+03	1.1588+03	1.1204+03	1.1118+03	8.6728+00	4.5301+03
18	1.1524+03	1.1585+03	1.1203+03	1.1118+03	8.4605+00	4.5301+03
19	1.1427+03	1.1438+03	1.1228+03	1.1180+03	4.7839+00	4.5964+03
20	1.1431+03	1.1439+03	1.1227+03	1.1179+03	4.8403+00	4.5964+03
21	1.1430+03	1.1439+03	1.1229+03	1.1179+03	4.9541+00	4.5964+03
22	1.1854+03	1.1905+03	1.1499+03	1.1404+03	9.5220+00	4.6431+03
23	1.1856+03	1.1906+03	1.1500+03	1.1403+03	9.6353+00	4.6431+03
24	1.1857+03	1.1907+03	1.1499+03	1.1402+03	9.6488+00	4.6431+03
25	1.2352+03	1.2419+03	1.1785+03	1.1630+03	1.5539+01	4.6042+03
26	1.2352+03	1.2422+03	1.1787+03	1.1631+03	1.5639+01	4.6042+03
27	1.2360+03	1.2424+03	1.1789+03	1.1634+03	1.5512+01	4.6042+03
28	1.2955+03	1.3015+03	1.1931+03	1.1633+03	2.9747+01	4.5284+03
29	1.2957+03	1.3013+03	1.1930+03	1.1632+03	2.9747+01	4.5284+03
30	1.2951+03	1.3013+03	1.1928+03	1.1636+03	2.9147+01	4.5284+03

## CONDENSING DATA REDUCTION

	237	238	240	243	246	247
	TNAM	CPNA	QNA	DTQL	QC	Q/AA
1	1.2619+03	3.0031-01	1.2472+04	1.1976+03	1.5574+04	5.2883+04
2	1.2619+03	3.0031-01	1.2220+04	1.1976+03	1.5322+04	5.2028+04
3	1.2619+03	3.0031-01	1.2355+04	1.1980+03	1.5459+04	5.2492+04
4	1.2157+03	3.0008-01	1.4720+04	1.1519+03	1.7633+04	5.9874+04
5	1.2158+03	3.0008-01	1.4701+04	1.1516+03	1.7613+04	5.9808+04
6	1.2158+03	3.0008-01	1.4701+04	1.1515+03	1.7613+04	5.9807+04
7	1.2213+03	3.0011-01	9.7013+03	1.1574+03	1.2637+04	4.2911+04
8	1.2212+03	3.0011-01	9.7983+03	1.1574+03	1.2734+04	4.3240+04
9	1.2212+03	3.0011-01	9.5848+03	1.1574+03	1.2521+04	4.2515+04
10	1.1669+03	3.0000-01	1.0337+04	1.1004+03	1.3043+04	4.4290+04
11	1.1668+03	3.0000-01	1.0453+04	1.1007+03	1.3161+04	4.4688+04
12	1.1668+03	3.0000-01	1.0395+04	1.1007+03	1.3102+04	4.4489+04
13	1.1667+03	3.0000-01	1.3181+04	1.0943+03	1.5863+04	5.3864+04
14	1.1667+03	3.0000-01	1.3335+04	1.0944+03	1.6017+04	5.4389+04
15	1.1667+03	3.0000-01	1.3065+04	1.0943+03	1.5747+04	5.3471+04
16	1.1162+03	3.0000-01	1.1653+04	1.0452+03	1.4143+04	4.8025+04
17	1.1161+03	3.0000-01	1.1787+04	1.0451+03	1.4277+04	4.8478+04
18	1.1161+03	3.0000-01	1.1498+04	1.0451+03	1.3988+04	4.7498+04
19	1.1204+03	3.0000-01	6.5966+03	1.0530+03	9.1171+03	3.0958+04
20	1.1203+03	3.0000-01	6.6745+03	1.0529+03	9.1947+03	3.1222+04
21	1.1204+03	3.0000-01	6.8313+03	1.0530+03	9.3519+03	3.1755+04
22	1.1452+03	3.0000-01	1.3263+04	1.0827+03	1.5900+04	5.3989+04
23	1.1451+03	3.0000-01	1.3421+04	1.0826+03	1.6057+04	5.4524+04
24	1.1451+03	3.0000-01	1.3440+04	1.0821+03	1.6074+04	5.4581+04
25	1.1707+03	3.0000-01	2.1463+04	1.1087+03	2.4202+04	8.2180+04
26	1.1709+03	3.0000-01	2.1602+04	1.1089+03	2.4342+04	8.2655+04
27	1.1712+03	3.0000-01	2.1426+04	1.1091+03	2.4167+04	8.2061+04
28	1.1782+03	3.0000-01	4.0412+04	1.1117+03	4.3163+04	1.4656+05
29	1.1781+03	3.0000-01	4.0411+04	1.1111+03	4.3160+04	1.4655+05
30	1.1782+03	3.0000-01	3.9597+04	1.1112+03	4.2346+04	1.4379+05

# CONDENSING DATA REDUCTION

	251	306	317	319	324	326
	WK	TWI T	Q/A T	TWO T	HCON T	NUC T
1	1.8260+01	1.2957+03	5.8742+04	1.2578+03	2.1640+04	6.1851-02
2	1.7964+01	1.2958+03	5.9226+04	1.2576+03	2.5107+04	7.1758-02
3	1.8124+01	1.2958+03	5.9004+04	1.2577+03	2.6164+04	7.4777-02
4	2.0545+01	1.2552+03	6.5063+04	1.2128+03	2.1360+04	6.0622-02
5	2.0521+01	1.2552+03	6.5002+04	1.2128+03	2.1429+04	6.0816-02
6	2.0522+01	1.2551+03	6.4742+04	1.2129+03	2.0545+04	5.8309-02
7	1.4703+01	1.2479+03	4.8739+04	1.2161+03	2.0481+04	5.8047-02
8	1.4815+01	1.2478+03	4.8588+04	1.2161+03	1.9741+04	5.5948-02
9	1.4567+01	1.2479+03	4.8916+04	1.2160+03	2.1633+04	6.1309-02
10	1.5050+01	1.1938+03	4.8001+04	1.1621+03	1.3001+04	3.6511-02
11	1.5185+01	1.1937+03	4.7506+04	1.1623+03	1.2439+04	3.4932-02
12	1.5117+01	1.1937+03	4.7662+04	1.1623+03	1.2607+04	3.5405-02
13	1.8328+01	1.2006+03	5.6378+04	1.1634+03	1.2096+04	3.4008-02
14	1.8507+01	1.2005+03	5.6365+04	1.1633+03	1.2157+04	3.4180-02
15	1.8195+01	1.2008+03	5.6899+04	1.1633+03	1.2853+04	3.6138-02
16	1.6217+01	1.1444+03	4.7882+04	1.1124+03	6.4400+03	1.8003-02
17	1.6370+01	1.1442+03	4.7491+04	1.1125+03	6.2182+03	1.7383-02
18	1.6039+01	1.1442+03	4.7825+04	1.1123+03	6.3395+03	1.7722-02
19	1.0435+01	1.1380+03	3.5067+04	1.1145+03	8.3700+03	2.3376-02
20	1.0525+01	1.1379+03	3.4654+04	1.1147+03	7.7126+03	2.1540-02
21	1.0704+01	1.1378+03	3.4640+04	1.1147+03	7.7341+03	2.1600-02
22	1.8315+01	1.1781+03	5.4795+04	1.1418+03	8.4482+03	2.3695-02
23	1.8497+01	1.1780+03	5.4620+04	1.1418+03	7.9890+03	2.2407-02
24	1.8516+01	1.1780+03	5.4662+04	1.1418+03	7.9359+03	2.2258-02
25	2.8099+01	1.2243+03	8.1616+04	1.1706+03	8.4826+03	2.3971-02
26	2.8262+01	1.2244+03	8.1239+04	1.1710+03	8.5990+03	2.4300-02
27	2.8062+01	1.2250+03	8.2046+04	1.1710+03	8.4677+03	2.3932-02
28	5.0600+01	1.2777+03	1.4046+05	1.1860+03	1.0324+04	2.9470-02
29	5.0596+01	1.2774+03	1.4037+05	1.1858+03	1.0023+04	2.8613-02
30	4.9640+01	1.2772+03	1.3980+05	1.1860+03	1.0022+04	2.8608-02

## CONDENSING DATA REDUCTION

	354	365	367	372	374	389
	TWI B	Q/A B	TWO B	HCON B	NUC B	TWI TC
1	1.2953+03	4.9432+04	1.2634+03	1.2876+04	3.6808-02	1.2985+03
2	1.2951+03	4.9068+04	1.2634+03	1.2591+04	3.5992-02	1.2986+03
3	1.2952+03	4.9379+04	1.2633+03	1.3051+04	3.7305-02	1.2986+03
4	1.2569+03	6.0758+04	1.2173+03	1.4669+04	4.1654-02	1.2579+03
5	1.2569+03	6.0421+04	1.2176+03	1.5562+04	4.4188-02	1.2578+03
6	1.2569+03	6.0556+04	1.2175+03	1.4979+04	4.2533-02	1.2578+03
7	1.2478+03	3.8799+04	1.2226+03	9.8768+03	2.8000-02	1.2505+03
8	1.2479+03	3.8943+04	1.2225+03	1.0453+04	2.9634-02	1.2504+03
9	1.2477+03	3.8446+04	1.2226+03	1.0000+04	2.8349-02	1.2505+03
10	1.1960+03	4.1972+04	1.1684+03	9.7821+03	2.7480-02	1.1962+03
11	1.1961+03	4.2108+04	1.1684+03	9.9771+03	2.8027-02	1.1960+03
12	1.1961+03	4.2302+04	1.1682+03	9.8381+03	2.7637-02	1.1961+03
13	1.2050+03	5.5631+04	1.1684+03	1.3211+04	3.7171-02	1.2030+03
14	1.2050+03	5.5264+04	1.1686+03	1.2941+04	3.6412-02	1.2029+03
15	1.2050+03	5.5539+04	1.1684+03	1.2998+04	3.6572-02	1.2033+03
16	1.1515+03	5.0200+04	1.1180+03	9.1780+03	2.5670-02	1.1465+03
17	1.1515+03	5.0282+04	1.1179+03	9.0903+03	2.5425-02	1.1464+03
18	1.1515+03	5.0547+04	1.1177+03	9.5291+03	2.6652-02	1.1464+03
19	1.1390+03	2.5802+04	1.1217+03	5.5717+03	1.5563-02	1.1401+03
20	1.1391+03	2.6074+04	1.1217+03	5.6081+03	1.5665-02	1.1400+03
21	1.1392+03	2.5885+04	1.1219+03	5.7290+03	1.6002-02	1.1400+03
22	1.1841+03	5.5924+04	1.1471+03	1.1713+04	3.2865-02	1.1805+03
23	1.1841+03	5.5792+04	1.1472+03	1.1393+04	3.1969-02	1.1803+03
24	1.1843+03	5.6172+04	1.1472+03	1.1843+04	3.3231-02	1.1803+03
25	1.2344+03	9.2807+04	1.1734+03	1.8111+04	5.1232-02	1.2268+03
26	1.2348+03	9.3039+04	1.1737+03	1.8722+04	5.2963-02	1.2270+03
27	1.2348+03	9.2800+04	1.1739+03	1.7594+04	4.9773-02	1.2275+03
28	1.2912+03	1.6743+05	1.1820+03	2.3595+04	6.7439-02	1.2806+03
29	1.2912+03	1.6772+05	1.1818+03	2.4056+04	6.8754-02	1.2803+03
30	1.2910+03	1.6703+05	1.1820+03	2.3532+04	6.7255-02	1.2801+03

# CONDENSING DATA REDUCTION

	399	401	405	406	408	424
	Q/A TC	TWO TC	TKC-TW	HCONTC	NUC TC	TWI BC
1	5.1279+04	1.2654+03	5.5766-01	9.1953+04	2.6285-01	1.2986+03
2	5.1770+04	1.2652+03	1.8216-01	2.8420+05	8.1237-01	1.2983+03
3	5.1545+04	1.2654+03	9.0881-02	5.6716+05	1.6211+00	1.2985+03
4	5.8242+04	1.2200+03	1.5312+00	3.8037+04	1.0797-01	1.2602+03
5	5.8182+04	1.2199+03	1.5163+00	3.8372+04	1.0892-01	1.2602+03
6	5.7918+04	1.2201+03	1.6338+00	3.5451+04	1.0063-01	1.2602+03
7	4.1747+04	1.2233+03	3.9461-01	1.0579+05	2.9986-01	1.2511+03
8	4.1595+04	1.2233+03	4.8563-01	8.5652+04	2.4278-01	1.2512+03
9	4.1925+04	1.2232+03	2.6538-01	1.5798+05	4.4778-01	1.2510+03
10	4.1702+04	1.1687+03	2.3707+00	1.7590+04	4.9404-02	1.1993+03
11	4.1201+04	1.1689+03	2.5209+00	1.6344+04	4.5904-02	1.1994+03
12	4.1357+04	1.1688+03	2.4711+00	1.6737+04	4.7006-02	1.1994+03
13	5.0127+04	1.1700+03	3.7497+00	1.3368+04	3.7597-02	1.2084+03
14	5.0114+04	1.1699+03	3.7597+00	1.3329+04	3.7487-02	1.2083+03
15	5.0654+04	1.1699+03	3.4884+00	1.4521+04	4.0837-02	1.2083+03
16	4.2214+04	1.1184+03	7.3512+00	5.7425+03	1.6056-02	1.1548+03
17	4.1819+04	1.1185+03	7.5984+00	5.5037+03	1.5389-02	1.1548+03
18	4.2157+04	1.1183+03	7.4094+00	5.6897+03	1.5909-02	1.1548+03
19	2.9274+04	1.1205+03	2.8947+00	1.0113+04	2.8246-02	1.1422+03
20	2.8854+04	1.1208+03	3.2140+00	8.9776+03	2.5075-02	1.1423+03
21	2.8841+04	1.1207+03	3.2358+00	8.9130+03	2.4895-02	1.1424+03
22	4.8808+04	1.1481+03	6.0561+00	8.0593+03	2.2608-02	1.1875+03
23	4.8632+04	1.1481+03	6.4446+00	7.5462+03	2.1169-02	1.1875+03
24	4.8675+04	1.1481+03	6.4979+00	7.4909+03	2.1014-02	1.1877+03
25	7.5470+04	1.1772+03	9.8994+00	7.6237+03	2.1555-02	1.2378+03
26	7.5086+04	1.1777+03	9.7632+00	7.6907+03	2.1745-02	1.2382+03
27	7.5898+04	1.1777+03	9.9297+00	7.6436+03	2.1614-02	1.2382+03
28	1.3458+05	1.1928+03	1.6234+01	8.2902+03	2.3689-02	1.2947+03
29	1.3450+05	1.1926+03	1.6619+01	8.0932+03	2.3126-02	1.2947+03
30	1.3392+05	1.1928+03	1.6368+01	8.1815+03	2.3376-02	1.2945+03

## CONDENSING DATA REDUCTION

	434	436	439	440	442	450
	Q/A BC	TWO BC	TK-TWI	HCONBC	NUC BC	PSI HD
1	5.5035+04	1.2631+03	1.0648+00	5.1686+04	1.4776-01	2.4546-01
2	5.4670+04	1.2631+03	1.1177+00	4.8912+04	1.3983-01	2.3791-01
3	5.4983+04	1.2630+03	1.0072+00	5.4591+04	1.5606-01	2.4237-01
4	6.7031+04	1.2165+03	1.3303+00	5.0386+04	1.4309-01	3.8687-01
5	6.6689+04	1.2168+03	1.0703+00	6.2311+04	1.7694-01	3.8609-01
6	6.6826+04	1.2167+03	1.2302+00	5.4322+04	1.5426-01	3.8592-01
7	4.4922+04	1.2218+03	9.7673-01	4.5992+04	1.3039-01	2.0746-01
8	4.5066+04	1.2218+03	7.7530-01	5.8128+04	1.6479-01	2.1059-01
9	4.4566+04	1.2219+03	8.8972-01	5.0089+04	1.4200-01	2.0376-01
10	4.8828+04	1.1671+03	1.2528+00	3.8974+04	1.0949-01	2.9521-01
11	4.8964+04	1.1671+03	1.1884+00	4.1203+04	1.1575-01	3.0057-01
12	4.9162+04	1.1670+03	1.2640+00	3.8894+04	1.0927-01	2.9785-01
13	6.2536+04	1.1672+03	1.3081+00	4.7806+04	1.3452-01	4.1776-01
14	6.2165+04	1.1674+03	1.3788+00	4.5087+04	1.2687-01	4.2615-01
15	6.2442+04	1.1672+03	1.3631+00	4.5808+04	1.2890-01	4.1166-01
16	5.7739+04	1.1163+03	2.5361+00	2.2767+04	6.3680-02	4.5334-01
17	5.7822+04	1.1162+03	2.6102+00	2.2153+04	6.1963-02	4.6165-01
18	5.8091+04	1.1161+03	2.3543+00	2.4675+04	6.9015-02	4.4361-01
19	3.3205+04	1.1201+03	1.3362+00	2.4851+04	6.9414-02	1.9984-01
20	3.3478+04	1.1200+03	1.3580+00	2.4652+04	6.8860-02	2.0285-01
21	3.3286+04	1.1202+03	1.2377+00	2.6893+04	7.5118-02	2.0989-01
22	6.3109+04	1.1457+03	1.9003+00	3.3210+04	9.3189-02	4.7113-01
23	6.2975+04	1.1458+03	2.0339+00	3.0963+04	8.6884-02	4.7979-01
24	6.3356+04	1.1457+03	1.8802+00	3.3696+04	9.4553-02	4.8054-01
25	9.9780+04	1.1723+03	2.6412+00	3.7779+04	1.0688-01	8.2570-01
26	1.0001+05	1.1725+03	2.4978+00	4.0039+04	1.1328-01	8.3550-01
27	9.9767+04	1.1727+03	2.7845+00	3.5829+04	1.0138-01	8.1969-01
28	1.7457+05	1.1809+03	5.4466+00	3.2050+04	9.1634-02	1.9186+00
29	1.7485+05	1.1807+03	5.3169+00	3.2887+04	9.4024-02	1.9158+00
30	1.7416+05	1.1809+03	5.3887+00	3.2319+04	9.2400-02	1.8500+00

# CONDENSING DATA REDUCTION

	451	452	453	610	611	613
	PI	PO	DPC	PIC	POC	DPCC
1	8.7287+00	8.7954+00	-6.6634-02	8.7639+00	8.8167+00	-5.2808-02
2	8.7160+00	8.7858+00	-6.9807-02	8.7501+00	8.8072+00	-5.7074-02
3	8.7076+00	8.7890+00	-8.1442-02	8.7424+00	8.8103+00	-6.7995-02
4	6.8576+00	7.0651+00	-2.0744-01	6.9148+00	7.0756+00	-1.6076-01
5	6.8559+00	7.0531+00	-1.9724-01	6.9130+00	7.0636+00	-1.5062-01
6	6.8594+00	7.0605+00	-2.0109-01	6.9164+00	7.0710+00	-1.5454-01
7	6.5502+00	6.6607+00	-1.1051-01	6.5793+00	6.6687+00	-8.9438-02
8	6.5518+00	6.6528+00	-1.0096-01	6.5815+00	6.6608+00	-7.9277-02
9	6.5468+00	6.6493+00	-1.0246-01	6.5752+00	6.6573+00	-8.2086-02
10	4.6850+00	4.8418+00	-1.5683-01	4.7264+00	4.8399+00	-1.1345-01
11	4.6837+00	4.8425+00	-1.5881-01	4.7260+00	4.8406+00	-1.1459-01
12	4.6850+00	4.8431+00	-1.5820-01	4.7269+00	4.8413+00	-1.1441-01
13	4.9106+00	5.1422+00	-2.3161-01	4.9724+00	5.1418+00	-1.6934-01
14	4.9065+00	5.1450+00	-2.3856-01	4.9697+00	5.1446+00	-1.7491-01
15	4.9119+00	5.1422+00	-2.3025-01	4.9728+00	5.1418+00	-1.6898-01
16	3.4275+00	3.6528+00	-2.2532-01	3.4945+00	3.6461+00	-1.5163-01
17	3.4284+00	3.6538+00	-2.2539-01	3.4969+00	3.6472+00	-1.5029-01
18	3.4275+00	3.6465+00	-2.1908-01	3.4929+00	3.6399+00	-1.4696-01
19	3.2394+00	3.2993+00	-5.9937-02	3.2663+00	3.2913+00	-2.5070-02
20	3.2462+00	3.3008+00	-5.4576-02	3.2735+00	3.2928+00	-1.9308-02
21	3.2442+00	3.3003+00	-5.6038-02	3.2726+00	3.2923+00	-1.9694-02
22	4.2890+00	4.5111+00	-2.2212-01	4.3598+00	4.5077+00	-1.4790-01
23	4.2951+00	4.5144+00	-2.1923-01	4.3673+00	4.5110+00	-1.4367-01
24	4.2976+00	4.5157+00	-2.1807-01	4.3698+00	4.5123+00	-1.4242-01
25	5.8624+00	6.2418+00	-3.7935-01	5.9965+00	6.2473+00	-2.5088-01
26	5.8592+00	6.2543+00	-3.9503-01	5.9951+00	6.2599+00	-2.6482-01
27	5.8941+00	6.2626+00	-3.6846-01	6.0265+00	6.2683+00	-2.4174-01
28	8.2561+00	8.8783+00	-6.2218-01	8.5978+00	8.9011+00	-3.0337-01
29	8.2682+00	8.8661+00	-5.9788-01	8.6095+00	8.8889+00	-2.7941-01
30	8.2521+00	8.8661+00	-6.1404-01	8.5801+00	8.8889+00	-3.0877-01

## CONDENSING DATA REDUCTION

	700	495	701	498	504	507
	X B	WKL B	X T	WKL T	NREF T	NREF B
1	2.4941-01	1.3706+01	8.0362-01	3.5860+00	4.3412+02	1.6597+03
2	2.4964-01	1.3480+01	8.0383-01	3.5239+00	4.2655+02	1.6322+03
3	2.5108-01	1.3573+01	8.0516-01	3.5313+00	4.2742+02	1.6435+03
4	2.6211-01	1.5160+01	8.1528-01	3.7949+00	4.4947+02	1.7977+03
5	2.6106-01	1.5164+01	8.1432-01	3.8104+00	4.5127+02	1.7980+03
6	2.6140-01	1.5157+01	8.1463-01	3.8041+00	4.5056+02	1.7973+03
7	2.5824-01	1.0906+01	8.1178-01	2.7673+00	3.2614+02	1.2862+03
8	2.5655-01	1.1014+01	8.1022-01	2.8116+00	3.3135+02	1.2989+03
9	2.5679-01	1.0826+01	8.1046-01	2.7609+00	3.2535+02	1.2766+03
10	2.6824-01	1.1013+01	8.2092-01	2.6951+00	3.0783+02	1.2595+03
11	2.6861-01	1.1106+01	8.2124-01	2.7144+00	3.1004+02	1.2702+03
12	2.6836-01	1.1060+01	8.2103-01	2.7055+00	3.0903+02	1.2650+03
13	2.7244-01	1.3335+01	8.2471-01	3.2128+00	3.6887+02	1.5339+03
14	2.7386-01	1.3438+01	8.2597-01	3.2207+00	3.6977+02	1.5458+03
15	2.7222-01	1.3242+01	8.2453-01	3.1926+00	3.6656+02	1.5231+03
16	2.8076-01	1.1664+01	8.3235-01	2.7188+00	3.0233+02	1.3001+03
17	2.8020-01	1.1783+01	8.3182-01	2.7531+00	3.0615+02	1.3134+03
18	2.7914-01	1.1562+01	8.3090-01	2.7121+00	3.0155+02	1.2885+03
19	2.5020-01	7.8245+00	8.0445-01	2.0407+00	2.2524+02	8.6399+02
20	2.4776-01	7.9170+00	8.0218-01	2.0820+00	2.2984+02	8.7427+02
21	2.4849-01	8.0445+00	8.0284-01	2.1105+00	2.3298+02	8.8833+02
22	2.6962-01	1.3377+01	8.2223-01	3.2558+00	3.6907+02	1.5191+03
23	2.6857-01	1.3529+01	8.2127-01	3.3059+00	3.7481+02	1.5366+03
24	2.6814-01	1.3552+01	8.2088-01	3.3166+00	3.7605+02	1.5391+03
25	2.6418-01	2.0676+01	8.1725-01	5.1352+00	6.0029+02	2.4221+03
26	2.6571-01	2.0753+01	8.1863-01	5.1259+00	5.9922+02	2.4314+03
27	2.6294-01	2.0683+01	8.1612-01	5.1600+00	6.0345+02	2.4238+03
28	2.5424-01	3.7736+01	8.0807-01	9.7119+00	1.1744+03	4.5710+03
29	2.5335-01	3.7778+01	8.0725-01	9.7527+00	1.1794+03	4.5758+03
30	2.5409-01	3.7027+01	8.0795-01	9.5336+00	1.1526+03	4.4845+03



APPENDIX E

ANALYSIS OF SOME OF THE ERRORS  
ASSOCIATED WITH THE MEASUREMENT OF  
TEMPERATURE DIFFERENCES  
IN THE 100 KW LOOP

G. L. Converse

## APPENDIX E

### Analysis of Some of the Errors Associated with the Measurement of Temperature Differences in the 100 KW Loop

There are several sources of error in the determination of the inside wall to fluid temperature difference in the 100 KW loop. The more important sources of error are the following:

1. Random errors in the measurement of outside wall and fluid temperatures.
2. Errors due to thermocouple drift.
3. Errors in the calculation of inside wall temperature due to the uncertainty in wall thermal conductivity.
4. Errors in the calculation of inside wall temperature caused by uncertainty in the heat flux.

Additional sources of error such as that due to uncertainty in the tube wall thickness are probably less important and were not considered.

Since, in general, two measurements of outside wall temperature are made at the exit of the tube while only a single outside wall temperature measurement is made at each station in the remainder of the tube, it was necessary to consider two cases. The calculational procedure together with a summary of the calculations will be given for each case.

Case I Measuring Station not at the Tube Exit (One outside wall thermocouple at the measuring station, and three well thermocouples located at the tube exit)

1. (a) Random error in the measurement of outside wall temperature.

This error was calculated from multiple digital readouts of the outside wall temperature at a given station. These calculations are summarized in the table below.

TABLE (1)  
RANDOM ERROR IN A SINGLE OUTSIDE WALL THERMOCOUPLE  
NOT AT THE TUBE EXIT

I.D. Date-Time-Run	X mv	Avg. X, $\bar{X}$ mv	$\delta X$ , $X - \bar{X}$ mv	$(\delta X)^2$ (mv) <sup>2</sup>	Probable Error of Each Case = $P_1, 2, 3$
8274-1620-1	14.681	14.687	-.006	$3.6 \times 10^{-5}$	.00643
8274-1620-2	14.682		-.005	$2.5 \times 10^{-5}$	.00643
8274-1620-3	14.698		.011	$12.1 \times 10^{-5}$	.00643
8274-2222-1	14.386	14.400	-.014	$19.6 \times 10^{-5}$	.01015
8274-2222-2	14.399		-.001	$0.1 \times 10^{-5}$	.01015
8274-2222-3	14.416		.016	$25.6 \times 10^{-5}$	.01015
8284-0238-1	14.369	14.355	.014	$19.6 \times 10^{-5}$	.00842
8284-0238-2	14.345		-.010	$10.0 \times 10^{-5}$	.00842
8284-0238-3	14.351		-.004	$1.6 \times 10^{-5}$	.00842

$$K = \Sigma \text{ no. occurrences} = 3$$

$$\Sigma (\delta X)^2 = 18.2 \times 10^{-5}, 45.3 \times 10^{-5}, 31.2 \times 10^{-5}$$

$$\text{Probable error of each case: } p_i = .6745 \sqrt{\frac{\Sigma (\delta X)^2}{K-1}}$$

$$\text{Probable error: } P = \sum_{i=1}^3 p_i / 3 = .0083368 \text{ mv}$$

$$\therefore p = 0.835^\circ\text{F (random error)}$$

1. (b) Random error in the measurement of the fluid temperature

Next the random errors in each of the three exit well thermocouples are calculated. Since the arithmetic average of the three exit well readings is used in the calculation of the wall to fluid temperature difference, the probable errors were combined to obtain the probable error in the average. In general, for independent error,

$$\text{if } z = f(x,y)$$

$$\text{then } P(z) = \sqrt{\left[P(x) \frac{\partial z}{\partial x}\right]^2 + \left[P(y) \frac{\partial z}{\partial y}\right]^2} \quad (1)$$

$$\text{Since } T_{f-\text{avg}} = (T_{f-1} + T_{f-2} + T_{f-3})/3$$

$$\text{then } P(T_{f-\text{avg}}) = \frac{1}{3} \sqrt{\left[P(T_{f-1})\right]^2 + \left[P(T_{f-2})\right]^2 + \left[P(T_{f-3})\right]^2}$$

This calculation is summarized in Table (2).

TABLE (2)

THE RANDOM ERROR OF THREE (3) EXIT WELL THERMOCOUPLES IN THE 100 KW LOOP

I.D. Date-Time-Run	X <sub>1</sub> mv	X <sub>2</sub> mv	X <sub>3</sub> mv	6X <sub>1</sub> mv	6X <sub>2</sub> mv	6X <sub>3</sub> mv	(6X <sub>1</sub> ) <sup>2</sup> (mv) <sup>2</sup>	(6X <sub>2</sub> ) <sup>2</sup> (mv) <sup>2</sup>	(6X <sub>3</sub> ) <sup>2</sup> (mv) <sup>2</sup>
8274-1620-1	14.551	14.669	14.622	.003	.002	.006	0.9x10 <sup>-5</sup>	0.4x10 <sup>-5</sup>	3.6x10 <sup>-5</sup>
8274-1620-2	14.547	14.666	14.618	-.001	-.001	.002	0.1x10 <sup>-5</sup>	0.1x10 <sup>-5</sup>	0.4x10 <sup>-5</sup>
8274-1620-3	14.546	14.665	14.607	-.002	-.002	-.009	0.4x10 <sup>-5</sup>	0.4x10 <sup>-5</sup>	8.1x10 <sup>-5</sup>
8274-2222-1	14.246	14.403	14.346	.004	.001	.011	1.6x10 <sup>-5</sup>	0.1x10 <sup>-5</sup>	12.1x10 <sup>-5</sup>
8274-2222-2	14.248	14.405	14.337	.006	.003	.002	3.6x10 <sup>-5</sup>	0.9x10 <sup>-5</sup>	0.4x10 <sup>-5</sup>
8274-2222-3	14.233	14.397	14.322	-.009	-.005	-.013	8.1x10 <sup>-5</sup>	2.5x10 <sup>-5</sup>	16.9x10 <sup>-5</sup>
8284-0238-1	14.218	14.369	14.311	.010	.002	.015	10.0x10 <sup>-5</sup>	0.4x10 <sup>-5</sup>	22.5x10 <sup>-5</sup>
8284-0238-2	14.201	14.365	14.287	-.007	-.002	-.009	4.9x10 <sup>-5</sup>	0.4x10 <sup>-5</sup>	8.1x10 <sup>-5</sup>
8284-0238-3	14.205	14.366	14.290	-.003	-.001	-.006	0.9x10 <sup>-5</sup>	0.1x10 <sup>-5</sup>	3.6x10 <sup>-5</sup>

$$K_1 = K_2 = K_3 = \text{no. occurrences} = 3$$

Average: (8274-1620)  $\bar{X}_1 = 14.548$ ,  $\bar{X}_2 = 14.667$ ,  $\bar{X}_3 = 14.616$ (8274-2222)  $\bar{X}_1 = 14.242$ ,  $\bar{X}_2 = 14.402$ ,  $\bar{X}_3 = 14.335$ (8284-0238)  $\bar{X}_1 = 14.208$ ,  $\bar{X}_2 = 14.367$ ,  $\bar{X}_3 = 14.296$ 

$$\Sigma(6X_1)^2 = 1.4 \times 10^{-5} \text{ mv}, \quad 13.3 \times 10^{-5} \text{ mv}, \quad 15.8 \times 10^{-5} \text{ mv}$$

$$\Sigma(6X_2)^2 = 0.9 \times 10^{-5} \text{ mv}, \quad 3.5 \times 10^{-5} \text{ mv}, \quad 0.9 \times 10^{-5} \text{ mv}$$

$$\Sigma(6X_3)^2 = 12.1 \times 10^{-5} \text{ mv}, \quad 29.4 \times 10^{-5} \text{ mv}, \quad 34.2 \times 10^{-5} \text{ mv}$$

TABLE (2) (Continued)

THE RANDOM ERROR OF THREE (3) EXIT WELL THERMOCOUPLES IN THE 100 KW LOOP

Probable error (each group):

$$\begin{aligned}
 p_1 &= .001785 \text{ mv}, \quad .005500 \text{ mv}, \quad .005995 \text{ mv} \\
 p_2 &= .0014308 \text{ mv}, \quad .0028216 \text{ mv}, \quad .0014308 \text{ mv} \\
 p_3 &= .0052464 \text{ mv}, \quad .0081779 \text{ mv}, \quad .0088202 \text{ mv}
 \end{aligned}$$

Probable error (each couple):

$$\begin{aligned}
 P_1 &= \sum_{i=1}^3 p_{1_i} / 3 = .004427 \text{ mv} \longrightarrow .444^\circ\text{F} \\
 P_2 &= \sum_{i=1}^3 p_{2_i} / 3 = .0018944 \text{ mv} \longrightarrow .190^\circ\text{F} \\
 P_3 &= \sum_{i=1}^3 p_{3_i} / 3 = .007415 \text{ mv} \longrightarrow .743^\circ\text{F}
 \end{aligned}$$

Probable error (all 3 couples):

$$P^* = \frac{1}{3} \sqrt{P_1^2 + P_2^2 + P_3^2} = .002947 \text{ mv} = 0.295^\circ\text{F} \text{ (random error)}$$

Random error in the outside wall to fluid temperature difference (1 wall and 3 well thermocouples):

$$P_{RN} = \sqrt{(p)^2 + (P^*)^2} = \pm .886^\circ\text{F}$$

These two errors (i.e., 1.(a) and 1.(b) above) have been combined in accordance with equation 1 above to obtain the random error in the outside wall to fluid temperature difference.

## 2. Errors due to thermocouple drift

The general procedure in calibrating the thermocouples in the 100 KW loop is to calibrate all thermocouples relative to a single well thermocouple (designated as B-5 and taken as the standard) both before and after testing. Since these relative calibrations are not in general the same, some thermocouple drift with time is implied. The average of these two calibrations is then used to correct the individual couple readings. Strictly speaking, this is not a random error and should be treated separately for each thermocouple in the analysis (as it is in making the thermocouple corrections). However, since this procedure would result in a different error curve for each thermocouple, in order to facilitate the analysis the thermocouple drift will be treated as a random error and thus independent of the particular thermocouple. It will then be treated as an independent error in the outside wall to fluid temperature difference and combined in accordance with equation 1 with the random error calculated above. This calculation is summarized in Table (3).

TABLE (3)

ERRORS DUE TO THERMOCOUPLE DRIFT (TREATED AS RANDOM ERRORS)

Thermocouple Number	Run 1 Before Test $X_1$ $^{\circ}\text{F}$	Run 2 Before Test $X_2$ $^{\circ}\text{F}$	Run 3 After Test $X_3$ $^{\circ}\text{F}$	Run 4 After Test $X_4$ $^{\circ}\text{F}$	$\bar{X}_1 =$ $\frac{X_1 + X_2}{2}$ $^{\circ}\text{F}$	$\bar{X}_2 =$ $\frac{X_3 + X_4}{2}$ $^{\circ}\text{F}$	$6X =$ $\frac{ X_1 - X_2 }{2}$ $^{\circ}\text{F}$	$(6X)^2$ $(^{\circ}\text{F})^2$
A20	4.45	3.66	9.38	5.45	4.055	7.415	1.680	2.8224
A21	2.04	2.50	1.06	3.10	2.27	2.08	.095	.009025
A22	-0.66	-0.049	-1.50	-0.28	-0.3545	-0.89	.26775	.07169
A23	0.17	0.58	-0.96	-1.37	0.375	-1.165	.77000	.5929
A24	4.61	2.94	2.45	2.80	3.775	2.625	.0575	.003306
A25	3.65	3.71	2.11	3.71	3.68	2.91	.385	.148225
B1	6.61	6.91	6.10	6.48	6.76	6.29	.235	.055225
B2	4.50	3.50	5.76	4.62	4.00	5.19	.595	.354025
B3	-0.31	-0.44	-0.24	-0.25	-0.375	-0.245	.065	.004225
B4	-6.29	-6.58	-6.26	-6.34	-6.435	-6.30	.0675	.004556

K = no. occurrences = 10

$$\Sigma(6X)^2 = 4.065577$$

Probable error:

$$P_{\text{DRIFT}} = .6745 \sqrt{\frac{\Sigma(6X)^2}{K-1}} = .45334^{\circ}\text{F}$$



Case II Measuring Station at the Tube Exit (Two Outside Wall Thermocouples and Three Exit Well Thermocouples)

These calculations are identical to those in Case I with the exception that the arithmetic average of two outside wall thermocouples is used in obtaining the outside wall temperature. The calculation of the probable random error in the average of these two couples is given in Table (4).

This error is combined with the previously calculated well thermocouple (fluid temperature) error, in accordance with equation 1 above, to obtain the random error in the outside wall to fluid temperature difference at the end of the heated length.

TABLE (4)  
RANDOM ERROR IN THE AVERAGE OF TWO  
OUTSIDE WALL THERMOCOUPLES

I.D. Date-Time-Run	$X_1$ mv	$X_2$ mv	$\sigma X_1$ mv	$\sigma X_2$ mv	$(\sigma X_1)^2$ (mv) <sup>2</sup>	$(\sigma X_2)^2$ (mv) <sup>2</sup>
8274-1620-1	14.770	14.776	.003	.011	$0.9 \times 10^{-5}$	$12.1 \times 10^{-5}$
8274-1620-2	14.765	14.765	-.002	.000	$0.4 \times 10^{-5}$	0
8274-1620-3	14.766	14.753	-.001	-.012	$0.1 \times 10^{-5}$	$14.4 \times 10^{-5}$
8274-2222-1	14.447	14.442	.003	.001	$0.9 \times 10^{-5}$	$0.1 \times 10^{-5}$
8274-2222-2	14.446	14.434	.002	-.007	$0.4 \times 10^{-5}$	$4.9 \times 10^{-5}$
8274-2222-3	14.440	14.448	-.004	.007	$1.6 \times 10^{-5}$	$4.9 \times 10^{-5}$
8284-0238-1	14.413	14.412	.010	.011	$10.0 \times 10^{-5}$	$12.1 \times 10^{-5}$
8284-0238-2	14.404	14.403	.001	.002	$0.1 \times 10^{-5}$	$0.4 \times 10^{-5}$
8284-0238-3	14.393	14.388	-.010	-.013	$10.0 \times 10^{-5}$	$16.9 \times 10^{-5}$

$$K_1 = K_2 = \Sigma \text{no. occurrences} = 3$$

Average: (8274-1620)  $\bar{X}_1 = 14.767$ ,  $\bar{X}_2 = 14.765$

(8274-2222)  $\bar{X}_1 = 14.444$ ,  $\bar{X}_2 = 14.441$

(8284-0238)  $\bar{X}_1 = 14.403$ ,  $\bar{X}_2 = 14.401$

$$\Sigma(\sigma X_1)^2 = 1.4 \times 10^{-5}, 2.9 \times 10^{-5}, 20.1 \times 10^{-5}$$

$$\Sigma(\sigma X_2)^2 = 26.5 \times 10^{-5}, 9.9 \times 10^{-5}, 29.4 \times 10^{-5}$$

Probable error (each group):

$$p_i = .001785 \text{ mv}, .002568 \text{ mv}, .006762 \text{ mv}$$

$$p_j = .0077635 \text{ mv}, .006711 \text{ mv}, .0081776 \text{ mv}$$

Average error (each couple):

$$p' = \sum_{i=1}^3 p_i / 3 = .003705 \text{ mv}$$

$$p'' = \sum_{j=1}^3 p_j / 3 = .0075507 \text{ mv}$$

TABLE (4) (Continued)

Probable error (both couples):

$$P_1 = \frac{1}{2} \sqrt{(p')^2 + (p'')^2} = .0084108/2 = .0042054 \text{ mv.}$$

$$P_1 = .421^\circ\text{F (random error)}$$

Random error in the calculation of the outside wall to fluid temperature difference at the test section exit:

$$P_{RX} = \sqrt{(P_1)^2 + (P^*)^2} = \pm .516^\circ\text{F}$$

Conclusion: Errors due to uncertainty in the thermal conductivity of the wall and the heat flux

These two errors can be conveniently treated together in the following manner.

$$T_{wi} - T_f = (T_{wo} - T_f) - q'' \left( \frac{D_o \ln(D_o/D_i)}{2k} \right) \quad (2)$$

From equations 1 and 2,

$$P(T_{wi} - T_f) = \sqrt{P(T_{wo} - T_f)^2 + \left[ q'' \frac{D_o \ln(D_o/D_i)}{2k} \right]^2 \left[ \left( \frac{P(q'')}{q''} \right)^2 + \left( \frac{P(k)}{k} \right)^2 \right]} \quad (3)$$

The probable percentage error in wall thermal conductivity is estimated as  $\pm 4\%$  based on the results obtained in Reference 12.

The estimated probable percentage error in heat flux is  $\pm 3\%$ .

$$\text{Then } \left( \frac{P(q'')}{q''} \right)^2 + \left( \frac{P(k)}{k} \right)^2 = (.04)^2 + (.03)^2 = (.05)^2$$

$$P(T_{wi} - T_f) = \sqrt{P(T_{wo} - T_f)^2 + (.05)^2 \left[ q'' \frac{D_o \ln(D_o/D_i)}{2k} \right]^2} \quad (4)$$

The probable error in the inside wall to fluid temperature difference is calculated from equation 4. A summary of the calculation is given in the table following.

TABLE (5)  
ERROR IN INSIDE WALL TO FLUID TEMPERATURE DIFFERENCE

①	Random error (1-non-exit couple)		0.886°F
②	Random error (2-exit couples)		0.516°F
③	Calibration error		0.45334°F
④	③ <sup>2</sup>		0.205517 (°F) <sup>2</sup>
⑤	① <sup>2</sup> + ④	$P_{T_{W_o}}^2$ (1 cpl.)	0.99051 (°F) <sup>2</sup>
⑥	② <sup>2</sup> + ④	$P_{T_{W_o}}^2$ (2 cpls.)	0.47177 (°F) <sup>2</sup>
⑦	Random error (in well cpls.)	$P_{T_{sat}}$	0.295°F
⑧	⑦ <sup>2</sup>		0.087025 (°F) <sup>2</sup>
⑨	⑤ + ⑧	$(P_{T_{W_o}-T_f})^2$ (1 cpl.)	1.077535 (°F) <sup>2</sup>
⑩	⑥ + ⑧	$(P_{T_{W_o}-T_f})^2$ (2 cpls.)	.558795 (°F) <sup>2</sup>

Thermal conductivity of Cb-1Zr:

$$k = 32 \text{ Btu/hr-ft-}^\circ\text{F at } 1800^\circ\text{F}$$

For a 3/4-inch nominal tube diameter

$$\ln(D_o/D_i) = .31306; \quad D_o = .08741667 \text{ ft}$$

$$\text{Let } F = \left[ \frac{D_o \ln(D_o/D_i)}{2k} \right]^2 = 4.57113 \times 10^{-10} \left( \frac{^\circ\text{F}}{\text{Btu/hr-ft}^2} \right)^2$$

TABLE (5) (Continued)  
ERROR IN INSIDE WALL TO FLUID TEMPERATURE DIFFERENCE

⑪ $q''$ $\frac{\text{Btu}}{\text{hr-ft}^2}$	⑫ $Fx(q'')^2$	⑬ ⑨ + ⑫	⑭ ⑩ + ⑫	⑮ $\sqrt{⑬}$ $(PT_{wi} - T_f)_1$	⑯ $\sqrt{⑭}$ $(PT_{wi} - T_f)_2$
0	0	1.077535	0.558795	1.038°F	0.74753°F
$2.5 \times 10^4$	0.2857	1.3632	0.8445	1.1676°F	0.91897°F
$5.0 \times 10^4$	1.1428	2.2203	1.7016	1.4900°F	1.30450°F
$7.5 \times 10^4$	2.5713	3.6488	3.1301	1.9102°F	1.7692°F
$1.0 \times 10^5$	4.5711	5.6486	5.1299	2.3767°F	2.2649°F
$1.25 \times 10^5$	7.1424	8.2199	7.7012	2.8671°F	2.7751°F
$1.5 \times 10^5$	10.2850	11.363	10.844	3.3709°F	3.2930°F

---

Although the above analysis is somewhat lacking in statistical rigor, it is felt that it may provide a somewhat better estimation of the error in the measurement of the inside wall to fluid temperature difference than can be obtained from an educated guess based on operating experience.

DISTRIBUTION FOR QUARTERLY AND FINAL REPORTS  
CONTRACT NAS3-2528  
January 1, 1964

NASA  
Washington, D.C. 20546  
Attn: William H. Woodward (RN)

NASA  
Washington, D.C. 20546  
Attn: Dr. Fred Schulman (RN)

NASA  
Washington, D.C. 20546  
Attn: James J. Lynch (RNP)

NASA  
Washington, D.C. 20546  
Attn: George C. Deutsch (RR)

NASA  
Ames Research Center  
Moffet Field, California 94035  
Attn: Librarian

NASA  
Goddard Space Flight Center  
Greenbelt, Maryland 20771  
Attn: Librarian

NASA  
Langley Research Center  
Hampton, Virginia 23365  
Attn: Librarian

NASA  
Lewis Research Center  
21000 Brookpark Road  
Cleveland, Ohio 44135  
Attn: Librarian (3-7)

NASA  
Lewis Research Center  
21000 Brookpark Road  
Cleveland, Ohio 44135  
Attn: Dr. Bernard Lubarsky (86-1)

NASA  
Lewis Research Center  
21000 Brookpark Road  
Cleveland, Ohio 44135  
Attn: Seymour Lieblein (7-1)

NASA  
Lewis Research Center  
21000 Brookpark Road  
Cleveland, Ohio 44135  
Attn: Warren H. Lowdermilk (106-1)

NASA  
Lewis Research Center  
21000 Brookpark Road  
Cleveland, Ohio 44135  
Attn: Dr. Louis Rosenblum (106-1)

NASA  
Lewis Research Center  
21000 Brookpark Road  
Cleveland, Ohio 44135  
Attn: Robert Siegel (49-2)

NASA  
Lewis Research Center  
21000 Brookpark Road  
Cleveland, Ohio 44135  
Attn: Robert Y. Wong (5-9)

NASA  
Manned Spacecraft Center  
Houston, Texas 77001  
Attn: Librarian

NASA  
George C. Marshall Space Flight Center  
Huntsville, Alabama 35812  
Attn: Librarian

NASA  
George C. Marshall Space Flight Center  
Huntsville, Alabama 35812  
Attn: Ernst Stuhlinger

NASA  
George C. Marshall Space Flight Center  
Huntsville, Alabama 35812  
Attn: Russell H. Shelton

NASA  
Lewis Research Center  
21000 Brookpark Road  
Cleveland, Ohio 44135  
Attn: I.I. Pinkel (86-5)

NASA  
Lewis Research Center  
21000 Brookpark Road  
Cleveland, Ohio 44135  
Attn: Solomon Weiss (54-1)

NASA  
Lewis Research Center  
21000 Brookpark Road  
Cleveland, Ohio 44135  
Attn: John E. Dilley (86-1)

NASA  
Lewis Research Center  
21000 Brookpark Road  
Cleveland, Ohio 44135  
Attn: Patent Counsel (77-1)

NASA  
Lewis Research Center  
21000 Brookpark Road  
Cleveland, Ohio 44135  
Attn: Harold J. Christenson (5-3)

NASA  
Lewis Research Center  
21000 Brookpark Road  
Cleveland, Ohio 44135  
Attn: Robert G. Dorsch (11-1)

NASA  
Lewis Research Center  
21000 Brookpark Road  
Cleveland, Ohio 44135  
Attn: Robert E. English (86-1)

NASA  
Lewis Research Center  
21000 Brookpark Road  
Cleveland, Ohio 44135  
Attn: James P. Lewis (11-1)

NASA  
Jet Propulsion Laboratory  
4800 Oak Grove Drive  
Pasadena, California 91103  
Attn: D. R. Bartz

NASA  
Western Operations Office  
150 Pico Boulevard  
Santa Monica, California 90406  
Attn: John Keeler

NASA  
Lewis Research Center  
21000 Brookpark Road  
Cleveland, Ohio 44135  
Attn: Daniel Bernatowicz (100-1)

NASA  
Lewis Research Center  
21000 Brookpark Road  
Cleveland, Ohio 44135  
Attn: Ruth N. Weltmann (86-5) (6)

NASA  
Lewis Research Center  
21000 Brookpark Road  
Cleveland, Ohio 44135  
Attn: H. G. Hurrell (100-1)

NASA  
Jet Propulsion Laboratory  
4800 Oak Grove Drive  
Pasadena, California 91103  
Attn: Librarian

NASA  
Lewis Research Center  
21000 Brookpark Road  
Cleveland, Ohio 44135  
Attn: D. Namkoong (86-1)

NASA  
Lewis Research Center  
21000 Brookpark Road  
Cleveland, Ohio 44135  
Attn: L. Gertsma (86-1)

NASA  
Lewis Research Center  
21000 Brookpark Road  
Cleveland, Ohio 44135  
Attn: Roger F. Mather (500-309)

NASA  
Scientific & Technical Information Facility  
Box 5700  
Bethesda, Maryland 20014  
Attn: NASA Representative (2)

NASA  
Scientific & Technical Information  
Washington, D.C. 20546  
Attn: Code AFFSS-A

Air Force Systems Command  
Aeronautical Systems Division  
Wright-Patterson Air Force Base, Ohio 45433  
Attn: R. J. Benzing (ASRCNL)

Air Force Systems Command  
Aeronautical Systems Division  
Wright-Patterson Air Force Base, Ohio 45433  
Attn: Bernard Chasman (ASRCEA)

Air Force Systems Command  
Aeronautical Systems Division  
Wright-Patterson Air Force Base, Ohio 45433  
Attn: George E. Thompson (ASRMFP-1)

Snap 50 Spur Office  
U.S. Atomic Energy Commission  
Washington, D.C. 20545  
Attn: Herbert D. Rothen  
NASA-AEC, Deputy

Snap 50 Spur Office  
U.S. Atomic Energy Commission  
Washington, D.C. 20545  
Attn: Gerald Leighton

U.S. Atomic Energy Commission  
Technical Reports Library  
Washington, D.C. 20545  
Attn: J. M. O'Leary (2)

U.S. Atomic Energy Commission  
Technical Information Service  
Extension  
P.O. Box 62  
Oak Ridge, Tennessee 37831 (2)

U.S. Atomic Energy Commission  
Washington, D.C. 20545  
Attn: R. M. Scroggins

U.S. Atomic Energy Commission  
Reactor Experiment Branch  
Washington, D.C. 20545  
Attn: T. W. McIntosh

Dr. James Hadley  
Head, Reactor Division  
Lawrence Radiation Laboratory  
Livermore, California

Argonne National Laboratory  
P.O. Box 299  
Lemont, Illinois 60439  
Attn: Librarian

Argonne National Laboratory  
9700 South Cass Avenue  
Argonne, Illinois 60440  
Attn: John F. Marchaterre

Brookhaven National Laboratory  
Upton, Long Island, New York 11973  
Attn: Librarian

Brookhaven National Laboratory  
Upton, Long Island, New York 11973  
Attn: Dr. O. E. Dwyer

Oak Ridge National Laboratory  
Oak Ridge, Tennessee 37831  
Attn: Herbert W. Hoffman



Oak Ridge National Laboratory  
Oak Ridge, Tennessee 37831  
Attn: W. D. Manly

U.S. Naval Research Laboratory  
Washington, D.C. 20390  
Attn: C. T. Ewing

Columbia University  
Department of Chemical Engineering  
New York, N.Y. 10027  
Attn: Dr. Charles F. Bonilla

Massachusetts Institute of Technology  
Cambridge, Massachusetts 02139  
Attn: Dr. Warren M. Rohsenow

University of Michigan  
Department of Chemical and  
Metallurgical Engineering  
Ann Arbor, Michigan 48103  
Attn: Dr. Richard E. Balzhiser

Southern Methodist University  
Engineering School  
Dallas, Texas 75222  
Attn: Dr. Harold A. Blum

University of Wisconsin  
Madison, Wisconsin 53706  
Attn: Dr. Max W. Carbon

Advanced Technology Laboratories  
Division of American Standard  
369 Whisman Road  
Mountain View, California 94040  
Attn: Library

Aerojet-General Corporation  
P.O. Box 296  
Azusa, California 91702  
Attn: Librarian (2)

Aerojet-General Nucleonics  
P.O. Box 77  
San Ramon, California 94583  
Attn: Librarian (2)

Aerojet-General Nucleonics  
P.O. Box 77  
San Ramon, California 94583  
Attn: Mr. Ken Johnson

AiResearch Manufacturing Company  
Sky Harbor Airport  
402 South 36th Street  
Phoenix, Arizona 85009  
Attn: Librarian (2)

AiResearch Manufacturing Company  
Sky Harbor Airport  
402 South 36th Street  
Phoenix, Arizona 85009  
Attn: E. A. Kovacevich

AiResearch Manufacturing Company  
9851-9951 Sepulveda Blvd.  
Los Angeles, California 90045  
Attn: Librarian

AiResearch Manufacturing Company  
9851-9951 Sepulveda Blvd.  
Los Angeles, California 90045  
Attn: James J. Killackey

Atomics International  
8900 DeSoto Avenue  
Canoga Park, California 91303  
Attn: Louis Bernath

Avco  
Research & Advanced Development  
Department  
201 Lowell Street  
Wilmington, Massachusetts 01800  
Attn: Librarian

Babcock and Wilcox Company  
Research Center  
Alliance, Ohio  
Attn: W. Markert, Jr.

Battelle Memorial Institute  
505 King Avenue  
Columbus, Ohio 43201  
Attn: Alexis W. Lemmon, Jr.

Curtiss-Wright Corporation  
Research Division  
Quehanna, Pennsylvania  
Attn: S. Lombardo

Electro-Optical Systems, Inc.  
Advanced Power Systems Division  
Pasadena, California  
Attn: Joseph Neustein

Euratom  
Common Research Center of Ispra  
Casella postale no. 1  
Ispra (Varese)  
Italy  
Attn: Dr. Bernard P. Milliot  
Heat Transfer Division

General Motors Corporation  
Allison Division  
Indianapolis, Indiana 46206  
Attn: Librarian

Geoscience Ltd.  
8686 Dunaway Drive  
La Jolla, California 92037  
Attn: H. F. Poppendiek

Hughes Aircraft Company  
Engineering Division  
Culver City, California 90230  
Attn: Tom B. Carvey, Jr.

Southwest Research Institute  
8500 Culebra Road  
San Antonio, Texas 78206  
Attn: Dr. W. D. Weatherford, Jr.

Marquardt Aircraft Company  
P.O. Box 2013  
Van Nuys, California  
Attn: Librarian

Materials Research Corporation  
Orangeburg, New York  
Attn: Vernon E. Adler

The Martin Company  
Nuclear Division  
P.O. Box 5042  
Baltimore, Maryland 21220  
Attn: Librarian

MSA Research Corporation  
Gallery, Pennsylvania 16024  
Attn: Frederick Tepper

Plasmadyne Corporation  
3839 South Main Street  
Santa Anna, California  
Attn: Librarian

Pratt & Whitney Aircraft  
400 Main Street  
East Hartford, Connecticut 06108  
Attn: Librarian (2)

Pratt & Whitney Aircraft  
400 Main Street  
East Hartford, Connecticut 06108  
Attn: Richard Curry

Pratt & Whitney Aircraft  
400 Main Street  
East Hartford, Connecticut 06108  
Attn: Eugene Szetela

Rocketdyne  
Canoga Park, California 91303  
Attn: Librarian

Headquarters  
Aeronautical Sys. Division  
Air Force Sys. Command  
United States Air Force  
WRIGHT PATTERSON AFB, Ohio  
ATTN: Information Processing Section  
Applications Laboratory  
Directorate of Mtls. & Processes

NASA-Lewis Research Center  
21000 Brookpark Road  
Cleveland, Ohio 44135  
Attn: Report Control Office, MS 5-5

Sundstrand Denver  
2480 West 70th Avenue  
Denver, Colorado 80221  
Attn: Librarian

Thompson-Ramo-Wooldridge, Inc.  
New Devices Laboratories  
7209 Platt Avenue  
Cleveland, Ohio 44115  
Attn: Librarian

Thompson-Ramo-Wooldridge, Inc.  
New Devices Laboratories  
7209 Platt Avenue  
Cleveland, Ohio 44115  
Attn: A. Ziobro

Union Carbide Nuclear Company  
P.O. Box X  
Oak Ridge, Tennessee 37831  
Attn: X-10 Laboratory Records  
Department (2)

United Nuclear Corporation  
Development Division  
5 New Street  
White Plains, New York  
Attn: Librarian

Westinghouse Electric Corporation  
Astronuclear Laboratory  
P.O. Box 10864  
Pittsburgh, Pennsylvania 15236  
Attn: Librarian

Westinghouse Electric Corporation  
Aero-Space Department  
Lima, Ohio 45801  
Attn: Librarian

California Institute of Technology  
Jet Propulsion Laboratory  
4800 Oak Grove Drive  
Pasadena, California 91103  
Attn: Mr. Gerald M. Kikin

A. L. Clarkson  
3325 Wilshire Blvd.  
General Electric Company  
Los Angeles, California 90005

Research Institute of Temple University  
4150 Henry Avenue  
Philadelphia, Pennsylvania 19144  
Attn: A. V. Grosse

Professor W. E. Hilding  
Department of Mechanical Engineering  
University of Connecticut  
Storrs, Connecticut 06268

Reactor Engineering Argonne Materials  
Laboratory  
Argonne, Illinois 60440  
Attn: Ralph P. Stein

Knolls Atomic Power Laboratory  
P.O. Box 1072  
Schenectady, New York 12301  
Attn: Document Librarian

General Electric Company  
P.O. Box 100  
Richland, Washington 99352  
Attn: Technical Information Operation  
Dr. T. T. Claudson

North American Aviation, Incorporated  
Atomics International Division  
Canoga Park, California  
Attn: Paul Cohn

Professor George A. Brown  
Engineering Projects Laboratory  
Massachusetts Institute of Technology  
Research Laboratory of Electronics  
Cambridge, Massachusetts 02139

General Dynamics Corporation  
General Atomic Division  
P.O. Box 608  
San Diego, California 92112  
Attn: Library (2)

Mr. Rudolph Rust  
Jet Propulsion Laboratory  
4800 Oak Grove Drive  
Pasadena, California